2020
Atomic, Molecular, and Optical Sciences Research PI Meeting

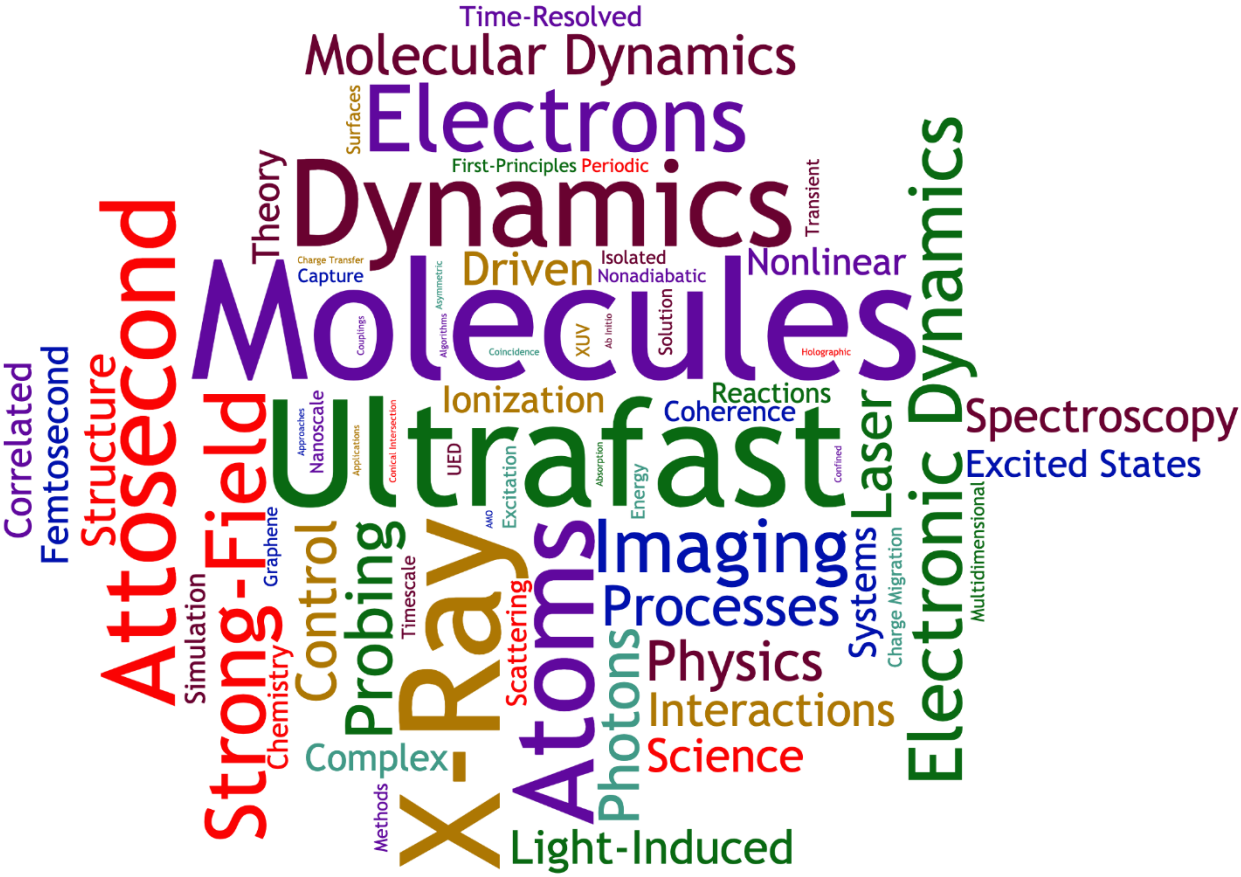

Virtual Meeting
October 26-28, 2020

U.S. DEPARTMENT OF ENERGY | Office of Science

Office of Basic Energy Sciences
Chemical Sciences, Geosciences & Biosciences Division

Page is intentionally blank.

Program and Abstracts

2020
Atomic, Molecular, and Optical Sciences Research PI Meeting

Virtual Meeting
October 26–28, 2020

Chemical Sciences, Geosciences, and Biosciences Division
Office of Basic Energy Sciences
Office of Science
U.S. Department of Energy

Cover Graphics: The input for the Wordclouds.com cover art is based on the titles of the abstracts for this year's meeting. The font is "Trebuchet MS."

The research grants and contracts described in this document are supported by the U.S. DOE Office of Science, Office of Basic Energy Sciences, Chemical Sciences, Geosciences and Biosciences Division.

Page is intentionally blank.

FOREWORD

This volume summarizes the 40th annual Research Meeting of the Atomic, Molecular and Optical Sciences (AMOS) Program sponsored by the U. S. Department of Energy (DOE), Office of Basic Energy Sciences (BES), and comprises descriptions of the current research sponsored by the AMOS program. The participants of this meeting include the DOE laboratory and university principal investigators (PIs) within the BES AMOS Program. The purpose of the annual PI meeting is to facilitate scientific interchange among the PIs and to promote a sense of program identity.

The AMOS program continues to advance fundamental, hypothesis-driven research in ultrafast chemical sciences, with emphasis on strong-field and x-ray physics and chemical dynamics. The program supports basic experimental and theoretical research aimed at understanding the structural and dynamical properties of atomic and molecular systems. The research targets fundamental interactions of photons and electrons with atomic and molecular systems to characterize and control their behavior. The foundational knowledge and techniques produced by this research portfolio constitute crucial contributions in support of the BES mission.

The AMOS program is vigorous and innovative, and enjoys strong support within the Department of Energy. This is due entirely to our scientists, the outstanding research they perform, and the relevance of this research to DOE missions. The AMOS community continues to explore new scientific frontiers relevant to DOE missions and the strategic challenges facing our nation and the world.

We are deeply indebted to the members of the scientific community who have contributed their valuable time toward the review of proposals and programs, either by electronic review of grant applications, panel reviews, or on-site and virtual reviews of our multi-PI programs. These thorough and thoughtful reviews are central to the continued vitality of the AMOS program.

We are privileged to serve in the management of this research program. In performing these tasks, we learn from the achievements and share the excitement of the research of the scientists and students whose work is summarized in the abstracts published on the following pages.

Many thanks to the staff of the Oak Ridge Institute for Science and Education (ORISE), in particular Linda Severs and Connie Lansdon, for their help in planning and executing this first *virtual* meeting of AMOS PIs. We also thank Teresa Crocket and Gwen Johnson in BES for their indispensable behind-the-scenes efforts in support of the BES/AMOS program.

Thomas B. Settersten
Jeffrey L. Krause
Chemical Sciences, Geosciences, and Biosciences Division
Office of Basic Energy Sciences
Office of Science
U.S. Department of Energy

Page is intentionally blank.

AGENDA

2020 Atomic, Molecular and Optical Sciences Research PI Meeting

Office of Basic Energy Sciences
U. S. Department of Energy
Virtual Meeting

Zoom Meeting ID and password: Registration required. Unique connection information will be sent to registered invitees.

All times are EDT (UTC-4)

Monday, October 26

12:45 pm **** Join Zoom Meeting ****

1:00 pm *BES/CSGB Update and Outlook*
Bruce C. Garrett, CSGB Division Director

1:30 pm *Welcome and Introductory Remarks*
Thomas B. Settersten, AMOS Program Manager

Session I New Project Introductions (3-minute, 1-slide summaries)

1:45 pm *ECRP: Atomic View of Molecular Photocatalysis using X-ray Lasers*
Amy Cordones-Hahn, SLAC National Accelerator Laboratory

ECRP: Probing Ultrafast XUV/x-ray Induced Electron Correlation in the Molecular Frame
Li Fang, University of Central Florida

Beating Electronic Decoherence
Wen Li, Wayne State University

Probing Molecular Wavepacket Evolution Using Multidimensional Coherent Spectroscopy
Steven Cundiff, University of Michigan

Dynamics of Two-Electron Atomic and Molecular Processes
Jean Marcel Ngoko Djiokap, University of Nebraska

2:00 pm **** Break ****

Monday, October 26 (continued)

Session II Small-Group Projects (30-minute presentations + 10-minute Q&A sessions)

2:20 pm *Coherent Probes of Molecular Charge Migration*
Kenneth J. Schafer, Mette Gaarde, Kenneth Lopata, Louisiana State University
Robert R. Jones, University of Virginia
Louis F. DiMauro, Ohio State University

3:00 pm *Imaging Ultrafast Charge Transfer Processes with Coincident Charged-Particle Spectroscopy*
Artem Rudenko, Daniel Rolles, and Loren Greenman, Kansas State University
Robin Santra, Deutsches Elektronen Synchrotron DESY

3:40 pm *Probing Nuclear and Electronic Dynamics in Ultrafast Ring-Conversion Molecular Reactions*
Martin Centurion, University of Nebraska
Peter M. Weber, Brown University
Kenneth Lopata, Louisiana State University
Artem Rudenko, Daniel Rolles, Kansas State University

4:20 pm *Theory and Simulation of Ultrafast Multidimensional Nonlinear X-ray Spectroscopy of Molecules*
Shaul Mukamel, University of California, Irvine
Marco Garavelli, Università di Bologna
Niranjan Govind, Pacific Northwest National Laboratory
Sergei Tretiak, Los Alamos National Laboratory

5:00 pm **** Break ****

Session III LCLS Informational Presentations

5:10 pm *LCLS-II X-ray Free-Electron Laser Facility at SLAC*
Robert W. Schoenlein
LCLS Deputy for Science, SLAC National Accelerator Laboratory

5:25 pm *MeV Ultrafast Electron Diffraction Facility at SLAC*
Xijie Wang
Director MeV-UED, SLAC National Accelerator Laboratory

5:40 pm *Q&A and Discussion*

5:55 pm **** Closing Remarks and Adjourn ****

Tuesday, October 27

12:45 pm	**** Join Zoom Meeting ****
Session IV	(20-minute presentations + 10-minute Q&A sessions)
1:00 pm	*Ultrafast AMO Physics in Strong Fields* **Philip H. Bucksbaum**, SLAC National Accelerator Laboratory
1:30 pm	*Complete Photoionization Spectroscopy in the Attosecond Regime* **Carlos Trallero**, University of Connecticut
2:00 pm	*Control of Molecular Dynamics: Algorithms for Design, Analysis and Implementation* **Herschel A. Rabitz**, Princeton University
2:30 pm	*Mapping Light-Induced Potentials, Bond Stabilization, and Light-Induced Conical Intersections in the Ro-Vibrational Dissociation Dynamics and Fragment-Kinetic-Energy-Release of Diatomic Molecular Ions* **Uwe Thumm**, Kansas State University
3:00 pm	**** Break ****
Session V	(20-minute presentations + 10-minute Q&A sessions)
3:15 pm	*Electronic and Nuclear Dynamics in Molecular Photoionization* **Robert R. Lucchese**, Lawrence Berkeley National Laboratory
3:45 pm	*Manipulating and Probing Ultrafast Atomic and Molecular Dynamics* **Robert R. Jones**, University of Virginia
4:15 pm	*Structure and Dynamics of Atoms, Ions, and Molecules: Light Driven Molecular Dynamics* **Itzik Ben-Itzhak**, Kansas State University
4:45 pm	*Getting the Whole Picture: First Results from Adding Feynman Phase to Strong-Field Virtual Detection* **Joseph Eberly**, University of Rochester
5:15 pm	**** Closing Remarks and Adjourn ****

Wednesday, October 28

12:15 pm **** Join Zoom Meeting ****

Session VI (20-minute presentations + 10-minute Q&A sessions)

12:30 pm *Early Career: X-ray Diffraction Imaging with Intense Sub-fs X-ray Pulses*
Tais Gorkhover, SLAC National Accelerator Laboratory

1:00 pm *Simulations of Non-linear Compton Scattering*
Francis Robicheaux, Purdue University

1:30 pm *X-ray Probes of Condensed Phase Photoinduced Dynamics*
Anne Marie March, Argonne National Laboratory

2:00 pm *Ultrafast X-ray Induced Phenomena*
Gilles Doumy, Argonne National Laboratory

2:30 pm *Ultrafast X-ray Studies of Chemical and Interfacial Dynamics*
Oliver Gessner, Lawrence Berkeley National Laboratory

3:00 pm **** Break ****

Session VII (20-minute presentations + 10-minute Q&A sessions)

3:15 pm *Generation of Optimized Ultrafast Extreme-Ultraviolet Beams for Applications in Energy Sciences*
Margaret Murnane, University of Colorado

3:45 pm *High-order Harmonic Generation in Solids*
Shambhu Ghimire, SLAC National Accelerator Laboratory

4:15 pm *Electron Dynamics in 2D Systems*
Tony F. Heinz, SLAC National Accelerator Laboratory

4:45 pm *Femtosecond and Attosecond Strong-Fields Processes in Two-Dimensional Finite Systems: Graphene and Graphene-Like Nanopatches and Polycyclic Molecules*
Vadym M. Apalkov, Georgia State University

5:15 pm *Closing Remarks*
Thomas B. Settersten, AMOS Program Manager

5:30 pm **** Adjourn ****

TABLE OF CONTENTS

Lawrence Berkeley National Laboratory

SLAC National Accelerator Laboratory

University Research Summaries (by PI)

Page is intentionally blank.

AMO Physics at Argonne National Laboratory

Gilles Doumy, Phay Ho, Anne Marie March, Stephen Southworth,
Linda Young
Chemical Sciences and Engineering Division
Argonne National Laboratory, Lemont, IL 60439
gdoumy@anl.gov, pho@anl.gov, amarch@anl.gov,
southworth@anl.gov, young@anl.gov

1 Overview

The Argonne AMO physics program explores the frontiers of x-ray physics as enabled by accelerator-based light sources and, in so doing, lays the foundation for ultrafast x-ray applications in other scientific domains. We utilize the novel properties of accelerator-based coherent x-ray sources, primarily the Advanced Photon Source (APS) synchrotron at Argonne and the Linac Coherent Light Source (LCLS) x-ray free-electron laser (XFEL) at SLAC in concert with ultrafast lasers, to create exotic and/or non-equilibrium states and to probe their rapidly evolving properties with atomic-scale spatial and temporal resolution. The experimental work is supported and complemented by theoretical developments, often taking advantage of massively parallel codes developed for the MIRA and THETA supercomputer at the Argonne Leadership Computing Facility (ALCF).

The program is structured in three complementary subtasks. The first subtask aims at a quantitative and predictive understanding of x-ray interactions with matter in the high-intensity limit. Here we explore new atomistic imaging approaches enabled by the most intense femtosecond and attosecond x-ray pulses. Our code developments build upon our knowledge base of the response of atoms and molecules, and the code was ported from MIRA to THETA supercomputer this year. We have uncovered the importance of transient resonant excitation in the unperturbed target as well as subsequently formed ions, and, have explored the use of incoherent imaging. These studies provide guidance for optimal conditions for serial single-shot coherent x-ray imaging of nanoscale samples. We have extended our studies beyond x-ray interaction with single particle samples to include propagation from the weak- to strong-field regimes in optically thick samples where substantial energy exchange between the sample and field leads to phenomena such as self-induced transparency and self-focusing.

In the second subtask we strive to understand and control the trajectory of ultrafast inner-shell excitations in molecular systems. We build upon our deep knowledge base of inner-shell phenomena in the energy domain and use ultrashort x-ray pulses from free-electron laser sources to explore inner-shell spectroscopies in the time domain - e.g. x-ray pump/x-ray probe photoelectron spectroscopy to observe time-evolving chemical shifts and stimulated x-ray Raman spectroscopies to create localized electronic excitations which are then probed to study the evolving charge densities. We are developing theoretical tools for high-precision predictions of photoelectron and photoabsorption spectra in small molecules. Tunable, intense, two-color attosecond pulses from XLEAP provide a revolutionary tool to investigate electron dynamics with x-ray non-linear spectroscopies. Energy domain access to multielectron processes occuring in the deepest inner shells of high-Z elements will be provided by a new photoelectron spectroscopy instrument at the APS.

The third subtask focuses on understanding molecular dynamics in condensed phases at the

atomic, molecular and electronic level. Here we use the APS to access the picosecond timescale and XFELs for femtosecond phenomena. Within this subtask we have developed sensitive high-repetition-rate methods to measure electronic and geometric changes of photo-excited molecules in solution in chemically relevant systems at the APS. Recent 500-fold improved efficiency of x-ray emission spectroscopy (XES) has extended implementation of "time-slicing" techniques with a ∼10-fold improved temporal resolution to XES. Extensive planning is underway for the APS Upgrade and the new beamline with rapidly interchangable monochromatic and broadband capabilities is eagerly anticipated along with enhanced pump laser capabilities. Finally, we have demonstrated the use of tunable soft x-rays from LCLS in the water window to observe the ultrafast birth and unique signature of the hydroxyl radical following impulsive ionization of pure liquid water and thus have introduced a new tool to study water radiolysis in complex environments.

2 X-ray Physics at the Intensity Frontier

2.1 X-ray Imaging Applications with Femtosecond and Attosecond Pulses

P. J. Ho, L. Young, S. H. Southworth, C. Knight[1], T. Gorkhover[2], S. Kuchel[2], C. Bostedt[3], A. Rudenko[4], D. Rolles[4], S.-K. Son[5], R. Santra[2,5], J. Hajdu[6], F. Maja[6] and other collaborators

Project Scope: The unprecedented intensity of XFELs enables exploration of a new frontier of light-matter interactions and the associated applications of imaging structure and chemical dynamics. We aim at a predictive understanding of the fundamental processes induced by intense x-ray pulses through a combined experimental and theoretical approach in systems of increasing complexity from atoms to molecules to clusters.

Recent Progress: Since the early vision for single-shot imaging experiments with XFELs [33], radiation induced damage has been an important topic. For atoms interacting with an intense XFEL pulse, early studies [34–39] have shown that sequential absorption [40] can be strongly enhanced through transient resonances. Recently, the interplay of resonant and relativistic effects was found to affect the charge state distributions from intense x-ray field ionization of heavy atom [6]. Beyond atoms, ultrafast charge transfer led to enhanced ionization in molecular ionization [41]. In the x-ray focus, extended systems are transformed into a highly excited state with a large fraction of delocalized electrons [42] and with strong electron-nuclear coupling [43].

Over the past years, our group has contributed to single particle imaging methods [2,3,5,7–12], including virtually contaminant-free sample delivery with an improved electrospray injector [7], imaging structural dynamics in laser heated nanoparticles [8] and ultracold rotating superfluid droplets [12], characterizing crystalline defects via angular correlations in the scattering images [9,10], coincidence imaging combining single-shot X-ray scattering with fluorescence and ion time-of-flight (TOF) spectroscopy [11] and a holographic approach [2].

During this past year, we published a paper on a combined experimental and theoretical study of x-ray diffractive imaging of sucrose clusters [13]. The scattering data was measured at LCLS using 180-fs, soft x-ray pulses. We found that near an absorption edge at 530 eV, there is a loss of scattering intensity close to a factor of 10 compared to the prediction from linear scattering theory. By performing Monte-Carlo/Molecular-Dynamics (MC/MD) calculations [45,46] of a 50-nm sucrose cluster on MIRA at the ALCF, our calculated results reveal that the anomalous scattering response reflects the signature of transient structures produced during the pulse.

This year, in collaboration with the group of Gorkhover, we investigated the scattering response of xenon clusters interacting with soft x-ray pulses (650 to 1500 eV) as a function of pulse duration (0.5 to 200 fs) and pulse energy. We experimentally explore the both resonant and non-resonant imaging in a new regime - with pulse durations below inner-shell decay timescales. This new regime is afforded by the broad bandwidth and sub-femtosecond capabilities of the XLEAP operation mode at LCLS. For theoretical analysis, we extended our MC/MD code to include relativistic and spin-orbit coupling corrections. By comparing the Ar time-of-flight (TOF) data with the calculated results from the Monte-Carlo rate equation [38], the experimental pulse energies of the sub-fs pulses were determined to be a few microJoules. We found that at 1.5 keV the Xe cluster scattering cross section is much higher than the cross section predicted from the linear scattering model. Our analysis shows that ion resonances [6, 13, 35, 38] are responsible for this increased cross section. A manuscript describing these results is being prepared for submission. In addition, in preparation for the arrival of AURORA, the first exascale computer at ALCF, we have ported our MC/MD code to THETA, which has a similar architecture to that of AURORA.

Future Plans: The sensitivity of the scattering response to the transient electronic structures near absorption edges suggest that both the pulse duration and photon energy can be exploited

for optimizing the scattering signal of SPI experiments. In collaboration with Gorkhover, we will perform experimental investigation of the resonant and non-resonant imaging processes using sub-fs pulses at LCLS. Theoretically we will continue to develop and use our MC/MD calculations for systems with heavier elements under realistic experimental pulse conditions. In addition, we plan to explore the effects of coherent electron dynamics, including Rabi oscillations, in resonant scattering.

2.2 Ultraintense, ultrashort pulse x-ray scattering in small molecules

Phay J. Ho, A. E. A. Fouda, K. Li[7], G. Doumy, L. Young

Project Scope: We study coherent x-ray scattering in small molecules from the linear to nonlinear regime. We explore the sensitivity of the coherent scattering channel to electron correlation effects in molecules and examine x-ray pump / x-ray probe methods that can directly probe x-ray induced ultrafast charge transfer and dissociation.

Recent Progress: The dream of performing single molecule imaging [33] via coherent x-ray scattering using "diffract-before-destroy" methodology with XFEL pulses has inspired many studies of x-ray-matter interactions at high intensities in free atoms [34–36,38,40], molecules [6], and small clusters [49]. These studies have generally focused on ion and electron spectra resulting from the dominant photoabsorption channel, leaving the coherent (elastic) scattering channel less explored. By contrast, coherent scattering has been the workhorse technique for studying larger targets in both the biological community [47,48] and the AMO physics community [13,42,43]. Here we bridge this gap by studying computationally coherent x-ray scattering in small molecules from the linear to the x-ray multiphoton regime.

Nonlinear x-ray absorption is readily reached by x-ray focusing and understanding the associated x-ray scattering pattern is of basic interest. Using the MC/MD method, we investigated non-resonant, hard x-ray scattering from 1,3-cyclohexadiene (CHD) at three x-ray energies: 5.6, 9.0 and 24 keV, motivated by the single spike operation demonstrations [50, 51], and the upcoming LCLS-HE. We calculated for three pulse durations 0.25, 2.5 and 25 fs. We observe that the shortest pulse duration allows extraction of molecular structure at fluences larger than the nominal saturation fluence — in accordance with the concept of "diffract-before-destroy". At the highest photon energy the inelastic channel is a bothersome background [45, 52], but is also the most readily discriminated via energy shift. In addition, we investigated hard x-ray scattering from CH_3I, where we find that x-ray coherent scattering can provide a *direct* visualization of the intramolecular charge transfer and dissociation processes that were previously deduced from ion charge state measurements [6].

While MC/MD calculations have shown to provide insights into non-linear x-ray interaction, they employ the independent atom model (IAM) for calculating the scattering response. As a first step toward computing molecular scattering response beyond IAM in the nonlinear x-ray regime, which requires tracking of a large number of core- and valence-excited states, we developed a code for calculating coherent x-ray scattering using *ab-initio* molecular wave functions. Using this code, we computed the static scattering responses of the ground state and core-excited states of CHD using molecular wave functions derived with HF and DFT theories (see Fig. 1). The paper describing the results of this study has been submitted for publication [53].

Future Plans: We plan to explore the feasibility to use CDI to study molecular bonding and electron correlation effects in a small molecule. We plan to extend our molecular scattering code by combining it with the rate equation and time-dependent Schrödinger equation approach to study the dynamical scattering response of molecules in intense x-ray pulses.

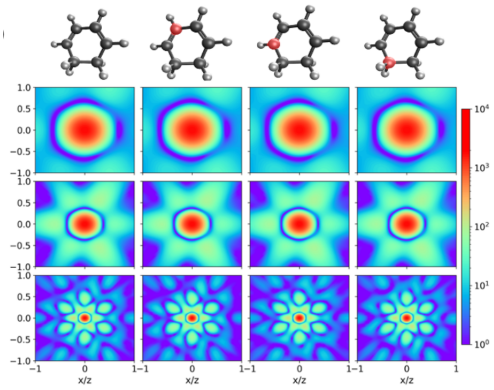

Figure 1: Scattering images of 1-3-cyclohexadiene simulated by DFT. The first column is the neutral ground state and the next three are core ionized states, the carbon with the core hole is indicated in red. The first second and third rows show photon energies of 5.6, 9 and 24 keV respectively.

2.3 X-ray imaging using higher-order correlations

P. J. Ho, L. Young, A. Fouda, C. Knight[1], and other collaborators

Project Scope: Coherent diffractive imaging (CDI) with XFEL pulses holds the promise to probe structure [4] and follow the dynamics of non-periodic entities with atomic resolution. However, this approach remains challenging due to sample damage during the pulse [45]. We aim to explore the potential of x-ray correlation methods as a high-resolution structural and dynamical probe by investigating the higher-order correlations associated with the fluorescence spectrum and speckle patterns from illuminated samples.

Recent Progress: Novel experimental spectroscopic and imaging techniques have been developed to exploit x-ray free-electron lasers (XFELs) for studying the structure and dynamics of non-periodic entities at atomic spatial resolution and femtosecond timescales. Recently, Classen and coworkers [54] proposed to use fluorescence intensity correlations, based on the principle of Hanbury Brown and Twiss effect [55], to image the 3D arrangement of an array of heavy atoms using intense x-ray pulses. By treating the heavy atoms as random light emitters, the second order correlation function $G_2(\vec{k}_1, \vec{k}_2)$ of the fluorescence intensity is related to the intensity of the Fourier transform of the distribution of the fluorescence emitters $\rho_f(\vec{r})$ by the following relation

$$G_2(\vec{k}_1, \vec{k}_2) = 1 + \left| \int d^3r \rho_f(\vec{r}) e^{i(\vec{k}_1 - \vec{k}_2)\cdot\vec{r}} \right|^2 \quad (1)$$

This past year, we published a paper [14] on the fluorescence dynamics of non-periodic systems subject to XFEL pulses as a function of system size using our MC/MD method on MIRA at the ALCF. We found that the cluster environment in an intense x-ray pulse leads to an enhanced $K\alpha$ and $K\alpha^h$ emission yield and extended emission time beyond the lifetime of the core-excited states.

This year we investigated the effectiveness of this fluorescence approach with intense x-ray pulses by computing the fluorescence intensity correlation, $G_2(\vec{k}_1, \vec{k}_2)$. In our investigation, Ar clusters were subjected to a 2-fs, 5-keV, 3.5×10^{11}-photons/μm^2 pulse. The 2-D fluorescence detector is assumed to have 1024×1024 pixels and is perpendicular to the incident x-ray beam. To compare the fluorescence imaging approach with the CXDI appproach, we focus on a subset of G_2, in which we choose a fixed $\vec{k}_1$ and vary only $\vec{k}_2$. We found that the fluorescence intensity correlation computed from the $K\alpha^h$ channel has a higher visibility/contrast in comparison to the $K\alpha$. This is because $K\alpha^h$ events take place within a narrower time window, when the degree of structural distortion is small. In comparison to the G_2 from these two channels, the computed coherent diffraction pattern has a lower contrast due to the background from delocalized electrons.

Future Plans: We plan to investigate the feasibility of achieving both atomic and elemental resolution in heterogeneous systems with fluorescence imaging. We note that there have been

experimental efforts within in the AMOS contractor group to measure G_2 on various targets at different XFEL facilities, and further experiments are being planned. Also, we plan to compute the full dataset of G_2 with more than 10^{12} values for feature detection on THETA.

2.4 X-ray transient absorption: from the weak- to strong-field regime

L. Young, K. Li[7], M. Gaarde[8], M. Labeye[8,9], P.J. Ho, G. Doumy, D. Koulentianos, S.H. Southworth, A.M. March, M. Meyer [10], T. Pfeifer[9], Z.-H. Loh[11], J.-E. Rubensson[6] and other collaborators

Project Scope: Understanding x-ray transient absorption from the weak- to strong-field regimes, as encountered at XFELs, is foundational for a complete understanding of nonlinear x-ray processes and also of practical importance. Here we focus on a quantitative understanding of deviations from a linear absorption model for propagation on resonances and develop the first 3D model in the x-ray regime. Such understanding may allow to tailor the temporal and spectral properties of a transmitted x-ray pulse and achieve a more complete understanding of x-ray attenuation and reshaping.

Recent Progress: Understanding fundamental x-ray/matter interactions at high intensity is a vibrant frontier enabled by the continued rapid development of x-ray free-electron lasers. Many early experiments involved understanding the interaction mechanisms [36, 40, 41] leading to x-ray damage resulting from stochastically varying self-amplified spontaneous emission pulses in the single atom/molecule regime. However, the propagation through thick resonant absorbing media, basic for studies in the solid state, solution phase and gases via transmission-based x-ray transient absorption, has been much less studied. XFELs now deliver nearly transform-limited pulses with sub-femtosecond duration at MHz repetition rates [56] over a wide range of x-ray energies thus universally enabling transient absorption studies near organic (C,N,O) and inorganic (transition metal and actinide) edges and the power density produces effects such as stimulated Raman scattering [57, 58], amplified spontaneous emission, pulse compression [59].

This year we completed and submitted for publication a theoretical study of temporal, spectral, and spatial reshaping of intense, ultrafast x-ray pulses propagating through a resonant medium [60]. Our calculations are based on the solution of a 3D Time-Dependent Schrödinger-Maxwell Wave Equation, with the incident x-ray photon energy on resonance with the core-level 1s-3p transition in neon. We studied the evolution of the combined incident and medium-generated field, including the effects of stimulated emission, absorption, ionization and Auger decay, as a function of the input pulse energy and duration. We found that stimulated Raman scattering between core-excited states $1s^{-1}3p$ and $2p^{-1}3p$ occurs at high x-ray intensity, and that the emission around this frequency is strongly enhanced when also including the response of the ion. We also explored the dependence of x-ray self-induced transparency (SIT) and self-focusing on the pulse intensity and duration.

A proposal to study resonant propagation and transient absorption from the weak- to strong-field regimes is awaiting scheduling at the EuXFEL SQS endstation. The implementation of this experiment is complex, requiring characterization of an incident SASE spectrum using a "cookiebox" photoelectron spectrometer in the undulator hall [61], replacement of the standard AQS endstation with a target cell chamber being designed and fabricated by the MPIK group, and addition of a transmission spectrometer from the Uppsala group. The high-resolution characterization of the incident SASE spectrum is being investigated by EuXFEL and Argonne/UChicago and employs a variant of ghost imaging techniques [62].

Future Plans: With beamtime at the EuXFEL, we plan to characterize the weak- to strong-field behavior for propagation through dense resonant media and test our theoretical model. Potential theoretical extensions to the 3D code include the inclusion of arbitrary polarization.

3 Ultrafast X-ray Induced Phenomena

3.1 Time-resolved chemical shifts

G. Doumy, S.H. Southworth, D. Koulentianos, P. J. Ho, A. Fouda, K. Li, A.M. March, L. Young, L. Cheng[12], J. Cryan[13], S. L. Sorensen[14], and other collaborators

Project Scope: The interaction of x-ray photons with inner shell electrons in molecules creates localized excitations that evolve rapidly, leading to charge redistribution, nuclear motion and eventually bond breaking. The availability at XFELs of two short x-ray pulses with different photon energies [63–65] and precisely controllable delay enables schemes where the first pulse interacts with the inner shell of one atomic site, and the second pulse then probes a different site. We aim to follow both the first steps of electron dynamics in the core-excited states and the evolution of the molecule after the first decay processes take place. This knowledge is crucial in understanding the photochemical behavior of these molecules upon x-ray absorption.

Recent Progress: The ability of synchrotrons to produce high average flux, high resolution soft x-ray radiation has been used for several decades to further the development of the ESCA technique (Electron Spectroscopy for Chemical Analysis) [66] and to study the possibility of site-selective photochemistry [67], by which selective excitation of a molecule could guide its dissociation paths. Powerful coincidence techniques have helped observe the outcome of site-selective ionization, as we used in our recent study on the molecule ethyl trifluoroacetate (known as the ESCA molecule for being a poster child of the sensitivity of the binding energy) [16]. Little site-selectivity was observed, and additional insights were only provided by theory, suggesting that it was the character of the dicationic states obtained after Auger decay that was the dominant factor, and not a fast equilibration of internal energy as suggested before. XFELs open the door to following these processes in real time.

Extending ESCA to time-resolved studies of x-ray induced dynamics was started in the group a few years ago with a pioneering experiment on the small molecule CO, exploiting the strong oxygen π^* resonance to provide good contrast between the two atomic sites for the pump and the probe in spite of the small difference in photon energies [68]. For the return of operation at LCLS, we were granted beamtime, now scheduled for November 2020. Using simple fluorinated hydrocarbon molecules as model targets, we will initiate electronic and nuclear dynamics by selectively ionizing a core electron at a carbon site, and follow the evolution of the system by x-ray photoemission spectroscopy at a Fluorine site by using a second, optimized pulse. At short delays between the two pulses, i.e. before Auger decay has taken place, we will probe core-excited molecules by producing double-core hole species.

The opportunity to use core-excited molecules to increase the chemical sensitivity of the ESCA method has been well documented, and the intense pulses from XFELs were quickly thought to provide a unique means to produce them in large amounts [69]. We have revisited the data from such an experiment, performed in the early days of LCLS operation on the molecule formamide [70]. This molecule is a model system with three different atomic sites with K-edges in the soft x-ray region, and we produced double core hole states using a single, intense x-ray pulse. The inability to selectively target each atomic site both reduces the efficiency of production and hampers the energy resolution greatly, preventing a meaningful comparison with theory.

We expect that our improved setup will produce cleaner and more precise data that should begin to test the accuracy of several different theoretical methods. Because photoemission is essentially an instantaneous process, we can expect that core-excited molecules will exhibit time-resolved chemical shifts before Auger decay takes place. It becomes critical to evaluate the initial binding energies precisely. In an ongoing collaboration with Lan Cheng, the highly accurate coupled-cluster

methods have been extended to core-excited molecules, using a differential measurement between a calculation of the ground state, and a calculation of the doubly core-excited state. A core-valence separation scheme is used, where virtual core orbitals are excluded from the coupled-cluster calculation. Benchmark calculations were performed on a series of small molecules, evaluating the effects of electron correlations by increasing the levels of excitation and studying the influence of the size of the basis set. Comparisons with previous experimental data obtained from XFELs and synchrotrons showed a good agreement, and calculations of the binding energies for the formation of two-site double core holes in the fluorinated hydrocarbons we will study at LCLS were reported [19]. While for single core hole ionization potentials a precision of 0.1 eV has been demonstrated [71], we expect a precision better than 0.5 eV for the double core hole states. Because these calculations are computationally expensive, it is also important to develop alternative methods using reduced basis sets in preparation for calculations involving nuclear dynamics. We have started on such a project on the formamide molecule, using restricted active space self consistent field (RASSCF) methods with good success in comparison with more expensive techniques [70].

Aside from photoemission, another natural probe of the molecular dynamics comes from recording the x-ray absorption spectrum, since it can often be easier to measure experimentally. X-ray absorption spectra are often more complicated than photoemission spectra, since they can involve multiple resonant states, including Rydberg states. When the molecule becomes larger, it can become difficult to assign the different spectral features to specific molecular sites. Here again, theoretical calculations are necessary to guide the interpretation. XAS spectra at the carbon K-edge were recorded for the ESCA molecule, and coupled-cluster calculations from Lan Cheng were able to reproduce the spectral features with excellent agreement both for the absolute energy and for the oscillator strength [72].

Future Plans: We will follow up on our upcoming experiment by expanding on two directions. First, obtaining better temporal resolution through the use of attosecond pulses, with 2-pulse, 2-color available for users starting next year. Second, we will take advantage of the high repetition rate of LCLS-II to perform measurements in coincidence to ascertain the location of the first ionization step.

3.2 Self-referenced measurement of electron dynamics

G. Doumy, A. Cavalieri[3], C. Bostedt[3], L. DiMauro[15], M. Meyer[10] and other collaborators

Project scope: Transposing the laser streaking methods from attophysics to XFEL studies has been an ongoing effort. While initially aimed at characterizing the x-ray pulse duration, those experiments have enabled a new, self referenced technique to measure the temporal properties of ultrafast electronic dynamics following inner-shell x-ray ionization with sub-femtosecond resolution.

Recent Progress: Laser streaking is currently the only demonstrated way to characterize the x-ray pulse duration at an XFEL. Successful demonstrations have been made using both linear and circular polarization for the intense laser field, using wavelengths ranging from the IR to THz [17, 73–75]. However, these methods suffer from the unavoidable temporal jitter between the two independent sources. Shot-to-shot compensation is possible to a precision of about 20 fs in the best conditions, much larger than the potential sub-femtosecond resolution of the streaking technique.

A self-referenced method can be envisioned by measuring concurrently the prompt photoemission signal and a signal from a delayed process, such as Auger decay. We have shown that this allows retrieving the phase of the streaking laser on a shot-to-shot basis, thus providing a timing jitter correction with femtosecond precision, as illustrated in Fig. 2. Despite the limited energy

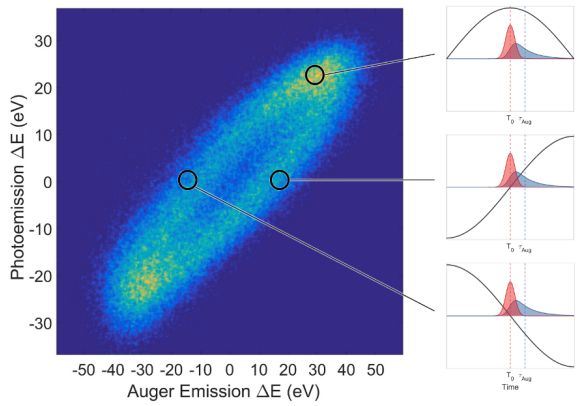

Figure 2: Correlation map generated from 80,000 single-shot streaking measurements in neon using a 17 μm streaking field, and 7 fs FWHM, 1130 eV ionizing X-ray pulses. Individual points in the scatter plot represent the kinetic energy shift of the photo- and Auger electron peaks in each shot. On the right, three sketches are shown, corresponding to three characteristic regions on the map. The sketches show the photoelectrons (red) and Auger electrons (blue) along with the streaking field (black), demonstrating the recovery of the phase of the streaking field. (Figure reproduced from Ref. [22])

resolution of this initial experiment, we also measured the delay between photoemission from the K shell of a neon atom and the Auger electron emission that results from the refilling of the core hole, with sub-femtosecond resolution. Surprisingly, this delay is longer than the core-hole lifetime, and can only be recovered by considering a full quantum mechanical model of the photoionization and subsequent Auger decay. The model shows that this quantum effect is significant when the x-ray pulse duration is on par with the decay lifetimes, but that using attosecond pulses such as produced by XLEAP would allow to neglect it [22].

Future Plans: Laser streaking is compatible with high-repetition-rate operation, and is the only demonstrated technique capable of correcting for the timing jitter between a laser and the XFEL pulses. Extension of this new method to molecular systems will be a challenging task but has the potential to become a standard technique at all soft x-ray XFEL beamlines.

3.3 Attosecond science at LCLS

G. Doumy, P. J. Ho, A.M. March, S.H. Southworth, L. Young, D. Koulentianos, K. Li, J. Cryan[13], P. Walter[13], A. Marinelli[13] and other collaborators

Project Scope: The success of the XLEAP project at LCLS to produce intense, sub-femtosecond pulses in the soft x-ray regime [56] is opening new areas of investigation, including non-linear interaction between the x-ray fields and atoms and molecules [76]. The ability to study electronic processes before decay processes or nuclear motion take place, coupled with the site-selectivity afforded by x-ray interaction will open a new window on observing electronic motion and electronic coherences.

Recent Progress: The success of the XLEAP initiative, and the unique availability at the LCLS, has been recognized as a great opportunity to launch a multi-year scientific campaign to establish the basis of attosecond science at XFELs. The effort is led by SLAC scientists, on the accelerator, beamline and photon science sides, and joined by multiple experimental and theoretical teams around the world. The effort focuses on using 2-pulse 2-color modes of operation with attosecond pulses in the soft x-ray regime. The first pulse will aim at creating electronic coherences, while the second pulse will attempt to probe processes such as charge migration.

Our group's involvement stems from years of experience as XFEL users, experience in attophysics using high harmonic sources and theoretical support. For the campaign, the main model molecule identified is para-amino-phenol. The first attosecond pulse will either attempt to produce electronic coherences by producing impulsive ionization of a set of inner valence orbitals, or

by stimulating x-ray Raman transitions with site selectivity. The second attosecond pulse will probe the electron density at a specific site in the molecule, using x-ray absorption as an observable, or photoemission spectroscopy. The experiment on impulsive ionization extends from work performed earlier at LCLS using our hemispherical electron analyzer [77] on isopropanol, using few-femtosecond pulses. The experiment on stimulated x-ray Raman transitions aims to produce neutral excited states, as demonstrated in NO gas [20].

Future Plans: While LCLS, and then LCLS-II will provide the first attosecond pulses, first at low repetition rate, and then up to MHz, other XFELs are aiming to offer such capabilites to users, including the upcoming soft x-ray line at Swiss-FEL, where very intense pulses may be possible.

3.4 High resolution electron spectroscopy of inner-shell resonance, threshold, and multiple core-hole processes

S. H. Southworth, D. Koulentianos, G. Doumy, A. M. March, C. Otolski, K. Li, P. J. Ho, L. Young, M. N. Piancastelli,[16], M. Simon,[16] and other collaborators

Project scope: Photoelectron and Auger electron spectroscopies excited by tunable synchrotron radiation are sensitive to electronic structure, photoionization dynamics, and core-hole decay mechanisms, topics that pose an enduring challenge for theorists. The intense, polarized, tunable, narrow-bandwidth x rays at the APS are ideal for Hard X-ray Photoelectron Spectroscopy (HAXPES) and we are developing a high resolution, high-collection-efficiency electron spectrometer, Scienta EW4000, for these studies.

Recent Progress:

The scientific program was initiated by collaborating with the group of M. Simon at the SOLEIL synchrotron facility using their HAXPES setup [78]. Measurements were made of the Ne *KK/K* double-to-single *K*-shell cross-section ratio over the 2.3-8 keV x-ray energy range. Double-*K* ionization necessarily involves electron correlation and illustrates key conceptual ideas that were well studied experimentally and theoretically in the case of He [79–81]. The goal of the Ne experiment is to observe variations of the *KK/K* ratio resulting from shakeoff and knockout mechanisms [81]. Unlike He, however, the *K*-shell photoelectrons escape from the core through the $2s^2 2p^6$ outer-shell electrons. Experiments on metal foils have suggested that *KK/K* ratios are modified by electron correlations with outer shells [82]. The Ne measurements will be compared with calculated *KK/K* ratios for both He-like Ne^{8+} and 10-electron Ne. The measurements complement the 2.3-keV measurement on the Auger electron spectrum of neon reported earlier that is rich with electron correlation effects [83].

The APS offers access to higher-energy x rays than the HAXPES setup at SOLEIL [78] enabling experiments on heavier atoms, deeper inner shells, and additional decay steps in vacancy cascades [18]. The first HAXPES experiments at the APS could include extending the Ne *KK/K* measurements to higher x-ray energies. Other early experiments will use high-resolution x-rays, such as provided by the Si(311) monochromator at beamline 7ID, to scan through Rydberg states and the ionization thresholds of Kr and Xe [18] and the 1s $\rightarrow$4p σ^* pre-edge resonance of CF_3Br. Those measurements will explore near-edge resonance and threshold phenomena, such as photoelectron recapture and photoelectron-Auger-electron energy transfers resulting from post-collision interactions [84].

We will also study multiple core-hole excitation and ionization in molecules [85,86]. Such states are produced by single-photon absorption and driven by electron correlation. Of particular interest are electronic states with one core ionized electron and one core excited electron. Simulating such highly correlated states presents challenges to theory [86, 87]. Multiple core-hole states in

molecules used in two-photon experiments at XFELs are additional targets of interest. We have recently remotely participated in a EuXFEL experiment led by our French collaborators focusing on the creation of double-core-hole states where one of the interactions is a resonant excitation (so-called $K^{-2}V$ states) in gas phase water.
Future Plans: The Auger electron spectra of neon recorded over 2.3 - 8 keV at SOLEIL will be analyzed to determine the *KK/K* ratio. The measurements will be compared with theoretical calculations for both 10-electron and helium-like neon to determine the effects of outer-shell electrons. Our electron spectrometer will be used for first experiments at the APS to investigate inner-shell resonance and threshold phenomena and highly-correlated multiple core-hole states of molecules.

3.5 Resonant inelastic x-ray scattering of actinide complexes

S. H. Southworth, G. Doumy, C. Otolski, A. M. March, A. E. A. Fouda, P. J. Ho, D. A. Walko,[17], R. E. Wilson,[18] and L. Cheng[12]

Project scope: The chemistry and electronic properties of actinide compounds are rich in variety due to the Z dependence of the 5f and 6d valence orbital energies [88,89]. The large nuclear charges result in strong relativistic effects acting on the atomic orbitals. Correlating the electronic and chemical properties of actinide compounds with their orbital structures is of both fundamental and practical interest. Theoretical calculations of their electronic structures and geometries require treatment of relativistic and many-electron interactions. The results of this research are relevant to Heavy Element Chemistry programs as well as fundamental atomic physics.
Recent Progress: Resonant inelastic x-ray scattering (RIXS) maps of four uranium compounds were measured across the 17165-eV U L_3 ($2p_{3/2}$) edge by recording the $L\beta_2$ ($4d_{5/2}$-$2p_{3/2}$) x-ray emission spectrum over 17150-17250 eV with 1 eV steps. The double-crystal monochromator at APS beamline 7ID was used with Si(311) crystals that produced an intense, tunable x-ray beam with an estimated bandwidth of ∼0.5 eV in the 17-18 keV range. For increased efficiency at high resolution, a multi-crystal x-ray emission spectrometer was used with 11 cylindrical Si(10 10 0) crystals and a pixelated area detector in von Hamos geometry [91].

The four compounds are UO_2, UO_3, Cs_2UCl_6, and $Cs_2UO_2Cl_4$. The compounds comprise two each of +4 and +6 U oxidation states with different ligand configurations. The experimental goal is to determine chemical shifts of U $2p_{3/2}$ →5f,6d resonances and $2p_{3/2}$ ionization energies to compare with high precision, relativistic electronic structure calculations [90].

The theoretical method-development work has extended our relativistic equation-of-motion coupled-cluster program for calculations of isolated molecules to include crystal fields. This has enabled calculations for qualitative understanding of ligand field splittings of 6d and 5f orbitals in the *L*-edge spectra of uranium compounds. The next theoretical development will be focused on a first efficient implementation of a core-valence separation scheme for spin-orbit equation-of-motion coupled cluster calculations of core-level spectroscopy. This will enable accurate treatment of spin-orbit coupling of 6d and 5f orbitals in these *L*-edge spectra.
Future Plans: The data analysis will be concluded with determinations of the pre-edge resonance and ionization energies and their chemical shifts. Theoretical developments are ongoing with the goal of determining and including the interactions needed for precise calculations of heavy element compounds.

4 X-ray Probes of Photo-excited Dynamics in Solution

4.1 Tracking the ligand exchange reaction of aqueous ferrocyanide using time-sliced synchrotron x-ray emission spectroscopy

A. M. March, G. Doumy, C. Otolski, S. H. Southworth, L. Young, W. Gawelda[10], G. Vanko[19], Z. Nemeth[19], D. R. Nascimento[20], A. Andersen[20], N. Govind[20]

Project Scope: The MHz-repetition-rate, optical-pump/x-ray-probe endstation at beamline 7ID at the Advanced Photon Source (APS), built by our group over the past several years, enables tracking of photophysical and photochemical reactions in solutions using both x-ray absorption and x-ray emission spectroscopies [23, 24, 26–29, 91–98]. With the high signal-to-noise ratios obtained, photoproducts with lifetimes as short as 10 ps can be studied. Such sub-pulse-duration temporal resolution is important for bridging the gap between the femtosecond regime accessible at XFELs and the >100 ps regime considered the domain of synchrotrons. Combining the strengths of both sources, the photochemistry of solvated transition metal complexes, of high interest for photocatalyis and solar energy conversion, can be studied on all the relevant timescales.
Recent Progress: Following up on our previous "time-slicing" x-ray absorption studies of the photo-induced ligand exchange reaction that occurs in aqueous solutions of ferrocyanide, $[Fe^{II}(CN)_6]^{4-}$ [28], we have extended the "time-slicing" technique to x-ray emission spectroscopy to track the spin changes that occur during the reaction. To obtain the requisite signal-to-noise ratio we used our newly developed MHz pink beam capabilities at 7ID [29]. In the time-slicing scheme, a short duration pump pulse is temporally scanned across a longer probe pulse while measurements are collected at several timepoints within the probe temporal profile. With sufficient signal-to-noise ratio and accurate knowledge of the probe temporal profile, the set of measurements can be analyzed to extract signatures of short-lived photoreaction intermediates.

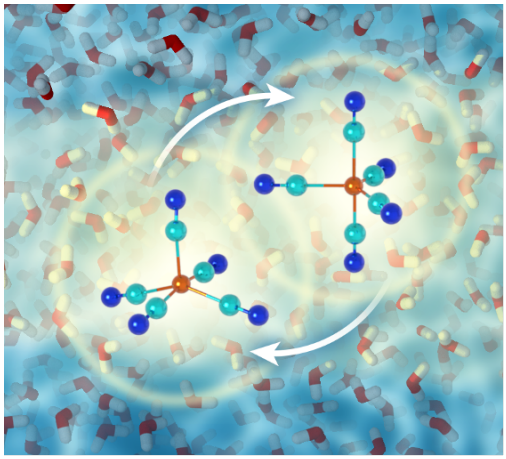

Figure 3: Illustration of the fluxional geometric changes that occur in the intermediate species involved in the photoaquation reaction in aqueous $[Fe(CN)_6]^{4-}$. Both geometries for this species are predicted to be triplet spin states [28].

The model for the reaction assumes a triplet state for the initial precursor to dissociation and for the pentacoordinated, 20 ps- lived intermediate, $[Fe^{II}(CN)_5]^{3-}$, that precedes aquation. We have measured the complete Fe 1s emission spectrum, including the Kα, Kβ, and valence-to-core regions. Our measurements confirm the triplet state of the pentacoordinated intermediate. Additionally, we have observed small spectral changes, compared to the ground state, for the aquated product $[Fe^{II}(CN)_5H_2O]^{3-}$ that demonstrate the sensitivities of the 1s emission spectrum to influences other than spin state and that provide a challenge for theoretical modelling. A manuscript reporting our observations is presently being prepared.
Future Plans: We plan to continue our exploration of the $[Fe^{II}(CN)_6]^{4-}$ aquation reaction, fo-

cusing on the picosecond timescale at the APS and the femtosecond timescale at an XFEL. The seemingly delicate balance between the fluctuating hydrogen bonding solvent environment and the d orbital energy levels of the complex inspires the question of whether we can alter the lifetime of the intermediate species by altering the hydrogen bonding network in the solvent, by addition of salts or solvent mixtures for example. The combined XAS/XES studies will greatly benefit from the new beamline at the APS (see Section 4.5). Additionally, the MHz optical transient absorption capabilities we are developing (see Section 4.3) will enable valuable preliminary observations before the x-ray measurements. We are investigating the feasibility of femtosecond x-ray spectroscopy measurements at an XFEL for observing the dynamics of the initial singlet to triplet transition that presumably occurs before ligand dissociation, and for observing experimentally the fluxional geometry changes that occur in the pentacoordinated intermediate after ligand dissociation.

4.2 Dynamics and coherence in ionized liquid water

L. Young, G. Doumy, S.H. Southworth, Y. Kumagai, A. Al Haddad[3], M.-F. Tu, A. M. March, P.J. Ho, Z.-H. Loh[11], J. E. Rubensson[6], L. Kjellsson[6], R. Santra[2,5], C. Arnold[5], R. Welsch[5], L. Inhester[5], W. Schlotter[13], A. Krylov[21], K. Nanda[21] and other collaborators

Project Scope: Time-resolved x-ray spectroscopies in the water window provide a powerful and unique probe for understanding valence and inner-shell hole dynamics, electronic coherence and proton transfer in ionized aqueous systems. These elementary processes are of fundamental importance as the initiators of radiation damage in condensed phases [99, 100].
Recent Progress: We reported our studies of valence hole dynamics in ionized liquid water in two publications [30, 31]. The novel methodologies associated with these studies, originally motivated by (a) the XFEL-enabled ultrafast probe of transient radicals associated with water radiolysis (H_2O^+,OH, H_3O^+, H_2O) and (b) the lack of knowledge about the fastest chemical reaction in water radiolysis, are readily generalizable to other situations and thus have led to new collaborations aimed at the understanding of radiolysis effects in the extreme environments associated with waste management at PNNL.

Our first paper [30] focused on following the kinetics of the proton transfer reaction and establishing the x-ray absorption signatures. We used fc-cvs-EOM-CCSD methods [103] to calculate relevant x-ray absorption signatures and x-ray transient absorption in the water window to follow the proton transfer reaction following impulsive strong-field ionization in pure liquid water: $H_2O^+ + H_2O \rightarrow OH + H_3O^+$. Calculations of the hole dynamics following ionization [30] using a quantum-mechanical (QM) description of a $(H_2O)_{12}^+$ cluster with a classical (MM) description of surrounding water molecules revealed that the x-ray absorption peak position of the valence hole resonance is sensitive to the local environment, specifically to the O—O distance of the specific oxygen atom involved in the proton transfer to its nearest neighbor. The timescale for the proton transfer was deduced by polarization-dependent transient absorption and agreed with present and earlier calculations [101, 102]. This paper was the subject of a joint press release by Argonne, SLAC, DESY and NTU and picked up by a number of news outlets including, Chemistry World and Optics and Photonics News.

Our second paper [31] reported on the acquisition and interpretation of the quasi-static RIXS (resonant inelastic x-ray scattering) spectrum of the important and chemically agressive hydroxyl radical. The quasi-static RIXS spectrum of the transient OH radical was isolated for time delays following ionization of 200 fs - 1.5 ps. We found that in sharp contrast to the single-photon UV spectrum, the two-photon RIXS spectrum of OH(aq) features two peaks corresponding to transitions between the OH orbitals. The energy difference between the elastic and inelastic peaks

corresponds to the X→A transition, which, in turn, roughly equals the energy gap between the 2σ and 1π orbitals. Thus, RIXS reveals intrinsic local electronic structure of solvated OH, which is *obscured* in the UV region by charge transfer (CT) transitions. An efficient theoretical framework was developed to model the RIXS spectra by our collaborators Krylov and Coriani [103, 105]. Our theoretical calculations, including solvent effects, compared well to our RIXS spectra of OH(aq) and also to the XES spectra of $OH^-(aq)$ [104]. Finally, we note that the spectrometer used in our study had a relatively low efficiency of 10^{-7} [106], an improved version is planned for the ChemRIXS endstation. The use of RIXS to identify transient intermediates with overlapping x-ray absorption spectra will be a very powerful tool in many studies. Its further implementation in studies of radiolysis will realize its potential at high repetition rate and with a more efficient x-ray emission spectrometer.

Future Plans: We have an approved, but not scheduled, experiment to extend our study to shorter timescales and thus capture the signature of H_2O^+. A second goal is to capture the x-ray spectroscopic signature of the solvated electron near the pre-edge feature, which will in turn shed light on the electronic structure of the solvated and pre-solvated electron [107, 108]. In the future, we plan to propose studies of local and non-local dynamics initiated by inner valence and core excitation using x-ray pump/x-ray probe techniques combined with x-ray transient absorption and RIXS.

4.3 Development of few-cycle optical transient absorption at MHz repetition rates for investigations of solution phase molecular dynamics

A. M. March, C. Otolski, G. Doumy, L. Young, J. E. Beetar[22], M. Chini[22]

Project Scope: Optical (UV to IR) transient absorption spectroscopy (OTA) remains an important complementary tool to x-ray spectroscopy for studies of solvated transition metal complexes. We will develop a MHz-repetition-rate OTA setup at the APS that can run concurrently with synchrotron x-ray experiments, in an optical-pump/x-ray-probe/optical-probe configuration, or as an independent OTA setup outside of x-ray beamtime. The setup will nominally have a temporal resolution of ∼300 fs. To achieve temporal resolution better than this, we will implement a hollow-core fiber and chirped mirror compressor that will enable reduction of the pump pulse duration to sub-20 fs in the visible and UV while maintaining the high repetition rate. Timescales <100 fs are important for enabling the investigation of structural dynamics, competitive reactive pathways, and controlled reactions of transition metal complexes.

Recent Progress: The components for developing the ∼300 fs resolution OTA have been ordered and delivered and are awaiting our return to the APS. Our efforts toward few-cycle temporal compression of MHz lasers began in February 2020 with a visit to our collaborator Michael Chini's lab at the University of Central Florida. There, a Pharos laser system similar to our own is used along with a hollow-core fiber and chirped mirror compressor to generate few-cycle infrared pulses for high-harmonic generation at high-repetition-rates for attoscience [109]. During the visit we conducted a series of pulse compression experiments demonstrating the ability to spectrally broaden a laser pulse in the visible wavelength range. In addition to a spectrally broadened visible light pulse, we observed, unexpectedly, a spectrally broad feature in the UV wavelength range. From our short investigation we hypothesize a sum-frequency-generation process in the hollow core fiber. The identity and mechanism of this process has yet to be fully explored and would lead to valuable insight for generating few-cycle visible and UV laser pulses. We are grateful for recently awarded equipment funds that enable the acquisition of the hollow core fiber, chirped mirrors, pulse picker and pulse characterization equipment for our setup at APS.

Future Plans: Implementation of the MHz OTA setup with ∼300 fs pulses will proceed once we return to the APS. Investigations to determine the best ways to generate the white-light probe and to detect the transient absorption changes at MHz rates will be our initial focus. Once completed, we will use the setup to explore the solvent dependence of the $[Fe^{II}(CN)_6]^{4-}$ aquation reaction (see Section 4.1 as well as to optically characterize an iron-based complex with photochromic ligands that will be the focus of planned x-ray studies (see Section 4.5). The implementation of the hollow-core fiber compression system will follow this work. We envision that the short-time dynamics involving the initial excitation of $[Fe^{II}(CN)_6]^{4-}$ and its transition from singlet to triplet could be a first study with the new sub-20 fs OTA setup. Additionally, we envision implementing a multi-pulse excitation to interrogate the short-lived singlet species and to control the dissociation reaction mechanism by accessing higher-lying potential energy surfaces.

4.4 Resonant x-ray absorption of strong-field-ionized CF_3Br

A. E. A. Fouda, P. J. Ho, R. W. Dunford, E. P. Kanter, B. Krässig, L. Young, E. R. Peterson[23], E. C. Landahl[24], L. Pan[25], D. R. Beck[26], and S. H. Southworth

Project Scope: Strong-field laser alignment and ionization processes in atoms and molecules can be studied by combining IR laser pulses with tunable synchrotron radiation. Theoretical treatments combine strong-field interactions, resonant x-ray absorption, and dissociative ionization of molecules.

Recent Progress: Understanding strong-field ionization in molecules requires treatment of geometric structure and orbital symmetries [110]. MO-tunneling theory accounts for alignment of the molecular frame and electron orbitals with respect to the polarization direction of the laser field. Strong field ionization in molecules also introduces photodissociation and ion fragmentation processes [111, 112]. In this work, we conducted an experimental and theoretical study of strong-field laser dynamics of CF_3Br followed by resonant x-ray absorption at the Br K-edge.

The experiments combined femtosecond IR laser pulses with tunable synchrotron radiation in a microprobe setup [113]. The experimental Br K-edge spectrum shows distinct resonances from 1s→4p,5p transitions of Br^{q+} (q=0-4) identified using relativistic configuration interaction calculations [114] and Hartree-Fock-Slater calculations [38, 46] with relativistic corrections [115]. In addition, time-dependent density functional theory (TDDFT) calculations identified x-ray absorption transitions from singly-charged molecular ions such as CF_3Br^+ and CF_2Br^+, but multiply-charged molecular ions are expected to dissociate prior to x-ray absorption.

To gain insight to the time-dependent charge separation and orbital characters leading to the q=1-4 charge states, *ab initio* molecular dynamics (AIMD) simulations were performed over a 60-fs period beginning with the neutral CF_3Br equilibrium geometry. The AIMD/DFT simulations provide snapshots of the evolving molecular geometries and orbital characters for each charge state.

The experimental x-ray absorption spectra show negligible variations between measurements with parallel and perpendicular laser and x-ray polarizations. This observation was explained using an atomic model for Br and in the AIMD simulations by calculating ionization rates with the laser polarization parallel and perpendicular to the C-Br axis.

Future Plans: A full report on this project is given in Ref. [116]. The experimental and theoretical methods used in this project will be applied to XFEL experiments on molecular ionization dynamics.

4.5 Pump-probe studies at the upcoming APS advanced spectroscopy beamline

A. M. March, C. Otolski, G. Doumy, S. H. Southworth, C. Otolski, L. Young, C. Elles[27], J. Blakemore[27], K. Mulfort[18], Z. Xie[18], X. Zhang[17], E. Kinigstein[17], S. Heald[17] and other collaborators

Scope: The APS Upgrade will bring higher brightness x-rays and finer fill patterns that will expand our x-ray spectroscopy studies to a broader range of timescales. Additionally, a new beamline is presently being constructed at Sector 25 that is devoted to advanced spectroscopy and that will enhance our studies greatly with the ability to easily interchange between monochromatic and broad-bandwidth x-ray operation. This will allow us to collect efficient XAS and XES pump-probe data in a single beamtime, rather than in two separate beamtimes that have often been a year or more apart. The new beamline will be commissioned before the dark period for the upgrade commences.

Recent Progress: Though the new beamline is not yet built, we report on two projects that are underway that will benefit from the new capabilities. The first is a study of a class of iron-containing complexes with photochromic ligands that are highly interesting for molecular electronics applications because their spin state can be switched using light at room temperature. Our objective is to use x-ray spectroscopy to understand details of the switching mechanism. We are collaborating with Karen Mulfort in the Solar Energy and Conversion Group at Argonne. The iron complex is presently being synthesized by her group. We will optically characterize the complex using our newly developed optical transient absorption setup and will have the first x-ray beamtime focusing on this complex this December.

The second project is an ongoing collaboration with the groups of Chris Elles and James Blakemore at the University of Kansas that aims to understand the photochemistry of a series of Mn-based CO_2 reduction catalysts, with form $Mn(CO)_3(bpy)Br$, bpy = 2,2-bipyridyl. These complexes suffer photodegradation under even mild ambient light but would otherwise be a promising alternative to toxic and expensive rhenium complexes. The systems are examples of complexes that require studies across multiple timescales, with bimolecular reactions occurring out to the microsecond timescale. We collected pump-probe EXAFS data at the Mn K-edge at various time delays during a beamtime in December 2019 and were able to probe changes on the picosecond to several tens of microseconds scales. Additionally, we probed the Br K-edge to identify changes from the point of view of the ligand. This work is being analyzed and prepared for publication.

Future Plans: At Sector 25 we have the opportunity to combine our pump-probe liquid-jet setup presently at Sector 7 with the one presently at Sector 11 and create a very powerful, versatile pump-probe endstation for XAS and XES studies from the picosecond timescale to milliseconds. Our collaboration with Sector 11 beamline scientist Xiaoyi Zhang and postdoc Eli Kinigstein has already begun through an LDRD to develop pump-probe x-ray spectroscopy using the 324 bunch fill pattern, which will provide a finer-spaced x-ray comb for pump, probe, probe, probe... studies to capture longer timescale chemistry. We will have our first XAS beamtime using 324-bunch mode at Sector 7 this December. In addition to our ongoing work on the Fe spin photoswitch complex and Mn catalysts mentioned above, we have several collaborative projects on Fe and Co complexes that are awaiting beamtime at APS and that will benefit greatly from the developments at Sector 25.

5 Affiliations of collaborators

[1]Argonne Leadership Computing Facility, Argonne National Laboratory, Lemont, IL
[2]Universität Hamburg, Hamburg, Germany

[3]Paul Scherrer Institute, Villigen, Switzerland
[4]Kansas State University, Manhattan, KS
[5]Center for Free-Electron Laser Science, DESY, Hamburg, Germany
[6]Uppsala University, Sweden
[7]University of Chicago, Chicago, IL
[8]Louisiana State University, Baton Rouge, LA
[9]Max Planck Institute for Nuclear Physics, Heidelberg, Germany
[10]European XFEL, Hamburg, Germany
[11]Nanyang Technological University, Singapore
[12]Johns Hopkins University, Baltimore, MD
[13]SLAC National Accelerator Laboratory, Menlo Park, CA
[14]Lund University, Lund, Sweden
[15]The Ohio State University, Columbus, OH
[16]Université Pierre et Marie Curie, Paris, France
[17]X-Ray Science Division, Argonne National Laboratory, Lemont, IL
[18]Chemical Sciences and Engineering Division, Argonne National Laboratory, Lemont, IL
[19]Wigner Research Centre for Physics, Hungarian Academy Sciences, Budapest, Hungary
[20]Pacific Northwest National Laboratory, Richland, WA
[21]University of Southern California, Los Angeles, CA
[22]University of Central Florida, Orlando, FL
[23]Massachusetts Institute of Technology, Lexington, MA
[24]DePaul University, Chicago, IL
[25]Cedarville University, Cedarville, OH
[26]Michigan Technological University, Houghton, MI
[27]University of Kansas, Lawrence, KS

References

Peer-Reviewed Publications Resulting from Subtask 1 (2018-2020)

[1] T. Osipov, C. Bostedt, J. C. Castagna, K. R. Ferguson, M. Bucher, S. C. Montero, M. L. Swiggers, R. Obaid, D. Rolles, A. Rudenko, J. D. Bozek, N. Berrah, "The LAMP instrument at the Linac Coherent Light Source free-electron laser," Review of Scientific Instruments **89**, 035112 (2018)

[2] T. Gorkhover, A. Ulmer, K. Ferguson, M. Bucher, F. Maia, J. Bielecki, T. Ekeberg, M.F. Hantke, B.J. Daurer, C. Nettelblad, J. Andreasson, A. Barty, P. Bruza, S. Carron, D. Hasse, J. Krzywinski, D.S.D. Larsson, A. Morgan, K. Mühlig, M. Müller, K. Okamoto, A. Pietrini, D. Rupp, M. Sauppe, Gijs van der Schot, M. Seibert, J.A. Sellberg, M. Svenda, M. Swiggers, N. Timneanu, D. Westphal, G. Williams, A. Zani, H.N. Chapman, G. Faigel, T. Möller, J. Hajdu, C. Bostedt, "Femtosecond X-ray Fourier holography imaging of free-flying nanoparticles", Nature Photonics **12**, 150–153 (2018).

[3] M. Sauppe, D. Rompotis, B. Erk, S. Bari,T. Bischoff, R. Boll, C. Bomme, C. Bostedt, S. Dörner,S. Düsterer, T. Feigl, L. Flückiger, T. Gorkhover, K. Kolatzki, B. Langbehn, N. Monserud, E. Müller, Jan P. Müller, C. Passow, D. Ramm, D. Rolles, K. Schubert, L. Schwob, B. Senfftleben, R. Treusch, A. Ulmer, H. Weigelt, J. Zimbalski, J. Zimmermann, T. Möller and D. Rupp,"XUV double-pulses with femtosecond to 650 ps separation from a multilayer-mirror-based split-and-delay unit at FLASH," J. Synchrotron Rad. **25**, 1517–1528 (2018).

[4] I. V. Lundholm, J. A. Sellberg, T. Ekeberg, Max F. Hantke, K. Okamoto, G. van der Schot, J. Andreasson, A. Barty, J. Bielecki, P. Bruza, M. Bucher, S. Carron, B. J. Daurer, K. Ferguson, D. Hasse, J. Krzywinski, D. S. D. Larsson, A. Morgan, Kerstin Mühlig,Maria Müller, C. Nettelblad, A. Pietrini, H. K. N. Reddy, D. Rupp, M. Sauppe, M. Seibert, M. Svenda, M. Swiggers, N. Timneanu, A. Ulmer, D. Westphal, G. Williams, A. Zani, G. Faigel, H. N.Chapman, T. Möller, C. Bostedt, J. Hajdu, T. Gorkhover, and F. R. N. C. Maia,"Considerations for three-dimensional image reconstruction from experimental data in coherent diffractive imaging," IUCrJ **5**, 531–541 (2018).

[5] Y. Kumagai, H. Fukuzawa, K. Motomura, D. Iablonskyi, K. Nagaya, S. Wada, Y. Ito, T. Takanashi, Y. Sakakibara, D. You, T. Nishiyama, K. Asa, Y. Sato,T. Umemoto, K. Kariyazono, E. Kukk, K. Kooser, C. Nicolas, C.

Miron, T. Asavei, L. Neagu, M. S. Schöffler, G. Kastirke, X. Liu, S. Owada, T. Katayama, T. Togashi, K. Tono, M. Yabashi, N. V. Golubev, K. Gokhberg, L. S. Cederbaum, A. I. Kuleff, and K. Ueda, "Following the Birth of a Nanoplasma Produced by an Ultrashort Hard-X-Ray Laser in Xenon Clusters", Phys. Rev. X **8**, 031034 (2018).

[6] B. Rudek, K. Toyota, L. Foucar, B. Erk, R. Boll, C. Bomme, J. Correa, S. Carron, S. Boutet, G. J. Williams, K. R. Ferguson, R. Alonso-Mori, J. E. Koglin, T. Gorkhover, M. Bucher, C. S. Lehmann, B. Krässig, S. H. Southworth, L. Young, C. Bostedt, K. Ueda, T. Marchenko, M. Simon, Z. Jurek, R. Santra, A. Rudenko, S-K. Son, and D. Rolles, "Relativistic and resonant effects in the ionization of heavy atoms by ultra-intense hard X-rays,"Nature Communications, **9**, 4200 (2018).

[7] J. Bielecki, M.F. Hantke, B.J. Daurer, H.K.N. Reddy, Hemanth, D. Hasse, D.S.D. Larsson, L.H. Gunn, M. Svenda, A. Munke, J.A. Sellberg, L. Flueckiger, A. Pietrini, C. Nettelblad, I. Lundholm, G. Carlsson, K. Okamoto, N. Timneanu, D. Westphal, O. Kulyk, A. Higashiura, G. van der Schot, N-T.D. Loh, T.E. Wysong, C. Bostedt, T. Gorkhover, B. Iwan, M.M. Seibert, T. Osipov, P. Walter, P. Hart, M. Bucher, A. Ulmer, D. Ray, G. Carini, K.R. Ferguson, I. Andersson, J. Andreasson, J. Hajdu, and F.R.N.C. Maia, "Electrospray sample injection for single-particle imaging with x-ray lasers," Science Advances **5** (2019). 10.1126/sciadv.aav8801

[8] T. Nishiyama, Y. Kumagai,A. Niozu, H. Fukuzawa, K. Motomura, M. Bucher, Y. Ito, T. Takanashi, K. Asa, Y. Sato, D. You, Y. Li, T. Ono, E. Kukk, C. Miron, L. Neagu, C. Callegari, M. Di Fraia, G. Rossi, D.E. Galli, T. Pincelli, A. Colombo, T. Kameshima, Y. Joti, T. Hatsui, S. Owada, T. Katayama, T. Togashi, K. Tono, M. Yabashi, K. Matsuda, C. Bostedt, K. Nagaya, and K. Ueda, "Ultrafast structural dynamics of nanoparticles in intense laser fields," Phys. Rev. Lett. **123**, 123201 (2019).

[9] T. Nishiyama et al., "Refinement for single-nanoparticle structure determination from low-quality single-shot coherent diffraction data," IUCrJ **7**, 10 (2020).

[10] A. Niozu et al., "Characterizing crystalline defects in single nanoparticles from angular correlations of single-shot diffracted X-rays," IUCrJ **7**, 276 (2020).

[11] T. Nishiyama et al., "Multispectroscopic Study of Single Xe Clusters Using XFEL Pulses," Appl. Sci.-Basel **9**, 10 (2019).

[12] S. M. O. O'Connell et al., "Angular Momentum in Rotating Superfluid Droplets," Phys. Rev. Lett. **124**, 215301 (2020).

[13] Phay J. Ho, Benedikt J. Daurer, Max F. Hantke, Johan Bielecki, Andre Al Haddad, Maximilian Bucher, Gilles Doumy, Ken R. Ferguson, Leonie Flükiger, Tais Gorkhover, Bianca Iwan, Christopher Knight, Stefan Moeller, Timur Osipov, Dipanwita Ray, Stephen H. Southworth, Martin Svenda, Nicusor Timneanu, Anatoli Ulmer, Peter Walter, Janos Hajdu, Linda Young, Filipe R.N.C. Maia and Christoph Bostedt, "The role of transient resonances for ultra-fast imaging of single sucrose nanoclusters", Nat. Commum. **11**:167 (2020).

[14] Phay J. Ho, Christopher Knight, and Linda Young, "Extended x-ray emission times of clusters in intense x-ray pulses", Phys. Rev. A **101**, 043413 (2020).

Peer-Reviewed Publications Resulting from Subtask 2 (2018-2020)

[15] L. Young, K. Ueda, M Gühr, P.H. Bucksbaum, M. Simon, S. Mukamel, N. Rohringer, K. Prince, C. Masciovecchio, M. Meyer, A. Rudenko, D. Rolles, C. Bostedt, M. Fuchs, D. Reis, R. Santra, H. Kapteyn, M. Murnane, H. Ibrahim, François Légaré, M. Vrakking, M. Isinger, D. Kroon, M. Gisselbrecht, A. L'Huillier, H. J. Wörner and S. R. Leone,"Roadmap on Ultrafast X-ray Atomic and Molecular Physics," J. Phys. B., **51** 032003 (2018).

[16] L. Inhester, B. Oostenrijk, M. Patanen, E. Kokkenen, S.H. Southworth, C. Bostedt, O. Travnikova, T. Marchenko, S.-K. Son, R. Santra, M. Simon, L. Young, and S. L. Sorensen, "Chemical understanding of the limited site-specificity in molecular inner-shell photofragmentation," J. Phys. Chem. Lett. **9**, 1156 (2018).

[17] M. C. Hoffmann, I. Grguras, C. Behrens, C. Bostedt, J. Bozek, H. Bromberger, R. Coffee, J. T. Costello, L. F. DiMauro, Y. Ding, G. Doumy, W. Helml, M. Ilchen, R. Kienberger, S. Lee, A. R. Maier, T. Mazza, M. Meyer, M. Messerschmidt, S. Schorb, W. Schweinberger, K. Zhang, A. L. Cavalieri, "Femtosecond profiling of shaped x-ray pulses," New J. Phys. **20**, 033008 (2018).

[18] S. H. Southworth, R. W. Dunford, D. Ray, E. P. Kanter, G. Doumy, A. M. March, P. J. Ho, B. Krässig, Y. Gao, C. S. Lehmann, A. Picón, L. Young, D. A. Walko, and L. Cheng, "Observing pre-edge K-shell resonances in Kr, Xe, and XeF_2," Phys. Rev. A **100**, 022507 (2019).

[19] X. Zheng, J. Liu, G. Doumy, L, Young, and L. Cheng "Hetero-site double core ionization energies with sub-eV accuracy from delta-coupled-cluster calculations." J. Phys. Chem. A **124**, 4413–4426 (2020).

[20] Jordan T. O'Neal, Elio G. Champenois,1 Solène Oberli, Razib Obaid, Andre Al-Haddad, Jonathan Barnard, Nora Berrah, Ryan Coffee, Joseph Duris, Gediminas Galinis, Douglas Garratt, James M. Glownia, Daniel Haxton, Phay Ho, Siqi Li, Xiang Li, James MacArthur, Jon P Marangos, Adi Natan, Niranjan Shivaram, Daniel S. Slaughter, Peter Walter, Scott Wandel, Linda Young, Christoph Bostedt, Philip H. Bucksbaum, Antonio Picón, Agostino Marinelli, and James P. Cryan, "Electronic Population Transfer via Impulsive Stimulated X-ray Raman Scattering with Attosecond Soft X-ray Pulses", Phys. Rev. Lett. **125**, 073203 (2020).

[21] Adam E. A. Fouda, Linsey C. Seitz, Dirk Hauschild, Monika Blum, Wanli Yang, Clemens Heske, Lothar Wein-

hardt, and Nicholas A. Besley, "Observation of Double Excitations in the Resonant Inelastic X-ray Scattering of Nitric Oxide", J. Phys. Chem. Lett. **11**, 7476–7482 (2020).

[22] D. C. Haynes, M. Wurzer, A. Schletter, A. Al-Haddad, C. Blaga, C. Bostedt, J. Bozek1, M. Bucher, A. Camper, S. Carron, R. Coffee,J. T. Costello,L. F. DiMauro, Y. Ding, K. Ferguson,I. Grgura, W. Helml, M. C. Hoffmann, M. Ilchen,S. Jalas, N.M. Kabachnik, A. K. Kazansky, R. Kienberger, A. R. Maier, T. Maxwell, T. Mazza, M. Meyer, H. Park, J. S. Robinson, C. Roedig, H. Schlarb,R. Singla1,F. Tellkamp, K. Zhang,G. Doumy, C. Behrens, A. L. Cavalieri, "Clocking Auger Electrons", Nature Physics - accepted

Peer-Reviewed Publications Resulting from Subtask 3 (2018-2020)

[23] M. Ross, A. Andersen, Z.W. Fox, Y. Zhang, K. Hong, J.-H. Lee, A. Cordones, A. M. March, G. Doumy, S. H. Southworth, M. A. Marcus, R. W. Schoenlein, S. Mukamel, N. Govind, M. Khalil, "Comprehensive Experimental and Computational Spectroscopic Study of Hexacyanoferrate Complexes in Water: From Infrared to X-ray Wavelengths," J. Phys. Chem. B **122**, 5075-5086 (2018).

[24] T. J. Penfold, J. Szlachetko, F. G. Santomauro, A. Britz, W. Gawelda, G. Doumy, A. M. March, S. H. Southworth, J. Rittmann, R. Abela, M. Chergui and C. J. Milne, "Revealing hole trapping in zinc oxide nanoparticles by time-resolved X-ray spectroscopy," Nature Communications **9**, 478 (2018).

[25] Y. Gao, R. Harder, S. H. Southworth, J. R. Guest, Z. Yan, X. Huang, L. E. Ocola, Y. Yifat, N. Sule, P.J. Ho, M. Pelton, N. F. Scherer, L. Young, "Three-dimensional optical trapping and orientation of microparticles for coherent diffractive imaging", Proc. Natl. Acad. Sci. **116**, 4018-4024 (2019).

[26] A. Britz, W. Gawelda, T. A. Assefa, L. L. Jamula, J. T. Yarranton, A. Galler, D. Khakhulin, M. Diez, M. Harder, G. Doumy, A. M. March, E. Bajnóczi, Z. Nemeth, M. Papai, E. Rozsalyi, D. Sarosine Szemes, H. Cho, S. Mukherjee, C. Liu, T. K. Kim, R. W. Schoenlein, S. H. Southworth, L. Young, E. Jakubikova, N. Huse, G. Vanko, C. Bressler, J. K. McCusker, "Using Ultrafast X-ray Spectroscopy To Address Questions in Ligand-Field Theory: The Excited State Spin and Structure of $[Fe(dcpp)^2]^{2+}$", Inorg. Chem., **58** 14, 9341-9350 (2019).

[27] M. W. Mara, D. S. Tatum, A. M. March. G. Doumy, E. G. Moore, K. N. Raymond, "Energy Transfer from Antenna Ligand to Europium(III) Followed Using Ultrafast Optical and X-ray Spectroscopy", J. Am. Chem. Soc., **141** 28, 11071-11081 (2019).

[28] A. M. March, G. Doumy, A. Andersen, A. Al Haddad, Y. Kumagai, M.-F. Tu, J. Bang, C. Bostedt, J. Uhlig, D. R. Nascimento, T. A. Assefa, Z. Nemeth, G. Vanko, W. Gawelda, N. Govind and L. Young, "Elucidation of the Photoaquation Reaction Mechanism in Ferrous Hexacyanide Using Synchrotron X-rays with Sub-Pulse-Duration Sensitivity", J. Chem. Phys., Special Topics: Ultrafast Spectroscopy and Diffraction from XUV to X-ray **151**, 144306 (2019).

[29] M.F. Tu, G. Doumy, A. Al Haddad, A. M. March, S. H. Southworth, L. Assoufid, Y. Kumagai, D. Walko, A. DiChiara, Z. Liu, B. Shi, L. Young and C. Bostedt, "Micro-Focused MHz Pink Beam for Time-Resolved X-ray Emission Spectroscopy", accepted in J. Synchr. Rad. **26**, 1956-1966 (2019).

[30] Z.-H. Loh, G. Doumy, C. Arnold, L. Kjellson, S. H. Southworth, A. Al Haddad, Y. Kumagai, M.-F. Tu, P. J. Ho, A. M. March, R. D. Schaller, M. S. Bin Mohd Yusof, T. Debnath, M. Simon, R. Welsch, L. Inhester, K. Khalili, K. Nanda, A. I. Krylov, S. Moeller, G. Coslovich, J. Koralek, M. P. Minitti, W. F. Schlotter, J.-E. Rubensson, R. Santra, L. Young, "Observation of the fastest chemical processes in the radiolysis of water", Science **367**, 179-182 (2020).

[31] L. Kjellsson, K. D. Nanda, J.-E. Rubensson, G. Doumy, S. H. Southworth, P. J. Ho, A. M. March, A. Al Haddad, Y. Kumagai, M.-F. Tu, R. D. Schaller, T. Debnath, M. S. Bin Mohd Yusof, C. Arnold, W. F. Schlotter, S. Moeller, G. Coslovich, J. D. Koralek, M. P. Minitti, M. L. Vidal, M. Simon, R. Santra, Z.-H. Loh, S. Coriani, A. I. Krylov and L. Young, "Resonant Inelastic X-Ray Scattering Reveals Hidden Local Transitions of the Aqueous OH Radical", Phys. Rev. Lett. **124**, 236001 (2020).

[32] Christopher J. Otolski, A. Mohan Raj, Vaidhyanathan Ramamurthy and Christopher G. Elles, "Spatial confinement alters the ultrafast photoisomerization dynamics of azobenzenes", Chemical Sciences **11**, 9513 - 9523, (2020).

Other cited references

[33] R. Neutze, R. Wouts, R. D. van der Spoel, E. Weckert, J. Hajdu,"Potential for biomolecular imaging with femtosecond X-ray pulses," Nature **406**,752 (2000).

[34] G. Doumy, C. Roedig, S.-K. Son, C. I. Blaga, A. D. Chiara, R. Santra, N. Berrah, C. Bostedt, J. D. Bozek, P. H. Bucksbaum, J. Cryan, L. Fang, S. Ghimire, J. M. Glownia, M. Hoener, E. P. Kanter, B. Krässig, M. Kuebel, M. Messerschmidt, G. G. Paulus, D. A. Reis, N. Rohringer, L. Young, P. Agostini, and L. F. DiMauro, "Nonlinear atomic response to intense ultrashort x rays," Phys. Rev. Lett. **106**, 083002 (2011).

[35] E. P. Kanter, B. Krässig, Y. Li, A. M. March, P. Ho, N. Rohringer, R. Santra, S. H. Southworth, L. F. DiMauro, G. Doumy, C. A. Roedig, N. Berrah, L. Fang, M. Hoener, P. H. Bucksbaum, S. Ghimire, D. A. Reis, J. D. Bozek, C. Bostedt, M. Messerschmidt, and L. Young, "Unveiling and driving hidden resonances with high-fluence, high-

intensity x-ray pulses," Phys. Rev. Lett. **107**, 233001 (2011).
[36] B. Rudek, S. K. Son, L. Foucar, S. W. Epp, B. Erk, R. Hartmann, M. Adolph, R. Andritschke, A. Aquila, N. Berrah, C. Bostedt, J. Bozek, N. Coppola, F. Filsinger, H. Gorke, et al., T. Gorkhover, H. Graafsma, L. Gumprecht, A. Hartmann, G. Hauser, S. Herrmann, He. Hirsemann, Pe. Holl, A. Hömke, L. Journel, C. Kaiser, N. Kimmel, F. Krasniqi, K. U. Kühnel, M. Matysek, M. Messerschmidt, D. Miesner, T. Möller, R. Moshammer, K. Nagaya, B. Nilsson, G. Potdevin, D. Pietschner, C. Reich, D. Rupp, G. Schaller, I. Schlichting, C. Schmidt, F. Schopper, S. Schorb, C. D. Schröter, J. Schulz, M. Simon, H. Soltau, L. Strüder, K. Ueda, G. Weidenspointner, R. Santra, J. Ullrich, A. Rudenko and D. Rolles, "Ultra-efficient ionization of heavy atoms by intense X-ray free-electron laser pulses," Nat. Photon. **6**, 858 (2012).
[37] B. Rudek, D. Rolles, S.-K. Son, L. Foucar, B. Erk *et al.*, "Resonance-enhanced multiple ionization of krypton at an x-ray free-electron laser," Phys. Rev. A **87**, 023413 (2013).
[38] P. J. Ho, C. Bostedt, S. Schorb, and L. Young, "Theoretical tracking of resonance-enhanced multiple ionization pathways in x-ray free-electron laser pulses," Phys. Rev. Lett. **113**, 253001 (2014).
[39] P. J. Ho, E. P. Kanter, and L. Young, "Resonance-mediated atomic ionization dynamics induced by ultraintense x-ray pulses,"Phys. Rev. A **92**, 063430 (2015).
[40] L. Young, E. P. Kanter, B. Krässig, Y. Li, A. M. March, S. T. Pratt, R. Santra, S. H. Southworth, N. Rohringer, L. F. DiMauro, G. Doumy, C. A. Roedig, N. Berrah, L. Fang, M. Hoener, P. H. Bucksbaum, J. P. Cryan, S. Ghimire, J. M. Glownia, D. A. Reis, J. D. Bozek, C. Bostedt, and M. Messerschmidt, "Femtosecond electronic response of atoms to ultra-intense x-rays," Nature **466**, 56 (2010).
[41] A. Rudenko, L. Inhester, K. Hanasaki, X. Li, S. J. Robatjazi, B. Erk, R. Boll, K. Toyota, Y. Hao, O. Vendrell, C. Bomme, E. Savelyev, B. Rudek, L. Foucar, S. H. Southworth, C.S. Lehmann, B. Kraessig, T. Marchenko, M. Simon, K. Ueda, K. R. Ferguson, M. Bucher, T. Gorkhover, S. Carron, R. Alonso-Mori, J. E. Koglin, J. Correa, G. J. Williams, S. Boutet, L. Young, C. Bostedt, S.-K. Son, R. Santra, D. Rolles, "Femtosecond response of polyatomic molecules to ultra-intense hard X-rays," Nature **546**, 129 (2017).
[42] T. Gorkhover, M. Adolph, D. Rupp, S. Schorb, S. W. Epp, B. Erk, L. Foucar, R. Hartmann, N. Kimmel, K.-U. Kühnel, D. Rolles, B. Rudek, A. Rudenko, R. Andritschke, A. Aquila, J.D. Bozek, N. Coppola, T. Erke, F. Filsinger, H. Gorke, H. Graafsma, L. Gumprecht, G. Hauser, S. Herrmann, H. Hirsemann, A. Hömke, P. Holl, C. Kaiser, F. Krasniqi, J.-H. Meyer, M. Matysek, M. Messerschmidt, D. Miessner, B. Nilsson, D. Pietschner, G. Potdevin, C. Reich, G. Schaller, C. Schmidt, F. Schopper, C.D. Schröter, J. Schulz, H. Soltau, G. Weidenspointner, I. Schlichting, L. Strüder, J. Ullrich, T. Möller, and C. Bostedt, "Nanoplasma dynamics of single large xenon clusters irradiated with superintense x-ray pulses from the Linac Coherent Light Source free-electron laser," Phys. Rev Lett. **108**, 245005 (2012).
[43] K. R. Ferguson, M. Bucher, T. Gorkhover, S. Boutet, H. Fukuzawa, J. E. Koglin, Y. Kumagai, A. Lutman, A. Marinelli, M. Messerschmidt, K. Nagaya, J. Turner, K. Ueda, G. J. Williams, P. H. Bucksbaum, and C. Bostedt, "Transient lattice compression in the solid-to-plasma transition," Science Advances **2**, 1500837 (2016).
[44] A. Aquila, A. Barty, C. Bostedt, S. Boutet, G. Carini, D. dePonte, P. Drell, S. Doniach, K. H. Downing, T. Earnest, and others, "The linac coherent light source single particle imaging road map," Struct. Dyn. **2**, 041701 (2015).
[45] Phay J. Ho, Chris Knight, Miklos Tegze, Gyula Faigel, C. Bostedt, and L. Young, "Atomistic 3D coherent X-ray imaging of non-biological systems," Phys. Rev. A **94**, 063823 (2016).
[46] Phay J. Ho, and Chris Knight, "Large-scale atomistic calculations of cluster in intense x-ray pulses," J. Phys. B: At. Mol. Opt. Phys. **50**, 104003 (2017).
[47] H. N. Chapman, A. Barty, M. J. Bogan, S. Boutet, M. Frank, S. P. Hau-Riege, S. Marchesini, B. W. Woods, S. Bajt, W. H. Benner et al., "Femtosecond diffractive imaging with a soft-X- ray free-electron laser," Nat. Phys. **2**, 839 (2006).
[48] M. M. Seibert, T. Ekeberg, F. R. N. C. Maia, M. Svenda, J. Andreasson, O. Jonsson, D. Odic, B. Iwan, A. Rocker, D. Westphal et al., "Single mimivirus particles intercepted and imaged with an X-ray laser," Nature (London) **470**, 78 (2011).
[49] B. F. Murphy, T. Osipov, Z. Jurek, L. Fang, S. K. Son, M. Mucke, J. H. D. Eland, V. Zhaunerchyk, R. Feifel, L. Avaldi et al., "Femtosecond X-ray-induced explosion of C60 at extreme intensity," Nat. Commun. **5**, 4281 (2014).
[50] S. Huang, Y. Ding, Y. Feng, E. Hemsing, Z. Huang, J. Krzy- winski, A. A. Lutman, A. Marinelli, T. J. Maxwell and D. Zhu, Phys. Rev. Lett. **119**, 154801 (2017).
[51] A. Marinelli, J. MacArthur, P. Emma, M. Guetg, C. Field, D. Kharakh, A. A. Lutman, Y. Ding and Z. Huang, Appl. Phys. Lett. **111**, 151101 (2017).
[52] J. M. Slowik, S.-K. Son, G. Dixit, Z. Jurek and R. Santra, New J. Phys. **16**, 073042 (2014).
[53] Phay J. Ho, Adam E. A. Fouda, Kai Li, Gilles Doumy, Linda Young, "Ultraintense, ultrashort pulse x-ray scattering in small molecules", Faraday Discussions - to be published. arXiv:2009.08870.
[54] A. Classen, K. Ayyer, H. N. Chapman, R. Röhlsberger and J. von Zanthier "Incoherent Diffractive Imaging via

Intensity Correlations of Hard X Rays," Phys. Rev. Lett. **119**, 053401 (2017).
[55] R. Hanbury Brown and R. Q. Twiss, "Correlation between Photons in two Coherent Beams of Light," Nature **177**, 27 (1956).
[56] J. Duris *et al.* "Tunable Isolated Attosecond X-ray Pulses with Gigawatt Peak Power from a Free-Electron Laser," Nat. Photon. (in press).
[57] C. Weninger, M. Purvis, D. Ryan, R. A. London, J. D. Bozek, C. Bostedt, A. Graf, G. Brown, J. J. Rocca, and N. Rohringer, "Stimulated Electronic X-Ray Raman Scattering," Phys.Rev. Lett. **111**, 233902 (2013).
[58] C. Weninger, N. Rohringer, "Stimulated resonant x-ray Raman scattering with incoherent radiation," Phys. Rev. A **88**, 053421 (2013).
[59] Y.-P. Sun, J.-C. Liu, C.-K. Wang, F. Gel'mukhanov,"Propagation of a strong x-ray pulse: Pulse compression, stimulated Raman scattering, amplified spontaneous emission, lasing without inversion, and four-wave mixing," Phys. Rev. A **81**, 013812 (2010).
[60] Kai Li, Marie Labeye, Phay J. Ho, Mette B. Gaarde, and Linda Young, "Resonant propagation of x-rays from the linear to the nonlinear regime", Phys. Rev. A. submitted. arXiv:2008.06920.
[61] J. Laksman et al., "Commissioning of a photoelectron spectrometer for soft X-ray photon diagnostics at the European XFEL, " J. Synchrotron Rad. **26**, 1010-1016 (2019).
[62] T. Driver et al., "Attosecond transient absorption spooktroscopy: a ghost imaging approach to ultrafast absorption spectroscopy", Phys. Chem. Chem. Phys. **22**, 2704-2712 (2020).
[63] A. A. Lutman, R. Coffee, Y. Ding, Z. Huang, J. Krzywinski, T. Maxwell, M. Messerschmidt, and H.-D. Nuhn, "Experimental demonstration of femtosecond two-color x-ray free-electron lasers," Phys. Rev. Lett. **110**, 134801 (2013).
[64] A. Marinelli, D. Ratner, A. A. Lutman, J. Turner, J. Welch, F.-J. Decker, H. Loos, C. Behrens, S. Gilevich, A. A. Miahnahri, S. Vetter, T. J. Maxwell, Y. Ding, R. Coffee, S. Wakatsuki, and Z. Huang, "High-intensity double-pulse X-ray free-electron laser," Nat. Commun. **6**, 6369 (2015).
[65] A. A. Lutman, T. J. Maxwell, J. P. MacArthur, M. W. Guetg, N. Berrah, R. N. Coffee, Y. Ding, Z. Huang, A. Marinelli, S. Moeller, and J. C. U. Zemella, "Fresh-slice multicolour X-ray free-electron lasers," Nat. Photon. **10** 745 (2016).
[66] K. Siegbahn, 'Electron Spectroscopy for Atoms, Molecules, and Condensed Matter', Rev. Mod. Phys. **54**, 709-728 (1982).
[67] W. Eberhardt, T. K. Sham, R. Carr, S. Krummacher, M. Strongin, S. L. Weng, and D. Wesner, Phys. Rev. Lett. **50**, 1038 (1983).
[68] A. Al Haddad, S. Oberli, G. Doumy, M.Bucher, S.Southworth, P.Ho, S.Pratt, L.Young, S.Moeller, D.Ray, R.Coffee, P. Stefan, M.Holmes, J.Krzywinski, T.Osipov, D.Ratner, P.Walter, A.Lutman, A.Marinelli, A.Picon and C.Bostedt, 'Mapping the electronic to nuclear relaxation of a molecular core-hole state with time-resolved photoelectron spectroscopy', in preparation
[69] R. Santra, N. V. Kryzhevoi and L.S. Cederbaum, 'X-Ray Two-Photon Photoelectron Spectroscopy: A Theoretical Study of Inner-Shell Spectra of the Organic Para-Aminophenol Molecule', Physical review letters **103** 013002 (2009)
[70] D. Koulentianos, A.E.A. Fouda, S.H. Southworth, J.D. Bozek, J. Küpper, R. Santra, N.V. Kryzhevoi, L.S. Cederbaum, C. Bostedt, M. Messerschmidt, N.Berrah, L. Fang, B. Murphy, T. Osipov, J.P. Cryan, J. Glownia, S. Ghimire, P.J. Ho, B. Krässig, D. Ray, Y. Li, E.P. Kanter, L. Young and G. Doumy, "High intensity x-ray interaction with a model bio-molecule system: double-core-hole states and fragmentation of formamide", submitted to J. Phys. B
[71] X. Zheng, L. Cheng, "Performance of Delta-Coupled-Cluster Methods for Calculations of Core-Ionization Energies of First-Row Elements," J. Chem. Theory Comput., **15**, 4945 (2019)
[72] S.L. Sorensen, X. Zheng, S.H. Southworth, M. Patanen, E. Kokkonen, B. Oostenrijk, O. Travnikova, T. Marchenko, M. Simon, C. Bostedt, G. Doumy, L. Cheng, L. Young, "From synchrotrons for XFELs: the soft x-ray near-edge spectrum of the ESCA molecule", submitted JPhysB
[73] W. Helml, A. R. Maier, W. Schweinberger, I. Grguras, P. Radcliffe, G. Doumy, C. Roedig, J. Gagnon, M. Messerschmidt,S. Schorb, C. Bostedt, and F. Grüner, L. F. DiMauro, D. Cubaynes, J. D. Bozek, Th. Tschentscher, J.T. Costello, M. Meyer, R. Coffee, S. Düsterer, A.L. Cavalieri, R. Kienberger, "Measuring the temporal structure of few-femtosecond free-electron laser X-ray pulses directly in the time domain," Nat. Photon., **8**, 950 (2014).
[74] S. Duesterer, P. Radcliffe, C. Bostedt, J. Bozek, A. L. Cavalieri, R. Coffee, J. T. Costello, D. Cubaynes, L. F. DiMauro, Y. Ding, G. Doumy, F. Grüner, W. Helml, W. Schweinberger, R. Kienberger, A. R. Maier, M. Messerschmidt, V. Richardson, C. Roedig, T. Tschentscher and M. Meyer,"Femtosecond x-ray pulse length characterization at the Linac Coherent Light Source free-electron laser" New J. of Phys., **13**, 093024 (2011).
[75] R. N. Coffee, J. P. Cryan, J. Duris, W. Helml, S. Li and A. Marinelli "Development of ultrafast capabilities for X-ray free-electron lasers at the linac coherent light source", **377**, Philosophical Transactions of the Royal Society A: Mathematical, Physical and Engineering Sciences (2019)

[76] S. Mukamel, D. Healion, Y. Zhang and J. Biggs, "Multidimensional attosecond resonant x-ray spectroscopy of molecules: lessons from the optical regime," Annu. Rev. Phys. Chem.., **64**, 101 (2013).
[77] T. Barillot, O. Alexander, B. Cooper, T. Driver, D. Garratt, S. Li, A. Al Haddad, A. Sanchez-Gonzalez, M. Agaker, C. Arrell, V. Averbukh, M. Bearpark, N. Berrah, C.Bostedt, J. Bozek, C. Brahms, P.H. Bucksbaum, G. Doumy, R. Feifel, L.J. Frasinski, S. Jarosch, A.S. Johnson, L. Kjellsson, P. Kolorenc, Y. Kumagai, E.W. Larsen, P. Matia-Hernando, M. Robb, J.-E. Rubensson, C. Sathe, R.J. Squibb, J.W.G. Tisch, K. Ueda, M. Vacher, D.J. Walke, T.J.A. Wolf, D. Wood, V. Zhaunerchyk, P. Walter, T. Osipov, A. Marinelli, T. Maxwell, R. Coffee, A. A. Lutman, J. P. Cryan, and J.P. Marangos, "Transient Hole Dynamics Resolved in Space and Time in the Isopropanol Molecule", submitted to Phys. Rev. X.
[78] D. Céolin *et al.*, "Hard X-ray photoelectron spectroscopy on the GALAXIES beamline at the SOLEIL synchrotron," J. Electron Spectrosc. Relat. Phenom. **190**, 188 (2013).
[79] J. A. R. Samson *et al.*, "Double photoionization of helium," Phys. Rev. A **57**, 1906 (1998).
[80] K. Hino *et al.*, "Double photoionization of helium using many-body perturbation theory," Phys. Rev. A **48**, 1271 (1993).
[81] T. Schneider *et al.*, "Separation and identification of dominant mechanisms in double photoionization," Phys. Rev. Lett. **89**, 073002 (2002).
[82] J. Hoszowska *et al.*, "Physical mechanisms and scaling laws of K-shell double photoionization," Phys. Rev. Lett. **102**, 073006 (2009).
[83] G. Goldsztejn *et al.*, "Experimental and theoretical study of the double-core-hole hypersatellite Auger spectrum of Ne," Phys. Rev. A **96**, 012513 (2017).
[84] T. Åberg and B. Crasemann, in Resonant Anomalous X-ray Scattering: Theory and Applications, edited by G. Materlik, C. J. Sparks, and K. Fischer (North-Holland, Amsterdam, 1994), p. 431.
[85] D. Koulentianos, S. Carniato, R. Püttner, G. Goldsztejn, T. Marchenko, O. Travnikova, L. Journel, R. Guillemin, D. Céolin, M. L. M. Rocco, M. N. Piancastelli, R. Feifel, and M. Simon, "Double-core-hole states in CH_3CN: pre-edge structures and chemical-shift contributions," J. Chem. Phys. **149**, 134313 (2018).
[86] S. Carniato, P. Selles, L. Andric, J. Palaudoux, F. Penent, M. Žitnik, K. Bučar, M. Nakano, Y. Hikosaka, K. Ito, and P. Lablanquie, "Single photon simultaneous K-shell ionization and K-shell excitation. I. Theoretical model applied to the interpretation of experimental results on H_2O," J. Chem. Phys. **142**, 014307 (2015).
[87] S. Carniato, "Theoretical simulation of $K^{-2}V$ inner-shell processes in Ne and Ar," J. Electron Spectrosc. **239**, 146931 (2020).
[88] T. Vitova *et al.*, "The role of the 5f valence orbitals of early actinides in chemical bonding," Nat. Commun. **8**, 16053 (2017).
[89] R. E. Wilson *et al.*, "Protactinium and the intersection of actinide and transition metal chemistry," Nat. Commun. **9**, 622 (2018).
[90] L. Cheng,"A study of non-iterative triples contributions in relativistic equation-of-motion coupled-cluster calculations using an exact two-component Hamiltonian with atomic mean-field spin-orbit integrals: Application to uranyl and other heavy-element compounds," J. Chem. Phys. **151**, 104103 (2019).
[91] A. M. March, T. A. Assefa, C. Boemer, C. Bressler, A. Britz, M. Diez, G. Doumy, A. Galler, M. Harder, D. Khakhulin, Z. Németh, M. Pápai, S. Schulz, S. H. Southworth, H. Yavas, L. Young, W. Gawelda, G. Vankó, "Probing transient valence orbital changes with picosecond valence-to-core X-ray emission spectroscopy," J. Phys. Chem. C, **121**, 2620 (2017).
[92] D. Moonshiram, C. Gimbert-Suriñach, A. Guda, A. Picon, C.S. Lehmann, X. Zhang, G. Doumy, A.M. March, J. Benet-Buchholz, A. Soldatov, A. Llobet, and S.H. Southworth "Tracking the Structural and Electronic Configurations of a Cobalt Proton Reduction Catalyst in Water," J. Am. Chem. Soc. **138**, 10586 (2016).
[93] G. Vankó, A. Bordage, M. Pápai, K. Haldrup, P. Glatzel, A. M. March, G. Doumy, A. Britz, A. Galler, T. Assefa, D. Cabaret, A. Juhin, T. B. van Driel, K. S. Kjær, A. Dohn, K. B. Møller, H. T. Lemke, E. Gallo, M. Rovezzi, Z. Németh, E. Rozsályi, T. Rozgonyi, J. Uhlig, V. Sundström, M. M. Nielsen, L. Young, S. H. Southworth, C. Bressler, and W. Gawelda, "Detailed characterization of a nanosecond-lived excited state: x-ray and theoretical investigation of the quintet state in photoexcited $[Fe(terpy)_2]^{2+}$, J. Phys. Chem C **119**, 5888 (2015).
[94] A. M. March, T. A. Assefa, C. Bressler, G. Doumy, A. Galler, W. Gawelda, E. P. Kanter, Z. Németh, M. Pápai, S. H. Southworth, L. Young, and G. Vankó, Feasibility of valence-to-core x-ray emission spectroscopy for tracking transient species," J. Phys. Chem. C **119**, 14571 (2015).
[95] C. Bressler, W. Gawelda, A. Galler, M. M. Nielsen, V. Sundström, G. Doumy, A. M. March, S. H. Southworth, L. Young, and G. Vankó, "Solvation dynamics monitored by combined X-ray spectroscopies and scattering: photoinduced spin transition in aqueous $[Fe(bpy)_3]^{2+}$," Faraday Discuss. **171**, 169 (2014).
[96] G. Vankó, A. Bordage, P. Glatzel, E. Gallo, M. Rovezzi, W. Gawelda, A. Galler, C. Bressler, G. Doumy, A. M. March, E. P. Kanter, L. Young, S. H. Southworth, S. E. Canton, J. Uhlig, V. Sundström, K. Haldrup, T. B. van Driel, M. M. Nielsen, K. S. Kjaer, and H. T. Lemke, "Spin-state studies with XES and RIXS: From static to ultrafast," J. Electron Spectrosc. Relat. Phenom. **188**, 166 (2013).

[97] K. Haldrup, G. Vankó, W. Gawelda, A. Galller, G. Doumy, A. M. March, E. P. Kanter, A. Bordage, H. Dohn, T. B. van Driel, K. S. Kjaer, H. T. Lemke, S. Canton, J. Uhlig, V. Sundström, L. Young, S. H. Southworth, M. M. Nielsen, and C. Bressler, "3. Guest-host interactions investigated by time-resolved x-ray spectroscopies and scattering at MHz rates: solvation dynamics and photoinduced spin transition in aqueous $Fe(bipy)_3^{2+}$," J. Phys. Chem. A **116**, 9878 (2012).

[98] A. M. March, A. Stickrath, G. Doumy, E. P. Kanter, B. Krässig, S. H. Southworth, K. Attenkofer, C. A. Kurtz, L. X. Chen, and L. Young, "Development of high-repetition-rate laser pump/x-ray probe methodologies for synchrotron facilities," Rev. Sci. Instrum. **82**, 073110 (2011).

[99] B. C. Garrett, D. Dixon *et al.* "Role of Water in Electron-Initiated Processes and Radical Chemistry: Issues and Scientific Advances", Chem. Rev. **105**, 355 - 389 (2005).

[100] E. Alizadeh, T. M. Orlando, L. Sanche, "Biomolecular damage induced by ionizing radiation: the direct and indirect effects of low-energy electrons on DNA," Annu. Rev. Phys. Chem. **66**, 379–398 (2015).

[101] E. Kamarchik, O. Kostko, J. M. Bowman, M. Ahmed, A. I. Krylov,"Spectroscopic signatures of proton transfer dynamics in the water dimer cation," J. Chem. Phys. **132**, 194311 (2010).

[102] O. Marsalek, C. G. Elles, P. A. Pieniazek, E. Pluhařová, J. VandeVondele, S. E. Bradforth, and P. Jungwirth, "Chasing charge localization and chemical reactivity following photoionization in liquid water," J. Chem. Phys. **135**, 224510 (2011).

[103] M.L. Vidal, X. Feng, E. Epifanovsky, A.I. Krylov, S. Coriani, "New and Efficient Equation-of-Motion Coupled-Cluster Framework for Core-Excited and Core-Ionized States,"J. Chem. Theo. Comp. **15**, 3117-3133 (2019).

[104] O. Fuchs, M. Zharnikov, L. Weinhardt, M. Blum, M. Weigand, Y. Zubavichus, M. Bär, F. Maier, J. D. Denlinger, C. Heske, M. Grunze, E. Umbach, "Isotope and Temperature Effects in Liquid Water Probed by X-Ray Absorption and Resonant X-Ray Emission Spectroscopy," Phys. Rev. Lett. **100**, 027801 (2008).

[105] K. Nanda, M. L. Vidal, R. Faber, S. Coriani, and A. I. Krylov, "How to stay out of trouble in RIXS calculations within equation-of-motion coupled-cluster damped response theory? Safe hitchhiking in the excitation manifold by means of core-valence separation," Phys Chem Chem Phys. **22**, 2629-2641 (2020).

[106] Y.-D. Chuang et al., "Modular soft x-ray spectrometer for applications in energy sciences and quantum materials," Rev. Sci. Instrum. **88**, 013110 (2017).

[107] J. M. Herbert, M. P. Coons, "The Hydrated Electron, "Annu. Rev. Phys. Chem. **68**, 447–472 (2017)

[108] A. P. Gaiduk, T. A. Pham, M. Govoni, F. Paesani and G. Galli"Electron affinity of liquid water," Nat. Comm. **9**, 247 (2018).

[109] J. Beetar, F. Rivas, S. Gholam-Mirzaei, Y. Liu, and M. Chini,"Hollow-core fiber compression of a commercial Yb:KGW laser amplifier," J. Opt. Soc. Am. B **36**, A33-A37 (2019).

[110] X. M. Tong, Z. X. Zhao, and C. D. Lin, "Theory of molecular tunneling ionization," Phys. Rev. A **66**, 033402 (2002).

[111] S. G. Sayres, M. W. Ross, and A. W. Castleman, Jr., "Ultrafast ionization and fragmentation of molecular silane," Phys. Rev. A **82**, 033424 (2010).

[112] C. Cheng, P. Vindel-Zandbergen, S. Matsika, and T. Weinacht, "Electron correlation in channel-resolved strong-field molecular double ionization," Phys. Rev. A **100**, 053405 (2019).

[113] L. Young, D. A. Arms, E. M. Dufresne, R. W. Dunford, D. L. Ederer, C. Höhr, E. P. Kanter, B. Krässig, E. C. Landahl, E. R. Peterson, J. Rudati, R. Santra, and S. H. Southworth, "X-ray microprobe of orbital alignment in strong-field ionized atoms," Phys. Rev. Lett. **97**, 083601 (2006).

[114] L. Pan and D. R. Beck, "The 1s photoabsorption transitions in Br I and Br II," J. Phys. B **39**, 4581 (2006).

[115] F. Herman and S. Skillman, *Atomic Structure Calculations* (Prentice-Hall, Englewood Cliffs, NJ, 1963.

[116] A. E. A. Fouda, P. J. Ho, R. W. Dunford, E. P. Kanter, B. Krässig, L. Young, E. R. Peterson, E. C. Landahl, L. Pan, D. R. Beck, and S. H. Southworth, "Resonant x-ray absorption of strong-field-ionized CF3Br", J. Phys. B, submitted (2020).

Page is intentionally blank.

J.R. Macdonald Laboratory Overview

The J.R. Macdonald Laboratory (JRML) focuses on the interaction of intense laser pulses with atoms and molecules for the purpose of understanding and even controlling the resulting ultrafast dynamics. The timescales involved range from attoseconds, necessary for studying electronic motion in matter, to femtoseconds and picoseconds for molecular vibration and rotation, respectively. We continue to harness the expertise within the Lab to further our progress in both understanding and control. The synergy afforded by the close interaction of theory and experiment within the Lab serves as a significant multiplier for this effort. To achieve our goals, we are advancing theoretical modeling and computational approaches as well as experimental techniques, such as particle imaging (COLTRIMS, VMI, etc.), molecular alignment, and high-harmonic generation.

Most of our research projects are associated with either "Strong-field and attosecond science" or "Correlated dynamics". These themes serve as broad outlines only, as the boundary between them is not always well defined. Similarly, in many cases it is hard to distinguish between improving theoretical and experimental tools and the resulting science discovery. A few examples are briefly mentioned below, while further details are provided in the individual abstracts of the PIs: I. Ben-Itzhak, C. Blaga, B.D. Esry, V. Kumarappan, C.D. Lin, D. Rolles, A. Rudenko, and U. Thumm.

Strong-field and attosecond science: Attosecond science is motivated by the idea of observing electronic motion in atoms and molecules on its natural timescale. One tool for this effort is attosecond pulses. These have recently become available at LCLS, and we have developed a new, more efficient theoretical approach to retrieve their properties. We have also worked to improve the retrieval algorithms for laser-induced electron diffraction (LIED) which goes hand-in-hand with our experimental LIED program. Strong-field dissociation of O_2^+ and strong-field ionization of O_2 were revisited. In the latter case, our techniques combining few-Kelvin targets with pump-probe imaging have allowed the observation of spin-dependent features.

Correlated dynamics: We have made extensive use of coincidence techniques to study correlated nuclear and electronic dynamics in a range of molecules from triatomics to simple rings, both in JRML and at FELs. Our native-frames approach has proven very adept at separating mechanisms and even electronic channels in the three-body breakup of these molecules. In particular, we have successfully applied the technique to polyatomics beyond triatomics. We have also taken advantage of techniques developed at JRML to measure the few-photon photoionization angular distributions from aligned CO_2 and C_2H_4. Our program to perform complementary experiments both in JRML and at FELs on the same molecules is also advancing with time-resolved studies of breakup in various species, especially the halomethanes with one or two halogen substitutions.

A significant fraction of this JRML research is done in collaboration with others, both at JRML and elsewhere. M. Dantus, E. Wells, R. Jones, and T. Weinacht are just a few of those that have enriched our program through collaboration. Similarly, some of us conduct experiments at free electron lasers, such as LCLS and FLASH, and at other facilities. Our group is well connected through such collaborations with many AMO groups across the world (ALS, ANL, BNL, FLASH, Univ. of Frankfurt, ICFO Barcelona, Univ. of Jena, LBNL, LCLS, Max-Born Institute–Berlin, Max-Planck Institutes for Quantum Optics and Kernphysik, The Ohio State University, PULSE- SLAC, and others), and we actively seek new collaborations.

As these abstracts are submitted, our newest laser system is on its way to JRML. This laser, nicknamed FLAME, is a robust, 3-kHz, 5-mJ system that will enable pump-probe coincidence measurements with wavelength conversion. The room and several experiments are awaiting its arrival. Many of our coincidence measurements will get an even bigger boost from the high-power 100-kHz-class system that we recently received funding for. These systems currently have a long lead time, however, such that it likely will not be in the Lab for 1–2 years.

With the arrival of the coronavirus, this year has proven as much a challenge to us as to everyone else. Kansas State University went into lockdown in the spring, leading us to shutdown experiements in the Lab for 2.5 months. Once we were able to reopen at the end of May, we did manage to bring our lasers back up and start our first experiment within a couple of weeks. But, between hiring freezes leaving several postdoc positions empty and the ongoing mitigation efforts, progress is still not at full speed. We will, however, continue to learn how to work in this new normal, keeping everyone safe and producing more exciting science.

Structure and Dynamics of Atoms, Ions, Molecules, and Surfaces: Molecular Dynamics with Ion and Laser Beams

Itzik Ben-Itzhak, J. R. Macdonald Laboratory, Physics Department, Kansas State University, Manhattan, KS 66506; ibi@phys.ksu.edu

Project Scope: *The goal of this part of the JRML program is to study and control molecular dynamics under the influence of ultrashort intense laser pulses. To this end, we typically study molecular ion beams and have a close collaboration between theory and experiment.*[1]

***Recent Progress*:** We focused our experimental work, employing 3D-momentum imaging techniques, on ion-beam and gas-phase targets, while continuing our collaborative research with others. A couple of examples are presented below.

Native frames: separating sequential from concerted three-body fragmentation

Travis Severt's PhD work, with others contributing to the different sub-projects within

During the fragmentation of polyatomic molecules, two or more bonds may break in a concerted manner (simultaneously) or sequentially (stepwise). Separating these competing processes has been a main goal toward improving the understanding of fragmentation dynamics [1]. A couple of years ago, we proposed the native-frames method (see Pub. [8] and Ref. [2]) to analyze three-body breakup and accomplish the goal above. Our analysis method is based on using relative momenta derived from Jacobi coordinates, which reduce the dimensionality of the problem. Moreover, this method enables systematic analysis that links the relative momenta to possible sequential breakup pathways and their respective center-of-mass reference frames. To identify and separate sequential breakup form concerted fragmentation one needs a signature, i.e. a feature in the measured spectra that distinguishes the two mechanisms from each other.

One example of such a signature is the uniform angular distribution associated with the second breakup step when the intermediate molecular fragment rotates long enough in the fragmentation plane. We demonstrated this method for both sequential fragmentation pathways of OCS^{3+}, i.e. breakup via $S^+ + CO^{2+}$ or $O^+ + CS^{2+}$ (Pub. [8] and Ref. [2]). Moreover, we reconstructed the distribution of sequential fragmentation events masked by competing breakup processes and separated the sequential and concerted breakup distributions in any plot created from the measured momenta.

Since then, we have extended our studies of three-body fragmentation induced by strong field laser pulses to other systems, such as CO_2 fragmentation into $C^+ + O^+ + O^+$, compared with the same channel studied by double ionization of a CO_2^+ beam [3]. For the CO_2^+ target, we also explored three-body fragmentation following single ionization, i.e. the $C^+ + O^+ + O$ and $C + O^+ + O^+$ channels, taking advantage of our ability to measure neutral fragments [4]. In Fig. 1 we show the yield of $C + O^+ + O^+$ breakup via a CO^+ intermediate, as a function of kinetic energy release (KER) in the second step and the angle between the relative momenta (see Pub. [1]). This sequential fragmentation, induced by 790-nm, 23-fs, ~10^{15}-W/cm^2 pulses, appears as the stripe centered about 0.5 eV and extending to zero degrees.

We have been also exploring the conditions leading to the uniform angular distributions by rotating intermediate molecules, and the resulting distributions when these conditions are not fulfilled [5].

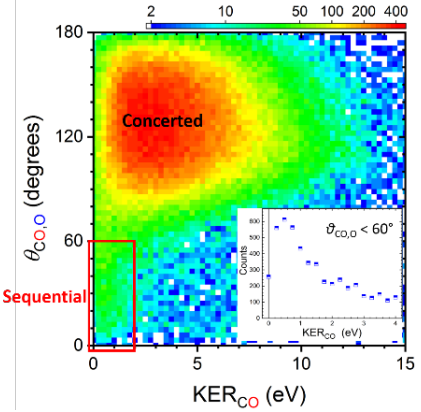

Figure 1. The $N(\mathrm{KER}_{CO}, \theta_{CO,O})$ distribution for $CO_2^+ \rightarrow C + O^+ + O^+$ fragmentation via the CO^+ intermediate molecule (Sequential breakup marked by the red box). (Inset) The KER in the second step, i.e. $CO^+ \rightarrow C + O^+$ breakup.

[1] In addition to the close collaboration with the theory group of *Brett Esry*, some of our studies are done in collaboration with others at JRML and elsewhere.

In addition, we implemented the native frames analysis method to distinguish sequential and concerted fragmentation of water and ammonia following double ionization by a single photon. These studies were carried out at the ALS in collaboration with others (from LBNL, UC Berkley, UC Davis, U. Frankfurt, Auburn U, UN Reno). In both cases two protons and two electrons were measured in coincidence, and the momentum of the remaining neutral fragment was evaluated using momentum conservation.

In the case of D_2O, the signature of sequential breakup, via an OD^+ intermediate predissociating into $D^+ + O$, is a uniform $N(\theta_{OD,D})$ distribution with a second step KER_{OD} smaller than 2.4 eV. This is the expected KER for predissociation of OD^+ via the metastable $a\,^1\Delta$ and $b\,^1\Sigma^+$ states [6]. Furthermore, we identify two pathways and the associated electronic states in the energy-correlation map shown in Fig. 2(a). Specifically, we separate the fragmentation of the $^1B^1$ and $2\,^1A^1$ states of D_2O^{2+} into the $a\,^1\Delta$ and $b\,^1\Sigma^+$ states of OD^+, respectively. Some of the OD^+ ions finally undergo predissociation to the $D^+ + O(^3P)$ limit. Moreover, the measured and calculated KER in each of these pathways are in very good agreement as shown in Fig. 2(b). This example demonstrates our ability to experimentally track sequential-fragmentation dynamics step-by-step and state selectively, enabling direct comparison with our molecular dynamics calculations [7].

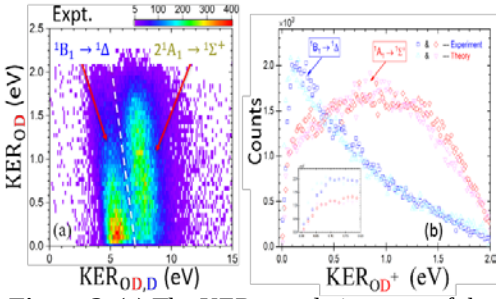

Figure 2. (a) The KER correlation map of the first and second fragmentation step of D_2O, and (b) the second step KER comparing theory and experiment. The inset shows the threshold behavior, where OD^+ dissociation is suppressed by the centrifugal barrier.

The ammonia fragmentation into $H^+ + H^+ + NH/(N+H) + 2e^-$, in contrast, forced us to search for another sequential breakup signature instead of the angular distribution that was found to be non-uniform. The energy sharing between the two protons is found to be nearly equal for the concerted breakup channels identified, while in contrast it is very asymmetric for the sequential fragmentation, $NH_3^{2+} \rightarrow H^+ + H + NH^+$ followed by $NH^+ \rightarrow H^+ + N$ (see Pub. [18]).

Importance of one- and two-photon transitions in the strong-field dissociation of NO^{2+}

Bethany Jochim, M. Zohrabi, B. Gaire, T. Uhlíková, K.D. Carnes, E. Wells, B.D. Esry, and I. Ben-Itzhak

In addition to our work on polyatomic molecules we kept exploring dissociation and ionization of diatomic molecules driven by ultrashort strong-field laser pulses. In this project we probed a metastable molecular dication, specifically NO^{2+}, introduced into the laser focus as a few keV beam [8]. Like the vibrationally cold CO^{2+} [9], the NO^{2+} cools in "flight" (~20 μs), to its electronic ground state while hign vibrational levels predissociate [see Fig. 3(b)], and then probed by laser pulses in the 10^{14} W/cm^2 range.

One may expect ionization to play an important role at this intensity range (see, e.g., Ref. [10]), however, our measurements indicate that dissociation into $N^+ + O^+$ dominates, while ionization is of the order of 1% or lower.

The main mechanisms leading to dissociation involve one and two-photon transitions between the *X* and *A* states, as shown in Fig. 3(a). Employing first order perturbation theory using the *X*–*A* transition dipole moment (inset), we reproduce the measured one-photon peak at about ~6.5 eV. These calculations show that $X\ ^2\Sigma^+(v = 5)$ to $A\ ^2\Pi(v = 9)$ photo-absorption is the dominant transition leading to $N^+ + O^+$ by rapid tunneling of the $A\,^2\Pi(v=9)$ state ($\tau = 14$ ps [11]). This interpretation is further supported by the measured angular distribution, shown in Fig. 4, which

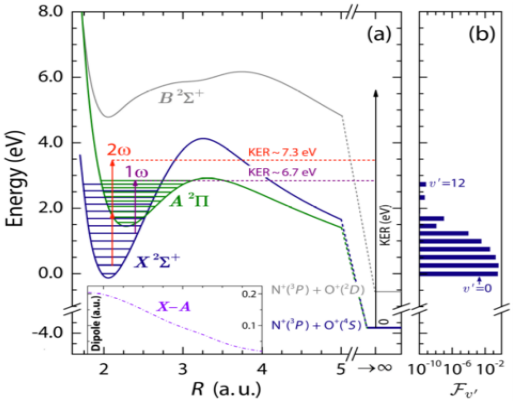

Figure 3. (a) Potentials of NO^{2+} (inset– *X*–*A* transition dipole moments) [8]. (b) Computed *X* vibrational population at the laser crossing.

nicely fits a $\sin^2\theta$ distribution expected for one-photon transitions with $\Delta\Lambda=1$, like the $X\ ^2\Sigma^+$ to $A\ ^2\Pi$ transitions. The higher KER peak (at about 7.5 eV) is consistent with two-photon absorption, namely $X\ ^2\Sigma^+$ to $A\ ^2\Pi$ to $X\ ^2\Sigma^+$, that is above the *A*-state barrier and therefore predissociates rapidly due to spin-orbit coupling between the *X* and *A* states. This two-photon transition nicely fits the expected $\sin^4\theta$ distribution. To conclude, NO^{2+} molecules preferentially dissociate perpendicular to the laser polarization at the 10^{14} W/cm^2 range, while ionization is only about 1% or lower.

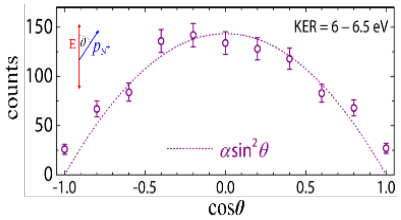

Figure 4. Angular distribution of one-photon *X* to *A* transitions leading to $N^+ + O^+$ dissociation.

***Future plans*:** We will continue to probe molecular-ion beams in a strong laser field, specifically investigating challenging two-color, pump-probe and CEP-dependence experiments. We will carry on our studies of more complex systems, including simple polyatomic molecules focusing on three-body breakup, bond-rearrangement, as well as hydrogen migration and elimination processes. To enable some of the studies involving imaging fragments with large mass difference, like proton elimination, we are upgrading the experimental setup used for coincidence momentum imaging. Specifically, we are adding a second position sensitive detector dedicated mainly to measuring the less massive ions.

References

1. C.E.M. Strauss and P.L. Houston, J. Chem. Phys. **94**, 8751 (1990)
2. T. Severt, J. Rajput, B. Berry, B. Jochim, P. Feizollah, B. Kaderiya, M. Zohrabi, U. Ablikim, F. Ziaee, Kanaka Raju P., D. Rolles, A. Rudenko, K.D. Carnes, B.D. Esry, and I. Ben-Itzhak, "Native frames: A new approach for separating sequential and concerted three-body fragmentation", Phys. Rev. A – in preparation
3. T. Severt *et al*. (CO_2 & CO_2^+), Phys. Rev. A – in preparation
4. I. Ben-Itzhak, P.Q. Wang, J.F. Xia, A.M. Sayler, M.A. Smith, K.D. Carnes, and B.D. Esry, Phys. Rev. Lett. **95**, 073002 (2005)
5. T. Severt *et al*. (out-of-plane rotation), Phys. Rev. A – in preparation
6. R. de Vivie, C.M. Marian, and S.D. Peyerimhoff, Chem. Phys. **112**, 349 (1987)
7. T. Severt[2], Z.L. Streeter[2], W. Iskandar, D. Reedy, K.A. Larsen, D. Call, E.G. Champenois, A. Gatton, B. Griffin, B. Jochim, R. Strom, M.M. Brister, A.L. Landers, D.S. Slaughter, R.R. Lucchese, J.B. Williams, Th. Weber, C.W. McCurdy, and I. Ben-Itzhak, "A concerted theory and experiment effort to track sequential fragmentation dynamics of water dications step by step and state selective", PNAS – in preparation
8. B. Jochim, M. Zohrabi, B. Gaire, T. Uhlíková, K.D. Carnes, E. Wells, B.D. Esry, and I. Ben-Itzhak, "Importance of one- and two-photon transitions in the strong-field dissociation of NO^{2+}", Phys. Rev. A – to be submitted soon
9. J. McKenna, A.M. Sayler, F. Anis, N.G. Johnson, B. Gaire, Uri Lev, M.A. Zohrabi, K.D. Carnes, B.D. Esry, and I. Ben-Itzhak, Phys. Rev. A **81**, 061401(R) (2010)
10. C. Cornaggia and Ph. Hering, Phys. Rev. A **62**, 023403 (2000)
11. R. Baková, J. Fišer, T. Šedivcová-Uhlíková, and V. Špirko, J. Chem. Phys. **128**, 144301 (2008)

Peer-Reviewed Publications Resulting from this Project (2018-2020)

18. K.A. Larsen, T.N. Rescigno, T. Severt, Z.L. Streeter, W. Iskandar, S. Heck, A. Gatton, E.G. Champenois, R. Strom, B. Jochim, D. Reedy, R. Moshammer, R. Dörner, A.L. Landers, J.B. Williams, C.W. McCurdy, R.R. Lucchese, I. Ben-Itzhak, D.S. Slaughter and Th. Weber, "Photoelectron and fragmentation dynamics of the $H^+ + H^+$ dissociative channel in NH_3 following direct single-photon double ionization", Phys. Rev. Res. – accepted.
17. "Ionization-induced sub-cycle metallization of nanoparticles in few-cycle pulses", Q. Liu, L. Seiffert, F. Süßmann, S. Zherebtsov, J. Passig, A. Kessel, S. Trushin, N.G. Kling, I. Ben-Itzhak, V. Mondes, C. Graf, E. Rühl, L. Veisz, S. Karsch, J. Rodríguez-Fernández, M.I. Stockman, J. Tiggesbäumker, K.-H. Meiwes-Broer, T. Fennel, and M.F. Kling, ACS Photonics – *almost* accepted.
16. "Control of electron recollision and molecular nonsequential double ionization", Shuai Li, Diego Sierra-Costa, Matthew J. Michie, Itzik Ben-Itzhak, and Marcos Dantus, Commun. Phys. **3**, 35 (2020).

[2] Equally contributing authors

15. "Strong-field control of H_3^+ production from methanol dications: Selecting between local and extended formation mechanisms", Naoki Iwamoto[2], Charles J. Schwartz[2], Bethany Jochim, Kanaka Raju P., Peyman Feizollah, J.L. Napierala, T. Severt, S.N. Tegegn, A. Solomon, S. Zhao, Huynh Lam, Tomthin Nganba Wangjam, V. Kumarappan, K.D. Carnes, I. Ben-Itzhak, and E. Wells, J. Chem. Phys. **152**, 054302 (2020).
JCP Special Topic on Ultrafast Molecular Sciences by Femtosecond Photons and Electrons – invited.
14. Experimental study of laser-induced isomerization dynamics of specific $C_2H_2^q$ ions", Bethany Jochim, M. Zohrabi, T. Severt, Ben Berry, K. J. Betsch, Peyman Feizollah, J. Rajput, E. Wells, K.D. Carnes, and I. Ben-Itzhak, Phys. Rev. A **101**, 013406 (2020).
13. "Symmetry breaking in the body-fixed electron emission pattern due to electron-retroaction in the photodissociation of H_2^+ and D_2^+ close to threshold", S. Heck, A. Gatton, K.A. Larsen, W. Iskandar, E.G. Champenois, R. Strom, A. Landers, D. Reedy, C. Dailey, J.B. Williams, T. Severt, B. Jochim, I. Ben-Itzhak, R. Moshammer, R. Dörner, D.S. Slaughter, and Th. Weber, Phys. Rev. Research **1**, 033140, (2019).
12. "Adaptive strong-field control of vibrational population in NO^{2+}", O. Voznyuk[2], Bethany Jochim[2], M. Zohrabi, Adam Broin, R. Averin, K.D. Carnes, I. Ben-Itzhak, and E. Wells, J. Chem. Phys. **151**, 124310 (2019).
11. "Strong-field induced bond rearrangement in triatomic molecules", S. Zhao, Bethany Jochim, Peyman Feizollah, Jyoti Rajput, F. Ziaee, Kanaka Raju P., B. Kaderiya, K. Borne, Y. Malakar, B. Berry, J. Harrington, D. Rolles, A. Rudenko, K.D. Carnes, E. Wells, I. Ben-Itzhak, and T. Severt, Phys. Rev. A **99**, 053412 (2019).
10. "Dependence on initial configuration of strong field-driven isomerization of C_2H_2 cations and anions", Bethany Jochim, Ben Berry, T. Severt, Peyman Feizollah, M. Zohrabi, Kanaka Raju P., E. Wells, K.D. Carnes, and I. Ben-Itzhak, J. Phys. Chem. Lett. **10**, 2320 (2019).
9. "Tracing intermolecular Coulombic decay of carbon-dioxide dimers and oxygen dimers after valence photo ionization", W. Iskandar, A.S. Gatton, B. Gaire, F.P. Sturm, K.A. Larsen, E.G. Champenois, N. Shivaram, A. Moradmand, J.B. Williams, B. Berry, T. Severt, I. Ben-Itzhak, D. Metz, H. Sann, M. Weller, M. Schöffler, T. Jahnke, R. Dörner, D. Slaughter, and Th. Weber, Phys. Rev. A **99**, 043414 (2019).
8. "Time-resolved imaging of bound and dissociating nuclear wave packets in strong-field ionized iodomethane", Y. Malakar, W.L. Pearson, M. Zohrabi, B. Kaderiya, Kanaka Raju P., F. Ziaee, S. Xue, A.T. Le, I. Ben-Itzhak, D. Rolles, and A. Rudenko – Phys. Chem. Chem. Phys. **21**, 14090 (2019).
7. "Bond rearrangement during Coulomb explosion of water molecules", M. Leonard, A. Max Sayler, K.D. Carnes, E.M. Kaufman, E. Wells, R. Cabrera-Trujillo, and B.D. Esry, and I. Ben-Itzhak, Phys. Rev. A **99**, 012704 (2019).
6. "H_2 roaming chemistry and the formation of H_3^+ from organic molecules in strong laser fields", Nagitha Ekanayake, Travis Severt, Muath Nairat, Nicholas P. Weingartz, Benjamin M. Farris, Balram Kaderiya, Peyman Feizollah, Bethany Jochim, Farzaneh Ziaee, Kurtis Borne, Kanaka Raju P., Kevin D. Carnes, Daniel Rolles, Artem Rudenko, Benjamin G. Levine, James E. Jackson, Itzik Ben-Itzhak, and Marcos Dantus, Nature Communications **9**, 5186 (2018).
5. "Dissociation dynamics of the water dication following one-photon double ionization II: Experiment", D. Reedy, J.B. Williams, B. Gaire, A. Gatton, M. Weller, A. Menssen, T. Bauer, K. Henrichs, Ph. Burzynski, B. Berry, Z. Streeter, J. Sartor, I. Ben-Itzhak, T. Jahnke, R. Dörner, Th. Weber, and A.L. Landers, Phys. Rev. A **98**, 053430 (2018).
4. "Resonance signatures in the body-frame valence photoionization of CF_4", K.A. Larsen, C. Trevisan, R. Lucchese, S. Heck, W. Iskandar, E. Champenois, A. Gatton, R. Moshammer, R. Strom, T. Severt, B. Jochim, D. Reedy, M. Weller, A. Landers, J.B. Williams, I. Ben-Itzhak, R. Dörner, D. Slaughter, C.W. McCurdy, Th. Weber, and T.N. Rescigno, Phys. Chem. Chem. Phys. **20**, 21075 (2018).
3. "State-selective dissociation dynamics of oxygen molecular ion studied with single-harmonic pump and infrared probe pulses", Y. Malakar, F. Wilhelm, D. Trabert, Kanaka Raju P., X. Li, W.L. Pearson, W. Cao, B. Kaderyia, I. Ben-Itzhak, and A. Rudenko, Phys. Rev. A **98**, 013418 (2018).
2. "Non-unique and non-uniform mapping in few-body Coulomb-explosion imaging", A.M. Sayler, E. Eckner, J. McKenna, B.D. Esry, K.D. Carnes, I. Ben-Itzhak, and G.G. Paulus, Phys. Rev. A **97**, 033412 (2018).
Selected for PRA Kaleidoscope Images: https://journals.aps.org/pra/kaleidoscope/pra/97/3/033412 March 2018
1. "Native frames: Disentangling sequential from concerted three-body fragmentation", Jyoti Rajput, T. Severt, B. Berry, B. Jochim, P. Feizollah, B. Kaderiya, M. Zohrabi, U. Ablikim, F. Ziaee, Kanaka-Raju P., D. Rolles, A. Rudenko, K.D. Carnes, B.D. Esry, and I. Ben-Itzhak, Phys. Rev. Lett. **120**, 103001 (2018).
Highlighted in Physics Today – online story: *Three-body fragmentation in a new frame by Johanna L. Miller*

Strong Field Excitation and Ionization: Low and High Energy Electron Rescattering Processes

Cosmin I. Blaga
J. R. Macdonald Laboratory, Physics Department, Kansas State University, Manhattan, KS, 66506
blaga@phys.ksu.edu

Project Scope

The scope of this JRML project is to develop ultrafast photoelectron metrologies as tools for molecular dynamics studies.

In recent years, my research interest has been focused on developing laser-driven electron diffraction (LIED) as an ultrafast imaging probe of molecular dynamics. For this purpose, we pursued the development of midinfrared ultrafast lasers that allowed us to leverage the λ^2- scaling law in order to generate high energy (> 100 eV) returning electron wave packets that possess the necessary resolving power to determine the location of atomic centers inside the parent molecular ion. These efforts were rewarded with steady progress, as we were able to observe molecular transformations from bond relaxations in diatomic molecules to cage deformations of fullerenes (a recent review of time-resolved ultrafast molecular can be found here [1]).

Although typical LIED probes use high energy electron-ion collisions, as dictated by the diffraction-limited process, arguably the vast majority of photochemical reaction triggered by visible or ultraviolet light only generate slow electrons (few eVs). Despite this obvious limitation, few years ago in a series of experiments undertaken at Ohio State in the group of Prof. Louis F. DiMauro, we demonstrated that as long as LIED is performed in the adiabatic limit (i.e. the Keldysh parameter was below 0.7), accurate electron-ion elastic differential cross-sections (DCS) could be retrieved from photoelectron angular distributions even for return energies of ~10 eV in the case of sodium when irradiated with 3-4 μm pulses. However, the resolving power of such low energy electrons was still diffraction limited, insufficient for atomic position determination but perhaps suitable in select cases for imaging larger molecular structures such as aromatic rings.

In a seminal result published a decade ago, Huismans *et al.* [2] demonstrated a novel holography method based on low energy photoelectrons. The experiments recorded low energy photoelectron angular distributions (PAD) from metastable xenon and identified holographic patterns formed by interference of various quantum electron trajectories. As at least one of these trajectories recollided with the parent ion, a de facto structural probing of the parent took place. Nonetheless, the resulting hologram was complicated and structural retrieval was not performed. Despite this, the result spurred a series of experiments and to date, various low energy electron holographic patterns and so-called quantum carpets have been observed in atomic and molecular targets.

In this project, during the last year we begin an investigation of low energy holographic signals observed in noble gases and select molecular targets. Our goal was to identify PAD

structures that were created by a small number of trajectories and investigate their suitability for structural retrieval while leveraging our LIED toolset. In essence, we aimed to identify those holographic patterns that fulfilled the following criteria: (i) were produced predominantly by a small number of quantum trajectories, (ii) at least one trajectory underwent recollision and (iii) the pattern was primarily ponderomotively driven and invariant to laser parameters since LIED requires a factorization formula that in the adiabatic limit allows us to extract e^--ion DCS that do not depend on the probing laser. Thus, we are now applying a more encompassing strategy to develop ultrafast molecular imaging metrologies based on electron rescattering at arbitrary recollision energies.

Recent Progress

a) High-Order Above Threshold Ionization Enhancements, LIED and electron holography. The 1994 discovery of the long high-order above threshold ionization (HATI) plateau in the photoelectron spectra of noble gases by Paulus et al. [3], confirmed not only the rescattering mechanism of strong field physics, but also identified a series of HATI plateau enhancements whose physical origin, even after 25 years, remains elusive [3-9]. A few years ago, while at Ohio State (DiMauro-Agostini Group) in collaboration with Louisiana State (Schaefer Group) the advent of intense tunable laser sources allowed us to revisit these enhancements, performing a series of experiments and numerical time-dependent Schrödinger equation (TDSE) simulations exploring a significantly expanded parameter space. Not surprisingly, the physical picture painted by these investigations was rich in complexity, various aspects of strong field ionization and excitation being present. However, few crucial takeaways from this project provided evidence that the rescattering aspect benefits from several key characteristics that could make it suitable for a simple holographic interpretation and LIED analysis. The first characteristic is *universality*. Upon exploring a significantly wider range of laser parameters and targets, we found yield enhancements in atoms and molecular targets (all noble gases, methane, ethane) and we have developed an empirical formula to predict for a given target what laser parameters are needed. Recently, several groups reported similar finding, identifying enhancements is targets as complex as formic acid [9]. A second characteristic we discovered was a precise ponderomotive scaling of the enhancement location. This suggests that the classical trajectory approximation in high-energy LIED might apply in this case as well. If so, quantitatively accurate *low-energy* DCS from PADs for low energy electrons might possibly be extracted from experimental data. We have performed a series of experiments in argon at various laser wavelength and our collaborators at Ohio State are working on extending these investigations to other noble gases. Finally, the third characteristic of HATI we're currently exploring at K-State is the holographic interpretation of the enhancement, based on previous theoretical work of Goreslavskii and Popruzhenko [5] and Frolov, Manakov and Starace [8]. In these works, the enhancement is interpreted as an interference between the well-known long and short trajectories. The connection with the reference and probe trajectories in electron holography [2] is immediate, as one recognizes that the difference between the long-short trajectory pair and reference-probe pair is merely semantical. At K-State, we are currently performing and analyzing PADs taken in argon irradiated with dichroic fields where the relative phase of two colors is the knob that controls the relative phase of the two dominating quantum trajectories. This all optical method will be combined with our LIED toolset to allow us to study

the electron wavepacket dynamics in the continuum and the recollision process. In closing, it is worth reiterating here that the electron metrology efforts outlined above are part of a larger, comprehensive collaborative effort conducted at K-State, OSU and LSU.

b) High-energy recollisions and a more robust LIED. During the last year we continued our long term international collaboration (KSU, OSU, IFCO-Barcelona, MPQ-Garching and Tohoku University, Japan) to apply LIED to the study of fullerenes. Unfortunately, experiments planned to take place in Barcelona were postponed repeatedly during the year due to the global COVID-19 pandemic. A separate C_{60} experiment planned to take place at LCLS has also been postponed. Nonetheless, despite these setbacks we are working with the theoretical group of CD Lin here at K-State towards developing a more robust LIED analysis and DCS retrieval from 2D PADs. The theoretical details of these efforts will be highlighted by the Lin Group. Here, it worth emphasizing that we are working with previously recorded raw experimental data taken at Ohio State that is either published (nitrogen and oxygen molecules [10]) or unpublished (carbon dioxide). This strategy will allow us to not only benchmark the expanded LIED version versus our old results, but it also gave our group members the opportunity to be productive and continue working remotely during the disruptive Spring and early Summer 2020 mandatory lab shutdown.

Future Plans

In the next few months we will focus our efforts to complete our electron-holography experimental investigations in argon outlined above. These investigations will be followed by a comprehensive LIED analysis and comparison with TDSE numerical simulations. If successful, we will immediately the new electron metrology to a molecular target, most likely methane and diatomics, with the aim at extracting low-energy DCS and investigate propagation phase delays between the two dominant trajectories. Finally, these results will be analyzed in conjunction with other holographic patterns observed in the PAD and look for connections and correlations between them, aiming to provide a more complete picture of PAD with the ultimate goal of providing novel time-resolved angular resolved photoelectron spectroscopy tools.

We are also looking forward to continue our international collaborations, awaiting the reopening of international travel and laser facilities to explore LIED and ultrafast molecular imaging of macromolecules (Barcelona and LCLS). At K-State, two new laser systems will arrive within the next year: a Ti:Sapphire 3 kHz laser funded by DOE will arrive within a few weeks and larger, high repetition laser operating at ~100 kHz (NSF-MRI) will arrive towards the end of 2021. These high repetition laser systems will be ideal tools for performing "ideal" LIED experiments, where UV pump pulses will photodissociate a target (such as CH_3I) that can be "seen" by an LIED probe. A third aligning pulse can also be employed to sharpen the image by removing the inherent averaging due to molecular orientation randomness.

References

[1] Junliang Xu, Cosmin I Blaga, Pierre Agostini, Louis F DiMauro, *Time-resolved Molecular Imaging*, J. Phys. B **49**, Issue 11, 112001 (2016).

[2] Y. Huismans *et al.*, *Time-Resolved Holography with Photoelectrons*, Science **331**, 61-64 (2010).

[3] G. G. Paulus et al., *Plateau in Above Threshold Ionization Spectra*, Phys. Rev. Lett. **72**, 2851 (1994).

[4] H. G. Muller and F. C. Kooiman, *Bunching and Focusing of Tunneling Wave Packets in Enhancement of High-Order Above-Threshold Ionization*, Phys. Rev. Lett. **81**, 1207 (1998).

[5] S. P. Goreslavskii and S. V. Popruzhenko, *Rescattering and quantum interference near the classical cut-offs*, J. Phys. B **32**, L531-L538 (1999).

[6] Joseph Wassaf, Valérie Véniard, Richard Taïeb, and Alfred Maquet, *Roles of resonances and recollisions in strong-field atomic phenomena: Above-threshold ionization*, Phys. Rev. A **67**, 053405 (2003).

[7] D. B. Milošević, E. Hasović, M. Busuladžić, A. Gazibegović-Busuladžić, and W. Becker, *Intensity-dependent enhancements in high-order above-threshold ionization*, Phys. Rev. A **76**, 053410 (2007).

[8] M. V. Frolov, N. L. Manakov, and A. T. Starace, *Analytic formulas for above-threshold ionization and detachment plateau spectra*, Phys. Rev. A **79**, 033406 (2009).

[9] C. Wang, Y. Tian, S. Luo, W. G. Roeterdink, Y. Yang, D. Ding, M. Okunishi, G. Prümper, K. Shimada, K. Ueda, and R. Zhu, *Resonance-like enhancement in high-order above-threshold ionization of formic acid*, Phys. Rev. A **90**, 023405 (2014).

[10] C. I. Blaga et al., *Imaging ultrafast molecular dynamics with laser-induced electron diffraction*, Nature **483**, 194-197 (2012).

Peer-review Publications Resulting from This Project

No publications to report.

Strong-field dynamics of few-body atomic and molecular systems

B.D. Esry
J. R. Macdonald Laboratory, Kansas State University, Manhattan, KS 66506
esry@phys.ksu.edu

Program Scope

My group's efforts are focused on developing novel analytical and numerical tools to more efficiently and more generally treat atoms and molecules in strong laser fields. Our goal is to advance the state-of-the-art to enable increasingly complicated processes and systems to be treated in an *ab initio* manner. We specialize in treating few-body systems with minimal approximations, using the results to validate general analytic approaches. Moreover, with more effective tools for such systems, we are able to explore a broader range of physical phenomena and can more realistically carry out quantitative comparisons with experiment for these highly non-perturbative processes.

1. Extracting total- and net-photon-number pathways in theory and experiment

Recent progress

One of the challenges to understanding strong-field phenomena sufficiently to predict outcomes without detailed calculation or explicit experiment is the lack of a simple, general, systematic picture. Our early success [1, 2] in developing such a picture for carrier-envelope phase (CEP) effects showed us, though, that it was possible.

Our "general theory" [1,2] is based on an exact representation of the time-dependent Schrödinger equation (TDSE). The simple picture that it produced — the interference of *net*-photon-number pathways — describes all known CEP experiments, whether they involve electronic motion, nuclear motion, or both. The representation we identified takes advantage of the fact that the TDSE depends parametrically on the CEP by transforming the wave function to a conjugate space, immediately suggesting even broader possibilities for parametric expansions.

With this idea in mind, time-dependent perturbation theory (TDPT) can be recognized as another example of a parametric expansion. When applied to strong-field phenomena, one concludes that it identifies *total*-photon-number pathways. The distinction between net and total photon numbers is, of course, relevant when many photons are exchanged with the field — as happens in a strong field.

We have combined both of these parametric expansions, thus enabling all possible quantum mechanical pathways to be labeled by their total- and net-photon number in an exact, *ab initio* manner. Whether this decomposition provides greater insight is a topic we continue to explore, and we provide here one example.

Our theory starts from the general form of time-dependent Schrödinger equation,

$$i\hbar\frac{d}{dt}|\Psi\rangle = \Big[H_0 + W(\epsilon,\varphi;t)\Big]|\Psi(t)\rangle, \qquad (1)$$

where H_0 is the field-free Hamiltonian and

$$W(\epsilon,\varphi;t) = \frac{\epsilon}{2}\Big[e^{i\varphi}v^\dagger(t) + e^{-i\varphi}v(t)\Big], \qquad (2)$$

is the laser-matter interaction. Here ϵ and φ represent the strength and carrier-envelope

phase (CEP), respectively, of the laser electric field, whereas $v(t)$ and $v^\dagger(t)$ carry the remainder of the dipole interaction. We expand the solution as

$$|\Psi(\epsilon,\varphi;t)\rangle = \sum_{m=0}^{\infty}\sum_{n=-m}^{m} \epsilon^m e^{in\varphi}|\psi_{m,n}(t)\rangle. \quad (3)$$

As stated above, the indices m and n can be interpreted as the total and net numbers of photons, respectively.

An observable such as the momentum distribution can be generally expressed as

$$\frac{dP}{d\mathbf{p}}(\epsilon,\varphi;t) = \sum_{\mu=0}^{\infty}\sum_{\nu=-\mu}^{\mu} \epsilon^\mu e^{i\nu\varphi}\frac{dP_{\mu,\nu}}{d\mathbf{p}}(t), \quad (4)$$

where

$$\frac{dP_{\mu,\nu}}{d\mathbf{p}} = \sum_{m,n}\langle\mathbf{p}|\psi_{\mu-\mathbf{m},\mathbf{n}-\nu}\rangle^*\langle\mathbf{p}|\psi_{\mathbf{m},\mathbf{n}}\rangle \quad (5)$$

with similar expressions for any other observable. Consequently, observables depend on the field strength and CEP through the sum μ=m+m' and difference ν=n-n', respectively, of the total and net photon numbers of the two interfering pathways $\langle\mathbf{p}|\psi_{\mu-\mathbf{m},\mathbf{n}-\nu}\rangle$ and $\langle\mathbf{p}|\psi_{\mathbf{m},\mathbf{n}}\rangle$.

We applied this formalism to the asymmetry of the photoelectron energy spectrum (PES) in multiphoton ionization. For simplicity, we used a one-dimensional model atom (soft Coulomb potential) with ground state energy −0.67 a.u. and a one-cycle Gaussian laser pulse (FWHM) at 50 nm. Its intensity was set to 1×10^{15} W/cm^2 at ϵ=1.

Figures 1(a) and 1(c) show the direction-resolved PES — *i.e.* to the left and right — as well as the CEP-averaged total PES, $\langle dP/dE\rangle$, at two intensities. The asymmetry,

$$A(\epsilon,\varphi;E) = \left[\frac{dP_L}{dE} - \frac{dP_R}{dE}\right] \Big/ \left\langle\frac{dP}{dE}\right\rangle, \quad (6)$$

shown in Figs. 1(c) and 1(d), is enhanced at low energies (EB1) and high energies (EB2) *between* neighboring broad multiphoton peaks [3].

In the figure, note: (i) that the peaks of $|A(\epsilon,\varphi;E)|$ shift to lower energy with increasing intensity, and (ii) that there is a shift in the φ oscillation from EB1 to EB2 for each intensity as well. These features can be rigorously and quantitatively attributed to specific contributions from $dP_{\sigma,\mu,\nu}/dE$ ($\sigma = L, R$) as defined in Eqs. (4) and (5).

We summarize the analysis of feature (i) here to demonstrate the approach. The numerator and denominator of Eq. (6) are decomposed into $A_{\mu,\nu}(E) = dP_{L,\mu,\nu}/dE - dP_{R,\mu,\nu}/dE$ and $dP_{\mu,0}/dE = dP_{L,\mu,0}/dE + dP_{R,\mu,0}/dE$, respectively. In EB1, $A_{3,\pm1}(E)$ dominates the numerator [cf. Figs. 2(a)–2(c)], whereas contributions of $dP_{2,0}/dE$ and $dP_{4,0}/dE$ to the denominator are comparable [cf. Figs. 2(d)–2(f)]. As ϵ increases, the relative contribution of $dP_{4,0}/dE$ increases, and the minimum of the denominator moves to lower E, causing the peaks of $|A(\epsilon,\varphi;E)|$ to shift. The shift in EB2 can be similarly explained in terms of $A_{5,\pm1}(E)$, $dP_{4,0}/dE$, and $dP_{6,0}/dE$.

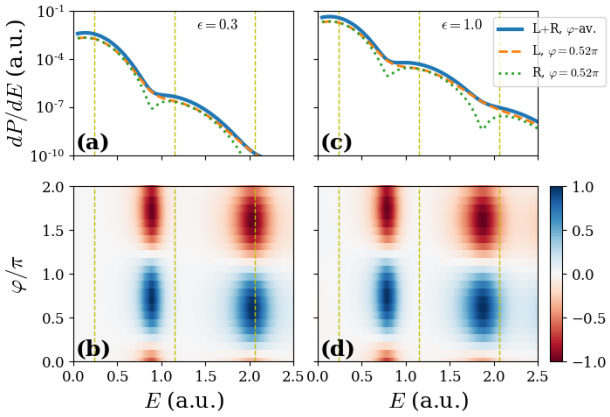

Figure 1: (a),(c) Direction-resolved PES at φ=0.52π and (b),(d) the asymmetry $A(\epsilon,\varphi;E)$ at (a),(b) $\epsilon = 0.3$ and (c),(d) 1.0.

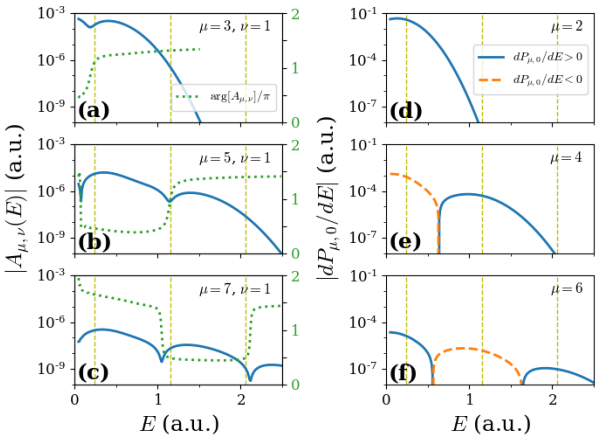

Figure 2: Number-of-photons pathway decomposition of left-right difference of PES (a)–(c) and CEP-averaged PES (d)–(f).

Future plans

We are still exploring the full interpretative power of this representation. We will thus apply it to a broader range of examples and look further and the meaning of the decompositions. One feature of the decomposition is that it can, in principle, be applied to experimentally measured observables to extract the components even for complex targets.

2. Using the photon-phase representation to extract the CEP from experiment

Recent Progress

Probably the most successful scheme for experimentally extracting the shot-by-shot CEP utilizes the left-right spatial asymmetry from Eq. (6) of the photoelectron spectrum following ionization of a xenon atom by a linearly polarized pulse. This asymmetry is then integrated over two separate energy ranges ΔE_i to give two asymmetries A_i, a parametric amplitude plot (PAP) is then made from these A_i (see Fig. 3), and the CEP is extracted using techniques based on empirical observations [4]

Utilizing only the one-dimensional φ decomposition from Eq. (3) above, however, we can write an exact, *ab initio* expression for $A_i(E)$. Explicitly, the full three-dimensional photoelectron distribution is

$$\frac{\partial^2 P}{\partial E \partial \theta_k} = \sum \mathcal{A}^*_{n'J'}(E)\mathcal{A}_{nJ}(E) \times Y_{J'0}(\theta_k)Y_{J0}(\theta_k)e^{i(n-n')\varphi}. \quad (7)$$

From this expression, $dP_{L,R}/dE$ can be obtained by integration over appropriate angles in each hemisphere. Note that Eq. (7) explicitly separates the CEP, angle, and energy dependence, and it puts all of the details of the system — xenon in this case — in the amplitudes

$$\mathcal{A}_{nJ}(E) = \sqrt{2\pi}(-i)^J e^{i\delta_J}\langle EJ|F_{nJ}(t_f)\rangle \quad (8)$$

where $F_{nJ}(t_f)$ is the radial wave function at the final time. Combining everything, we have an exact expression for the PAP in terms of the amplitudes $\mathcal{A}_{nJ}(E)$.

For low intensities, where the CEP-dependence of the asymmetries is dominated by the interference of pathways differing by a single photon, $\Delta n{=}n{-}n'{=}1$ in Eq. (7), our resultant expression reproduces the experimental observation that the asymmetry is sinusoidal in the CEP, resulting generally in an elliptical PAP. In this limit, we have produced an exact formula for CEP extraction.

At higher intensities, our theory shows that higher-order contributions — *i.e.* $\Delta n{\geq}3$, leading to higher frequency terms in Eq. (7) — will drive the PAP from an ellipse towards the "phase potato" shape often seen in experiment. In this more complicated regime, we have suggested an algorithm for extraction of the CEP that can potentially

provide improvements over current experimental techniques.

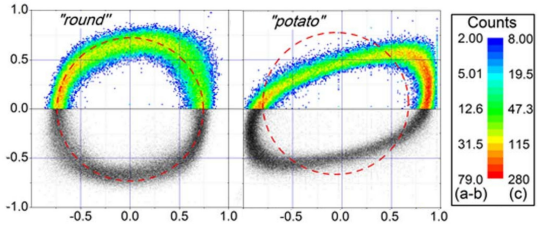

Figure 3: Experimental PAPs adapted from Ref. [5].

Future Plans

This effort was one of our first to use our parametric formalism to extract information from experiment. We are working on the next step to find methods to extract the photon-pathway amplitudes $\mathcal{A}_{nJ}$ from an experimental spectrum. The ability to find these amplitudes would provide greater insight into which physical processes contribute to each feature in an experimental spectrum, even for complex systems. This knowledge could, in turn, provide valuable information about how to tailor a pulse to enhance or remove specific features.

References

[1] V. Roudnev and B. D. Esry, Phys. Rev. Lett. **99**, 220406 (2007).

[2] J. J. Hua and B. D. Esry, J. Phys. B **42**, 085601 (2009).

[3] E. Cormier and P. Lambropoulos, Eur. Phys. J. D **2**, 15 (1998).

[4] T. Wittmann, B. Horvath, W. Helml, M. G. Schatzel, X. Gu, A. L. Cavalieri, G. G. Paulus, and R. Kienberger, Nature Physics **5**, 357 (2009).

[5] A. M. Sayler, T. Rathje, W. Müller, K. Rühle, R. Kienberger, and G. G. Paulus, Opt. Lett. **36**, 1 (2011).

Peer-Reviewed Publications Resulting from this Project (2018–2020)

[P4] "Native frames: disentangling sequential from concerted three-body fragmentation," J. Rajput, T. Severt, B. Berry, B. Jochim, P. Feizollah, B. Kaderiya, M. Zohrabi, U. Ablikim, F. Ziaee, Kanaka Raju P., D. Rolles, A. Rudenko, K. D. Carnes, B. D. Esry, and I. Ben-Itzhak, Phys. Rev. Lett. **120**, 103001 (2018).

[P3] "Nonunique and nonuniform mapping in few-body Coulomb-explosion imaging," A. M. Sayler, E. Eckner, J. McKenna, B. D. Esry, K. D. Carnes, I. Ben-Itzhak, and G. G. Paulus, Phys. Rev. A **97**, 033412 (2018).

[P2] "An optimized absorbing potential for ultrafast, strong-eld problems," Y. Yu and B. D. Esry, J. Phys. B **51**, 095601 (2018).

[P1] "Bond rearrangement during Coulomb explosion of water molecules," M. Leonard, A. M. Sayler, K. D. Carnes, E. M. Kaufman, E. Wells, R. Cabrera-Trujillo, B. D. Esry, and I. Ben-Itzhak, Phys. Rev. A **99**, 012704 (2019).

Controlling rotations of asymmetric top molecules: methods and applications

Vinod Kumarappan
James R. Macdonald Laboratory, Department of Physics
Kansas State University, Manhattan, KS 66506
vinod@phys.ksu.edu

Program Scope

The goal of this program is to improve molecular alignment methods, especially for asymmetric top molecules, and then use well-aligned molecules for further experiments in ultrafast molecular physics. We use multi-pulse sequences for 1D alignment and orientation, and for 3D alignment of molecules. Our main focus now is to further develop our method for extracting orientation-resolved information from rotational wavepacket dynamics, particularly for asymmetric top molecules. We are particularly interested in applying this method to obtain molecular frame photo-ion and photoelectron angular distributions, and to extract the complex dipole responsible for high-harmonic generation.

Recent Progress

In the past several years we have focused on using the time evolution of the molecular axis distributions in board rotational wavepackets to extract angle-dependent information. Our primary method is to fit time-dependent signals in pump-probe experiments to molecular axis distribution moments calculated using TDSE simulation of the rotational wavepacket. The fit parameters then provide us with angular information. We have applied this method, which we call Orientation Resolution using Rotational Coherence Spectroscopy (ORRCS) to high harmonic generation and strong field ionization and fragmentation of several molecules. During this year we have focused on studying the role of spin in the ionization and fragmentation of triplet oxygen and on analyzing ion and electron momentum distributions using ORRCS. The ion momentum analysis allowed us to quantify the breakdown of the axial recoil approximation in the fragmentation of CO_2 [2], and we were able to extract photoelectron momentum distributions as a function of the lab-frame alignment angle of N_2, CO_2 and C_2H_4.

Strong-field ionization and fragmentation of triplet oxygen:

Oxygen is a well-know example of a molecule with a triplet ground state where Hund's case (b) applies. Nuclear rotational angular momentum is coupled to the electronic spin angular momentum and each rotational energy level is split into a spin triplet. Although both rotational and Raman spectroscopy of these states is well studied and understood, no signatures of this structure has been measured in non-resonant alignment experiments to the best of our knowledge. Consequently, the role of spin in the strong-field ionization of oxygen hasn't been studied either, although several experiments have investigated the angle dependent SFI of oxygen.

The most important reason for this situation is that spin-rotation coupling is only important for small values ($\lesssim 7$) of the total angular momentum quantum number J and therefore a cold molecular beam must be used. But angle-dependent SFI rates of oxygen agree with predictions from MO-ADK and there has been little follow-up since the first measurements. During the last year we have used an Evan-Lavie value to produce oxygen at a few K to study the role of spin-rotation

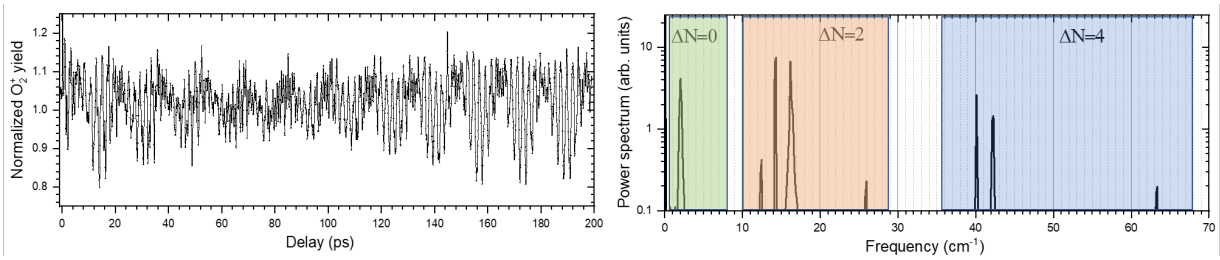

Figure 1: Left: Delay-dependent O_2^+ ionization yield. The alignment pulse was 210 fs, 6 TW/cm^2, and the ionization pulse was 40 fs, 40 TW/cm^2. Right: Fourier spectrum of the ionization yield. The $\Delta N = 2$ lines correspond to transitions from the $N = 0$ triplet states, and a single line from $N = 3$ state. The $\Delta N = 0$ and 4 lines can arise from multiple pathways that are not resolved in this scan.

coupling in SFI. We measure the delay-dependent yield of O_2^+ in pump-probe experiment, where the pump non-resonantly aligns the molecules and the probe singly ionizes them. Since the rotational motion is coupled to the spin of the lone-pair electrons, alignment also excites spin dynamics in the molecules, and we find that the yield is sensitive to this coupled spin-rotation dynamics.

The immediate consequence of reducing the rotational temperature of the molecules to few K is that the alignment dynamics is no longer periodic since the energies of the states in the wavepacket are not commensurate. An example is shown in Fig. 1, where the non-periodicity of single-ionization yield is apparent. The Fourier transform of this signal shows not only purely rotational coherences ($\Delta N = 2$ and $\Delta J = 2$, where N and J are nuclear and total angular momentum, respectively), but also mixed spin-rotation ($\Delta N = 2$ and $\Delta J = 0, 1$) as well as pure spin coherences ($\Delta N = 0$, at ~ 2 cm^{-1}). The observed $\Delta N = 2$ lines match very well with the known Raman spectrum of the molecule and the $\Delta N = 4$ are likely to contain several unresolved combinations of two Raman transitions. Note that the presence of these lines in the FFT spectrum shows not only that the pump pulse excites these coherences, but also that SFI is sensitive to them. The pure spin coherence is interesting from this perspective. It is possible that this coherence is not truly a spin effect at all — the small-J states are only approximately Hund's case (b) (the approximation becomes better with increasing values of J) and the true eigenstates involved are mixtures of spin and rotation.

In order to better understand the role of spin-rotation dynamics in SFI of oxygen, we solve the TDSE using an effective Hamiltonian. Since the rotational and Raman spectroscopy of oxygen is well studied, spin-spin and spin-rotation coupling parameters are known. By calculating the time-dependent expectation values of $P_L(\cos\theta)$ for the molecular axis distribution and constructing the expected delay dependence of the ionization based on the the angle dependence of SFI measured with high-temperature samples (where spin doesn't matter), we will test how much of the delay-dependence can be understood in terms of the angle-dependence of the ionization rate.

Photoelectron angular distributions from few-photon ionization

In this project, we align molecules using a non-resonant pump pulse at 790 nm, ionize them with 261 nm (third harmonic) pulse, and then measure the photoelectron angular distributions (PADs) as a function of pump-probe delay. Our goal is to extract photoelectron angular distribution as a function of the angle between the molecular axis and the laser polarization from these delay dependent measurements in which pump and probe are polarized in the same directions. In order to extract this angle dependence of the PADs, we first decompose the measured lab-frame momentum distribution in a Gaussian radial basis and Legendre polynomial angular basis, and fit the delay dependence of the fit coefficients to the delay-dependent expectation values of molecular axis

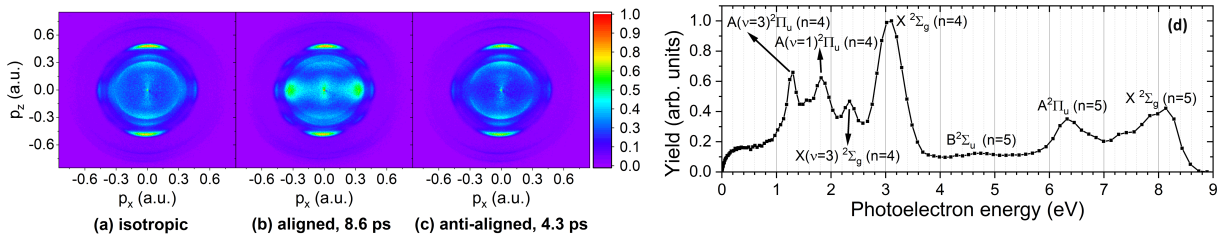

Figure 2: (a)–(b) Photoelectron momentum spectra of nitrogen ionized by 261 nm pulses measured with a VMI spectrometer. The pump pulse was blocked for (a). Delay-integrated photoelectron energy spectrum. n is the number of photons.

distributions moments. These moments are calculated using a rigid-rotor TDSE code. We applied this procedure recently to ion momentum distributions in the strong-field fragmentation of CO_2, where we were able to quantify the break down of axial recoil.

An example of the results of the analysis for electrons in shown in Fig. 3. After Abel inversion (using pBasex) of the photoelectron spectrum measured with a VMI spectrometer, four-photon ionization to the $X^2\Sigma_g$ ground state of the cation is selected from the energy spectrum. The momentum distribution is for this channel is decomposed into Legendre a polynomial basis by the pBasex algorithm; panel (a) shows the ORRCS fit to the delay dependence of these coefficients. From the fit coefficients we can extract the angle-dependence of the ionization rate (shown in panel (b)) and a differential photoionization cross section (DCS) — it is differential in the polar molecular alignment angle θ relative to the laser polarization and the polar angle of the electron momentum θ_k, but the azimuthal angles are averaged over due to the axial symmetry of the experiment. This differential cross section is shown in panel (c). Finally, panels (d) and (e) show a comparison between the extracted DCS and measured data at the peaks of alignment and antialignment, where molecules have a narrow distribution around $\theta = 0°$ and $90°$, respectively. Note that our analysis retrieves the DCS at all angles θ.

Similar analysis has been completed for the other channels labeled in Fig. 2, and for ionization of CO_2 and C_2H_4. A manuscript describing the analysis method and results is in the final stages of preparation.

Future plans

JRML has recently received funding for two new lasers — a 15 W, 3 kHz Ti:Sapphire system (funded by this program) that is scheduled to arrive before this PI meeting and a high-power, high-repetition-rate system (funded by an NSF MRI grant lead by Artem Rudenko) with an anticipated installation date late in 2021. In preparation for the latter, we are planning to build a continuous jet source. In order to reach a few K rotational temperature, we will use a cryogenic He jet and entrain a molecular sample introduced early in the supersonic expansion stage. When combined with a COLTRIMS setup, this source will enable us to combine strong molecular alignment with coincidence momentum measurements to make high resolution molecular frame measurements. The development of an HHG-based source for single-photon ionization of molecules was paused by lab shutdown in the spring. The apparatus is now being constructed and we expect to commission it in the next couple of months. We plan to extract alignment-dependent photoelectron angular distributions for linear and asymmetric top molecules using this setup. With Bret Esry's help, we have made progress in speeding up our asymmetric-top TDSE code and will continue to implement further improvements.

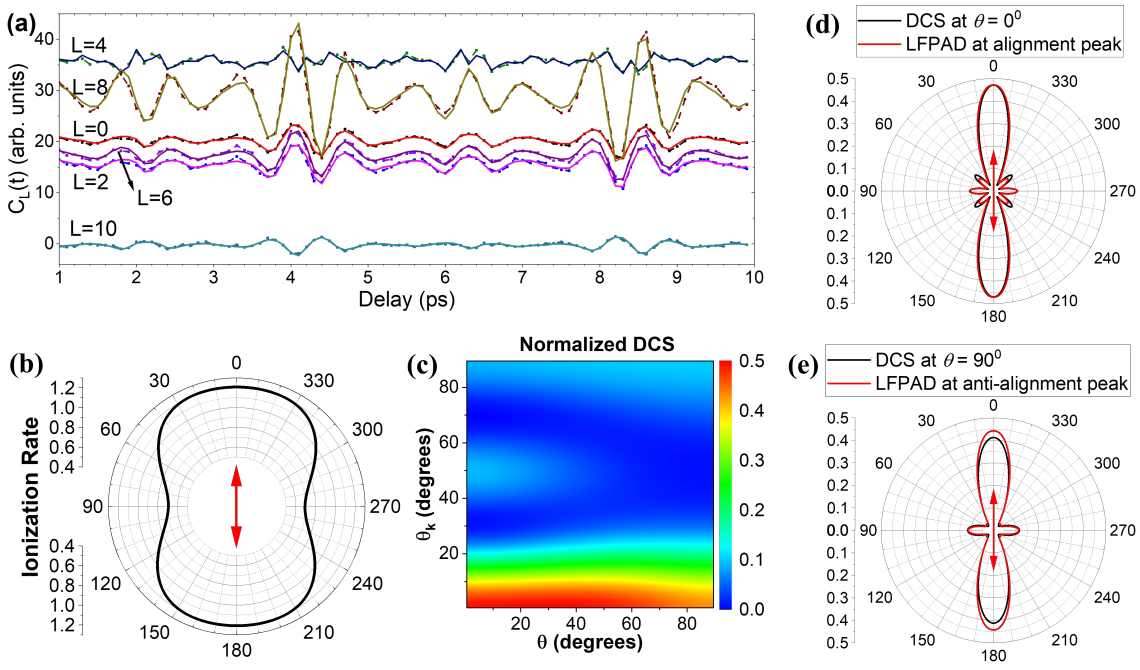

Figure 3: (a) Legendre decomposition of the angular distribution of electron from four-photon ionization of nitrogen to the $X^2\Sigma_g$ ground state of the cation as a function of pump-probe delay. Solid lines are fits. (b) Angle dependence of the ionization rate retrieved from the fit to the $L = 0$ coefficient. (c) Differential cross section as a function of molecular alignment angle θ and electron momentum direction θ_k in the laboratory frame. (d) and (e) Comparison of the extracted differential cross section with data at alignment and anti-alignment peaks, where the molecular axis distribution is tightly confined near $\theta = 0°$ and $\theta = 90°$, respectively. The laser probe laser polarization is vertical both cases.

Peer-Reviewed Publications Resulting from this Project (2018-2020):

[1] Iwamoto, Naoki and Schwartz, Charles J. and Jochim, Bethany and Raju P., Kanaka and Feizollah, Peyman and Napierala, J. L. and Severt, T. and Tegegn, S. N. and Solomon, A. and Zhao, S. and Lam, Huynh and Wangjam, Tomthin Nganba and Kumarappan, V. and Carnes, K. D. and Ben-Itzhak, I. and Wells, E., "Strong-field control of H_3^+ production from methanol dications: Selecting between local and extended formation mechanisms ", J. Chem. Phys. **152**, 054302 (2020).

[2] Huynh Lam, Suresh Yarlagadda, Anbu Venkatachalam, Tomthin Nganba Wangjam, Rajesh K. Kushawaha, Chuan Cheng, Peter Svihra, Andrei Nomerotski, Thomas Weinacht, Daniel Rolles and Vinod Kumarappan, "Angle-dependent strong-field ionization and fragmentation of carbon dioxide measured using rotational wave-packets", Phys. Rev. A (accepted).

Strong field rescattering physics and attosecond physics

C. D. Lin
J. R. Macdonald Laboratory, Kansas State University
Manhattan, KS 66506
e-mail: cdlin@phys.ksu.edu

Program Scope:

We investigated the interaction of ultrafast intense lasers and attosecond pulses with atoms and molecules. Our major efforts are to identify experiments and theoretical retrieval methods where structure information of the molecules or attosecond pules can be accurately obtained. In this report we emphasize: (a) methods to extract bond lengths from laser-induced electron spectra; (b) methods to retrieve amplitude and phase of single molecule harmonics; and (3) retrieval of attosecond pulses from angle-integrated electron spectra and retrieval of single shots from LCLS light sources. Theoretical methods that support JRML experiments are also addressed.

1. Retrieval of molecular structure from Laser induced electron diffraction experiments

Recent progress

Since our pioneering article [R1] in 2010 establishing the theoretical foundation of laser-induced electron diffraction (LIED), two groups, one at Ohio State University, and another at ICFO in Barcelona, have been the main drivers of such experiments. The progress has been slow because LIED requires mid-infrared (MIR) lasers. With such lasers more available recently, more laboratories have now devoted to LIED experiments.

So far retrieval of molecular bond lengths from the LIED experiments have been carried out by extracting the electron scattering differential cross section (DCS) in the laser frame from the angular distribution of photoelectrons in the laboratory frame. The momenta in the two frames are related by the vector potential of the laser at the time of rescattering. To extract the DCS from the momentum spectra in the laboratory frame is laborious, in particular, since LIED signals are weak. In spite of such difficulties, LIED experiments on a few small molecules have been carried out and many interesting results have been reported, including evidences of change of molecular bond lengths as the laser wavelength is varied.

As the LIED is being pushed to more complex molecules and toward dynamic systems where the molecules are first excited by another laser to create vibrational wave packets, a more efficient retrieval method is required. In the last year, we have been working on toward such a robust method. Using the raw photoelectron spectra measured from OSU and ICFO, we have been investigating how to best retrieve the molecular bond lengths from the laboratory photoelectron angular distributions directly. Since structure retrieval is an "art", and the independent atom model (IAM) is valid only in a limited region of the electron momentum, criteria for extracting smoothed experimental data for retrieval have to be established.

For small molecules, we have re-analyzed the earlier data for N_2, O_2, CO_2 and H_2O, including some unpublished data using different wavelengths. Consistent results with prior reported bond lengths have been obtained. A full report on this new method is under preparation. A small portion of the application of this method to OCS experiment has been submitted for publication and is under review.

Future plans

With Cosmin Blaga joining the J. R. MacDonald Laboratory (JRML) recently, LIED will be an essential part of the JRML program. Collaboration with the ICFO group will continue. They have experimental data that have not been analyzed yet. At this time, our intention is to first reanalyze the C_{60} data reported in [R2]. It is understood that additional experiment on this system is being planned. Clearly, as the complexity is increased, a possible proof-of-principle experiment is to study isomers where diffraction is expected to be different. Since isomers of $C_2H_2Cl_2$ have been used in high-order harmonic generation, it may serve as a possible target for LIED.

The holy grail of ultrafast dynamic imaging of molecules of course is to monitor the change of atomic configurations in time. Tremendous technical challenges remain, but an exploration of the feasibility from the theoretical simulations appears to be timely in the coming years. To this end, we will learn how to simulate nuclear vibrational wave packets for molecules which will allow us to generate theoretical diffraction images. Analysis of such theoretical data may guide future planning of such experiments.

2. Retrieval of amplitude and phase of single molecule harmonics from HHG spectra generated from aligned linear molecules

Recent progress

High-order harmonic signals generated in molecules are the consequence of coherent superposition of complex laser-induced transition dipoles $d(\theta, \omega)$ with each fixed-in-space molecule; here θ is the angle of the molecular axis with respect to the laser polarization axis and ω is the harmonic energy. In rotational coherent spectroscopy, the fixed-in-space $d(\theta, \omega)$ in the molecular frame can be extracted by measuring harmonics generated by a probing laser from the rotational molecular wave packet that has been prepared by a prior pump laser. By varying the time delay between the two lasers, methods have been utilized to extract the θ dependence of both the amplitude and phase of each individual harmonic, but it is an outstanding problem that the relative phase between harmonics cannot be retrieved. In a recent paper [**Pub_A1**], we reported that this limitation has been removed. We showed that with the additional measurement of harmonic spectra versus pump-probe angles at one fixed time delay, the resulting two two-dimensional input harmonic spectra (time-delay and pump-probe angle) would enable the full retrieval of the complex transition dipole $d(\theta, \omega)$, using a retrieval method based on machine learning algorithms. We demonstrated this method on N_2 and CO_2. This method would bypass the need of using RABITT that requires an additional IR pulse in order to extract the phase of harmonics. Furthermore, the phase retrieved using our method can be directly related to the full energy and angular dependent transition dipole which is the most basic and complete elementary parameters that describe the interaction of light and molecules. Such complete information cannot be obtained in standard photoionization experiments.

Future plans

The results reported in [Pub_A1] has been demonstrated with theoretical data. It has been tested with experimental data initially but it was decided that there is too much information in the paper. It was recommended by the referee that a full description of the experiment and presentation of the data are needed. We are currently preparing the retrieval using experimental data for N_2 and CO_2. Further studies for these two molecules with different wavelengths of the probe laser or with different pump (aligning) laser would also be of great interest in order to demonstrate the power of the present retrieval method. Further application of this technique to other linear molecules would be of great interest. Extension of the method to nonlinear molecules has not yet been explored.

3. Retrieval of attosecond pulses using full angular streaking spectra and for single-shot angular streaking spectra from LCLS

Recent progress

Characterization of attosecond pulses generated either by harmonic generation or at any free-electron laser facilities like LCLS is important in attosecond science but have been grossly neglected.

For isolated single attosecond pulses, the standard FROG-CRAB method is not applicable to attosecond pulses less than about 100 as since the method is limited to small bandwidth. We have developed a PROBP (**P**hase **R**etrieval **o**f **B**roadband **P**ulse) [R3] method which can be applied to broadband pulses. In 2019 we have developed the so-called PROBP-AC method which can be applied to attosecond pulses down to about a few tens attoseconds. This work was published in [Pub_A5] this year.

To determine the spectral phase of an attosecond pulse, the so-called streaking spectra are obtained by measuring photoelectron spectra generated by the attosecond pulse in the presence of a time-delayed IR pulse. Both pulses are co-linearly polarized in the same direction, and only photoelectrons emitted along the same direction are used for the spectral phase characterization. This widely used method is not favorable from the experimental viewpoint since the collected signal is weighted by a volume element sin θ in the polarization direction. It has been suggested that one way to increase the signal is to collect all the electrons up to about 90^0. However, photoelectrons away from $\theta=0^0$ are also generated by $m \neq 0$ magnetic sub-states of the target, and the standard strong field approximation also needed to be modified. In [Pub_A3], we extend the PROBP method for retrieving attosecond pulses using photoelectrons that have been collected over a large angular range, thus providing a more accurate tools for retrieving the spectral phase of attosecond pulses down 50 as.

I reported our attosecond pulses retrieval method at the 2019 DOE contractors' meeting. After the meeting I was approached by colleagues from LCLS and was made aware of characterization of attoseconds generated at LCLS beamlines. After reaching James Cryan and educated by what issues they have, we decided to take a look at the problem.

We have constructed the algorithm needed to retrieve the single attosecond pulses, reported in their 2020 paper in [R4]. We have retrieved 188 shots in a few days which is faster than the method reported in [R4]. It is hoped that our new approach will be used to analyze the single shot data from these light sources. The work described for the LCLS data has been completed. It is in the process of drafting a report for publication.

Future plans

It is not yet clear how we will proceed from here after this project is completed. Another run at LCLS is scheduled where the spectral bandwidth will be measured. If such information is available, the number of parameters to be retrieved will be reduced. It would then decrease the time to achieve convergence and to increase the accuracy.

References

R1. Junliang Xu, Zhangjin Chen, A. T. Le and C. D. Lin, Phys. Rev. A.82, 033403 (2010)

R2. H. Fuest et al., Phys. Rev. Lett. 122, 053002 (2019).

R3. Xi Zhao et al., Phys. Rev. A95, 033418 (2017).

R4. J. Duris et al., Nat. Photonics 14, 30 (2020).

Eleven Most Recent Publications (out of 22 articles from 2018-2020)

A1. "Retrieval of full angular and energy dependent complex transition dipoles in molecular frame from laser-induced high-order harmonic signals with aligned molecules", Bincheng Wang, Yanqing He, Xi Zhao, Lixin He, Pengfei Lan, Peixiang Lu, and C. D. Lin, **Phys. Rev. A101**, 063417 (2020).

A2. "Optimally spatial separation of high-order harmonics from infrared driving laser with an annular beam in the overdriven regime", Cheng Jin, Xiangyu Tang, Baochang Li, Kan Wang, and C. D. Lin, **Phys. Rev. Applied**, 14, 014057 (2020).

A3. "Investigation of isolated attosecond pulse reconstruction from angular integrated photoelectron streaking spectra", Xi Zhao, Changli Wei, Su-Ju Wang, Bincheng Wang, and C. D. Lin, **J. Phys. B53**, 154002 (2020).

A4. "Analysis of THz generation by multi-color laser pulses with various frequency ratios", Zhaoyan Zhou, Zhihui Iv, Dongwen Zhang, Zengxiu, and C. D. Lin, **Phys. Rev. A101**,043422 (2020).

A5. "Metrology of time-domain soft X-ray attosecond pulses and re-evaluation of pulse durations of three recent experiments", Xi Zhao, Su-Ju Wang, Wei-Wei Yu, Hui Wei, Changli Wei, Bincheng Wang, Jigen Chen, and C. D. Lin, **Phys. Rev. Applied**, 13, 034043 (2020).

A6. "Shaping attosecond pulses by controlling the minima in high-order harmonic generation through alignment of CO_2 molecules", Cheng Jin, Su-Ju Wang, Xi Zhao, S-F Zhao and C. D. Lin, **Phys. Rev. A101**, 013429 (2020).

A7. Robust control of the minima of high-order harmonics by fine-tuning the alignment of CO_2 molecules for shaping attosecond pulses and probing molecular alignment", Cheng Jin, Su-Ju Wang, Song-Feng Zhao, Anh-Thu Le, and C. D. Lin, Phys. Rev. A102, 013108 (2020).

A8. "Imaging an isolated water molecule using a single electron wave packet", Xinyao Liu, Kasra Amini, Tobias Steinle, A. Sanchez, M. Shaikh, B. Belsa, J. Steinmetzer, Anh-Thu Le, R. Moshammer, T. Pfeifer, J. Ullrich, R. Moszynski, C.D. Lin, S. Gräfe, Jens Biegert, **J. Chem. Phys**. **151**, 024306 (2019).

A9. "Imaging the Renner–Teller effect using laser-induced electron diffraction", K. Amini, M Sclafani, T. Steinle, Anh-Thu Le, A. Sanchez, C. Müller, J. Steinmetzer, Lun Yue, J Ramón M. Saavedra, M. Hemmer, M. Lewenstein, R. Moshammer, T. Pfeifer, M. G Pullen, J. Ullrich, B. Wolter, R. Moszynski, F J García de Abajo, CD Lin, S. Gräfe, Jens Biegert, **PNAS, 116**, 8173 (2019).

A10. "Method for spectral phase retrieval of single attosecond pulses utilizing the autocorrelation of photoelectron streaking spectra, "Wei-Wei Yu, Xi Zhao, Hui Wei, Su-Ju Wang, C. D. Lin", **Phys. Rev. A 99**, 033403 (2019).

A11. "Pulse-duration dependence of the double-to-single ionization ratio of Ne by intense 780-nm and 800-nm laser fields: Comparison of simulations with experiments", Zhangjin Chen, Lina Zhang, Yali Wang, Oleg Zatsarinny, Klaus Bartschat, Toru Morishita, C. D. Lin, **Phys. Rev. A 99**, 043408 (2019).

Imaging Ultrafast Electronic and Nuclear Dynamics in Polyatomic Molecules

Daniel Rolles
J.R. Macdonald Laboratory, Physics Department, Kansas State University,
Manhattan, KS 66506, rolles@phys.ksu.edu

Program Scope: *This program focuses on imaging nuclear and electronic dynamics during photochemical reactions by means of femtosecond pump-probe experiments with laboratory-based laser sources and free-electron lasers, complemented by experiments with 3rd generation synchrotrons. The aim of the experiments is to test the suitability of different wavelengths and techniques for probing molecular dynamics, and to study exemplary ultrafast reactions in gas-phase molecules with the goal of clarifying their reaction mechanisms and pathways.*

Recent Progress: Most of my group's research in the last year combined experiments with our laboratory laser sources at the J.R. Macdonald Lab (JRML) with larger-scale collaborative efforts at the free-electron lasers LCLS, FLASH, FERMI, SACLA, and the European XFEL, and at the ALS synchrotron radiation facility. We applied our expanded range of pump wavelengths from the deep UV to the XUV to initiate nuclear and electronic dynamics in polyatomic molecules and probed these dynamics using electron and ion spectroscopy techniques. Other experiments focused on exploring the link between molecular geometry and the experimentally observed momentum correlations between fragments ions produced by different ionization probes (strong-field, single-photon XUV/X-ray, and multi-photon XUV/X-ray) in order to establish the experimental and conceptual requirements for using Coulomb explosion imaging as a probe of ultrafast nuclear dynamics. Our work resulted in 7 published and accepted papers to date in 2020 (see Refs. 1-7); some examples of more recent and yet unpublished results are presented in the following.

(i) Wavelength-dependent photodissociation dynamics in halomethanes, *F. Ziaee, K. Borne, S. Bhattacharyya, A. Rudenko, D. Rolles, B. Erk[1], F. Allum[2], M. Burt[2], M. Brouard[2], P.H. Bucksbaum[3], R. Forbes[3] et al.; [1]DESY, Hamburg, Germany; [2]Oxford University, UK; [3]PULSE Institute, SLAC, Stanford.*

We have extended our previous studies of the ultrafast photodissociation of halomethanes [15,17,28,29] to deep-UV excitation at 200 nm, conducting closely related experiments both at JRML and at FLASH. In particular, we have focused on the dissociation of CH_3I after B-band photoabsorption (see Fig. 1) and on multiple bond cleavage in CH_2IBr and CH_2ICl. Figure 1 shows a measurement of the predissociation lifetime of the $^3E_1/^3E_2$ Rydberg states in CH_3I [5]. In an experiment at SACLA in Feb 2020, we have also revisited the charge transfer dynamics in inner-shell ionized CH_3I after dissociative ionization at 800-nm with significantly improved temporal resolution as compared to previous studies [Erk *et al.*, Science **345**, 288-291 (2014)] and are working on a similar experiment using our HHG XUV source at JRML. Furthermore, we have investigated the dissociative ionization and Coulomb explosion of $CHBr_3$ using an 800-nm pump-probe coincidence experiment at JRML.

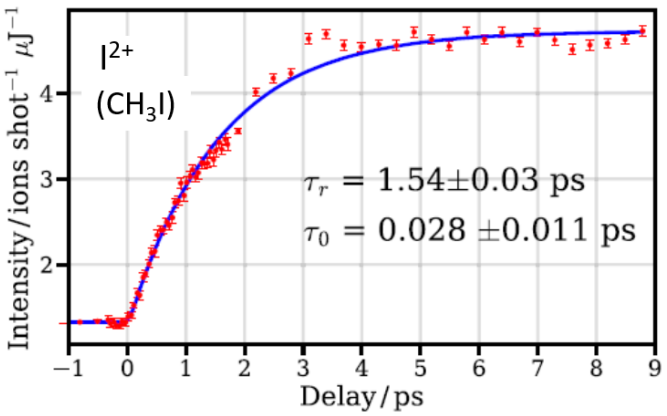

Figure 1: *Time-resolved yield of low-energy I^{2+} ions produced after XUV inner-shell ionization of CH_3I as a function of delay between a 200-nm pump and the 95-eV probe pulse (from Ref. [5]).*

(ii) Momentum-resolved electron-ion coincidence experiments with synchrotron radiation, *S. Pathak, S. Bhattacharyya, K. Borne, X. Li, J. Tross, T. Severt, C. Trallero[1], N. Berrah[1] et al.; [1]University of Connecticut.*

Being able to experimentally distinguish and quantify small and localized geometric changes in gas-phase molecules is a key ingredient for our time-resolved experiments exploring ultrafast chemical dynamics. An important class of such geometry changes is the production and/or interconversion of different conformers, i.e., molecules with the same chemical formula but different geometrical structures caused by rotation around a single bond. In an experiment performed at the Advanced Light Source (ALS), we have shown that the momentum correlation of fragment ions produced after inner-shell photoionization of 1,2-dibromoethane ($C_2H_4Br_2$) can be used to distinguish the geometries of two conformational isomers (see Fig. 2a) and to quantify their relative abundance. The experiment was performed at 140 eV photon energy, resulting predominantly in Br(*3d*) ionization and leading to double and triply charged final states. Using the *native frames* method [25], which we recently developed at JRML, we can disentangle sequential and concerted breakup pathways contributing to the $C_2H_4^+ + Br^+ + Br^+$ triple coincidence channel, and use the momentum correlations in the latter (see Fig. 2b) to identify *anti* and *gauche* conformers and to determine their relative abundance in the molecular beam. The sensitivity of the method to quantify these abundances is then established by measuring the relative abundance change with sample temperature (Fig. 2c), which agrees well with calculations. This level of sensitivity is crucial for many of our ongoing time-resolved experiments at JRML and XFELs and for future studies of the interconversion of conformers, where the quantitative determination of small changes in conformer population is essential.

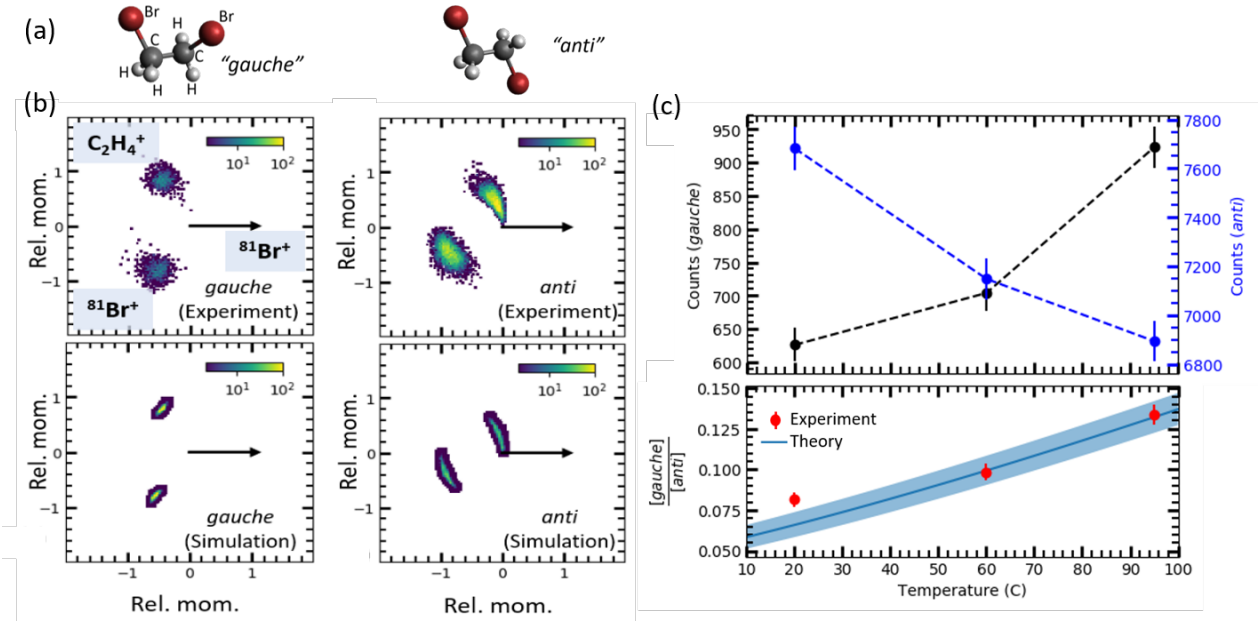

Figure 2: *(a) Gauche* and *anti* conformations of 1,2-dibromoethane ($C_2H_4Br_2$). (b) Experimentally determined and simulated momentum correlation (Newton plots) for *gauche* and *anti* conformers. (c) Experimentally determined abundance of *gauche* (black) and *anti* (blue) conformer (top) and conformer ratio (bottom) as a function of sample temperature compared to theoretical expectations. The blue band represents the uncertainty of the theoretical ratio when assuming an uncertainty of +/- 10˚C in the sample temperature. *(Pathak et al., submitted).*

In addition to the above Coulomb explosion imaging experiments on conformers and other molecular systems of interest with synchrotron radiation, we have performed similar experiments using strong-field ionization at JRML and using X-ray multi-photon ionization at the European XFEL. We have also used the ALS to study interatomic Coulombic decay in endohedral fullerenes in collaboration with the Berrah group [2], and we have continued high-resolution electron spectroscopy studies of CH_3I at SOLEIL in collaboration with the PULSE Institute and several other international collaborators [6,19,20].

Future Plans: In the next months, we will have several experimental campaigns at LCLS, FLASH, FERMI, the SLAC MeV-UED facility, and the European XFEL, most of which had been postponed due to the COVID shutdown and are now all being rescheduled in rapid succession. At LCLS, the main emphasis is on the recommissioning and Early Science experiments with the new TMO end-station and on attosecond experiments performed within the SLAC-led attosecond campaign. Most of the experiments at the other facilities involve using the Coulomb explosion imaging technique and variable pump wavelengths, as described above, to probe nuclear and electronic dynamics in a range of gas-phase molecules. At JRML, my group is in charge of integrating a newly purchased 3-kHz, 5-mJ femtosecond laser system into our lab's multi-user operations. The laser will drive a deep-UV TOPAS and several XUV HHG sources that will allow multi-color pump-probe experiments and electron-ion and ion-ion coincidence detection using our typical coincidence techniques. First experiments with the new laser are planned for this fall.

Peer-Reviewed Publications Resulting from this Project in the Last Three Years (2018-2020):

1. S. Pathak, …, J. Tross, …, D. Rolles, *Tracking the ultraviolet-induced photochemistry of thiophenone during and after ultrafast ring opening*, Nat. Chem. **12**, 795-800 (2020).
2. R. Obaid, …, U. Ablikim, …, D. Rolles, …, N. Berrah, *Interatomic Coulombic decay in endohedral fullerene at the 4d → 4f resonance*, Phys. Rev. Lett. **124**, 113001 (2020).
3. A. Benediktovitchy, …, D. Rolles, …, N. Rohringer, *Amplified spontaneous emission in the extreme ultraviolet by expanding xenon clusters*, Phys. Rev. A **101**, 063412 (2020).
4. H. Lam, …, A. Venkatachalam, …, T. Weinacht, D. Rolles, and V. Kumarappan, *Angle-dependent strong-field ionization and fragmentation of carbon dioxide measured using rotational wave-packets*, Phys. Rev. A, in press (2020).
5. R. Forbes, …, F. Ziaee, D. Rolles, M. Burt, *Time-resolved site-selective imaging of predissociation and charge transfer dynamics: the CH_3I B-band*, J. Phys. B., in press (2020).
6. R. Forbes, A. De Fanis, D. Rolles, ..., D.M.P. Holland, *Photoionization of the I 4d and valence orbitals of methyl iodide*, J. Phys. B **53**, 155101 (2020).
7. T. Kierspel, …, D. Rolles, A. Rudenko, …, J. Küpper, *X-ray diffractive imaging of controlled gas-phase molecules: Toward imaging of dynamics in the molecular frame*, J. Chem. Phys. **152**, 084307 (2020).
8. N. Berrah, …, D. Rolles, …, R. Santra, *Femtosecond-resolved observation of the fragmentation of buckminsterfullerene following X-ray multiphoton ionization*, Nature Physics **15**, 1279–1283 (2019).
9. D. J. Wilson, A. M. Summers, …, D. Rolles, A. Rudenko, C. A. Trallero-Herrero, *An intense, few-cycle source in the long-wave infrared*, Scientific Reports **9**, 6002 (2019).
10. L. Mercadier, …, A. Rudenko, D. Rolles, J. R. Crespo Lopez-Urrutia, and N. Rohringer, *Evidence of Extreme Ultraviolet Superfluorescence in Xenon*, Phys. Rev. Lett. **123**, 023201 (2019).
11. S. Zhao, B. Jochim, P. Feizollah, J. Rajput, F. Ziaee, Kanaka Raju P., B. Kaderiya, K. Borne, Y. Malakar, B. Berry, J. Harrington, D. Rolles, A. Rudenko, K.D. Carnes, E. Wells, I. Ben-Itzhak, and T. Severt, *Strong-field-induced bond rearrangement in triatomic molecules*, Phys. Rev. A **99**, 053412 (2019).
12. K. Toyota, …, N. Berrah, …, D. Rolles, A. Rudenko, R. Santra, *xcalib: a focal spot calibrator for intense X-ray free-electron laser pulses based on the charge state distributions of light atoms*, J. Synch. Rad. **26**, 1017-1030 (2019).

13. A. V. Golovin, …, D. Rolles, *The effect of elliptical polarization in MSXα calculations of the molecular-frame photoelectron angular distributions of CO C(1s) ionization*, Eur. Phys. J. D **73**, 131 (2019).
14. U. Ablikim, …, S. Augustin, S. Pathak, …, N. Berrah, and D. Rolles, *A Coincidence Velocity Map Imaging Spectrometer for Ions and High-Energy Electrons to Study Inner-Shell Photoionization of Gas-Phase Molecules*, Rev. Sci. Instr. **90**, 055103 (2019).
15. Y. Malakar, …, B. Kaderiya, Kanaka Raju P., F. Ziaee, S. Xue, A.T. Le, I. Ben-Itzhak, D. Rolles, and A. Rudenko, *Time-resolved imaging of bound and dissociating nuclear wave packets in strong-field ionized iodomethane*, Phys. Chem. Chem. Phys. **21**, 14090-14102 (2019).
16. N. Ekanayake, M…, T. Severt, P. Feizollah, B. Jochim, B. Kaderiya, Kanaka Raju P., F. Ziaee, K. Borne, K.D. Carnes, D. Rolles, A. Rudenko, I. Ben-Itzhak, B.G. Levine, J.E. Jackson, and M. Dantus, *H_2 roaming chemistry and the formation of H_3^+ from alcohols in strong laser fields*, Nature Communications **9**, 5186 (2018).
17. F. Allum, …, A. Rudenko, …, F. Ziaee, M. Brouard, T. Marchenko, D. Rolles, *Coulomb explosion imaging of CH_3I and CH_2ClI photodissociation dynamics*, J. Chem. Phys. **149**, 204313 (2018).
18. B. Rudek, …, R. Santra, A. Rudenko, S.-K. Son, and D. Rolles, *Relativistic and resonant effects in the ionization of heavy atoms by ultra-intense hard X-rays*, Nature Communications **9**, 4200 (2018).
19. R. Forbes, ..., D. Rolles, ..., J. G. Underwood, D.M.P. Holland, *Photoionization of the iodine 3d, 4s, and 4p orbitals in methyl iodide*, J. Chem. Phys. **149**, 144302 (2018).
20. R. Forbes, ..., D. Rolles, ..., J. G. Underwood, D.M.P. Holland, *Auger electron angular distributions following excitation or ionization of the I 3d level in methyl iodide*, J. Chem. Phys., J. Chem. Phys. **149**, 094304 (2018).
21. M. Sauppe, …, D. Rolles, ..., T. Möller, D. Rupp, *XUV double-pulses with femtosecond to 650 picoseconds separation from a multilayer mirror based split-and-delay unit at FLASH*, J. Synchr. Rad. **25**, 1517-1528 (2018).
22. B. Erk, …, D. Rolles, *CAMP@FLASH - An End-Station for Imaging, Electron- and Ion-Spectroscopy, and Pump-Probe Experiments at the FLASH Free-Electron Laser*, J. Synchr. Rad. **25**, 1529 (2018).
23. D. Rolles, R. Boll, B. Erk, D. Rompotis, B. Manschwetus, *An Experimental Protocol for Femtosecond NIR/UV-XUV Pump-Probe Experiments with Free-Electron Lasers*, Journal of Visualized Experiments **140**, e57055 (2018).
24. T. Kierspel, …, D. Rolles, …, J Küpper, *Photophysics of indole upon x-ray absorption*, Phys. Chem. Chem. Phys. **20**, 20205 – 20216 (2018).
25. J. Rajput, T. Severt, B. Berry, B. Jochim, P. Feizollah, B. Kaderiya, M. Zohrabi, U. Ablikim, F. Ziaee, Kanaka Raju P., D. Rolles, A. Rudenko, K.D. Carnes, B.D. Esry, and I. Ben-Itzhak, *Native frames: Disentangling sequential from concerted three-body fragmentation*, Phys. Rev. Lett. **120**, 103001 (2018).
26. T. Osipov, ..., D. Rolles, A. Rudenko, J. D. Bozek, N Berrah, *The LAMP Instrument at the Linac Coherent Light Source Free-Electron Laser*, Rev. Sci. Instr. **89**, 035112 (2018).
27. L. Young, …, A. Rudenko, D. Rolles, …, *Roadmap of Ultrafast X-ray Atomic and Molecular Physics*, J. Phys. B: At. Mol. Opt. Phys. **51**, 032003 (2018).
28. K. Amini, …, A. Rudenko, … D. Rolles, R. Boll, *Photodissociation of Aligned CH_3I and $C_6H_3F_2I$ Molecules probed with Time-Resolved Coulomb Explosion Imaging by Site-Selective Extreme Ultraviolet Ionization*, Struct. Dyn. **5**, 014301 (2018).
29. F. Brauβe, …, A. Rudenko, …, A. Rouzée, D. Rolles, *Time-resolved inner-shell photoelectron spectroscopy: From a bound molecule to an isolated atom*, Phys. Rev. A **97**, 043429 (2018).
30. M. Fisher-Levine, R. Boll, F. Ziaee, …, A. Nomerotski, D. Rolles, *Time-resolved ion imaging at free-electron lasers using TimepixCam*, J. Synchr. Rad. **25**, 336-345 (2018).

Imaging ultrafast light-induced dynamics with coincident charged-particle momentum spectroscopy

Artem Rudenko
J. R. Macdonald Laboratory, Department of Physics, Kansas State University, Manhattan, KS 66506 rudenko@phys.ksu.edu

Program Scope: The main goals of this research are to understand basic physics of (non-linear) light-matter interactions in a broad span of wavelengths, from terahertz and infrared to XUV and x-ray domains, and to apply the knowledge gained for real-time imaging of ultrafast photo-induced reactions. These goals are being pursued using both, lab-based laser and high-harmonic sources, and external facilities, free-electron lasers (FEL) and synchrotrons. The program aims at studying light-induced phenomena in systems of increasing complexity, from isolated atoms to small and mid-size molecules, and small nanoscale objects. Currently, the main focus is on time-domain studies of ultrafast light-induced electronic and nuclear dynamics in molecules, and on developing new strong-field and X-ray imaging schemes for these studies.

Recent Progress:

1. UV-induced photoprocesses in halomethanes: imaging transient reaction intermediates and three-body dissociation*, B. Kaderiya, F. Ziaee, K. Borne, Y. Malakar, Kanaka Raju P., T. Severt, S. Pathak, S. Bhattacharyya, I. Ben-Itzhak, D. Rolles, A. Rudenko.*

Following our earlier time-resolved experiments on strong-field [P15] and single-photon induced [P4-P6] dynamics in halomethanes, during the last year we focused on utilising three-body Coulomb explosion imaging (CEI) for mapping the reaction pathways triggered by the interaction with UV light. In particular, we have studied photodissociation and molecular halogen elimination from CH_2I_2 and CH_2IBr triggered by 45 fs, 266 nm ultraviolet (UV) pulses and employing multiple ionization by intense 25 fs, 800 nm near-infrared (NIR) pulses as a probe. Fig. 1 displays an exemplary set of CE maps obtained in such experiment on CH_2I_2 (diiodomethane) for the final state with five electrons removed. Here, the measured yield of the I^{++}+I^{++}+ CH_2^+ three-body breakup channel is shown as a function of the measured kinetic energy release (KER) and the angle between the momentum vectors of the two doubly-charged iodine ions for different UV-NIR delays. The distribution at zero delay closely resembles the pattern produce by the NIR pulse alone since the UV pump pulse at the intensities used here does not contribute to multiple ionization. The lower-energy fragments appearing at larger delays reflect different channels of UV-induced dissociation, with the Coulomb repulsion energy decreasing as the molecular bond(s) elongate. However, already at 100 fs delay, an interesting additional feature appears at rather large angles, within the marked region 1. According to our classical CE simulations, this area, which is nearly empty at zero delay, corresponds to the fragmentation of a CH_2I–I isomer of diiodomethane. As illustrated in the inset, the number of events in this area rises within the first 150 fs, then decreases again, becoming rather small at 600 fs and reducing to nearly zero at 10 ps. This behavior most likely reflects the transient formation of the CH_2I–I isomer, which was discussed in [R1] for neutral and in [R2] for cationic states of diiodomethane. With increasing delay,

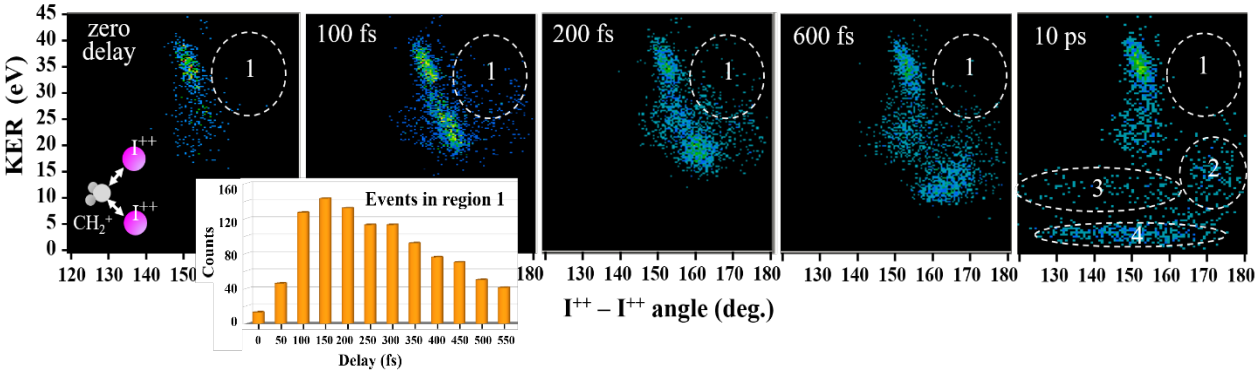

Figure 1: *Three-particle CE maps of UV-induced CH_2I_2 photodynamics at five different delay between 266 nm UV pump (~$1{\cdot}10^{14}$ W/cm^2) and 800 nm NIR probe ($5{\cdot}10^{14}$ W/cm^2) pulses. Different regions marked with numbers in the figure correspond to different fragmentation pathways triggered by the pump pulse (see text). Inset shows the number of events in region 1 in the 50 fs delay windows centered at the indicated delay value.*

the events from region 1 propagate towards lower KERs, asymptotically approaching either region 2, where both iodine ions are essentially emitted back to back (180°), or region 3, which covers a broad range of smaller angles. Based on the delay-dependent sum energies of the two iodine ions, we can assign these two regions to the pathways involving either I_2/I_2^+ elimination (region 2) or $CH_2I + I$ dissociation, either neutral or ionic (region 3). Our analysis suggests that each of these regions contains events resulting from the transient isomer formation and its subsequent decay, besides the dominant contributions from "direct" I_2/I_2^+ or I/I^+ ejection channels.

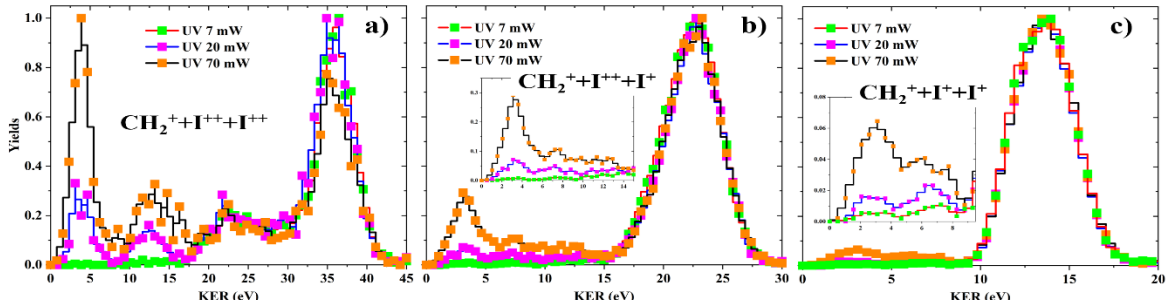

Figure 2: *The KER distributions for three different three-body CE channels of CH_2I_2 measured at 10 ps delay between the UV pump and NIR probe pulses for three different UV powers. The highest UV power (70 mW) corresponds to the intensity of ~$1{\cdot}10^{14}$ W/cm^2 used in Fig. 1. The NIR intensity is kept at $8{\cdot}10^{14}$ W/cm^2 (same as in Fig. 1).* ***a)*** *$CH_2^+ + I^{++} + I^{++}$ channel (same as in Fig. 1);* ***b)*** *$CH_2^+ + I^{++} + I^+$ channel;* ***c)*** *$CH_2^+ + I^+ + I^+$ channel.*

Another interesting feature can be observed at 10 ps delay in region 4, at the KER values below 5 eV. This structure is also clearly visible in Fig. 2a, which shows the 1D KER spectrum for the same $CH_2^+ + I^{++} + I^{++}$ channel at 10 ps delay (same as Fig. 1) for three different UV pump intensities. The only way the three-body CE of CH_2I_2 after removal of five electrons can lead to such low KER is if the three fragments are far away from each other at the time the probe pulse arrives, such that the contribution from Coulomb repulsion becomes small. Therefore, this low-KER feature reflects the three-body dissociation triggered by the pump – the process that is difficult to access by spectroscopic probing techniques. This interpretation is supported by the KER measurements for three-body CE of the quadruply- and triply-charged molecules shown in Fig. 2b and 2c, respectively. While all other KER features shift to significantly lower values for lower charge states, the peak below 5 eV remains at nearly the same position for all three channels.

2. Coulomb explosion imaging of polyatomic molecules at XFELs*, X. Li, R. Boll[1], T. Jahnke[2], D. Rolles, A. Rudenko et al.* *[1] European XFEL, Hamburg; [2] University of Frankfurt.*

In parallel to time-resolved CEI experiments at the JRML, we pursue further developments of this approach at XFEL facilities, where even higher charge states can be created during the ultrashort XFEL pulse duration. During the last year, we have achieved significant progress in this direction at the European XFEL, demonstrating the possibility of full 3D geometry reconstruction for CH_3I [R3] and visualizing the structure of more complex ring molecules containing an iodine marker [R4]. These results, which demonstrate the capability of the CEI approach to capture nuclear geometry, including the positions of hydrogen atoms, paves the way for a number of novel pump-probe experiments on photoinduced molecular dynamics.

3. State-selective analysis of XUV-induced molecular dynamics*, S.J. Robatjazi, S. Pathak, W.L. Pearson, Kanaka Raju P., A. Venkatachalam, D. Rolles, A. Rudenko.*

Ultrashort XUV pulses produced by high-harmonics generation (HHG) can be efficiently used to excite electronic and nuclear wave packets in highly excited or ionic molecular states, and to probe them in the time domain. One of the key challenges here is identifying particular states contributing to the dynamics. We employ coincident photoelectron-photoion imaging with a double-sided VMI spectrometer for state-specific analysis of molecular dynamics triggered by broadband, ~25 fs HHG pulses. Fig. 3 depicts the results of such an experiment on a CO_2 molecule. Here, an XUV pump pulse consisting mainly of the 13th harmonic of 800 nm NIR laser (selected by a combination of Al and Sn filters) ionizes the neutral CO_2 and populates one of the four low-lying cationic states (see Fig. 3a), which is then probed via dissociation by the 25 fs 800 nm pulse at ~$1{\cdot}10^{13}$ W/cm^2. While the upper $C\ ^2\Sigma_g^+$ state is predissociative and can dissociate without the probe pulse, its population upon CO_2 photoionization at ~ 20 eV is less than 3% of the total photoinization yield [R5]. Fig. 2c displays the measured delay-dependent yield of CO^+ ions. Since at our

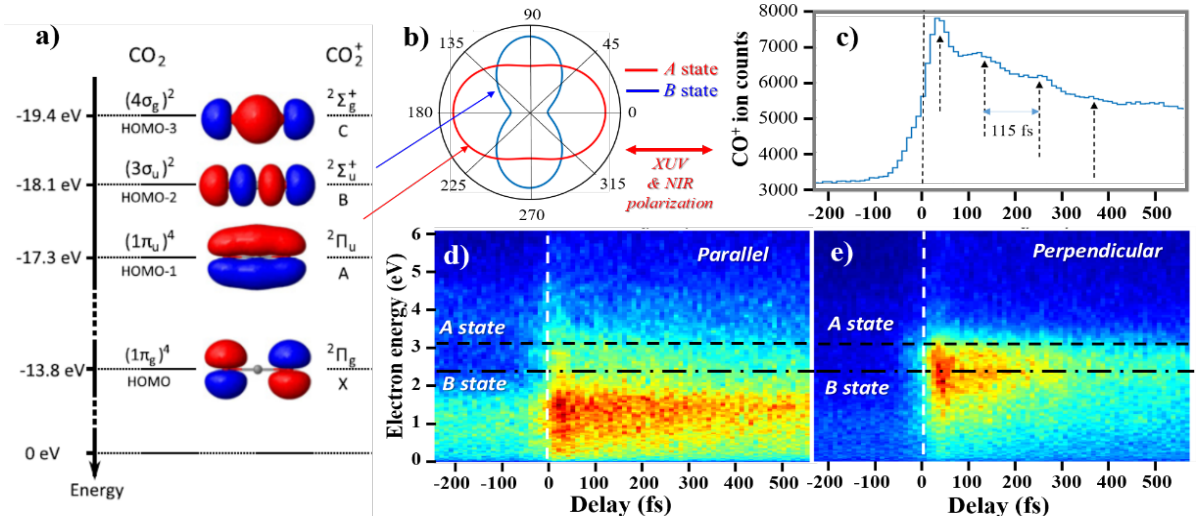

Figure 3: ***a)*** *A diagram of four lowest CO_2^+ electronic states.* ***b)*** *The simulated electron angular distributions for the $A^2\Pi_u$ and $B^2\sum_u^+$ final states at $\hbar\omega \approx 20$ eV (from [R5]).* ***c)*** *Yield of the detected CO^+ ions as a function of the delay between the XUV pump and the NIR probe pulses (both pulses linearly polarized in the horizontal direction).* ***d)*** *Kinetic energy spectrum of the photoelectrons detected on coincidence with CO^+ ions and emitted in the direction parallel (within ±15°) to the XUV and NIR polarization.* ***e)*** *Same as* ***d)*** *but for electron emitted perpendicular to the light polarization. Horizontal lines mark the highest electron energies expected for the ionization to the $A^2\Pi_u$ and $B^2\sum_u^+$ by the central photon energy of the XUV pulse ($\hbar\omega = 20.4$ eV).*

NIR intensity the dissociation from the ground cationic state $X^2\Pi_g$, which requires the absorption of at least 4 NIR photons, is rather unlikely, the CO^+ signal is dominated by the superposition of $A^2\Pi_u$ and $B^2\sum_u^+$ states probed by the NIR pulse. Similar to the results of [R6], the CO^+ yield exhibit sharp rise and then decays, displaying a clear oscillatory structure of ~115 fs periodicity. In [R6] the overall signal decay was explained by the rotational dynamics following alignment-selective initial photoionization to the $B^2\sum_u^+$, whereas the oscillation was seen as a coherent motion of the electronic population between the $B^2\sum_u^+$ and $A^2\Pi_u$,states driven by the vibronic coupling. We take a more detailed look into the formation of this curve by considering the delay-dependent photoelectron spectra measured in coincidence with CO^+ ions in Fig 3d and 3e. Because of different symmetries of *A* and *B* states, the electron emission along the XUV polarization direction is dominated by the former, whereas in the perpendicular direction, the latter is expected to provide a stronger contribution (see Fig. 3b). While the data for perpendicular direction (Fig. 3e) indeed manifest the main contribution at the energies corresponding to the ionization to the lowest vibrational states of $B^2\sum_u^+$, the spectrum for parallel direction (Fig. 3d) is dominated by the low-energy electrons (<2 eV). The most likely reason for this is that the low-lying vibrational states of $A^2\Pi_u$ require at least two NIR photons for dissociation. As a consequence, the position of the dominant photoelectron band in Fig. 3d shifts towards higher vibrational levels (and, thus, lower electron energies), which are accessible by one NIR photon.

Future Plans: We plan to continue research activities in all three areas outlined above. For lab-based CEI experiments, the next step will be to study photoinduced dynamics as a function of the UV pump wavelength. This will be realized exploiting a new TOPAS system delivering tuneable UV light down to 190 nm, which is currently being installed at the JRM. The efforts in the experiments at XFELs will focus on applying the demonstrated CEI machinery to time-resolved experiments. A proposal for applying this technique for imaging strong-field induced vibrational wave packets in iodomethane has been approved for beamtime at the European XFEL in 2020, but due to Covod-19 interruptions is currently planned for February 2021. Finally, time-resolved electron-ion coincidence experiments with JRML HHG sources will focus on bond rearrangement. H_3 formation and hydrogen migration dynamics in alcohol molecules, following our earlier NIR-only measurements [P10].

References

[R1] V. A. Borin et al., *Direct photoisomerization of CH_2I_2 vs. $CHBr_3$ in the gas phase: a joint 50 fs experimental and multireference resonance-theoretical study*, Phys. Chem. Chem. Phys. **18**, 28883 (2016).

[R2] A. Cartoni et al., *VUV Photofragmentation of CH_2I_2: The $[CH_2I{-}I]^{\bullet+}$ Iso-diiodomethane Intermediate in the I-Loss Channel from $[CH_2I_2]^{\bullet+}$*, J. Phys. Chem. A **119**, 3704 (2015).

[R3] X. Li, A. Rudenko, ..., D. Rolles, M. Meyer, T. Jahnke and R. Boll, *Coulomb explosion imaging of small polyatomic molecules with ultrashort x-ray pulses*, in preparation (2020).
[R4] R. Boll, J. Schaefer, …, X. Li, D.Rolles, ..., A.Rudenko, M. Meyer, R. Santra and T. Jahnke, *X-ray induced Coulomb explosion images complex single molecules*, in preparation (2020).
[R5] M. R. F. Siggel et al., *Shape-resonance-enhanced continuum-continuum coupling in photoionization of CO_2*, J. Chem. Phys. **99**, 1556 (1993).
[R6] H. Timmers, Z. Li, N. Shivaram, R. Santra, O. Vendrell, and A. Sandhu, *Coherent Electron Hole Dynamics Near a Conical Intersection* Phys. Rev. Lett. **113**, 113003 (2014).

Peer-Reviewed Publications Resulting from this Project (2018-2020):

[P1] J. Rajput, T. Severt, B. Berry, B. Jochim, P. Feizollah, B. Kaderiya, M. Zohrabi, U. Ablikim, F. Ziaee, Kanaka Raju P., D. Rolles, A. Rudenko, K.D. Carnes, B.D. Esry, and I. Ben-Itzhak, *Native frames: Disentangling sequential from concerted three-body fragmentation*, Phys. Rev. Lett. **120**, 103001 (2018).
[P2] T. Osipov, Ch. Bostedt, …, D. Rolles, A. Rudenko, J. D. Bozek, N Berrah, *The LAMP Instrument at the Linac Coherent Light Source Free-Electron Laser*, Rev. Sci. Intr. **89**, 035112 (2018).
[P3] L. Young, … A. Rudenko, D. Rolles, C. Bostedt, …, S. R. Leone, *Roadmap of Ultrafast X-ray Atomic and Molecular Physics*, J. Phys. B: At. Mol. Opt. Phys. **51**, 032003 (2018).
[P4] K. Amini, …, A. Rudenko, …, D. Rolles, and R. Boll, *Photodissociation of Aligned CH_3I and $C_6H_3F_2I$ Molecules probed with Time-Resolved Coulomb Explosion Imaging by Site-Selective Extreme Ultraviolet Ionization*, Struct. Dyn. **5**, 014301 (2018).
[P5] F. Braußе, …, A. Rudenko, …, D. Rolles,, *Time-resolved inner-shell photoelectron spectroscopy: From a bound molecule to an isolated atom*, Phys. Rev. A **97**, 043429 (2018).
[P6] F. Allum, …, A. Rudenko, …, F. Ziaee, M. Brouard, T. Marchenko, D. Rolles, *Coulomb explosion imaging of CH_3I and CH_2ClI photodissociation dynamics*, J. Chem. Phys. **149**, 204313 (2018).
[P7] Y. Malakar, F. Wilhelm, D. Trabert, Kanaka Raju P., X. Li, W. L. Pearson, W. Cao, B. Kaderiya, I. Ben-Itzhak, and A. Rudenko, *State-selective dissociation dynamics of an oxygen molecular ion studied with single-harmonic pump and infrared-probe pulses*, Rhys. Rev. A **98**, 013418 (2018).
[P8] B. Rudek, …, R. Santra, A. Rudenko, S.-K. Son, and D.Rolles, *Relativistic and resonant effects in the ionization of heavy atoms by ultra-intense hard X-rays*, Nature Comm. **9**, 4200 (2018).
[P9] B. Erk, ..., A. Rudenko, … D. Rolles, *CAMP@FLASH - An End-Station for Imaging, Electron- and Ion-Spectroscopy, and Pump-Probe Experiments at FLASH Free-Electron Laser*, J. Synchr. Rad., **25**, 1529 (2018).
[P10] N. Ekanayake, M. Nairat, N.P. Weingartz, B.M. Farris, T. Severt, P. Feizollah, B. Jochim, B. Kaderiya, Kanaka Raju P., F. Ziaee, K. Borne, K.D. Carnes, D. Rolles, A. Rudenko, I. Ben-Itzhak, B.G. Levine, J.E. Jackson, and M. Dantus, *H_2 roaming chemistry and the formation of H_3^+ from alcohols in strong laser fields*, Nature Communications **9**, 5186 (2018).
[P11] D.J. Wilson, A.M. Summers, S. Zigo, S.-J. Robatjazi, J. Powell, D. Rolles, A. Rudenko, C.A. Trallero-Herrero, *An intense, few-cycle source in the long-wave infrared*, Scientific Reports **9**, 6002 (2019).
[P12] L. Mercadier, …, A. Rudenko, D. Rolles, J.R. Crespo Lopez-Urrutia, and N. Rohringer, *Evidence of Extreme Ultraviolet Superfluorescence in Xenon*, Phys. Rev. Lett. **123**, 023201 (2019).
[P13] S. Zhao, B. Jochim, P. Feizollah, J. Rajput, F. Ziaee, Kanaka Raju P., B. Kaderiya, K. Borne, Y. Malakar, B. Berry, J. Harrington, D. Rolles, A. Rudenko, K.D. Carnes, E. Wells, I. Ben-Itzhak, and T. Severt, *Strong-field-induced bond rearrangement in triatomic molecules*, Phys. Rev. A **99**, 053412 (2019).
[P14] K. Toyota, …, N. Berrah, …, D. Rolles, A. Rudenko, R. Santra, *xcalib: a focal spot calibrator for intense X-ray free-electron lasers based on the charge state distributions of light atoms*, J. Synch. Rad. **26**, 1017 (2019).
[P15] Y. Malakar, W.L. Pearson, M. Zohrabi, B. Kaderiya, Kanaka Raju P., F. Ziaee, S. Xue, A.T. Le, I. Ben-Itzhak, D. Rolles, and A. Rudenko, *Time-resolved imaging of bound and dissociating nuclear wave packets in strong-field ionized iodomethane*, Phys. Chem. Chem. Phys. **21**, 14090-14102 (2019).
[P16] G. Schmid, ..., A. Rudenko, J. Ullrich, Th. Pfeifer, and R. Moshammer, *Terahertz-Field-Induced Time Shifts in Atomic Photoemission*, Phys. Rev. Lett. **122**, 073001 (2019).
[P17] H. Fukuzawa, …, A.Rudenko, C. Miron, H. Kono, and K. Ueda, *Real-time observation of X-ray-induced intramolecular and interatomic electronic decay in CH_2I_2*, Nature Comm. **10**, 2186 (2019).
[P18] J.A. Powell, A.M. Summers, Q. Liu, S.J. Robatjazi, P. Rupp, J. Stierle, C. Trallero-Herrero, M.F. Kling, and A. Rudenko, *Interplay of pulse duration, peak intensity, and particle size in laser-driven electron emission from silica nanospheres*, Optics Express **27**, 27124 (2019).
[P19] T. Kierspel, …, D. Rolles, A. Rudenko, …, J. Küpper, *X-ray diffractive imaging of controlled gas-phase molecules: Toward imaging of dynamics in the molecular frame*, J. Chem. Phys. **152**, 084307 (2020).
[P20] Y.-C. Cheng, …, D. Rolles, A. Rudenko, …, M. Gisselbrecht, *Imaging multiphoton ionization dynamics of CH3I at a high repetition rate XUV Free-Electron Laser* J. Phys. B: At. Mol. Opt. Phys., accepted (2020).

Controlling and imaging the dynamics in small molecules

Uwe Thumm

J.R. Macdonald Laboratory, Kansas State University, Manhattan, KS 66506, thumm@phys.ksu.edu

Project scope: To develop conceptual, analytical, and numerical tools to (i) predict the effects of intense pulses of light in the IR to soft X-ray frequency range on the bound and free electronic and nuclear dynamics in small molecules, (ii) image their laser-controlled nuclear and electronic molecular dynamics, and (iii) extend our investigations on dimers to examine the coupling between nuclear degrees of freedom in trimers.

Recent progress: Molecular ionization in short intense light pulses can excite ro-vibrational nuclear wave packets that propagate coherently in several electronic states of the residual molecular ions. Near the ion's intrinsic (external-field-free) and light-induced avoided crossings the nuclear probability amplitude adiabatically follows or diabatically crosses field-dressed Born-Oppenheimer (BO) potential surfaces (Fig. 1). This excited bound and dissociative nuclear wave-packet motion is being scrutinized in experiments and theoretical modeling at JRML [1,S1,R1-R9]. Following up on our numerical modeling of dissociative ionization (DI) of oxygen [1,R2,R3,R9], nitrogen [R9], carbon-monoxide [R9], and noble-gas [R2,R10] dimers, based on the propagation of nuclear wave packets in one degree of freedom, the internuclear distance R, we extended the scope of our investigations, (i) addressing the coupling between nuclear degrees of freedom and (ii) increasing the number of included BO channels. Addressing open questions [R3-R7] in the interpretation of in-house single pulse [R6,R7] and IR- [R9] or EUV- [R5] pump - IR-probe experiments, we examined the light-induced ro-vibrational nuclear dynamics in O_2^+.

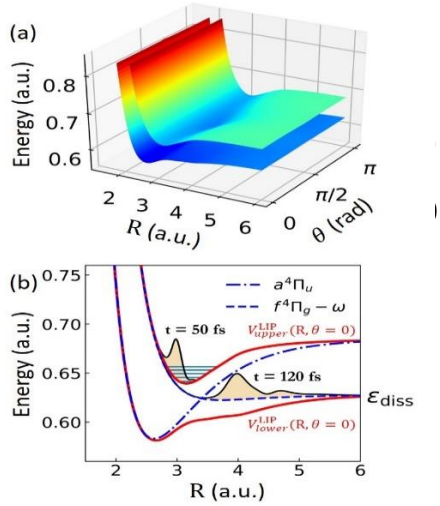

Fig. 1. Light-induced Floquet potentials V_{lower}^{LIP} and V_{upper}^{LIP} for the two-channel model of O_2^+ in an 800 nm cw external field with a peak intensity of 10^{13} W/cm^2.

(a) Field-dressed potential energy surfaces as a function of the internuclear distance R and the molecular alignment angle θ.
(b) Corresponding field-dressed Floquet curves along the laser-polarization direction θ = 0 (solid red) and field-free BO potential energy curves for the $O_2^+(a\ ^4\Pi_u)$ (blue dash-dotted curve) and $O_2^+(f\ ^4\Pi_g)$ state (blue dashed curve). The lowest vibrational levels, v=1-4, in V_{upper}^{LIP} (R, θ = 0) are indicated as turquoise horizonal lines. Snapshots of the nuclear motion are shown as the nuclear probability density in the upper state at the peak of the 40 fs (FWHIM) probe laser pulse (at t = 50 fs after the wave packet was launched) and after the pulse has passed (at t = 120 fs).

1. Molecular bond stabilization in the strong-field dissociation of O_2^+: We assumed rapid ionization of O_2 molecules in the pump pulse launches a ro-vibrational nuclear wave packet ψ(R, θ, t=0) in the $O_2^+(a\ ^4\Pi_u)$ state [1,R3-R5] and examined the rotational and vibrational dynamics of O_2^+ exposed to probe-pulse electric fields E(t) for conditions realized in contemporary pump-probe experiments. We solved the time-dependent Schrödinger equation (TDSE) in BO approximation for an initial distribution of randomly aligned molecular ions in the rotational ground state, based on field-free potential curves and dipole couplings we calculated using the quantum-chemistry code GAMESS [R1]. To reveal rotational excitation effects in O_2^+, we compared results from 2D ro-vibrational (treating the internuclear distance R and molecular orientation angles θ as dynamical variables) with 1D propagation calculations (in R) at fixed θ [1,R11]. In the 1D model we introduce E_{eff} = E(t) cos θ as an effective probe-pulse electric field. We

propagated $\psi(R, \theta, t)$ through a 50 fs delayed IR probe pulse and followed its evolution subject to IR-field-induced dipole couplings between the $a\ ^4\Pi_u$ and dissociative $f\ ^4\Pi_g$ states of O_2^+ [Fig. 1(b)].

For fixed peak intensities, our numerical results show that total, angle-integrated $O_2^+ \rightarrow O(^3P) + O^+(^4S^0)$ dissociation yields do not monotonically increase with increasing infrared-probe pulse duration [1]. We find this pulse-duration-dependent stabilization to be consistent with the transient trapping of nuclear probability density in a light-induced (bond-hardening) potential-energy well and robust against rotational excitation. We analyzed this stabilization effect and underlying bond-hardening mechanism (i) in the time domain, by following the evolution of partial nuclear probability densities associated with the dipole-coupled $O_2^+(a\ ^4\Pi_u)$ and $O_2^+(f\ ^4\Pi_g)$ states, and (ii) in the frequency domain, by examining ro-vibrational quantum-beat spectra for the evolution of the partial nuclear probability densities associated with these states. This analysis reveals the characteristic timescale for bond-hardening in O_2^+ and explains the onset of bond stabilization for sufficiently long pulse durations.

2. Signatures in KER spectra of transient nuclear probability trapping: Following the ro-vibrational dynamics of the initial pump-laser-excited cationic nuclear wave packet, while accounting for the dipole coupling between the $O_2^+(a\ ^4\Pi_u)$ and $O_2^+(f\ ^4\Pi_g)$ electronic states in 800 nm, 40 fs probe-laser pulses with peak intensities of 10^{13} to 10^{14} W/cm^2, we calculated angle-resolved KER spectra. These reveal energy- and angle-dependent fringe structures [S1] that shift downward as the molecular alignment angle θ increases from 0 to $\pi/2$. For the lowest considered peak intensity, 10^{13} W/cm^2, Fig. 2 shows identical O^+ fragment KER spectra resulting from 1D and 2D calculations, indicating that rotational excitations in the probe pulse are irrelevant. The energy spacing between the KER peaks of about 0.1 eV agrees with the vibrational-level spacing in the field-free $O_2^+(a\ ^4\Pi_u)$ state [R1,R4,R6,R9].

The Floquet light-induced potentials (LIP) V_{lower}^{LIP} and V_{upper}^{LIP} in Fig. 1, despite being calculated for continuum-wave (cw) fields $E_{eff}(E_0,\theta) = E_0 \cos\theta$ and fixed alignment angles θ at the peak electric field strength E_0 of the probe pulse, give valuable insights for understanding the dissociation dynamics of O_2^+ in strong *pulsed* probe fields. As a measure for the influence of transient bond-hardening wells on the fragment KER, we take as a guide the few lowest vibrational states in V_{upper}^{LIP} with energies $\{\varepsilon_\upsilon{}^{LIP}(E_0,\theta)\}$ [Fig. 1(b)]. To identify the transient trapping of the O_2^+ nuclear wave packet, we relate the dependence of the O^+ fragment yield on E_0 and θ in our TDSE-calculated KER spectra to the vibrational energies $\{\varepsilon_\upsilon{}^{LIP}(E_0,\theta)\}$ relative to the dissociation limit ε_{diss} for one-photon dissociation into the $O_2^+(f\ ^4\Pi_g)$ channel,

$$\varepsilon_\upsilon{}^{KER}(E_0,\theta) = \varepsilon_\upsilon{}^{LIP}(E_0,\theta) - \varepsilon_{diss}\ . \qquad (1)$$

Within this interpretation, we assume that part of the nuclear wave packet is first promoted into the upper Floquet curve at the peak of the probe-laser pulse and dissociates to emerge after the passage of the probe pulse in the field-free $O_2^+(f\ ^4\Pi_g)$ channel at large R. Since LIPs strongly depend on the pulse intensity and profile, this allows us to identify dynamical effects due to the transient trapping of the nuclear wave packet.

To analyze the *angle dependence of the fringes* in the KER spectra, we compare our TDSE results with the vibrational energies in Eq. (1), indicated as superimposed black dashed curves in Fig. 2(b,c). The θ dependence of the fringes in the TDSE-calculated spectra is qualitatively reproduced by the Floquet prediction. The fringes disappear if the cations are aligned perpendicularly to the probe-laser polarization (at $\theta = \pi/2$), consistent with the vanishing E_{eff} and bond-hardening well. Thus, the angular dependence in E_{eff} translates into a downward shift of the vibrational spectrum in V_{upper}^{LIP}, which follows the energy shifts of the fringes in the KER spectrum. This suggests that the fringe structures contain information about the dissociation dynamics through associated field-dressed potentials.

The angle-dependent shifts in the KER fringes increase for larger probe-pulse peak intensities I_0 and follow, in their overall trend, the Floquet vibrational energies in Eq. (1) [Figs. 2(b,c), 3(a-c)]. This is a manifestation

of transient O_2^+ nuclear-probability-density trapping during dissociation. The difference between the 1D and 2D results increases with I_0 and is most pronounced near $\theta = \pi/2$. This indicates the higher importance of rotational excitations for dissociation near $\pi/2$ and increasing probe-pulse intensity.

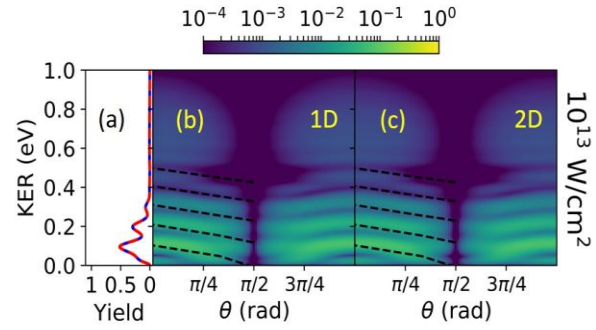

Fig. 2. **(a)** Angle-integrated KER spectra for 40 fs probe pulses with a peak intensity of 10^{13} W/cm^2 without (1D, dashed red curve) and including rotational excitations (2D, solid blue curve). **(b,c)** Corresponding angle-resolved KER spectra from (b) 1D and (c) 2D calculations, normalized to the respective maximal fragment yields in Fig. 3(c). Black dashed lines show the lowest five vibrational levels in the Floquet light-induced bond-hardening well according to Eq. (1).

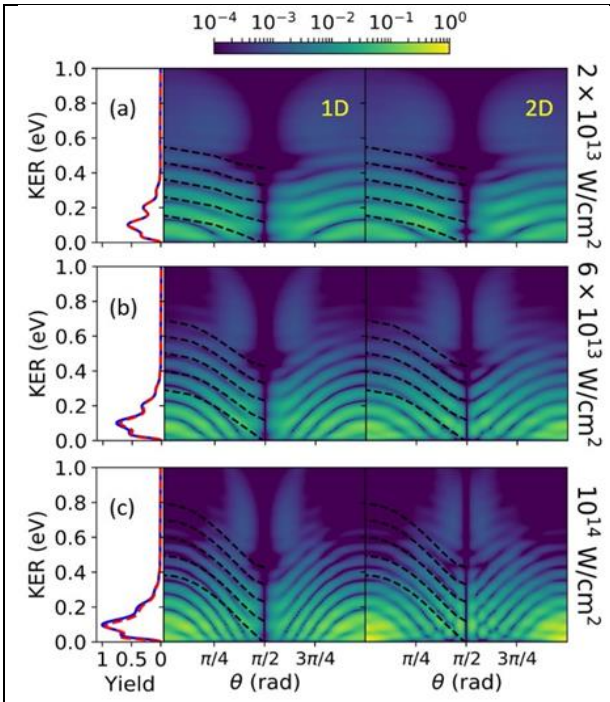

Fig. 3. (a-c) As Fig. 2 for probe-laser-pulse peak intensities of (a) $2x10^{13}$, (b) $6x10^{13}$, and (c) 10^{14} W/cm^2. All spectra are normalized to the respective maximal fragment yields in (c). **(d-f)** Fragment angular distributions P(θ), obtained by integrating the respective yields in (a-c) over KERs between 0.2 and 0.3 eV, for the intensities in (a-c), respectively, and normalized to the maximum in (f). Results from 1D and 2D TDSE calculations are represented as dashed red and solid blue curves, respectively.

3. Imprint of the light-induced conical intersection (LICI) on the nuclear dynamics: Examining the ro-vibrational dynamics of the dissociating O_2^+ cation near the LICI of the LIP surfaces at $\theta = \pi/2$ [Fig. 1(a)], we identified related angle-dependent structures in the KER spectra, suggesting a means for assessing the significance of LICIs in molecular dissociation pathways [S1]. Figures 3(d-f) show normalized fragment angular distributions P(θ) with pronounced modulations, predicted by both, 1D and 2D calculations, that reflect the fringe structures in the angle-resolved KER spectra. The modulation frequencies vary strongly over the range of considered intensities, indicating their overall sensitivity to the associated LIPs. The modulations predicted by the 2D calculations are shifted toward larger angles, as compared to the 1D results. These shifts are attributed to rotational motion towards the LICI and become prominent at higher intensities. While we primarily trace the intensity dependence of P(θ) to transient trapping of the vibrational nuclear motion, we expect diffraction effects in the nuclear dynamics near the LICI, recently found in the dissociation of H_2^+ [R13], to also contribute to specific angle-dependent structures in the O^+ fragment distribution at larger angles $\theta \leq \pi/2$.

Future plans: In collaboration with JRML experimentalists, we plan to continue the outlined studies and investigate (i) field-induced molecular orientation and stabilization effects, allowing for finite initial rotational temperatures of the molecular gas, by incoherent sampling over Maxwell-Boltzmann-distributed cation initial rotational states and phenomenologically including the laser-alignment of the neutral parent molecules, (ii) the bound and dissociative dynamics in O_2 and CO_2 molecules after single ionization in XUV pulses delivered by the newly developed single-high-harmonic source [R5], and (iii) the impact of focal volume averaging on the O_2^+ fragment KER spectra reported under points 2 and 3 above [1,S1,R5,R6]. We further intend to (iv) extend the reported calculations to the dissociative ionization of N_2 and CO and (v) develop a complementary quantum-trajectory approach [R12,R13] to scrutinize the imprint of the LICI on P(θ) reported under point 3 above [S1]. To examine the light-induced nuclear dynamics in $CO_2^{(o,+)}$, we will obtain potential energy surfaces and dipole-couplings using GAMESS [1,R1], as a basis for quantifying ro-vibrational and light-induced couplings between two [R14] (later all three) normal (stretching and bending) modes in multi-dimensional QB [R8] and KER spectra [S1].

Peer-reviewed publications (2018-2020)

[1] P. M. Abanador, T. Pauly, and U. Thumm, *Molecular bond-stabilization in the strong-field dissociation of O_2^+*, Phys. Rev. A **101**, 043410 (2020).

[2] J. Li and U. Thumm, *A semiclassical approach for solving the time-dependent Schrödinger equation in inhomogeneous pulses of electromagnetic radiation*, Phys. Rev. A **101**, 013411 (2020).

[3] Q. Liao, W. Cao, Q. Zhang, K. Liu, F. Wang, P. Lu, and U. Thumm, *Distinction of electron dispersion in time-resolved photoemission spectroscopy*, Phys. Rev. Lett. **125**, 043201 (2020).

[4] M. J. Ambrosio and U. Thumm, *Spatiotemporal analysis of a final-state shape resonance in interferometric photoemission from Cu(111) surfaces*, Phys. Rev. A **100**, 043412 (2019).

[5] F. Navarrete, M. Ciappina, and U. Thumm, *Crystal-momentum-resolved contributions to high-order harmonic generation in solids*, Phys. Rev. A **100**, 033405 (2019).

[6] E. Saydanzad, J. Li, and U. Thumm, *Spatiotemporal imaging plasmonic fields near metallic nanoparticles beyond the diffraction limit*, Phys. Rev. A **98,** 063422 (2018).

[7] J. Li, E. Saydanzad, and U. Thumm, *Imaging plasmonic fields near Au nanospheres with spatiotemporal resolution*, Phys. Rev. Lett. **120**, 223903 (2018).

[8] M. J. Ambrosio and U. Thumm, *Energy-resolved attosecond interferometric photoemission from Ag (111) and Au (111) surfaces*, Phys. Rev. A **97**, 043431 (2018).

Submitted manuscripts

[S1] P. Abanador, and U. Thumm, *Characterization of light-induced potentials in the strong-field dissociation of O_2^+*, Phys. Rev. A.

References

[R1] M. Magrakvelidze, C.M. Aikens, and U. Thumm, Phys. Rev. A **86**, 023402 (2012).

[R2] M. Magrakvelidze, A. Kramer, K. Bartschat, and U. Thumm, J. Phys. B **47**, 124003 (2014).

[R3] P. Cörlin, …, U. Thumm, T. Pfeifer, and R. Moshammer, Phys. Rev. A, **91**, 043415 (2015).

[R4] S. Xue, H. Du, B. Hu, C. D. Lin, and A.-T. Le, Phys. Rev. A **97**, 043409 (2018).

[R5] Y. Malakar, F. Wilhelm, …, I. Ben-Itzhak, and A. Rudenko, Phys. Rev. A **98**, 013418 (2018).

[R6] M. Zohrabi, J. McKenna, …, C. L. Cocke, and I. Ben-Itzhak, Phys. Rev. A **83**, 053405 (2011).

[R7] A. M. Sayler, …, K. D. Carnes, B. D. Esry, and I. Ben-Itzhak, Phys. Rev. A **75**, 063420 (2007).

[R8] M. Winter, R. Schmidt, and U. Thumm, New J. Phys. **12**, 023023 (2010).

[R9] S. De, …, U. Thumm, …, I. Ben-Itzhak, and C. L. Cocke, Phys. Rev. A **84**, 043410 (2011).

[R10] J. Wu, M. Kunitski, …, U. Thumm, and R. Dörner, Phys. Rev. Lett. **111**, 023002 (2013).

[R11] A. Tóth, A. Csehi, G. J. Halász, and Á. Vibók, Phys. Rev. A **99**, 043424 (2019).

[R12] G. J. Halász, A. Vibók, and L. S. Cederbaum, J. Phys. Chem. Lett. **6**, 348 (2015).

[R13] A. Natan, M. R. Ware, …, O. Heber, and P. H. Bucksbaum, Phys. Rev. Lett. **116**, 143004 (2016).

[R14] H. Timmers, Z. Li, …, R. Santra, O. Vendrell, and A. Sandhu, Phys. Rev. Lett. **113**, 113003 (2014).

Atomic, Molecular and Optical Sciences (AMOS) at the Lawrence Berkeley National Laboratory

Oliver Gessner (PI), Co-Investigators: Martin Head-Gordon, Stephen R. Leone, Robert R. Lucchese, C. William McCurdy, Daniel M. Neumark, Thomas N. Rescigno, Daniel S. Slaughter, Thorsten Weber

Chemical Sciences Division, Lawrence Berkeley National Laboratory, Berkeley, CA 94720
OGessner@lbl.gov, MHead-Gordon@lbl.gov, SRLeone@lbl.gov, RLucchese@lbl.gov, CWMcCurdy@lbl.gov, DMNeumark@lbl.gov, TNRescigno@lbl.gov, DSSlaughter@lbl.gov, TWeber@lbl.gov

Project Scope: The AMOS Program at LBNL seeks to answer fundamental questions in atomic, molecular and chemical sciences that are central to the mission of the Department of Energy's Office of Science. The Program consists of a variety of closely coupled experimental-theory efforts, united by the overarching goal to provide deep insight into the physics and chemistry of the fundamental interactions that drive key chemical processes in simple molecules, complex molecular systems, and molecules in complex environments. Major areas of emphasis include inner-shell excitation, photoionization, multiple-ionization and dissociation dynamics of small molecules as well as time-resolved studies of the flow of charge and energy in atoms and molecules in the gas phase, in the condensed phase, and at interfaces. Experiments apply a broad span of existing and emerging tools based on combinations of laboratory- and facility-scale pulsed XUV and X-ray light sources and electron beams with state-of-the-art experimental techniques. Table-top femtosecond and attosecond XUV and X-ray light sources, X-ray free electron lasers, synchrotron radiation, and low-energy electron beams are employed in combination with transient XUV and X-ray absorption and photoemission spectroscopy, XUV nonlinear and four-wave mixing spectroscopy, electron and ion momentum imaging, coincidence techniques, ultrafast X-ray scattering and coherent diffractive imaging, as well as ultrafast electron diffraction. The theory component of the Program focuses on the development of new methods for solving, from first-principles, complex multi-atom and multi-electron processes that play key roles in the dynamics of the systems under investigation. The close coupling between experiment and theory as well as the complementary nature of the different activities within a single program provide a framework to tackle problems across a broad range of timescales, system sizes and, in particular, complexity, that are otherwise intractable.

The Atomic, Molecular and Optical Sciences Program at LBNL consists of three subtasks:

1. **Photon- and Electron-Driven Processes in Atoms and Small Molecules**
2. **Photon-Driven Processes in Complex Molecular Systems and Molecules in Complex Environments**
3. **First-Principles Theory of Dynamics and Electronic Structure**

The co-investigators participate in multiple subtasks, collaborating and using common techniques in studies in which experiment and theory are tightly integrated.

Subtask 1: Photon and Electron Driven Processes in Atoms and Small Molecules

S. R. Leone, R. R. Lucchese, C. W. McCurdy, D. M. Neumark, T. Rescigno, D. S. Slaughter, and Th. Weber

Attosecond Dynamics

The attosecond dynamics group develops new nonlinear spectroscopy methods with attosecond extreme ultraviolet (XUV) pulses produced by high harmonic generation (HHG) for time-domain measurements of ultrafast electronic dynamics in atoms and molecules. These experiments probe electronic wavepacket propagation excited by an attosecond XUV pulse using two independently controlled few-cycle near-infrared (NIR) pulses. Accurate measurements of electronic dynamics using attosecond transient absorption spectroscopy (ATAS) are limited by overlapping signals from many NIR-induced processes. The attosecond group developed a new method that overcomes this challenge by exploiting the phase-matching condition of four-wave mixing (4WM) signals using a noncollinear beam geometry in which each pulse has a unique wavevector. 4WM signals are emitted with angle dependence according to specific combinations of the incident wavevectors, enabling background-free characterization of electronic, vibrational, and vibronic dynamics in atoms and molecules (Cao *et al.* **2018** *Phys. Rev. A* 97, 023401; Warrick *et al.* **2018** *Faraday Discuss*. 212, 157–174). A refined understanding of the nonlinear signal generation, achieved in collaboration with theorists M. Gaarde and K. Schafer at Louisiana State University, demonstrated a time-dependent accumulation of an AC Stark phase grating (Fidler *et al.* **2019** *Nat. Comm.* 10, 1384). These developments enabled the first demonstration of XUV multidimensional spectroscopy (Marroux *et al.* **2018** *Sci. Adv.* 4, eaau3783).

Attosecond Transient Absorption and XUV Wave Mixing Studies *(Leone, Neumark, Lucchese, McCurdy)*

Recent Progress*:* Current work uses the enhanced signal specificity of the wave-mixing technique to understand shorter-lived, more complex electronic dynamics. 4WM studies directly measured the lifetimes of multiple $^2P_{1/2}$ *ns/d* autoionizing states in krypton that are obscured in the ATAS data, demonstrating the technique's ability to accurately measure ultrafast decaying states (Fidler *et al.* **2019** *J. Chem. Phys.* 151, 114305). Measurements at the iodine $N_{4,5}$ pre-edge of ICl show orbital alignment-dependent core-excited state lifetimes, indicating that non-local decay channels involving the chlorine atom enhance the decay rates for core-hole states aligned parallel with the molecular axis (Marroux *et al.* **2020** *Nat. Comm. submitted*).

Recent investigations on O_2, focusing on the 3s Rydberg state in a series converging to the ionic c $^4\Sigma_u^-$ state, show the power of attosecond 4WM to measure single state dynamics with few femtosecond lifetimes. The spectrum at pulse overlap (Fig. 1-1a) shows the ATAS signal in the direction of the XUV pulse at ~0 mrad and the 4WM signals, spatially isolated at ~1.5-2.8 mrad angular divergence. The 3s Rydberg state supports v=0 and 1 vibrational levels at 20.85 eV and 21.05 eV, respectively. Due to the proximity of these states to ionic states and the predissociative potential, the 3s Rydberg state includes competing autoionization and dissociation decay channels. While extensive studies on the higher Rydberg states exist, no previous time-domain measurement of the 3s Rydberg dynamics has been possible due to its few-femtosecond lifetime. The phase matching condition can spatially distinguish pathways relying on two separate NIR interactions (Λ- or V-type) from those requiring two interactions with one NIR pulse (ladder-type) by altering the beam crossing angles. Using 4WM with different angles between the XUV and NIR_1 (18 mrad) and NIR_2 (13 mrad) pulses, the Λ-type pathway isolates the 3s Rydberg state (Fig. 1-1a, green box) dynamics from the ladder-type pathway of higher-lying states (Fig. 1-1a, grey box). Fitting the Λ-type signals determines 5.8 ± 0.5 fs (Fig. 1-1b) and 4.3 ± 0.7 fs (Fig. 1-1c) lifetimes for the v=0 and v=1 states,

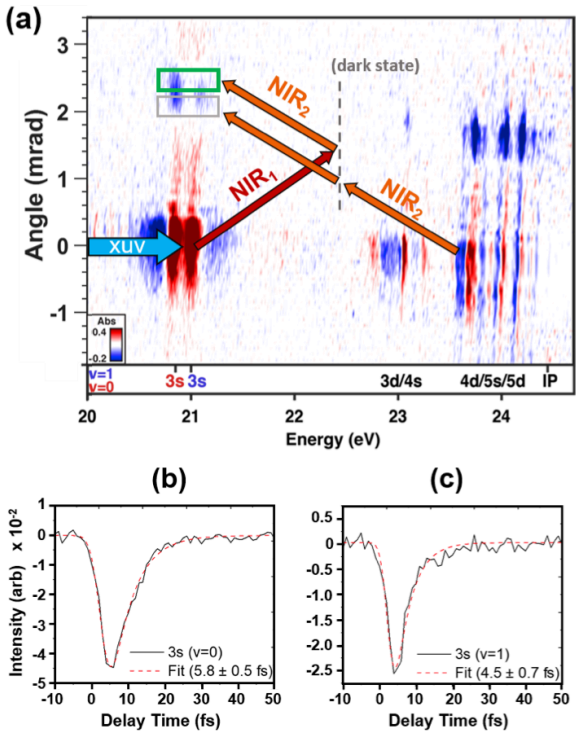

Fig. 1-1. Four-wave mixing in O_2. (a) ATA signal (~0 mrad) showing convoluted absorption (red) and emission (blue) features with complex Fano line shapes. Spatially-isolated wave-mixing signals with ladder ($\vec{k}_{signal} = \vec{k}_{XUV} - \vec{k}_{NIR2} - \vec{k}_{NIR2}$) and Λ-pathways ($\vec{k}_{signal} = \vec{k}_{XUV} + \vec{k}_{NIR1} - \vec{k}_{NIR2}$) phase matching conditions are overlaid (arrows). The Λ-pathways for the 3s Rydberg v=0 and 1 are angularly separated and integrated around 2.5 mrad (green box) for lifetime extraction. The lifetimes are determined to be (b) 5.8 ± 0.5 fs for v=0 and (c) 4.5 ± 0.7 fs for v=1.

respectively. In collaboration with C.W. McCurdy and R.R. Lucchese from the LBNL AMOS theory team, calculated results of 5.6 fs and 4.8 fs, respectively, match the experimental values very well, while also providing deeper insight into the dominant decay mechanisms. Although the tunneling barrier for predissociation might initially appear to explain the different lifetimes, the theoretical results suggest autoionization dominates the decay processes for both vibrational states. The calculations show that autoionization lifetimes can change significantly with internuclear distance. This work has provided the first molecular excited state lifetime extracted with XUV wave-mixing and the first in-depth characterization of the O_2 3s Rydberg decay dynamics.

Concurrent research is extending XUV wave-mixing to investigate increasingly complex ultrafast electronic dynamics. Angularly diffuse XUV beams were successfully used as a reference field in a self-heterodyned noncollinear wave-mixing experiment on helium (Fidler *et al.* **2020** *J. Phys. Photonics* 2, 034003). The intrinsic reference field amplified the detected wave-mixing emission from the helium 1s*np* states to clearly identify at least eight light induced states, whereas previous homodyned experiments observed only one light induced state. Wavepacket dynamics of Ar inner valence ($3s^{-1}np$) autoionizing Rydberg states (26.6-29.5 eV) are being studied with XUV wave-mixing and multidimensional spectroscopies. Nontrivial coherent oscillations in the wave-mixing spectra suggest that the wavepacket is a complex composition of inner valence excited states. XUV-NIR multidimensional spectroscopy is being used to characterize the inner valence excited state wavepacket. Most recently, 4WM emission of the Na^+ $L_{2,3}$ transitions ($^2P_{1/2}$ and $^2P_{3/2}$ inner shell states) were measured in NaCl crystalline thin films. The Na^+ 2p orbital to Rydberg-like core-level states directly report on high-energy core exciton dynamics of NaCl. These proof-of-principle experiments demonstrate that 4WM signals from inner shell atomic states can provide fundamental insight into the dynamics of extended many-electron systems.

Future Plans: A new high-energy laser will be installed, and apparatus renovations will be performed to facilitate core-excited state studies at shorter wavelengths. Increased pulse energy from the new laser will improve XUV photon flux above 50 eV and allow broadband UV pulses to be used freely in new experimental configurations. For example, wave-mixing experiments on $4d^{-1}6p$ core-excited states of iodine-containing molecules will be possible. Bond-length dependent core-hole lifetime measurements in CH_3I will use a 266 nm pulse to trigger iodine dissociation followed by an XUV-UV-UV wave-mixing pulse sequence. The inter-nuclear distance dependence of non-local decay mechanisms will be directly measured and will serve as a benchmark for future theoretical models. Incorporating a high-energy optical parametric amplifier to drive the HHG process will

produce tabletop soft X-rays reaching the chemically relevant carbon K-edge (~300 eV) photon energies. Multidimensional wave-mixing spectroscopies using soft X-rays will probe ultrafast core-excited state dynamics with the exquisite sensitivity and specificity of atomic K-shell absorption edges in organic molecules. For example, a predicted doubly excited state in formaldehyde ($1s, n\rightarrow(\pi^*)^2$) is one-photon forbidden and only limited experimental confirmation exists of the energy and dynamics of this state. Multidimensional experiments enabled by a 4WM pulse sequence will access this doubly excited dark state, revealing its energetic location and lifetime. These future developments will provide an incisive picture of otherwise inaccessible electronic and nuclear dynamics governing chemical reactions.

Ultrafast Excited State Dynamics Probed by Multidimensional Momentum Imaging

Particle angle- and energy resolved molecular photoionization measurements are sensitive to the coupled motion of electrons and nuclei as well as their ionization and fragmentation mechanisms. In particular, Molecular and Recoil Frame Photoelectron Angular Distributions (M/RFPADs), i.e. the body-fixed frame electron emission patterns in molecules, sensitively interrogate the molecule from within and shed light on fundamental properties such as symmetry, particle correlation and entanglement, energy transfer between electrons and nuclei as well as vibrational dynamics such as bending and stretching of the molecular backbone, which are at the core of many photochemical reactions and the focus of our studies. We investigate these phenomena in high detail via electron-ion coincidence measurements in momentum space, which we pursue in single, double, and quadruple ionization experiments of small quantum systems with COLd Target Recoil Ion Momentum Spectroscopy (COLTRIMS). Experiments utilize single XUV synchrotron light pulses, 2-VUV photon absorption schemes with intense tabletop high harmonic generation, and soft X-ray pulses at free electron lasers. Our studies focus on fundamentally important systems ranging from isolated atoms (Ar) to small polyatomic molecules (N_2, O_2, D_2O, and NH_3) that are within reach of both complete experimental characterization and accurate theoretical treatment and interpretation, enabling tight coupling of the experimental and the theoretical thrusts, which directly complement, inspire, and inform each other.

Photoelectron and Fragmentation Dynamics of NH_3 Following Direct Single-Photon Double Ionization *(Lucchese, McCurdy, Rescigno, Slaughter, Weber)*

Recent Progress: Due to its complexity, the detailed investigation of dissociation processes of polyatomic molecules still remains a challenge. We have performed state-selective COLTRIMS experiments at the Advanced Light Source (ALS) together with Multi-Reference Configuration Interaction (MRCI) calculations on the Photo Double Ionization (PDI) of ammonia (NH_3) molecules. First, we focused on the $H^+ + H^+$ dissociation channel of NH_3 following direct valence PDI at 61.5 eV (Larsen *et al.* July **2020** *submitted to Phys. Rev. R*), where the two photoelectrons and two protons were measured in coincidence on an event-by-event basis, extending our previous experiments on water (Reedy *et al.* **2018** *Phys. Rev. A* 98, 053430). From the dication Potential Energy Surface (PES) cuts, derived from the MRCI calculations, we identified four participating dication electronic states that lead to the $H^+ + H^+$ fragmentation. The PDI yield as a function of the Kinetic Energy Release (KER) and the relative angle, measured between the momentum vectors of the two emitted protons, indicate that three of the four dication states, namely the $(2a_1^{-1}, 3a_1^{-1})^1A_1$, $(1e^{-2})^1A_1$, and $(1e^{-2})^3A_2$ states, dissociate via a concerted mechanism, while the fourth state $(1e^{-2})^1E$ dissociates via a sequential process, with the intermediate ro-vibrationally excited NH^+ fragment ion decaying through an intersystem crossing that leads to a four-body breakup. Two of the dication states, i.e. the $(2a_1^{-1}, 3a_1^{-1})^1A_1$ and $(1e^{-2})^1A_1$ states, exhibit concerted bending and stretching dissociation mechanisms that fragment near the ground state geometry (axial recoil approximation applies). The third state, i.e. the $(1e^{-2})^3A_2$ state, undergoes appreciable evolution in its molecular geometry and an

asymptotic electron transfer from H to NH^+ at distances greater than 18 Bohr (!) in the dissociating dication, preceding the three-body breakup. This long-range electron transfer is reminiscent of a previously observed dissociative electron attachment mechanism investigated by our group (Rescigno *et al.* **2016** *Phys. Rev. A* 93, 052704). Differences between the MRCI calculations, which do not take internal excitations into account, and the measured KER suggest that the neutral NH fragment in each of the three-body dissociation channels is indeed highly ro-vibrationally excited.

We also state-selectively analyzed the $NH_2^+ + H^+$ and $NH^+ + H + H^+$ fragmentation channels after PDI of NH_3 for the same photon energy of 61.5 eV (Larsen *et al.* July **2020** *submitted to J. Phys. B: At. Mol. Opt. Phys.*). With help from the LBNL AMOS theory group, five dication states, $(3a_1^{-2})^1A_1$, $(3a_1^{-1}, 1e^{-1})^3E$, $(3a_1^{-1}, 1e^{-1})^1E$, $(1e^{-2})^3A_2$, and $(1e^{-2})^1E$ are identified as active in this photon energy range and assigned to the two different breakup channels in the measured electron-ion energy correlation maps. Three of these dication states dissociate into ro-vibrationally excited ionic fragments, where the $(3a_1^{-1}, 1e^{-1})^1E$ and $(3a_1^{-1}, 1e^{-1})^3E$ dication states lead to hot NH_2^+ fragments, while the $(1e^{-2})^3A_2$ dication state leads to a hot NH^+ fragment. Our measurement identifies three dication electronic states that dissociate to form $NH_2^+ + H^+$ fragments, which are populated via direct PDI as well as through autoionization. We find that the initial excitation in one of these dication states, the $(3a_1^{-2})^1A_1$ state, undergoes intersystem crossing preceding dissociation. In the three-body dissociation of NH_3^{2+}, we identified three dication states contributing to the $NH^+ + H^+ + H$ fragmentation channel, two of which are distinct from the states of the two-body breakup channel. In contrast to the two-body fragmentation channel, the three dication states contributing to the three-body breakup are found to directly dissociate without any non-adiabatic transitions preceding the fragmentation. The dissociation of the three dication states leading to three-body fragmentation resulted in different breakup signatures due to the neutral H atom. We observe that the range of angles spanned between the two photoions, following the PDI to the $(3a_1^{-1}, 1e^{-1})^1E$ and $(1e^{-2})^3A_2$ dication states, is broader than in the $(1e^{-2})^1E$ state. The range of kinetic energies spanned by the neutral H fragment is broader in the $(1e^{-2})^1E$ dication state compared to the $(3a_1^{-1}, 1e^{-1})^1E$ and $(1e^{-2})^3A_2$ dication states. We also observe a difference in the correlation between the kinetic energy of the neutral H and the measured relative angle between the NH^+ and H^+ photoions (see Fig. 1-2). The dashed silver lines in Fig. 1-2

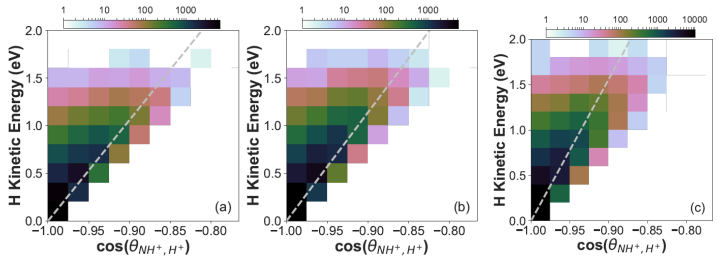

Fig. 1-2. The $NH^+ + H^+ + H$ three-body fragmentation yield after PDI of NH_3 at 61.5 eV as a function of the cosine of the measured relative angle between the NH^+ and H^+ fragment momentum vectors and the kinetic energy of the neutral H fragment for the three dication states: (a) $(3a_1^{-1}, 1e^{-1})^1E$, (b) $(1e^{-2})^3A_2$, and (c) $(1e^{-2})^1E$. The dashed silver lines indicate the decreasing influence, from participant to spectator, of the neutral H fragment.

are intended to guide the eye towards the slope of the features and improve the visibility of the energy-angle correlations. We also analyzed the relative electron-electron angular distribution of all dication electronic states, while integrating over all possible electron-electron energy sharing cases, and for the special scenario of equal electron-electron energy sharing. The distributions indicate the dominance of a knock-out PDI mechanism in all cases, as the relative electron-electron angles mainly peak between 115 and 180°, similar to the kinematics reported for the PDI of atoms (He) and small molecules (D_2 and H_2O) for comparable excess energies, which are governed by Two-Step 1 (TS 1) ionization processes.

Future Plans: Next, we will investigate the preferred orientations of water and ammonia molecules for excitation of specific dication states with respect to the light polarization vector. We will analyze

the angular distributions of the dissociation fragments for the direct and sequential ionization reactions employing laboratory and native frame coordinate systems. This will enable us to identify the relevant state- and breakup-specific body-fixed (sub)frames and produce the respective electron-pair emission patterns, which will provide deeper insight into the influence of electron-electron correlation, charge transfer, electron-nuclei interaction, and symmetry (selection rules) in the double ionization process. These investigations will eventually enable the study of PDI-induced dissociation processes of even more complex molecular structures in high detail such as (deuterated) methanol (CH_3OD), which is the simplest molecule containing a hydroxyl and a methyl group. Methyl groups can be deprotonated, while polar hydroxyl groups seek to form hydrogen bonds, making methanol an excellent candidate to study intramolecular proton transfer. In future experiments at the ALS, we will track the HOD^+ formation channel in 3D-momentum space with the goal to identify the dication states and fragmentation pathways that are relevant for this process. PhotoIon-PhotoIon COincidence (PIPICO) time-of-flight spectra, electron-ion energy correlation maps, and RFPADs will enable us to isolate most of the expected active 13 singlet and 9 triplet dication states, track proton and hydrogen elimination, H_3^+ formation, coupled electron-nuclear motion, and sequential ionization processes.

Angle- and Energy-Resolved Non-Resonant One-Color Two-Photon Single Ionization of Atomic and Molecular Targets *(Lucchese, McCurdy, Rescigno, Slaughter, Weber)*

Recent Progress: By using a high harmonic generation driver in the near-UV regime from frequency-doubling the 800 nm output of a 30 mJ Ti:Sapph. laser system, we can produce more than 10 nJ of 9.3 eV VUV photons per pulse with < 30 fs pulse duration. This is sufficient to drive resonant and non-resonant nonlinear processes in atomic and molecular gas targets. Although the repetition rate of this laser system is currently limited to 50 Hz, we are able to perform coincident electron-ion 3D-momentum spectroscopy experiments on non-resonant 2-photon XUV ionization processes of individual atoms and molecules. Applying these extraordinary capabilities, which complement FEL-type COLTRIMS experiments towards lower photon energies, we initiated a new thrust that focuses on *coherence and particle correlation in 2-photon XUV excited state dynamics* of atoms and small molecules. In particular, we were able to extract angular asymmetry parameters (β_2 and β_4) from measured electron and ion angular distributions in the laboratory frame, in order to study the role of dark states, electron-electron correlation, continuum resonances, and electron-nuclear coupling. For non-resonant two-photon single-ionization (NOTPSI) of Ar, we find that the observed photoelectron emission pattern can be explained by interference between different p and f partial wave components of the photoelectron scattering wave function, which add destructively along the polarization direction of the ionizing VUV field (Larsen *et al.* **2020** *Phys. Rev. A* 101, 061402(R)). Comparison of our measurements against previous calculations (Pan and Starace **1991** *Phys. Rev. A* 44, 324) reveals that the photoionization dynamics are evidently influenced by electron-electron correlation effects. However, it appears that the level of electron-electron correlation accounted for in the Coulomb correlated HF calculations is not sufficient to reach complete agreement with the experimental results. Our measurements serve as a benchmark for future *ab initio* theoretical treatments of NOTPSI dynamics in multi-electron systems. A particular challenge in this regard is the inclusion of continuum-continuum coupling in the calculations, which is expected to be important in reproducing the PAD in non-resonant regions. More generally, the investigation and understanding of continuum states and resonances as well as couplings, transitions, and decays of continuum states remain a challenge for experiment and theory alike, while the ability to interpret spectroscopic signals in future XFEL experiments will depend critically on the capability to accurately describe these states.

Driven by the challenge to understand continuum states and continuum resonances, we used two 9.3 eV photons from intense femtosecond VUV pulses, resonant within the Schumann-Runge continuum in the intermediate excitation step, to study the decay of metastable and optically dark continuum resonances of molecular oxygen at 18.6 eV excitation energy (Larsen *et al.* **2020** *J. Chem. Phys.* 153, 021103). These resonances are parity-forbidden in single-photon experiments and have not been studied before experimentally or theoretically. Since scattering through such resonances often weakly competes with the stronger direct ionization process, studying them in detail is difficult. We overcame some of these challenges through the use of photo-fragment ion detection. Specifically, together with the LBNL AMOS theory team we performed a combined experimental and theoretical study on the photodissociation dynamics of $O^+ + O^-$ ion-pair formation in O_2 following resonant 2-VUV-photon absorption, where the resulting O^+ ions are detected using 3-D momentum imaging. In this experiment, a dipole-allowed parallel transition to the $B^3\Sigma_u^-$ state is excited by the first VUV photon. This valence state is weakly mixed with the $E^3\Sigma_u^-$ Rydberg state. A second VUV photon from within the same pulse populates continuum resonances lying below the dissociative ionization threshold, which can decay by predissociation to ion-pair states, interrupting and competing with molecular autoionization. As illustrated in Fig. 1-3, the KER-dependent photoion angular distributions and their respective anisotropy parameters (β_2 and β_4) provide clear indications for

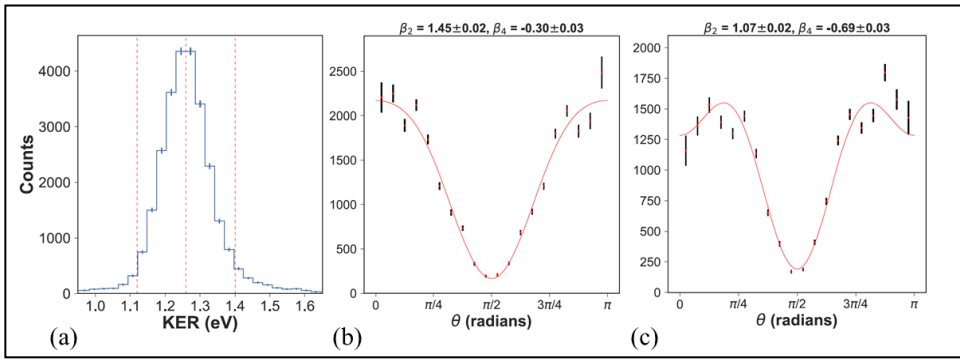

Fig. 1-3. (a) KER of the ion-pair formation from O_2, following resonant two-photon absorption at 9.3 eV. (b,c) Energy-resolved O^+ photoion angular distributions for the low (b) and high (c) KER regions as indicated in (a) by the dashed red lines.

the participation of two optically dark and nearly degenerate continuum resonances of different symmetry. The PADs reveal that these resonances are excited by a mixture of parallel-parallel (||-||) and parallel-perpendicular (||-⊥) 2-VUV-photon transitions, where both decay by coupling to the ion-pair formation states of the same total symmetry via internal conversion. This collaborative work demonstrates that energy- and angle-resolved fragment ion momentum imaging can be highly sensitive to the symmetry of predissociative electronic states in the ionization continuum.

Future Plans: We are in the process of extending our combined experimental and theoretical energy- and angle-resolved studies on the photoionization dynamics of non-resonant one-color two-photon single valence ionization to non-dissociating N_2^+ molecular cations. In this case, the 2-VUV-photon single-ionization of N_2 populates the $X^2\Sigma_g^+$, $A^2\Pi_u$, and $B^2\Sigma_u^+$ ionic states, where the photoelectron angular distributions associated with the $X^2\Sigma_g^+$ and $A^2\Pi_u$ states both vary rapidly with changes in photoelectron kinetic energy of only a few hundred meV. At this point, we tentatively attribute the rapid evolution in the photoelectron angular distributions to the excitation and decay of dipole-forbidden autoionizing resonances in the photoionization continuum that belong to series of different symmetries, all of which are members of the Hopfield series, and compete with the direct two-photon single ionization. The anisotropy parameters β_2 and β_4 will be extracted from experiments, while the LBNL AMOS theory team will approximate this process by one-photon single ionization calculations from a selected excited state of neutral N_2 (e.g. the $b^1\Pi_u$ state of N_2 for the $A^2\Pi_u$ ionic state of N_2^+) as a resonant intermediate. This project will provide a deeper understanding of the role of dipole-forbidden autoionizing resonances in non-resonant one-color two-photon single

ionization of diatomic molecules, in particular with respect to interference and competition between this sequential ionization mechanism and direct 2-VUV-photon single ionization.

Double Core-Hole Generation in O_2 Molecules Using an X-ray Free-Electron Laser *(Weber)*

Recent Progress: In collaboration with the Frankfurt group (R. Doerner), DOE BES-AMOS PIs from KSU and LBNL (Rolles, Rudenko, Weber) employed a newly built COLTRIMS endstation at the EuXFEL and measured the first molecular frame photoelectron angular distributions of the second photoelectron (MF2ndPADs) emitted by double core-hole ionization in O_2 molecules (Kastrike *et al.* **2020** *Phys. Rev. X* 10, 021052). More recently, single-site and two-site double core-holes (ss-DCH and ts-DCH) were identified in electron-ion energy correlation maps of the $O_2^+ + O_2^+$ breakup (not shown here), which is produced by absorption of two 670 eV photons from a short (25fs) X-ray pulse about 120 eV above the oxygen K-edge, followed by two single Auger decays (Kastrike *et al.* Aug. **2020** accepted for pub. in *Phys. Rev. Lett.*). The respective MF2ndPADs were retrieved for ~30 eV and ~110 eV 2nd photoelectrons, related to the ss-DCH and the ts-DCH ionization process, respectively, for both parallel and perpendicular orientation of the molecule relative to the X-ray polarization axis. The results shown in Fig. 1-4 are integrated over the emission direction of the 1st K-shell photoelectron (~127 eV). The respective MF2ndPADs were modeled within the frozen-core (blue line) and relaxed-core (red-line) Hartree-Fock approximations. In the case of the ts-DCH creation, the two approximations yield very similar angular emission distributions, which are both in good agreement with the measured data. For the ss-DCH creation, the relaxed-core Hartree-Fock approximation results in a good agreement between theory and experiment, while the frozen-core Hartree-Fock approximation fails. This happens because, in the latter approximation, the σ-shape resonance of the second photoelectron occurs at kinetic energies where the second ss-DCH photoelectrons are observed in the experiment. This is not surprising as one-particle Hartree-Fock approximations usually fail at molecular shape resonances, and contributions from different partial waves start to distinctly alter the computed angular distributions. Indeed, the theoretical MF2ndPAD, depicted in Fig. 1-4a by the blue curve (frozen-core Hartree-Fock), exhibits an enhanced contribution from σ-waves, i.e. it overestimates the electron emission along the molecular axis

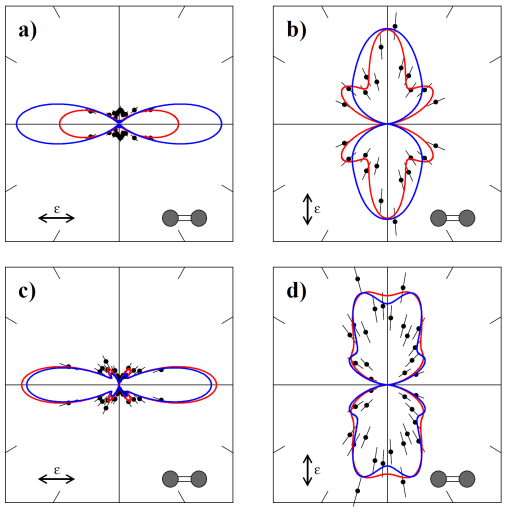

Fig. 1-4. Black points: MF2ndPADs of the second electron emitted during the ss-DCH (a & b) and ts-DCH (c & d) creation for horizontal (left column) and vertical (right column) orientation of the molecular breakup of O_2 into $O^{2+} + O^{2+}$ (horizontal) with respect to the light polarization axis after absorption of two 670 eV photons. Curves: theoretical modeling using the frozen-core (blue) and relaxed-core (red) Hartree-Fock approximations.

Future Plans: The EuXFEL results inspire first experiments at the future dynamic reaction microscope (DREAM) endstation at LCLS-II during its Early Science campaign in summer 2022. With an X-ray pulse repetition rate of ~100 kHz, MF2ndPADs for ss-DCH and ts-DCH creation can be measured for specific emission angles between the 2nd photoelectron and the 1st K-photoelectron, while being differential in the orientation of the molecular axis and the polarization vector. This highly differential insight will enable us to study the role of electron-electron correlation and the influence of symmetry in the quadruple ionization process of diatomic molecules employing two X-ray photons.

Investigations of Dynamics in Transient Anions Formed by Electron Attachment

Transient anions formed by electron attachment to polyatomic molecules can exhibit highly-coupled electronic and nuclear motion, which is often rooted in conical intersections between metastable electronic states. Dissociative Electron Attachment (DEA) is an electron-molecule reaction in which free electron energy is efficiently converted into nuclear degrees of freedom such as dissociation and vibrational excitation. The flow of energy and charge within the molecular anion provides rich information on fundamental chemistry beyond the Born-Oppenheimer approximation and has relevance to applications involving reactive anionic and radical species that are often produced by dissociation.

Mechanisms of Electron Attachment and Dissociation Dynamics in Formamide *(Slaughter, Weber, Rescigno, Lucchese, McCurdy)*

Recent Progress: Low energy electrons interact with formamide via Feshbach resonances, the lowest of which was recently proposed to have a singly occupied valence orbital that is electronically stabilized by a high dipole moment (Li *et al.* **2019** *Phys. Rev. Lett.* 122, 073002). This is contrary to the more common DEA mechanism at similar incident energy energies in other small polyatomic molecules, such as formic acid (Griffin *et al.* **2020** *J. Phys.: Conf. Series* 1412, 052004; Slaughter *et al.* **2020** *Phys. Chem. Chem. Phys.* 22, 13893), where a diffuse Rydberg or valence orbital is doubly occupied and stabilized below the potential energy of the parent neutral state by electron-electron correlation. Electronic stabilization is essential in DEA resonances to allow dissociation to compete with autodetachment. The measured and calculated NH_2^- angular distributions for incident electron energies between 5.3 eV to 6.8 eV (the 6.3 eV case is depicted as an example in the right panel of Fig. 1-5) show that electron attachment occurs via one of two Feshbach resonances. The resonances have A′ and A″ symmetries, corresponding to the excitation of the highest or second-highest occupied orbital, respectively, and double occupation of a Rydberg orbital. The calculated angular distribution for the A″ resonance (black curve in right panel of Fig. 1-5) provides better agreement with the experiment at 6.3 eV. A similar comparison at lower electron attachment energies below 6.3 eV (not shown here) indicates the increasing contribution from the A′ resonance (green dashed curve), with rotation of the C-N recoil axis during dissociation. This work was performed in collaboration with J. Williams (University of Nevada, Reno) and A. Moradmand (Cal. State Maritime Academy), and the results are reported in an article recently accepted for publication (Panelli *et al.* **2020** *Phys Rev. Research*).

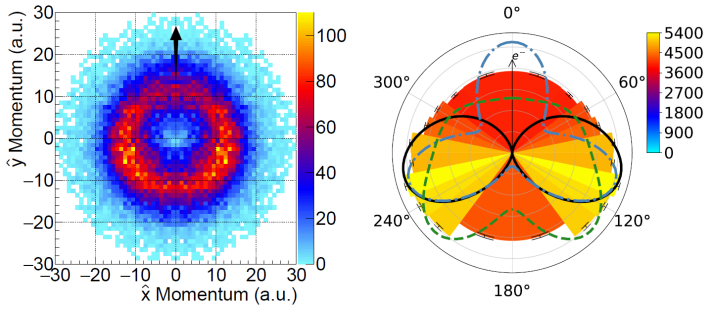

Fig. 1-5. NH_2^- fragment distributions from DEA to formamide at 6.3 eV electron attachment energy. Left: Laboratory-frame momentum image. The electron is incident in the +y-direction. Right: Measured (solid colors) and calculated (lines) angular distributions of NH_2^-. The color scale and radial extent indicate the ion yield in arbitrary units. Calculations for two Feshbach resonances of A″ (black line) and A′ (blue dot-dashed line) symmetry are shown. For the A′ resonance, a 30° rotation of the recoil axis toward larger O-C-N angles leads to a more isotropic NH_2^- angular distribution (green dashed line).

Future Plans: The next system of fundamental importance that we will target for dynamical studies by fragment momentum imaging is nitromethane. Nitromethane is the simplest organic-nitro molecule with important applications in the manufacture of fuels and explosives and as an industrial

solvent. It is also one of the simplest molecules that can bind an electron in either of two fundamentally different ways (Sommerfeld **2002** *Phys. Chem. Chem. Phys.* 4, 2511; Kunin *et al.* **2016** *Phys. Chem. Chem. Phys.* 18, 33226) in either valence- or dipole-bound resonances below 1 eV. Investigating the fragmentation dynamics of these low-energy resonances by 3D anion momentum imaging is expected to reveal important details about the influence of large dipole moments on the dynamics of DEA and the underlying dissociation mechanisms. Higher resonant attachment energies around 4.5 eV, 5.9 eV, and 9.5 eV have been found by mass spectrometry (Walker *et al.* **2001** *Int. J. Mass spectrom.* 205, 171; Alizadeh *et al.* **2008** *Int. J. Mass spectrom.* 271, 15) to produce O^-, OH^-, CN^-, and NO_2^- along with several other minor fragmentation channels. Conservation of momentum requires that the lighter fragments (e.g. O^-) receive higher kinetic energies, which tends to produce finer structures in the measured angular distributions. We therefore expect rich information in the 3D momentum of those fragments to reveal an even higher level of detail on the electron attachment mechanisms and anion dissociation dynamics. This work complements the DOE-EPSCOR project in collaboration with Martin Centurion "*Capturing Ultrafast Electron Driven Chemical Reactions in Molecules*", which will explore anion resonances by pump-probe photo-fragment and photoelectron spectroscopy.

Subtask 2: Photon Driven Processes in Complex Molecular Systems and Molecules in Complex Environments

O. Gessner, M. Head-Gordon, S. R. Leone, D. M. Neumark, D. S. Slaughter, Th. Weber

Probing Delayed C–I Bond Fission in the UV Photochemistry of 2-Iodothiophene with Ultrafast Core-to Valence Transient Absorption Spectroscopy *(Gessner, Leone, Neumark)*

Femtosecond time-resolved transient XUV absorption (TXA) spectroscopy is used to monitor photodissociation dynamics from the perspective of well-defined reporter atoms. Experiments using a laboratory-based high-order harmonic generation (HHG) setup are complemented by high-level *ab initio* calculations of XUV spectroscopic fingerprints of possible reaction intermediates and products.

Recent Progress: For sulfur-containing compounds, the importance of triplet states in their photochemistry is gaining increasing recognition, as intersystem crossing (ISC) can significantly perturb the dynamics and number of surface crossings. Spectral signatures of ring closed vs. ring open dissociation pathways will be explored through comparison with *ab initio* core absorption spectra, in combination with molecular dynamics calculations, to unlock a detailed atomic-scale picture of the dissociation dynamics. In an exploratory study, we probe electronic and structural changes during the UV-induced dissociation of 2-iodothiophene using a 268 nm pump pulse and an ~50 eV XUV probe pulse that promotes iodine 4d core-to-valence transitions in search of evidence for ring-opening as a precursor step to fragmentation. The transient absorption spectra shown in Fig. 2-1A are obtained by integrating the measured XUV absorption changes $\Delta A(E,\Delta t)$ over separate pump-probe time-delay ranges as indicated in the figure legend. The time-dependent behavior of the XUV transient absorption spectra is explored in Fig. 2-1B by inspecting key spectral regions using the same colors as marked by horizontal, color-coded bars in Fig. 2-1A. An important observation is that following UV excitation, the 2-iodothiophene parent molecule population bleach continues to increase up to delays of ~1 ps. Absorption changes in this energy window correspond to molecular, rather than atomic, iodine species and conclusively show that the dissociation requires several hundred femtoseconds to complete. This conclusion is further supported by the delayed appearance of neutral I atoms, beginning to rise only after ~100 fs have elapsed, and gradual changes in the asymptotic yield can be seen up until ~1 ps. A global fit allows overlapping spectral features of the time-resolved spectra to be decomposed into their transient spectral contributions and to provide a

consistent description of various transient intensities for fixed energies within a single kinetic model (solid lines in Fig. 2-1B).

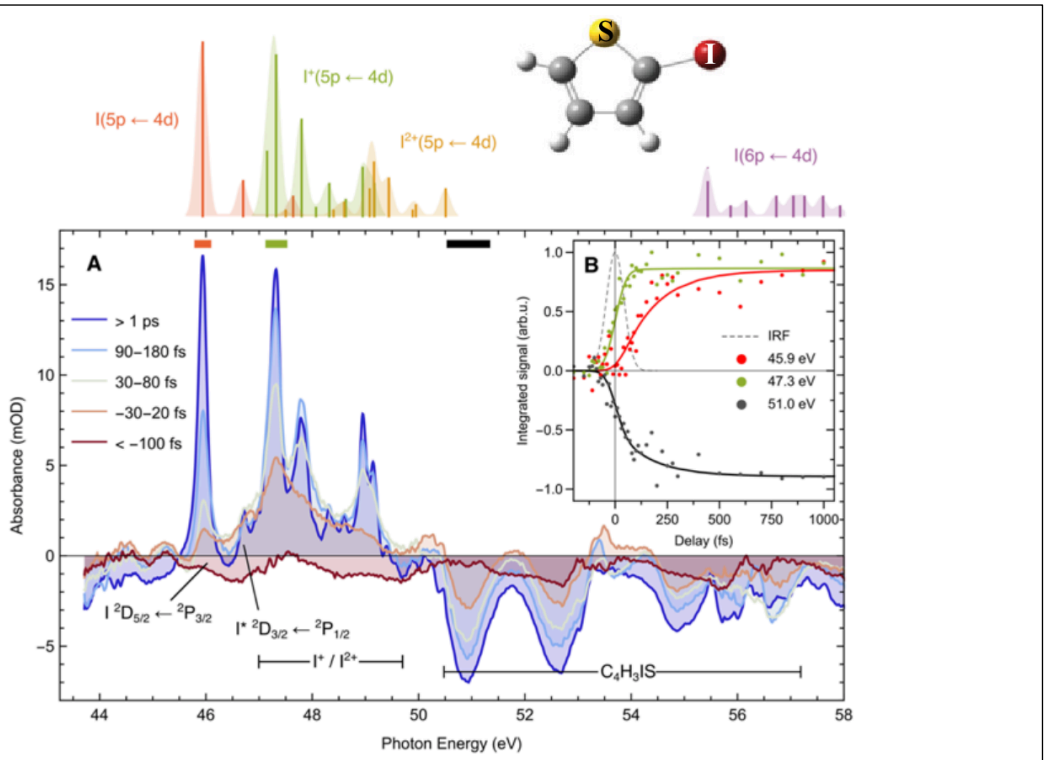

Fig. 2-1. (A) UV pump – XUV probe transient absorption spectra at the iodine 4d edge of 2-iodothiophene. Negative-going signal at energies >50 eV corresponds to depletion of the parent molecule. At very early times [-30–+20] fs (orange), a broad feature associated with a short-lived species near 48 eV is observed, at intermediate delays [90–180] fs (light blue), pronounced asymmetry in the neutral I atom near 46 eV is observed, while after >1 ps (blue) the asymptotic products are formed. Color-coded bars indicate the energies selected to illustrate time-dependent spectral trends in panel B. (B) Circular points are measured data using the same color codes (energies specified in legend). The solid lines correspond to the result of a global fit analysis. The instrument response function (IRF) measured in xenon is overlaid (dashed gray). Literature np←4d absorbance spectra for both iodine atoms and ions are shown at the top of the figure, as a stick spectrum and after Gaussian convolution (O'Sullivan *et al.* **1996** *Phys. Rev. A* 53, 3211–3226).

Future Plans: A modified version of a recently developed, high-precision *ab initio* theory for inner-shell excitation energies will be used to support interpretation of the recorded transient XUV spectroscopic fingerprints (Hait and Head-Gordon **2020** *J. Phys. Chem. Lett.* 11, 775–786). A complementary viewpoint of the dynamics from the perspective of the sulfur and carbon atoms will be enabled by expanding the photon energy range of the high-harmonics setup using a high-power optical parametric amplifier (OPA). Commissioning of the OPA is imminent and components for a corresponding high-pressure HHG setup have been ordered. Complementing the HHG-based TXA experiments, an ultrafast electron diffraction (UED) experiment at SLAC National Accelerator Laboratory has been granted experimental time, which is scheduled for November 2020. The UED experiment will concentrate on UV-induced dynamics in bromoform, in order to provide a direct comparison for the information provided by TXA and UED techniques, following our recent femtosecond XUV absorption study of this system (Toulson *et al.* **2019** *Struct. Dyn.* 6, 054304).

XUV Ultrafast Transient Polarization Spectroscopy (X-UTPS)

The aim of this thrust is to establish a new multidimensional, polarization-based nonlinear XUV and X-ray spectroscopy method to monitor ultrafast gas- and condensed-phase chemical dynamics with high detail. Ultrafast Transient Polarization Spectroscopy (UTPS) (Thurston *et al.* **2020** *Rev. Sci.*

Instrum. 91, 053101) employs a four-wave mixing (4WM) scheme to probe both the real and imaginary parts of the 3rd-order nonlinear response of excited electronic states in molecules by exploiting the Optical Kerr Effect (OKE) in the time domain. The unique sensitivity of intensity-dependent refractive index (χ^3) processes to electronic structure, electronic and vibrational coherences, and the correlated motion of electrons and holes provides access, for example, to dynamics near conical intersections, even if there is no change in electronic binding energies. The central goal of this effort is to push the unique strengths of nonlinear techniques based on 3rd-order optical responses into the XUV and X-ray regime, labeled X-UTPS. The inclusion of inner-shell electronic resonances and absorption edges in X-UTPS is expected to provide access to atomic site-specific information including local electronic dynamics within a molecule under conditions where other inner-shell techniques are less sensitive. Thus, X-UTPS will complement both linear and other nonlinear XUV- and X-ray spectroscopy techniques, with a particular emphasis on larger molecules and liquids.

Ultrafast Dynamics of Excited Electronic States in Nitrobenzene Measured by UTPS *(Weber, Slaughter)*

Recent Progress: We recently developed a NIR implementation of UTPS (Thurston *et al.* **2020** *Rev. Sci. Instrum.* 91, 053101) and demonstrated the capability of the technique to measure the 3rd-order nonlinear optical response of excited electronic states in liquid nitrobenzene. This application of the technique (see sketch in Fig. 2-2) uses one 780 nm femtosecond pump pulse to excite the liquid nitrobenzene sample to the first singlet excited electronic state by 2-NIR-photon absorption (pump), and a pair of 780 nm non-resonant femtosecond pulses (Kerr gate and probe) to detect changes in the 3rd-order nonlinear optical susceptibility. The Kerr gate induces a transient birefringence through the intensity dependent refractive index (χ^3), and the probe pulse interacts with this birefringence, resulting in a change in the polarization of the very same pulse. The OKE signal produced in this 4WM scheme is sensitive to the collective motion of electrons and nuclei, *i.e.* electronic and vibrational coherences. Phase matching between the Kerr gate and probe pulses produces the OKE signal colinear with the probe pulse. The polarization of the probe and signal are orthogonal, and hence they can be well separated using polarizing optics.

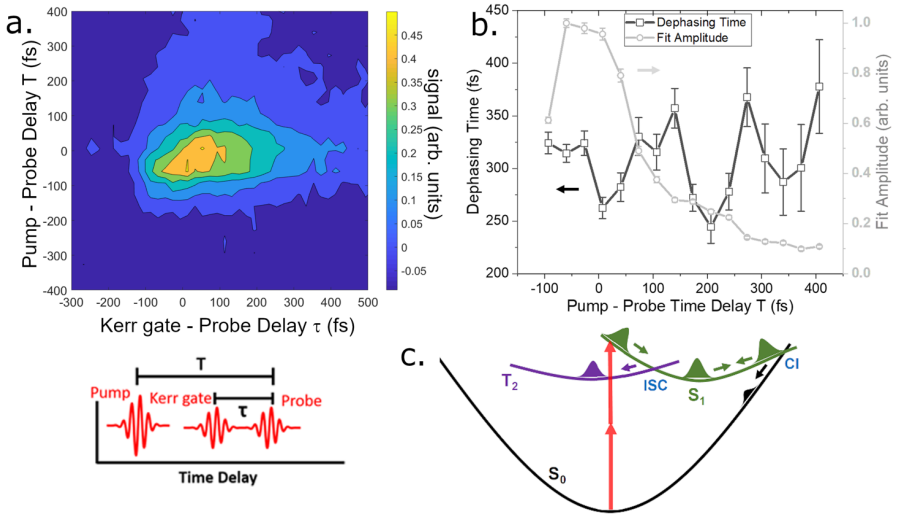

Fig. 2-2. (a) Measured 2D time-resolved UTPS spectrum of nitrobenzene after excitation to the S_1 state by two 1.6 eV photons from the NIR pump pulse. Explanation of pump-probe delay *T* and Kerr gate-probe delay *τ*. (b) Amplitude and dephasing times for the S_1 excited state wavepacket, extracted from exponential fits of the 2D data for each pump-probe delay *T*. (c) Nitrobenzene, following photoexcitation to S_1, decays to the ground electronic state via two pathways: a conical intersection (CI) with the ground electronic state S_0, or intersystem crossing (ISC) to the triplet manifold (T_2), followed by another ISC (not shown) to S_0.

Dynamics of excited liquid nitrobenzene (Thurston *et al.* **2020** *J. Phys. Chem. A* 124, 2573–2579) is probed within the first few hundred femtoseconds following 2-NIR-photon excitation at 780 nm. The excitation by two NIR photons in the pump pulse creates a wavepacket in the S_1 state that undergoes nonradiative decay via two competing pathways involving either a conical intersection

(CI) with S_0 or intersystem crossing (ISC) with T_2. Fig. 2-2a shows the time-dependence of the measured 3rd-order response for delays T between pump and probe and delays τ between the Kerr gate and the probe pulse (see timing sketch in Fig. 2-2a). The pump-probe signal decays in a little more than T=300 fs after excitation to S_1. The Kerr gate-probe delay τ-dependence measures a different decay that is due to dephasing of the initially coherent wavepacket on the excited electronic state. Dephasing can be caused by decoherence, which is induced by coupling between two or more vibrational or dissociative degrees of freedom. Fitting a single exponential to these decay times for each value of the pump-probe delay T, we extract the dephasing times, shown in Fig. 2-2b. The dephasing times oscillate in T with a period of 185 fs, which we associate with a response to periodic motion on the S_1 state, as the nuclear wavepacket spreads on the S_1 potential energy surface and decays through a CI to S_0, or by ISC to T_2 (Fig. 2-2c). In collaboration with LBNL theorist Liang Tan (Molecular Foundry) we have employed the sum-over-states method to calculate relative values of the effective 3rd-order response $\chi^{(3)}_{eff}$ for the S_1 and T_2 excited states and the S_0 ground electronic state for the relevant geometries identified in previous electronic structure calculations (Giussani *et al.* **2017** *J. Chem. Theory. Comput.* 13, 2777–2788). Importantly, we found that $\chi^{(3)}_{eff}$ is unique for each electronic state, even for the degeneracies at the CI and ISC geometries (Fig. 2-2c). This work demonstrates the sensitivity of UTPS to femtosecond dynamics on excited electronic states, and the potential for UTPS to resolve dynamics involving two or more electronic states, even near geometries where the states are degenerate.

Future Plans: Current and near-future efforts are directed at bringing UTPS to the XUV regime. The first experiments employing XUV pulses will establish a simple 2-pulse scheme, where the 2-color OKE will be investigated for N_2 in a femtosecond 4WM experiment. This will allow us to develop and test the essential instrumentation on previously-investigated dynamics (Warrick *et al.* **2018** *Faraday Discuss.* 212, 157–174) of excited bright ungerade and dark gerade electronic states in N_2, by 2-color NIR + XUV 4WM, while working towards future X-UTPS experiments. A new experimental setup is under development for the existing 1 kHz XUV HHG beamline.

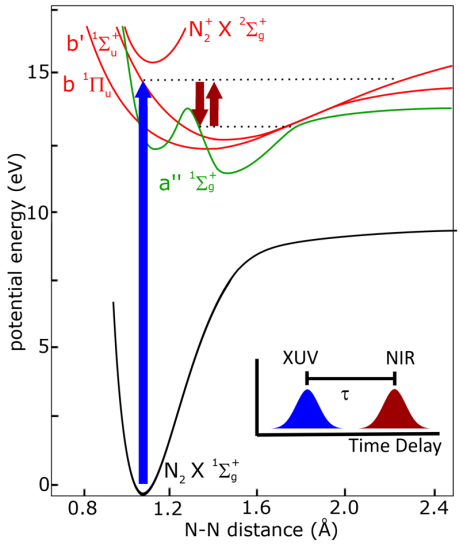

Fig. 2-3. A 14 eV pulse pump initiates a wavepacket on the b $^1\Pi_u$, b′ $^1\Sigma_u^+$, c $^1\Pi_u$, and c′ $^1\Sigma_u^+$ excited electronic states (c and c' states not shown). The interaction with the NIR pulse, which has a variable delay τ, produces a four-wave mixing signal in the probe direction due to the OKE. The signal will be sensitive to electronic states resonant with the NIR pulse, such as the a″ $^1\Sigma_g^+$ dark state.

A resonant 14 eV XUV pulse (~20 fs duration) and a NIR pulse (~40 fs duration) will be focused in a noncolinear geometry into a windowless gas cell containing N_2. The cell is housed in a vacuum endstation connected to the existing XUV beamline. The linear polarization of the NIR pulse is tilted by 45°, using a half-wave plate, relative to the linear XUV polarization. When the NIR pulse is scanned a few femtoseconds before or after the XUV pulse, we will measure OKE signals emitted in the same direction as the XUV pulse, carrying information on the dynamic coupling between the ground electronic state, the b $^1\Pi_u$, b′ $^1\Sigma_u^+$, c $^1\Pi_u$, as well as the c′ $^1\Sigma_u^+$ XUV-excited electronic states, and the a″ $^1\Sigma_g^+$ dark state, in 2-NIR-photon down-up (V) transitions (see Fig. 2-3, c and c' states not shown to avoid congestion). Dynamics involving higher lying Rydberg states may also be observed due to up-down (Λ) 2-NIR-photon transitions from the XUV excited state. The XUV + NIR 4WM signal,

arising from the OKE, will be emitted in the XUV propagation direction with the polarization orthogonal to the probe pulse. The signal spectrum will be analyzed as a function of time delay τ between the XUV and NIR pulses using a rotatable multi-mirror broadband XUV polarizer (Yang *et al.* **2007** *J. Appl. Phys.* 101, 053114) and an XUV spectrometer.

Extending UTPS to XUV probe photon energies is very demanding. Multiple efforts are currently underway to address several experimental and theoretical challenges. To analyze the polarization of the XUV signal, a reflective polarizer, based on existing designs of multiple reflections from metallic or multilayer mirrors, will be deployed to enable high transmission > 5% and high extinction ratios > 95% for 8-40 eV photon energies (Yang *et al.* **2007** *J. Appl. Phys.* 101, 053114). The existing XUV spectrometer and a new high-sensitivity CCD camera will enable the polarization-dependent UTPS spectrum to be detected and analyzed. With guidance from the LBNL AMOS PIs McCurdy, Lucchese, and Head-Gordon, we will use existing electronic structure codes, such as the Dalton package, to calculate the resonant and non-resonant 3rd-order response of small molecules. Further development of the sum-over-states theory and computational methods will also be achieved in collaboration with LBNL theorist Liang Tan (Molecular Foundry) to determine the frequency and molecular structure-dependence of the non-resonant 3rd-order optical response in more complex molecules.

Time-Resolved X-ray Photoelectron Spectroscopy Studies of Interfacial Energy- and Charge-Transfer Processes in Heterogeneous Light-Harvesting Systems *(Gessner)*

In this effort, time-resolved X-ray photoelectron spectroscopy (TRXPS) techniques are developed and applied to unravel fundamental processes underlying the conversion of photon energy into mobile charges and chemical transformations using heterogeneous light harvesting systems. Studies encompass photoinduced charge dynamics at molecule-semiconductor interfaces, energy- and charge-transfer in organic heterojunctions, as well as photodynamics in nanoplasmonic light harvesters. Synchrotron-based picosecond TRXPS studies are complemented by campaigns at X-ray Free Electron Lasers (XFELs) to access the femtosecond regime.

Recent Progress: As the demand for renewable energy technologies grows, so does the need for a deeper understanding of the fundamental processes underlying the photovoltaic and photocatalytic efficiencies of emerging solar light-harvesting concepts. A particularly prominent system is comprised of the wide bandgap semiconductor TiO_2, sensitized with Au nanoparticles (NPs). While TiO_2 exhibits promising photocatalytic properties, it is unfortunately poorly suited to absorb visible light due to its large bandgap. Sensitization with AuNPs provides a solution, with absorption due to localized surface plasmon resonances readily tunable across a significant fraction of the solar spectrum, by using NPs of

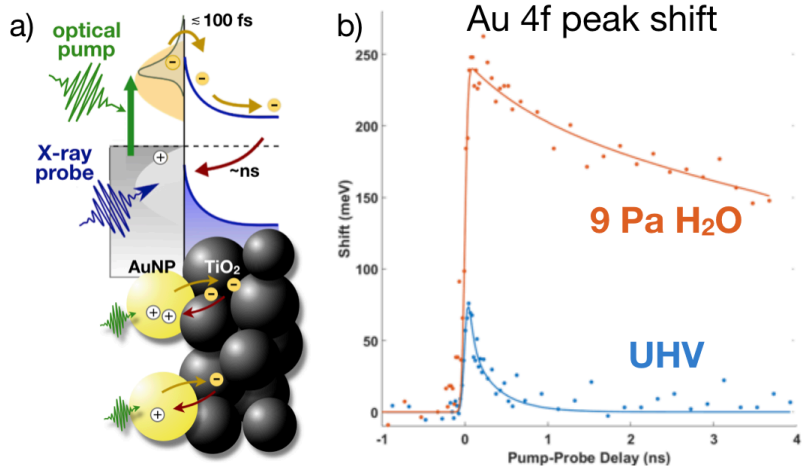

Fig. 2-4. Feasibility test of ambient pressure TRXPS. a) Concept of optical-pump/X-ray-probe TRXPS experiment of photoinduced charge transfer in AuNP sensitized TiO_2. b) Time dependent shift of the Au 4f photolines under both UHV (blue) and water vapor enriched (orange) environments.

different sizes. AuNPs can also act as catalytic reaction centers, for example, during photoelectrochemical (PEC) water splitting to produce hydrogen. Following the successful application of picosecond TRXPS to monitor and quantify photoinduced charge transfer dynamics in AuNP-sensitized, nanoporous TiO_2 substrates (Borgwardt *et al.* **2020** *J. Phys. Chem. Lett.* 11, 5476–5481), first steps have been undertaken to extend the application of TRXPS toward more realistic, application-inspired sample conditions. Fig. 2-4a outlines the concept of the optical-pump/X-ray-probe TRXPS experiment: a visible pump pulse tuned to the plasmon resonance of the AuNPs initiates charge-injection dynamics, which are monitored by recording XPS spectra of time-delayed X-ray pulses. Fig. 2-4b compares the time-dependent peak shifts of the Au 4f doublet recorded under UHV conditions (blue) and with 9 Pa of water vapor present in the experimental chamber (orange). Large differences in the Au 4f photoresponses are readily apparent. Both the maximum shift and the relaxation timescales differ significantly for wet and dry interfacial conditions. These preliminary results suggest that adsorbed and/or reactive species may play an important role for interfacial charge dynamics in nanoplasmonic light harvesting systems, strongly supporting the need for experiments under *in situ* conditions to capture electronic dynamics underlying the chemical function of the interface.

A combination of picosecond TRXPS, UV-photoemission spectroscopy, and optical absorption spectroscopy is used to gain detailed spatiotemporal insight into photoinduced charge populations, band structures, and electric fields at the interface between a nanocrystalline ZnO substrate and adsorbed N3 dye molecules. Detailed modeling of transient shifts in chromophore (C1s/Ru3d) and electron acceptor (Zn3d) associated photolines is underway to gain access to delayed charge injection from interfacial trap states, photoinduced interfacial electric fields, and a detailed picture of the spatiotemporal evolution of the space charge layer within the semiconductor electrode.

A femtosecond TRXPS experiment at the FLASH Free Electron Laser provides unprecedented, real-time insight into photo-induced charge generation in an organic light-harvesting system by dissociation of interfacial charge-transfer states in a planar heterojunction formed by a copper-phthalocyanine (CuPc) chromophore/donor domain and a C_{60} electron acceptor phase. The study complements previous picosecond TRXPS experiments on the same system, which revealed a surprisingly high efficiency of charge generation from energetically low-lying triplet excitons (Roth *et al.* **2019** *Phys. Rev. B* 99, 020303(R)). The latest femtosecond time-resolved experiment lends further support to the emerging concept of charge generation from energetically disfavored interfacial charge-transfer excitons and directly determines the exciton dissociation efficiency (Roth *et al.* **2020** *Nat. Commun. submitted*, arXiv:2009.08745).

Future Plans: A self-consistent model to describe all available steady-state and time-resolved data on the interfacial band structure and photoinduced dynamics in the N3-ZnO system will be completed. The goal is to provide a comprehensive description of the entire electron-injection/charge recombination cycle with picosecond temporal resolution and sub-nm spatial sensitivity to interfacial band structures.

TRXPS studies of photoinduced charge transfer in nanoplasmonic light harvesting systems will be extended in two directions, higher temporal resolution and *in situ* conditions for interfacial chemistry. A recently submitted proposal for experimental time at FLASH has been shortlisted for potential beamtime in 2021. The experiment aims to provide a better understanding of the mechanism by which plasmonic excitations couple to charge-transfer and, ultimately, charge-separated configurations on femtosecond timescales. At the Advanced Light Source (ALS), a proposal to conduct near ambient-pressure TRXPS studies of photoinduced charge transfer and chemical dynamics in water-covered AuNP-TiO_2 has received an excellent ranking, which will hopefully result in experiments in 2021 upon further recovery of more extended user operation at the ALS.

Dynamics in Helium Nanodroplets *(Gessner, Neumark)*

This effort combines laboratory-based, HHG-driven experiments and XFEL-based campaigns to gain deeper insight into ground- and excited-state dynamics in pure and doped helium nanodroplets. Owing to the relatively simple electronic structure of He atoms, pure droplets are particularly well suited to test our understanding of the emergence of collective electronic properties and associated dynamics in complex systems from their atomic constituents. Weak-field excitations in neutral droplets are studied by HHG-enabled femtosecond time-resolved photoelectron imaging, strong-field and X-ray-induced high-charge configurations by single-pulse X-ray coherent scattering and ion spectroscopy at XFELs. The XFEL based techniques are also used to study highly quantum-enabled and collective ground-state phenomena.

Recent Progress: Laboratory-based efforts were severely hampered by a combination of facilities failures, public safety power shutoff (PSPS) events, laser failures, and COVID-19 induced shelter-in-place orders. Nevertheless, significant progress has been made to achieve an XUV pump resonant with the main absorption feature of the helium droplets, which is the prime target of the next series of experiments. With the recent reopening of LBNL, work is underway to resume the status of the apparatus prior to the shutdown, and to proceed with experiments to monitor energy- and charge-transfer in highly excited, doped nanodroplets.

Coherent X-ray scattering studies at the LCLS elucidated the mechanisms by which fast rotating superfluids approach the behavior of classical rigid-body rotors (O'Connell *et al.* **2020** *Phys. Rev. Lett.* 124, 215301), as well as the impact of the superfluid vs normal fluid nature of ^{4}He and ^{3}He, respectively, on droplet hydrodynamics (Verma *et al.* **2020** *Phys. Rev. B* 102, 014504). Most recently, activities were extended to studies at the European XFEL (EuXFEL) in Hamburg. Due to COVID-19 restrictions, the campaign was conducted almost entirely through remote access from the U.S., Austria, Switzerland, and Germany, the first beamtime of its kind at this facility. The experiment at the SQS instrument aims to study equilibrium distributions of surface charges on highly charged helium nanodroplets by ultrafast coherent diffractive imaging (CDI). Charges are being tracked by Xe dopant clusters. Several hundred CDI images were recorded under various charge and doping conditions. The analysis is ongoing.

An LCLS experimental campaign on pure and xenon doped helium droplets aims to gain deeper insight into the charging and relaxation dynamics of atomic clusters exposed to intense X-ray pulses. The combination of single-pulse X-ray diffraction patterns and ion time-of-flight (TOF) spectra, recorded in coincidence, provides significantly better-defined experimental conditions compared to conventional, cluster ensemble- and X-ray intensity-averaged studies. From each scattering image, the droplet size and the number of X-ray photons incident on the particular droplet are derived, while ion TOF spectra provide information on energy buildup and release in the droplets. The combined information gives access to the degree of charging of individual droplets and the degree of inner- versus outer-ionization during the pulse-droplet interaction. Fig. 2-5 shows ion TOF spectra sorted horizontally by the original cluster size and vertically by the number of trapped electrons normalized to the number of cluster atoms. As the number of trapped electrons in the droplet increases, there is a marked decrease in the presence of weakly bound He_n^+ clusters, and as the number of trapped electrons further increases, He^+ and He_2^+ increase in intensity and width, indicating a marked increase in initial ion kinetic energy. This study of ion TOF spectra allows us to study the transition from a weakly ionized cluster to a plasma with a trapping potential, and to explore Coulomb explosion dynamics. Note that a conventional ion TOF experiment would average over all spectra shown in Fig. 2-5, considerably reducing the amount of information that may be gained.

Future Plans: Analysis of the pure droplet data on intense X-ray induced ionization dynamics will be extended to those from xenon-doped droplets. The experiment was conducted at 840 eV, a photon

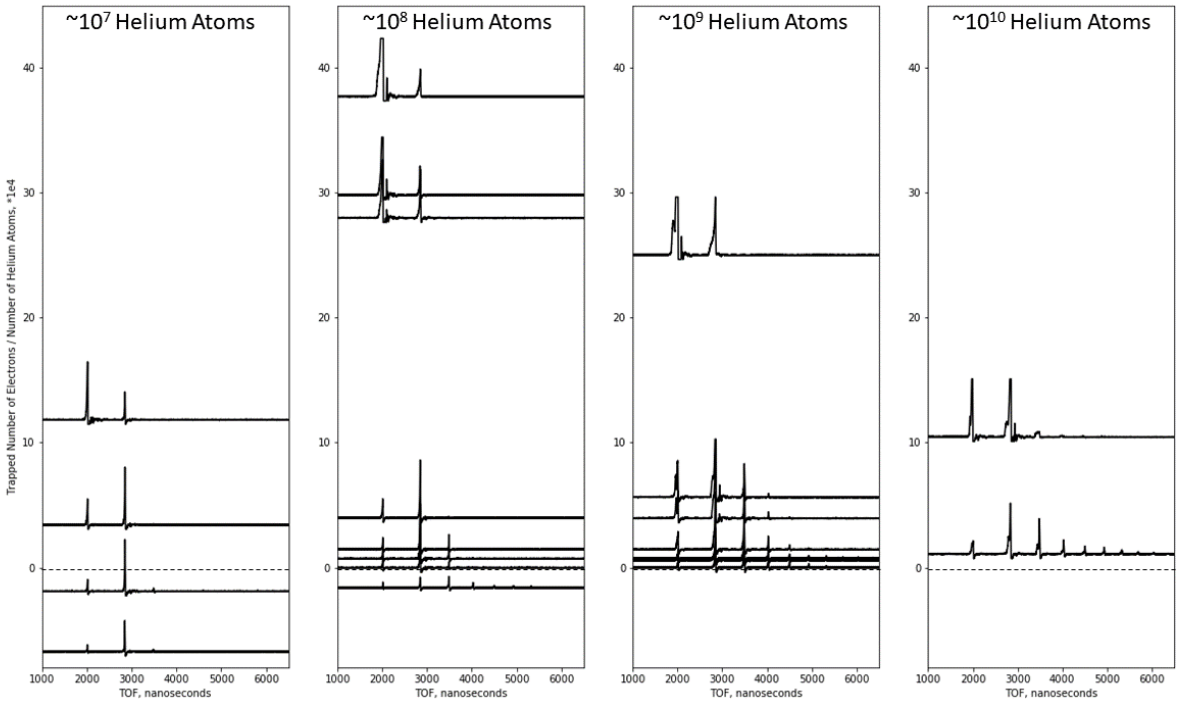

Fig. 2-5. Coincident TOF-CDI experiment on cluster charging in intense X-ray fields: Droplet ion TOF spectra are vertically sorted by the number of trapped electrons, normalized to the number of helium atoms. The dashed line corresponds to the transition from outer- to inner-ionization, i.e., the point at which enough ionized electrons have left the cluster such that the cluster Coulomb potential prevents any other ionized electrons from leaving the cluster. The panels correspond to different droplet size regimes as indicated. Conventional ion TOF spectroscopy averages over all spectra shown in all panels.

energy at which the Xe dopant absorbs much stronger than the helium host. Initial analysis of xenon doped droplets yields different underlying physics in contrast with pure droplets. Ultimately, the understanding gained from single-pulse X-ray interactions with pure and doped helium droplets will be employed to disentangle the ultrafast dynamics induced in an X-ray-pump/X-ray-probe scheme that was applied during an LCLS experiment. Laboratory-based HHG-driven experiments will be resumed as soon as possible.

Subtask 3: First-Principles Theory of Dynamics and Electronic Structure

M. Head-Gordon, C. W. McCurdy, R. R. Lucchese, T. N. Rescigno

Simultaneous Treatment of Short Pulse Ionization and Nuclear Motion *(Lucchese, McCurdy)*

Recent Progress: We have demonstrated a new capability for treating electronic excitation and short pulse ionization simultaneously with nuclear motion that is based on the correlated Schwinger variational method for photoionization developed by Lucchese and coworkers. Ionizing probe pulses in femtosecond and attosecond scale experiments produce photoelectrons and, in many cases, atomic ions resulting from dissociation of the resulting molecular cation. Calculations treating electronic excitation and nuclear motion simultaneously require accurate calculation of dipole coupling amplitudes between the electronic states as well as between bound electronic states and the photoionization continuum. The nuclear dynamics are seen only through the lens of the photoionization process, whose description requires accurate, correlated theoretical methods. The numerical Schwinger variational codes of the LBNL AMOS group give us a near-unique capability to compute accurate photoionization amplitudes including high-level treatments of correlation both in the target

and ionization continuum for small systems. Using those couplings in a calculation that propagates wave packets on the potential curves for the electronic states of the molecule and the ion that are coupled by the pulses (currently in one dimension), we have demonstrated in *ab initio* calculations on the lithium hydride molecule how the pump/probe delay dependence of the photoelectron spectrum, the MFPAD, and the kinetic energy release into $Li + H^+$ dissociation reveal the details of nuclear motion on the intermediate bound electronic states of LiH. All the features of the time dependence of the KER in Fig. 3-1 have been explained. A manuscript describing the new methodology and these results has been submitted.

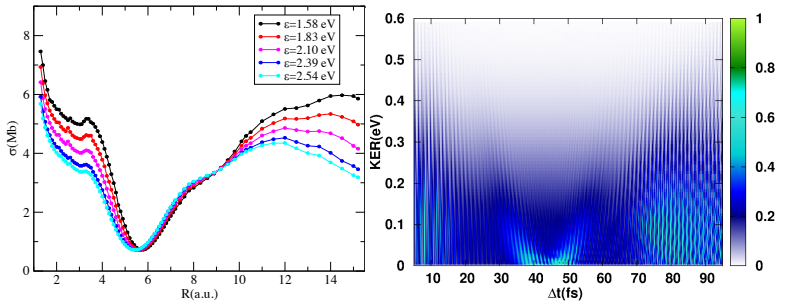

Fig. 3-1. Left: Total photoionization cross section of LiH as a function of internuclear distance from 5 state Schwinger variational close-coupling calculations for different photoelectron energies showing persistent minimum near six Bohr. Right: Kinetic energy release (KER) of $Li + H^+$ integrated over photoelectron energy for 400 nm, 5 fs probe and pump pulses as a function of delay. As the wave packet crosses the region near 6 Bohr, the dissociative ionization signal nearly disappears.

Future Plans: This capability was developed for application to other diatomic and linear systems accessible to laser-based momentum-imaging experiments at LBNL. We will explore new pump/probe experiments with N_2, O_2, CO and CO_2, which are accurately described by the numerical Schwinger method, and predict the signatures of their nonadiabatically coupled excited state dynamics in photoionization and dissociative photoionization in preparation for joint experimental and theoretical ultrafast studies at LBNL.

Coupled Nuclear-Electronic Dynamics in O_2 Inner-Valence Excited States Based on the Numerical Schwinger Method and the Local Complex Potential Model *(Lucchese, McCurdy)*

Recent Progress: In four-wave mixing experiments in the AMOS program at LBNL, Dan Neumark and Steve Leone have measured the lifetimes of the two metastable vibrational states of the 3s σ_g Rydberg state of the series converging to the $c^4\Sigma_u^-$ state of O_2^+. They applied transient wave-mixing spectroscopy with an attosecond XUV pulse to measure the lifetime of these states. Lifetimes of 5.8±0.5 fs and 4.5±0.7 fs are determined for the v = 0 and v = 1 states, respectively. These states can both autoionize and dissociate by tunneling, for which the lifetimes for the corresponding ion vibrational state are computed as 16 ps and 170 fs respectively. The LBNL experiment raises the question of what causes the difference in the observed lifetimes. A single tunneling width in the

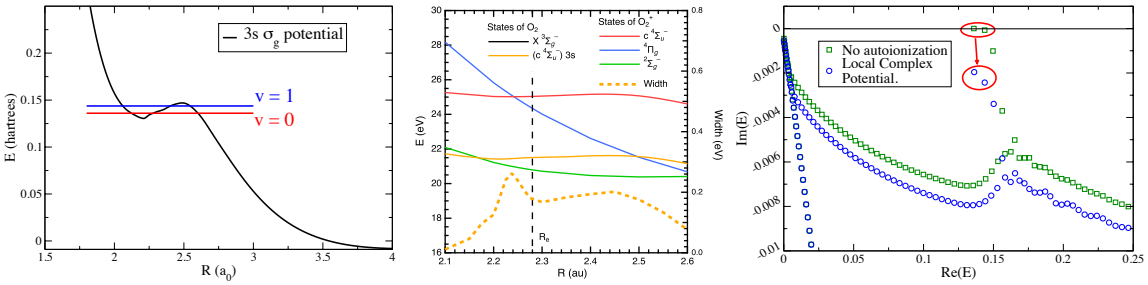

Fig. 3-2. Left: Real part of the potential curve of the 3s σ_g Rydberg state of the series converging to the $c^4\Sigma_u^-$ state of O_2^+. Middle: Schwinger 8-channel calculation of autoionization width as a function of internuclear distance, showing the O_2^+ ionization thresholds crossing the autoionizing 3s σ_g Rydberg state. Right: Exterior scaling calculation of complex resonance energies including dynamical coupling of vibration and autoionization (circled blue points are metastable state energies).

usual sum of partial widths for the two processes, $\Gamma = \Gamma_{\mathrm{autoion}} + \Gamma_{\mathrm{tunnel}}$, cannot reproduce the observed lifetimes if they both have the same contribution from autoionization, $\Gamma_{\mathrm{autoion}}$. We performed eight-channel close-coupling calculations using the numerical Schwinger method over the range of internuclear distances involved in these dynamics, and fit a Fano profile to the autoionizing feature in the photoionization cross section to calculate both the width and position of the 3s σ_g Rydberg state as a function of internuclear distance, shown in Fig. 3-2. Using those data, we then calculated the lifetimes in the local complex potential model, $V(R) = E_{\mathrm{res}}(R) - i\Gamma(R)/2$, used previously at LBNL to describe dissociative attachment. That model handles decay due to autoionization, but not tunneling dissociation. However, solving the resulting Schrödinger equation with exterior complex scaling treats both dissociative nuclear motion and ionization and allowed the calculation of the total lifetime with dynamical coupling of the two decay mechanisms. Total lifetimes of 6.2 fs and 5 fs were found for the two vibrational states, within the error bars of the measurement. The total lifetimes were found to be extremely sensitive to tiny shifts of the potentials, revealing that the sampling of the R-dependent lifetimes by the vibrational wave functions provides a mechanism for the coupling of vibration and autoionization. A manuscript is in preparation.

Double Photoionization of Water by One Photon *(McCurdy, Lucchese, Rescigno)*

Recent Progress: We are continuing a major effort to calculate and observe the angular dependence in the body frame of one-photon double photoionization of water. This will be the first such observation and *ab initio* calculation of this process for a polyatomic molecule. In the first set of experiments we reported (Streeter *et al.* **2018** *Phys. Rev. A* 98, 053429 and Reedy *et al.* **2018** *Phys. Rev. A* 98**,** 053430), we suggested a two-step process, in which states of the OH^+ cation are produced that are then predissociated by spin-orbit coupling to another state. We simulated that two-step process completely and identified the two dynamical pathways responsible for it. The original experimental data has been reanalyzed by the Kansas State group led by Itzik Ben-Itzhak using the "native frames" method, which detects the presence of sequential processes in a COLTRIMS experiment, and a joint manuscript is in preparation.

Future Plans: We are making multiple improvements to the computational algorithms we previously applied to double photoionization of H_2 to make it possible to solve this challenging problem. New coincidence data has been taken at the ALS from which the TDCS will be extracted, and these comparisons will be the first of their kind on a polyatomic molecule. This work is being done in collaboration with Prof. Frank Yip (California State University, Maritime), who has participated in the visiting faculty program (VFP) at LBNL in recent summers. A new propagation technique and a novel method for extracting the double photoionization probabilities from the two-electron wave packet are being tested.

Two-Photon Ionization in Molecules *(Lucchese, Rescigno, McCurdy)*

Recent Progress: To support experimental work at LBNL that uses an HHG-based high-power VUV light source and coincidence particle detection, we have developed tools that allow us to compute two-photon ionization processes within a weak field approximation, including photoelectron asymmetry parameters and the positions and lifetimes of Rydberg autoionizing states. Using the Schwinger variational method, the first application was the resonant two-photon excitation of O_2 leading to ion pair production (Larsen *et al.* **2020** *J. Chem. Phys.* 153, 021103) with a second manuscript on the two-photon ionization of N_2 in preparation. For these systems, the first photon does not have enough energy to ionize the system, so that it is possible to treat the intermediate state using a sum of discrete states, which can be extended into the continuum without the necessity of treating field-induced continuum-continuum coupling.

Future Plans: We will extend the Schwinger variational codes for linear molecule photoionization to allow for the efficient computation of photoionization from many intermediate states. The intermediate states will be obtained by diagonalizing the coupled-channel Hamiltonian that is used in the scattering calculation, using a basis set composed of Gaussian type functions in each channel. It will be possible to complete these calculations with an effort that will be comparable to that of a scattering calculation and will not depend on the number of intermediate states for which dipole transition matrix elements to the ionized states are needed.

Validity of the Static Exchange in Core Ionization *(Lucchese, Rescigno, McCurdy)*

Recent Progress: RFPADs from core ionization of molecules containing symmetry equivalent atoms can probe the relative rates of Auger decay and fragmentation compared to the rate of hopping of the vacancy between the equivalent atoms. If the molecule fragments rapidly so that the atomic ion emitted corresponds to the ion where the hole was initially located, then one can obtain a good representation of the RFPAD by a calculation where just one localized hole state is considered. We found that (Marante *et al.* **2020** *Phys. Rev. A* 102, 012815), for a system such as the F 1*s* ionization in CF_4, the fully coupled channel calculation with delocalized hole states yielded the same RFPAD as when the hole states were transformed to the equivalent four local hole states. We additionally found that in the localized hole basis, channel coupling was negligible, in contrast to the delocalized hole representation.

Core-Hole Localization in CCl_4 *(Lucchese, Rescigno, McCurdy)*

Recent Progress: Our study of F K-edge ionization in CF_4 (McCurdy *et al*. **2017** *Phys. Rev. A* 95, 011401(R)) showed unambiguous evidence of hole localization. LBNL experiments at the ALS on CCl_4 found that ionization from the Cl 2p orbital, but not from the 2s orbital, results in fragmentation to the two-body $CCl_3^+ + Cl^+$ channel following Auger decay, allowing COLTRIMS measurements in the recoil frame. The question is whether those distributions show a similar signature of core hole localization that we saw in CF_4. Our preliminary close-coupling calculations using the complex Kohn method were plagued by lack of convergence and extreme sensitivity to the Gaussian and Coulomb function basis sets employed. Two recent developments from work done in collaboration with Prof. Cynthia Trevisan of Cal State Maritime have helped solve these problems. Using an extension of the effect of hole localization on the channel coupling discussed above, in the case of Cl 2p ionization in CCl_4, we have been able to reduce the number of coupled channels from 12, the total number of Cl 2p orbitals, to 3, the number of 2p orbitals on one Cl, by localizing the hole state on one center. The problem of basis set dependence was solved by carrying out single-channel calculations using both the basis set Kohn method and our recently developed overset grid-based Kohn method, which can produce fully converged benchmark results. We discovered that standard contracted Gaussian basis sets do not have the flexibility needed to describe ionization from core orbitals in heavier atoms, but that suitable addition of uncontracted tight orbitals in the scattering basis, coupled with high partial-wave continuum functions, are critical in achieving numerical convergence. Fig. 3-3

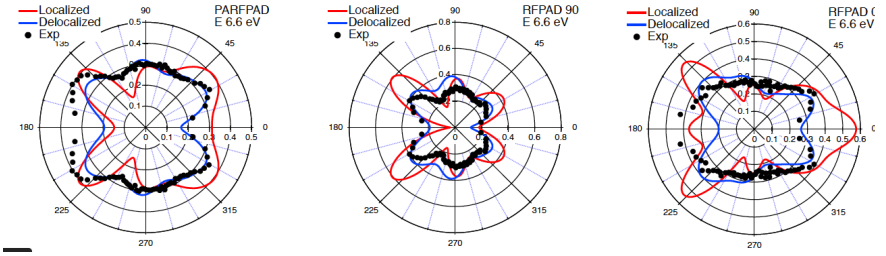

Fig. 3-3. RFPADs for Cl 2p ionization in CCl_4 at 6.6 eV photoelectron energy. Experiment is compared with theoretical calculations using both localized and delocalized core-holes. Right: photon polarization parallel to dissociation axis; center: polarization perpendicular to dissociation axis; left: results integrated over all polarization directions.

compares our most recent calculations with experiment at a photoelectron energy of 6.6 eV. We show RFPADs for Cl 2p ionization with photon polarization both parallel and perpendicular to the axis of dissociation, as well as integrated over all directions. For the localized calculations, we place a vacancy on the dissociating chlorine and couple the $2p_x$, $2p_y$ and $2p_z$ channels, while for the delocalized calculations we keep the same dissociation axis but place the vacancy on each of the other symmetry equivalent chlorines and sum the cross sections incoherently. We find, in stark contrast to CF_4, that the delocalized hole calculations give the best agreement with experiment.

Future Plans: Additional electronic structure calculations will be needed to clarify why hole localization is evidently less dominant in CCl_4 than in CF_4. In addition, we will examine whether spin-orbit coupling, which is significant in Cl 2p ionization and which was not considered in our calculations, can modify the results.

Development of the Overset Grid Scattering Code *(Lucchese, Rescigno, McCurdy)*

Recent Progress: After successfully completing the implementation of the overset-grid method to molecular photoionization (Marante *et al.* **2020** *Phys. Rev. A* 102, 012815), we have applied this code to the CCl_4 Cl 2*p* ionization problem as discussed above. In addition, we have begun to implement a new method based on the overset grid where we use a global spectral representation based on the discrete variable representation in a product basis of radial and angular basis functions. This will remove the artificially high partial-wave expansion needed to accurately describe the switching functions used in the previous implementation.

Future Plans: Based on the global spectral representation, we will extend the overset-grid code to treat multi-channel calculations, initially using a single-configuration representation of the target states. This will allow for applications to problems of core ionization for p-shells where at least a three-channel approximation is needed even with the decoupling obtained by using the localized hole representation.

Shape Resonance in NO Photoionization and Time Delays *(Lucchese)*

Recent Progress: In attosecond experiments on the photoemission from molecules, the time delay associated with the emission can be characterized by the energy derivative of the phase of the photoionization dipole amplitude (PDA). Of particular current interest is the dependence of such phases and derivatives in the molecular frame. With dissociative photoionization it is now possible to obtain such information experimentally in a one-photon experiment where the phase of the PDA in one direction can be referenced to that in a different direction. In the case of a resonant process, such as a shape resonance, the reference phase can be taken to be from photoemission in a non-resonant symmetry. We have considered the case of the dissociative photoionization of NO leading to the $c\ ^3\Pi$ state of NO^+, which has a σ^* shape resonance. Applying a multi-channel form of the Fano resonance line-shape formalism to photoionization results from the Schwinger variational code, it is possible to separate the resonant and non-resonant contributions to the PDA, as shown in Fig. 3-4. Through an analysis of the resulting phases and their energy derivatives, we found photoemission time

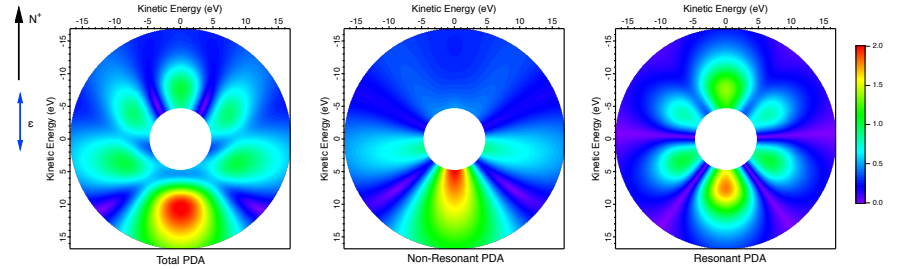

Fig. 3-4. Decomposition of the magnitude of the PDA for the ionization of NO to the $c\ ^3\Pi$ state of NO^+, as a function of photoelectron emission direction (N+ emitted in the upward vertical direction) and photoelectron energy in eV. The polarization is also in the vertical direction in the plots.

delays of the resonant contribution of 237 as that, when modulated by interference with the non-resonant scattering, leads to total emission delays of +295 as to -446 as, depending on the direction of emission and photoelectron kinetic energy. A manuscript is in preparation discussing these results with a comparison to experimental data of D. Dowek, University of Paris.

Dissociative Attachment of Electrons to Formic Acid and Formamide *(Rescigno, McCurdy, Lucchese)*

Recent Progress: Together with Prof. Cynthia Trevisan of Cal State Maritime, who has participated in the Berkeley Lab Undergraduate Faculty Fellowship (BLUFF) program in recent summers, we have completed an extensive theoretical study of dissociative attachment to formic acid (HCOOH). We have identified several doubly-excited (Feshbach) anion states that are responsible for H^- production in the 6-9 eV electron energy range. The lowest of these ($^2A'$) can produce H^- by either CH or OH break. A second resonance ($^2A''$) can produce H^- plus an excited formyloxyl radical (HCOO•). We have also determined that a higher resonance of $^2A'$ symmetry, though not directly accessible in the 6-9 eV range, can be accessed through a conical intersection with the lowest $^2A'$ resonance and produce another excited formyloxyl radical. A joint experimental/theoretical study detailing these findings was published in PCCP (Slaughter *et al.* **2020** *Phys. Chem. Chem. Phys.* 22, 13893).

Dissociative electron attachment to the formamide molecule, $HCONH_2$, is expected to proceed by mechanisms similar to those we studied in the case of formic acid and indeed, our recent theoretical studies have shown this to be the case. Our findings contrast sharply with a recent study (Li *et al.* **2019** *Phys. Rev. Lett.* 122, 073002), which proposed a dipole-assisted resonance mechanism for DEA to formamide, where the incident electron promotes an electron in an occupied orbital to an unoccupied valence orbital before being itself captured into a diffuse dipole-bound state. NH_2^- anions from DEA are observed to be formed in a 5.3-6.8 eV energy range. We find two Feshbach resonances in this range of $^2A'$ and $^2A''$ symmetry, respectively. The calculated angular distributions we find for these resonances are compared with experiment (see discussion in Subtask 1) in Fig. 3-5. As the electron energy is increased from 5.3 to 6.8 eV, the ion angular distributions change from mostly isotropic to peaked at about 105°. The latter behavior is well described by the $^2A''$ entrance amplitude, calculated assuming axial recoil. On the other hand, the distributions computed using the $^2A'$ resonance assuming axial recoil bear little resemblance to observations, although under a rotation of the recoil axis by 30° we get a more isotropic distribution closer to what is observed at lower energies. This argues for two overlapping resonances, one leading to prompt dissociation, well described assuming axial recoil, the other pointing to an internal geometric change of the anion prior to dissociation. Our joint experimental/theoretical study has been accepted for publication in *Phys. Rev. Research*.

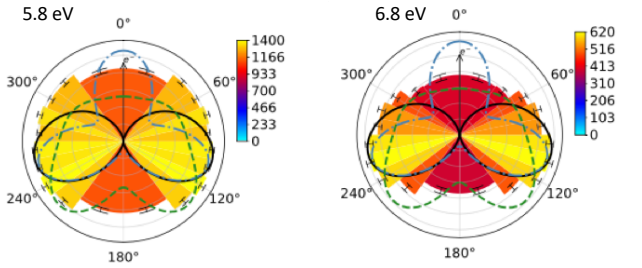

Fig. 3-5. NH2-/HCONH2 at 5.8 and 6.8 eV. Comparison of theory and experiment. Solid line: DEA via $^2A''$ resonance; dashed-dot line: DEA via $^2A'$ resonance, assuming axial recoil; dashed-line: DEA via $^2A'$ resonance with a 30° rotation toward larger O-C-N angles.

Future Plans: O- and H- from DEA to formamide are observed in the 10.0-11.5 eV electron energy range. We plan to look for doubly-excited states at these higher energies, but hasten to add that this energy range lies above the ionization energy of formamide, which makes the calculations quite challenging.

State-Targeting DFT for Excited States, Including Core Excitations *(Head-Gordon)*

Recent Progress: Many excited states of molecules can be quite well described using ground state DFT with a restricted open-shell Kohn-Sham (ROKS) framework. This includes states for which TDDFT fails to give reasonable results, like charge-transfer excited states, or as discussed below, core excitations. The ROKS energy is a minimum only for the lowest excited state; higher excited states are saddle points. We have therefore very recently developed a new algorithm (Hait *et al*. **2020** *J. Chem. Theory Comput.* 16, 1699−1710), that performs square gradient minimization (SGM) to reliably find the higher saddle points. SGM is proving to be robust and efficient (only 3 times the cost of a standard DFT calculation). This algorithm is the key to our recent breakthrough on accurately computing DFT core-excited states.

Using SGM, we have achieved a breakthrough in the accuracy that we can achieve for core excitation energies at low computational cost (Hait *et al*. **2020** *J. Phys. Chem. Lett.* 11, 775–786). We have shown that core excitations can be very accurately computed using ground state density functionals, by finding saddle points, rather than minima, of the restricted open shell DFT energy functional in orbital space. The modern SCAN and ωB97X-V functionals predict the K-edge of C, N, O, and F to an RMS error of ~0.3 eV (see Fig. 3-6). Equally good results are obtained for L-edge spectra of third row elements, when a perturbative spin−orbit correction is used. This high accuracy can be contrasted with normal TDDFT, which typically has > 10 eV error and requires translation of computed spectra to align with experiment. The new approach is computationally tractable (same scaling as ground-state DFT) and can be applied to geometry optimizations or even *ab initio* molecular dynamics of core-excited states. *It is hard to overstate the potential significance of this development for routine calculations of core-excited states*. The main limitation of the method is cases where there is essential configuration interaction between more than two determinants in the core excitation, which appears to be rare for species with singlet ground states.

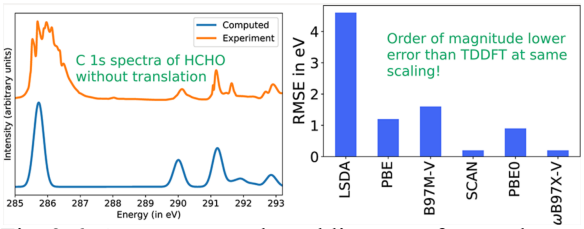

Fig. 3-6. A new approach enabling use of ground state DFT for core excited states can be remarkably accurate (e.g. SCAN, wB97X-V functionals, at right; unshifted spectra at left). This method finds saddle points of the restricted open shell Kohn-Sham (ROKS) energy, using the new SGM algorithm.

Future Plans: We are extending ROKS to treat excitations in radicals. This should enable us to also evaluate core level excitations (K shell for first row elements, also L shell for heavier elements) for open shell systems, potentially with accuracy as good as reported above. To date, we have included spin-orbit and relativistic corrections separate from our calculations, using atomic values. We are starting to think about direct inclusion of the spin-orbit terms. Additionally, the ROKS approach is ready for molecular chemical applications so we have initiated collaborations with the Leone and Gessner experimental groups on systems where they have recently obtained data.

State-Targeting Coupled Cluster Theory for Doubly Excited States, Including Double Core Hole States *(Head-Gordon)*

Recent Progress: We have revisited the idea of using the coupled-cluster (CC) ground state formalism to target excited states (Lee *et al*., **2019** *J. Chem. Phys.* 151, 214103). Our main focus was targeting doubly excited states and double core hole states. Typical equation-of-motion (EOM) approaches for obtaining these states struggle without higher-order excitations than doubles. We showed that by using a non-Aufbau determinant optimized via the maximum overlap method, the CC ground state solver can target higher energy states. Furthermore, just with singles and doubles (i.e., CCSD), we demonstrated that the accuracy of ΔCCSD and ΔCCSD(T) (triples) far surpasses

that of EOM-CCSD for doubly excited states. The accuracy of ΔCCSD(T) is nearly exact for doubly excited states considered in this work. An example is shown below in Fig. 3-7 for the lowest doubly excited state of formaldehyde, showing more than a 4 eV improvement over conventional EOM-CCSD. For double core hole states, we used an improved ansatz for greater numerical stability by freezing core hole orbitals. The improved methods, core valence separation (CVS)-ΔCCSD and CVS-ΔCCSD(T), were applied to the calculation of the double ionization potential of small molecules. Even without relativistic corrections, we observed qualitatively accurate results with CVS-ΔCCSD and CVS-ΔCCSD(T). The tools and intuition developed in this work may serve as a stepping stone toward directly targeting arbitrary excited states using ground state CC methods.

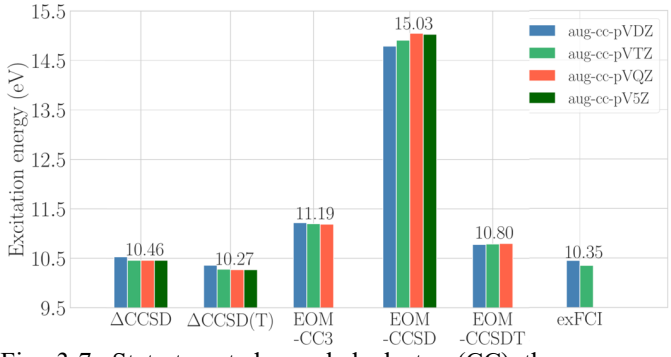

Fig. 3-7. State-targeted coupled cluster (CC) theory versus equation-of-motion (EOM)-CC calculations at the singles and doubles (SD) and triples (T) levels for the excitation energy from the ground state to the doubly excited state of formaldehyde, in various basis sets, versus the exact full configuration interaction (FCI) results. It is evident that ΔCCSD greatly outperforms EOM-CCSD, and even outperforms the much more costly EOM-CC3 and EOM-CCSDT methods, showing the value of the state-targeting approach.

Future Plans: Inspired by our success for double excitations, we intend to seek a generalization of the method to describe open shell singlet excited states. If successful, this will be a wavefunction counterpart to the ROKS methods discussed above.

Direct Targeting of Core-Excited States via Non-Orthogonal Single Excitation CI *(Head-Gordon)*

Recent Progress: The creation of a core hole either due to excitation or ionization leads to dramatic orbital relaxation effects such as contraction of the valence shell towards the core. While it is common to capture such effects through brute force approaches, a potentially more natural and economical framework is offered by non-orthogonal CI (NOCI) treatment. For this purpose, we have recently defined and implemented the non-orthogonal configuration interaction singles (NOCIS) method for calculating core-excited states of closed-shell molecules (Oosterbaan *et al*. **2018** *J. Chem. Phys.* 149, 044116). NOCIS is a black-box variant of NOCI (that in itself makes NOCIS a very rare variant of NOCI), which uses A different core-ionized determinants for a molecule with A atoms of a given element to form single substitutions. The use of core-ionized determinants permits natural inclusion of orbital relaxation effects. In addition, NOCIS has a number of other desirable properties: NOCIS is variational, spin-pure, size-consistent, and delivers multiple states. We have extended the NOCIS theory to doublet radicals, yielding promising results with an accuracy comparable to those obtained for closed shell ground states (Oosterbaan *et al.* **2019** *J. Chem. Theory Comput*. 15, 2966–2973). To obtain such accuracy required extra sets of optimized orbitals for the configuration(s) that promote from the core K-shell of interest to the half-occupied valence orbital. We observed that CI between determinants on a single atomic center is much stronger than CI between determinants on different centers, which motivated the development of a single center (1C) approximation to NOCIS that neglects the off-diagonal elements of the Hamiltonian (Oosterbaan *et al.* **2020** *Phys. Chem. Chem. Phys.* 22, 8182–8192). Interestingly, 1C-NOCIS for closed shell molecules reduces to the venerable static exchange approximation (STEX), while it is a natural generalization to core excitations of molecules in open shell states. With greatly improved computational efficiency, and the same accuracy, 1C-NOCIS is our preferred form of the theory for most purposes.

Future Plans: The main factor limiting the accuracy of 1C-NOCIS (and NOCIS itself) is its neglect of dynamical electron correlation (NOCIS includes only essential electron correlations). We are thinking about tractable approaches for including dynamic electron correlation, perhaps based on our non-orthogonal MP2 approach. Additionally, as a higher accuracy alternative, we are exploring the applicability of coupled cluster theory targeted at core-excited states. This will be an unconventional approach that can potentially capture orbital relaxation and all main correlation effects, while still being applicable to medium-sized molecules.

Analysis of Valence and Charge Transfer States in Photochemical Bond-Breaking by TDDFT *(Head-Gordon)*

Recent Progress: The analysis of bond-breaking by single reference methods such as DFT using spin-polarization is textbook material, but, rather surprisingly, there has been no such analysis for excited state methods such as TDDFT. We have recently filled this gap, by reporting analysis and numerical experiments for excited states associated with single bond-breaking with some remarkable discoveries such as valence excited states that exhibit sharp kinks at the Coulson-Fischer point, followed by separation to an incorrect asymptote despite use of spin-polarized orbitals! This is illustrated in Fig. 3-8 comparing exact solution versus time-dependent Hartree-Fock for the hydrogen molecule in a minimal basis. The behavior of TDDFT is similar. This work should inform the selection and design of methods for photochemical bond-breaking.

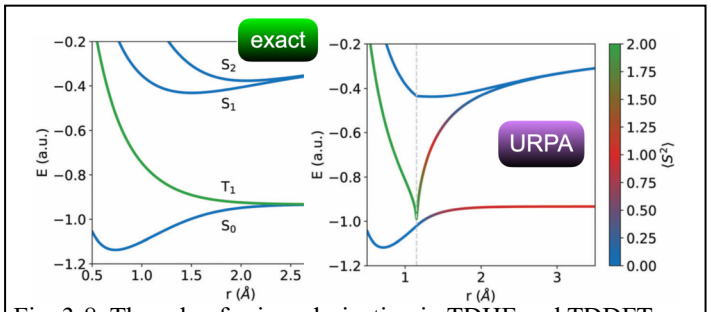

Fig. 3-8. The role of spin-polarization in TDHF and TDDFT excited states is assessed by comparing TDHF (i.e. RPA) states for H2 against exact solutions in a minimal basis. While the ground state is qualitatively correct, the M_s=0 triplet excitation energy collapses to zero at the Coulson-Fischer point, and then changes character to become a charge-transfer excited state towards dissociation.

The Role of Spin Polarized Orbitals in Strong-Field Ionization *(Head-Gordon, McCurdy)*

Recent Progress: As an initial step of a collaboration between McCurdy and Head-Gordon on time-dependent approaches to describing strong molecule-field interactions, we have begun exploring the existence of generalized Coulson-Fischer points associated with strong-(static) field ionization of atoms and molecules. Comparison of spin-restricted Hartree-Fock (RHF) versus spin-unrestricted Hartree-Fock (UHF) relative to accurate benchmark calculations on the model problem of field-induced ionization of 2-4 electron atoms shows that UHF is qualitatively superior for the first ionization in He and Be. We are in the process of writing up these results, which we think will have implications for the role of unrestriction in time-dependent electron dynamics in strong fields.

Peer Reviewed Publications Resulting from this Program (2018–2020)

1. Cao, W.; Warrick, E. R.; Fidler, A.; Leone, S. R.; Neumark, D. M., Excited-state Vibronic Wave-packet Dynamics in H_2 Probed by XUV Transient Four-wave Mixing. *Phys. Rev. A* **2018**, *97* (2), 023401, DOI 10.1103/PhysRevA.97.023401.
2. Ge, Q.; Head-Gordon, M., Energy Decomposition Analysis for Excimers Using Absolutely Localized Molecular Orbitals within Time-Dependent Density Functional Theory and Configuration Interaction with Single Excitations. *J. Chem. Theory Comput.* **2018**, *14* (10), 5156–5168, DOI 10.1021/acs.jctc.8b00537.
3. Ge, Q.; Mao, Y.; Head-Gordon, M., Energy Decomposition Analysis for Exciplexes Using Absolutely Localized Molecular Orbitals. *J. Chem. Phys.* **2018**, *148*, 064105, DOI 10.1063/1.5017510.

4. Hoshino, M.; Kato, H.; Kuze, N.; Tanaka, H.; Fukuzawa, H.; Ueda, K.; Lucchese, R. R., Changes in Site-specific Shape Resonances in Nitrogen K-Shell Photoionization Of N_2O Induced by Vibrational Excitation. *J. Phys. B: At. Molec. Opt. Phys.* **2018**, *51* (6), 065402, DOI 10.1088/1361-6455/aaaeb3.
5. Hvizdos, D.; Vana, M.; Houfek, K.; Greene, C. H.; Rescigno, T. N.; McCurdy, C. W.; Curık, R., Dissociative Recombination by Frame Transformation to Siegert Pseudostates: A Comparison with a Numerically Solvable Model. *Phys. Rev. A* **2018**, *97* (2), 022704, DOI 10.1103/PhysRevA.97.022704.
6. Kostko, O.; Xu, B.; Ahmed, M.; Slaughter, D. S.; Ogletree, D. F.; Closser, K. D.; Prendergast, D. G.; Naulleau, P.; Olynick, D. L.; Ashby, P. D.; Liu, Y.; Hinsberg, W. D.; Wallraff, G. M., Fundamental Understanding of Chemical Processes in Extreme Ultraviolet Resist Materials. *J. Chem. Phys.* **2018**, *149* (15), 154305, DOI 10.1063/1.5046521.
7. Kraus, P. M.; Zürch, M.; Cushing, S. K.; Neumark, D. M.; Leone, S. R., The Ultrafast X-ray Spectroscopic Revolution in Chemical Dynamics. *Nat. Rev. Chem.* **2018**, *2* (6), 82–94, DOI 10.1038/s41570-018-0008-8.
8. Larsen, K.; Trevisan, C.; Lucchese, R.; Heck, S.; Iskandar, W.; Champenois, E.; Gatton, A.; Moshammer, R.; Strom, R.; Severt, T.; Jochim, B.; Reedy, D.; Weller, M.; Landers, A.; Williams, J. B.; Ben-Itzhak, I.; Dörner, R.; Slaughter, D.; McCurdy, C. W.; Weber, T.; Rescigno, T. N., Resonance Signatures in the Body-frame Valence Photoionization of CF_4. *Phys. Chem. Chem. Phys.* **2018,** *20* (32), 21075–21084, DOI 10.1039/C8CP03637C.
9. Marroux, H. B. J.; Fidler, A. P.; Neumark, D. M.; Leone, S. R., Multidimensional Spectroscopy with Attosecond Extreme Ultraviolet and Shaped Near-Infrared Pulses. *Sci. Adv.* **2018**, *4* (9), eaau3783, DOI 10.1126/sciadv.aau3783.
10. Martin, L.; Bello, R. Y.; Hogle, C. W.; Palacios, A.; Tong, X. M.; Sanz-Vicario, J. L.; Jahnke, T.; Schöffler, M.; Dörner, R.; Weber, T.; Martín, F.; Kapteyn, H. C.; Murnane, M. M.; Ranitovic, P., Revealing the Role of Electron-Electron Correlations by Mapping Dissociation of Highly Excited D_2^+ Using Ultrashort XUV Pulses. *Phys. Rev. A* **2018**, *97* (6), 062508, DOI 10.1103/PhysRevA.97.062508.
11. Oosterbaan, K. J.; White, A. F.; Head-Gordon, M., Non-orthogonal Configuration Interaction with Single Substitutions for the Calculation of Core-Excited States. *J. Chem. Phys.* **2018**, *149* (4), 044116, DOI 10.1063/1.5023051.
12. Ranitovic, P.; Sturm, F. P.; Tong, X. M.; Wright, T. W.; Ray, D.; Zalyubovskya, I.; Shivaram, N.; Slaughter, D. S.; Belkacem, A.; Weber, T., Attosecond Coherent Control of Oxygen Dissociation by XUV-IR Laser Fields Using Three-Dimensional Momentum Imaging. *Phys. Rev. A* **2018**, *98* (1), 013410, DOI 10.1103/PhysRevA.98.013410.
13. Reedy, D.; Williams, J. B.; Gaire, B.; Gatton, A.; Weller, M.; Menssen, A.; Bauer, T.; Henrichs, K.; Burzynski, P.; Berry, B.; Streeter, Z. L.; Sartor, J.; Ben-Itzhak, I.; Jahnke, T.; Doerner, R.; Weber, T.; Landers, A. L., Dissociation Dynamics of the Water Dication Following One-photon Double Ionization II: Experiment. *Phys. Rev. A* **2018**, *98* (5), 053430, DOI 10.1103/PhysRevA.98.053430.
14. Streeter, Z. L.; Yip, F. L.; Rescigno, T. N.; Lucchese, R. R.; Gervais, B.; McCurdy, C. W., Dissociation Dynamics of the Water Dication Following One-photon Double Ionization I: Theory. *Phys. Rev. A* **2018**, *98* (5), 053429, DOI 10.1103/PhysRevA.98.053429.
15. Waitz, M.; Bello, R. Y.; Metz, D.; Lower, J.; Trinter, F.; Schober, C.; Keiling, M.; Lenz, U.; Pitzer, M.; Mertens, K.; Martins, M.; Viefhaus, J.; Klumpp, S.; Weber, T.; Schmidt, L. P. H.; Williams, J. B.; Schöffler, M. S.; Serov, V. V.; Kheifets, A. S.; Argenti, L.; Palacios, A.; Martín, F.; Jahnke, T.; Dörner, R., Erratum: Imaging the Square of the Correlated Two-Electron Wave Function of a Hydrogen Molecule. *Nat. Commun.* **2018**, *9*, 2259, DOI 10.1038/s41467-018-04740-5.
16. Warrick, E. R.; Fidler, A. P.; Cao, W.; Bloch, E.; Neumark, D. M.; Leone, S. R., Multiple Pulse Coherent Dynamics and Wave Packet Control of the N_2 a" $^1\Sigma_g^+$ Dark State by Attosecond Four Wave Mixing. *Faraday Discuss.* **2018**, *212*, 157–174, DOI 10.1039/C8FD00074C.
17. Yost, S. R.; Head-Gordon, M., Efficient Implementation of NOCI-MP2 Using the Resolution of the Identity Approximation with Application to Charged Dimers and Long C-C Bonds in Ethane Derivatives. *J. Chem. Theory Comput.* **2018**, *14* (9), 4791–4805, DOI 10.1021/acs.jctc.8b00697.

18. Young, L.; Ueda, K.; Gühr, M.; Bucksbaum, P. H.; Simon, M.; Mukamel, S.; Rohringer, N.; Prince, K. C.; Masciovecchio, C.; Meyer, M.; Rudenko, A.; Rolles, D.; Bostedt, C.; Fuchs, M.; Reis, D. A.; Santra, R.; Kapteyn, H.; Murnane, M.; Ibrahim, H.; Légaré, F.; Vrakking, M.; Isinger, M.; Kroon, D.; Gisselbrecht, M.; L'Huillier, A.; Wörner, H. J.; Leone, S. R., Roadmap for Ultrafast X-ray Atomic and Molecular Physics. *J. Phys. B: At. Mol. Opt. Phys.* **2018**, *51* (3), 032003, DOI 10.1088/1361-6455/aa9735.
19. Zeller, S.; Kunitski, M.; Voigtsberger, J.; Waitz, M.; Trinter, F.; Eckart, S.; Kalinin, A.; Czasch, A.; Schmidt, L. P. H.; Weber, T.; Schöffler, M.; Jahnke, T.; Dörner, R., Determination of the He-He, Ne-Ne, Ar-Ar, and H_2 Interaction Potential by Wave Function Imaging. *Phys. Rev. Lett.* **2018**, *121*, 083002, DOI 10.1103/PhysRevLett.121.
20. Bello, R. Y.; Yip, F. L.; Rescigno, T. N.; Lucchese, R. R.; McCurdy, C. W., Role of Initial-State Electron Correlation in One-Photon Double Ionization of Atoms and Molecules. *Phys. Rev. A* **2019**, *99*, 013403, DOI 10.1103/PhysRevA.99.013403.
21. Boll, D. I. R.; Fojón, O. A.; McCurdy, C. W.; Palacios, A., Angularly Resolved Two-Photon Above-Threshold Ionization of Helium. *Phys. Rev. A* **2019**, *99,* 023416, DOI 10.1103/PhysRevA.99.023416.
22. Champenois, E. G.; Greenman, L.; Shivaram, N.; Cryan, J. P.; Larsen, K. A.; Rescigno, T. N.; McCurdy, C. W.; Belkacem, A.; Slaughter, D. S., Ultrafast Photodissociation Dynamics and Nonadiabatic Coupling between Excited Electronic States of Methanol Probed by Time-Resolved Photoelectron Spectroscopy. *J. Chem. Phys.* **2019**, *150* (11), 114301, DOI 10.1063/1.5079549.
23. Fidler, A. P.; Camp, S. J.; Warrick, E. R.; Bloch, E.; Marroux, H. J. B.; Neumark, D. M.; Schafer, K. J.; Gaarde, M. B.; Leone, S. R., Nonlinear XUV Signal Generation Probed by Transient Grating Spectroscopy with Attosecond Pulses. *Nat. Commun.* **2019**, *10* (1), 1384, DOI 10.1038/s41467-019-09317-4.
24. Fidler, A. P.; Marroux, H. B. J.; Warrick, E. R.; Bloch, E.; Cao, W.; Leone, S. R.; Neumark, D. M., Autoionizing Dynamics of $(^2P_{1/2})ns/d$ States in Krypton Probed by Noncollinear Wave Mixing with Attosecond Extreme Ultraviolet and Few-Cycle Near Infrared Pulses. *J. Chem. Phys.* **2019**, *151* (11), 114305, DOI 10.1063/1.5113912.
25. Fukuzawa, H.; Lucchese, R. R.; Liu, X.-J.; Sakai, K.; Iwayama, H.; Nagaya, K.; Kreidi, K.; Schöffler, M. S.; Harries, J. R.; Tamenori, Y.; Morishita, Y.; Suzuki, I. H.; Saito, N.; Ueda, K., Probing Molecular Bond-Length Using Molecular-Frame Photoelectron Angular Distributions. *J. Chem. Phys.* **2019**, *150* (17), 174306, DOI 10.1063/1.5091946.
26. Geneaux, R.; Marroux, H. J. B.; Guggenmos, A.; Neumark, D. M.; Leone, S. R., Transient Absorption Spectroscopy Using High Harmonic Generation: A Review of Ultrafast X-ray Dynamics in Molecules and Solids. *Philos. Trans. R. Soc. A* **2019**, *377* (2145), 20170463, DOI 10.1098/rsta.2017.0463.
27. Gessner, O.; Vilesov, A. F., Imaging Quantum Vortices in Superfluid Helium Droplets. *Annu. Rev. Phys. Chem.* **2019**, *70*, 173–198, DOI 10.1146/annurev-physchem-042018-052744.
28. Hait, D.; Rettig, A.; Head-Gordon, M., Beyond the Coulson-Fischer Point: Characterizing Single Excitation CI and TDDFT for Excited States in Single Bond Dissociations. *Phys. Chem. Chem. Phys.* **2019**, 21, 21761–21775, DOI 10.1039/c9cp04452c.
29. Heck, S.; Gatton, A.; Larsen, K. A.; Iskandar, W.; Champenois, E. G.; Strom, R.; Landers, A.; Reedy, D.; Dailey, C.; Williams, J. B.; Severt, T.; Jochim, B.; Ben-Itzhak, I.; Moshammer, R.; Doerner, R.; Slaughter, D. S.; Th. Weber, Symmetry Breaking in the Body-Fixed Electron Emission Pattern Due to Electron-Retroaction in the Photodissociation of H_2^+ and D_2^+ Close to Threshold. *Phys. Rev. R* **2019**, 1, 033140, DOI 10.1103/PhysRevResearch.1.033140.
30. Iskandar, W.; Gatton, A. S.; Gaire, B.; Sturm, F. P.; Larsen, K. A.; Champenois, E. G.; Shivaram, N.; Moradmand, A.; Williams, J. B.; Berry, B.; Severt, T.; Ben-Itzhak, I.; Metz, D.; Sann, H.; Weller, M.; Schoeffler, M.; Jahnke, T.; Dörner, R.; Slaughter, D.; Weber, T., Tracing Intermolecular Coulombic Decay of Carbon-Dioxide Dimers and Oxygen Dimers after Valence Photoionization. *Phys. Rev. A* **2019**, *99* (4), 043414, DOI 10.1103/PhysRevA.99.043414.

31. Lee, J.; Small, D. W.; Head-Gordon, M., Excited States via Coupled Cluster Theory without Equation-of-Motion Methods: Seeking Higher Roots with Application to Doubly Excited States and Double Core Hole States. *J. Chem. Phys.* **2019**, *151*, 214103, DOI 10.1063/1.5128795.
32. Lucchese, R. R.; Rescigno, T. N.; McCurdy, C. W., The Connection between Resonances and Bound States in the Presence of a Coulomb Potential. *J. Phys. Chem. A* **2019**, *123* (1), 82–95, DOI 10.1021/acs.jpca.8b10715.
33. Mahl, J.; Neppl, S.; Roth, F.; Borgwardt, M.; Saladrigas, C.; Toulson, B. W.; Cooper, J. K.; Rahman, T.; Bluhm, H.; Guo, J.; Yang, W.; Huse, N.; Eberhardt, W.; Gessner, O., Decomposing Electronic and Lattice Contributions in Optical Pump – X-ray Probe Transient Inner-Shell Absorption Spectroscopy of CuO. *Faraday Discuss.* **2019**, *216*, 414–433, DOI 10.1039/C8FD00236C.
34. Okunishi, M.; Ito, Y.; Sharma, V.; Aktar, S.; Ueda, K.; Lucchese, R. R.; Dnestryan, A. I.; Tolstikhin, O. I.; Inoue, S.; Matsui, H.; Morishita, T., Rescattering Photoelectron Spectroscopy of the CO_2 Molecule: Progress Towards Experimental Discrimination Between Theoretical Target-Structure Models. *Phys. Rev. A* **2019**, *100*, 053404, DOI 10.1103/PhysRevA.100.053404.
35. Oosterbaan, K. J.; White, A. F.; Head-Gordon, M., Non-Orthogonal Configuration Interaction with Single Substitutions for Core Excited States: An Extension to Doublet Radicals. *J. Chem. Theory Comput.* **2019**, *15*, 2966–2973, DOI 10.1021/acs.jctc.8b01259.
36. Plunkett, A.; Harkema, N.; Lucchese, R. R.; McCurdy, C. W.; Sandhu, A., Ultrafast Rydberg-State Dissociation in Oxygen: Identifying The Role of Multielectron Excitations. *Phys. Rev. A* **2019**, *99* (6), 063403, DOI 10.1103/PhysRevA.99.063403.
37. Roth, F.; Neppl, S.; Shavorskiy, A.; Arion, T.; Mahl, J.; Seo, H. O.; Bluhm, H.; Hussain, Z.; Gessner, O.; W. Eberhardt, Efficient Charge Generation from Triplet Excitons in Metal-Organic Heterojunctions. *Phys. Rev. B* **2019**, *99* (2), 020303, DOI 10.1103/PhysRevB.99.020303.
38. Schnorr, K.; Bhattacherjee, A.; Oosterbaan, K. J.; Delcey, M. G.; Yang, Z.; Xue, T.; Attar, A. R.; Chatterley, A. S.; Head-Gordon, M.; Leone, S. R.; Gessner, O., Tracing the 267 Nm-Induced Radical Formation in Dimethyl Disulfide Using Time-Resolved X-ray Absorption Spectroscopy. *J. Phys. Chem. Lett.* **2019**, *10*, 1382–1387, DOI 10.1021/acs.jpclett.9b00159.
39. Toulson, B. W.; Borgwardt, M.; Wang, H.; Lackner, F.; Chatterley, A. S.; Pemmaraju, C. D.; Neumark, D. M.; Leone, S. R.; Prendergast, D.; Gessner, O., Probing Ultrafast C–Br Bond Fission in the UV Photochemistry of Bromoform with Core-to-Valence Transient Absorption Spectroscopy. *Struct. Dyn.* **2019**, *6*, 054304, DOI 10.1063/1.5113798.
40. Ueda, K.; Sokell, E.; Schippers, S.; Aumayr, F.; Sadeghpour, H.; Burgdörfer, J.; Lemell, C.; Tong, X.-M.; Pfeifer, T.; Calegari, F.; Palacios, A.; Martin, F.; Corkum, P.; Sansone, G.; Gryzlova, E. V.; Grum-Grzhimailo, A. N.; Piancastelli, M. N.; Weber, P. M.; Steinle, T.; Amini, K.; Biegert, J.; Berrah, N.; Kukk, E.; Santra, R.; Müller, A.; Dowek, D.; Lucchese, R. R.; McCurdy, C. W.; Bolognesi, P.; Avaldi, L.; Jahnke, T.; Schöffler, M. S.; Dörner, R.; Mairesse, Y.; Nahon, L.; Smirnova, O.; Schlathölter, T.; Campbell, E. E. B.; Rost, J.-M.; Meyer, M.; Tanaka, K. A., Roadmap on Photonic, Electronic and Atomic Collision Physics: I. Light–matter Interaction. *J. Phys. B: At. Molec. Opt. Phys.* **2019**, *52* (17), 171001, DOI 10.1088/1361-6455/ab26d7.
41. Veyrinas, K.; Saquet, N.; Marggi Poullain, S.; Lebech, M.; Houver, J. C.; Lucchese, R. R.; Dowek, D., Dissociative Photoionization of NO across a Shape Resonance in the XUV Range Using Circularly Polarized Synchrotron Radiation. *J. Chem. Phys.* **2019**, *151*, 174305, DOI 10.1063/1.5121620.
42. Wu, E. C.; Ge, Q.; Arsenault, E. A.; Lewis, N. H. C.; Gruenke, N. L.; Head-Gordon, M.; Fleming, G. R., Two-Dimensional Electronic-Vibrational Spectroscopic Study of Conical Intersection Dynamics: An Experimental and Electronic Structure Study. *Phys. Chem. Chem. Phys.* **2019**, *21* (26), 14153–14163, DOI 10.1039/c8cp05264f.
43. Borgwardt, M.; Mahl, J.; Roth, F.; Wenthaus, L.; Braußе, F.; Blum, M.; Schwarzburg, K.; Liu, G.; Toma, F.M.; Eberhardt, W.; Gessner, O., Photoinduced Charge Carrier Dynamics and Electron Injection Efficiencies in Au Nanoparticle-Sensitized TiO_2 Determined with Picosecond Time-Resolved X-ray

Photoelectron Spectroscopy. *J. Phys. Chem. Lett.* **2020**, *11* (14), 5476–5481, DOI: 10.1021/acs.jpclett.0c00825.

44. Douguet, N.; Fonseca dos Santos, S.; Rescigno, T. N., Inner-Shell Photodetachment of C_n^- Ions. *Phys. Rev. A,* **2020**, *101*, 033411, DOI 10.1103/PhysRevA.101.033411.
45. Fidler, A.P.; Warrick, E.R.; Marroux, H.J.B.; Bloch, E.; Neumark, D.M.; Leone, S.R., Self-Heterodyned Detection of Dressed State Coherences in Helium by Noncollinear Extreme Ultraviolet Wave Mixing with Attosecond Pulses. *J. Phys. Photonics* **2020**, *2*, 034003, DOI: 10.1088/2515-7647/ab869c.
46. Hait D.; Head-Gordon, M., Highly Accurate Prediction of Core Spectra of Molecules at Density Functional Theory Cost: Attaining Sub-electronvolt Error from a Restricted Open-Shell Kohn-Sham Approach, *J. Phys. Chem. Lett.* **2020**, *11*, 775–786, DOI 10.1021/acs.jpclett.9b03661.
47. Hait, D.; Head-Gordon, M., Excited State Orbital Optimization via Minimizing the Square of the Gradient: General Approach and Application to Singly and Doubly Excited States via Density Functional Theory, *J. Chem. Theory Comput.* **2020**, *16*, 1699–1710, DOI 10.1021/acs.jctc.9b01127.
48. Kastirke, G.; Schoeffler, M.; Weller, M.; Rist, J.; Boll, R.; Anders, N.; Baumann, T.M.; Eckart, S.; Erk, B.; De Fanis, A.; Fehre, K.; Gatton, A.; Grundmann, S.; Grychtol, P.; Hartung, A.; Hofmann, M.; Ilchen, M.; Janke, C.; Kircher, M.; Kunitski, M.; Li, X.; Mazza, T.; Melzer, N.; Montano, J.; Music, V.; Nalin, G.; Ovcharenko, Y.; Pier, A.; Rennhack, N.; Rivas, D.E.; Doerner, R.; Rolles, D.; Rudenko, A.; Schmidt, J.; Siebert, N.; Strenger, D.; Trabert, I.; Vela-Perez, R.; Wagner, Th.; Weber, J.B.; Williams, P.; Ziolkowski, P.; Schmidt, L.Ph.H.; Czasch, A.; Ueda, K.; Trinter, F.; Meyer, M.; Demekhin, P.V.; Jahnke, T., Double Core-Hole Generation in O_2 Molecules using an X-ray Free-Electron Laser: Molecular-Frame Photoelectron Angular Distributions. *Accepted for publication in Phys. Rev. Lett.* **August 2020**.
49. Kastirke, G.; Schöffler, M.S.; Weller, M.; Rist, J.; Eckart, S.; Fehre, K.; Grundmann, S.; Hartung, A.; Hofmann, M.; Janke, C.; Kircher, M.; Trabert, D.; Vela-Perez, I.; Nalin, G.; Mel-zer, N.; Anders, N.; Pier, A.; Strenger, N.; Siebert, J.; Kunitski, M.; Dörner, R.; Gatton, A.; Williams, J. B.; Weber, T.; Li, X.; Rudenko, A.; Rolles, D.; Erk, B.; Wagner, R.; Music, V.; Rennhack, N.; Montaño, J.; Ovcharenko, Y.; Ziolkowski, P.; Rivas, D.E.; Baumann, T.M.; Schmidt, P.; Grychtol, P.; Ilchen, M.; Fanis, A.D.; Mazza, T.; Boll, R.; Schmidt, L.P.H.; Czasch, A.; Trinter, F.; Meyer, M.; Ueda, K.; Demekhin, P.V.; Jahnke, T., Photoelectron Diffraction Imaging of a Molecular Break-up using an X-ray Free-Electron Laser. *Phys. Rev. X* **2020**, *10*, 021052, DOI: 10.1103/PhysRevX.10.021052.
50. Larsen K.A.; Slaughter, D.S.; Weber. Th., Angle-Resolved Nonresonant Two-Photon Single Ionization of Argon using 9.3-eV Photons Produced via High-Order Harmonic Generation. *Phys. Rev. A* **2020**, *101*, 061402(R), DOI: 10.1103/PhysRevA.101.061402.
51. Larsen, K.A.; Lucchese, R.R.; Slaughter, D.S.; Weber, T., Distinguishing Resonance Symmetries with Energy-Resolved Photoion Angular Distributions from Ion-Pair Formation in O_2 Following Two-Photon Absorption of a 9.3 eV Femtosecond Pulse. *J. Chem. Phys.* **2020**, *153*, 021103, DOI: 10.1063/5.0013485.
52. Marante, C.A.; Greenman, L.; Trevisan, C.S.; Rescigno, T.N.; McCurdy, C.W.; Lucchese, R.R., Validity of the Static-Exchange Approximation for Inner-Shell Photoionization of Polyatomic Molecules. *Phys. Rev. A* **2020**, *102*, 012815, DOI: 10.1103/PhysRevA.102.012815.
53. Mizuno, H.; Oosterbaan, K.J.; Menzl, G.; Smith, J.; Rizzuto, A.M.; Geissler, P.L.; Head-Gordon, M.; Saykally, R.J., Revisiting the $\pi \rightarrow \pi^*$ Transition of the Nitrite Ion at the Air/Water Interface: A Combined Experimental and Theoretical Study. *Chem. Phys. Lett.* **2020,** *751*, 137516, DOI: 10.1016/j.cplett.2020.137516.
54. Mudrich, M.; LaForge, A. C.; Ciavardini, A.; O'Keeffe, P.; Callegari, C.; Coreno, M.; Demidovich, A.; Devetta, M.; Fraia, M. D.; Drabbels, M.; Finetti, P.; Gessner, O.; Grazioli, C.; Hernando, A.; Neumark, D. M.; Ovcharenko, Y.; Piseri, P.; Plekan, O.; Prince, K. C.; Richter, R.; Ziemkiewicz, M. P.; Möller, T.; Eloranta, J.; Pi, M.; Barranco, M.; Stienkemeier, F., Ultrafast Relaxation of Photoexcited Superfluid He Nanodroplets. *Nat. Commun.* **2020**, *11* (1), 1–7, DOI 10.1038/s41467-019-13681-6.

55. O'Connell, S.M.O.; Tanyag, R.M.P.; Verma, D.; Bernando, C.; Pang, W.; Bacellar, C.; Saladrigas, C.A.; Mahl, J.; Toulson, B.W.; Kumagai, Y.; Walter, P.; Ancilotto, F.; Barranco, M.; Pi, M.; Bostedt, C.; Gessner, O.; Vilesov, A.F., Angular Momentum in Rotating Superfluid Droplets. *Phys. Rev. Lett.* **2020**, *124* (21), 215301, DOI: 10.1103/PhysRevLett.124.215301.
56. O'Neal, Jordan T.; Champenois, Elio G.; Oberli, Soléne; Obaid, Razib; Al-Haddad, Andre; Barnard, Jonathan; Berrah, Nora; Coffee, Ryan; Duris, Joseph; Galinis, Gediminas; Garratt, Douglas; Glownia, James M.; Haxton, Daniel; Ho, Phay; Li, Siqi; Li, Xiang; MacArthur, James; Marangos, Jon P.; Natan, Adi; Shivaram, Niranjan; Slaughter, Daniel S.; Walter, Peter; Wandel, Scott; Young, Linda; Bostedt, Christoph; Bucksbaum, Philip H.; Picón, Antonio; Marinelli, Agostino; Cryan, James P., Electronic Population Transfer via Impulsive Stimulated X-ray Raman Scattering with Attosecond Soft-X-ray Pulses. *Phys. Rev. Lett.* **2020**, *125*, 073203, DOI: 10.1103/PhysRevLett.125.073203. Selected as a Feature Article.
57. Oosterbaan, K.J.; White, A.F.; Hait, D.; Head-Gordon, M., Generalized Single Excitation Configuration Interaction: An Investigation into the Impact of the Inclusion of Non-Orthogonality on the Calculation of Core-Excited States. *Phys. Chem. Chem. Phys.* **2020**, *22*, 8182–8192, DOI: 10.1039/C9CP06592J.
58. Panelli, G.; Moradmand, A.; Griffon, B.; Swanson, K.; Weber, Th.; Rescigno, T.N.; McCurdy, C.W.; Slaughter, D.S.; Williams, J.B., Investigating Resonant Low-Energy Electron Attachment to Formamide: Dynamics of Model Peptide Bond Dissociation and other Fragmentation Channels. *Accepted for publication in Phys. Rev. R* **August 2020**.
59. Roy, P.P.; Shee, J.; Arsenault, E.A.; Yoneda, Y.; Feuling, K.; Head-Gordon, M.; Fleming, G.R., Solvent Mediated Excited State Proton Transfer in Indigo Carmine. *J. Phys. Chem. Lett.* **2020**, *11*, 4156−4162, DOI: 10.1021/acs.jpclett.0c00946.
60. Schiffmann, A.; Toulson, B.W.; Knez, D.; Messner, R.; Schnedlitz, M.; Lasserus, M.; Hofer, F.; Ernst, W.E.; Gessner, O.; Lackner, F., Ultrashort XUV Pulse Absorption Spectroscopy of Partially Oxidized Cobalt Nanoparticles. *J. Appl. Phys.* **2020**, *127* (18), 184303, DOI: 10.1063/5.0004582.
61. Slaughter, D.; Weber, Th.; Belkacem, A.; Trevisan, C.; Lucchese, R.; McCurdy, C.W.; Rescigno, T., Selective Bond-Breaking in Formic Acid by Dissociative Electron Attachment. *Phys. Chem. Chem. Phys.* **2020**, *22*, 13893–13902, DOI: 10.1039/D0CP01522A. *Selected for the collection: 2020 PCCP HOT Articles.*
62. Thurston, R.; Brister, M.; Tan, L.; Champenois, E.; Bakhti, S.; Muddukrishna, P.; Weber, T.; Belkacem, A.; Slaughter, D.; Shivaram, N., Ultrafast Dynamics of Excited Electronic States in Nitrobenzene Measured by Ultrafast Transient Polarization Spectroscopy. *J. Phys. Chem. A* **2020**, *124* (13), 2573–2579, DOI: 10.1021/acs.jpca.0c01943.
63. Thurston, R.; Brister, M.M.; Belkacem, A.; Weber, T.; Shivaram, N.; Slaughter, D.S., Time-Resolved Ultrafast Transient Polarization Spectroscopy to Investigate Nonlinear Processes and Dynamics in Electronically Excited Molecules on the Femtosecond Time Scale. *Rev. Sci. Instrum.* **2020**, *91*, 053101, DOI: 10.1063/1.5144482.
64. Verma, D.; O'Connell, S.M.O.; Feinberg, A.J.; Erukala, S.; Tanyag, R.M.; Bernando, C.; Pang, W.; Saladrigas, C.; Toulson, B.; Borgwardt, M.; Shivaram, N.; Lin, M.-F.; Haddad, A.A.; Jäger, W.; Bostedt, C.; Walter, P.; Gessner, O.; Vilesov, A.F., Shapes of Rotating Normal Fluid ^{3}He Versus Superfluid ^{4}He Droplets in Molecular Beams. *Phys. Rev. B* **2020**, *102* (1), 014504, DOI: 10.1103/PhysRevB.102.014504.
65. Yip, F.L.; McCurdy, C.W.; Rescigno, T.N., Hybrid Gaussian--Discrete-Variable Representation for Describing Molecular Double-Ionization Events. *Phys. Rev. A* **2020**, *101* (6), 063404, DOI: 10.1103/PhysRevA.101.063404.

PULSE Ultrafast Chemical Science

P.H. Bucksbaum, D.A. Reis, K. Gaffney, T. Heinz, T. Martinez, T. Wolf, A. Natan, J. Cryan, S. Ghimire, A. Cordones-Hahn, E. Hohenstein, SLAC National Accelerator Laboratory, 2575 Sand Hill Rd. MS 59, Menlo Park, CA 94025. Email phb@slac.stanford.edu

Project Scope:

The PULSE Ultrafast Chemical Science program develops ultrafast chemical physics research at SLAC that is enabled by SLAC's x-ray and relativistic electron facilities, including LCLS-II, SSRL, Ultrafast Electron Diffraction (UED). Our overarching goal is to establish research at SLAC that makes optimal use of these unique tools for fundamental discoveries and new insights in ultrafast chemical science.

Recent Progress:

Our recent research illustrates this close connection between the advanced facilities at SLAC and advanced research in PULSE. Here are just a few recent examples:

Gaffney and Cordones-Hahn have been exploring ways to study solution phase chemical dynamics directly using SLAC's rapidly developing capabilities in UED. They have commissioned a new liquid-yet endstation and have performed the first solution-phase UED experiments. The MeV electrons from UED together with ultra-thin liquid jet technology can overcome the challenge of strong absorption and scattering of electrons from the solvent.

James Cryan and his team have used focused soft x-rays at LCLS to perform the first experiments on impulsive stimulated x-ray Raman scattering (ISXRS). Impulsive scattering is widely used in ultrafast chemistry to create rovibrational coherences that track the course of energy flow within a molecule by exciting it with a broadband ultrashort kick. Strong ultrafast x-ray pulses can extend this method to valence electronic coherences that are initiatied in the vicinity of atomic core levels in molecules. This is the first successful attempt to see this process. It made good use of the broad bandwidth (5.5 eV FWHM) attosecond x-ray pulses tuned near the oxygen $1s \rightarrow 2\pi^*$ resonance of nitric oxide (NO), and probed by a time-delayed UV pulse to measure the excited states that are produced.

The two distinguishing advantages of this highly collaborative ultrafast chemical science program are the on-site presence of unique ultrafast x-ray and electron facilities, and our connection to Stanford University. These help to keep us competitive on an international level.

Our Ultrafast Chemical Science programs, along with highlights of recent research and future, are described fully in the abstracts for those subtasks, which follow this overview. Here we concentrate on cross-cutting themes, and overall management.

Management Structure: This Ultrafast Chemical Science program, directed by Professor Phil Bucksbaum. is in the Chemical Sciences Division directed by Kelly Gaffney, within the SLAC Energy Sciences Directorate, directed by Tony Heinz.

The intellectual vitality of our Ultrafast Chemical Science program is assisted greatly by its membership in a parallel Stanford University organizational unit, the Stanford PULSE Institute, directed by David Reis.

The PIs and co-PIs who receive their research support from this program are:

Professor Philip Bucksbaum, AMO Physics, the FWP director;
Professor David Reis, Nonlinear x-ray science, deputy director;
Professor Kelly Gaffney, Physical Chemistry;
Professor Tony Heinz, Optical Physics
Professor Todd Martinez, Theoretical Physical Chemistry;
Research Scientist Dr. Thomas Wolf, Physical Chemistry;
Research Scientist Dr. Adi Natan, AMO Physics;
Research Scientist Dr. Amy Cordones-Hahn, Chemistry;
Research Scientist Dr. James Cryan, AMO Physics;
Research Scientist Dr. Shambhu Ghimire; Nonlinear x-ray optics;
Research Scientist Dr. Ed. Hohenstein, Theoretical Chemistry

The program is organized into nine subtasks:

1. UTS: Ultrafast Theory and Simulation (Martinez, Hohenstein)
2. ATO: Attoscience (Cryan, Bucksbaum)
3. SPC: Solution Phase Chemistry (Cordones-Hahn, Gaffney)
4. NPI: Non-periodic X-ray Imaging (Natan)
5. SFA: Strong Field AMO Physics (Bucksbaum, Natan, Cryan)
6. NLX: Nonlinear X-Ray Science (Reis)
7. EDN: Electron Dynamics on the Nanoscale (Heinz)
8. EIM: Excitations in Molecules (Wolf)
9. HHG: High Harmonics in Optical Media (Ghimire)

***Awards Prizes, and other Honors**:*

1. **Fellowships** (2017-2020):
   Todd Martinez: Election to International Academy of Quantum Molecular Science, 2017
   David Reis: Elected Fellow in the Optical Society, 2019
   Tony Heinz: Clarivate Citation Laureate in Physics (one of three), 2019
   James Cryan: Elected Fellow in the American Physical Society, 2020

2. **Awards and Prizes** (2017-2020):
   Philip Bucksbaum: American Physical Society, Norman F. Ramsey Prize, 2020
   Amy Cordones Hahn: DOE Early Career Award, 2020
   Tony Heinz: Optical Society, Meggers Award, 2020

3. **New membership in NASEM** (2017-2020):
   Todd Martinez: Election to the National Academy of Sciences, 2019

Personnel changes: Tais Gorkhover, who was a DOE Early Career recipient in the AMOS program and a SLAC Panofsky Fellow, accepted a tenured faculty position at the University of Hamburg this year. Postdoctoral Fellow Ruaridh Forbes accepted a staff position in the Laser Division of LCLS. Both continue to be active participants in PULSE research. Ed Hohenstein has joined the Ultrafast Theory and Simulation subtask.

PULSE Ultrafast Chemical Science Major themes: Ultrafast science has emerged as one of the primary arenas for scientific progress across all areas of BES, and it has also now been established as a primary mission focus for SLAC.[1] PULSE has been advancing this area for more than a decade and so we are in a good position to claim leadership in selected broad areas of the field. Our primary aim this year has been to focus on early science opportunities at LCLS-II which began operations in August 2020, and at UED, which has also begun operations following the general laboratory shutdown due to the pandemic:

- Sub-femtosecond frame rates for femtosecond movies will capture the motion of electrons within molecules, using some methods that have not been possible without the improved characteristic of the LCLS-II linac and x-ray laser.
- Ultrafast methods with Angstrom resolution to record chemistry at the level of the intramolecular bonds.
- multiphoton x-ray interactions to explore the new capabilities of x-ray nonlinear spectroscopy.

These tasks are well-embedded in the themes of the BESAC 2017 report *Opportunities for Basic Research at the Frontiers of XFEL Ultrafast Science* (a.k.a. *Ultrafast Roundtable Report*), [2] and also line up with the BESAC 2015 report, *Challenges at the Frontiers of Matter and Energy: Transformative Opportunities for Discovery Science,*[3] especially the section on *Imaging Matter across Scales,* and *Harnessing Coherence in Light and Matter.* The tasks are also in line with the 2004 report *Directing Matter and Energy: Five Challenges for Science and the Imagination* (a.k.a. *Grand Challenges Report*)[4] where our work is particularly relevant for the *Energy and Information on the Nanoscale* and *Control at the Level of Electrons* challenges. The nine subtask abstracts will discuss these themes further, but we like to cast them in three phrases that capture the essence of the opportunities. These are:

• Imaging on the nanoscale in space and the femtoscale in time.

• The architecture of light conversion chemistry.

• Harnessing coherence on the eV scale in time, space, and field strength.

Space allocations: Most of our research activities take place in laboratories in SLAC Building 40a. SLAC currently provides office space for our research groups, and also allocates approximately 10,000 square feet to research laboratories and a computer room for this FWP. Additional space exists in the new SLAC Arriaga Science Center for future opportunities.

Collaborations: In addition to strong links to LCLS, we also have collaborative connections to other outside research labs, including DESY, the Lawrence Berkeley Laboratory, the Center for Free Electron Lasers (CFEL) in Hamburg, and other BES-AMOS groups at the University of Michigan, Kansas State University, Stony Brook University, the Ohio State University, the University of Connecticut, Louisiana State University, Northwestern University.

Knowledge transfer to LCLS: The transfer of knowledge to and from LCLS is extremely fluid and critical to our success. Much of our research creates benefits for LCLS by providing new

[1] http://www-group.slac.stanford.edu/oa/strategic.htm
[2] https://science.energy.gov/~/media/bes/pdf/reports/2018/Ultrafast_x-ray_science_rpt.pdf
[3] https://science.energy.gov/bes/efrc/research/transformative-opportunities/
[4] https://science.energy.gov/~/media/bes/pdf/reports/files/Directing_Matter_and_Energy_rpt.pdf

research methods and research results, and in addition there are several more direct transfers of our research product to help LCLS:

- We work closely with instrument development teams at LCLS for the development of the next-generation LCLS-II instruments. This year particularly strong collaborations involve the new TMO instrument, the XLEAP attosecond instruments, and lasers for TMO and CXI.
- We have assisted in the development of laser and timing tools currently at LCLS.
- Some of our postdocs and students have transferred to permanent staff positions at LCLS. This year Dr. Ruaridh Forbes made this transition.
- We connect LCLS to the Stanford PULSE Institute, since all of our staff are members of PULSE, PULSE assists LCLS in student and postdoctoral recruitment and mentorship.
- PULSE conducts an annual Ultrafast X-ray Summer School to train students and postdocs about LCLS science opportunities. This year the UXSS was completely via video conference, and for this reason attracted a record number of students and other attendees. We have also been tracking the connections between former attendees and publications from LCLS experiments, and find that the UXSS has been the starting point for a large fraction of the groups who are now part of the LCLS user community.

UTS: Ultrafast Theory and Simulation (Todd J. Martínez, PI), SLAC National Accelerator Laboratory, 2575 Sand Hill Road, Menlo Park, CA, 94025,

toddmtz@slac.stanford.edu

Program Scope: This program is focused on developing and applying new methods for describing molecular dynamics on electronically excited states, as well as the interaction of molecules with radiation fields. We continue to develop and apply the *ab initio* multiple spawning (AIMS) method that solves the electronic and nuclear Schrodinger equations simultaneously from first principles, including the treatment of cases where the Born-Oppenheimer approximation breaks down (e.g. around conical intersections where two or more electronic states are exactly degenerate). We are working to extend this methodology to incorporate the effects of novel pump and probe pulses using high energy photons, including those obtained from modern x-ray sources such as LCLS. We are also extending these approaches to predict and interpret diffraction signals from ultrafast electron and X-ray experiments. Primary application areas include understanding the behavior of molecular excited states in paradigmatic phenomena such as light-induced isomerization, excited state proton transfer, and excitation energy transfer.

Recent Progress: *Ultrafast Electron Diffraction of Pyridine:* We have initiated numerous collaborations with the ultrafast electron diffraction team centered at SLAC. In a recent study, we have explored the femtosecond electron diffraction of photoexcited pyridine. Up until now, one of the major difficulties of UED is that only nuclear dynamics could be extracted from the signal. This is complementary to optical spectroscopies, which primarily see electronic changes (modulated by the motion of the nuclei). Ideally, one would like to observe *both* electronic and nuclear dynamics in the *same* experiment, *and* one would like the corresponding signals to be independent. In principle, the UED experiment measures the time-evolving electronic/nuclear charge density. Therefore, information about the electronic dynamics is encoded in the signal. Furthermore, the elastic and inelastic components of the UED signal are relatively easy to disentangle. In collaboration with SLAC experimentalists, we endeavored to find a way to use a single UED experiment to expose electronic and nuclear dynamics independently.

We previously (Parrish, et al. J. Chem. Theo. Comp. 2019) developed a scheme for computing the UED signal by scattering off the charge density determined from quantum chemistry, in contrast to the independent atom model (IAM) analysis which is usually performed (and takes as input the nuclear positions only, effectively using parameterized atomic electron densities). Unfortunately, the diffraction signal from ground and excited electronic states is often difficult to distinguish in an experiment (since relatively few electrons are involved in the excitation). However, we extended this scheme to compute both the elastic and inelastic components of the diffraction signal from direct scattering off the electronic and nuclear charge densities. The primary contributor to the inelastic signal comes from the electron correlation component of the electronic density (because it depends directly on the two-body reduced density matrix). This provides an opportunity to distinguish electronic states with widely differing electron correlation (such as open shell configurations compared to closed shell configurations). As shown in Figure 1, the inelastic and elastic signals are easy to separate in the experimental signal for pyridine and furthermore the inelastic signal tracks the excited state population (Yang, et al., Science 2020).

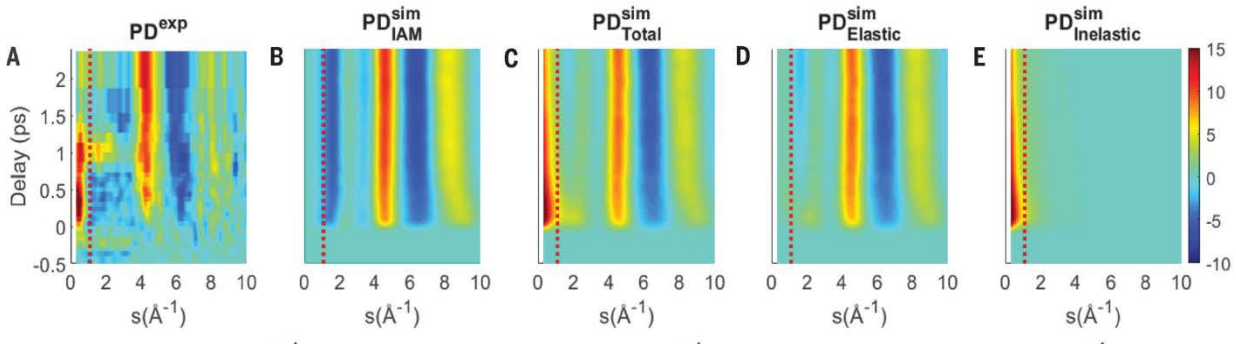

Figure 1. Time-resolved percentage difference (relative to unexcited sample) electron diffraction signals for pyridine after excitation to the S_1 state: a) experimentally measured, b) computed with IAM, c) computed with *ab initio* scattering using the electronic density of the ground and excited electronic states, d) the elastic component of the *ab initio* scattering signal, and e) the inelastic component of the *ab initio* scattering signal. Only the full *ab initio* scattering signal is able to capture the low s transient (which is dominated by electronic state-dependent inelastic scattering that is inaccessible to IAM). The calculations show that this low s signal is diagnostic of the population in S_1.

Development of the hole-hole Tamm-Dancoff approximated density functional theory (hhTDA). We have developed a new electronic structure method that is ideally suited for studying ultrafast nonadiabatic dynamics involving low-lying ππ* and nπ* excited states. The hhTDA method starts from a DFT reference state with two additional electrons occupying the LUMO. The ground and excited states are then created by annihilating two electrons from this space. This generates single and double excitations from all occupied orbitals to the LUMO. This method has several important advantages in the context of ultrafast dynamics: all excited states are treated on equal footing so conical intersections between all pairs of states are properly described, the method is capable of describing wavefunctions with multireference character, dynamic electron correlation is included through the DFT reference state, and finally the computational cost of this method is comparable to that of TDDFT, so it can be applied to large molecules and dynamics simulations. We have developed a highly optimized GPU implementation of this method along with analytic gradients and nonadiabatic coupling vectors. This program has been interfaced with AIMS dynamics to allow on-the-fly evaluation of the potential energy surfaces needed in these simulations (Yu, et al. J. Chem. Theory Comput. 2020).

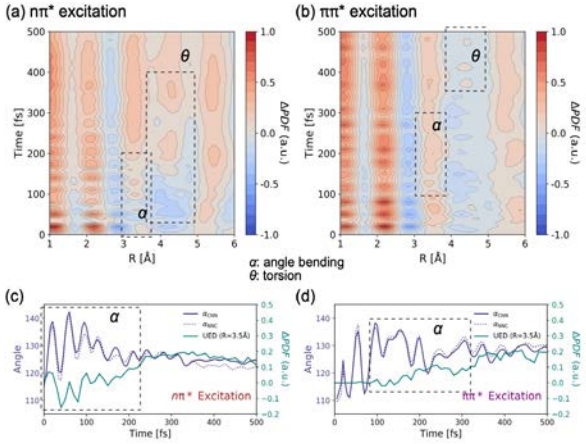

Figure 2. Simulated ultrafast electron diffraction signals after photoexcitation of azobenzene to its S_1 nπ* state (left) and to its S_2 ππ* state (right). These simulations were performed using hhTDA to generate the potential energy surfaces. We predict that the difference in deactivation mechanisms can be identified in by the changes in density in the 3-5 Å region.

We have found the hhTDA method to make quite accurate predictions of electronic excitation energies (within a few tenths of an eV from experiment) as well as the relative energies of

critical points on excited state potential energy surfaces (Bannwarth, et al. J. Chem. Phys. 2020). In particular, we have found hhTDA to perform well for the lowest two excited states of azobenzene (seen in Figure 2). This has allowed us to make quantitatively correct predictions of the photoisomerization yield resulting from excitation to each of these states. Further, we are able to extract time resolved spectroscopic observables (here, we show the UED signal) thus making these predictions directly testable by experiment.

In addition to UED observables, hhTDA has the advantage that core-excited states are treated equivalently to valence-excited states. Therefore, it is also possible to evaluate time-resolved X-ray absorption spectra (TRXAS) from our hhTDA simulations. We have begun preliminary investigations along these lines. Our initial results indicate that hhTDA is capable of resolving pre-edge features in TRXAS spectra.

Future Plans: Over the next year, we will further develop the hh-TDA method and explore its application to X-ray core-level spectroscopies such as XAS. We will also expand our efforts in collaboration with SLAC UED experimentalists to explore excited state dynamics in liquid phase, exploiting the liquid jet sample setup which is being developed in connection with the UED apparatus. We will simulate femtosecond diffraction for a number of molecules in advance of the experiments in order to establish the predictiveness of the current tools. In fact, the results shown above were carried out independently of the experiments they are being compared to and there are no adjustable parameters. Nevertheless, the theory and simulation data was obtained in parallel with the experiment and the agreement would be more persuasive if we carried out simulations in advance of the experiments. This will of course become more difficult as we progress to excited state dynamics in liquids, but we view this as a necessary step to clearly expose possible inadequacies in the theory.

References: Peer-Reviewed Publications Resulting from this Project (2018-2020)

Curchod, B. F. E. and T. J. Martínez, (2018). Ab Initio Nonadiabatic Quantum Molecular Dynamics.
Chem. Rev. 118:3305.

Boguslavskiy, A. E., O. Schalk, N. Gador, W. J. Glover, T. Mori, et al. (2018). Excited state non-adiabatic dynamics of the smallest polyene, trans 1,3-butadiene. I. Time-resolved photoelectron-photoion coincidence spectroscopy. J. Chem. Phys. 148:164302.

Glover, W. J., T. Mori, M. S. Schuurman, A. E. Boguslavskiy, O. Schalk, A. Stolow, and T. J. Martínez. (2018). Excited state non-adiaabtic dynamics of the smallest polyene, trans 1,3-butadiene. II. Ab initio multiple spawning simulations. J. Chem. Phys. 148:164303.

Yang, J., X. Zhu, T. J. A. wolf, Z. Li, J. P. F. Nunes, R. Coffee, J. P. Cryan, M. Guehr, K. Hegazy, T. F. Heinz, K. Jobe, R. Li, X. Shen, T. Veccione, S. Weathersby, K. J. Wilkin, C. Yoneda, Q. Zheng, T. J. Martínez, M. Centurion, and X. Wang. (2018). Imaging CF3I conical intersection and photodissociation dynamics with ultrafast electron diffraction. Science 361:64.

Li, T. E., A. Nitzan, M. Sukharev, T. Martínez, H.-T. Chen, and J. E. Subotnik. (2018). Mixed quantum-classical electrodynamics: Understanding spontaneous decay and zero-point energy. Phys. Rev. A. 97:032105.

Sachse, T., T. J. Martínez, B. Dietzek, and M. Presselt. (2018). A Program for Automatically Predicting Supramolecular Aggregates and Its Application to Urea and Porphin. J. Comp. Chem. 39:763.

Hollas, D., L. Sistik, E. G. Hohenstein, T. J. Martínez, and P. Slavicek. (2018). Nonadiabatic Ab Initio Molecular Dynamics with Floating Occupation Molecular Orbital-Complete Active Space Configuration Interaction Method. J. Chem. Theo. Comp. 14:339.

Mignolet, B., B. F. E. Curchod, F. Remacle, and T. J. Martínez. (2019). Sub-Femtosecond Stark Control of Molecular Photoexcitation with Near Single-Cycle Pulses. J. Phys. Chem. Lett. 10:742.

Sachse, T., T. J. Martínez, M. Presselt. On Combining the Conductor-like Screening Model and Optimally-tuned Range-separated Hybrid Density Functionals. (2019). J. Chem. Phys. 150:174117.

Timmers, H., X. Zhu, Z. Li, Y. Kobayashi, M. Sabbar, M. Hollstein, M. Reduzzi, T. J. Martínez, D. M. Neumark, and S. R. Leone. Disentangling conical intersection and coherent molecular dynamics in methyl bromide with attosecond transient absorption spectroscopy. (2019). Nature Comm. 10:3133.

Wilkin, K. J., R. M. Parrish, J. Yang, T. J. A. Wolf, P. F. Nunes, M. Guehr, R. Li, X. Shen, Q. Zheng, X. Wang, T. J. Martínez, and M. Centurion. (2019). Diffractive Imaging of Dissociation and Ground-State Dynamics in a Complex Molecule. Phys. Rev. A 100:023402.

Parrish, R. M. and T. J. Martínez. (2019). Ab Initio Computation of Rotationally-Averaged Pump-Probe X-Ray and Electron Diffraction Signals. J. Chem. Theo. Comp. 15:1523.

Wolf, T. J. A., D. M. Sanchez, J. Yang, R. M. Parrish, J. P. F. Nunes, M. Centurion, R. Coffee, J. P. Cryan, M. Guehr, K. Hegazy, A. Kirrander, R. K. Li, J. Ruddock, X. Shen, T. Veccione, S. P. Weathersby, P. M. Weber, K. Wilkin, H. Yong, Q. Zheng, X. J. Wang, M. P. Minitti, and T. J. Martínez. (2019). The Photochemical Ring-Opening of 1,3-cyclohexadiene Imaged by Ultrafast Electron Diffraction. Nature Chem. 11:504.

Wolf, T. J. A., R. M. Parrish, R. H. Myhre, T. J. Martínez, H. Koch, M. Guehr. (2019). Observation of Ultrafast Intersystem Crossing in Thymine by Extreme Ultraviolet Time-Resolved Photoelectron Spectroscopy. J. Phys. Chem. A 123:6897.

Yu, J. K., R. Liang, F. Liu, T. J. Martínez. (2019). First-Principles Characterization of the Elusive I Fluorescent State and the Structural Evolution of Retinal Protonated Schiff Base in Bacteriorhodopsin. J. Amer. Chem. Soc. 141:18193.

Erickson, B. A., Z. N. Heim, E. Pieri, E. Liu, T. J. Martínez, D. M. Neumark. (2019). Relaxation Dynamics of Hydrated Thymine, Thymidine, and Thymidine Monophosphate Probed by Liquid Jet Time-Resolved Photoelectron Spectroscopy. J. Phys. Chem. A 123:10676.

Liekhaus-Schmaltz, C., X. Zhu, G. A. McCracken, J. P. Cryan, T. J. Martínez, P. H. Bucksbaum. (2020). Strictly non-adiabatic quantum control of the acetylene dication using an infrared field. J. Chem. Phys. 152:184302.

Weir, H., M. Williams, R. M. Parrish, E. G. Hohenstein, T. J. Martínez. (2020). Nonadiabatic Dynamics of Photoexcited cis-Stilbene Using Ab Initio Multiple Spawning. J. Phys. Chem. B 124:5476.

Van den Berg, J. L., K. I. Neumann, J. A. Harrison, H. Weir, E. G. Hohenstein, T. J. Martínez, R. N. Zare. (2020). Strong, Nonresonant Radiation Enhances Cis-Trans Photoisomerization of Stilbene in Solution. J. Phys. Chem. A 124:5999.

Bannwarth, C. J. K. Yu, E. G. Hohenstein, T. J. Martínez. (2020). Hole-Hole Tamm-Dancoff-approximated density functional theory: A highly efficient electronic structure method incorporating dynamic and static correlation. J. Chem. Phys. 153:024110.

Yu, J. K., C. Bannwarth, E. G. Hohenstein, T. J. Martínez. (2020). Ab Initio Nonadiabatic Molecular Dynamics with Hole-Hole Tamm-Dancoff Approximated Density Functional Theory. J. Chem. Theo. Comp. 16:5499.

Duan, H.-G., A. Jha, X. Li, V. Tiwari, H. Ye, P. K. Nayak, X.-L. Zhu, Z. Li, T. J. Martínez, M. Thorwart, R. J. D. Miller. (2020). Intermolecular vibrations mediate ultrafast singlet fission. Sci. Adv. 6:eabb0052.

Yang, J., X. Zhu, J. P. F. Nunes, J. K. Yu, R. M. Parrish, T. J. A. Wolf, M. Centurion, R. Li, Y. Liu, B. Moore, M. Niebuhr, S. Park, X. Shen, S. Weathersby, T. Weinacht, T. J. Martínez, X. Wang. (2020). Simultaneous observation of nuclear and electronic dynamics by ultrafast electron diffraction. Science 368:885.

Curchod, B. F. E., W. J. Glover, T. J. Martínez. (2020). SSAIMS – Stochastic-Selection Ab Initio Multiple Spawning for Efficient Nonadiabatic Molecular Dynamics. J. Phys. Chem. A 124:6133.

List, N. H., A. L. Dempwolff, A. Dreuw, P. Norman, T. J. Martínez. (2020). Probing competing relaxation pathways in malonaldehyde with transient X-ray absorption spectroscopy. Chem. Sci. 11:4180.

ATO: Attosecond Science

PIs: James Cryan and Phil Bucksbaum
jcryan@slac.stanford.edu, phb@slac.stanford.edu
Stanford PULSE Institute, SLAC National Accelerator Laboratory
2575 Sand Hill Rd. Menlo Park, CA 94025
Participants: Taran Driver, Andrei Kamalov, Siqi Li, Agostino Marinelli,
Jordan O'Neal, Anna Wang

Project Scope: All photochemical transformations are initially driven by electron motion. Thus in order to more fully understand photon driven chemistry, we would like to track the evolution of electrons on their intrinsic timescale. For isolated molecules in the gas phase, this natural timescale is in the attosecond domain.

The ATO task is focused on understanding how coherent superpositions of electronic states evolve in time, and how these superpositions couple to other degrees of freedom in the molecular system. Moreover, the ability to measure real-time information of electron dynamics on attosecond timescales leads to a number of open-ended questions. For example, the nature of the information that is encoded in attosecond measurements, and how this information can be retrieved from the measurement, is still an active field of study. What role does coherent electron motion (on the attosecond scale) play in the chemistry (longer timescale nuclear motion) of a molecule?

Recent Progress

Creating and Probing Electronic coherences in molecules: In FY2019 we demonstrated the generation of isolated, GW-scale, soft x-ray (SXR) attosecond pulses with an X-ray free electron laser [Duris2020]. These pulses are intense enough to drive nonlinearities in molecular systems. A simple nonlinear technique for driving electronic motion, impulsive stimulated X-ray Raman scattering~(ISXRS), involves a single impulsive interaction to produce a coherent superposition of electronic states. We have demonstrated the ability of attosecond SXR pulses to produce valance excited states in the prototypical molecular system nitric oxide~(NO) using a time-delayed UV pulse to probe the valence excited states [O'Neal2020]. The impulsive excitation is resonantly enhanced by the oxygen $1s\text{->}2p\pi^*$ resonance, and we observe an excitation fraction nearly 3% following the interaction with the attosecond X-ray pulse.

ISXRS is not the only method for preparing non-stationary electronic states: impulsive ionization of inner valence electrons has been proposed as a method for creating a coherent superposition of ionic excited states. In comparison to ISXRS, impulsive ionization is more easily realized, but provides less control of the non-stationary state and lacks site-specificity of the excitation. Never-the-less, in a collaboration led by Jon Marangos (Imperial College) we have used an x-ray pump/x-ray probe scheme to investigate ultrafast hole dynamics in isopropanol [Barillot2020]. Combining the measurements with *ab intio* calculations of the ionization dynamics we can develop a complete picture of the electron dynamics following ionization of an inner valence hole.

Exploiting Noise in the Machine: In FY2020 the ATO task devoted significant effort in trying to understand the best way to extract information from the data collected at XFEL facilities. We make full use of the natural fluctuations of SASE XFEL pulses by correlating changes in the measured shot-to-shot x-ray spectrum with the single-shot yield of measured photoproducts. Extracting information from the correlated data set using the alternating direction method of multipliers (ADMM), we have made sub-bandwidth measurement of x-ray absorption spectra (XAS) [Driver2020] and x-ray photoelectron spectra (XPS) [Li2020]. In upcoming beamtimes we will

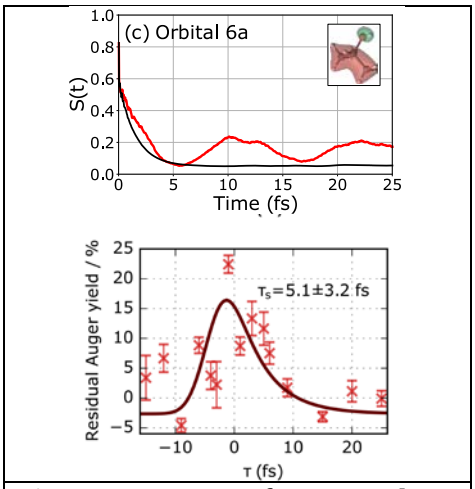

Figure 1 – Decay of Inner Valence Vacancy in Isopropanol - The upper panel shows the hole survival probability for ionization of the 6a inner valence orbital following sudden ionization. The colored curve corresponds to a mixture (1:1) of the two lowest conformers of the molecule. The black curves correspond to the averaged dynamics over geometries sampled over the spread of zero-point energy. The lower panel shows the time-dependent yield of Auger electrons detected when an x-ray probe pulse is resonantly tuned to the 1s->6a transition in the cation. The decay of the Auger signal is a signature of the dynamics of the inner valence hole and decays on a similar timescale.

exploit these site-specific observables to follow ultrafast charge motion in another prototypical system aminophenol (NH_2-C_6H_4-OH).

Electron Correlation in Attosecond Photoemission: In addition to developing methods for studying ultrafast electron dynamics with XFELs we employ table-top, HHG-based attosecond pulse sources to study the photoemission process in the time domain. We combine attosecond interference measurements with calculations of photoionization matrix elements to demonstrate how multi-electron dynamics affect photoionization time delays in carbon dioxide (CO_2) [Kamalov2020]. Attosecond photoionization has been primarily interpreted within the single-particle approximation, even for multi-electron systems. However, in molecular CO_2, electron correlation is observed to affect the time delays through two mechanisms: autoionization of molecular Rydberg states and accelerated escape from a continuum shape resonance.

Attosecond X-ray Photoemission: In order to diagnose the isolated attosecond pulses described above, we adapted the angular streaking (or atto-clock) method developed by Hartmann *et al.* [Hartmann2018] to work with isolated attosecond pulses. A circularly polarized, infrared (IR) laser field is temporally and spatially overlapped with the X-ray pulse and the combined interaction of the fields produces photoelectrons where the temporal properties of the X-ray pulse are mapped onto the photoelectron momentum distribution [Li2018]. In addition, to diagnosing the x-ray temporal waveform, this streaking technique can be used to study the temporal dynamics of x-ray ionization of *K*-shell electrons. Absorption of a high-energy photon creates a "hole" in the inner valence or core levels which results in electronic rearrangement on extremely fast timescales. This rearrangement leads to de-excitation of the system, often through the ejection of an energetic electron in the so-called Auger effect. There can also be sub-femtosecond interactions between the molecular ion and the initial outgoing electron produced by X-ray ionization. For example, transient trapping of the photoelectron wavepacket by the molecular potential leads to a large increase in the absorption cross-section just above the *K*-shell ionization edge. This feature has been dubbed the shape resonance. We have used the angular streaking technique to probe both of these absorption phenomena directly in the time domain using attosecond SXR pulses.

Time-Resolving Molecular Auger Decay: When tuned to the vicinity of a near-edge resonance, broad bandwidth attosecond x-ray pulses will coherently populate multiple core-excited resonances creating an electronic wavepacket in the core-excited molecule. As the core-excitation decays, the Auger emission from the different states in the core-excited wavepacket will interfere producing a beat in the Auger emission. We have successfully resolved this quantum beat, by directly measuring the temporal profile of the emitted Auger wavepacket. This is the first demonstration of time-resolved Auger emission that goes beyond extracting an exponential decay lifetime for the emission process. By tuning the central frequency, we can alter the core-excited wavepacket and thus alter

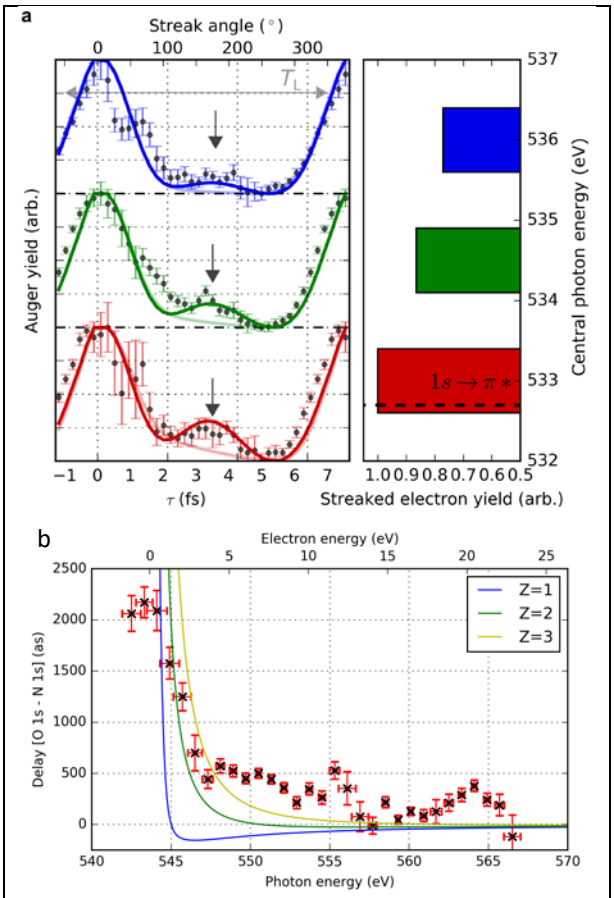

Figure 2 – Angular Streaking of X-ray Photoemission. Panel (a) shows the measured Auger emission in the presence of a 2.4 um streaking laser field (black dots). Looking as a function of angle between the streaking laser direction and Auger emission direction we can map out the temporal profile of the Auger emission. Comparing to a simple model with (dark lines) and without (transparent lines) interference between core-excited states, we clearly resolve the quantum beat in the Auger emission resulting from the coherent superposition of core-excited states. Panel (b) shows the relative photoemission delay between oxygen *K*-shell and nitrogen *K*-shell photoelectrons (black x). The solid curves show the expected Wigner delay for different effective ionic charge states.

the beat in the Auger emission as shown in Fig. 2. In follow-up experiments we hope to further resolve the electronic coherence and study the coupling of the coherence to nuclear motion on timescales shorter than the Auger lifetime.

***K*-shell Photoemission delays:** We have measured the photoionization delay between different *K*-shell continua: The N $(1s)^{-1}$ and O $(1s)^{-1}$ continuum in nitric oxide (NO). The nitrogen *1s* electrons provide a reference wavepacket to remove features induced by the phase of the ionizing x-ray pulse. Scanning near threshold we observe many features in the relative photoemission delay, likely related to the $2p\pi^*$ shape resonance. We are currently collaborating with Sasha Landsman (OSU) to model the two-color photoemission process in NO. We have also made measurements of valence ionization of NO using our table-top HHG source. Comparing the results of the two measurements we find there are stark differences in the delay of low kinetic energy electrons. These differences likely arise due to the localized (delocalized) nature of the valence *1s* (valence) orbital being ionized. As shown in Fig. 2, the *K*-shell photoemission has better agreement for a model with higher ionic charge due to the high level of localization of the initial *1s* orbital.

Future Plans

In the next calendar year, we will begin our attosecond campaign at the Linac Coherent Light Source. This is a multi-beamtime experiment with the goal of performing real-time measurements of attosecond electron dynamics and subsequent coupling to nuclear motion using the soft X-ray attosecond capabilities described above. Our measurements will demonstrate the control and observation of coherent electronic motion on its natural, attosecond, timescale and explore how the coherence affects the subsequent motion of the nuclei to drive chemical change. The campaign will provide pioneering insights into the coherent motion of electrons and how this drives chemical change, producing incisive X-ray observables against which theory can be directly tested on an unprecedented level of detail with particular emphasis on the atomic site-specific information content of X-ray transitions.

We will also continue our efforts in using angular streaking to explore attosecond photoemission delays in X-ray ionization. We will study the complicated many-body problem of correlated electron dynamics using the model process of photoemission.

References and Preprints:

[Barillot2020] Barillot *et al.* "Transient Hole Dynamics Resolved in Space and Time in the Isopropanol Molecule." under review in PRX

[Driver2020] Driver *et al.* "Attosecond transient absorption spooktroscopy: a ghost imaging approach to ultrafast absorption spectroscopy." Physical Chemistry Chemical Physics **22**, 2704-2712 (2020)

[Duris2020] J. Duris *et al.* "Tunable isolated attosecond X-ray pulses with gigawatt peak power from a free-electron laser." Nature Photonics **14**, 30-36 (2020)

[Hartmann2018] N. Hartmann *et al.*, "Attosecond time–energy structure of X-ray free-electron laser pulses," *Nat. Photonics*, vol. 12, no. 4, pp. 215–220, Apr. 2018.

[Li2018] Siqi Li *et al.* "Characterizing isolated attosecond pulses with angular streaking." Optics Express **26** 4531-4547 (2018).

[Li2020] Siqi Li *et al.* "Two-dimensional correlation analysis for X-ray photoelectron spectroscopy." under review in Jouranl of Phys. B.

[Kamalov2019] Kamalov *et al.* "Electron correlation effects in attosecond photoionization of CO_2." Physical Review A **102**, 023118 (2020)

Peer-Reviewed Publications Resulting from this Project (2018-2020):

1. Andrei Kamalov, Anna L. Wang, Philip H. Bucksbaum, Daniel J. Haxton, James P Cryan "Electron correlation effects in attosecond photoionization of CO_2." Physical Review A **102**, 023118 (2020)
2. Jordan T. O'Neal, Elio G. Champenois, *et int.* James P. Cryan "Electronic Population Transfer via Impulsive Stimulated X-Ray Raman Scattering with Attosecond Soft-X-Ray Pulses." Physical Review Letters **125**, 073203 (2020)
3. Taran Driver, Siqi Li, Elio G. Champenois, Joseph Duris, Daniel Ratner, Thomas J. Lane, *et int.* Agostino Marinelli and James P. Cryan "Attosecond transient absorption spooktroscopy: a ghost imaging approach to ultrafast absorption spectroscopy." Physical Chemistry Chemical Physics **22**, 2704-2712 (2020)
4. Joseph Duris, Siqi Li, Taran Driver, Elio G. Champenois, James P. MacArthur, *et int.* James P. Cryan, Agostino Marinelli "Tunable isolated attosecond X-ray pulses with gigawatt peak power from a free-electron laser." Nature Photonics **14**, 30-36 (2020)
5. Ryan N Coffee, James P Cryan, Joseph Duris, Wolfram Helml, Siqi Li, Agostino Marinelli "Development of ultrafast capabilities for X-ray free-electron lasers at the linac coherent light source." Philosophical Transactions of the Royal Society A **377**, 20180386 (2019).
6. Daniel Ratner, James P Cryan, Thomas J Lane, Siqi Li, G Stupakov "Pump-probe ghost imaging with SASE FELs." Physical Review X **9**, 011045(2019)
7. Siqi Li, EG Champenois, R Coffee, Z Guo, K Hegazy, A Kamalov, A Natan, J O'Neal, T Osipov, M Owens III, D Ray, D Rich, P Walter, A Marinelli, JP Cryan, "A co-axial velocity map imaging spectrometer for electrons." AIP Advances **8**, 115308 (2018)
8. Jie Yang, Xiaolei Zhu, Thomas JA Wolf, Zheng Li, J Pedro F Nunes, Ryan Coffee, James P Cryan, Markus Gühr, Kareem Hegazy, Tony F Heinz, Keith Jobe, Renkai Li, Xiaozhe Shen, Theodore Veccione, Stephen Weathersby, Kyle J Wilkin, Charles Yoneda, Qiang Zheng, Todd J Martinez, Martin Centurion, Xijie Wang, "Imaging CF3I conical intersection and photodissociation dynamics with ultrafast electron diffraction." Science **631**, 64-67 (2018)
9. Siqi Li, Zhaoheng Guo, Ryan N Coffee, Kareem Hegazy, Zhirong Huang, Adi Natan, Timur Osipov, Dipanwita Ray, Agostino Marinelli, James P Cryan, "Characterizing isolated attosecond pulses with angular streaking." Optics Express **26** 4531-4547 (2018).

SPC: Solution Phase Chemistry, Kelly Gaffney (PI), Amy Cordones-Hahn (PI)
SLAC National Accelerator Laboratory, 2575 Sand Hill Rd., Menlo Park, CA, 94025
Email: gaffney@slac.stanford.edu, acordon@slac.stanford.edu

Project Scope

Harnessing the strong optical absorption and photocatalytic activity of inorganic complexes depends on our ability to control fundamental physical and chemical phenomena associated with the non-adiabatic dynamics of electronic excited states. Internal conversion and intersystem crossing events governed by non-adiabatic interactions between electronic states critically influence the electronic excited state chemistry. Conventional wisdom predicts dynamics to occur with a hierarchy of time scales – vibrational energy redistribution followed first by internal conversion, and then by intersystem crossing. Contrary to conventional wisdom, ultrafast time-domain studies have shown that spin-state transitions can compete with spin-conserving electronic state transitions and both types of electronic-state transitions can occur on the time scale of vibrational energy redistribution.

There is a clear need for a new conceptual framework that can supplant the conventional wisdom for understanding electronic excited-state dynamics. The incisive observation of the electronic excited state dynamics is an essential step towards this objective. To achieve this experimental objective, the Solution Phase Chemistry (SPC) sub-task focuses on the application of ultrafast x-ray methods to the study of electronic excited state dynamics of inorganic molecules in complex chemical environments. More specifically, we endeavor to:

- Identify how excited state electron and spin density distributions control non-radiative relaxation with time resolved measurements, simple ligand exchange reactions, and simulation.
- Determine the importance of site-specific interactions between solvent and solute in electronic excited-state relaxation dynamics with ultrafast time-resolved measurements and molecular simulation.

Achieving these scientific objectives also requires development of ultrafast x-ray and electron methods. Our previous research has emphasized the development of simultaneous hard x-ray diffuse scattering (XDS) and x-ray emission spectroscopy (XES) as probes of charge, spin, and metal-ligand bonding dynamics in electronic excited states. We currently focus on methods that will be transformed by LCLS-II, in particular soft x-ray Resonant Inelastic X-ray Scattering (RIXS) as a probe of metal-ligand covalency in electronic excited states, and the extension of ultrafast electron diffraction (UED) to solution phase dynamics.

Recent Progress

***Mechanistic understanding and control of electronic relaxation dynamics in 3d coordination complexes* (Jay 2018; Kjaer 2018; Kjaer 2019; Kunnus 2020a; Kunnus 2020b; Ledbetter 2020; Norell 2018; Tatsuno 2019):** The strength of the interaction between charge transfer and metal-centered excited states controls the rate and mechanism for electronic excited state relaxation dynamics in 3d transition metal complexes. To gain a mechanistic understanding of these processes, our approach has been to disentangle the nuclear and electronic structure dynamics of MLCT excited states in iron coordination complexes using simultaneous hard x-ray

WAXS and Fe K-edge XES (Kjaer 2019).This work initially focused on the archetypical photo-induced spin crossover complex iron tris-2,2'-bipyridine ($[Fe(bpy)_3]^{2+}$. By separating the measurement of nuclear and electronic dynamics, we have been able to identify the mean Fe-ligand bond length where transitions between metal-centered triplet (^{3}MC) and quintet (^{5}MC) states occur (Kjaer 2019).

More recently, in pursuit of long-lived charge transfer excited states, we have begun investigating the excited state dynamics of iron carbene complexes as photosensitizers and photocatalysts (Kunnus 2020b; Tatsuno 2019). The Fe-C bond of organometallic Fe carbene complexes generates a strong ligand field that destabilizes MC excited states, resulting in MLCT lifetimes ≥100 ps. We applied simultaneous hard x-ray WAXS and Fe Kα and Kβ XES to investigate the dynamics of an Fe carbene photosensitizer, $[Fe(bmip)_2]^{2+}$ where bmip = 2,6-bis(3-methyl-imidazole-1-ylidine)-pyridine, induced by MLCT excitation (Kunnus 2020b). This measurement shows temporal oscillations in the XES and XSS difference signals with the same 278 fs period oscillation. These oscillations originate from an Fe-ligand stretching vibrational wavepacket on a ^{3}MC excited state surface. Our observations demonstrate that MC excited states remain a viable relaxation challenge, even for the large ligand field carbenes. From a methodological perspective, this study demonstrates an unexpected sensitivity of the Kα XES to molecular structure, which originates from a small change in the average Fe-ligand bond length in the initial (1s) and final (2p) core-ionized states of the Kα emission process. In our prior studies we have assumed the x-ray emission signal is insensitive to the details of the molecular structure. Clearly, this assumption does not apply to the strongly covalent Fe carbenes and we hope to determine the prevalence of vibronic effects in hard x-ray emission spectroscopy.

Further mechanistic studies of excited state relaxation in Fe model photosensitizers focused on the mixed ligand complex $[Fe(bpy)(CN)_4]^{-4}$, where the incorporation of CN ligands is known to destabilize MC states, similarly to the aforementioned carbene ligands, and extend the MLCT lifetime. By combining ultrafast Fe K-edge XES and optical spectroscopy (Kjaer 2018), we identified the solvent-dependent relaxation pathways that result in a relatively long-lived MLCT state (aprotic solvents) or meta-stable ^{3}MC state (protic solvents), thus establishing our ability to tune the MLCT lifetime by varying experimental conditions. More recent work on this class of Fe mixed-ligand complexes has focused on ligand control of MLCT lifetimes, using polypyridyl ligand modifications as a pathway to controlling excited state relaxation processes (Kunnus 2020a). These studies have used a novel combination of ultrafast optical spectroscopy and Fe L-edge resonant inelastic x-ray scattering (RIXS) to demonstrate that the MLCT relaxation mechanism transitions from one mediated by metal-centered excited states at large chemical driving force to one driven by vibrational tunneling in the Marcus inverted region at lower chemical driving force. These findings strongly indicate that successful design of ligands for long MLCT lifetimes requires both reducing the chemical driving force and minimizing the charge transfer induced distortions of the electron accepting ligand. These finding are directing the next steps of this research project.

Development of Liquid Phase Ultrafast Electron Diffraction (UED) methods **(Koralek 2018; Nunes 2020)*:*** We have collaborated with SLAC's Ultrafast Electron Diffraction (UED) facility on the development and commissioning of a new liquid-jet endstation for the first solution-phase UED experiments (Nunes 2020). While electron diffraction had previously been applied to

understanding the ultrafast structural dynamics of isolated gas phase molecules and solid-state materials systems, the strong attenuation of the electron beam in liquids precluded measurements of solution-phase and solvated molecule dynamics. The new endstation overcomes this challenge by coupling the MeV electrons available at UED with newly developed ultra-thin in-vacuum liquid sheet jets (Koralek 2018). In the first liquid-phase UED experimental run (Nunes 2020), we successfully measured the static electron diffraction of a wide range of liquid-phase samples, probed the photo-induced structural changes of liquid water under conditions ranging from vibrational to strong field excitation, and resolved the photodissociation of solvated I_3^-. Future developments will focus on the extending the UED capabilities to measure excited state structural dynamics of dilute solvated molecules, such as the Fe complexes described above.

Future Plans

Controlling MLCT excited state lifetimes in 3d coordination complexes **(Kjaer 2018; Kjaer 2019; Koroidov 2018; Kunnus 2020a; Kunnus 2020b; Ledbetter 2020; Norell 2018; Tatsuno 2019)*:*** New systems aimed at suppressing spin crossover relaxation in Fe-based materials will be explored through ultrafast optical absorption, WAXS, XES, and RIXS measurements. We will approach this goal using targeted ligand design to stabilize the MLCT or destabilize MC excited states. We will continue to target newly designed polypyridyl ligands in Fe mixed-ligand complexes that both lower the energy of the MLCT states and decrease the structural distortions that enhance MLCT-to-ground state relaxation. We will also focus on identifying the role of strong metal-ligand covalency in dictating the excited state relaxation mechanisms of Fe carbenes and of a new class of Fe complexes incorporating amido donor ligands, thought to mix strongly with the Fe d orbitals.

Preparing for science enabled by LCLS-II **(Biasin 2018; Cordones 2018; Jay 2018; Källman 2020; Koralek 2018; Norell 2018; Kong, 2019; Haldrup, 2019):** The SPC sub-task emphasizes the development and application of unique research infrastructure at SLAC to the objectives described above. For LCLS-II, we are collaborating with LCLS in the development of the chemRIXS endstation for solution phase ultrafast RIXS. We propose using ultrafast RIXS to investigate electronic excited state PCET and electronic excited state dynamics of 3d transition metal complexes. For PCET reactions, we will leverage the ability of x-ray spectroscopy to provide an atom specific fingerprint of the H or proton site, while the studies of transition metal complexes will focus on the interplay between the electron density distribution and excited state relaxation dynamics.

References

Peer-Reviewed Publications Resulting from this Project (2018-2020)

Asakura, K., K. J. Gaffney, C. Milne, et al. (2020). XFELs: cutting edge X-ray light for chemical and material sciences. *Phys. Chem. Chem. Phys.* **22**: 2612.

Biasin, E., T. B. van Driel, G. Levi, et al. (2018). Anisotropy enhanced X-ray scattering from solvated transition metal complexes. *J. Synchrotron Radiat.* **25**: 306.

Cordones, A. A., J. H. Lee, K. Hong, et al. (2018). Transient metal-centered states mediate isomerization of a photochromic rutheniumsulfoxide complex. *Nature Comm.* **9**.

Haldrup, K., G. Levi, E. Biasin, et al. (2019). Ultrafast X-ray scattering measurements of coherent structural dynamics on the ground-state potential energy surface of a diplatinum molecule. *Phys. Rev. Lett.* **122**: 063001.

Jay, R. M., J. Norell, S. Eckert, et al. (2018). Disentangling Transient Charge Density and Metal-Ligand Covalency in Photoexcited Ferricyanide with Femtosecond Resonant Inelastic Soft X-ray Scattering. *J. Phys. Chem. Lett.* **9**: 3538.

Källman, E., M. Guo, M. G. Delcey, et al. (2020) Simulations of valence excited states in coordination complexes reached through hard X-ray scattering. *Phys. Chem. Chem. Phys.* **22**: 8325.

Kjaer, K. S., K. Kunnus, T. C. B. Harlang, et al. (2018). Solvent control of charge transfer excited state relaxation pathways in [Fe(2,2 '-bipyridine)$(CN)_4]^{2-}$. *Phys. Chem. Chem. Phys.* **20**: 4238.

Kjaer, K. S., T. B. van Driel, T. C. B. Harlang, et al. (2019). Finding Intersections between Electronic Excited State Potential Energy Surfaces with Simultaneous Ultrafast X-ray Scattering and Spectroscopy. , *Chem. Sci.*, **10**: 5749.

Kong, Q. Y., M. G. Laursen, K. Haldrup, et al. (2019). Initial Metal-Metal Bond Breakage Detected by fs X-ray Scattering in the Photolysis of $Ru_3(CO)_{12}$ in cyclohexane at 400 nm, *Photochem. Photobio. Sci.* **18**: 319.

Koralek, J. D., J. B. Kim, P. Bruza, et al. (2018). Generation and characterization of ultrathin free-flowing liquid sheets. *Nature Comm.* **9**.

Koroidov, S., K. Hong, K. S. Kjaer, et al. (2018) Probing the Electron Accepting Orbitals of Ni-Centered Hydrogen Evolution Catalysts with Non-Innocent Ligands by Ni and S Edge X-Ray Absorption, *Inorg. Chem.* **57**: 13167.

Kunnus, K., L. Li, C. J. Titus, et al. (2020a). Chemical control of competing electron transfer pathways in iron tetracyano-polypyridyl photosensitizers. *Chem. Sci.* **11**: 4360.

Kunnus, K., M. Vacher, T. C. B. Harlang, et al. (2020b). Vibrational wavepacket dynamics in Fe carbene photosensitizer determined with femtosecond X-ray emission and scattering. *Nat. Commun.* **11**: 634.

Ledbetter, K., M. E. Reinhard, K. Kunnus, et al. (2020). Excited state charge distribution and bond expansion of ferrous complexes observed with femtosecond valence-to-core x-ray emission spectroscopy. *J. Chem. Phys.* **152:** 074203.

Norell, J., R. M. Jay, M. Hantschmann, et al. (2018). Fingerprints of electronic, spin and structural dynamics from resonant inelastic soft X-ray scattering in transient photo-chemical species. *Phys. Chem. Chem. Phys.* **20**: 7243.

Nunes, J. P. F, K. Ledbetter, M. Lin, et al. (2020). Liquid-phase mega-electron-volt ultrafast electron diffraction. *Struc. Dyn.* **7**: 024301.

Tatsuno, H., K. Kjaer, K. Kunnus, et al. (2019) Hot Branching Dynamics in a Light-Harvesting Iron Carbene Complex Revealed by Ultrafast X-ray Emission Spectroscopy. *Angewandte Chemie* **59**: 364.

NPI: Non-Periodic Ultrafsat X-ray Imaging

Adi Natan, SLAC National Accelerator Laboratory, Menlo Park, CA 94025

natan@slac.stanford.edu

Project Scope : The NPI subtask goal is to image atomic motion and transient structure dynamics of molecules in the gas and condensed phase using ultrafast hard x-ray scattering. We develop experimental and computational methods to measure, analyze and understand how to image dynamics in molecular systems of various complexity, help LCLS develop effective science protocols for x-ray diffractive scattering experiments, demonstrate important new capabilities as soon as they become feasible at LCLS and leverage development of new modalities and detection schemes.

Recent Progress: Preparing for LCLS-II capabilities, we are developing several experimental and analysis approaches to advance the field of molecular movies using ultrafast x-ray scattering. We are developing a computational-experimental approach that combines the information about the detector and measurement limitations with scattering simulations of the relevant part of the phase space we would like to resolve, namely atomic species and distance ranges. The result is a representation that can be used to deconvolve and super-resolve multiple real-space motions de-novo and uncover details that are otherwise not resolvable with a typical Q range. We validate the method with various "ground truth" calculations where we solve the time dependent Schrodinger equation (TDSE) for light-molecule interaction for a wide range of excitations, and use the solutions as inputs of a scattering simulation that include measurement limitations . An example that demonstrates the method on simulated data is shown in Fig 1, where we calculate a the outcome of a "typical" complex excitation scheme that include dynamics in three electronic states in Iodine (X, B, C) induced by a pair of time delayed optical pulses of different wavelengths. For simplicity, we will use the angle averaged atomic positions of such a calculation (Fig 1a) to simulate scattering signals that are limited in Q range similar to typical experimental conditions (1 $Å^{-1}$ < Q < 4 $Å^{-1}$). Transforming the data to real-space using the sine-transform, will reveal the limitation in resolution as well as additional artifacts due to the finite Q range (Fig 1c). Deconvolving based on the representation mentioned correctly recovers the positions and amplitudes of the simulated data (Fig 1d).

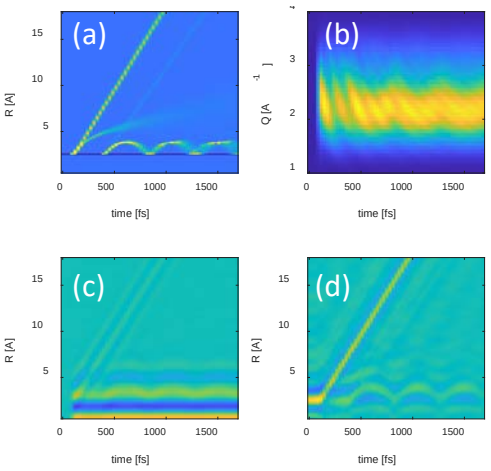

Fig 1 - Deconvolving simulated scattering data from a finite detector. (a) TDSE calculation on I_2 molecules following 480 and 530 nm pulses (30 fs, $7*10^{10}$ W/cm^2) that excite X to B and C states. (b) simulated scattering signal (angle averaged) using the TDSE with a finite Q range, similar to experiments. (c) a sine-transform of the data in (b) is unable to capture the dynamics details. (d) Deconvolution-based analysis where the measurement limitations and atomic distance ranges are included captures de-novo the details in (b) and improves the resolution limit set by the finite Q range by a factor of ~6.

Developing this method will not only impact our analysis of future experiments, but is already making an impact being used in current analysis efforts, where we are able to resolve dynamics not seen previously in the gas and condensed phase from previous experiments. We demonstrate this approach and resolve complex and strong field excitation dynamics of Iodine in the gas phase from data collected in a previous LCLS beam time. We uncover multiple dissociation pathways

of strongly driven Iodine and are able to resolve several ballistic type dissociations pathways that result from unbound potentials, as well as diffusive type dissociation, where the wavepacket is dissociated from a bound state and is dispersed around the outer turning point of the potential curve on from which it is dissociating from, as can be seen in Fig 2.

A similar effect is also capture in the TDSE in Fig 2, where the first pulse at t=100 fs induce two dissociations, one from the unbound C state that has a ballistic trajectory, and the other from the B state, that is strongly dispersed (diffusive trajectory) by the potential curve.

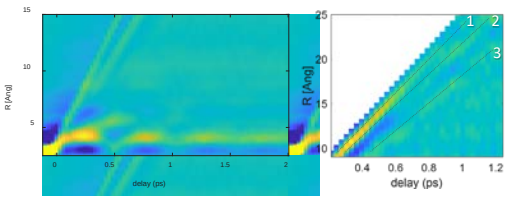

Fig 2 - Deconvolving measured time-resolved scattering signal of I_2. (left) Real-space angle averaged charge density position as function of probe delay of excited I_2. The excitation pulse was 520 nm, 50 fs duration, ~$2*10^{11}$ W/cm^2. We can see damped vibrations, diffusive and ballistic dissociations (See text). (right) inspecting larger spatial distances we can resolve three dissociation process with velocities of (1) 20.5, (2) 18.6, and (3) 16.2 $\pm$0.4 Å/*ps*.

We also are developing a generalization of this approach to account for any anisotropy order of a scattering signal, where we decompose the scattering signal to a Legendre basis and obtain the deconvolution procedure of each order separately. It is easy to show that each photon absorbed will generally contribute an additional (even) Legendre order, however a n-photon process will have projections on all the lower orders. We prove that for the general case of an nth-photon process, the corresponding representation and the deconvolution are robust and will behave like the 0th order for most practical purposes, with the difference that in a 2D-array detector, the angle resolution (hench the order degree) is ultimately limited by the pixel size and scattering angle. We develop an algorithm to treat the general case where signals are composed of several anisotropy orders, by mapping the projections from the nth order representation to all lower orders and peeling their effect until the anisotropy signals represent a single order process. We are implementing this technique to analyze strongly driven molecular iodine that exhibit high-order scattering anisotropy and use that information to disentangle the states and number of photons involved, to create a real-space angle resolved molecular movie of the excited system.

In the case of solution phase ultrafast scattering, most experiments analysis rely on models that consider a single pathway reaction to interpret that data. It is therefore important to develop de-novo approaches that can reveal multiple process for excited systems in complex environments. We are implementing our deconvolution approach and show we can disentangle several types of dynamics of excited Iodine in Methanol (Fig 3). We observe two dissociation signals, one from the solute and one from the solute-cage (I-O, I-C), as well as recombination. By analyzing the real-space isotropic and anisotropic contributions we trace motion relaxation and transition to equilibrium solvent-solute distances. We observe how motion changes from ballistic to diffusive in timescales of 400 fs, and distances of 4-5 A, and redistribute in the environment via rovibrational solute-cage coupling. We support our results

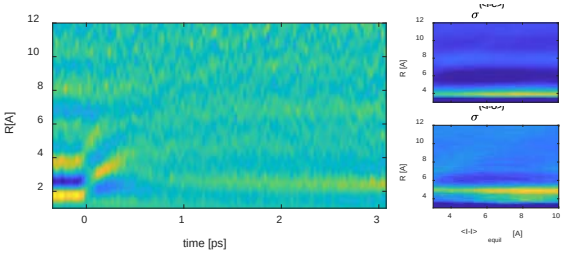

Fig 3 - Deconvolving measured time-resolved scattering signal of I_2 in methanol. (left) Real-space angle averaged charge density position as function of probe delay. (right) the calculated equilibrium distances of I-C and I-O pair correlations as function of the I-I distance. (see text)

with calculating the equilibrium positions of the different solvent-solute pair-correlations that contribute and obtain agreement for the build up at longer time delays.

We have also made progress in analyzing and understanding the photo-physics of $Fe[CO]_5$ data. This was aided by developing tools for the analysis of time-resolved scattering data in dynamic noise conditions based on high-dimensional correlation and prediction analysis of the different experimental parameters. This approach allows to extrapolate an effective instantaneous background representation at the single shot level and further reduce the noise variance. This is important with the challenging dynamic fluorescence background that $Fe[CO]_5$ has. We resolve time dependent dissociation dynamics and relaxation and are currently in the process to correlate our analysis with spectroscopic data. We expect that this will also be invaluable to future LCLS-II experiments at larger Q-range and for generic samples where we expect weaker signals with more challenging background channels.

We are continuing to collaborate with ATO subtask to use attosecond X-ray pulse characterization using angular streaking to uncover electronic motions. Initial experiments in the soft x-ray regime demonstrated this approach, capturing attosecond x-ray pulse pairs, observe electronic population transfer via impulsive Raman in the x-ray regime, and time resolve the molecular Auger decay. Developing this method will enable potential hard x-rays scattering experiments in the attosecond regime to establish the x-ray probe properties as well as relative phase between two attosecond x-ray pulses in a single shot. Such information will open the way to develop new imaging modalities, that will allow the combination of spectroscopy and imaging in attosecond – angstrom scales, for studying and imaging electronic motion in excited systems.

Future Plans: We were granted LCLS beam time to study ultrafast solvation and coherent dynamics with high-energy X-rays, collaborating with the SPC and EIM subtasks, and with researchers from DTU. This beam time was postponed to Run 19 due to the covid-19 situation. We plan to harness the new LCLS capabilities combining high-energy X-rays with extreme brilliance and time resolution to robustly characterize the non-equilibrium properties of molecules in the condensed phase with atomic scale resolution in time and space. Until now, having access to only low-Q data made disentangling significantly overlapping signals arising from different parts of the system unfeasible. With LCLS-II, this limitation will be alleviated by extending the photon energy up to 25 keV and the Q-range to >12 $Å^{-1}$, enabling the solute scattering difference signal to be robustly distinguished from other solvent and solute-solvent (cage) difference signals. It will also enable higher fidelity in the structural analysis, and the ability to measure not only the centroid of wave packets, but also their dynamical widths. We plan to demonstrate how the high Q-range and anisotropic scattering signal can be used to directly measure the ultrafast solvation dynamics of the model photocatalysts PtPOP ($[Pt_2(POP)_4]^{4-}$, and IrDimen ($[Ir_2(dimen)_4]^{2+}$. These complexes provide ideal systems for demonstrating the ability of high-*Q* ultrafast scattering and QM/MM simulations to decompose ultrafast solvation dynamics into specific changes in the solute-solvent pair distribution function with a particular focus on how electronic excited states change the interaction between the solvent and photo-catalytically active metal sites. We will also use previously measured PtPOP scattering data in low-Q range to validate the deconvolution approach both for the isotropic and anisotropic case, and compare with the study's QM/MM model with the aim to uncover additional dynamics originating from other atom pairs.

We also prepare for a Run 18 LCLS beam time, where will extend our efforts to map the interactions involving multiple degrees of freedom in the triatomic CS_2 and polyatomic CH_2IBr, with precision, and in all the relevant dimensions. The goal is to excite and view the evolving complex polyatomic intramolecular motion with sufficient fidelity and to demonstrate the ability of ultrafast X-ray scattering to for discovery science, as well as confirmation of theory and models.

We are continuing our effort to develop a way resolve in energy X-ray scattering such that inelastic and elastic parts of the scattering process can be accessed independently, and consequently, to allow to disentangle the contribution of electronic coherent motions, or coherences from charge density populations. We have designed and ordered a diced crystal analyzer to study the way we can tailor different bandwidth acceptance of different aspect ratios of the diced crystal elements, with the aim to resolve <1eV bandwidth at energy shifts of a few eV around >10 keV photons. This analyzer will be used in the imaging mode rather than in the focusing mode to obtain all the momentum vector components. We expect to use this approach first in a synchrotron study in 2021 to demonstrate speckle contrast enhancement via energy resolved imaging.

Peer-Reviewed Publications Resulting from this Project (2018-2019):

S. Li, R. Coffee, Z. Guo, A. Natan, K. Hegazy, et al, **A Co-axial Velocity Map Imaging Spectrometer for Electrons,** AIP Advances, 8(11), 115308 (2018).

G. Porat, G. Alon, S. Rozen, O. Pedatzur, M. Kruger, et al, **Attosecond time-resolved photoelectron holography**, Nat. Communications 9 (1), 2805 (2018).

S. Li, Z. Guo, R. N. Coffee, K. Hegazy, Z. Huang, et al, **Characterizing isolated attosecond pulses with angular streaking**, Opt. Express 26 (4), 4531-4547 (2018).

M. R. Ware, J. M. Glownia, A. Natan, J. P. Cryan, and P. H. Bucksbaum, **On the limits of observing motion in time-resolved x-ray scattering** Philos. Trans. Royal Soc. A, 377(2154), 20170477 (2019)

M. R. Ware, J. M. Glownia, N. Al-Sayyad, J. T. O'Neal, and P. H. Bucksbaum, **Characterizing dissociative motion in time-resolved x-ray scattering from gas-phase diatomic molecules**, Physical Review A 100, 033413 (2019)

J. Duris, S. Li, T. Driver, E. G. Champenois, J. MacArthur, et al, **Tunable Isolated Attosecond X-ray Pulses with Gigawatt Peak Power from a Free-Electron Laser**, *Nature Photonics* 14 (1), 30-36 (2020).

T. Driver, S. Li, E. G. Champenois, J. Duris, D. Ratner, et al, **Attosecond Transient Absorption Spooktroscopy: a ghost imaging approach to ultrafast absorption spectroscopy,** *Physical Chemistry Chemical Physics* (2020).

T. Kierspel, A. Morgan, J. Wiese, T. Mullins, A. Aquila, et al, **X-ray diffractive imaging of controlled gas-phase molecules: Toward imaging of dynamics in the molecular frame**. *Journal of Chemical Physics*, 152 (8), 084307 (2020).

P H Bucksbaum, M R Ware, A Natan, J P Cryan, J M Glownia, **Characterizing multiphoton excitation using time-resolved X-ray scattering**, *Physical Review X* 10 (1), 011065 (2020)

O'Neal, Jordan T., et al. **Electronic population transfer via impulsive stimulated x-ray Raman scattering with attosecond soft-x-ray pulses,** *Physical Review Letters* 125 7 073203 (2020).

SFA: Strong Field AMO Physics

PIs: Phil Bucksbaum and Adi Natan
Stanford PULSE Institute, SLAC National Accelerator Laboratory
2575 Sand Hill Rd. Menlo Park, CA 94025
phb@slac.stanford.edu, natan@slac.stanford.edu

Participants: *Phil Bucksbaum, Ruaridh Forbes, Nick Werby, Ian Gabalski, Adi Natan, James Cryan, David Reis. Collaborators: Mike Glownia, Mike Minitti, Matt Ware, Thomas Wolf, Nanna Holmgaard, Todd Martinez (PULSE); Robert Luccese (LBNL); Peter Weber (Brown); Carla Faria, Andrew Maxwell (UCL).*

Project Scope*:* The Strong Field AMO task investigates the dynamics and control of atoms and molecules in externally applied strong coherent electromagnetic fields, from optical to x-ray frequencies. We study strong-field excitation of external and internal quantum coherences in molecules to gain a deeper understanding of strong-field ionization and field-induced changes in symmetry and topology as well as strong-field quantum control. This is particularly relevant for focused beams from x-ray FELs, since they are a source of some of the strongest electromagnetic fields available, up to kilovolts per Angstrom. It also has close connections to attosecond science, since strong fields induce rapid evolution of small quantum systems.

Recent Progress

Strong-field attosecond electronics: Elastic rescattering structures in strong-field ionization. Strong-field ionization by optical or infrared focused lasers occurs at field strengths in the vicinity of 1v/Å. The gross features of the ionization such as ATI, strong-field cutoffs, and inelastic process leading to high harmonics have been explored for decades, the intricate electron momentum spectra observed in velocity-map images such as Fig. 1 have a number of features that have eluded simple explanation because of many overlapping and interfering quantum electronic processes. Clearly identifying these processes would yield insights into the strong-field attosecond quantum dynamics of strongly-driven electrons, so this is of great interest to this research community.

Quantum calculations predict complex sub-cycle interferences that have attracted wide interest. Experimental searches for these features must overcome the significant challenge that a highly controlled 1- to 2-cycle pulse is difficult to realize in the laboratory, whereas sub-cycle features produced by longer pulses are dominated by above-threshold ionization (ATI), a signature of multi-cycle interference. We have developed a simple and effective technique to recover sub-cycle features in the momentum distributions for atoms and small molecules subject to strong-field ionization. We overcome these difficulties by first decomposing the momentum distributions in a Legendre basis, and then directly filtering the one-dimensional radial coefficients. This method reveals interference structures in unprecedented detail. We can resolve new structures that have not previously been noted in earlier literature.

Among the features that we have discovered using this analysis are finer modulations superimposed on the well-known prominent holographic features, such as the spider-like interferences, as seen in Fig. 1. Coulomb-quantum orbit strong field calculations are currently underway in a collaboration with Carla Faria and Andrew Maxwell of the University College London to see how these features might be related to subcycle electron trajectories. These analysis methods allow isolation of subcycle interference effects to facilitate a detailed comparison.

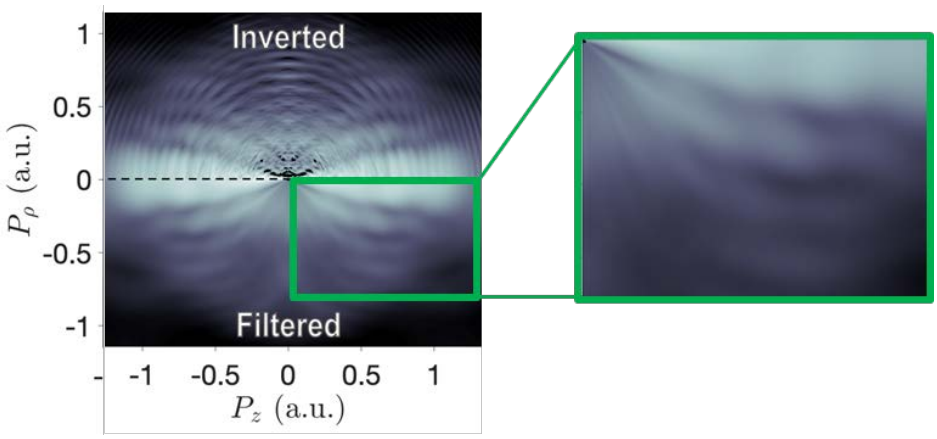

Fig. 1: Filtering technique applied to argon: Removal of the multicycle interferences (i.e. ATI) that dominate the Abel inverted data (top left) reveals subcycle structure that was previously difficult to separate (bottom left). The expanded view (right) shows modulations, which are evidence for subcycle interference.

Electrons that return within about one optical cycle following strong-field laser-induced photoionization can also scatter elastically or inelastically in the field, and the sudden momentum change then can lead to momenta above the field-induced momentum A_0. This scattering momentum is typically beyond the cutoff for laser-induced diffraction, since the typical $\hbar/p$ for strong-field ionization at 800nm is much greater than a bond length. Nonetheless these rescattering features are highly structured in patterns that depend on the target. Simple SFA trajectory maps show that these features are likely due to the "long trajectories" in field ionization (Fig. 2).

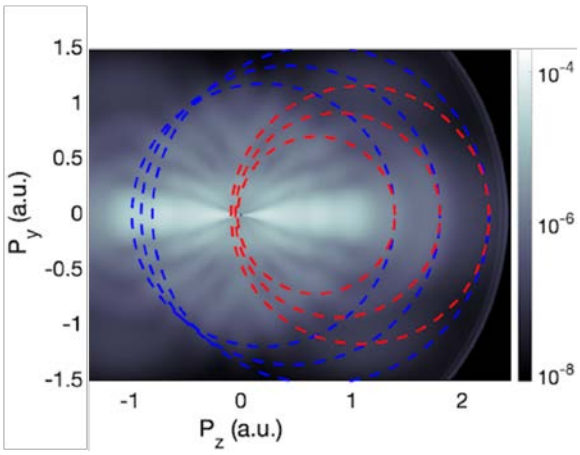

Fig. 2. Rescattering rings in subcycle strong-field scattering VMI maps extend beyond the circle of scattering defined by the laser-induced momentum A_0, where most of the strong-field ionized electrons are found. In the image of ionization from Ar shown at left, the red circles trace scattering from the "long trajectories" that return to the cation, and the blue circles trace rescattering by the short trajectories. The data appear to follow the long trajectories, as expected.

We have been working with Robert Lucchese of LBNL to analyze these features to explore whether we can see the effects of the scattering potential distorted by the strong field.

X-ray scattering signatures of early-time accelerations in molecular dissociation

Hard x-ray elastic scattering from transiently excited molecules produces time-resolved x-ray scattering (TRXS) data $S(Q,\tau)$, where Q is the momentum transfer and as a function of pump-probe delay. A standard goal is to view this data as a "molecular movie" $S(R,\tau)$ by performing a Fourier transform on Q to form the molecular spatial autocorrelation function. However, this view suffers from congestion, since different modes of motion tend to overlap in space and time. To overcome this we have developed frequency resolved x-ray scattering (FRXS)

analysis, where TRXS data are Fourier transformed along the τ-axis to form the complex scattering function $S(Q,\omega)$. This work has now been extended to the study of strong-field processes, shown in Fig. 3.

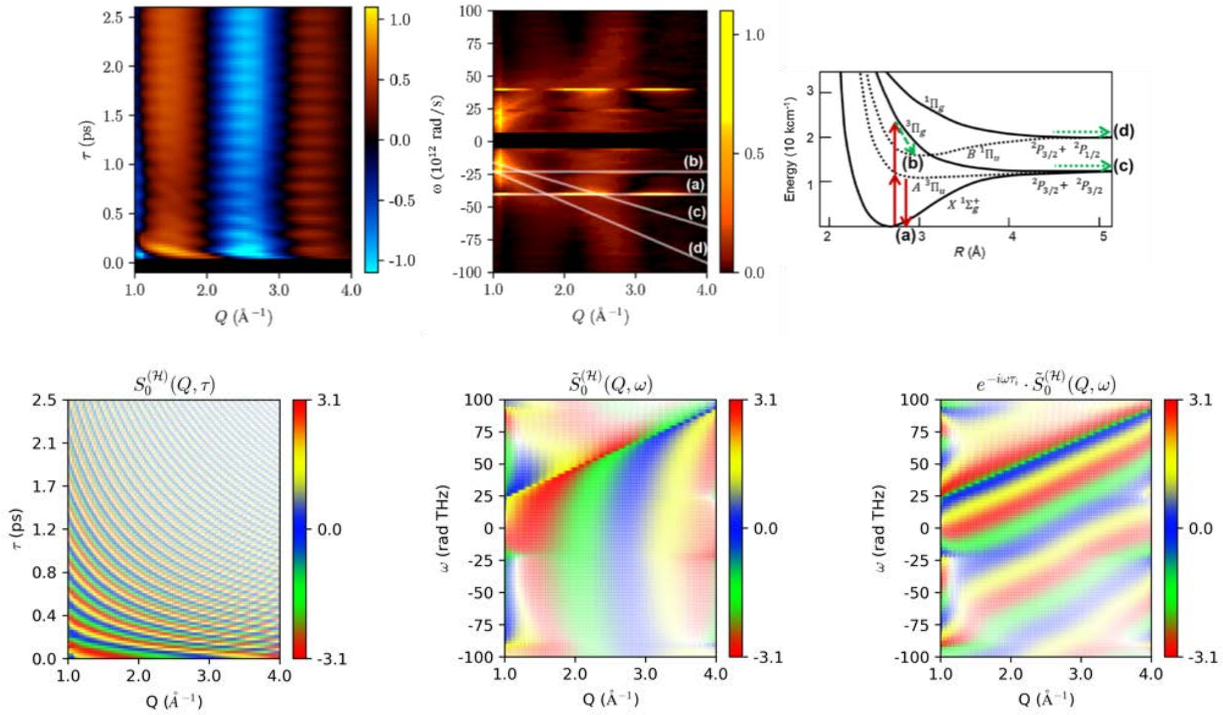

Fig. 3. Top, left to right: TRXS data from intense 800nm excitation of molecular iodine; FXRS power spectrum of the same data, with four channels indicated (a) through (d); each process labeled on a simplified iodine potential energy diagram. Bottom, left: simulation of Hilbert-transformed dissociation TRXS data. Bottom center: FRXS analysis of the same data. Note that the Hilbert transform eliminates the mirror image for negative frequencies. Bottom right: Time translation of the FRXS data by an amount specific to the terminal velocity of this dissociation yields a transformed map whose phase evolution normal to the dissociation feature is related to the acceleration felt by the dissociating atom.

X-ray scattering probes of strong-field processes: This year we completed our first FRXS analysis of strong-field nonlinear processes excited in molecular iodine. In addition to dominant excitation channels associated with stimulated Raman scattering (SRS) and two-photon dissociation, we also found some unexpected weaker channels of nonlinear excitation, including two weaker dissociation and vibrational excitation channels: A weak vibration was assigned to the three-photon process of spontaneous hyper-Raman excitation; and a weak dissociation was shown to require two-photon absorption to an transient intermediate state, followed by intersystem crossing to the final dissociation channel. This mixing can be assisted by the presence of the strong field.

X-ray scattering probes of accelerated motion: We have recently extended this work to study the early-time non-uniform motion that occurs in transitions from bound to dissociative states. The transient acceleration appears in FXRS as diffuse scattering patterns with characteristic phase evolution. We have developed a set of transformations that isolate individual channels to measure the early-time accelerated motion. This procedure is used to analyze diatomic iodine X-ray scattering data with multiple dissociations, and the ability of this technique to characterize

early-time accelerations of one dissociation channel even in the presence of another dissociation is demonstrated.

Collaboration to provide 200nm ultrafast pump pulses for CXI at LCLS: Strong field investigations using x-ray scattering will benefit from shorter wavelength excitation sources, and also shorter time duration pulses. We have therefore collaborated this year with the Peter Weber group at Brown University to implement 200 nm and sub-30 fs pump capabilities at the CXI end station. This will be commissioned later this month, in time for use in Run 18 in 2020.

Future Work

Molecular movies: We are leading a Run 18 LCLS experiment that will use TXRS to explore dynamics in photoexcited polyatomic molecules. We will study intermodal interactions of polyatomic molecules involving bends, stretches, dissociation, and roaming reassociation using photoexcitation by femtosecond pulses of ultraviolet laser radiation and probing with LCLS hard x rays. Our target molecules are CS2 and CH2BrI. This work also involves collaboration with several theory groups for modeling and simulation: Adam Kirrander (Edinburgh); Todd Martinez (PULSE); and Gopal Dixit (Mumbai).

Strong-field ionization attosecond dynamics: We are renovating our VMI apparatus to upgrade it for use at 100 kHz. This should give us the capability of exploring ultrafast dynamics with very high electron momentum imaging capabilities. Science goals that have been inaccessible at lower repetition rates include observation of two-electron momentum correlations; and coherent control of electron motion on the attosecond time scale.

Peer-Reviewed Publications Resulting from this Project (2018-2020)[1–10]

1. Porat, G. *et al.* Attosecond time-resolved photoelectron holography. *Nat. Commun.* **9**, 2805 (2018).
2. Young, L. *et al.* Roadmap of ultrafast x-ray atomic and molecular physics. *J. Phys. B At. Mol. Opt. Phys.* **51**, 032003 (2018).
3. Ware Matthew R., Glownia James M., Natan Adi, Cryan James P. & Bucksbaum Philip H. On the limits of observing motion in time-resolved X-ray scattering. *Philos. Trans. R. Soc. Math. Phys. Eng. Sci.* **377**, 20170477 (2019).
4. Ware, M. R., Glownia, J. M., Al-Sayyad, N., O'Neal, J. T. & Bucksbaum, P. H. Characterizing dissociative motion in time-resolved x-ray scattering from gas-phase diatomic molecules. *Phys. Rev. A* **100**, 033413 (2019).
5. Ware, M. R. From Time-resolved to Frequency-resolved X-ray Scattering. (Stanford University, 2019).
6. Kierspel, T. *et al.* X-ray diffractive imaging of controlled gas-phase molecules: Toward imaging of dynamics in the molecular frame. *J. Chem. Phys.* **152**, 084307 (2020).
7. Bucksbaum, P. H., Ware, M. R., Natan, A., Cryan, J. P. & Glownia, J. M. Characterizing Multiphoton Excitation Using Time-Resolved X-ray Scattering. *Phys. Rev. X* **10**, 011065 (2020).
8. Driver, T. *et al.* Attosecond transient absorption spooktroscopy: a ghost imaging approach to ultrafast absorption spectroscopy. *Phys. Chem. Chem. Phys.* **22**, 2704–2712 (2020).
9. Duris, J. *et al.* Tunable isolated attosecond X-ray pulses with gigawatt peak power from a free-electron laser. *Nat. Photonics* **14**, 30–36 (2020).
10. Gabalski, I., Ware, M. & Bucksbaum, P. X-ray scattering signatures of early-time accelerations in iodine dissociation. *J. Phys. B* (2020) (accepted for publication).

NLX: Nonlinear X-ray Science

David A. Reis
Stanford PULSE Institute, SLAC National Accelerator Laboratory,
Menlo Park, CA 94025 dreis@slac.stanford.edu

Project Scope:

In the NLX *program, we are focused on the nonlinear optics of short-wavelength, ultra-fast coherent radiation.* We seek to understand strong-field and multi-photon interactions and exploit them to probe electronic structure at the atomic-scale in space and time. We are interested in fundamental interactions, with a primary focus on coherent non-sequential processes such as wave-mixing and two-photon Compton scattering using hard x rays. In the upcoming funding period, we propose experiments on x-ray and optical wave-mixing to image the strong-field- driven attosecond electronic dynamics responsible for solid-state high-harmonic generation. We will also explore the bound-state contribution to two-photon Compton scattering. The new scattering mechanism holds promise as a nonlinear photons-in/photon-out method of achieving simultaneous chemical specificity and atomic-scale structure in low Z materials. Our program is synergistic with other strong-field investigations in PULSE and makes use of the unprecedented intensities at hard x-ray wavelengths of LCLS and SACLA free-electron lasers. The results could have a profound impact on future light sources such as the LCLS-II.

Recent Progress:

Non-sequential two-photon interactions at x-ray wavelengths became possible with the advent of the LCLS free-electron laser. Much of the focus in this program has been the exploration of fundamental nonlinear x-ray interactions and their use for measurements of chemical and materials dynamics. However, we have also historically studied fundamentals of strong-field high-harmonics generation (HHG) in solids. Much of this work continues through collaborations with other subtasks (Ghimire and Heinz), although we are also interested in using x-ray nonlinear optical mixing and other x-ray methods for studying the microscopic properties of HHG. One such experiment, in collaboration with Hermann Dürr's group used x-ray absorption spectroscopy to study the correlated electron material NiO under the conditions where high-harmonics are generated. The results are currently under review (submitted version on the ArXiv) and show ultrafast modifications to the electronic structure, showing a change in the balance between electron hoping and Coulomb repulsion.

We have also submitted results on two-photon resonant x-ray scattering from metallic Fe and Cu (submitted version on the Arxiv) and are in the process of responding to referee reports. In these studies, we have identified and characterized a new mechanism of two-photon, multi-electron scattering with significantly larger cross-section compared to other effects that we have studied, such as two-photon half-resonant absorption and anomalous nonlinear Compton scattering. We see rich behavior of the two-photon differential cross-section, including two-electron Raman scattering when the photon energy approaches the sequential 1s double core-threshold, and a competition between two-electron, one photon florescence and two-electron, two-photon Raman scattering as we exceed the edge. The results could present a new approach for understanding electron correlation effects in

highly excited materials, as well as potentially give access to new information about valence electron structure through multi-photon RIXS.

The above-mentioned affect was first observed in experiments aimed at two-photon excitation of the ^{57}Fe nuclear resonance near 14.4 keV. In a series of experiments at LCLS and SACLA we looked for delayed emission associated with excitation and then de-excitation of the relatively long-lived nuclear isomer state (used in Mössbauer spectroscopy and nuclear resonant scattering experiments). To date we have only been able to set an upper limits on the generalized two-photon cross-section. We have been working with the Pallfy group in Heidelberg on the theory and hope to submit a manuscript soon

Future Plans:

Future measurements are aimed at a better understanding of novel x-ray matter interactions and development of novel spectroscopies of materials both under strong optical and x-ray fields.

Submitted (ArXiV)

Johann Haber, Andreas Kaldun, Samuel W. Teitelbaum, Alfred Q.R. Baron, Philip H. Bucksbaum, Matthias Fuchs, Jerome B. Hastings, Ichiro Inoue, Yuichi Inubushi, Dietrich Krebs, Taito Osaka, Robin Santra, Sharon Shwartz, Kenji Tamasaku, David A. Reis, Nonlinear resonant X-ray Raman scattering, https://arxiv.org/abs/2006.14724

Strong-field physics in three-dimensional topological insulators, Denitsa Baykusheva, Alexis Chacón, Dasol Kim, Dong Eon Kim, David A. Reis, Shambhu Ghimire, https://arxiv.org/abs/2008.01265

Ultrafast modification of the electronic structure of a correlated insulator, O. Vaskivskyi, P Thunström, S Ghimire, R Knut, J Söderström, L Kjellsson, D Turenne, RY Engel, M Beye, J Lu, AH Reid, W Schlotter, G Coslovich, M Hoffmann, G Kolesov, C Schüßler-Langeheine, A Styervoyedov, N Tancogne-Dejean, MA Sentef, DA Reis, A Rubio, SSP Parkin, O Karis, J Nordgren, J-E Rubensson, O Eriksson, HA Dürr, https://arxiv.org/abs/2008.11115.

Peer-Reviewed Publications Resulting from this Project (2018-2020)

[1] G. Vampa, J. Lu, Y. S. You, D. R. Baykusheva, M. Wu, H. Liu, K. J. Schafer, M. B. Gaarde, D. Reis, and S. Ghimire. Attosecond synchronization of extreme ultraviolet high harmonics from crystals. Journal of Physics B 53(14): 144003 2020 (Collaborative with HHG subtask).

[2] D. Krebs, D. A. Reis, and R. Santra. Time-dependent QED approach to x-ray nonlinear Compton scattering. Physical Review A, 99(2):022120, 2019.

[3] J. Lu, E. F. Cunningham, Y. S. You, D. A. Reis, and S. Ghimire. Interferometry of dipole phase in high harmonics from solids. Nature Photonics, **13**:96–100, 2019. (Collaborative with Ghimire ECA)

[4] S. Ghimire and D. A. Reis. High-harmonic generation from solids Nature Physics, **15**(2):197–197, 2019. (Collaborative with Ghimire ECA)

[5] D. Popova-Gorelova, D. A. Reis, and R. Santra. Theory of x-ray scattering from laser-driven electronic systems. Physical Review B, **98**(22):224302, 2018.

[6] Y. S. You, E. Cunningham, D. A. Reis, and S. Ghimire. Probing periodic potential of crystals via strong-field re-scattering. Journal of Physics B: Atomic, Molecular and Optical Physics, **51**(11):114002, 2018. (Collaborative with Ghimire ECA)

[7] M. Fuchs and D. A. Reis. Hard x-ray nonlinear optics, in L. Young, K. Ueda, M. Gühr, P. H. Bucksbaum, M. Simon, S. Mukamel, N. Rohringer, K. C. Prince, C. Masciovecchio, M. Meyer, A. Rudenko, D. Rolles, C. Bostedt, M. Fuchs, D. A. Reis, R. Santra, H. Kapteyn, M. Murnane, H. Ibrahim, F. L´egar´e, M. Vrakking, M. Isinger, D. Kroon, M. Gisselbrecht, A. L'Huillier, H. J. Wörner, and S. R. Leone. Roadmap of ultrafast x-ray atomic and molecular physics. Journal of Physics B: Atomic, Molecular and Optical Physics, **51**(3):032003, 2018.

Page is intentionally blank.

Electron Dynamics on the Nanoscale

Tony F. Heinz, PI
SLAC National Accelerator Laboratory, 2575 Sand Hill Road, Menlo Park, CA 94025
Email: tony.heinz@stanford.edu

Project Scope

In this component of the SLAC ultrafast chemical science research program, we investigate the dynamics of electron motion and electronically excited states in nanostructured systems, intermediate in scale between small molecules and bulk materials. We are currently focusing on electrons in atomically thin two-dimensional (2D) layers of van-der-Waals crystals and heterostructures, using transition metal dichalcogenide semiconductors as model systems. Our research makes use of complementary spectroscopic techniques to probe radiative and non-radiative relaxation pathways after photoexcitation, including the role of Coulomb interactions and vibrational coupling as manifest in exciton formation, exciton-exciton and exciton-carrier interactions, intervalley scattering, and exciton radiative decay. The role of the external environment in modifying the electronic states and their dynamics has also been a focus of recent attention, as are heterostructures composed of atomically thin 2D van der Waals layers combined with other 2D layers with controlled relative crystallographic orientation. 2D van der Waals layers, with their lack of chemical reactivity, can be combined in a wide variety of structures simply by mechanical assembly to provide a set of customizable systems in which to investigate underlying principles of excited-state dynamics.

Recent Progress

We have focused on the elucidation of dynamics of excited states in atomically thin transition metal dichalcogenide (TMDC) layers in the class of MX_2 (M = Mo, W and X = S, Se, Te). These systems provide models for the behavior of electrons in two-dimensional (2D) semiconducting van-der-Waals layers, which are prototypes for laterally delocalized electronic states with strong vertical localization. The systems have attracted great interest because of their strong and anomalous excitonic interactions, their strong spin-orbit interactions, as well as the possibility of accessing the valley degree of freedom through their valley circular dichroism and of constructing diverse heterostructures from multiple layers. Through control of the relative crystallographic orientation of the different layers it is also possible to influence the dynamics and electronic properties of the combined system, notably generating moiré effects and localized potentials.

Our recent research within this program has examined the diverse influence and coupling of additional layers surrounding a semiconductor layer on its electronic properties and electron dynamics. One such interaction involves the role of a second layer in the crystallographic bilayer in altering exciton dynamics through modified electron-phonon coupling; a second new interlayer exciton states that are created when two semiconductor monolayers with different band gaps are combined to form a type-II heterostructure involves studying the significant influence of the dielectric screening of the environment induced by stacked external layers on the excited states of a monolayer. Additional activities within this project, including contributions to ultrafast excited-states dynamics of dissociating molecules probed by ultrafast electron diffraction and electronic dynamics in bulk semiconductors.

Here we highlight a new experimental approach in our research which provides direct access to the momentum-space characteristics of excitons, namely, time-resolved angularly-resolved photoemission spectroscopy (tr-ARPES). These studies have been carried out in collaboration with the group of Keshav Dani at the Okinawa Institute of Science and Technology (OIST), which was facilitated by his sabbatical visit to SLAC/Stanford during the past year. The initial results of this study on excitons in monolayer 2D semiconductors has been accepted for publication in *Science*.

Time-resolved ARPES for probing excitons

Time-resolved ARPES has been established as a powerful probe of electron dynamics in solids. It allows one to determine the energy and momentum of photoexcited carriers and to track their temporal evolution following an ultrafast excitation pulse. For 2D systems, the mapping of momentum of the photoemitted electrons to crystal momentum is especially simple. What has not, however, been addressed is the use of tr-ARPES to investigate *excitons*. Indeed, there has been discussion in the community about what, if anything, one should measure in photoemission for a system populated by excitons. As we have examined theoretically, the correct view of photoemission from excitons is that one obtains a distribution of photoemitted electrons that reflects the state of both the electron within the exciton and the state of the hole that remains in the material following the photoemission process.

At a basic level, the ARPES spectrum reveals the valley in momentum space in which the electron in the exciton resides. This is information is not available from conventional optical probes such as (time-resolved) absorption or emission spectroscopy. Further, tr-ARPES is provides strong response not only for direct excitons (where the electron and hole reside in valleys with the same momenta), but also for indirect excitons. At a more detailed level, the width of the exciton ARPES spectrum reflect the momentum-space width of the excitonic state, which corresponds to the real-space correlation of the electron and hole in the exciton. The dispersion of the exciton tr-ARPES spectrum is determined by the hole dispersion relation for cold excitons and also by the exciton dispersion relation for excitons with meaningful kinetic energy.

Direct observation of bright and momentum-dark excitons in monolayer WSe_2

Using the capabilities at OIST for tr-ARPES using femtosecond XUV pulses to access electrons across the full Brillouin zone, we investigated excitons in photoexcited WSe_2 monolayers. Fig. H1 shows schematically the measurement scheme and the valleys at the top of the valence band and the bottom of the conduction band. Since the energies of the K and Q valleys in the conduction band are expected to be similar, both KK excitons (hole at K valley, electron at K valley) and KQ excitons may be stable following photoexcitation. Each species is expected in to give rise to a distinct ARPES signal based on the momentum of the electron. While there has been indirect evidence of the creation of KQ excitons through scattering of photogenerated KK excitons, no direct momentum-sensitive technique has been available to determine directly the nature of photoexcited states.

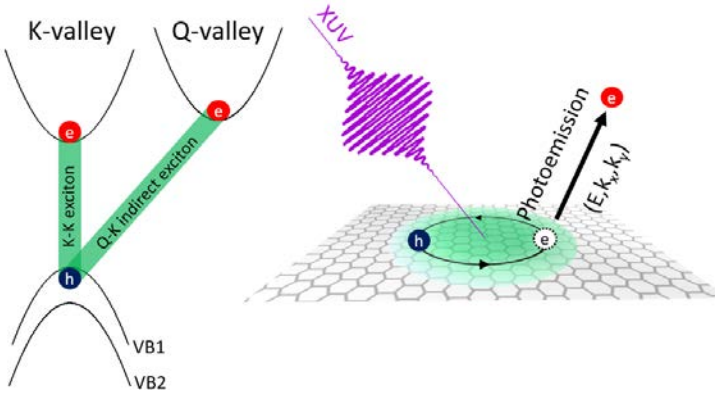

Fig. H1: Schematic illustration of the tr-ARPES measurement (right) and of the WSe_2 band structure, showing the highest energy parts of the valence band and the lowest energy parts of the conduction band.

Key results from the tr-ARPES measurement are presented in Fig H2 where the spectrum of photoemitted electrons is displayed against their momentum. The dotted lines are the calculated quasiparticle calculated band structure for monolayer WSe_2. For the sample without photoexcitation, we observe photoemission from electrons in the valence band (A). After resonant photoexcitation at a delay time of about 1 ps, we observe additional emitted electrons near the K and Q valleys of the conduction band. The existence of emission near the K and Q valleys in the conduction band is a direct signature for the creation of KK and KQ excitons. The energy of the emitted electrons is seen to lie below the corresponding conduction band. This is the consequence of the large exciton binding energies, of several hundred meV, present in this monolayer semiconductor. In addition to providing a direct demonstration of the presence of KK and KQ excitons, these measurements allow us to examine the dynamics of intervalley exciton scattering

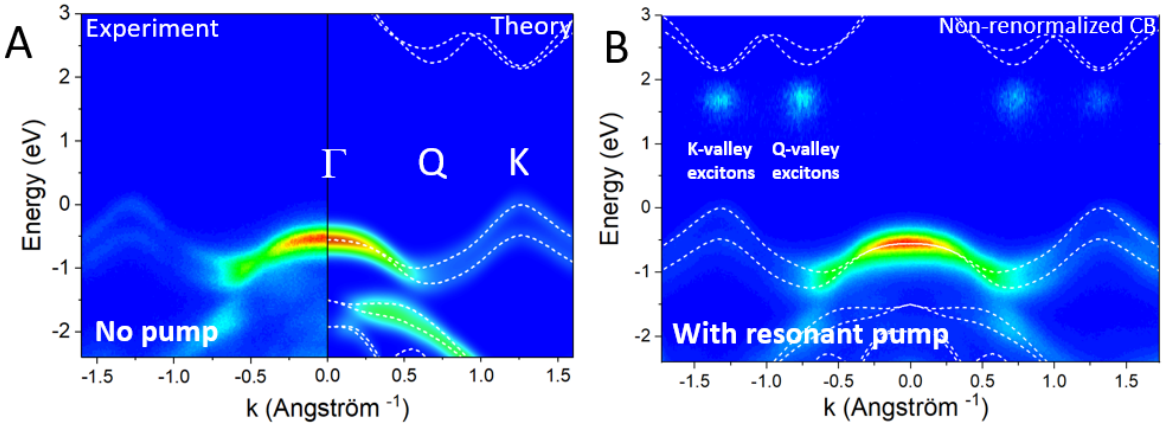

Fig. H2. tr-ARPES spectra from monolayer WSe_2 prior to photoexcitation (A) and ~1 ps after resonant photoexcitation. The color encodes the intensity of the emission. The dashed lines are the calculated valence and conduction bands, split by the spin-orbit interaction.

In addition to providing a direct demonstration of the presence of KK and KQ excitons, these measurements allow us to examine the dynamics of intervalley exciton scattering. For resonant photoexcitation through a direct band transition, we only create KK excitons. Indeed, this is what is observed initially during photoexcitation. Then on a time scale of 100 fs, we observe the buildup of the KQ excitons through intervalley phonon scattering induced by phonons.

Future Plans

Several important extensions of the tr-ARPES measurements presented above are planned. One direction is imaging of the exciton wavefunction in momentum space through optimized determination of the width and dispersion of the exciton ARPES emission feature. In addition, we will apply this approach to examine interlayer charge transfer, the formation of interlayer excitons in 2D semiconductor heterostructures, and the dependence of these phenomena on relative crystallographic orientation. Extension of these studies to probe charge transfer with transitions from core-levels using soft x-ray photons are also planned to provide an atomic-level view of charge transfer dynamics. Another research direction to be pursued in collaboration with co-PIs Shambhu Ghimire and David Reis is electron dynamics in the strong-field regime induced by intense ultrafast pulses and manifested in nonperturbative nonlinear response.

Peer-Reviewed Publications Resulting from this Project (2018-2020)

1. J. Madéo, M. K. L. Man, C. Sahoo, M. Campbell, V. Pareek, E. L. Wong, A. Al Mahboob, N. S. Chan, A. Karmakar, B. M. K. Mariserla, X. Li, T. F. Heinz, T. Cao, K. M. Dani, "Directly visualizing the momentum forbidden dark excitons and their dynamics in atomically thin semiconductors," *Science* (in press).
2. O. Karni, E. Barre, S. C. Lau, R. Grillen, E. Y. Ma, B. Kim, K. Watanabe, T. Taniguchi, J. Maultzsch, K. Barmak, R. H. Page, and T. F. Heinz, "Infrared interlayer exciton emission in MoS_2/WSe_2 heterostructures," *Phys. Rev. Lett.* **123**, 247402 (2019).
3. A. Raja, L. Waldecker, J. Zipfel, Y. Cho, S. Brem, J. D. Ziegler, M. Kulig, T. Taniguchi, K. Watanabe, E. Malic, T. F. Heinz, T. C. Berkelbach, and A. Chernikov, "Dielectric disorder in two-dimensional materials," *Nature Nanotech.* **14**, 832-837 (2019).
4. G. Vampa, H. Liu, T. F. Heinz, and D. A. Reis, "Disentangling interface and bulk contributions to high-harmonic emission from solids," *Optica* **6**, 553-556 (2019).
5. C. Jin, E. Y. Ma, O. Karni, E. C. Regan, F. Wang, and T. F. Heinz, "Ultrafast dynamics in van der Waals heterostructures," *Nature Nanotech.* **13**, 994-1003 (2018).
6. A. Raja, M. Selig, G. Berghäuser, J. Yu, H. M. Hill, A. F. Rigosi, L. E. Brus, A. Knorr, T. F. Heinz, E. Malic, and A. Chernikov, "Enhancement of exciton-phonon scattering from monolayer to bilayer WS_2," *Nano Lett.* **18**, 6135-6143 (2018).
7. J. K. Kim. X. Shi, M. J. Jeong, J. Park, H. S. Han, S. H. Kim, Y. Guo, T. F. Heinz, S. Fan, C.-L. Lee, J. H. Park, and X. Zheng, "Enhancing Mo:$BiVO_4$ Solar Water Splitting with Patterned Au Nanospheres by Plasmon-Induced Energy Transfer," *Adv. Eng. Mater*. **8**, 1701765 (2018).
8. J. Yang, X. Zhu, T. J. A. Wolf, Z. Li, J. P. F. Nunes, R. Coffee, J. P. Cryan, M. Gühr, K. Hegazy, T. F. Heinz, K. Jobe, R. Li, X, Shen, T. Veccione, S. Weathersby, K. J. Wilkin, C. Yoneda, Q. Zheng, T. J. Martinez, M. Centurion, and X. Wang "Imaging CF_3I conical intersection and photodissociation dynamics with ultrafast electron diffraction," *Science* **361**, 64-67 (2018).
9. G. Wang, A. Chernikov, M. M. Glazov, T. F. Heinz, X. Marie, T. Amand, and B. Urbaszek, "Colloquium: Excitons in atomically thin transition metal dichalcogenides," *Rev. Mod. Phys*. **90**, 021001 (2018).

EIM: Excited States in Isolated Molecules

Thomas Wolf

SLAC National Accelerator Laboratory, 2575 Sand Hill Road, Menlo Park, CA 94025

thomas.wolf@slac.stanford.edu

Project Scope

Our interest is the investigation of elementary chemical processes in isolated molecules on their natural time scale of femtoseconds and picoseconds. We are especially interested in non-Born-Oppenheimer approximation (non-BOA) dynamics, because of its importance for light harvesting, atmospheric chemistry and DNA nucleobases photoprotection. For this purpose, we use time resolved spectroscopy with extreme ultraviolet (EUV) light from laboratory-based high harmonic generation (HHG) and soft x-rays (SXR) from the Linac Coherent Light Source (LCLS). Those techniques allow a site and element specific access to non-BOA dynamics. We complement spectroscopic investigation methods with gas phase ultrafast electron diffraction (UED).

Recent Progress

We have expanded on our studies of excited state dynamics of nucleobases with soft X-ray spectroscopy. In an earlier publication (Wolf *et. al.*, Nat. Commun. 8, 29 (2017)), we have demonstrated selective sensitivity of near-edge X-ray absorption fine structure (NEXAFS) spectroscopy at the oxygen K-edge to population in the nπ* state of thymine. We now investigated the associated photon energy dependent transient resonant Auger spectra. The ground state spectra (Fig. 1 a)) show strong signatures at the photon energies of the π* resonances (531.4 and 532.2 eV). Broad and intense peaks centered at 485 eV and 507 eV electron kinetic energy can be assigned to spectator decay channels. Additionally, participator decay signatures can be identified as intensity modulations of the photolines (weak features from valence ionization with linear photon energy-dependence in Fig. 1a)) in the region of the π* resonances. The transition from resonant Auger spectra through the Rydberg resonance series close to the oxygen K edge to non-resonant Auger spectra is obvious by a shift of

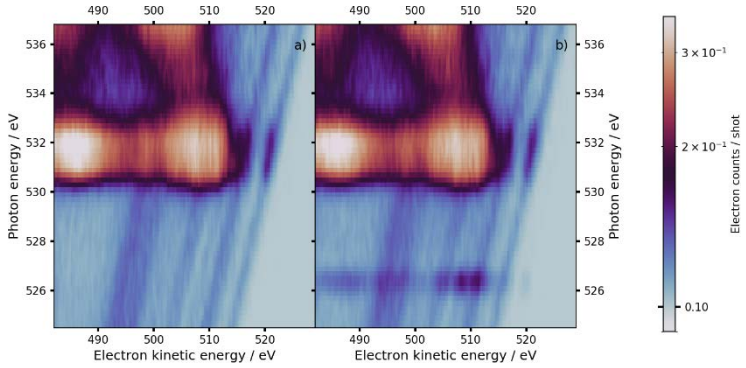

Figure 1: a) Photon energy-dependent resonant Auger electron spectra of the nucleobase thymine at the oxygen edge. b) Same as a), but 4 ps after optical excitation by an ultrashort UV pulse. Note the logarithmic color scale

the spectator decay signatures to lower electron kinetic energies.

The photon energy dependent resonant Auger spectra of thymine 4 ps after UV excitation (see Fig. 1 b)) show additional resonant Auger signatures at a photon energy of 526 eV, red-shifted by approximately the UV photon energy from the ground state π* resonances (see Fig. 1 b)). They correspond to Auger decay of the nπ* state signature from our earlier NEXAFS spectra and are to our knowledge the first observation of resonant Auger decay from a valence-excited state.

The nπ* state resonant Auger spectrum exhibits two relatively intense maxima at similar electron kinetic energies as the spectator decay signatures in the ground state resonant Auger spectra at the π* resonances. This can be expected since the intermediate core-excited state is identical for both transitions. Additionally, we observe a weak signature in the nπ* state resonant Auger spectrum at electron kinetic energies beyond the ground state photolines (at 520 eV electron kinetic energy / 526.5 eV photon energy in Fig. 1 b)) which corresponds to participator decay. The final singly charged state corresponding to this participator decay signature is identical with the final state of transient valence photoelectron spectra of the nπ* state. Thus, the signature allows direct connection of the transient NEXAFS observable with transient valence photoelectron spectroscopy. We, furthermore, observe weak transient Auger signatures at larger delay times which we associate with population transfer from the nπ* state to a ππ* triplet state.

We have, furthermore, made progress on the analysis of an experiment investigating photoinduced ring-opening in the molecule α-phellandrene at SLAC's Mega-electron-volt ultrafast electron diffraction (UED) facility. This study builds up on our recently published study on the analog ring-opening reaction in 1,3-cyclohexadiene (Wolf *et al.* Nat. Chem., 11, 504 (2019)). Compared to 1,3 cyclohexadiene, α-phellandrene exhibits an isopropyl substituent at one of the carbon atoms at the site of the ring-opening reaction. The substitution lifts the symmetry of the six-membered ring system and gives rise to 6 conformer structures, 3 conformers with axial orientation and 3 conformers with equatorial orientation of the isopropyl group to the 6-membered ring. We only observe the conformers with equatorial orientation in static diffraction experiments. Preliminary *ab-initio* wavepacket simulations performed by the PULSE UTS subtask (PI Todd Martinez) suggest that ring-opening dynamics are conformer specific. Evidence for this can also be found in our experimental results.

Future Plans

We plan to continue our studies of the interplay between electronic and nuclear degrees of freedom during ultrafast structural dynamics in molecules in the gas phase. Our proposal for studying an isomer of α-phellandrene, α-terpinene, which differs in the substitution sites of the cyclohexadiene ring, was granted experimental time at SLAC's UED facility. We additionally received beamtime at LCLS for complementary structural dynamics studies with higher time resolution using hard X-rays. Moreover, we will perform the first optical pump/ soft x-ray probe user experiment to study of ultrafast excited state dynamics in the new TMO endstation at LCLS.

Peer-Reviewed Publications Resulting from this Project (2018-2020):

- O. Schalk, D. Townsend, T. J.A. Wolf, D. M.P. Holland, A. E. Boguslavskiy, M. Szöri, A. Stolow, **Time-resolved photoelectron spectroscopy of nitrobenzene and its aldehydes**, Chem. Phys. Lett., 691, 379 (2018).
- R. H. Myhre, T. J. A. Wolf, L. Cheng, S. Nandi, S. Coriani, M. Gühr, H. Koch, **A theoretical and experimental benchmark study of core-excited states in nitrogen**, J. Chem. Phys, 148, 064106 (2018).
- H. Xiong, L. Fang, N. G. Kling, T. J. A. Wolf, E. Sistrunk, R. Obaid, M. Gühr, N. Berrah, **Fragmentation of endohedral fullerene $Ho_3N@C_{80}$ in an intense femtosecond near-infrared laser field**, Phys. Rev. A, 96, 023419 (2018).
- J. Yang, X. Zhu, T. J. A. Wolf, Z. Li, J. P. F. Nunes, R. Coffee, J. Cryan, M. Gühr, K. Hegazy, T. F. Heinz, K. Jobe, R. Li, X. Shen, T. Veccione, S. Weathersby, K. J. Wilkin, C. Yoneda, Q. Zheng, T. J. Martinez, M. Centurion, X. Wang, **Imaging CF3I conical intersection and photodissociation dynamics by ultrafast electron diffraction,** Science, *361*, 64 (2018).
- F. Holzmeier, T. J. A. Wolf, C. Gienger, I. Wagner, J. Bozek, S. Nandi, C. Nicolas, I. Fischer, M. Gühr, R. F. Fink, **Normal and Resonant Auger Spectroscopy of Isocyanic Acid HNCO,** J. Chem. Phys., *149*, 034308 (2018).
- A. Battistoni, H. A. Dürr, M. Gühr, T. J. A. Wolf, **A tilted pulse-front setup for femtosecond transient grating spectroscopy in highly non-collinear geometries,** J. Opt., *20*, 095501 (2018).
- T. J. A. Wolf, D. M. Sanchez, J. Yang, R. M. Parrish, J. P. F. Nunes, M. Centurion, R. Coffee, J. P. Cryan, M. Gühr, K. Hegazy, A. Kirrander, R. K. Li, J. Ruddock, X. Shen, T. Veccione, S. P. Weathersby, P. M. Weber, K. Wilkin, H. Yong, Q. Zheng, X. J. Wang, M. P. Minitti, T. J. Martínez, **The photochemical ring-opening of 1,3-cyclohexadiene imaged by ultrafast electron diffraction,** Nat. Chem. 11, 504 – 509, (2019).
- T. J. A. Wolf, M. Gühr, **Photochemical Pathways in Nucleobases measured with an X-ray FEL**, Philos. Trans. Royal Soc. A, 377, 20170473 (2019).
- K. Wilkin, R. Parrish, J. Yang, T. J. A. Wolf, P. Nunes, M. Guehr, R. Li, X. Shen, Q. Zheng, X. Wang, T. J. Martinez, M. Centurion, **Diffractive imaging of dissociation and ground state dynamics in a complex molecule,** Phys. Rev. A, 100, 023402 (2019).
- T. J. A. Wolf, R. M. Parrish, R. H. Myhre, T. J. Martínez, H. Koch, M. Gühr, **Observation of Ultrafast Intersystem Crossing in Thymine by Extreme Ultraviolet Time-resolved Photoelectron Spectroscopy,** *J. Phys. Chem. A*, 123, 6897 (2019).
- N. Berrah, A. Sanchez-Gonzalez, Z. Jurek, R. Obaid, H. Xiong, R. J. Squibb, T. Osipov, A. Lutman, L. Fang, T. Barillot, J. D. Bozek, J. Cryan, T. J. A. Wolf, D. Rolles, R. Coffee, K. Schnorr, S. Augustin, H. Fukuzawa, K. Motomura, M. Niebuhr, M. Guehr, L. J. Frasinski, R. Feifel, C-P. Schulz, K. Toyota, S.-K. Son, K. Ueda, T. Pfeifer, J.P. Marangos and R. Santra, **X-ray multiphoton ionization of molecules: Femtosecond-resolved observation of delayed fragmentation and evaporation of neutral atoms** , Nat. Phys., 15, 1279 (2019).

- R. Obaid, K. Schnorr, T. Wolf, T. Takanashi, N. Kling, K. Kooser, K. Nagaya, S. Wada, L. Fang, S. Augustin, D. You, E. Campbell, H. Fukuzawa, C. Schulz, K. Ueda, P. Lablanquie, T. Pfeifer, E. Kukk, N. Berrah, **Photo-ionization and fragmentation of Sc3N@C80 following excitation above the Sc K-edge,** J. Chem. Phys., 151, 104308 (2019).
- J. Duris, S. Li, T. Driver, E. G. Champenois, J. MacArthur, A. A. Lutman, Z. Zhang, P. Rosenberger, R. Coffee, G. Coslovich, J. M. Glownia, G. Hartmann, W. Helml, A. Kamalov, J. Knurr, J. Krzywinski, M.-F. Lin, M. Nantel, Adi Natan, J. O'Neal, N. Shivaram, P. Walter, A. Wang, T. Wolf, J. Z. Xu, M. F. Kling, P. H. Bucksbaum, A. Zholents, Z. Huang, J. P. Cryan, A. Marinelli, **Tunable Isolated Attosecond X-ray Pulses with Gigawatt Peak Power from a Free-Electron Laser**, Nat. Photonics, 14, 30 (2019).
- L. Inhester, Z. Li, X. Zhu, N. Medvedev, T. J. A. Wolf, **Characterization of chemical bond dissociation using femtosecond core-level electron spectroscopy**, J. Phys. Chem. Lett., 10, 6536 (2019).
- X. Shen, J. Pedro F. Nunes, J. Yang, K. Jobe, R. Li, M.-F. Lin, B. Moore, M. Niebuhr, S. Weathersby, T. J. A. Wolf, C. Yoneda, M. Gühr, M. Centurion, X. Wang, **Femtosecond gas-phase mega-electron-volt ultrafast electron diffraction**, Struct. Dyn., 6, 054305 (2019).
- Y. Liu, S. L. Horton, J. Yang, J. P. F. Nunes, X. Shen, T. J. A. Wolf, R. Forbes, C. Cheng, B. Moore, M. Centurion, Kareem Hegazy, R. Li, M.-F. Lin, A. Stolow, P. Hockett, T. Rozgonyi, P. Marquetand, X. Wang, T. Weinacht, **Spectroscopic and Structural Probing of Excited State Molecular Dynamics with Time-Resolved Photoelectron Spectroscopy and Ultrafast Electron Diffraction**, Phys. Rev. X, 10, 021016 (2020).
- T. Driver, S. Li, E. G. Champenois, J. Duris, D. Ratner,TJ Lane, P. Rosenberger, A. Al-Haddad, V. Averbukh, T. Barnard, N. Berrah, C. Bostedt, P. H. Bucksbaum, R. Coffee, L. F. DiMauro, L. Fang, D. Garratt, A. Gatton, Z. Guo, G. Hartmann, D. Haxton, W. Helml, A. LaForge, A. Kamalov, M. F. Kling, J. Knurr, M.-F. Lin, A. A. Lutman, J. P. MacArthur, J. P. Marangos, M. Nantel, A. Natan, R. Obaid, N. H. Shivaram, A. Schori, P. Walter, A. Wang, T. J. A. Wolf, A. Marinelli, J. P. Cryan, **Attosecond Transient Absorption Spooktroscopy: a ghost imaging approach to ultrafast absorption spectroscopy**, 22, 2704 (2020).
- R. Obaid, H. Xiong, S. Augustin, K. Schnorr, U. Ablikim, Andrea Battistoni, Thomas J. A. Wolf, R. C. Bilodeau, T. Osipov, K. Gokhberg, D. Rolles, A. C. LaForge, N. Berrah, I**ntermolecular Coulombic decay in endohedral fullerene at the 4d → 4f resonance**, Phys. Rev. Lett., 124, 113002 (2020).
- J. P. F. Nunes, K. Ledbetter, M. Lin, M. Kozina, D. P. DePonte, E. Biasin, M. Centurion, C. J. Crissman, M. Dunning, S. Guillet, K. Jobe, Y. Liu, M. Mo, X. Shen, R. Sublett, S. Weathersby, C. Yoneda, T. J. A. Wolf, J. Yang, A. A. Cordones, X. J. Wang, L**iquid-phase Mega-electron-volt ultrafast electron diffraction**, Struct. Dyn., 7, 024301 (2020).
- J. Yang, X. Zhu, J. P. F. Nunes, J. K. Yu, R. M. Parrish, T. J. A. Wolf, M. Centurion, M. Gühr, R. Li, Y. Liu, B. Moore, M. Niebuhr, S. Park, X. Shen, S. Weathersby, T. Weinacht, T. J. Martinez, X. Wang, **Simultaneous observation of nuclear and electronic dynamics by ultrafast electron diffraction**, Science, 368, 885 (2020).

HHG: Frontier in High-order Harmonic Generation

Shambhu Ghimire, SLAC National Accelerator Laboratory
2575 Sand Hill Rd, Menlo Park, CA, 94025
shambhu@slac.stanford.edu

Scope of the program

A new field of research has emerged following the observation of nonperturbative high-order harmonic generation (HHG) in bulk crystals subjected to intense mid-infrared laser fields [Ghimire2010]. The interests are in developing solid-state HHG as an ultrafast probe of the source material [Vampa2015, You2017a] such that it can provide a new window to view intense laser-matter interactions with sub-cycle resolution, and in the possibility of stable attosecond pules in compact setups [Li2020]. These applications require a clear understanding of the underlying microscopic mechanism as well as propagation effects. In the condensed phase, field-driven electrons are never far from the atomic cores, so the usual strong-field approximation is no longer a good approximation. Consequently, the three-step recollision model [Corkum1993], which successfully describes atomic HHG, becomes questionable in describing the HHG process and related strong-field phenomena in dense optical media. The main fundamental questions we are addressing in this program are: (i) how the novel HHG mechanism in solids compares to its well-studied gas phase cousins, (ii) can HHG become an atomic-scale probe of the source material, (iii) how do the time-domain profiles of harmonics look like and would that information be useful to determine the relative contribution from multiple HHG channels and in attosecond pulse metrology in condense matter systems.

Recent Progress

Recollision physics in dense media: Strong-field-controlled recollisions have been utilized in attosecond clocking of several physical processes including charge dynamics in molecules in the gas phase systems. Recently we explored similar possibilities in bulk crystals by performing attosecond clocking of extreme ultraviolet (XUV) harmonics. Here, a qualitative difference to the atomic case is that (i) one has to consider the influence of the periodic potential in the driven motion of the electron and (ii) the hole also moves. Attosecond clocking of electron-hole recollision are shown schematically in figure **a)**. Note that the electron and hole move

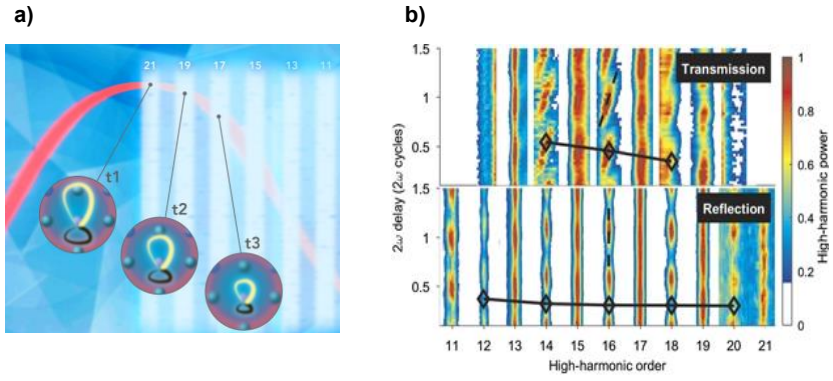

Figure1 ***a)*** *illustration of quantum orbits of electrons and holes at t1, t2 and t3.* ***b)*** *Attosecond clocking of electron-hole recollisions is performed by introducing a phase-delayed weak second-harmonic field and analyzing the modulations in even-order harmonics. The solid line connects the minima/maxima of even-orders indicating attosecond delays in recollisions associated to corresponding harmonic orders.*

in opposite directions because of their opposite charge and then they are turned around subsequently to recollide. The size of their quantum orbit depends on their initial phase with respect to the peak of the laser field. Recollisions produce XUV photons, whose energy is determined by the energy of electron and hole, limited by the maximum bandgap of the source material [Ghimire2019].

The emission of XUV burst every half-cycle of the laser-field corresponds to the odd-order harmonics separated by twice the photon energy of the driving laser field in the frequency domain. For attosecond clocking of high harmonics, we use a weak second-harmonic field ($\leq$1% in intensity) to gently perturb these quantum orbits. Depending on the delay between the fundamental and second harmonic laser field, the consecutive half-cycles can be slightly asymmetric such that the inversion symmetry is broken, which results in the generation of even-order harmonics, as shown in figure **b)**. For a delay scan (vertical axis), the intensity of even-order gets strongly modulated, however, (up to 1% limit of the second harmonic field) the odd-order do not show appreciable changes.

Propagation effects: We compare measurements in two configurations; first, we use a typical transmission geometry and, then we use a recently discovered reflection configuration [Vampa2018] under otherwise similar laser conditions such that the peak fields inside the sample remains the same. We find that the experimental data in the reflection mode agrees reasonably well with the results from the generalized re-collision model [Vampa2015] extended her for the XUV wavelength range. Here the relative locations of minima/maxima in even order harmonics represent the attosecond clocking of corresponding recollisions. We extract a minimum atto-chirp of 11 ± 44 as/eV (lower limit) at $\sim$15 eV. We note that the intra-band channel of solid-state HHG would not exhibit such a harmonic order dependent delay and essentially no chirp is expected in that channel. In the transmission mode, the slope is larger (upper figure in **b)** and harmonics are broader as well as are shifted in photon energy as a function of the delay. We attribute this behavior to the broader (by about 30 percent) and blue-shifted spectrum of the fundamental pulse measured after the sample. Such propagation effects are unique challenges attributed to the high-density of the source material as they are not typically observed in atomic HHG. Our full report on this topic has been recently published [Vampa2020].

Use of the LCLS to probe novel HHG physics: We use transient x-ray absorption spectroscopy (XAS) at the LCLS to explore microscopic dynamics relevant to HHG. We use a prototypical strongly correlated electron system NiO as source material. First, we studied crystal-orientation dependence on HHG, where we found that harmonic generation efficiency is much stronger along Ni-O bond directions (cubic direction) than to Ni-Ni or O-O bond directions (diagonal direction). Then, we probed time-resolved absorption using soft-x-rays at the LCLS by tuning their photon energy around Ni and O K-shell absorption edges. We find dynamical changes on O K-edge while Ni K-edge is largely unaffected. Also, the x-ray absorption is higher along the cubic direction compared to the diagonal direction, as the anisotropy in HHG. We note that x-ray pulses are much longer than half-cycle of the optical laser field. Even in such conditions, where measurements only provide average effects, we observed robust transient absorption signals around the O K-edge. A full report on this topic is under review [Granas2020]. We plan to extend these measurements to attosecond X-ray pulses that are now available at the LCLS.

Perspective in Attosecond Science: Our perspective on attosecond science based on the generation of high harmonics from gases and solids is now published in *Nature Communications* [Li2020]. The paper summarizes how the recent developments in ultrafast, long-wavelength lasers have enabled solid-state HHG research as well as the extension of harmonic spectrum from atomic targets in the soft-x-ray wavelength range to the "water window". The paper surveys the challenges in dispersion compensation and pulse characterization that are unique to the soft-x-ray wavelength range. It also discusses how solid-state HHG has emerged as a spectroscopic tool to probe the electronic structure and dynamics of solid materials.

Synergistic activities: We continue synergistic activities with the EDN sub-task lead by *Heinz* group on exploring strong-field-driven processes in atomically thin two-dimensional crystals and heterostructures. We collaborate with the NLX sub-task lead by *Reis* group as well as with other PULSE and LCLS groups. We plan to use the table-top soft-x-ray HHG source that is being developed collaboratively by the LCLS laser group and PULSE staff.

Planned Research

In the next few years, we will perform multi-dimensional high-harmonic spectroscopy and RABBITT experiments to measure the crystal-orientation dependent spectral phase of high harmonics from wide bandgap dielectrics. A string of experimental surprises on fundamental high-harmonic responses are still emerging, which includes orthogonally polarized even-order harmonics on non-centrosymmetric materials such as atomically thin MoS_2[Liu2017]. We plan to investigate its origin such as the potential role from Berry curvature and related topological properties of materials [Baykusheva2020]. We will conduct element-specific transient absorption spectroscopy using attosecond X-ray pulses at the LCLS. These experiments provide complementary information that is difficult to obtain from all-optical methods.

Journal Publications (2018-2020)

1. Jie Li, Jian Lu, Andrew Chew, Seunghwoi Han, Jialin Li, Yi Wu, Shambhu Ghimire, and Zenghu Chang "**A Prospective on Attosecond Science based on high harmonic generation from gases and solids**", Nature Communications 11, 2748 (2020).
2. Giulio Vampa, Jian Lu, Yong Sing You, Denitsa R. Baykusheva, Mengxi Wu, Hanzhe Liu, Ken J. Schafer, David A. Reis, Mette B. Gaarde and Shambhu Ghimire, "**Attosecond synchronization of extreme ultraviolet high harmonics from crystals**", J. Phys. B, 53, 14 (2020).
3. Yuanmu Yang, Jian Lu, Alejandro Manjavacas, Ting S. Luk, Hanzhe Liu, Kyle Kelley, Jon-Paul Maria, Evan Runnerstrom, Michael B. Sinclair, Shambhu Ghimire, Igal Brener, "***High-harmonic generation from an epsilon-near-zero material****", Nature physics*, DOI: 10.1038/s41567-019-0584-7, 2019.
4. Jian Lu, Eric Cunningham, YongSing You, David A. Reis and Shambhu Ghimire, "***Interferometry of dipole phase in high harmonics from solids***". Nature Photonics 13,96-100, 2019.

5. YongSing You, Jian Lu, Eric Cunningham, Cristian Roedel and Shambhu Ghimire, "***Crystal orientation-dependent polarization state of high-order harmonics***", Optics Letters 44, 3, 53-533, 2019
6. Shambhu Ghimire and David A. Reis "***Review: high-order harmonic generation from solids***", Nature Physics, 15, 10-16, 2019
7. Shambhu Ghimire, "***Locking the waveform with a quartz crystal***" NATURE PHOTONICS 12 (5), 256-257, 2018
8. YongSing You, Eric Cunningham, David Reis and Shambhu Ghimire, "***Probing periodic potential of the crystal via strong-field re-scattering***", J. Phys. B: At. Mol. Opt. Phys. 51, 114002, 2018
9. Giulio Vampa, YongSing You, Hanzhe Liu, Shambhu Ghimire, and David Reis, "***Observation of backward high-harmonic emission from solids***" Optics express 26 (9), 12210-12218, 2018 (ECA not lead)
10. Mengxi Wu, YongSing You, Shambhu Ghimire, David Reis, Dana Browne, Kenneth J Schafer, and Mette Gaarde, "***Orientation dependence of temporal and spectral properties of high-order harmonics in solids***", Physical Review A 96 (6), 063412, 2018 (ECA not lead)

References and pre-print

1. [Baykusheva2020] Baykusheva D. et al. "Strong-field physics in three-dimensional topological insulators"
2. [Corkum1993] Corkum, P. "Plasma perspective on strong field multiphoton ionization" Phys. Rev. Lett. **71,** 1994–1997 (1993).
3. [Ghimire2011] Ghimire, S. et al. "Observation of high-order harmonic generation in a bulk crystal" Nat. Phys. **7,** 138–141 (2011).
4. [Ghimire2012] Ghimire, S. et al. "Generation and propagation of high-order harmonics in crystals" Phys. Rev. A **85,** 043836 (2012).
5. [Granas2020] O. Grånäs *et al.*, Ultrafast modification of the electronic structure of a correlated insulator, arXiv2008.11115
6. [Liu2017] Liu et al., "Observation of high harmonics from an atomically thin semiconductor", Nature Physics 13, 262, 2017
7. [Ndabahimiye2016] Ndabashimiye, G. et al. "Solid-state harmonics beyond the atomic limit" Nature 534, 520–523 (2016).
8. [Vampa2015] Vampa, G. *et al*. "Linking high harmonics from gases and solids" Nature 522, 462–464 (2015).
9. [You2017a] Ghimire S. *et al.* , "Anisotropic high harmonic generation in bulk crystals", Nature Physics 13, 345-349, (2017)
10. [You2017b]Y.You *et al.*, "Laser waveform control of extreme ultraviolet high harmonic generation in solids", Optics Letters 42, 9, (2017)

Early Career: Atomic View of Molecular Photocatalysis using X-Ray Lasers

Amy Cordones-Hahn
SLAC National Accelerator Laboratory
2575 Sand Hill Rd., Menlo Park, CA, 94025
acordon@slac.stanford.edu

Project Scope:

Molecular photocatalysts have the potential to deliver an alternative sustainable method to produce fuels or other value-added chemicals using solar energy. Identifying the molecular properties that influence their excited state reactivity is a critical first step to creating new and efficient photocatalysts. This research program aims to pinpoint and control the electronic excited state reaction pathways of transition metal complex photocatalysts.

Nickel-based hydrogen-evolving catalysts with 'non-innocent' ligands, known to actively participate in the electron and proton transfer reactions of the catalyst, will serve as platforms to identify how catalyst charge distribution influences the excited state character and reaction mechanism. Achieving the ultimate goal of controlling photocatalytic reactivity first requires the ability to identify and manipulate the excited state charge distribution, relaxation mechanism, and geometry of the reaction site, which may involve metal or ligand atoms. These requirements inform the technical approach of this research, which exploits the atomic specificity and ultrafast time-resolution of X-ray spectroscopy at the Linac Coherent Light Source (LCLS) X-ray free electron laser.

Ultrafast X-ray spectroscopy probing metal and ligand atomic sites will be used to map the excited state charge distributions, determine the transient catalyst structures, and differentiate the mechanistic roles of metal vs. ligand reactive sites. Through these experiments, this research will establish: 1) how catalyst excited states initiate electron and proton transfer reactions, 2) the specific role of metal vs. ligand atom reactive sites, and 3) how to use ligand composition to influence critical excited state properties and reactivity. This novel approach using ultrafast X-ray methods to identify excited state reaction pathways and inform catalyst design will lead to new classes of molecular photocatalysts that efficiently convert solar energy to high value chemicals.

Future Plans:

The early part of this research program will focus on an established class of Ni-based molecular electrocatalysts for hydrogen evolution that contain 'non-innocent' ligands. We will first establish how the presence of strongly covalent ligands influence the electronic excited state character and relaxation mechanisms of the catalysts. The typical charge transfer and metal-centered excited state character assignments lack precision in this case, as the catalysts are characterized by strong metal-ligand covalency and highly delocalized frontier orbitals. Therefore, ultrafast soft x-ray spectroscopy probes of the metal atom L-edges and ligand atom K-

edges will be essential to identify the distribution of charge and spin in the reactive excited states of the catalysts. We will identify how these properties are influenced by the ligand composition by changing the coordinating atoms of the ligand and by incorporating electron donating and withdrawing groups. The high repetition rate of LCLS-II will enable these soft x-ray spectroscopy studies of dilute catalyst solutions.

We will also focus on identifying the light driven electron and proton transfer reaction mechanisms of this same class of molecular catalysts. We will identify the metal or ligand-based reactive sites of the photocatalysts by mapping how charge is localized following photoreduction and by identifying the proton binding sites. Again, soft x-ray spectroscopy probes sensitive to the metal or ligand atomic charge and protonation state will enable sensitivity to these properties on the slower timescales of chemical reactivity. We will identify how the changes in ligand composition described above influence not only excited state character, but also photochemical reaction pathway.

The later stages of this program will build on the understanding of how covalent ligands influence excited state character, dynamics, and reactivity (established as described above). We will systematically tune ligand design in order to promote more reactive excited states (e.g., ones that localize charge on the reactive site of the catalyst) and extend their lifetimes. Besides the ligand design strategies described above, we will also explore heteroleptic complexes that undergo excited state charge transfer from one ligand to another.

Peer-Reviewed Publications Resulting from this Project (Project start date: 09/2020):

No publications to report.

Early Career: Time-resolved imaging of non-equilibrium electron dynamics with novel X-ray holographic approaches

Tais Gorkhover, SLAC National Accelerator Laboratory 2575 Sand Hill Rd, Menlo Park, CA, 94025
taisgork@slac.stanford.edu

Scope of the program

The ability to follow transient structural changes is essential for understanding and controlling non-equilibrium phenomena such as catalytic reactions, ultrafast phase transitions, and energy transfer from light to matter. These processes often evolve from a complex interplay between rapid electronic and nuclear motions at the nanoscale, which are hardly accessible with conventional microscopic methods. State-of-the-art imaging tools often require long exposure times to achieve high spatial resolution and thus, their sensitivity to short-lived phenomena is limited. Ultrafast spectroscopic methods can provide valuable information about transient states, but the signal ambiguity often increases with the complexity and heterogeneity of the sample. The capabilities offered by current and next-generation X-ray laser facilities, such as the Linac Coherent Light Source (LCLS) and its successor, LCLS II, offer the potential to directly visualize ultrafast dynamics with high spatial and temporal resolutions. This research program is developing ultrafast X-ray diffraction imaging approaches that exploit these cutting-edge X-ray sources to advance the fundamental understanding of non-equilibrium processes in complex nanoscale systems.

Recent Progress

Observation of two-photon interference in incoherent X-ray fluorescence imaging. A very recent theoretical publication suggests that incoherent diffraction imaging (IDI) with X-ray fluorescence will eventually enable creating three-dimensional (3D) maps of nanospecimen with atomic resolution, high chemical contrast, and sub-fs temporal resolution. In addition, IDI bears the promise of overcoming several fundamental limitations inherent to coherent X-ray diffraction imaging (CDI) as there are three major potential advantages compared to CDI [Classen2017]. First, the structure is determined from fluorescence, which has orders of magnitude higher cross sections than elastic scattering in the hard X-ray domain. Second, fluorescence is being emitted into 4π so that in theory the full 3D structure can be determined without rotating the sample and without the need of high dynamic range detectors. Third, the method carries a spectroscopic component as it is highly element selective and very sensitive to changes in the fluorescence line shape. Overall, IDI bears the potential to increase the state-of-art capabilities of hard X-ray diffraction imaging. The experimental implementation of this technique is still challenging.

IDI is based on two-photon interference which can be detected on a one or two dimensional detector using second order correlation function g(2). One crucial requirement for high contrast in two-photon interference is spatially incoherent, but temporally coherent radiation, such as monochromatic thermal light. Another candidate is X-ray fluorescence excited by ultrashort FEL pulses on a timescale comparable to the fluorescence coherence time. If the fluorescence

photons are being recorded within their coherence time, the relative phases of the scattered photons can be considered as stable, allowing the observation of stationary speckle pattern similar to the observation of Hanbury Brown and Twiss [Hanbury1956, 1956a]. The patterns will fluctuate and spatially vary over several exposures, yet the autocorrelation of the intensity distribution calculated for each short exposure is insensitive to the random phase variations of the emission, and will continuously build up for several exposures [Classen2017]. By calculating the second order correlation function g(2) of the speckles over the multitude of exposures, the structure factor of the sample (or the Fourier transform the sample´s structure) will appear.

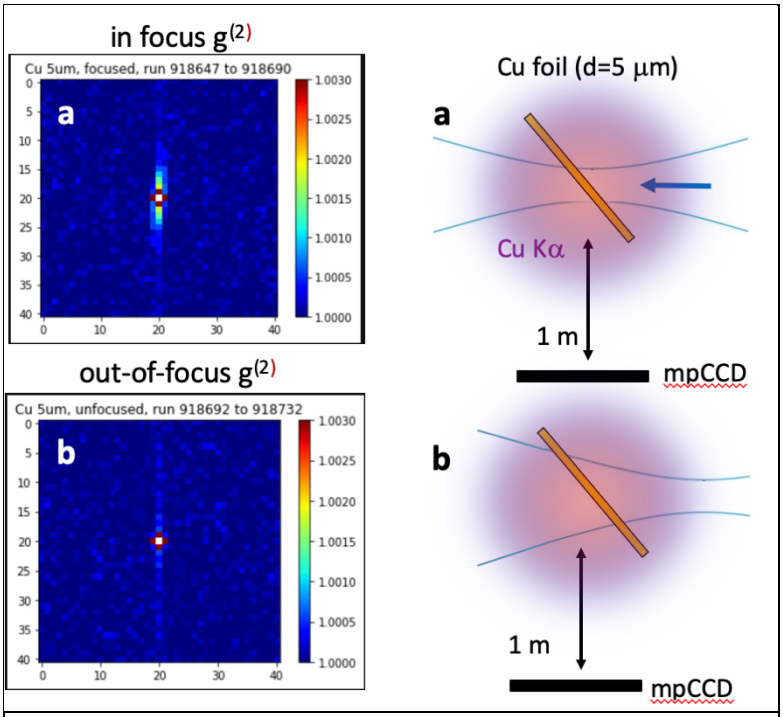

Figure 1: g(2) calculated from K_α fluorescence stemming from a Cu foil placed into the FEL focus. Right panel: experimental setup, the blue arrow pointing into the FEL direction. Left panel: measured g(2) which reflects the intersection between the foil and the FEL focus in Fourier space.

In FY 2020 we have achieved several milestones towards the experimental application of IDI. First, we have carried out a 5 x 12 hours experiment at the Spring-8 Angstrom Free Electron Laser facility (SACLA) in February 2020 Japan. During this experiment we successfully observed two-photon interference from a Cu foil placed into the FEL nanofocus in a setup displayed on the right hand side of figure 1. The K-alpha fluorescence from the Cu film is captured by a two-dimensional mpCCD detector with 1024 X 1024 pixels located 1 m from the foil and rotated 90 degrees relative to the X-ray FEL direction. The Cu foil surface has been placed on a scanning stage so that the FEL was hitting a fresh spot during every exposure and the fluorescence was being recorded for thousands of X-ray FEL shots. After filtering the data exclusively on the highest FEL pulse energies, we calculated the second order correlation function g(2) from a subset of fluorescence images as shown on the left side of figure 1. In this case, g(2) reflects the Fourier transform of the FEL focal volume on the Cu foil as projected on the mpCCD. The X-axis corresponds to direction along the FEL beam or the foil thickness in this case. The Y-axis mirrors the vertical projection of the FEL spot size on the foil.

In case a), the foil has been carefully positioned into the center of the FEL focus which follows a Gaussian intensity distribution with full width half maximum (FWHM) d-vertical = 150 nm. In case b), the foil has been placed 4 X Rayleigh lengths further downstream from the minimum FEL focus spot. Here, the FEL spot must be greater than 800 nm FWHM in in vertical direction. In case a), the bright central spot along Y-axis in g(2) (displayed on the left panel) is 10 – 12 pixel in

momentum space which corresponds to the expected d-vertical = 150 nm in real space. The X-extension of the g(2) spot is minimal as the foil thickness is around 5 micrometers and thus, too thick for the field of view of about 500 nm in this measurement. In case b) both directions cannot be resolved as they are greater than the field-of-view. The difference in g(2) between a) and b) is remarkable as it clearly demonstrates that using X-ray fluorescence IDI one can resolve features smaller than 200 nm even when looking at angles where structural information from coherent diffraction pattern (CDI) cannot be expected. The complete data set which contains different foil materials and thicknesses is currently under analysis and is expected to guide future signal-to-noise ratio (SNR) considerations of IDI. Due to several experimental restrictions, the contrast of the measurement presented in figure 1 was very low as shown on the color scale. The observed values of g(2) ranged between 1.000 and 1.003. This low contrast was sufficient for the identification of the FEL focal volume but the contrast further degraded during additional measurements of fluorescence from nanoparticles and crystallin samples.

Second, we carried out numerical simulations which were dedicated to the improvement of contrast in future studies. The main findings from the simulation indicate that the contrast can be improved by a factor > 20 if the pulse duration can be shorted from 10 fs to 0.5 fs. In addition, undersampling at the SACLA experiment degraded the signal by an additional factor of 5. Finally, IDI on nanoparticles seems to benefit from diluted samples which is different from CDI. Third, we are preparing to address all three aspects during our next scheduled LCLS beam time and to greatly benefit from the availability of sub-fs X-ray pulses.

Diffraction imaging with XUV higher harmonics generated from a solid state sample We used XUV higher-harmonics generation from a solid to record CDI images of 100 nm small Si nanospheres in collaboration with Dr. Giulio Vampa, Dr. Shambhu Ghimire and Prof. David Reis. The nanoparticles were spin coated on a thin MgO crystal piece and illuminated with intense IR pulses. The first measurements conducted in Sep 2020 suggest that we observe coherent XUV diffraction patterns from the nanosamples and the this method might be used for table-top time-resolved imaging of nanoparticles. Further work is needed to confirm the results and evaluate the capabilities of this method.

Attosecond imaging and transient resonances One general limitation in coherent diffraction imaging (CDI) with X-ray FELs is the generally low X-ray diffraction cross section of matter. This results in low brightness of the images in higher scattering angles and restricts the quality and the achievable spatial resolution. In addition X-ray absorption, which degrades the sample, occurs usually much more likely than the desired elastic scattering. This enforces a trade-off between damage and required brightness of the image. Even in diffraction-before-destruction CDI X-ray damage is regarded as detrimental as it leads to ionization and bleaching of the sample even before structural damage can occur. In contrast, our recent study demonstrates that under certain conditions X-ray damage can in fact increase the coherent scattering cross section of samples through transient resonances. Our main observation is exhibited in figure 2.

In this measurement we recorded tens thousands of single exposure CDI images of Xe nanoparticles at different photon energies and used the brightness of the images to calculate the effective scattering cross section per Xe atom at the highest X-ray fluences. Our data set contains three different pulse durations, figure 2 exhibit an exemplary photon energy scan which was recorded with 5 fs short FEL pulses near Xe 3d resonance. The solid blue curve illustrates the scattering cross section expected from synchrotron data, each point represents a single measurement of the scattering cross section from a single nanoparticle and the dashed curve shows the normalized calculation performed by Dr. Phay Ho (ANL). Surprisingly, at the 3d resonance around 700 eV the measured scattering cross section is below the expected value, but this trend is reversed at 1500 eV. Here, the heavily ionized Xe clusters scatter more efficiently as the Xe ions resonance shifts from 700 eV to greater X-ray energies. The diffraction patterns from Xe nanoparticles (not shown here) at 1500 eV do not indicate degradation of the image in contrast to previous observations of ionic resonances. Our data and corresponding simulation (developed by Dr. Phay Ho and Prof. Linda Young from ANL) strongly suggest that ionic resonances can increase the brightness and thus, the quality of CDI images in a predictable and controlled manner, and are most beneficial when applied in combination with intense sub-fs FEL pulses.

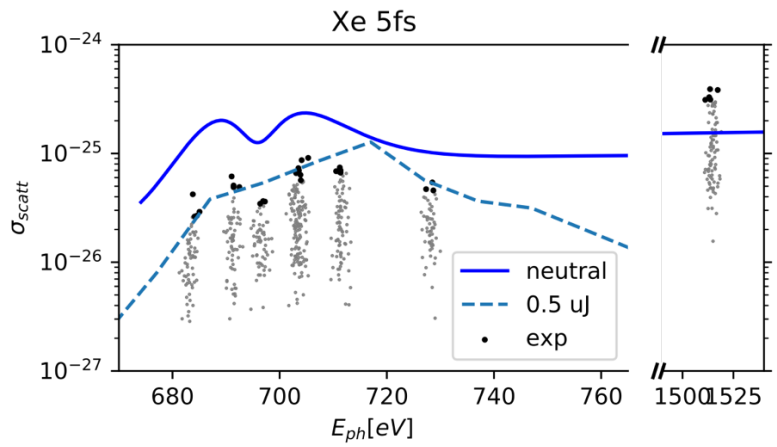

Figure 2. X-ray scattering cross section σ per atom of Xe nanospheres injected into an intense 5 fs X-ray FEL pulse at different photon energies.

Peer-Reviewed Publications Resulting from this Project (project start date 09/2018)

No publications to report

References:

[Classen2017] Classen, Anton, et al. *Phys. Rev. Lett.* 119.5 (2017): 053401.

[Hanbury1956] R. Hanbury Brown and R. Q. Twiss, *Nature* (London) 178, 1046 (1956).

[Hanbury1956a] R. Hanbury Brown and R. Q. Twiss, *Nature* (London) 177, 27 (1956).

Early Career: Ultrafast Dynamics of Molecules on Surfaces Studied with Time-Resolved XUV Photoelectron Spectroscopy

Thomas K. Allison
Departments of Chemistry and Physics
Stony Brook University, Stony Brook, NY 11794-3400
email: thomas.allison@stonybrook.edu

Program Scope

The capture and storage of solar energy involves the separation and steering of electrons and holes created by the absorption of light. In dye-sensitized solar cells and organic photovoltaics, electrons are injected from a photo-excited molecule into a semiconductor. In heterogeneous photo-catalysis, excitation of the electrons in a solid can cause reactions on the surface, storing the photon's energy in chemical bonds. In both cases, the dynamics of charge separation and subsequent reactions are complex and often involve multiple intermediate states. The main objective of this work is to provide important fundamental insight into these dynamics using time-resolved photoelectron spectroscopy to track the motion of electrons, holes, and nuclei at molecule/surface interfaces. An ancillary objective is also developing the required instrumentation.

Recent Progress

Photoemission spectroscopy using synchrotron radiation is one of the most important methods for establishing relationships between structural and electronic properties at surfaces, with core and valence level shifts providing information about charge transfer, electronic screening, and the geometrical structure of molecules at surfaces. Angle-resolved photoemission (ARPES) provides momentum-space information about molecular orbitals of adsorbates, energy dispersion of surface states at the interface, the band structure of the underlying solid. The quasi-CW nature of synchrotron radiation ($\sim$100 ps pulses at MHz repetition rates), which produces few photoelectrons per pulse, is essential for surface experiments where electrons emerge from a small volume of space at the surface, and space charge/image charge effects can blur and shift the photoelectron spectrum.

The ideal XUV light source for extending photoemission techniques to the time domain would have the flux and multi-MHz repetition rate of a synchrotron, but with ultrashort pulse durations. Many groups around the world have been working towards this goal using a variety of platforms. At Stony Brook, we have developed this ideal light source using cavity-enhanced high-harmonic generation and have achieved a setup with sufficient flux and tuning range to enable challenging surface science experiments at the endstation.

The light source was running reliably from Dec. 2017 to Aug. 2019 and in that time we made a lot of progress, publishing breakthrough papers which are now widely cited [1, 2] and getting the new time-of-flight momentum microscope (TOF k-mic) from the Schönhense group in Mainz [3] up and running, as presented in our 2019 abstract. During this time, graduate student Peng Zhao completed his dissertation work [4]. In Aug./Sept. 2019 we also obtained preliminary pump-probe data with the setup, showing progress towards our technical goal of perturbative-pump time-resolved ARPES from a small area of the sample (μ-ARPES) with acquisition times of only minutes per pump-probe/delay.

Unfortunately, we have not been able to get back to these pump-probe experiments since this time due to a number of reasons including COVID-19. Long Island was hit particularly hard with COVID-19 in March and all lab activities ceased on March 21 and did not resume until June, and even still have not fully resumed. Below are some of the other technical problems that have delayed pump-probe experiments, and our solutions to these problems.

Problem 1, Personnel Turnover: Previously, this project has been mainly driven by the work of graduate student Peng Zhao and postdoc Chris Corder. Both left in the summer of 2019.

Solution 1: New Personnel: Graduate student Jin Bakalis has carrier on the project and in the winter

of 2019-2020 was joined by two new postdocs, Sergey Chernov and Alice Kunin. Both have extensive experience with photoelectron spectroscopy, have hit the ground running, and have also adapted well to the constraints of COVID.

Problem 2, Oscillator Troubles: Mode-locked laser oscillators for cavity-enhancement applications must operate with substantially lower optical phase noise than in nearly all other frequency comb applications, even many of those in precision measurement contexts. This is due to the narrow $\sim$100 kHz linewidths of long enhancement cavities of even modest finesse. Our home-built Yb:fiber oscillators based on nonlinear polarization evolution (NPE) [5] can achieve the necessary specifications, but using NPE for the mode-locking mechanism can present problems with long-term stability. Also, we have observed the Yb:fiber used in our oscillators to photo-darken over time. The NPE oscillator has long been the weakest link in the system. Over summer 2019, we observed the performance of our NPE oscillator degrade such that frequency locking to the enhancement cavity became noisy and unstable, with ultimate oscillator death occurring in Sept. 2019.

Solution 2, Laser front-end upgrades: Since nothing works without the oscillator, in the fall of 2019, we decided to tackle this problem with a multi-pronged approach. First, we replaced the fiber assembly in the Yb:fiber oscillator and carefully optimized the net cavity dispersion to again achieve low phase noise. Second, we constructed a new polarization-maintaining Yb:fiber pre-amplifier to boost the power from the oscillator. This lessens the number of simultaneous constraints the oscillator need satisfy. Third, in consultation with the program manager we have used DOE funds to purchase a new all-polarization-maintaining Er:fiber oscillator from Menlo Systems, which can be coherently shifted to the 1 μm Yb wavelength using a combination of nonlinear Er-doped fiber amplifiers and highly-nonlinear fiber as described in [6]. We have implemented this solution on another project and observed it to be very reliable. Currently we are still operating with the rebuilt Yb:fiber oscillator but we have completed shifting the new Menlo comb to 1 μm and are ready to execute the swap at the next opportunity. Both new oscillators run at 61 MHz repetition rate, which enables easier pulse picking (either photoelectrons or pump pup pulses), compared to our previous 88 MHz.

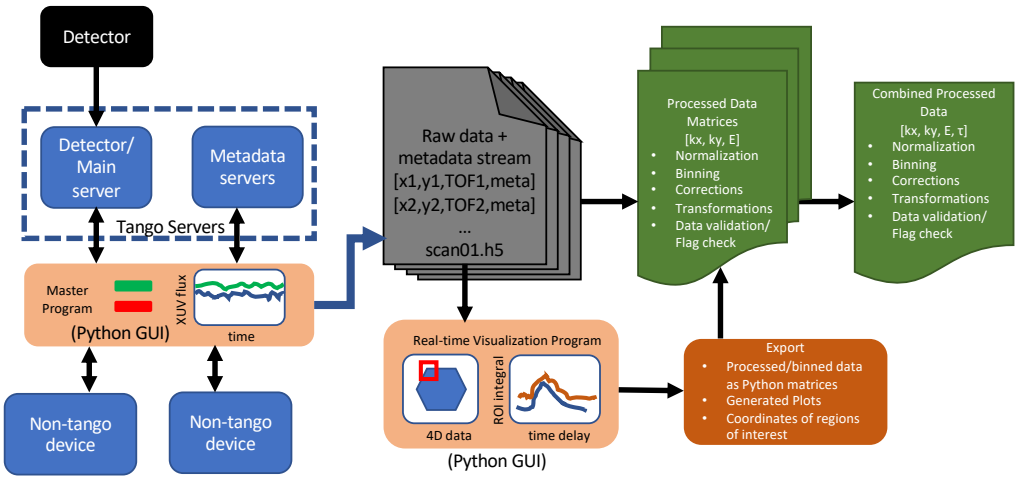

Figure 1: **Data acquisition and visualization pipeline:** Tango servers interact with the DLD and other instruments which collect metadata. A Python-based program runs pump/probe scans and streams the data to HDF5 files. These files are then simultaneously read by a real-time visualization program using the single writer multiple reader (SWMR) feature of HDF5. The visualization program (screenshot in figure 2) allows selection of regions of interest (ROI) in the 4-dimensional data set and the construction of various projections, for example counts in a region (k_x, k_y, E)-space vs. pump/probe delay.

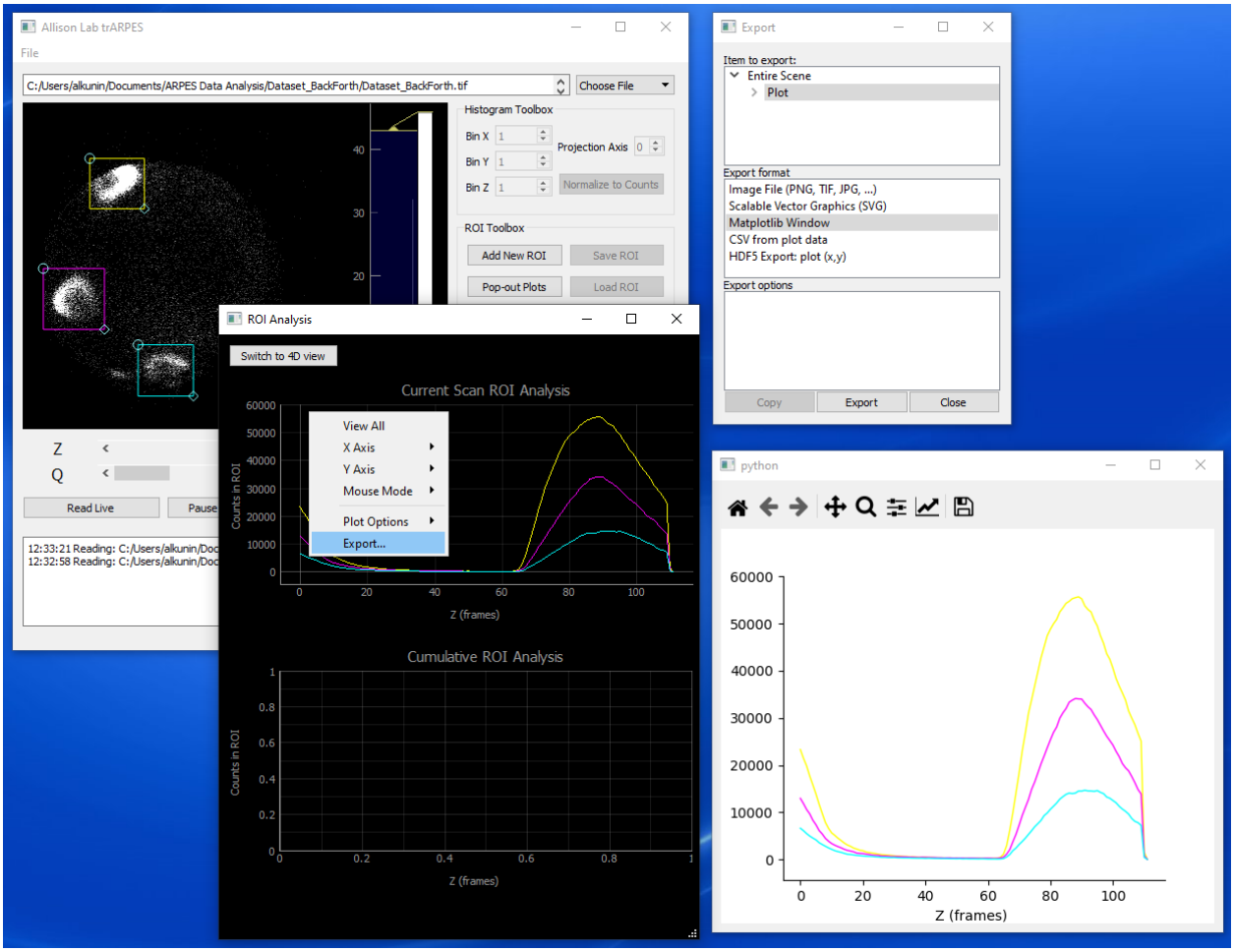

Figure 2: **Data Visualization Software**: Screenshots of the data-visualization program in action. Partial projections are extracted from multiple projections of ARPES data from a single domain of a highly-ordered pyrolytic graphite sample.

Problem 3, Software: The combination of our new light source and the TOF k-mic represents a roughly four order of magnitude increase in the attainable data rates for time-resolved ARPES. Once doing real pump-probe experiments with the TOF k-mic, it immediately became apparent that the software provided with the instrument's delay-line detector (Surface Concepts GmbH) was woefully inadequate to handle this data rate. This is due to the way the default software saves the data and the way it is allows the user to visualize it. Pump-probe experiments in general require continuous data streaming with minimal dead time due to changing parameters (i.e. pump/probe delay). For ARPES measurements of small differential signals, it is also important to incorporate simultaneously acquired metadata (e.g. pump-probe delay, XUV flux, sample conditions, pump power, etc.) into the main data stream (photoelectron hits). At high count rates, the overall raw data stream is order 10 MB/s, which presents a manageable, but also nontrivial challenge for online storage and multi-dimensional visualization. On-line visualization is necessary to monitor that the experiment is working, the sample is not damaged, etc. The surface concepts software had barely enough functionality to recored static 3D data cubes (k_x, k_y, E), but would save data slowly and also did not provide options for incorporating metadata.

As others in Europe are also implementing TOF k-mics at HHG sources and FELs, this software/big data problem has become recognized worldwide. Indeed, we participated in an entire workshop devoted

solely to how to handle the massive amount of ARPES data that can be generated with these next-generation analyzers [7], and entire papers dedicated to the software/big data problem have been recently published [8, 9] .

Solution 3, Software Development: Improving the k-mic software has always been on our to-do list, but the restrictions of the COVID-19 pandemic brought it to the forefront. In April, we began work on a multi-pronged upgrade of the software and have now arrived at a new suite of codes that form a data acquisition and analysis pipeline illustrated in figures 1 and 2. We have worked on the front-end data acquisition (based on the Tango server framework [10]) in collaboration with Yves Acremann at ETH Zürich. Overall, this new suite of codes enables real-time acquisition, visualization, and storage with less than 50 ms of dead time between parameter changes.

Synergistic activities enabled by this project: The large amount of technical work we have done on this project has enabled us to make unique contributions to other efforts in developing time-resolved ARPES instrumentation. The PI was recruited to be a major contributor in the development of a new ultrafast laser user facility being constructed at the Ohio State University, the NSF NeXUS. The PI is also now a collaborator on a nascent effort to bring a TOF k-mic to LCLS-II. While it is mainly our hard-won experience that is helping these other projects, some aspects of our AMOS-funded project such as software can be directly ported to these larger efforts.

Future Plans

We are currently working on resuming pump-probe experiments using the new software upgrades, hardware upgrades, and new personnel.

Peer-Reviewed Publications Resulting from this Project (2018-2020)

C. Corder, P. Zhao, J. Bakalis, X. L. Li, M. D. Kershis, A. R. Muraca, M. G. White, and T. K. Allison. Ultrafast extreme ultraviolet photoemission without space charge. *Structural Dynamics* **5**, 054301 (2018). DOI:10.1063/1.5045578

References

[1] Christopher Corder et al. "Ultrafast extreme ultraviolet photoemission without space charge". In: *Structural Dynamics* 5.5 (2018), p. 054301.

[2] Christopher Corder et al. "Development of a tunable high repetition rate XUV source for time-resolved photoemission studies of ultrafast dynamics at surfaces". In: *Proc.SPIE* 10519 (2018), pp. 10519 –10519 –7.

[3] K. Medjanik et al. "Direct 3D mapping of the Fermi surface and Fermi velocity". In: *Nat Mater* 16.6 (June 2017), pp. 615–621.

[4] Peng Zhao. "An advanced instrument for time- and angle-resolved photoemission spectroscopy". PhD thesis. Stony Brook University, 2019.

[5] Xinlong Li et al. "High-power ultrafast Yb:fiber laser frequency combs using commercially available components and basic fiber tools". In: *Review of Scientific Instruments* 87.9, 093114 (2016), p. 093114.

[6] Anthony Catanese et al. "Mid-infrared frequency comb with 6.7 W average power based on difference frequency generation". In: *Opt. Lett.* 45.5 (2020), pp. 1248–1251.

[7] *https://th.fhi-berlin.mpg.de/meetings/fairdi2020/index.php?n=Meeting.Satellite*.

[8] Rui Patrick Xian et al. *An open-source, end-to-end workflow for multidimensional photoemission spectroscopy*. 2020.

[9] Conrad Stansbury and Alessandra Lanzara. "PyARPES: An analysis framework for multimodal angle-resolved photoemission spectroscopies". In: *SoftwareX* 11 (2020), p. 100472. ISSN: 2352-7110.

[10] *https://www.tango-controls.org/*.

Early Career: New correlated numerical methods for attosecond molecular single and double ionization

Luca Argenti
Department of Physics and CREOL, the College of Optics & Photonics
University of Central Florida, Orlando, FL32816
e-mail: Luca.argenti@ucf.edu

Project Scope

Continuous advances in the XUV and soft-x-ray ultrafast technologies, pursued at large free-electron-laser facilities as well as in several attosecond laboratories around the world, have extended the range of attosecond-pulse parameters to shorter durations, larger intensities, energies, and repetition rates. New XUV-pump XUV/soft-x-ray-probe schemes, in which the duration of both light-matter interaction stages is short, have drastically enhanced the time resolution with which ionization can be steered and monitored. Soft-x-ray probes can excite core electrons, thus monitoring the valence dynamics with high spatial resolution. X-ray pulses in the water window have extended the scope of attosecond spectroscopy to aqueous matrices. Photoelectrons from core orbitals are scattered by neighboring nuclei, thus encoding the geometry of the target molecule. In molecules with tightly bound pairs of equivalent atoms, such as N_2 or C_2H_2, core photoelectrons give rise to characteristic double-slit interference fringes that mirror the evolution of molecular geometry and charge migration. XUV pulses can even release two or more electrons, which, if detected in coincidence, give direct information on the concerted motion of electrons in the ground as well as in excited states. The theoretical description of these processes is essential to track the motion of correlated electron pairs, and, ultimately, to control ultrafast dynamics in matter. Until computational tools for molecular single and double ionization will be available, the "attosecond revolution" will remain incomplete.

This project concerns the merge of hybrid-basis close-coupling approaches with state-of-the-art numerical techniques for the single- and double-ionization continuum, and for correlated parent-ion bound states, to describe both single- and double-escape processes from poly-electronic molecules. The resulting code is here referred to as ASTRA (AttoSecond TRAnsitions). No general method to solve the secular problem above the second ionization threshold has been established yet. Whereas recent interfaces of quantum-chemistry codes to hybrid Gaussian-B-spline close-coupling (CC) space are promising, more advanced methods are required to describe the multi-photon double-ionization processes targeted by upcoming attosecond experiments. For this reason, we will develop and integrate the numerical tools for the representation of free-electron pairs with electronic-structure molecular packages to lay the foundation of a new hybrid CC program for the time-dependent description of molecular single and double-ionization processes, with a quantitative account of light-driven static and dynamic electronic correlation. Most of the fundamental quantities needed to carry out this program (hybrid integrals and high-order transition density matrices) are not available yet. Computing and incorporating them in scalable programs is a major theoretical, computational and algorithmic challenge. Successfully tackling this challenge will allow us to directly image correlated motion in matter, thus opening the way to a transformative expansion of attosecond science.

Recent Progress

During the first year of the project, which started September 1st 2019, we have made progress in several directions scheduled in the original proposal, which are listed below.

i) Quadrature algorithms for the mono and bi-electronic integrals in a hybrid basis, based on a modified Becke's scheme.

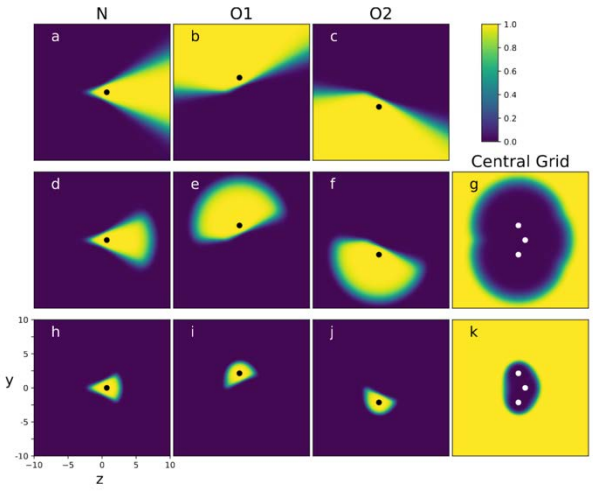

Figure 1: Original and modified Becke's weight distributions for NO_2 molecule (solid circles indicate the position of the nuclei). The original Becke scheme defines atomic weights that in general do not vanish at infinity (a-c). The weight can be localized based on switch-off functions centered on the individual atoms (d-f) or on a global molecular function, based on the nuclear potential (h-j). In either case, a complementary weight is defined presiding over the asymptotic region, which is regular at each and every nucleus location, and which is mostly insensitive to the short-range features of the molecular structure.

A common way to evaluate electronic integrals for polyatomic molecules is to use Becke's partitioning scheme [Becke1988] in conjunction with multi-center grids of comparable size. Becke scheme, however, is efficient only for integrands that fall off rapidly at large distances, such as those approximating bound electronic states. States in the electronic continuum, however, do not meet this criterion. To overcome the limitation of the original quadrature, we have developed a modified version of Becke's scheme that applies to molecular photoionization and electron-molecule scattering. In the modified scheme, the original atomic weights in Becke's partition of unity are smoothly switched off outside the molecular region. The atomic integrals are evaluated on radial grids, centered on each atom, and with a radius of the order of few bond lengths. A central master grid is used to evaluate the complementary weight contribution in the interstitial region and at long range. The accuracy of the method has been benchmarked with test calculations of the norm of Gaussian Type Orbitals, Yukawa potentials, and Spherical Bessel functions. A manuscript on this subject has been submitted and is currently under revision [H. Gharibnejad, N. Douguet, B. I. Schneider, J. Olsen, L. Argenti, A Multi-Center Quadrature Scheme for the Molecular Continuum, *submitted*].

ii) Transition density matrices between ionic states with arbitrary D_{2h} symmetry and multiplicity. We have collaborated with Jeppe Olsen to extend the general configuration-interaction code LUCIA, so that it can generate one-, two-, and three-body transition density matrices (TDM) [McWeeny1969] between ionic states with arbitrary (possibly, different) symmetry and multiplicity, using the formalism of string-based determinant expansions of wave functions [Olsen1988]. LUCIA is now able to give in formatted output all TDMs up to second order, as well as a number of subsidiary quantities, such as matrix elements between ionic states augmented with active orbitals, between spin-uncoupled states, and for selected spin magnetic quantum numbers. From these data, it is possible to deduce the underlying invariant (reduced) TDMs, with which matrix elements between arbitrary close-coupling states can be obtained.

iii) Framework code. We have written a framework code for the calculation of arbitrary matrix elements between close-coupling states, concerning the logistics of group symmetry, multiplicity, close-coupling-space composition, naming conventions, storage and loading conventions, etc.

iv) Spin-coupled formulas. We have derived the formulas for the matrix elements of one-body and two-body operators between spin-coupled single-ionization states in terms of reduced ionic transition density matrices of first order (A, B), second order (P, Q), (as well as third order, which

however concerns only matrix elements computed entirely within LUCIA, and which are then omitted here), suitably contracted with angular-algebra factors to match the spin coupling of the ionization states (primes and *x* indicate summation over active and inactive orbitals, respectively):

$$\langle A,p;S\Sigma|\hat{O}|B,q;S\Sigma\rangle = \delta_{S_A S_B} S_{pq} \Pi_{S_A}^{-1} \langle A\|\hat{O}\|B\rangle + \delta_{AB} o_{pq} + \sum_r{}' \left(B^{BA}_{pr} o_{rq} + o_{pr} B^{BA}_{rq} \right) +$$

$$+ 2 \left(\sum_x o_{xx} \right) B^{BA}_{pq} + \sum_{rs}{}' o_{rs} P^{BA}_{ps,qr}.$$

$$\langle A,p;S\Sigma|\hat{H}|B,q;S\Sigma\rangle = \delta_{AB} (S_{pq} E_A + \tilde{h}_{pq}) + \sum_r{}' \left(B^{BA}_{pr} \tilde{h}_{rq} + \tilde{h}_{pr} B^{BA}_{rq} \right) +$$

$$+ \delta_{S_A S_B} \sum_{rs}{}' [pq|rs] A^{BA}_{sr} + \sum_{rs}{}' [ps|rq] B^{BA}_{sr} + \sum_{rs}{}' \left([pa|rs] Q^{BA}_{sa,rq} + [qa|rs] Q^{BA}_{sp,ra} \right)$$

$$\tilde{h}_{pq} = h_{pq} + 2J^{\mathrm{core}}_{pq} - K^{\mathrm{core}}_{pq}, \qquad J^{\mathrm{core}}_{pq} = \sum_x^{\mathrm{core}} [pq|xx], \qquad K^{\mathrm{core}}_{pq} = \sum_x^{\mathrm{core}} [px|xq].$$

These formulas are currently being tested.

v) Provisional hybrid integrals. The hybrid integrals as of point i) will still require some work to be completed. In the meanwhile, we have built an interface to the hybrid polycentric-Gaussian – B-spline integral library, recently published with the UKRmol+ molecular scattering code [Masin2020], as a temporary scaffolding while the new hybrid-integral code is being developed. The integrals have already been successfully used in a prototype CI-singles code for the Rydberg states of the N_2 molecule (see point vi).

vi) Prototype CI-Single (CIS) close-coupling code. We have written an ad hoc prototype code for the calculation of the Rydberg states of the N_2 molecule in a close-coupling basis, using the CIS approxiamation, in order to establish a validation chain between 1) UKRmol+, 2) the "elementary" CIS Prototype code, and 3) the general ASTRA code, based on TDM. The first link already works. We are currently finalizing ASTRA (see point iv), to be fed with the elementary CIS TDMs.

vii) Annual meeting. In March 7-12, 2020 (shortly before COVID lockdown), we held the one-week meeting between the internal and external collaborators to this project, to align our efforts.

viii) Personnel. We have hired a postdoctoral fellow, Dr. Juan Martín Randazzo, an established and tenured researcher at the Argentinian Research Council (CONICET), with a background in molecular double ionization, who has taken a two-year leave from his institution to join our effort, starting the end of January 2020. Dr. Randazzo has been actively involved in, and has contributed to, all the stages of the project, and in particular points v) and vi).

ix) Extension of the XCHEM benchmark. The XCHEM code, of which the PI is a co-developer, will be used as a benchmark for the development of the ASTRA code. To this end, XCHEM needed some revisions. During Fall 2019, the PI has made remarkable progress, in collaboration with one of Martín's co-workers. We have entirely rewritten the calculation of the scattering states, the diagonalization of the Hamiltonian for the confined system with ScaLapack, the projection of arbitrary wave packets on scattering states, and the calculation of the molecular-frame photoelectron angular distributions (MFPADs) as well as the corresponding laboratory-frame observable for randomly oriented molecules. Test calculations have been done on the channel-resolved MFPADs of the CO molecule (a manuscript is currently in preparation). The figure illustrates preliminary results for the MFPAD for different parent ions and field polarization.

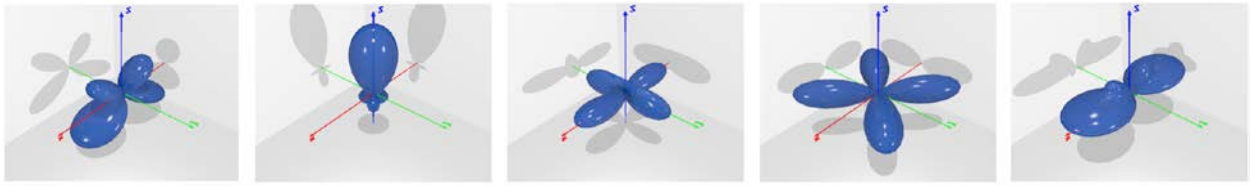

(a) $A^2\Pi(B_1)$ ($\vec{E}$ = z axis) (b) $X^2\Sigma^+$ ($\vec{E}$ = z axis) (c) $A^2\Pi(B_1)$ ($\vec{E}$ = x axis) (d) $A^2\Pi(B_2)$ ($\vec{E}$ = x axis) (e) $X^2\Sigma^+$ ($\vec{E}$ = x axis)

In conclusion, at the moment we are on track with the roadmap set in the proposal.

Future Plans

We expect to complete the first benchmark calculation of N_2 Rydberg states with ASTRA within the CIS approximation, to validate the overall code structure, and to refine those calculation with the use of well correlated N_2^+ ions, within ASTRA TDM formalism, by the end of 2020. During the second year, we should be able to make sufficient progress with the new code for the hybrid integrals, to replace the current scaffolding interface to the UKRmol+ hybrid-integral library. This will allow us to consider with equal accuracy molecular conformations in which atoms are close or far apart, either because of the sheer number of atoms in the molecule, because the molecule is loosely bound (e.g., rare-gas clusters), or because it is close to dissociation. We plan to hire a second postdoctoral fellow (the process has been delayed, due to the ongoing pandemic), to complete the calculation of the hybrid bi-electronic integrals, and their transformation to an orthogonal basis. Once the structural codes (Hamiltonian and dipole matrix elements) are complete and reliable, we will progressively add to the ASTRA suite programs to evaluate stationary scattering states, Siegert states, to solve the time-dependent Schödinger equation in the presence of external fields, and to analyze the photoelectron spectra and optical response. The PI has already implemented the corresponding algorithms in polyelectronic atoms and, indeed, in the XCHEM molecular code. Some care will be dedicated to parallelize the codes. At that point, the resulting general single-ionization codes (fixed nuclei), should be competitive with any other time-dependent single-ionization code on the market, which we plan to use as benchmarks. Once these tests are completed successfully, we will be in the position of implementing the (demanding!) extension of ASTRA to treat double-ionization processes.

References:

[Becke1988] A. D. Becke, J. Chem. Phys. **88**, 2547 (1988).
[Helgaker2000] T. Helgaker, P. Jørgensen, and J. Olsen. *Molecular Electronic-Structure Theory* (Chichester, UK, 2000), 1st edn.
[Helgaker2012] T. Helgaker, S. Coriani, P. Jørgensen, K. Kristensen et al., Chem. Rev. **112**, 543 (2012).
[Marante2017] C. Marante, M. Klinker, I. Corral, J. Gonzalez-Vazquez, L. Argenti, and F. Martin. J. Chem. Theory Comput. **13**, 499 (2017).
[Masin2020] Z. Masın, *et al.*, Comp. Phys. Commun. **249**, 107092 (2020)
[McWeeny1969] R. McWeeny and B. T. Sutcliffe. *Methods of molecular quantum mechanics* (Academic Press, London, 1969), 2 edn.
[Olsen1988] J. Olsen, B. O. Roos, P. Jørgensen, and H. J. A. Jensen. J. Chem. Phys. **89**, 2185 (1988).

Peer-Reviewed Publications Resulting from this Project (Sep2019-2020): One manuscript submitted, currently under review [see point i)].

Attosecond dynamics driven by ultrashort laser pulses

Principal Investigator: Andreas Becker

JILA and Department of Physics, University of Colorado at Boulder,
440 UCB, Boulder, CO 80309-0440

andreas.becker@colorado.edu

Project Scope

The quest for studying dynamics in matter on ultrashort timescales has driven the development of a variety of technologies in ultrafast science. The most prominent among these are ultrashort electron pulses, femtosecond laser pulses, X-ray free electron lasers, and currently one of the shortest of all these probes, attosecond light pulses (1 as = 10^{-18} s). Substantial progress in controlling electron dynamics and the coupling between electron and nuclear dynamics in highly nonlinear processes driven by femtosecond laser pulses enabled the first realization of sub-femtosecond pulses in 2001. Nowadays, the controlled electron dynamics over a subcycle of the driving laser pulse allows for the emission of coherent light at extreme ultraviolet and soft X-ray wavelengths on a suboptical cycle time scale, i.e. on the attosecond time scale, through the process of high-harmonic generation.

Measurements on the attosecond timescale have been under ongoing rapid development for about a decade. One of the open challenges is the realization of a conventional pump-probe spectroscopy set-up using two isolated attosecond laser pulses, in which time resolution would be achieved by the delay and durations of the two pulses. So far, the intensity of attosecond laser pulses has however been too low to achieve significant attosecond pump-probe signals. Using the knowledge how to manipulate and control electron dynamics with laser pulses, a variety of spectroscopic techniques with and without the application of attosecond pulses has been developed and applied to temporally resolve dynamical processes on the attosecond time scale [DOE1].

With the work in our projects we seek to provide theoretical support related to the establishment of ultrafast optical techniques as tools to uncover new insights in the temporal resolution of ultrafast dynamics in atoms and molecules and strong-field nonlinear processes, such as excitation, ionization and high harmonic generation, in general. One of the exciting recent developments in this area is the development of a polarization control over the generated ultrashort pulses. This creates new possibilities for imaging on ultrafast time scales and has renewed, in general, the interest in the interaction of atoms and molecules with laser light of variable polarization, ranging from linear via elliptical to circular.

Recent Progress

Recent developments undertaken and accomplishments completed in the research projects can be summarized as follows.

A. Excitation with Bichromatic Circularly Polarized Laser Pulses

Excitation of atoms (and molecules) is known to play an important role in many strong-field processes. Previously within this project we have studied the distributions over the orbital angular momentum number in Rydberg states due to the interaction with a linearly polarized laser pulse [DOE4]. Impact of pulse parameters such as the pulse duration, peak intensity and the carrier-envelope phase have been analyzed. Part of our theoretical predictions are in agreement with the results of a recent experimental work [1].

Over the last year we have extended our theoretical studies on this topic to the superposition of two circularly polarized laser pulses, which recently has seen an upsurge in activity in strong-field experiment and theory. In a recent experiment on strong-field ionization by a bichromatic circularly polarized pulse it has been shown that the probability to ionize an atom is significantly enhanced if the two fields are counter-rotating as compared to co-rotating fields [2]. The experimental observations were interpreted as due to the increased density of excited states accessible for resonant enhanced multiphoton ionization in the case of counter-rotating fields. Studies of the excited state distributions over the quantum numbers (principal, angular momentum, magnetic) can shed further light on the role of excited states in the pathways to ionization since excitation in a resonant multiphoton process should rely on the spin-angular momentum selection rules for the absorption of circularly polarized photons.

We have therefore studied the excitation of hydrogen atom by bichromatic circularly polarized laser pulses using numerical solutions of the time-dependent Schrodinger equation [DOE8]. The results are in agreement with the selection rules for multiphoton processes in such fields, namely excited states are populated in which orbital angular momentum and magnetic quantum numbers are either both odd or both even, independent of the relative helicity, peak intensity, and pulse duration of the pulses. For co-rotating pulses the results show that excitation predominantly proceeds to states with magnetic quantum number of the same helicity as the laser pulses. A surprising result of our analysis was that besides pathways via direct photon absorption a transfer of population among the Rydberg states via Lambda-type transitions occurs. In the case of counter-rotating pulses the largest excitation probability is found for Rydberg states that differ in magnetic quantum number by Δm = -3 or Δm = +3. This pattern allows to estimate how many photons from each of the two bichromatic fields have been absorbed. Finally, we have confirmed that a population in Rydberg states beyond a maximum orbital angular quantum number is unlikely, which has been previously reported for the interaction with linearly polarized laser pulses [3].

B. Asymmetries in the Ionization with Ultrashort Pulses

In another thrust of our work we focus on few-photon ionization of atoms with ultrashort pulses. The general renewed interest in this topic is driven by the recent rapid technical development in the production of deep-ultraviolet and extreme-ultraviolet pulses using high harmonic generation (HHG) and free-electron lasers (FEL). The ongoing quest in shortening pulses at these wavelengths towards the single-cycle regime in duration are achieved via large spectral bandwidths (e.g., [4]). Such broadband energy pulses give rise to competition between one- and two-photon (as well as three-photon) ionization processes for emission at a given energy.

Previously, we have shown the effect of the difference between the central frequencies of the spectral distributions of the vector potential and the electric field of an ultrashort laser pulse on various light induced processes, such as excitation, ionization and high harmonic generation [DOE5]. Over the last year we have focused on the analysis of photoelectron angular distributions and related anisotropy parameters for the competition of one- and two-photon ionization of helium atom and other rare gas atoms in an ultrashort EUV laser pulse, using numerical results from the time-dependent Schrodinger equation. In the work we make use of single-active electron potentials previously developed within this project [DOE9].

First, we have explored the competition between the two processes for an atom prepared in the ground state as function of the pulse duration, peak intensity, central frequency and photoelectron energy [DOE7]. In the results obtained for fixed pulse parameters the transition and interference between the processes can be observed in the even and odd beta-parameters, respectively, while the onset of the impact of three-photon ionization is observed at high peak intensities. We have also shown that the transition can be still seen via the even anisotropy

parameters in pulses without carrier-to-envelope stabilization as well as in free-electron laser pulses with fluctuating pulse shape.

While studies of quantum systems in a single state are important, very interesting physics arises from the systems in superposition states. Currently, it is the superposition of atomic or molecular electronic states and the related attosecond electron dynamics that is the focus of the present project and other studies in the field. Unlike for the ionization of a quantum system prepared in the ground state, conventional anisotropy and asymmetry parameters are not well suited to provide comprehensive tools for the analysis of photoionization from atomic superposition states. Therefore, an extension of the toolbox for the characterization of the states and the identification of competing pathways is desirable. We have proposed a new set of generalized asymmetry parameters which are sensitive to interference effects in the photoionization of atomic systems in superposition states [DOE10]. These new parameters can be used to identify the interplay of competing linear and nonlinear pathways at low and high intensities, as well as at ultrashort pulse durations. The application and relevance of the parameters has been tested using state-of-the-art numerical solutions of the time-dependent Schrödinger equation.

C. Imaging of Electron Dynamics with Pulses of Variable Polarization

As mentioned before, one of the exciting recent developments in attosecond laser pulse technology is the development of polarization control for the generated ultrashort pulses [5]. This creates new possibilities for imaging electron dynamics on ultrafast time scales. In the third thrust of our project we therefore analyze the prospects of the application of these pulses for time resolution of electron dynamics. To this end, we currently study the reconstruction of a wavepacket and the corresponding electron dynamics in an atom via photoelectron angular distributions in a pump-probe scheme as a function of time delay. Specifically, we focus on dynamics related to the superposition of excited states which lead to a so-called ring current in the atom, that is characterized by the circulation of electron density about the center of the atom. In strong-field physics such ring currents have recently attracted much attention in theory and experiment. Our method is based on the interferences between one-photon transitions from ground and excited states as well as the two-photon pathway from the ground state (see also section B). In the reconstruction predictions of first- and second-order perturbation theory are used to determine the unknown phases and amplitudes from the photoelectron angular distributions, which we simulate via solutions of the time-dependent Schrodinger equation in the single-active-electron approximation. In our analysis of the results we study how the relevance of each pathway for the reconstruction as a function of peak intensity and pulse duration can be identified. As in other recent projects we also plan to analyze the applicability and limits of the reconstruction method with respect to variations in the laser parameters.

Future Plans

We plan to continue our studies in the three thrusts outlined above. For the interaction of atoms with bicircular laser pulses we currently further analyze the Lambda transitions between Rydberg states, which we have identified as a mechanism for a repopulation among states with different magnetic quantum numbers. Such processes are also known to provide a means for controlling the transfer between states. We intend to apply the newly proposed set of generalized asymmetry parameters to a broader range of atomic systems and laser parameters. We further plan to analyze in more detail the relation of these asymmetry parameters to the conventional beta-parameters. In our studies of spectroscopic methods to image electron dynamics we plan to finalize the analysis of the imaging of ring currents by testing the limits and applicability of the proposed method. Then, we intend to extend our focus to spectroscopic methods involving the superposition of laser pulses with variable polarization. Finally, we have started studies on the application of the cross-correlation method in time-delayed laser pulses.

Besides an analysis of the results for the ionization (auto- and cross-correlation) signal we intend to compare the method with other techniques that use time-delayed pulses but rely on the observation of the radiation generated by the two pulses.

References

[1] D. Chetty et al., Phys. Rev. A **101**, 053402 (2020).

[2] C.A. Mancuso et al., Phys. Rev. A **96**, 023402 (2017).

[3] D.G. Arbo et al., Phys. Rev. A **78**, 013406 (2008).

[4] M. Galli et al., Opt. Lett. **44**, 1308 (2019).

[5] P.C. Huang at al., Nat. Photon. **12**, 349 (2018).

Peer-Reviewed Publications Resulting from this Project (2018-2020)

[DOE1] A. Jaron-Becker and A. Becker, *Attosecond Spectroscopy,* Encyclopedia of Modern Optics (2nd Edition), edited by R. Guenther and D. Steel (Oxford: Elsevier, 2018) pp. 233-243.

[DOE2] C. Goldsmith, A. Jaron-Becker, and A. Becker, *Effect of attochirp on attosecond streaking time delay in photoionization of atoms,* Journal of Physics B: Atomic, Molecular and Optical Physics **51**, 025601 (2018).

[DOE3] C. Goldsmith, J. Su, A. Jaron-Becker, and A. Becker, *Analysis of absorption time delays in resonant and non-resonant two-photon ionization,* Journal of Physics B: Atomic, Molecular and Optical Physics **51**, 155602 (2018).

[DOE4] J. Venzke, R. Reiff, Z. Xue, A. Jaron-Becker, and A. Becker, *Angular momentum distribution in Rydberg states excited by a strong laser pulse*, Physical Review A **98**, 043434 (2018).

[DOE5] J. Venzke, T. Joyce, Z. Xue, A. Becker, and A. Jaron- Becker, *Central frequency of of few-cycle pulses in strong-field processes*, Physical Review A **98**, 063409 (2018).

[DOE6] C. Goldsmith, A. Jaron-Becker, and A. Becker, *Attosecond Streaking Time Delays: Finite-Range Interpretation and applications,* Applied Sciences **9**, 492 (2019).

[DOE7] J. Venzke, A. Jaron-Becker, and A. Becker, *Ionization of Helium with ultrashort laser pulses,* Journal of Physics B: Atomic, Molecular and Optical Physics **53**, 085602 (2020).

[DOE8] J. Venzke, Y. Gebre, A. Becker, and A. Jaron-Becker, *Pathways to excitation of atoms with bicircular laser pulses,* Physical Review A **101**, 053425 (2020).

[DOE9] R. Reiff, T. Joyce, A. Jaron-Becker and A. Becker, *Single-active electron calculations of high-order harmonic generation from valence shells for quantitative comparison with TDDFT calculations,* Journal of Physics Communications **4**, 065011 (2020).

[DOE10] J. Venzke, A. Becker, and A. Jaron-Becker, *Asymmetries in ionization of atomic superposition states by ultrashort laser pulses,* Scientific Reports **10**, 161164 (2020).

Molecular Dynamics Imaging from Within at the Femto- and Atto-Second Timescale using FELs

Nora Berrah,
Physics Department, University of Connecticut, Storrs, CT 06268
e-mail:nora.berrah@uconn.edu

Project Scope

The goal of our research program is to investigate *fundamental interactions between ultrafast photons and molecular systems* to advance our quantitative understanding of electron correlations, charge transfer and many body phenomena. Our research investigations focus on probing, on femtosecond and attosecond time-scale, multi-electron interactions, and tracing nuclear motion in order to understand and ultimately control energy and charge transfer processes from electromagnetic radiation to matter. Most of our work is carried out in a strong partnership with theorists.

Our current interests include: **1)** Time-resolved molecular dynamics investigations using x-ray pump-x-ray probe techniques using free electron lasers (FELs), such as the LCLS x-ray FEL at SLAC National Laboratory but also at FERMI, Italy, SACLA, Japan, FLASH-II and XFEL in Hamburg, Germany. Our current experiments allow us to probe physical and chemical processes that happen on femtosecond time scale. **2)** The study of non-linear and strong field phenomena in the soft and hard x-ray regime. **3)** Investigations of electron dynamics in molecules at the attosecond timescale with the new XLEAP capability at LCLS-II. We use IR/UV table-top lasers at UConn and the ALS synchrotron facility to prepare our FELs experiments. We present below results completed and in progress this past year and plans for the immediate future.

Recent Progress

1) Intermolecular Coulombic Decay in Endohedral Fullerene at the 4d ➔ 4f Resonance

Interatomic Coulombic decay (ICD) [a] is, unlike the Auger process, a nonlocal electronic decay mechanism which occurs when local electronic decay is energetically forbidden; it offers an ultrafast decay path where energy is transferred with a neighboring atom leading to its ionization. It is characterized by the transfer of the excess energy from the excited species to the neighbor and is driven by the correlation between the electrons located on the neighboring species. Hence, ICD investigations impacts fundamental understanding of energy transfer between electronic degrees of freedom and relaxation processes resulting from long range correlation effects.

ICD impacts molecular photodissociation and can efficiently quench fast nuclear rearrangements in the excited states of molecules [b]. As part of the cascades initiated by X-ray absorption, ICD can damage the environment a few fs after the photon impact [c]. Non-local electronic decay channels, like ICD, have been aggressively pursued theoretically [a,b,c] and are considered an important component in photochemistry and radiation chemistry. ICD has been investigated in various system but not in endohedral

fullerenes which are unique targets to observe charge transfer because molecules can be confined within a hollow spherical carbon molecular cage. Discovered around the same time as C_{60}, endohedral fullerenes with confined metal species have received broad interest in chemistry and condensed matter physics due to their unique ionization and fragmentation mechanisms upon photon excitation.

Endohedral fullerenes were predicted to exhibit strong intermolecular decay channels [d] upon inner-shell ionization through intermolecular Coulombic decay but this prediction was never experimentally verified, motivating our experimental investigation.

We carried out inner-shell ionization of gas-phase $Ho_3N@C_{80}$ (where @ indicates that Ho_3N is contained within the C_{80} cage). At photon energies above the 4d resonance threshold of Ho^{3+}, the carbon cage is effectively transparent, due to the low photoabsorption cross section, while the holmium atoms have a relatively large photoabsorption cross section. We used our ALS velocity-map imaging (VMI) technique [Pub8] that enabled ion-electron coincidence measurements as well as measurements of the kinetic energy of the detected particles. For the present experiment, we evaporated $Ho_3N@C_{80}$ in its gas phase at about 900 K using an effusive oven giving a target density of ~ 10^8 cm^{-3}.

We observed intermolecular Coulombic decay in endohedral fullerenes, $Ho_3N@C_{80}$, and have shown that ICD processes, subsequent to inner-shell ionization, are much stronger than local, intra-atomic Auger decay by forming multiple charge states of $(Ho^{3+})_3N^{3-}@C_{80}^{6-}$around the 4d ➔ 4f transitions. From the electron kinetic energy (eKE) distribution in coincidence with different parent and fragmented ions, we measured the signatures of the predicted ICD [d] between the holmium and the cage, and cascade Auger-ICD between the holmium ions. Furthermore, we observed the dominance of 5s /5 p photoelectron lines in the $Ho_3N@C_{80}^{+}$ spectrum. Because of the 4d-4f resonance, the 5s/5p orbitals are resonantly enhanced, opening the ICD channels at around 30 eV. Additionally, cascade type ICD also played an important role in the formation of triply charged complexes. These cascade processes warrant further investigation at higher x-ray photon energies for metal-cage complexes, which can act as a prototypical system to study radiation induced damage in the high-intensity regime accessed by FELs. Our work validated theory and reported unexpected results [Pub1].

We had established the possibility to carry out time resolved experiments on endohedral fullerenes with FELs [Pub6] and this work carried out with X-rays at the ALS [Pub1] prepares and motivates further experiments with FELs. In fact, we have a collaborative approved beamtime in the spring of 2021 at LCLS-II, using attosecond X-ray pulses. We will be using our oven system and our technique to generate the endohedral fullerenes. Specifically, the experiment will use the angular streaking technique with XLEAP (Pub2, Pub4) to study electronic dynamics related to the influence of the confinement by the carbon cage.

References

[a] L. S. Cederbaum, J. Zobeley, and F. Tarantelli, Phys. Rev. Lett. **79**, 4778 (1997)
[b] G. Jabbari, K. Sadri, L. S. Cederbaum, and K. Gokhberg, J. Chem. Phys.**144**, 164307 (2016)].
[c] V. Stumpf, K. Gokhberg, and L. S. Cederbaum, Nat. Chem. **8**, 237 (2016)
[d] V. Averbukh and L. S. Cederbaum, Phys. Rev. Lett. 96, 053401 (2006)

Future Plans.

The principal areas of investigation planned for the coming year are:

1) Prepare the time-resolved beamtime experiment using the SLAC UED facility regarding molecular ring opening. Our beamtime was scheduled for August 2019 but because of Covid-19, it was rescheduled to January 2021. **2)** Prepare the time-resolved beamtime regarding the experiment that will investigate intermolecular interactions of molecular iodine solvated in small water clusters. The experiment will be at the FLASH-II FEL using a COLTRIMS system to measure electron-ion-ion coincidences paired with high rep rate. This experiment prepares us to use the future high rep rate at LCLS-II. **3)** Finish the analysis and write the publication of our non-linear physics experiment on Ar and H_2S at EU-XFEL carried out on October 2019. **4)** Continue the analysis of the FLASH-II FEL, time-resolved ultrafast dynamics experiment, subsequent to the ionization of giant C_{60} resonances in the XUV regime. These resonances consists of strongly correlated electrons. The experiment was carried out Oct, 2019. **5)** Continue the data analysis of our April 2019 experiment on single and double H-migration at the FLASH FEL Hamburg, Germany. The experiment used high repetition FEL pulses paired with a Reaction Microscope (REMI/COLTRIM) instrument similar to the one being built at LCLS-II, called DREAM. The last two projects carried out at FLASH-II will prepare us for the research we plan to conduct at LCLS-II after 2021 with the high repetition rate using the DREAM and the LAMP end-stations.

Peer-Reviewed Publications Resulting from this Project (2018-2020).

1. Razib Obaid, Hui Xiong, Sven Augustin, Kirsten Schnorr, Utuq Ablikim, Andrea Battistoni, Thomas J. A.Wolf, Rene C. Bilodeau, Timur Osipov, Kirill Gokhberg, Daniel Rolles, Aaron C. LaForge and Nora Berrah, "Intermolecular Coulombic decay in endohedral fullerene at the 4d→ 4f resonance", Phys. Rev Lett. **124** (11), 113002, DOI: 10.1103 (2020).
2. Jordan T. O'Neal, Elio G. Champenois, Razib Obaid, Andre Al-Haddad, Jonathan Barnard, Nora Berrah, Ryan Coffee, Joseph Duris, Gediminas Galinis, Douglas Garratt, Daniel Haxton, Phay Ho, Siqi Li, Xiang Li, James MacArthur, Jon Marangos, Adi Natan, Niranjan Shivaram, Daniel S. Slaughter, Peter Walter, Scott Wandel, Linda Young, Christoph Bostedt, Philip H. Bucksbaum, Agostino Marinelli, and James P. Cryan, "Electronic Population Transfer via Impulsive Stimulated X-ray Raman Scattering with Attosecond Soft X-ray Pulses"(Accepted to Phys. Rev. Lett.)
3. N. Berrah, A. Sanchez-Gonzalez, Z. Jurek, R. Obaid, H. Xiong, R. J. Squibb, T. Osipov, A. Lutman, L. Fang, T. Barillot, J. D. Bozek, J. Cryan, T. J. A. Wolf, D. Rolles, R. Coffee, K. Schnorr, S. Augustin, H. Fukuzawa, K. Motomura, N. Niebuhr, L. J. Frasinski, R. Feifel, C. P. Schulz, K. Toyota, S.-K. Son, K. Ueda, T. Pfeifer, J.P. Marangos and R. Santra, "X-ray multiphoton ionization of molecules: Femtosecond-resolved observation of delayed fragmentation and evaporation of neutral atoms", Nature Physics 15, 1279 (2019).
4. Taran Driver, Siqi Li, Elio G. Champenois, Joseph Duris, Daniel Ratner, TJ Lane, Philipp Rosenberger, Andre Al-Haddad, Vitali Averbukh, Toby Barnard, Nora Berrah, Christoph Bostedt, Philip H. Bucksbaum, Ryan Coffee, Louis F. DiMauro, Li Fang, Douglas Garratt, Averell Gatton, Zhaoheng Guo, Gregor Hartmann, Daniel Haxton, Wolfram Helm Aaron LaForge, Andrei Kamalov, Matthias F. Kling, Jonas Knurr, Ming-Fu Lin, Alberto A. Lutman, James P. MacArthur, Jon P. Marangos, Megan Nante, Adi Natan, Razib Obaid, Niranjan H. Shivaram, Avaid Schori, Peter Walter, Anna Wang, Thomas J. A. Wolf, Agostino Marinelli, and

James P. Cryan, “Attosecond Transient Absorption Spooktroscopy: a ghost imaging approach to ultrafast absorption spectroscopy” Phys. Chem. Chem. Phys., 2019, DOI: 10.1039/c9cp03951a

5. Stephane Carniato, Patricia Selles, Anthony Ferté, Nora Berrah, Alan Wuosmaa, Motoyoshi Nakano, Yasumasa Hikosaka, Kenji Ito, Matjaž Žitnik, Klemen Bučar, L. Andric, J. Palaudoux, Francis Penent, and Pascal Lablanquie, "Double-core ionization photoelectron spectroscopy of C_6H_6 . Breakdown of the “intuitive” ortho-meta-para binding energy ordering of $K^{-1}K^{-1}$ states". Chem. Phys. 151, 214303 (2019).
6. Razib Obaid, Kirsten Schnorr, Thomas J. A. Wolf, Tsukasa Takanashi, Nora G. Kling, Kuno Kooser, Kiyonobu Nagaya, Shin-ichi Wada, Li Fang, Sven Augustin, Daehyun You, Eleanor E. B. Campbell, Hironobu Fukuzawa, Claus-Peter Schulz, Kiyoshi Ueda, Pascal Lablanquie, Thomas Pfeifer, Edwin Kukk, and Nora Berrah, “Photoionization and fragmentation of $Sc_3N@C_{80}$ following excitation above the Sc K-edge at SACLA” J. Chem. Phys. **151**, (2019).
7. Koudai Toyota, Zoltan Jurek, Sang-Kil Son, Hironobu Fukuzawa, Kiyoshi Ueda, Nora Berrah, Benedikt Rudek, Daniel Rolles, Artem Rudenko, and Robin Santra, “*xcalib*: a focal spot calibrator for intense X-ray free-electron laser pulses based on the charge state distributions of light atoms,” *J. Synchrotron Radiat.* **26**, 1017–1030 (2019).
8. U. Ablikim, C. Bomme, T. Osipov, H. Xiong, R. Obaid, R. C. Bilodeau, N. G. Kling, I. Dumitriu, S. Augustin, S. Pathak, K. Schnorr, D. Kilcoyne, N. Berrah, and D. Rolles “A coincidence velocity map imaging spectrometer for ions and high-energy electrons to study inner-shell photoionization of gas-phase molecules” Rev. Sci. Instrum. **90**, 055103 (2019).
9. Eva Lindroth, Francesca Calegari, Linda Young, Marion Harmand, Nirit Dudovich, Nora Berrah and Olga Smirnova “Challenges and opportunities in attosecond and XFEL science”, *Nature Reviews Physics* **1**, 107–111 (2019).
10. Kiyoshi Ueda, Emma Sokell, Stefan Schippers, et al., Nora Berrah, Edwin Kukk, Robin Santra, Alfred Müller, Danielle Dowek, Robert Lucchese, Bill McCurdy, et al., Jan-Michael Rost, Michael Meyer and Kazuo A. Tanaka “Roadmap on photonic, electronic and atomic collision physics I. Light-matter interaction” in press, J. of Phys. B **52**, Number 17, 171001 (2019).
11. Soroush D. Khosravi, Michael M. Bishop, Amy M. LaFountain, Daniel B. Turner, George N. Gibson, Harry A. Frank, and Nora Berrah, “Addition of a Carbonyl End Group Increases the Rate of Excited-State Decay in a Carotenoid via Conjugation Extension and Symmetry Breaking” J. Phys. Chem. B, 122, **48**, 10872-10879 (2018).
12. Razib Obaid, Christian Buth, Georgi L. Dakovski, Randolf Beerwerth, Michael Holmes, J. Aldrich, Ming-Fu Lin, Michael Minitti, Timur Osipov, William Schlotter, Lorenz S. Cederbaum, Stephan Fritzsche, and Nora Berrah, “LCLS in - photon out: fluorescence measurement of neon using soft x-rays” J. Phys. B: At. Mol. Opt. Phys. **51**, 034003 (2018).
13. C. Buth, R. Beerwerth, R. Obaid, N. Berrah, L. Cederbaum and S. Fritzsche “Neon in ultrashort and intense x rays from free electron lasers", J. Phys. B **51**, 055602 (2018).
14. Hui Xiong, Li Fang, Timur Osipov, Nora G. Kling, Thomas J. A. Wolf, Emily Sistrunk, Razib Obaid, Markus Gühr, and Nora Berrah, “Fragmentation of endohedral fullerene $Ho_3N@C_{80}$ in an intense femtosecond near-infrared laser field”, Phys. Rev. A **97**, 023419 (2018).
15. Timur Osipov, Christoph Bostedt, J-C Castagna, Ken R Ferguson, Maximilian Bucher, Sebastian C Montero, Michelle L Swiggers, Razib Obaid, Daniel Rolles, Artem Rudenko, John D Bozek, and Nora Berrah, “The LAMP Instrument at the Linac Coherent Light Source Free-Electron Laser”, Rev. of Sci. Instr., **89**(3), 035112 (2018). 'Editor's pick' section.
16. Kasra Amini et al., “ Photodissociation of aligned CH_3I and $C_6H_3F_2I$ molecules probed with time-resolved Coulomb explosion imaging”, Structural Dynamics, **5**, (2018) (in press)
17. N. Berrah, “Fullerene Dynamics with X-Ray Free-Electron Lasers” Book chapter in Fullerenes and Relative Materials, Edited by Natalia Kamanina, and Published by, IntechOpen. ISBN: 978-953-51-5591-1 (2018).
18. Li Fang, Edwin Kukk, Nora Berrah,” Book Chapter in 'Advances in Optics: Reviews' Book Series, Vol. 2, e-ISBN: 978-84-697-9438-8, (2018).

Imaging Structural Dynamics in Isolated Molecules with Ultrafast Electron Diffraction

PI: Martin Centurion
Department of Physics and Astronomy, University of Nebraska, Lincoln, NE 68588-0299
martin.centurion@unl.edu

Program Scope or Definition

This project aims to investigate photochemical reactions at the molecular level by observing how the molecular structure changes upon light absorption. The project relies on ultrafast electron diffraction to image photo-induced reactions in isolated molecules with atomic resolution. A sample of molecules in the gas phase is excited by a femtosecond laser pulse, and the structure is probed by a femtosecond electron pulse. The scattering pattern of the probe electrons contains information on the structure of the molecule, and under certain conditions an image of the molecule can be retrieved with atomic resolution.

Introduction

In photo-induced molecular reactions light can be converted into chemical and kinetic energy on femtosecond time scales. Observing the motion of atoms and the resulting transient structures during these processes is essential to understand them. Diffraction methods are an ideal tool because they are directly sensitive to the spatial distribution of charge, and are thus complementary to spectroscopic methods that probe the energy landscape. We have implemented ultrafast electron diffraction (UED) with femtosecond temporal resolution to observe structural dynamics in isolated molecules.

A gas-phase diffraction experiment comprises four major parts: i) An electron gun that delivers short pulses on a target, ii) a laser that triggers both the electron gun and the photochemical reaction, iii) a sample delivery system that creates a gas jet target in a vacuum environment, and iv) a detection system. Two different systems will be used in this project. The first is the MeV electron gun at the ASTA test facility at SLAC National Lab. This RF photoelectron gun produces femtosecond electron pulses in an energy range between 2 MeV and 5 MeV, with a repetition rate of 180 Hz. We have designed and constructed an experimental chamber for gas phase diffraction experiments, in collaboration with the group of Xijie Wang at SLAC. The main advantage of using MeV electrons is that they are relativistic, which minimizes the velocity mismatch between laser and electrons and also the pulse spreading due to Coulomb forces. The velocity mismatch has been a major limitation in the temporal resolution of UED experiments with sub-relativistic pulses. Experiments will also be performed in the PI's lab at UNL using a photoelectron gun that combines a DC accelerator with an RF compression cavity. Electrons are accelerated to an energy of 90 keV and then temporally compressed at the target position by a small RF cavity, at a repetition rate of 5 kHz. This setup includes an optical system to deliver laser pulses with a tilted intensity front on the sample. The tilted pulses will serve to compensate the velocity mismatch of laser and electrons through the sample to reach femtosecond resolution. The setup at SLAC is expected to reach better temporal resolution due to the use of relativistic electron pulses, while the setup at UNL is expected to reach a better spatial resolution due to the higher average beam current that will allow for capturing the scattering at larger angles.

Recent Progress

Over the last year we have continued the data analysis on the proton transfer reaction in nitrophenol, carried out a new UED experiment at SLAC on the cis-trans isomerization of Stilbene, tested and commissioned multiple sample delivery methods for the SLAC MeV UED user run (started 8/2020).

Analysis and interpretation of proton-transfer UED experimental data: We have continued the analysis and interpretation of the proton transfer reaction in 2-Nitrophenol (2NP). In this reaction, we aim to capture the structural dynamics that follow a proton transfer from the hydroxyl to the nitro group. Previous results have reported multiple channels, including dissociation of the nitro group, and rotations and vibrations of the nitro group [Ernst et al, J. Phys. Chem. A 119, 9225 (2015)], but these spectroscopic measurements did not have direct access to the structure. We are collaborating with the group of T. Martinez at Stanford who is carrying out simulations of the reaction. We are working to improve on the data analysis methods of previous experiments, such that we can extract the full time-dependent structures from the experimental data and identify the dominant structural rearrangements, and then make a comparison with theory in terms of what are the main motions and time scales. We are using a genetic algorithm to find the structural changes that generate the diffraction signal. So far this approach has proven successful at identifying the end products of the reaction and the main modes that are activated by the proton transfer.

Developing and commissioning sample delivery methods for the SLAC MeV-UED user facility. In collaboration with the SLAC MeV-UED group, we have tested multiple sample delivery methods in preparation for the first MeV-UED gas phase user run. In previous runs, it proved difficult to deliver samples with low vapor pressure. Problems included clogging of sample, unstable delivery and not sufficient density in the jet. We have systematically tested the operation of multiple different delivery methods, which can be applied to samples with different characteristics. Pulsed nozzles were found to successfully deliver sample using an in-vacuum sample container (short distance to the nozzle) with a high pressure of helium as a carrier gas flowing through the sample. Several methods of continuous sample delivery were also successfully tested: a continuous nozzle, a continuous slit nozzle (increases the path length) and a flow cell. The pulsed nozzle consumes less sample, while the slit nozzle and flow cell increase the interaction length and thus the scattering signal. The commissioning schedule had to be modified due to Covid19 restrictions, so we did not extensively test the sample delivery during UED experiments. Two successful tests were carried out, one was an experiment on photoexcited Cyclohexadiene (CHD) with the flow cell. The previous (published) UED study of CHD was carried out with a pulsed nozzle. The total scattering signal with the flow cell increased by more than an order of magnitude compared to the pulsed nozzle, and similar time-dependent changes were observed, confirming sample delivery and laser-electron spatial and temporal overlap. A second successful UED test was with cis-Stilbene, which had been unsuccessfully tried twice in the last few years. This time the sample delivery worked well using the pulsed valve with a high pressure of helium as a carrier gas.

Data analysis of the isomerization of cis-Stilbene: We have started the preliminary analysis of the UED experiment on cis-Stilbene. The data before time-zero matches well with the known static structure of cis-Stilbene, which shows successful sample delivery. We see a clear time-dependent signal at time-zero, with components both at low and high momentum transfer. The analysis of the late time delays (> 1ps) shows that the diffraction signal cannot be matched well to the structures of the known end products, trans-Stilbene and DHP. So far we have used only static structures for the simulation of end products so the mismatch could be due to the formation of end products with high vibrational amplitudes, or due to the formation of other products. The data analysis is still preliminary but confirms that we have captured structural changes. Figure 1 shows a preliminary analysis of the data, showing a time dependent signal appearing at both low and high momentum transfer, a clear indication of structural changes.

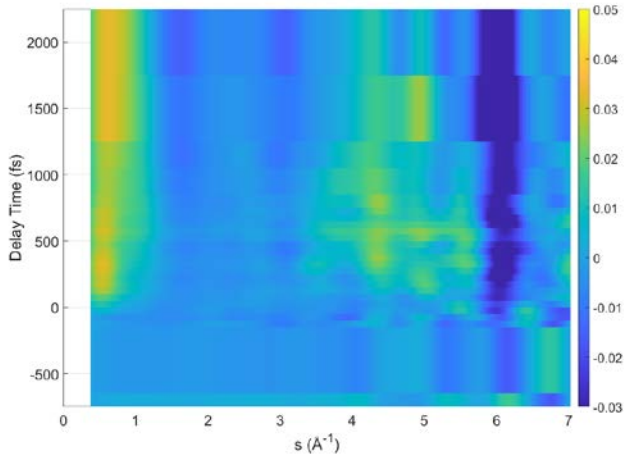

***Figure 1**. Preliminary diffraction signal analysis for the isomerization of cis-Stilbene. The plot shows the changes in the modified molecular scattering signal (sM), as a function of time (vertical) and momentum transfer (horizontal). The region (s < 0.3 Angstrom^{-1}) is not accessible experimentally so was left blank.*

MeV-UED from liquid samples (LUED): The analysis of the first MeV-UED experiment from a thin liquid jet was finished and submitted for publication (see publication #7 below). This experiment demonstrated the capability to record UED patterns from liquids, using a thin sub-micrometer liquid jet, with a resolution on the order of 200 fs.

Collaborations: We have collaborated on two other UED experiments. In the first, led by J. Yang of SLAC, investigated the dynamics of photoexcited Pyridine. This study demonstrated, for the first time, that UED can capture changes in both nuclear and electronic structures. Observing both nuclear and electronic dynamics simultaneously will be a great asset to capture non Born-Oppenheimer dynamics and to determine absolute time delays between electronic photoexcitation and nuclear motion. The second, led by the group of T. Weinacht at Stonybrook, used time-resolved photoelectron spectroscopy (TRPES) and UED to investigate the electronic and nuclear dynamics in the photodissociation of diiodomethane (CH2I2). This study combined two experimental method and theory to fully capture the dynamics. As a follow up to the Pyridine UED experiment, we have applied and were granted and XFEL beam time at LCLS to perform ultrafast X-ray diffraction (UXRD) (PI is Thomas Wolf). One of the goals of this beam time is to combine UED with UXRD data to disentangle the electronic and nuclear contributions to the diffraction signal.

Future plans

Over the next year, we expect to finalize the analysis and interpretation of the proton transfer UED data, and submit a manuscript for publication. We will continue with the data analysis of the UED data on the isomerization reaction of cis-Stilbene that we acquired earlier this year. Our setup at UNL was negatively impacted by the Covid19 shutdown but we expect to have it in operation this year. We are participating as collaborators in several ongoing and planned UED beam times this year. We will also apply for new gas phase UED and UXRD beam times at the next opportunity.

Peer-Reviewed Publications Resulting from this Project (2018-2020)

1. J. Yang, X. Zhu, T. J.A. Wolf, Z. Li, J. P. F. Nunes, R. Coffee, J. P. Cryan, M. Gühr, K. Hegazy, T. F. Heinz, K. Jobe, R. Li, X. Shen, T. Veccione, S. Weathersby, K. J. Wilkin, C. Yoneda, Q. Zheng, T. J. Martinez, M. Centurion, X. Wang "Imaging CF3I conical intersection and photodissociation dynamics with ultrafast electron diffraction" *Science* 361, 64 (2018).

2. A. T. Le, M. Centurion and C. D. Lin, "Elements of Structure Retrieval in Ultrafast Electron and Laser-induced Electron Diffraction from Aligned Polyatomic Molecules" In *Attosecond Molecular Dynamics*, Chapter 13 (RSC Publishing, London,2018).

3. T. J. A. Wolf, D. M. Sanchez, J. Yang, R. M. Parrish, J. P. F. Nunes, M. Centurion, R. Coffee, J. P. Cryan, M. Gühr, K. Hegazy, A. Kirrander, R. K. Li, J. Ruddock, X. Shen, T. Vecchione, S. P. Weathersby, P. M. Weber, K. Wilkin, H. Yong, Q. Zheng, X. J. Wang, M. P. Minitti & T. J. Martínez, "The photochemical ring-opening of 1,3-cyclohexadiene imaged by ultrafast electron diffraction" *Nature Chemistry* 11, 504 (2019).

4. K.J. Wilkin, R. M. Parrish, J. Yang, T. J. A. Wolf, J. P. F. Nunes, M. Guehr, R. Li, X. Shen, Q. Zheng, X. Wang, T. J. Martinez, M. Centurion, "Diffractive imaging of dissociation and ground-state dynamics in a complex molecule" *Phys. Rev. A* 100, 023402(2019).

5. S. Schippers, E. Sokell, F. Aumayr, H. Sadeghpour, K. Ueda, I. Bray, K. Bartschat, A. Murray, J. Tennyson, A. Dorn, M. Yamazaki, M. Takahashi, N. Mason, O. Novotný, A. Wolf, L. Sanche, M. Centurion, Y. Yamazaki, G. Laricchia, C. M Surko, J. Sullivan, G. Gribakin, D. Wolf Savin, Y. Ralchenko, R. Hoekstra,and G. O'Sullivan "Roadmap on photonic, electronic and atomic collision physics: II. Electron and antimatter interactions" *Journal of Physics B*: At. Mol. Opt. Phys. 52 171002 (2019).

6. X. Shen, J. P. F. Nunes, J. Yang, R. K. Jobe, R. K. Li, Ming-Fu Lin, B. Moore, M. Niebuhr, S. P. Weathersby, T. J. A. Wolf, C. Yoneda, M. Guehr, M. Centurion and X. J. Wang, "Femtosecond gas-phase mega-electron-volt ultrafast electron diffraction" *Structural Dynamics* 6, 054305 (2019).

7. 24. J. P. F. Nunes, K. Ledbetter, M. Lin, M. Kozina, D. P. DePonte, E. Biasin, M. Centurion, C. J. Crissman, M. Dunning, S. Guillet, K. Jobe, Y. Liu, M. Mo, X. Shen, R. Sublett, S. Weathersby, C. Yoneda, T. J. A. Wolf, J. Yang, A. A. Cordones, and X. J. Wang "Liquid-phase mega-electron-volt ultrafast electron diffraction" *Structural Dynamics* 7, 024301 (2020).

8. 25. Yusong Liu, Spencer L. Horton, Jie Yang, J. Pedro F. Nunes, Xiaozhe Shen, Thomas J. A. Wolf, Ruaridh Forbes, Chuan Cheng, Bryan Moore, Martin Centurion, Kareem Hegazy, Renkai Li, Ming-Fu Lin, Albert Stolow, Paul Hockett, Tamás Rozgonyi, Philipp Marquetand, Xijie Wang, and Thomas Weinacht, "Spectroscopic and Structural Probing of Excited-State Molecular Dynamics with Time-Resolved Photoelectron Spectroscopy and Ultrafast Electron Diffraction" *Phys. Rev. X* 10, 021016(2020).

9. 16. Jie Yang, Xiaolei Zhu, J. Pedro F. Nunes, Jimmy K. Yu, Robert M. Parrish, Thomas J. A. Wolf, Martin Centurion , Markus Gühr, Renkai Li, Yusong Liu , Bryan Moore, Mario Niebuhr , Suji Park, Xiaozhe Shen , Stephen Weathersby , Thomas Weinacht , Todd J. Martinez, Xijie Wang, "Simultaneous observation of nuclear and electronic dynamics by ultrafast electron diffraction" *Science* 368, 885–889 (2020) .

Capturing Ultrafast Electron Driven Chemical Reactions in Molecules

PI: Martin Centurion
Department of Physics and Astronomy, University of Nebraska, Lincoln, NE 68588-0299
martin.centurion@unl.edu

Co-PIs: Daniel S. Slaughter, Robert R. Lucchese and C. William McCurdy
Chemical Sciences Division, Lawrence Berkeley National Laboratory, Berkeley, CA 94720

Program Scope

The goals of this project, which started on September 15, 2018, are to develop experimental tools to investigate the dynamics of dissociative electron attachment (DEA) reactions in real time. In a DEA reaction, the attachment of a low energy electron to a molecule results in bond breaking and the fragmentation of the molecule. A new instrument has been designed and is under construction to perform time-resolved photoelectron and photo-fragment spectroscopy following electron transfer from an iodide anion to a molecule within a mass-selected molecular dimer. The experiments proposed here will establish the experimental tools to interrogate the dynamics of dissociative electron attachment on the fundamental timescales of the nuclear motion, by simultaneously probing the valence electronic structure and the fragmentation pathways.

Introduction

Low energy (few eV) electrons are readily generated in the interaction of radiation with matter, and these electrons can in turn interact with molecules and drive a large number of chemical processes in atmospheric, radiation and plasma chemistry. One of these fundamental processes is dissociative electron attachment, where a low energy electron attaches to a molecule, forming a transient anion that dissociates. The metastable transient anion system evolves from the electronic continuum, so dissociation competes with autodetachment. These reactions can take place on femtosecond time scales and exhibit strong coupling between electronic and nuclear motion. The breakdown of the Born-Oppenheimer approximation makes it highly challenging to accurately describe the dynamics with existing quantum chemistry methods. It is also very challenging to observe these reactions experimentally on the relevant timescale, due to the difficulty in delivering few-eV electron pulses on a sample to trigger the reaction with femtosecond resolution.

We are developing a new instrument to do momentum- and time-resolved measurements of dissociative electron attachment reactions by combining two experimental methodologies: time resolved photoelectron imaging spectroscopy and coincidence momentum imaging of the photoelectron and the mass-resolved reaction fragments. The experiments proposed here will establish the required tools to interrogate these dynamics on the fundamental timescales of the nuclear motion. Initial experiments will focus on anion fragment mass spectrometry and fragment momentum imaging, followed by time resolved photoelectron spectroscopic measurements of photodetached electrons. Near-future developments include momentum imaging experiments of both photoelectrons and neutral fragments in coincidence. The coincidence measurements will allow us to assign the measured valence electron binding energies to specific fragmentation channels. The experiments will be supported by theoretical calculations of the electron attachment and dissociation processes.

Recent Progress

In our design, we have separated the instrument in three major parts: The anion cluster source, the time of flight region and the detection chamber. We have successfully characterized the ion beam using cations and anions formed in electron collisions with carbon dioxide, installed and tested the time of flight (TOF) electrodes and channeltron detector, and designed and constructed a mass selector and a reflectron mass spectrometer. We have constructed the gas delivery system to deliver the gas mixtures needed to produce iodide-molecule clusters. In addition, significant simulation work has been carried out on the performance of the TOF mass selecting system and the reflectron mass spectrometer module to analyze charged fragments following the intra-dimer electron transfer by a laser pulse.

Anion source: The anion source has been designed and tested using carbon dioxide as a test gas. This chamber contains a pulsed gas nozzle to generate the desired clusters, an electron beam to generate anions through collisions, and a skimmer to select and transport the central part of the beam to the time of flight electrodes. A continuous electron gun is used to ionize the gas coming out of the nozzle. In order to produce the iodide-molecule clusters for our experiment, a gas jet with a mixture of three gases will be intersected by the electron beam. For first experiments, the gases will be Argon, CF_3I or CH_3I, and nitromethane (CH_3NO_2). The argon gas, upon impact, generates a large number of low energy electrons by ionization. The iodine-containing molecules break up upon electron impact and provide the iodide anions, which attach to the nitromethane as the iodide-nitromethane anion cluster. We have constructed a sample delivery system to produce the required gas mixtures, which is based on two bubblers where the different chemicals can be stored and have high pressure argon flow through. The sample delivery system has been installed and leak tested.

Time-of-flight (TOF): The anions generated in the source pass through a skimmer to enter into the TOF chamber. Steering and focusing electrodes have been installed to guide the anion beam into the TOF region. First experiments were done with CO_2 as a test sample. Cation and anion beams have been generated and transported to the TOF chamber. The beam current is measured and optimized using a Faraday cup that sits after the TOF electrodes, such that with the TOF electrodes grounded the beam passes through into the Faraday cup. With this measurement we have optimized the direction and focusing of the electron beam and the opening time of the gas nozzle time. The Faraday cup was also used to measure the travel time of the ion packets from the source to the TOF region, such that the time of the extraction field pulse applied to the TOF electrodes can be synchronized with the time of arrival of the ions. The TOF system comprises three electrodes, the third of which is kept grounded. The first two are switched on using a high voltage pulse at the time when the ions reach the center of the electrodes. The maximum voltage determines the final energy of the ions after acceleration, while the difference in voltage between the first two electrodes determines the position of the temporal focus of the packet. We have successfully tested the TOF using CO_2 gas. Figure 1 shows the trace from the first successful test of our TOF, using a beam of CO_2 cations produced by electron impact ionization, with the assignments for different fragments. The experimental results are in good agreement with simulations. The performance of the TOF was simulated using the SIMION software package. The simulations were used to optimize the TOF voltages such that the temporal focus overlaps with the detector, and to calculate the time or arrival of the different fragments.

Detection: The detection chamber will include three devices: a mass gate to select a single anion from the incoming anion beam, a reflectron mass spectrometer that will measure the fragments produced by the

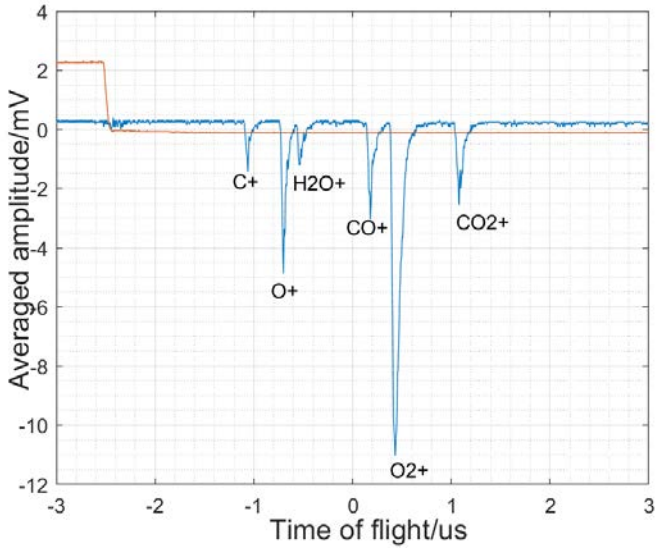

Figure 1. Time of flight trace of cation fragments produced by electron impact ionization of CO_2. The figure shows the voltage response decoupled from the channeltron detector, without amplification. The water peak is attributed to contamination of the sample line. We have used this to optimize the temporal focusing of the TOF. The TOF spectrum of the fragments was simulated using SIMION and found to be in good agreement with the measurement.

photoattachment-dissociation reactions and a VMI spectrometer to study photodetachment by one or two laser pulses. First experiments will be performed with a single laser pulse to measure charged fragments with the reflectron, and in the second phase the VMI will be installed for pump-probe time-resolved experiments. Simulations were carried out to inform the design of the mass selected anion beam (consisting of a time-of-flight spectrometer and a mass gate), reflectron and VMI spectrometer.

A mass selector will be used to select the desired anion clusters, and reject the rest of the beam. The mass selector consists of a set of electrodes which are normally held at a high (negative) voltage to reject the incoming ion beam. A voltage pulse applied on the mass selector electrodes will be timed to allow only a selected fragment to pass. The selected ions will be excited by a laser pulse, and the fragmentation will initially be studied using a simple and compact reflectron spectrometer to analyze the anion fragment. The performance of the system comprising the TOF and the reflectron has been simulated using SIMION, and shows that a mass resolution of approximately 2% of the mass of the fragment can be achieved. The reflectron uses six electrodes, with the voltages optimized using two parameters, a linear and a quadratic component to the voltage step between electrodes. This allows for a simple configuration of the device. The time resolution can be optimized for low or high masses simply by changing the maximum voltage of the device. The design of the reflectron, aided by simulations, has been completed, and the reflectron spectrometer has been constructed (see Figure 2). The reflectron is mounted at an angle of six degrees with respect to the incoming anion beam. The performance of the device is very sensitive to the angle of incidence of the anions, so it is mounted on a rotational feedthrough to allow for fine tunning of the angle. While the reflectron will capture the fragmentation products, a velocity map imaging (VMI) detector will capture the electrons produced in the competing processes of photodetachment. A first design for the VMI has been produced but needs to be optimized after the final parameters of the anion beam are measured.

Future plans

The immediate plans are to commission the mass gate and the reflectron spectrometer and the recently installed sample delivery system to select specific anion clusters by their mass. The nitromethane-iodide

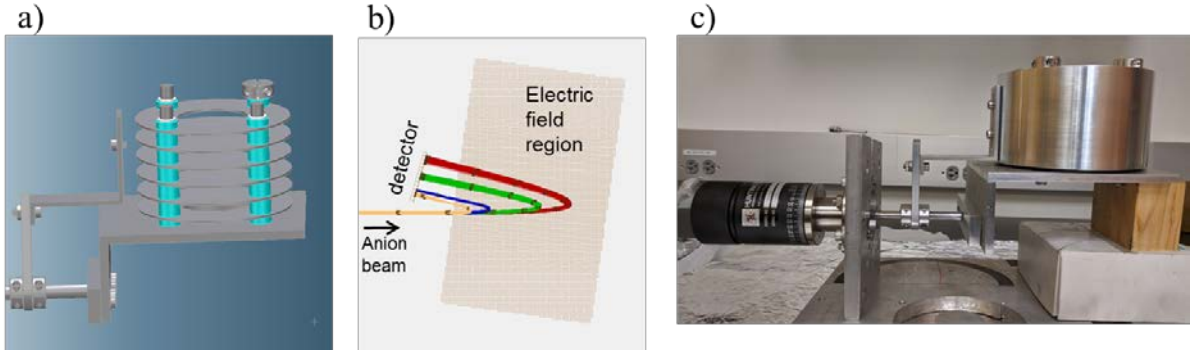

Figure 2. a) CAD design of the reflectron time of flight spectrometer containing six parallel electrodes. b) SIMION simulated trajectories of parent anion $I^-.CH_3NO_2$ and the fragments I^-, CNO^- and O^- through the electric fields. All fragments can be well resolved in the simulations c) The fabricated device, with a shield around the electrodes to prevent stray fields from interfering with the incoming anion beam.

anions will be produced using a mixture of argon, trifluoroiodomethane and nitromethane. We will first optimize the production of the desired clusters by adjusting the relative pressures of the gases and tuning the electron beam energy. We expect that many anion species will be produced, and we will use the mass gate to select one, such as the iodide-nitromethane dimer. We will then perform first photoattachment experiments using a femtosecond laser pulse to study intracluster electron transfer from iodide to nitromethane, by detecting the anion fragments using the reflectron spectrometer. We will also perform anion fragment momentum imaging experiments to study dissociative attachment of free electrons to nitromethane using the ion momentum microscope and a low-energy electron beam at LBNL. This will allow us to answer an important scientific question in this project: can photoattachment with an ultrashort laser pulse, and electron attachment with an external electron beam, proceed in similar reaction pathways? We will investigate how the laser-triggered fragmentation compares with the external electron beam as a function of the electron beam energy. This will mark a significant step in the development of an atomic photocathode, i.e. a localized source of photoelectrons that could be used to trigger electron-driven reactions with femtosecond resolution. Following these first experiments we will complete the construction of the VMI photoelectron spectrometer, such that both fragments and electrons can be measured in a single experiment. The next step will be to perform time-resolved experiments using two laser pulses, one to trigger the reaction and the second to photodetach the electron can capture the evolution of the dissociation process. The idea of capturing electron-driven dynamics in molecules with femtosecond resolution was identified as a science opportunity at the SLAC Workshop on “New science opportunities enabled by LCLS-II X-ray Lasers” in 2015.

Peer-Reviewed Publications Resulting from this Project (2018-2020)

None.

Probing nuclear and electronic dynamics in ultrafast ring-conversion molecular reactions

PD/PI: Martin Centurion[1]. PIs: Kenneth Lopata[2], Daniel Rolles[3], Artem Rudenko[3], Peter Weber[4]
[1]Department of Physics and Astronomy, University of Nebraska, Lincoln, NE 68588-0299, *martin.centurion@unl.edu*
[2]Department of Chemistry, Louisiana State University, Baton Rouge, LA 70803
[3]J.R. Macdonald Laboratory, Department of Physics, Kansas State University, Manhattan, KS, 66506
[4]Department of Chemistry, Brown University, Providence, R.I. 02912

Program Scope or Definition

This project, which started on August 15, 2019, is in collaboration with the groups of Daniel Rolles and Artem Rudenko at Kansas State University, Peter Weber at Brown University and Kenneth Lopata at Louisiana State University. A series of ultrafast photo-triggered ring-opening and ring-closing reactions are investigated, with the goal of developing general rules that can be applied to understand and predict the outcome of a large class of reactions. We will do this by focusing on a set of exemplary reactions and by applying multiple complimentary time-resolved pump-probe techniques and computational models to capture a complete picture of the dynamics. The work over the first two years focuses on the strained multi-ring reaction in the conversion of quadricyclane to norbornadiene and the possible formation of a four-membered ring in the conversion of cycloocta-1,3-diene to bicyclo [4.2.0]oct-7-ene. A unique aspect of this project is the combination of multiple state-of-the-art probing methods that provide complementary information along with theoretical models to interpret experiments and build a more complete picture of the dynamics.

Introduction

One of the research priorities for the Chemical Sciences, Geosciences, and Biosciences Division within the US DOE Basic Energy Sciences Program is to develop and implement novel tools to probe the dynamics of electrons and nuclei that underlie chemical bonding and reactivity, and to elucidate structural dynamics responsible for chemical transformations. After many successful proof-of-principle studies performed with a variety of ultrafast methods in recent years, the next important strategic step is a concerted effort to employ several of the new and complementary techniques on a specific class of photochemical reactions. Application of complementary methods, coupled with a coordinated computational model and data analysis, is expected to yield significant new insights into the reaction dynamics and pathways.

The interconversion between different ring structures is an important theme in organic synthesis. Ring conversion reactions change the number of atoms in organic ring structures, and are therefore essential in the creation of a large number of cyclic molecular motifs. They involve a range of chemical transformations including redistribution of charges, creation or release of ring strain, making or breaking of aromaticity or electron conjugation, and the conversion between simple and complicated multi-ring motives. Ring interconversion reactions are an important theme in organic synthesis, industrial chemistry, chemical biology and pharmacology. Photochemically induced electrocyclic reactions in particular are widely seen in nature in the

synthesis of natural products, and have tremendous commercial applications in the synthesis of pharmaceuticals. They featured prominently in the development of the Woodward-Hoffman rules that aim to rationalize pericyclic reactions, and play an important role in the photo-induced vision mechanism and the light-induced formation of previtamin D. To date, only a few select model systems have been studied using advanced time-resolved spectroscopic and scattering methods. Consequently, many aspects of the nuclear and electron dynamics of ring interconversion reactions remain unknown.

The experimental portfolio includes ultrafast electron and X-ray diffraction experiments that are directly sensitive to the nuclear and electronic structures of molecules. Ionization-based methods are also sensitive to the electronic and nuclear structures, and additionally to the energies of the orbitals, electronic states and vibrational states of the molecule. The ultrafast ionization-based experiments include ion mass spectrometry, Coulomb explosion imaging, photoelectron spectroscopy, and Rydberg fingerprint spectroscopy. All experiments are carried out in the PIs laboratories and at large-scale facilities such as the XFEL and MeV electron sources at SLAC National Lab and the XFEL at DESY in Hamburg.

Recent Progress

Over the first year of this project, we have carried out multiple experiments in our local university laboratories, applied for and obtained beam time for multiple UED and XFEL experiments, and performed numerical simulations to support the experiments. All of the experiments carried out so far have been highly collaborative with people from two or three different universities participating. The progress is described in the following split up by research topic. We are planning to use multiple different measurements for each reaction being investigated, and some of the experiments have already taken place, while others are planned for the near future. Most of the data analysis and interpretation is still preliminary.

I. Interconversion of quadricyclane (QD) to norbornadien (NB)

The interconversion of quadricyclane (QD) to norbornadiene (NB) (Figure 1) involves highly strained, and thus energetic, molecular structures and therefore finds applications in photochemical energy conversion and storage schemes. We have performed Rydberg spectroscopy experiment on the QD to NB reaction and on the reverse reaction of NB to QD at Brown University (BU), with the participation of a postdoctoral scholar from the University of Nebraska – Lincoln (UNL). We have also performed MeV-UED experiments at SLAC National Lab on the QD to NB reaction with the participation of group member from Kansas State University (KSU), BU and UNL. Our collaborator Adam Kirrander from Edinburgh University is currently carrying out quantum chemical calculations of the reaction dynamics and end products. As described in the Future Work section, we also have time-resolved valence photoelectron and ion spectroscopy experiments at the FERM FEL in Trieste (Nov/2020) and ultrafast hard x-ray diffraction at the LCLS XFEL (Dec/2020) on the

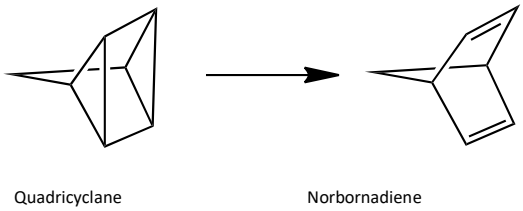

Figure 1: The interconversion of quadricyclane to norbornadiene.

same reaction. When taken together, the Rydberg and photoelectron spectroscopy experiments will provide detailed information on the electronic dynamics, while the UED and x-ray diffraction experiments will provide complementary information on the nuclear motion and possibly also the time scales for electronic dynamics.

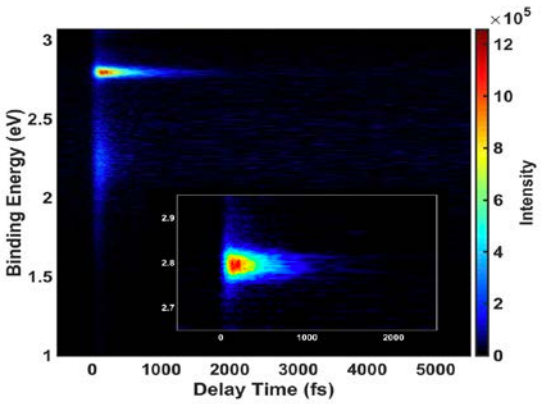

Figure 2. Time-resolved photoelectron spectra of NB upon excitation at 200 nm and probed with 403 nm photons. The inset shows the time dependence on an expanded time window.

I.1. QD and NB Rydberg spectroscopy.

The electronic excitation of QD creates a vacancy in a highly strained three-membered ring, which then enables the electron dynamics that leads to the formation of the NB with less-strained five- and six-membered rings. The reaction involves an ultrafast mechanism that unfolds on 100 fs time scales [Rudakov2012].

In prior spectroscopic studies, we investigated the time-resolved Rydberg electron binding energy spectrum of the ring transformation of QD to NB. The measurement revealed the dynamics and the time-evolving dispersion as the molecule crosses electronic surfaces. Excitation at 208 nm prepares QD in the 3p state, which quickly (τ_1 = 320 fs) decays to the lower 3s state. In that state, QD isomerizes to NB with a time constant of τ_2 = 136 fs, and the NB so generated reacts with τ_3 = 394 fs. The energies of the spectral peaks depend on time, revealing a structural evolution while the molecule reacts. A careful analysis also shows that the peak widens with time, suggesting that the wavepacket spreads as the molecule relaxes its structure.

In order to create a unified data set with the other measurements, we repeated the Rydberg experiments with 200 nm excitation. We also investigated the reverse reaction, the conversion of NB to form QD upon excitation. Figure 2 shows the first spectra so obtained, revealing a dynamic evolution out of the initially prepared 3s Rydberg state on a sub-picosecond time range. No signal is observed that can be attributed to QD. Therefore, unlike the reaction of the QD entity, the NB converts presumably to the ground electronic state of the NB/QD system, rather than converting to the higher-energy Rydberg state of the QD. The QD → NB reaction in the Rydberg state appears to be a one-way reaction on the present time scales.

I.2. QD MeV-UED experiments

The UED study of quadricyclane, carried out in Sept/2020, aims to capture structural rearrangements that occur during the conversion to NB and resolve the structure of the vibrationally hot NB photoproduct. The sample was optically pumped with 30 uJ of 200 nm light, and the ensuing dynamics were probed using 3.7 MeV electrons. Based on the amplitude of the scattering signal on the picosecond timescale, we estimate the excitation percentage to be approximately 3%.

The UED signal over the first picosecond is shown in Fig. 3a as percentage difference signal of change in intensity divided by intensity of the ground state signal ($\Delta I/I$). The data show features which span 8 $Å^{-1}$ and appear shortly after time-zero with an onset timescale of approximately

400 fs. This timescale is consistent with the estimate for the formation and subsequent internal

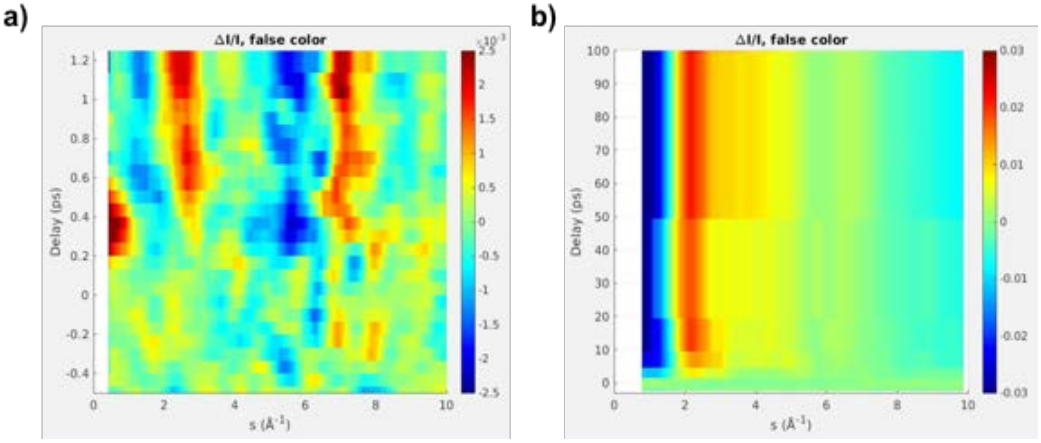

Figure 3: Time-dependent difference signal (ΔI/I) showing the a) ultrafast and b) picosecond dynamics of quadricyclane.

conversion of NB to its ground state. These data also reveal a fast transient feature at low momentum transfer ($s < 1$ Å^{-1}) with a 240 fs onset and a lifetime of approximately 400 fs, which agrees with the timescales observed in the Rydberg spectroscopy experiment. This feature is particularly interesting, as for a molecule the size of QD, this region of the momentum transfer spectrum does not typically encode structural information. In fact, under the independent atomic model, simulations of the expected photoproducts for QD:NB interconversion cannot reproduce such a feature. The nature of this feature can be confirmed by the ultrafast x-ray diffraction experiments planned for later this year, since the elastic contributions are similar for electrons and x-rays, but the inelastic scattering signal is different. We have also ongoing theoretical simulations to help us interpret the diffraction signals. The structural dynamics of the QD:NB system over longer timescales were also captured in our UED experiment. The difference diffraction signal at time delays above 5 ps shows strong features at momentum transfer values below 4 Å^{-1}. Further analysis is needed to interpret the diffraction signals in real space and to determine the nature of structural changes and transient structures.

II. Ring-Opening and ring-closing dynamics of cycloocta-1,3-diene (COD)

Ring conversion reactions play a crucial role in the conversion of light into mechanical and chemical energy. In organic chemistry, the study of this class of reactions has led to the development of the Woodward-Hoffman rules, which rationalize and predict the stereochemistry of pericyclic reaction. The study of model systems which undergo photo-triggered ring conversion reactions using time-resolved techniques aims to extend these general rules to the atomic scale. Cycloocta-1,3-diene (COD) is one of these model systems. The photoexcitation of COD is believed to lead to either: ring-opening and formation of octa-1,3-diene, or ring closing and formation of the four-membered ring bicyclo [4.2.0]oct-7-ene. Using MeV-UED and UXRD, we aim to capture the electronic and nuclear dynamics that take place during the ring conversion, retrieve the structure of photoproducts and determine the abundance of different reaction pathways. The UED experiments were carried out in Sept/2020, and the UXRD experiments at LCLS are scheduled for Dec/2020. We are also planning to carry out Rydberg

spectroscopy experiments and time-resolved coincident ion momentum spectroscopy experiments on COD next year.

In the MeV UED study of cycloocta-1,3-diene, the sample was optically pumped with 15 uJ of 200 nm, resulting in an excitation percentage of approximately 4%, based on the amplitude of the changes in the diffraction signal.

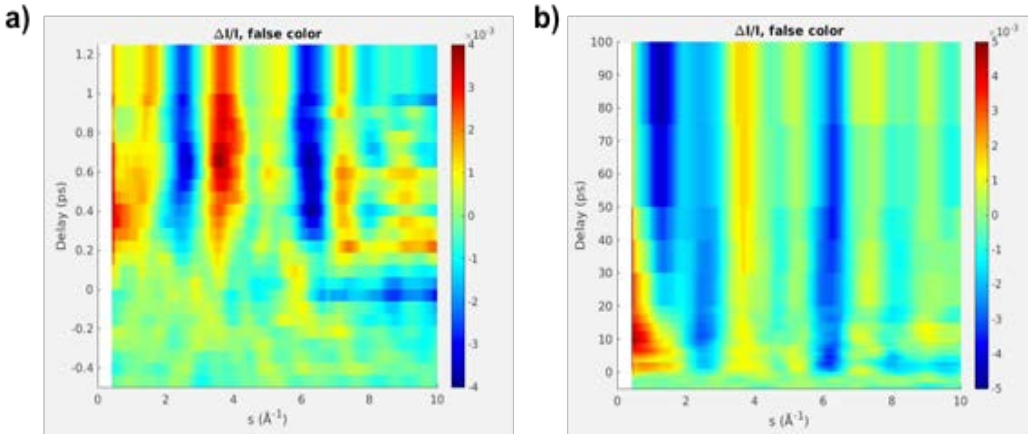

Figure 4: Time-dependent difference signal (ΔI/I) showing the a) ultrafast and b) picosecond dynamics of cycloocta-1,3-diene.

The UED signal over the 1 picosecond timescale (Fig. 4a) reveals several features with an onset timescale of approximately 400 fs, most notoriously the onset of a peak at 3.8 $Å^{-1}$ and the bleaches at 2.5 and 6.5 $Å^{-1}$. These features are qualitatively consistent with the simulated difference signal for many of the expected outcomes of a photoexcited COD, *i.e.* vibrationally hot COD, cis-trans isomerized COD and octa-1,3-diene. Further analysis and theoretical input will be needed to assign features to specific structural motifs and thus determine the dominant relaxation pathways for COD. These will take place over the next few months. At low momentum transfer ($s < 1$ $Å^{-1}$), our data show a transient onset with signal characteristic, *i.e.* position, intensity and timescale, consistent with the presence of electronic structure dynamics. Detailed simulations of the contribution of electronic structure to the total scattering signal are required to validate and assign the nature of this signal. The longer timescale dynamics of COD were also captured by our UED experiment (see Fig 4b). Over the 100 ps timescale, the data show a transient peak at small angles (low momentum transfer) which lasts ~40 ps, the delayed bleach of a feature at 1.5 $Å^{-1}$, and the sharpening of the peak at 3.5 $Å^{-1}$ towards later time delays. These indicate that the structural rearrangements are not completed on the femtosecond time scales.

III. Fragmentation of laser-ionized toluene

The focus of this sub-project is to determine the rate of formation of the tropylium cation by laser ionization of toluene, but we also aim to answer the more general question of what products are formed during the ionization. This task requires a multimodal approach from the beginning. Time-of-flight mass spectroscopy experiments can determine many of the fragments that are

formed and their relative yield, but cannot distinguish between fragments of the same mass but different geometry. For example, the detection of a mass corresponding to $C_7H_7^+$ could correspond either to tropylium or benzyl. Diffraction measurements, on the other hand, can distinguish between products with the same mass and different structures, but struggle to accurately determine the identity of fragments when there are many fragments and the relative yield is unknown. Therefore, we aim to combine the two measurements, using the TOF data to determine what are the most predominant fragments and thus reduce the parameter space, and then use the UED data to determine the structures. This project also presents a new challenge, in that diffraction from ions cannot be simulated using the independent atom model, which has been the basis of most data analysis in electron diffraction experiments. Thus, theory contribution to this project is essential in order to provide calculated fragment structures and ab-initio scattering calculations to compare with the data. The TOF mass spectroscopy experiments have been carried out at KSU, and the UED measurements at UNL, again in a highly collaborative effort with researcher from BU, KSU and UNL participating in the measurements. The ab-initio scattering simulations were carried out at BU. We are now in the process of merging the information from the two measurements together, and using the theoretical scattering patterns to fit the data and determine what fragments are present.

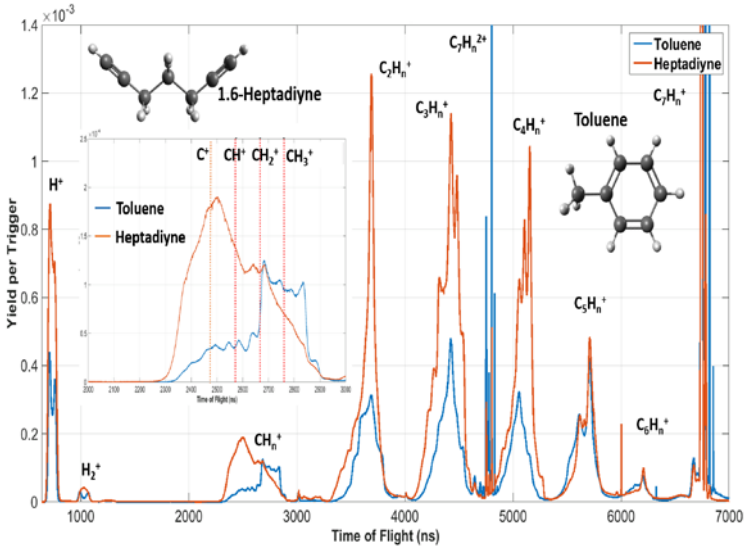

Figure 5: Ion time-of-flight spectra from ionization and fragmentation of toluene and 1,6-heptadiyne by 25 fs, 800 nm pulses at 130 TW / cm^2. The inset shows an enlarged view of the region containing CH_n^+ ions (n = 0-3)

III.1. Coulomb explosion imaging and ion spectrometry experiments

Within the first year of the project, experiments at KSU have focused on (1) exploring the Coulomb explosion imaging (CEI) as a probing scheme for ring-conversion reactions and (2) obtaining a detailed picture of strong-field induced ionization and fragmentation of several C_7H_8 isomers, in particular, toluene, in order to find optimal conditions for UED and XFEL experiments aimed at studying ring-conversion dynamics in ionic states, and to facilitate the interpretation of the results of these experiments. This work combined laser experiments at KSU, and the analysis of the data obtained in the first CEI experiments at the European XFEL.

The experiments at KSU were performed with 25 fs, 800 nm laser pulses and employed the momentum-resolving coincident ion spectrometry setup to characterize molecular ionization and fragmentation. The targets for these experiments included toluene, heptadiyne, quadricyclane (QD), norbornadiene (NB) and cyclohexadiene (CHD). For each of these targets, we have

extracted time-of-flight (TOF) mass spectra, branching ratios between fragments, and double-to-single ionization yields from the recorded ion data. For toluene, the measurements were carried out for a set of different laser intensities ranging from 30 to 220 TW/cm^2, and the corresponding data have been used to guide the modeling and fitting of the UNL UED data on laser-ionized toluene. Two exemplary TOF mass spectra for toluene and 1,6-heptadiyne, illustrating the fragmentation of ring and chain isomers, respectively, are shown in Figure 5. The mass spectra for both molecules are clearly different, which is particularly reflected in a very different emission patterns for CH_n^+ fragments (highlighted in the inset) and in a much higher fraction of bound doubly charge parent ions for heptadiyne.

In order to understand the mechanisms of the molecular breakup and to explore the potential of the CEI technique to visualize the differences in molecular geometry, we studied the characteristic breakup patterns of different molecular charged states, exploiting the coincident momentum imaging capabilities of the KSU setup. An interesting preliminary finding of this comparative experiment is that the kinetic energy release (KER) for several strong dicationic fragmentation channels is almost identical for all studied isomers, as illustrated in Figure 6, where the KER of the two-body breakup channel involving CH_3^+ ejection is shown for all 5 studied molecules. There, only the CHD (C_6H_8) manifest a clearly different two-peak KER distribution, whereas the spectra for all C_7H_8 isomers are very similar. This suggests that substantial structural rearrangement might occur in the dications before fragmentation, and indicates that higher charge states and many-body breakup are needed to reveal the differences in nuclear geometry.

Correspondingly, we have explored the possibility of retrieving information about the geometric structure of the toluene and heptadiyne molecules using the three-body breakup of triply-charged final state. Figure 7 shows preliminary results of this experiment in the form of a fragment ion

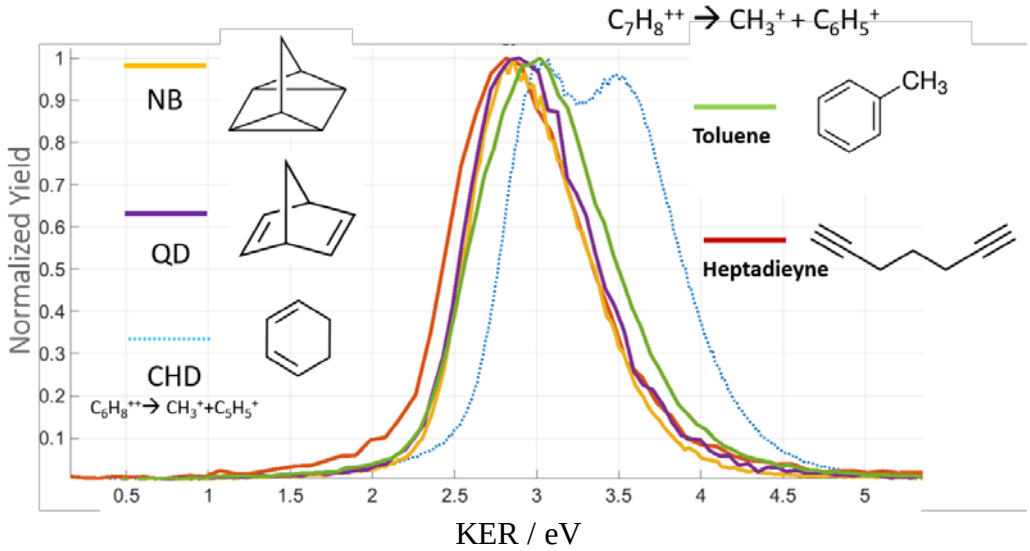

Figure 6: Fragment ion kinetic energy release (KER) for the $CH_3^+ + C_6H_5^+$ coincidence channel following strong-field induced ionization of four C_7H_8 isomers: norbornadiene (NB), quadricyclane (QC), toluene, and heptadiene with ~25-fs, 800-nm pulses at a peak intensity of ~500 TW/cm^2. The KER for the $CH_3^+ + C_5H_5^+$ channel for cyclohexadiene (CHD) is shown for comparison.

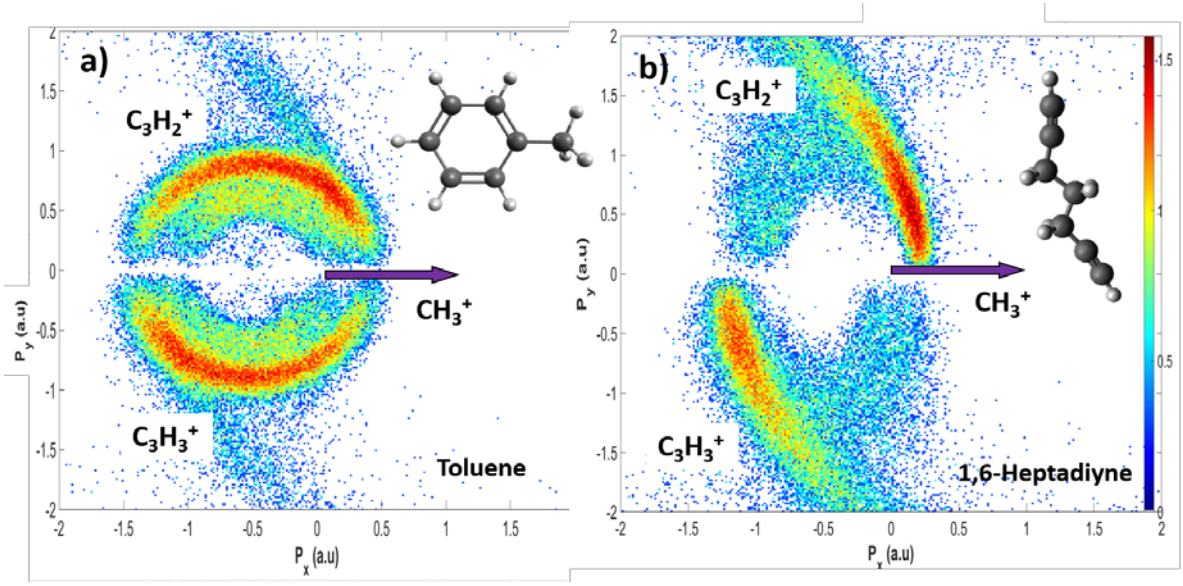

Figure 7: Fragment ion momentum correlation plot ('Newton plot') for the $CH_3^+ + C_3H_2^+ + C_3H_3^+$ coincidence channel following strong-field induced ionization of (a) toluene and (b) heptadiene with ~25-fs, 800-nm pulses at a peak intensity of ~500 TW/cm^2.

momentum correlation plots ('Newton plots') for the $CH_3^+ + C_3H_2^+ + C_3H_3^+$ coincident channel for (a) toluene and (b) heptadiyne, with the CH_3^+ momentum vector pointing to the right. In contrast to Figure 6, the molecular breakup for a ring and a chain isomer looks very different for this tricationic three-body fragmentation channel. While the pronounced circular structure in the Newton plot for toluene in (a) is a signature of a predominantly sequential breakup of the trication following the CH_3^+ ejection [Rajput18], the breakup is mainly concerted for heptadiyne, with both heavy fragments preferentially emitted back to back. More detailed data analysis of these data is still in progress and is expected to provide a set of reference data for the planned European XFEL experiment on toluene and heptadiyne. For the same purpose, the KSU team has also performed momentum-resolved electron-ion-ion coincidence experiments on toluene and other ring molecules after inner-shell ionization with synchrotron radiation at the Advanced Light Source. The results will guide the upcoming XFEL experiment and well as future UED and XFEL proposals and planned time-resolved coincidence experiments with the new TOPAS at KSU.

III.2 UED experiments on ionized toluene

We have performed UED measurements on strong-field ionized toluene molecules at UNL. These are, to our knowledge, the first UED experiments on ions. These experiments present unique challenges in that there can be a distortion of the electron beam due to interaction with macroscopic electromagnetic fields due to plasma formation, and that the diffraction signal from ions cannot be calculated using the independent atom model. We have observed that the electron beam is distorted, but the distortion is localized to a fairly small region around the center of the

diffraction pattern, and that the distortion is very anisotropic. We were able to remove this effect by a combination of blocking the region where the distortion is strong and by removing anisotropic components from the diffraction signal. The experimental UED patterns were compared by ab-initio scattering calculations, since calculation using the independent atom model gave very poor results. The molecules were ionized by a 50 femtosecond laser pulse with a peak intensity of 110 TW/cm^2 and diffraction patterns were acquired at relative time delays of -5ps, 5 ps, 10 ps and 15 ps after the ionization. For each time step, the diffraction signal was accumulated for 100 minutes. Recording the diffraction patterns at this time steps allows us determine if the fragmentation products are still evolving on the picosecond scale.

Figure 8 shows the diffraction difference signal, rescaled to the difference modified molecular scattering. A difference signal is generated by subtracting a reference diffraction pattern recorded at -5ps (electrons arriving before the laser) to focus on the changes to the pattern. A simulated signal is then fit to the diffraction data (red line in Figure 7). The simulated signal is generated by first selecting a subset of all possible fragments, based on the most prevalent fragments observed in the ion mass spectrometry experiments. The fragments are: $C_4H_3^+$-C_3H_2, $C_6H_5^+$-CH_3, $C_5H_5^+$-C_2H_3, toluene+, benzylium cation -H, CHT+ and the tropylium cation-H. The fragments are assumed to come in pairs. All pairs were included in the simulations. The tropylium and CHT+ fragments produce very similar diffraction signals, so they were merged together in the calculations. Second, the diffraction signal for each of this fragments is calculated using the ab-initio scattering code. The calculated signals are then fit to the data, using the relative yield of each fragment pair as a free parameter in the fit. The results of the UED fits will be compared with the measured yields in the mass spectrometry measurements. A preliminary comparison shows reasonable agreement,however, some important things that still need to be worked out to make a more quantitative comparison. The results of the UED measurements show that the fragments are still changing on the picosecond time scales, most likely due to formation of initially very hot fragments. The ion mass spectrometry measurements, however, are measured after a very long time, most likely after the structural changes are finished. Based on the comparison, we expect that we should be able to determine which of the fragments are still changing on picosecond scales. We also need to analyze in more details the relative yield from single and double ionization. This will be extracted from the ionization data set, and included in the UED fits to produce more accurate results. The results show that approximately 12% of the

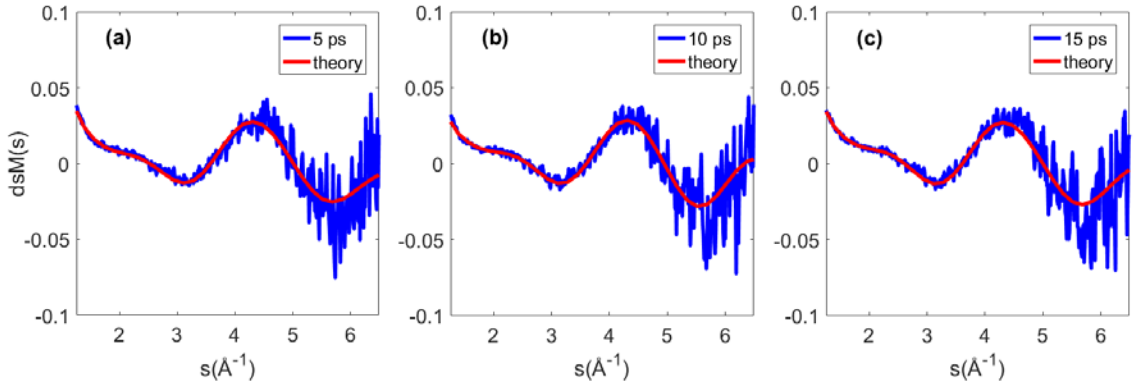

Figure 8. Experimental ΔsM signal from UED measurements (blue lines) and calculated fit (red lines) for time delays for a) 5 ps, b) 10 ps, c) 15 ps.

molecules in the diffraction volume are ionized, and that the most prevalent fragment is toluene+ accounting for about 70% of the total ions.

III.3. Calculation of structures and electron scattering signals

When the high-energy electrons are scattered from a molecular system, they interact with both the electrons and nuclei of the molecule. The electron scattering intensity can be therefore described as a function of the electron density and the nuclear distribution in the molecule. To correctly account for those interactions, within the First-Born approximation the elastic electron scattering signal consists of three terms,

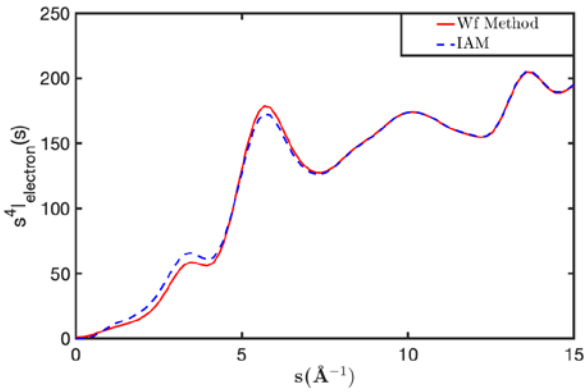

Figure 9: Calculated elastic electron scattering patterns for toluene(+) cations using a wavefunction description of the electron density (red solid line) and the Independent Atom model approach (blue dashed line). The differences between both methods mainly appear at low values of *s*, as a consequence of the inaccurate description by IAM when treating charged systems.

$$s^4 I_{electron}(s)/I_{Ruth}(s) = I_{ee}(s)[\rho(\boldsymbol{r})] + I_{ne}(s)[\rho(\boldsymbol{r}), \boldsymbol{R}] + I_{nn}(s)[\boldsymbol{R}] \qquad (1)$$

where s is the momentum transfer vector, I_{Ruth} is the Rutherford cross-section that describes the scattering of an electron by a free electron, $\rho(\boldsymbol{r})$ is the electron density, $\boldsymbol{R}$ are the nuclear coordinates, and I_{ee}, I_{ne} and I_{nn} are the *electron-electron*, *nuclear-electron* and *nuclear-nuclear* interaction terms in the electron scattering process, respectively. Each of the terms in Equation (1) is rotationally averaged to correspond to an isotropic electron scattering intensity from a randomly oriented molecular ensemble.

To simulate the electron scattering intensity using the three terms outlined above, one may use approximations such as Independent Atom Model (IAM), treating the electron density $\rho(\boldsymbol{r})$ as a sum of spherical atomic densities centered at the atom positions $\boldsymbol{R}$. However, this approximation neglects the charge distribution over the molecule, i.e. all chemical bonding, and it produces inaccuracies when charged species are considered. To overcome this problem, the electron scattering intensities have been calculated using accurate wavefunctions for each molecular species present in the experimental sample.

When considering the toluene ionization and subsequent photofragmentation, all 20 possible molecular fragments should be considered, both in their cationic and neutral forms. Each molecular fragment geometry has been optimized in its ground electronic state by using a multiconfigurational approach. The molecular wavefunctions and atomic positions have been used, following Equation (1), to obtain the total electron scattering signal. The first two terms, $I_{ee}(s)[\rho(\boldsymbol{r})]$ and $I_{ne}(s)[\rho(\boldsymbol{r}), \boldsymbol{R}]$, have been calculated using the analytic approach outlined in before[Wang1994, Zotev2020], while $I_{nn}(s)[\boldsymbol{R}]$ has been treated as a coherent sum of atomic charges centered at atomic positions $\boldsymbol{R}$.

The calculated electron scattering intensities describe the molecular electron distribution, bonding and electronic states adequately. This representation of the scattering process thus

enhances the accuracy beyond that achieved by the IAM (Figure 9) and it constitutes a powerful and versatile tool to analyze the experimental results described in this report. The natural directions to improve the existing method would include a more accurate description of the scattering process going beyond the First-Born approximation and the inclusion of vibrational corrections to the wavefunction. These supplementary considerations will be developed going forward and they will be part of our future research outcomes.

IV. X-ray scattering for probing electron and nuclear dynamics

In conjunction with planned future X-ray ionization/X-ray scattering experiments, we have developed a theoretical framework for simulating the dynamics and resulting scattering signals in molecules following inner-shell ionization. Since X-rays scatter exclusively from electrons, these measurements selectively probe the density distribution changes during a reaction. This includes both modulations in the scattering due to nuclear rearrangement as well as changes to the inelastic scattering resulting from charge density dynamics. Thus, in addition to resolving the ring-opening dynamics, X-ray scattering can in principle also resolve the attosecond electronic density reorganization immediate before nuclear rearrangement. Elucidating this process is critical, as it is predicted to affect the ring-opening and fragmentation pathways, for example, by dictating which bonds break during the reaction. Due to the complexity of the scattering signals, simulations are necessary for interpretation of the resulting scattering patterns.

To address this, we have performed first-principles simulations to compute the scattering for a range of geometries. Here, we use density functional theory (DFT) for electronic charge distribution followed by a Fourier transform of the electronic density to compute scattering. Our preliminary work show that the scattering is modulated both changes in the nuclear geometry as well as by the creation of a core-hole itself (even without nuclear motion). As with X-ray absorption, these effects are predicted to be element specific, which makes this technique ideal for rings containing heteroatoms. We have also begun to quantify the sensitivity of X-ray scattering to charge density redistribution for the case of a frozen geometry. This serves as a first step towards simulating ring-opening processes, and will support future proof-of-principle attosecond experiments. We have developed a scheme for simulating these quantities using time-dependent density functional theory (TDDFT) with atom-centered basis sets. It has been shown [Hermann2020] that inelastic X-ray scattering is primarily sensitive to the rate of change of the density, $\partial_t \rho(\boldsymbol{r}, t)$, rather than the instantaneous density itself ($\rho(\boldsymbol{r}, t)$). Drawing on a probability continuity argument ($\partial_t \rho(\boldsymbol{r}, t) = -\nabla \cdot j(\boldsymbol{r}, t)$), attosecond X-ray scattering experiments can thus be viewed as probes of diverging electron current rather than density or holes. To compute these currents in ring-molecules, we propagate the 1-particle density matrix following sudden core-hole ionization, with the field-free current density ($j(\boldsymbol{r}, t)$) then computed via the derivatives of the atom-centered basis functions:

$$j(\boldsymbol{r}, t) = -i \sum_{\mu,\nu}^{N} \left[P_{\nu\mu}(t) \phi_\mu \nabla \phi_\nu - P_{\mu\nu}(t) \phi_\nu \nabla \phi_\mu \right]$$

where N is the number of basis functions, $P(t)$ is the density matrix, and $\phi(\boldsymbol{r})$ are the atomic orbitals. We have implemented this in the parallelized *NWChem* software package.

Our preliminary results show that inner-shell ionization of a ring-shaped molecule results in complicated density redistribution that is likely detectable with X-ray scattering. Fig. 10, for example, shows a snapshot of the resulting currents in the oxazole molecule (C_3H_3NO) 0.3 fs following creation of an oxygen core-hole. Although somewhat distinct from the other molecular targets in this project, this system is an ideal starting point due to the presence of two heteroatoms (nitrogen, oxygen), as well as three chemically unique carbon atoms. In this case, there are significant convergent/divergent fluxes near the core-hole, as well as concerted ring-current throughout the molecule. Interestingly, these curled ring currents, unlike linear density oscillations, are significantly divergent and thus expected to yield a significant scattering signal modulation. We have a manuscript in preparation detailing these simulation and scattering computations, as well as results relating geometry, core-hole, and density current effects on X-ray scattering signals.

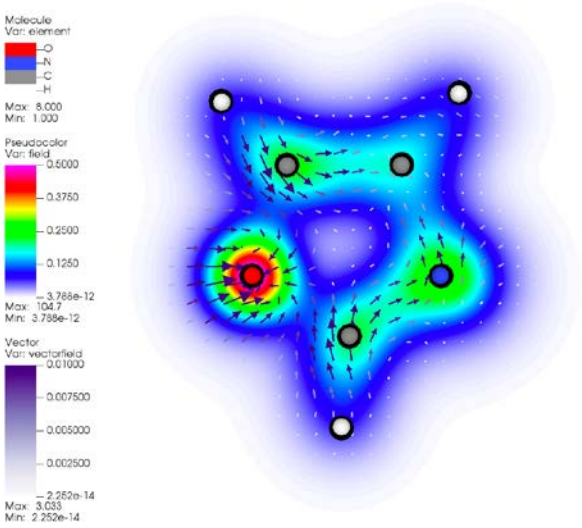

Figure 10: A snapshot of the electron density (colorscale) and electron current density (arrows) 1 Å above the plane of the oxazole molecule 0.3 fs after inner-shell ionization from the oxygen 1s orbital. The highly convergent currents around the core-hole, and curved ring currents throughout the molecule are predicted to be visible to X-ray scattering. This enables measurement of the initial stages of a ring-opening reaction at the attosecond time scale.

Future plans

Over the next year, a large effort will be dedicated to continuing the data analysis and interpretation of the experiments described above. In addition, new experiments are planned both in local labs and at large-scale facilities. By the end of this year or beginning of next year, we should have four different experimental methods applied to the QD reaction. We will focus on the data analysis of this experiments and combining the results at the data interpretation stage to build a complete picture of the nuclear and electronic dynamics based on the different probing mechanisms. This will only be possible with the different methods applied to the same molecule. We will also carry out Rydberg spectroscopy measurements and time-resolved coincident ion momentum imaging experiments on COD to complement the UED experiments that already took place and the XFEL experiment that is scheduled for the end of this year.

Over the last few months, the KSU team has investigated a significant effort into retrofitting and preparing the lab space and purchasing optics and other equipment for the new TOPAS that will be driven by half of the output of a new 30-fs, 3-kHz, 5-mJ Ti:Sa laser, both of which are scheduled to be delivered and installed in early October. Using the tunable deep-UV and UV pulses from the TOPAS as a pump and the other half of the 800-nm pulses from the Ti:Sa as a probe, we plan to perform time- and momentum-resolved ion coincidence experiments of various ring rearrangement reactions, e.g. in QD, NB, COD, in order to complement the experiments on the same targets performed using different ultrafast techniques within this project. The UNL team is also preparing to install a new TOPAS system that will allow us to perform UED measurements with a continuously variable excitation wavelength. This will introduce an important new capability which will be enabled by the tunable wavelength and high repetition rate UED instrument: determining how the dynamics and reaction products depend on the excitation wavelength. The TOPAS will be pumped using a fraction of the pulse energy of an existing 50 fs, 5 kHz, 2 mJ laser system. In conjunction with these experiments, the LSU team will perform strong-field ionization simulations to assist in predicting fragmentation yields as a function of laser intensity. Additionally, our scattering methodologies will be extended to help simulate UED signals, by using DFT to compute the densities of the systems along predicted reaction pathways. Finally, we expect to complete the ultrafast X-ray scattering simulations, which will form the basis for designing future attosecond X-ray scattering experiments—both for predicting signal modulations, and for suggesting ring systems to focus on. Building on this, we will also being work on simulating X-ray scattering probed-dynamics in the molecules targeted in this project (e.g., QD, NB, COD).

Scheduled experiments at Large scale facilities:

1. *FERMI beamtime on QD (Nov 12-14, 2020):*

In order to investigate the electronic relaxation pathways and geometric rearrangements in the very early stages after the UV-excitation of quadricyclane, which is beyond the temporal resolution of the MeV-UED experiment, we will use time-resolved valence photoelectron and ion spectroscopy at the FERM FEL in Trieste. The experiment is scheduled to be conducted at the LDM beamline on Nov 12-14, 2020.

The electronic excitation of QD at 200 nm creates a vacancy in the highly strained three-membered ring, which then enables the electron dynamics that lead to the formation of NB with less-strained five- and six-membered rings (see Figure 11), along with the formation of other reaction products produced through competing channels. According to prior work done by one of the PIs of this grant (Weber), the reaction involves an ultrafast mechanism that unfolds on a time scale of a few hundred femtoseconds [*Rudakov2012*]. While some information about the ultrafast dynamics

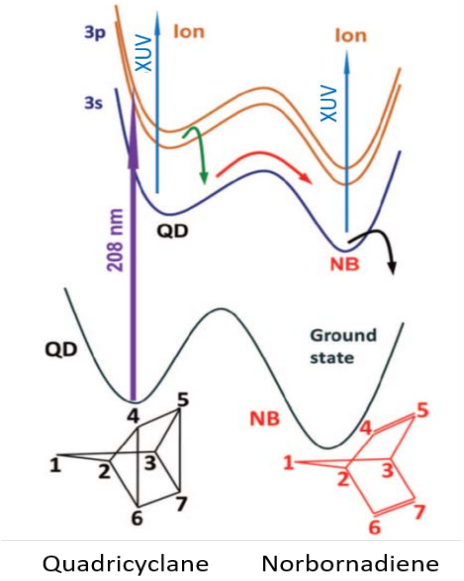

Figure 11: Interconversion of quadricyclane to norbornadiene. The reaction is triggered by a UV pulse and probed by an XUV pulse. Figure adapted from [*Rudakov2012*].

during this reactions is known from time-resolved photoelectron spectroscopy and mass spectrometry [*Rudakov2012, Fuß2002*], the former experiment, due to its limited photon energy, was only able to follow the dynamics in the most highly excited product states. Using the FERMI FEL as a probe, such time-resolved photoelectron spectroscopy measurements can now be performed at higher photon energies, making it possible to probe the entire electronic de-excitation process all the way back to the electronic ground state and, in particular, to probe competing reaction channels as well as the subsequent further decay of the photoproducts. The applicability of FEL-based TRPES has been demonstrated, e.g., in a recent experiment performed by the Rolles group at the FERMI FEL in Trieste investigating the UV-induced ring-opening reaction in thiophenone [*Pathak2020*].

2. LCLS LU79: Molecular Nuclear and Electron Dynamics on Complex Energy Landscape

These experiments aim to observe the same reactions in QD and COD that were investigated with UED, but with X-ray scattering instead of electron scattering. The combined application of both electron and x-ray scattering is expected to yield insights that either method alone could not achieve. Status: LU79 was selected for beam time at LCLS. It is still scheduled for December 2020, but will likely be postponed because the hard X-ray energies will not be available at LCLS in time.

3. European XFEL: Coulomb explosion imaging of ultrafast ring-conversion reactions

The KSU team participated in CEI experiments on iodine-containing ring molecules at the European XFEL. In these experiments, charge states much higher than in the KSU laser measurements described above could be reached. Correspondingly, the Newton plots similar to those shown in Figure 7 directly reveal the ring structure of the molecules, including the number of the hydrogen atoms and their positions in the ring [Boll2020]. These breakthrough results pave the way for employing CEI as a probe for time-resolved imaging of ring-conversion reactions resolving not only the motion of heavier atoms but also hydrogens. However, one of the key steps for implementing this approach is its demonstration for systems without heavy atom markers like iodine. In order to test this for the comparative example of toluene and 1,6-hemptadiyne discussed above and to study ring rearrangement in strong-field ionized toluene, we submitted the beamtime proposal entitled *"Coulomb explosion imaging of ultrafast ring-conversion reactions"* for the European XFEL. The proposal was approved and was initially scheduled for May 2020. Because of the ongoing pandemic, the experiment was postponed and is currently expected to be rescheduled for February 2021.

Peer-Reviewed Publications Resulting from this Project (Project start date: 08/2019)

"Ultrafast X-ray and Electron Scattering of Free Molecules: a Comparative Evaluation" Lingyu Ma, Haiwang Yong, Joseph D. Geiser, Andrés Moreno Carrascosa, Nathan Goff, and Peter M. Weber, Structural Dynamics, **7**, 034102 (2020); PMCID: PMC7316516; https://doi.org/10.1063/4.0000010.

References

[Boll2020] R. Boll, J. Schäfer, B. Richard, K. Fehre, G.R Kastirke, M. Abdullah, N. Anders, T.M. Baumann, A. Czasch, S. Eckart, B.Erk, A.De Fanis, L. Foucar, S. Grundmann, P. Grychtol,

A. Hartung, M. Hofmann, M. Ilchen, L. Inhester, C. Janke, Z. Jurek, M. Kircher, K. Kubicek, M,Kunitski, X. Li, T. Mazza, S. Meister, N. Melzer, J. Montano, V. Music, G. Nalin, Y. Ovcharenko, C. Passow, A.Pier, N. Rennhack, J. Rist, D.E. Rivas, D. Rolles, I. Schlichting, L.Ph.H. Schmidt, P. Schmidt, M.S. Schöffler, J. Siebert, N. Strenger, D. Trabert, F. Trinter, I. Vela-Perez, R. Wagner, P.Walter, M. Weller, P. Ziolkowski, R. Dörner, S.-K. Son, A. Rudenko, M. Meyer, R. Santra, and T.Jahnke, "X-ray induced Coulomb explosion images complex single molecules", in preparation.

[Fuß2002] Fuß, W, Puspa, K. K., Schmid, W. E. and Trushin, S. A., 'Ultrafast [2+2]-cycloaddition in norbornadiene', Photochem. Photobiol. Sci., 1, 60-66 (2002).

[Hermann2020] G. Hermann, V. Pohl, G. Dixit, J. C. Tremblay, 'Probing Electronic Fluxes via Time-Resolved X-Ray Scattering', Phys. Rev. Lett. 124, 013002 (2020)

[Pathak2020] S. Pathak, L.M. Ibele, …, D. Rolles, 'Tracking the ultraviolet-induced photochemistry of thiophenone during and after ultrafast ring opening', Nat. Chem. 12, 795-800 (2020).

[Rajput2018] J. Rajput, T. Severt, B. Berry, B. Jochim, P. Feizollah, B. Kaderiya, M. Zohrabi, U. Ablikim, F. Ziaee, Kanaka Raju P., D. Rolles, A. Rudenko, K.D. Carnes, B.D. Esry, and I. Ben-Itzhak, Native frames: Disentangling sequential from concerted three-body fragmentation, Phys. Rev. Lett. 120, 103001 (2018).

[Rudakov2012] F. Rudakov and P. M. Weber, 'Ultrafast structural and isomerization dynamics in the Rydberg-exited Quadricyclane: Norbornadiene system', Journal of Chemical Physics 136, 134303 (2012).

[Rudakov2012] F.. Rudakov and P. M. Weber, 'Ultrafast structural and isomerization dynamics in the Rydberg-exited Quadricyclane: Norbornadiene system', Journal of Chemical Physics 136, 134303 (2012).

[Wang1994] Jiahu Wang and Vedene H. Smith, Evaluation of cross sections for {X}-ray and high-energy electron scattering from molecular systems, Int. J. Quant. Chem. 1994, 52, 1145--1151

[Zotev2020] N. Zotev, A. M. Carrascosa, M. Simmermacher and A. Kirrander, Excited Electronic States in Total Isotropic Scattering from Molecules, Journal of Chemical Theory and Computation, 2020,16,2594–2605.

Page is intentionally blank.

Early Career: Probing Attosecond Bound Electron Dynamics Driven by Strong-Field Light Transients

Michael Chini
Department of Physics and CREOL, the College of Optics & Photonics
University of Central Florida, Orlando, FL 32816
E-mail: Michael.Chini@ucf.edu

Program Scope

The ability to measure and control ultrafast dynamics in electronically excited states of molecular systems has opened new frontiers in the study of internal energy conversion, charge transfer, and coupling of electronic and nuclear degrees of freedom. Recently, such control has been extended to the attosecond (1 attosecond = 10^{-18} seconds) regime, owing to the development of carrier-envelope phase-stabilized few-cycle lasers and isolated attosecond extreme ultraviolet (XUV) pulses. This project aims to use innovative laser techniques to reconstruct the time-dependent quantum mechanical wave packets initiated by strong-field excitation in bound electronic states of gas-phase atoms and molecules, and to control their dynamic evolution on attosecond to few-femtosecond (1 femtosecond = 10^{-15} seconds) timescales.

Recent Progress

Measurement and control of electronic motion requires time-resolved spectroscopic techniques with attosecond precision. In this project, coherent wave packet dynamics will be triggered using strong-field near-infrared light transients, with durations close to (or potentially below) a single optical cycle. The dynamics will be followed using optical spectroscopies based on the interference of the coherence emission with an isolated attosecond pulse produced via high-order harmonic generation.

As a first step towards our goal, we have demonstrated nonlinear compression[1] of a Yb:KGW amplifier (400 μJ pulse energy, 280 fs pulse duration, 50 kHz repetition rate) to a duration of 1.6 optical cycles, through the use of a hollow-core fiber filled with N_2O gas and a chirped mirrors-based compressor (Fig. 1). While Yb-based laser technology offers significant advantages over other femtosecond laser platforms in terms of high average power, excellent power and pointing stability, and low thermal load, the long pulse durations (typically ~300 fs) have prevented their widespread application to attosecond science. However, we have found that "delayed" nonlinearities, such as those associated with rotational alignment in molecular gases[2], can serve to dramatically enhance spectral broadening when driven by these relatively long pulses, enabling extreme compression of the pulses from ytterbium lasers. In the last year, we generated coherent supercontinuum spectra exceeding two optical octaves using a N_2O-filled hollow-core fiber[3]. The spectral phase of the supercontinuum was found to be well-behaved, and pulses of 5.8 fs (1.6 optical cycles at the central wavelength of 1074 nm) were compressed using chirped mirrors (Fig. 2a, 2b). The full bandwidth of the supercontinuum supports field transients with below one cycle duration.

Additionally, we have demonstrated the effectiveness of the 1.6-cycle source for attosecond pulse generation, through the observation of an XUV supercontinuum in the high-order

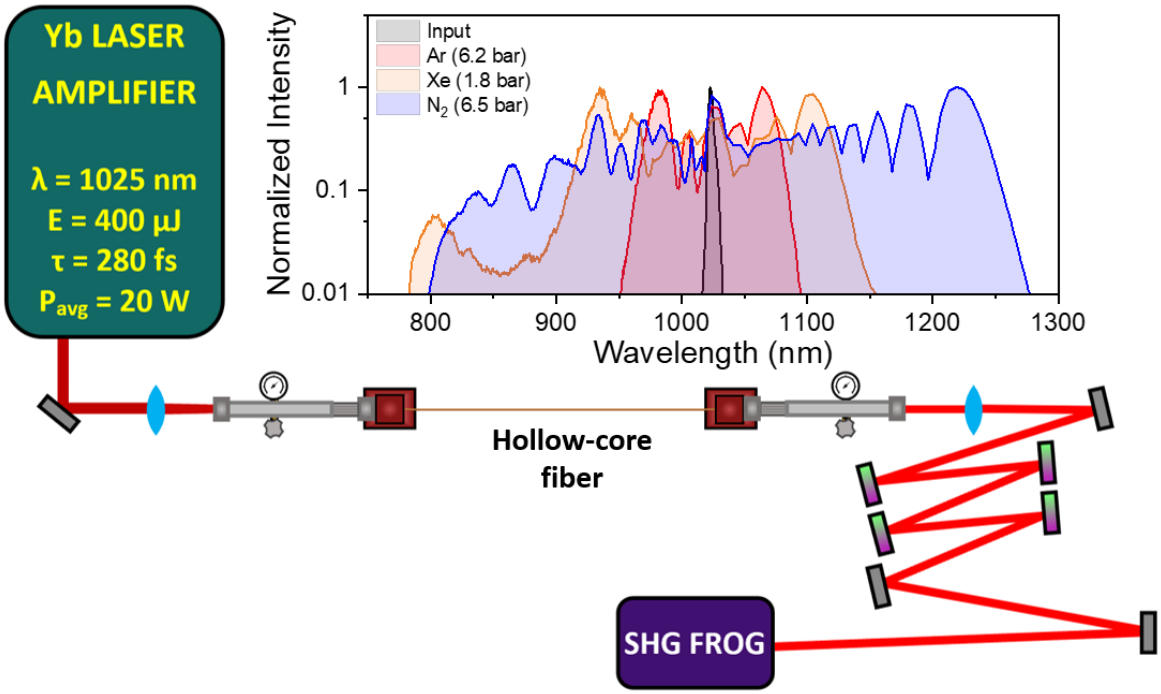

Figure 1: Schematic of the pulse compression setup. Inset: characteristic spectra using different gas media.

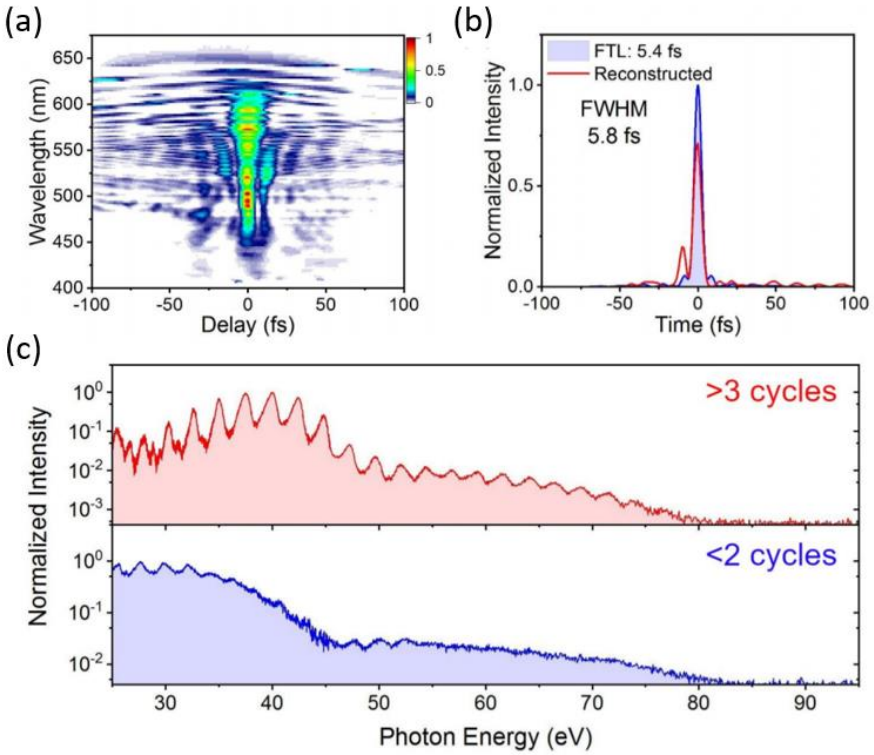

Figure 2: Pulse compression and high harmonic generation. (a) Experimental FROG trace and (b) retrieved pulse envelope following compression in N_2O-filled hollow-core fiber. (c) XUV spectra generated from pulses compressed in Xe (top) and N2O (bottom).

harmonic spectrum (Fig. 2c). Briefly, high-order harmonics were generated by focusing the 1.6-cycle pulses, as well as >3-cycle pulses generated using a xenon-filled hollow-core fiber, through an argon-filled gas cell. While the XUV spectra exhibited harmonic peaks up to the harmonic cut-off at ~80 eV when harmonic generation was driven with the longer input pulses, the 1.6-cycle pulses yielded a supercontinuum. Importantly, these measurements were performed by averaging the XUV spectrum over many laser shots, with randomly varying carrier-envelope phase (CEP). CEP-dependent measurements originally planned for this year have been delayed due to the COVID-19 pandemic, as we have been unable to lock the CEP of our laser oscillator since lab operations restarted after lengthy shutdowns.

Finally, we have begun construction of our experimental setup for time-resolved attosecond spectroscopy. The procurement of the vacuum chambers for housing the XUV focusing mirror and the target gas, and thus the construction of the instrument, were unfortunately delayed due to COVID-19 shutdowns. However, these critical parts have now arrived, and we will soon be able to begin the proposed attosecond strong-field transient interference spectroscopy (ASTIS) measurements. Critically, the versatile instrument will also allow us to perform attosecond experiments in transient absorption[4], interferometry[5], and photoelectron imaging[6] modes.

The research outcomes described above have also led to some work which, while somewhat beyond the scope of the original proposal, will have significant benefits to the program. These include a collaborative project with Linda Young, Anne Marie March, and Gilles Doumy (Argonne National Laboratory) to produce few-cycle pulses in the visible (~515 nm central wavelength) and ultraviolet (~343 nm central wavelength) regions of the spectrum, as well as studies of how rotational decoherence associated with repetitive laser heating of the molecular gas can affect nonlinear propagation, supercontinuum generation, and pulse compression. Results from these studies are expected to lead to improvements in both the peak intensity and average power of isolated attosecond sources, due to favorable scaling of the high-order harmonic flux with shorter wavelength driving lasers and the potential to drive attosecond sources using kilowatt-class industrial-grade femtosecond lasers. They will also allow us to drive XUV coherences in different regimes (e.g. multiphoton vs tunneling excitation) by varying the driving laser wavelength.

Future Plans

In the next year, we aim to characterize isolated attosecond pulses and XUV coherences using *in situ* perturbations of the driving laser field. This requires that we first characterize the carrier-envelope phase (CEP) stability of the compressed pulses, and measuring the CEP dependence of both the high-order harmonic spectrum and the XUV free-induction decay driven by the 1.6-cycle pulses. These measurements can be completed using our existing XUV spectrometer. We are considering a novel method to characterize CEP dependence using the attosecond light house technique, in the event that CEP stability cannot be regained in the coming months. Finally, we will construct and test our new experimental setup for time-resolved attosecond spectroscopy.

References

1. J. E. Beetar, F. Rivas, S. Gholam-Mirzaei, Y. Liu, and M. Chini, “Hollow-core fiber compression of a commercial Yb:KGW laser amplifier,” J. Opt. Soc. Am. B **36**, A33-A37 (2019).
2. J. K. Wahlstrand, Y.-H. Cheng, and H. M. Milchberg, “Absolute measurement of the transient optical nonlinearity in N_2, O_2, N_2O, and Ar,” Phys. Rev. A **85**, 043820.
3. J. E. Beetar, M. Nrisimhamurty, T.-C. Truong, G. C. Nagar, Y. Liu, J. Nesper, O. Suarez, F. Rivas, Y. Wu, B. Shim and M. Chini “Multioctave supercontinuum generation and frequency conversion based on rotational nonlinearity” Sci. Adv. **6**, eabb5375 (2020).
4. R. Geneaux, H. J. B. Marroux, A. Guggenmos, D. M. Neumark, and S. R. Leone, "Transient absorption spectroscopy using high harmonic generation: a review of ultrafast X-ray dynamics in molecules and solids," Phil. Trans. R. Soc. A 377, 2145 (2019).
5. D. Azoury, O. Kneller, S. Rozen, B. D. Bruner, A. Clergerie, Y. Mairesse, B. Fabre, B. Pons, N. Dudovich & M. Kruger, “Electronic wavefunctions probed by all-optical attosecond interferometry.” Nature Photonics. 13, 54-59 (2019).
6. M. J. J. Vrakking, “Attosecond imaging.” Phys. Chem. Chem. Phys., 16, 2775 (2014).

Peer-Reviewed Publications Resulting from this Project (Project start date: 08/2018)

1. J. E. Beetar, M. Nrisimhamurty, T.-C. Truong, G. C. Nagar, Y. Liu, J. Nesper, O. Suarez, F. Rivas, Y. Wu, B. Shim & M. Chini “Multioctave supercontinuum generation and frequency conversion based on rotational nonlinearity” Sci. Adv. **6**, eabb5375 (2020).

Probing electron and vibrational excitations, and their interactions, using coherent multidimensional techniques

Steven T. Cundiff
Department of Physics, University of Michigan, Ann Arbor, MI 48109
cundiff@umich.edu

Project Scope: This project will develop and demonstrate multidimensional coherent spectroscopy (MDCS) [1] techniques to fully map wave-packet dynamics in simple molecules. The MDCS techniques will allow the wave-packet evolution to be recorded continuously. The initial experiments will be performed using the existing MDCS apparatus in the lab to record the evolution of the wave-packet's energy. A version that is compatible with using an XFEL as a probe will be developed. Using the XFEL will allow the evolution of the position of the wave-packet, not just its energy, to be determined [2].

Recent Progress: This is a new project with a start date of August 15, 2020. Funding has only become available in mid-September. We are currently focused on designing the iodine vapor cell for the first experiments and identifying the laser system to be procured that will enable the study of iodine.

Future plans: The science goals for the first three years of the project will focus on answering the following questions:

- Can the evolution of the energy of a wave packet in a diatomic molecule be fully mapped using multidimensional coherent spectroscopy?
- Can wave packets on different potential energy surfaces be separated using coherent techniques?
- Can these methods be adapted to using an XFEL as a probe to map the internuclear distance of the wave packet rather than just the energy?
- Do these methods open the door to studying wave packet dynamics in more complex molecules?

A first technical step is to replace the existing laser system as the current system is beyond its operating lifetime and thus at risk of imminent failure. The need to replace the laser system is also an opportunity to upgrade it to meet the needs of the proposed experiments. Specifically the replacement laser systems, based on using Yb gain media, will operate a 1 MHz repetition rate, matching the planned repetition rate for the future LCLS upgrade. In addition the OPA will be replaced by a NOPA, which provides greater optical bandwidth.

The goal of the first phase of the project is to use 2D coherent spectroscopy (2DCS) to provide a complete and detailed map the energetic evolution of wave-packets, starting with simple molecules with known potential energy surfaces. Building on this initial step, we will attempt to invert the problem and seek to use the wave-packet dynamics to characterize the potential energy surfaces to develop a tool for measuring the surfaces in molecules where they are not known. We will also look at molecules that have more complex electronic structure, for example, many potential energy surfaces that can be simultaneously excited, avoided crossings and conical intersections that result in non-adiabatic dynamics.

The key concept is that a 2D coherent spectrum correlates the frequency at which the nonlinear signal is emitted with the corresponding absorption energy, even though the optical pulses that produce the initial excitation and stimulate the final signal are broadband. By scanning the waiting time, T, between the initial

pulse pair that creates the excitation and the third pulse the stimulates the signal, it will then be possible to map the energy shift between excitation and emission, even if there are multiple wavepackets evolving simultaneously. This method is directly analogous the tracking the energetic shifts during spectral diffusion of excitons [3]. These data will provide continuous tracking of the energy of a wave-packet. However, the data will not directly measure the position of the wavepacket, the position will have to be inferred from the potential energy surfaces. To directly measure the position of the wave-packet will require using the diffraction pattern provided by a time-resolved hard X-ray probes, as can be done at the LCLS and discussed below.

Although the 2DCS data will not directly give the position of the wave-packet, it may be possible to infer the position of the wave-packet through kinematics. Since the 2DCS tracks the change in potential energy of the wave-packet, the velocity of the wave-packet can be estimated since the change in kinetic energy is equal to the change in potential energy, the velocity can be determined and integrated to get the position. The confounding factor will be that the measured potential energy is the difference between the electronic states, not the absolute potential energy, thus the ground state potential energy curve must be taken into account. However, the excitation process will also launch a wavepacket in the electronic ground state through a Raman process. If this packet can be simultaneously tracked, it may be possible to fully determine both surfaces.

The deconvolution procedure demonstrated by the PI's group [4] will be essential for removing the "blurring" effects of the optical response in the 2D coherent spectra.

The initial experiments will be performed in iodine to connect with the previous pump-probe measurements [5] and the LCLS experiments [2] and because its transition energies are a good match for the wavelengths produced by the laser system. However, the large changes in the potential energy surfaces mean that even the enhance bandwidth of the NOPA will be insufficient to probe the wavepacket dynamics over a large enough range of nuclear motion, thus we will look at using continuum generation to produce even more bandwidth, either for all pulses, or just the final pulse plus local oscillator.

Once we have established the basic concepts using iodine, we will investigate other simple molecules, specifically those with more complicated potential energy surfaces than iodine. The exact molecule will be determined once the initial results on iodine are obtained. One set of possibilities are alkali metal dimers as the PI's lab has experience with making vapor cells for these species atomic species, which always contain some fraction of the atoms bound in dimers.

A 3D coherent spectrum allows individual pathways to be isolated and characterized [6]. The concept of a well-defined pathway applies when a discrete level picture applies. In a molecular system this is the case when there are well define vibrational levels for the ground and electronically excited state. The oscillations evident in prior work show that is the case in iodine. However there are also clearly non-oscillatory components corresponding motion of the wavepacket that is not vibrational. In this situation, the wavepacket will disperse. The dispersion of the wavepacket with time corresponds to a loss of internal coherence, which will also be revealed by a 3D coherent spectrum.

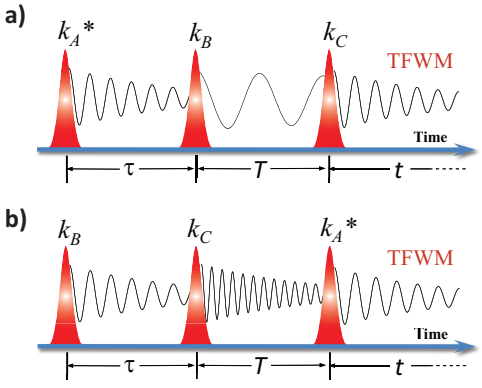

Figure 1: Examples of the typical pulse sequences used in MDCS. (a) Pulse sequence corresponding to the generation of a photon echo, often called a 'single-quantum' spectrum. During time period T vibrational coherences can contribute to the overall phase of the emitted signal. (b) Pulse sequence for observing 'double-quantum coherences' that are signatures of interactions among excitations if no real doubly excited state exists.

A sequence of 2D coherent spectra, which are generated by Fourier transforming with respect to delays τ and t shown in Fig. 1, as a function of the waiting time T between the second and third pulses. While these data sets will be a function of three dimensions, they do

not necessarily allow the generation of a full 3D *coherent* spectrum. To do so requires that the overall phase be stable between successive 2D spectra such that the real and imaginary parts are properly defined and the Fourier transform with respect to T produces the appropriate sign for the frequencies.

We will take full 3D coherent spectra on iodine to start with, again to connect to the prior work, both by others and in previous section. By analyzing the lineshapes in a 3D space we will be able to separate the effects of dephasing versus anharmonicity in the potential surfaces on the dispersal of the wave-packets. For unbound wave-packets, there will not be distinct peaks in the 3D spectra, nevertheless an analysis of the spectrum will allow the dispersion of the wave-packet due purely to deterministic evolution on the potential energy surface to be separated from lost internal coherence due to dephasing processes.

In some situations a 3D spectrum can also distinguish between wave-packets on the ground state potential versus the electronically excited state potential. If the thermal excitation of the higher vibrational modes of the ground-state potential is minimal, then the Raman coherence in the ground state must evolve at a negative frequency, whereas those in the excited state can evolve with either positive or negative frequency. Thus the positive frequency components must be due to excited state Raman coherences and the difference between positive and negative frequency components are due to the ground state Raman coherences.

The work described thus far will be purely optical, in the sense that the excitation and observable signal are all optical. While these experiments can provide unprecedented detail in mapping the evolution of the energy of a wave-packet, by monitoring the frequency and phase of the emitted signal, they do not directly measure the inter-nuclear separation of the molecule. Directly measuring the inter-nuclear separation can be achieved by using diffraction of hard x-ray pulses from an XFEL, however that data does not indicate the origin of the wave-packet, which can be done with multidimensional coherent methods, as described in the previous sections.

To marry multidimensional coherent methods with x-ray probes, requires a different approach than used by our current apparatus. The current apparatus uses excitation beams with distinct directions, such that their interference results in a spatial modulation of the excited state populations, which forms the grating that is mapped into the absorption and acts as a diffraction grating to scatter the final pulse into the signal directions. The resulting spatially inhomogeneous excited state populations would give spatially varying x-ray diffraction patterns, which would average out. To overcome this problem, fully collinear beams are needed to realize a spatially uniform excitation. The simplest implementation is to use pulse pair for the excitation in an experiment similar to that performed by Glownia et al. [2]. The challenge will be to separate the diffraction due to the pulse pair rather than the individual pulses. This can be realized by exploiting the sensitivity to the relative phase of the two pulses and cycling the phase such that the signals due to the individual pulses cancel, whereas that due to the pair adds constructively.

There have been several approaches to using fully collinear excitation pulses to implement multidimensional coherent spectroscopy. A very early implementation used a pulse shaper to generate 4 phase locked pulses and a fluorescence signal as the observable [7]. Another approach uses a pulse shaper to generate a phase locked pulse pair and a separate beam as a probe, which also acts as the local oscillator [8]. The use of acousto-optic based pulse shapers, such as the commercially available 'Dazzler' are limited to low repetition rates of 30 kHz and below, which makes them incompatible with the planned upgrade to LCLS. Static pulse shapers based on liquid crystal spatial light modulators are a possibility, but are relatively inefficient and have limitations on handling high power pulses. Thus neither of these seem like a good option and in the following sections we propose to alternate approaches.

We propose that as part of this project we will develop methods that are compatible with using LCLS to probe nuclear motion. The goal would not be a full MDCS experiment, but rather using a phase locked pulse pair to replace the excitation pulse and show the phase cycling can be used with LCLS diffraction experiments to tag the initial excitation energy of the observed wave-packet. Two methods are described in the following sections. The first is simpler and could be used for initial demonstrations of the concept of excitation with a phase-locked pulse pair. The second method is targeted at the future upgrade of LCLS to a

repetition rate of 1 MHz. The basic concepts would be demonstrated in the PI's laboratory using an optical probe, rather than an x-ray probe. Where appropriate, the relevant apparatus would be built in a modular fashion such that it could be shipped to SLAC and used with laser sources available there. Of course, doing so would require a successful proposal for beam time on a future LCLS run.

Peer-Reviewed Publications resulting from this project (Project start date: 08/2020**):** None

References

[1] S. T. Cundiff and S. Mukamel, "Optical multidimensional coherent spectroscopy," Phys. Today **66**(7), 44 – 49 (2013). URL http://dx.doi.org/10.1063/PT.3.2047.

[2] J. M. Glownia, A. Natan, J. P. Cryan, R. Hartsock, M. Kozina, M. P. Minitti, S. Nelson, J. Robinson, T. Sato, T. van Driel, G. Welch, C. Weninger, D. Zhu, and P. H. Bucksbaum, "Self-Referenced Coherent Diffraction X-Ray Movie of Angstrom-and Femtosecond-Scale Atomic Motion," Phys. Rev. Lett. **117**(15), 153,003 (2016).

[3] R. Singh, M. Richter, G. Moody, M. E. Siemens, H. Li, and S. T. Cundiff, "Localization dynamics of excitons in disordered semiconductor quantum wells," Phys. Rev. B **95**(23), 235,307 (2017).

[4] M. Richter, R. Singh, M. Siemens, and S. T. Cundiff, "Deconvolution of optical multidimensional coherent spectra," Sci. Adv. **4**(6), eaar7697 (2018).

[5] R. Bowman, M. Dantus, and A. Zewail, "Femtosecond transition-state spectroscopy of iodine: From strongly bound to repulsive surface dynamics," Chem. Phys. Lett. **161**(4-5), 297–302 (1989).

[6] H. Li, A. D. Bristow, M. E. Siemens, G. Moody, and S. T. Cundiff, "Unraveling quantum pathways using optical 3D Fourier-transform spectroscopy," Nature Commun **4**, 1390 (2013).

[7] P. Tian, D. Keusters, Y. Suzaki, and W. Warren, "Femtosecond phase-coherent two-dimensional spectroscopy," Science **300**, 1553–1555 (2003).

[8] E. M. Grumstrup, S.-H. Shim, M. A. Montgomery, N. H. Damrauer, and M. T. Zanni, "Facile collection of two-dimensional electronic spectra using femtosecond pulse-shaping technology," Opt. Expr. **15**, 16,681–16,689 (2007).

Understanding and Controlling Strong-Field Laser Interactions with Polyatomic Molecules

DOE Grant No. DE-SC0002325

Marcos Dantus, dantus@msu.edu
Department of Chemistry and Department of Physics and Astronomy, Michigan State University, East Lansing MI 48824

1. Project Scope

Advances in our understanding of laser-matter interactions allow us to think about strategies for not only observing but also *controlling* the different processes and reactions that follow these interactions. Our program focuses on the chemical processes occurring in polyatomic molecules under intense laser excitation. Efforts on quantum control of electronic, vibrational, and rotational dynamics of molecules prior to and during strong-field interactions are in line with the Grand Challenge questions that have been proposed in recent DOE- and NSF-sponsored workshops. Recently, we have sharpened our focus towards better understanding and controlling of ultrafast hydrogen migration processes occurring in organic molecules under strong fields. These processes, which occur following single and double ionization, include the formation of neutral hydrogen molecules, and involve the making and breaking of multiple chemical bonds that result in the formation of H_3^+, H_2O^+, H_3O^+, and CH_5^+. Our studies have provided the first evidence for roaming chemical reactions initiated by ion precursors, resulting in the first time-resolved measurements of this type of reaction mechanism. Our work, in collaboration with other groups within the DOE AMOS group, is improving the quantum mechanical descriptions of relatively unknown chemical reactions that involve roaming of neutral fragments.

2. Recent Progress

(a) Quantum Coherent Control of H_3^+ Formation in Strong Fields

M. Michie, N. Ekanayake, N. P. Weingartz, J. Stamm, and M. Dantus. *J. Chem. Phys.* **150**, 044303 (2019).

Strong-field laser-matter interactions are well understood for isolated atoms and diatomic molecules, yet our understanding falls short when polyatomic molecules are involved. Similarly, quantum coherent control (QCC) of laser-matter interactions is well known for two- and three-photon resonant transitions, but not understood in cases with higher order transitions. Here, we consider the simplest approach to QCC, namely the use of a single spectral phase step, on a chemical process requiring strong-field double ionization. The goal is to determine if QCC can be used to control strong-field laser-matter interactions involving higher order 7- to 16-photon excitation. We find that indeed the spectral phase step provides a significant and unexpected method to control the yield of H_3^+ and its coincidence ion HCO^+ following the double ionization of methanol (see Fig. 3).

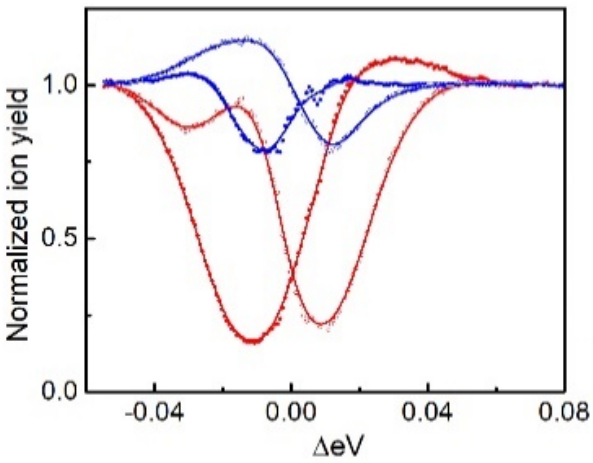

FIG. 1. *The yield of H_3^+(red) and its coincidence ion HCO^+ (blue) detected as a function of scanning a positive or negative $3\pi/4$ phase step phase across the spectrum. The ion yields are normalized to their value when TL pulses are used. Notice that in some cases the ion yield exceeds that obtained for TL pulses.*

(b) Control of electron recollision and molecular nonsequential double ionization

S. Li, D. Sierra-Costa, M. J. Michie, I. Ben-Itzhak and M. Dantus, *Commun. Phys.* **3**, 35 (2020).

Intense laser pulses lasting a few optical cycles, are able to ionize molecules via different mechanisms. One such mechanism involves a process whereby within one optical period an electron tunnels away from the

molecule and is then accelerated and driven back as the laser field reverses its direction, colliding with the parent molecule and causing correlated nonsequential double ionization (NSDI). Here we report control over NSDI via spectral-phase pulse shaping of femtosecond laser pulses. The measurements are carried out on ethane molecules using shaped pulses. We find that the shaped pulses can enhance or suppress the yield of dications resulting from electron recollision by factors of 3 to 6. This type of shaped pulses is likely to impact all phenomena stemming from electron recollision processes induced by strong laser fields such as above threshold ionization, high harmonic generation, attosecond pulse generation, and laser-induced electron diffraction.

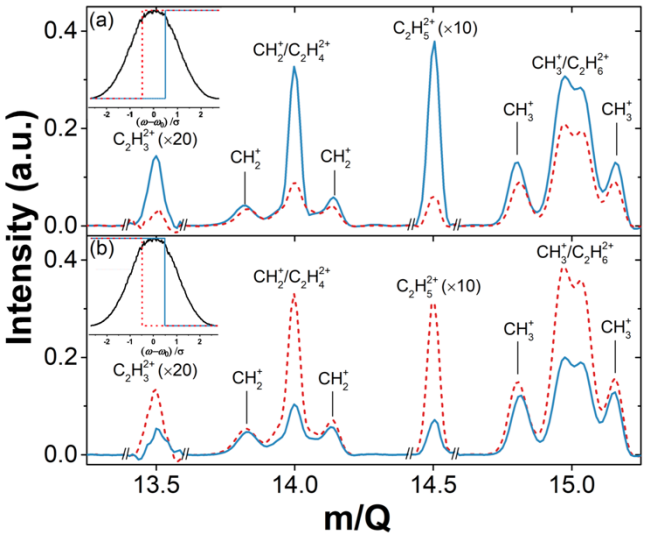

FIG 2. *Portion of the mass spectrum of ethane showing the fragment ions with m/Q between 13 and 15.5 obtained using shaped pulses. (a) Laser spectra for two different shaped pulses with a positive ¾π phase step in either the high energy (blue line) or low energy (red-dashed line) portion of the laser spectrum (see inset diagrams showing their location at ±σ/2 relative to ω_0). (b) Spectra for negative ¾π phase step in either the high energy (blue line) or low energy (red-dashed line) portion of the laser spectrum. Notice the phase step serves to enhance or suppress the yield of doubly charged fragment ions associated with non-sequential double ionization, and that the effect is reversed upon changing the sign of the phase step. The four spectra, shown as measured (without normalization), were obtained within the span of 30 min under identical conditions except for the frequency where the phase step is located.*

3. Future Plans

i. We are collaborating with Prof. Jean Marcel Ngoko, Dr. Dian Peng, and Dr. Hua-Chieh Shao (formerly from Tony Starace's group) on simulating the tunnel ionization process numerically and analytically. Their results on helium ionization match our experimental results. We are preparing a joint publication.

Relative difference

$$\delta = \frac{\phi^+ - \phi^-}{\left(\phi^+ + \phi^-\right)/2}$$

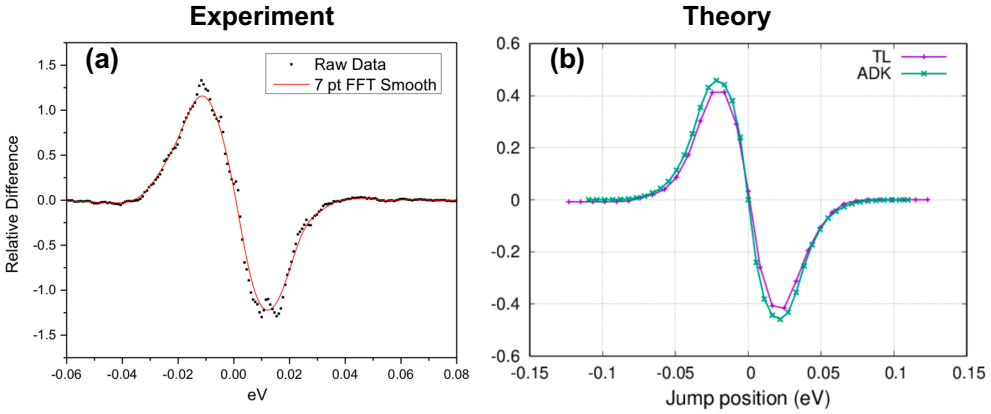

ii. We have obtained time resolved data regarding the formation of H_3^+ from ethane. We find H_3^+ on average forms in 490 ± 80 fs, while D_3^+ forms in 530 ± 80 fs. We are collaborating with Prof. Benjamin Levine on molecular dynamics simulations. We find that double ionization of ethane leaves the doubly charged ion

with a significant amount of excess energy which causes very large amplitude motion of the hydrogen atoms. This leads to both H migration and H_2 roaming. We are preparing the results for publication.

iii. With the goal of following changes in molecular structure that occur soon after single- or double-ionization of ethane, we have obtained rotational coherence transients from multiple fragment ions. The rotational revivals observed correspond to $C_2H_6^+$, $C_2H_5^+$, $C_2H_4^+$, $C_2H_3^+$,and $C_2H_6^{2+}$, $C_2H_5^{2+}$, $C_2H_4^{2+}$. We are in the process of simulating results for six different fragment ions and extracting the molecular structure of these species which are far from equilibrium. We will then compare our results to molecular dynamics simulations.

iv. We are collaborating with Prof. Eric Wells on simulating the observed enhancement of H_3^+ from ethane as a function of chirp. Based on simulating the shaped laser pulses we are now able to explain the reason why the observed a greater yield of H_3^+ when using negatively chirped pulses, an experiment that other research groups try to replicate (including ours) but failed.

These projects will provide clarity to reports in the literature related to the ethane in strong fields. Future work will address larger molecules and take advantage of our ability to use shaped femtosecond pulses in order to discriminate between tunnel ionization, multiphoton ionization, or non-sequential double ionization. While hydrogen migration in large organic molecules during strong field interactions has been studied, we find of particular interest the formation of neutral H_2, which roams the parent ion and abstracts an additional proton to form H_3^+. While carrying out these fundamental projects, we have discovered an extremely sensitive method for ultrafast pulse metrology with milliradian spectral phase resolution. We are finalizing the theory and experiments related to this finding and plan to publish the work and apply for a patent simultaneously.

5. Peer-Reviewed Publications Resulting from this Project (2018-2020)

1. S. Li, D. Sierra-Costa, M. J. Michie, I. Ben-Itzhak and M. Dantus, "Control of electron recollision and molecular nonsequential double ionization," *Commun. Phys.* **3**, 35 (2020).

2. M. J. Michie, N. Ekanayake, N. P. Weingartz, J. Stamm, and M. Dantus, "Quantum coherent control of H_3^+ formation in strong fields" *J. Chem. Phys.* **150**, 044303 (2019).

3. N. Ekanayake, M. Nairat, N. P. Weingartz, M. J. Michie, B. G. Levine, and M. Dantus, "Substituent effects on H_3^+ formation via H_2 roaming mechanisms from organic molecules under strong-field photodissociation" *J. Chem. Phys.* **149**, 244310 (2018).

4. N. Ekanayake, T. Severt, M. Nairat, N. P. Weingartz, B. M. Farris, B. Kaderiya, P. Feizollah, B. Jochim, F. Ziaee, K. Borne, K. Raju P., K. D. Carnes, D. Rolles, A. Rudenko, B. G. Levine, J. E. Jackson, I. Ben-Itzhak, and M. Dantus, "H_2 roaming chemistry and the formation of H_3^+ from organic molecules in strong laser fields," *Nat. Commun.* **9**, 5186 (2018).

Page is intentionally blank.

PROGRAM TITLE: ATTOSECOND, IMAGING AND ULTRA-FAST X-RAY SCIENCE

PI: Louis F. DiMauro
Department of Physics
The Ohio State University
Columbus, OH 43210
dimauro.6@osu.edu

1.1 PROJECT SCOPE

This grant's aim is to explore the realm of ultrafast dynamics using different complementary tools. In one thrust, we explore and exploit fundamental aspects of generation and measurement of high harmonic and attosecond pulses to access fundamental atomic and molecular processes. A second thrust provides a natural link to our attosecond effort via the same underlying strong field physics, laboratory infrastructure and technical approach. The strong field driven "self-imaging" method uses elastic scattering of the field-driven electron wave packet as an alternative route for spatial-temporal imaging in the gas phase. In 2011, the viability of this approach for achieving femtosecond timing and picometer spatial resolution was demonstrated in a collaboration between OSU and KSU groups. A third thrust is the implementation of an AMO science program using the ultra-fast, intense x-rays available at LCLS XFEL. The objective is the study of fundamental atomic processes, x-ray nonlinear optics and the development of methods for time-resolved x-ray physics. Our overall objective is advancing these methods as robust tools for imaging and probing electron dynamics thus producing the complete molecular movie.

Progress over the past year includes efforts on five projects: (1) construction of a new specialized instrument for advancing strong field physics using attosecond pulses, (2) dynamical spatial-temporal imaging of the C_{60} fullerene, (3) measurement of the spectral phases around multiple autoionizing states, (4) development of a high-average power mid-infrared (MIR) laser and (5) clocking Auger electrons at the LCLS. The following sections will present a description of projects (1), (4) and (5).

1.2 PROGRESS IN FY2020

Our strong field program over the last several years has focused on using long wavelength generated harmonics. We are interested in addressing three basic questions related to attosecond physics. First, can high harmonic and attosecond spectroscopy extract atomic/molecular structure? Second, what is really being measured? Finally, can attosecond techniques simulate basic strong-field physics?

The Strong Field Simulator. In typical strong field ionization experiments, a single high-intensity laser allows bound electrons to tunnel into the continuum, ionizing the atomic or molecular target, and drives the trajectory of that electron far from the parent ion. Electron trajectories that return to interact with the parent ion are of particular interest due to the many physical phenomena attributed to them: elastic (LIED) and inelastic (NSDI, RESI) scattering or recombination (HHG). The standard 3-step view of strong field ionization is illustrated in Fig. 1(a).

Recently, we have introduced the strong field simulator (SFS) method to explore a wide variety of strong field processes [see Fig. 1(b)], which is enabled by the combination of an intense, low-frequency laser field with a precisely synchronized attosecond source. The key feature of the SFS method is that it breaks open the familiar 3-step scenario of ionization followed by acceleration and rescattering in a strong laser field into its component parts, delegating ionization to the attosecond field and introducing the ionization time as the key variable in the SFS measurement. This in turn makes the influence of the laser intensity, responsible for acceleration and rescattering, more directly accessible in the experiment. Figure 1 provides a brief tutorial to this approach.

In 2018, we initiated a set of proof-of-principle measurements to demonstrate the viability of the SFS approach. The experiment used three key principles, (i) a sufficiently long wavelength (≥ 1 μm) laser field was used to exploit the λ^2-scaling of the ponderomotive potential to ensure that high-energy rescattering events were driven while not promoting significant MIR ionization, (ii) the use of precisely phase-locked MIR and attosecond pulse train (APT) fields and (iii) low-order harmonic APT to promote near threshold single-photon atomic ionization at a constant rate.

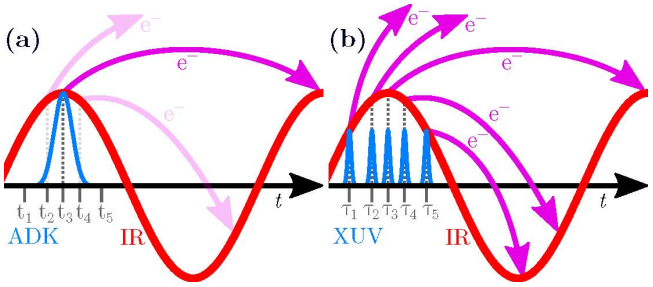

Figure 1: Comparison between (a) ordinary strong field processes and (b) the SFS approach. The MIR laser field as a function of time is shown in red. Five different example electron trajectories are schematically shown in magenta. Their initial point corresponds to their ionization time (t_1 to t_5) and t_3 to t_5 are illustrative trajectories with classical returns. In (a), the exponential tunneling rate (ADK blue curve) confines the ionization time around the field extremes. The shading is indicative of the tunneling rate, i.e., lighter means less. In (b), the ionization time is experimentally chosen by the delay τ_i of the XUV pulse relative to the NIR field. A few different delays are illustrated. The key point is that choosing τ_i in the SFS approach mimics a strong field process initiated at t_i but at constant ionization rate.

We employed an existing attosecond apparatus, not ideal for this experiment, to collect photoelectron spectra as a function of the delay between the XUV and MIR pulses. The delay spectra showed an overall structure, which oscillated at 2ω, or twice each cycle of the MIR field. In addition, there was also a strong energy dependence to the oscillating phase with manifests two energy regions with opposing sign. Our collaborator, Prof. Ken Schafer (LSU), performed TDSE modelling. The simulations reproduced the primary features of our experiments and provided physical insight. Ultimately, this initial study showed that we had achieved the quantum path control key to the SFS scheme and reinforced our confidence for future investment. A joint OSU/LSU paper is under review at PRX.

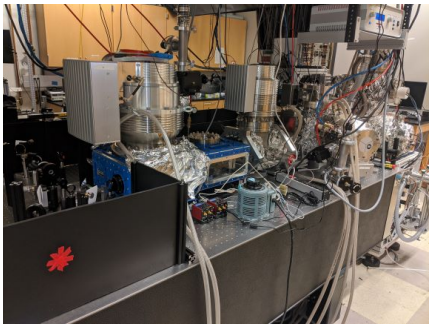

Figure 2: The SFS apparatus at OSU in August 2020. The key design elements include the use of a pulsed gas valve, narrower vacuum apertures and spherical dielectric XUV mirrors.

Having validated the SFS approach, we have completed the design and assembly of a new beamline optimized for SFS experiments (see Fig. 2). We focused on improving three criteria which were lessons learned from our initial experiments: (1) increased XUV flux in the interaction region (signal enhancement), (2) reduced background contamination in our detection chamber (noise) and (3) improved interferometric stability (temporal resolution). Criterion (1) is addressed by the addition of a pulsed gas valve which allows for higher gas density used to produce XUV HHG. In addition, Xenon gas will be used to generate near-threshold harmonics, resulting in a typical increase of the XUV flux by a factor of 10 compared to Argon gas. Previously, the largest source of contamination in the detection chamber was caused by the continuous flow of gas used in HHG. As such, (2) is resolved by a combination of the pulsed gas valve – reducing the amount of gas entering the vacuum system – and tighter vacuum apertures to choke the gas flow through the apparatus. Criterion (3) is aided by keeping this apparatus closer to the laser system and building the entire beamline at a lower height profile with respect to the optical table. We have also added a new important capability by using a multi-layer spherical mirror (MLSM) to focus the XUV and MIR pulses. These mirrors are engineered to have a narrow band reflection efficiency (~5 eV FWHM), with a central energy of 25, 35, or 45 eV depending on choice of mirror. This will allow us to selectively filter the photon energies of the XUV pulse train, and correspondingly the initial kinetic

energy of the photoionized electron wave packet adding another dimension to explore in the SFS scheme. In addition, the MLSM will produce a smaller XUV beam waist compare to the past experiments thus enabling a more uniform intensity profile of the dressing field.

The laboratory reopened in July 2020 following the OSU COVID shutdown, the SFS apparatus has been fully commissioned for vacuum integrity, photoelectron spectrometer performance and high harmonic generation. The MLSM shows a reflectivity consistent with the expected 5 eV bandwidth at 25 eV. Currently, the stability of the temporal and spatial overlap between phase-locked MIR and APT fields is being characterized. Once verified, the scientific campaigns will be underway.

High harmonic generation in the water window. Part of the purview of this grant is the advancement of attosecond technology for robust and broad applications. Through our DOE program, we have introduced the concept of scaling towards longer wavelength for achieving higher photon energy (cutoff) and shorter attosecond pulses. Although mid-infrared (MIR) generation (1-4 μm) based on nonlinear processes have been a productive approach, it remains noncompetitive source compared to the quality of the NIR light from CPA-based titanium sapphire (TiSapp) systems (0.8 μm).

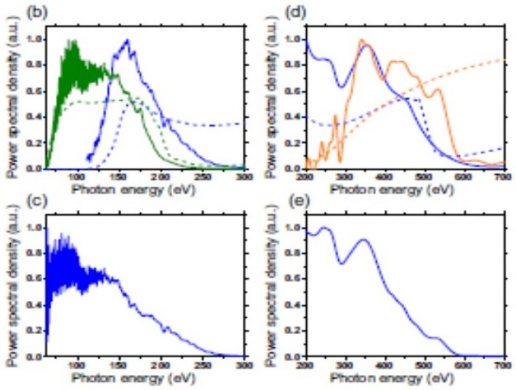

Figure 3: Soft x-ray HHG driven by the OSU 2.4 μm CPA laser system. (b) Spectra generated in Ar and measured with Zr (green solid curve) and Sn (blue solid curve) filters. The corresponding filter transmission is shown with dashed lines. (c) Combined results from (b) after correction for the filter transmission. (d) Spectra generated in Ne and measured with Sn (blue solid curve) and Al (orange solid curve) filters. The corresponding filter transmission is shown with dashed lines. (e) Combined results from (d) after correction for the filter transmission.

During the past year, we have demonstrated and applied a Cr^{2+}:ZnSe laser amplifier delivering 7 mJ, 100 fs pulses at 1 kHz repetition rate and 2.4 μm central wavelength with excellent energy stability and beam quality [7A]. The CPA system supports direct lasing at 2.4 μm and uses Holmium fiber laser pumps, making it competitive in performance and cost with TiSapp except with MIR operation. We showed that the pulses can be post-compressed to 39 fs, 6.2 mJ and 115 GW peak power using a novel nonlinear compression scheme. It enables reliable post-compression in a compact and simple setup even at the multi-mJ pulse energy level without any additional dispersion management due to soliton-like regime in the anomalous dispersion range. The system was successfully applied to generate soft x-ray HHG in the water window up to 0.6 keV (see Fig. 3). In addition to HHG applications, due to the very good pulse quality and mid-IR wavelength, the demonstrated system will enable efficient (significantly more efficient compared to ~1 μm) pumping of a sub-mJ-level 6–12 μm OPA, which will advance strong field physics into LWIR regime.

Clocking Auger electrons at the LCLS. Intense X-ray free-electron lasers (XFELs) can rapidly excite matter, leaving it in inherently unstable states, which decay on femtosecond timescales. As the relaxation occurs primarily via Auger emission, excited state observations are constrained by Auger decay. *In situ* measurement of this process is therefore crucial, yet it has thus far remained elusive at XFELs due to inherent timing and phase jitter, which can be orders of magnitude larger than the timescale of Auger decay.

One common attosecond metrology, the streaking method, has been successfully deployed on many tabletop experiments. To translate this method onto an XFEL platform, we have conducted a series of LCLS campaigns aimed at mitigating the jitter issue. To do so, we have developed an novel approach termed *self-referenced attosecond streaking* that provides sub-femtosecond resolution in spite of jitter, enabling time-domain measurement of the delay between photo- and Auger emission in atomic neon

excited by intense, femtosecond pulses at the LCLS. Using a fully quantum-mechanical description that treats the ionization, core-hole formation and Auger emission as a single process, we have measured the Auger decay lifetime of 2.2 + 0.2 -0.3 fs for the neon KLL decay channel. The paper is accepted in Nature Physics [8A] and available on the archives.

This successful demonstration of its efficacy, self-referenced streaking will enable experimentalists to take advantage of the extreme-intensity X-ray pulses at XFELs while simultaneously exploiting the unrivalled time resolution provided by attosecond streaking spectroscopy. In conjunction with the technique, the measurement was made possible via the application of a consistent quantum model of Auger decay. Through the application of this advanced model, we demonstrated that the older *ad hoc* two-step model significantly overestimates the extracted lifetime. This will have major ramifications for future studies of Auger decay, especially those applying our self-referenced streaking to make the measurement at XFELs.

1.3 Future Plans

Strong field simulator: Using the newly constructed SFS apparatus, we will perform a series of novel experiments along the SFS scheme. (i) Study the non-sequential double ionization in Helium using a dielectric mirror centered at 25eV – close to Helium's ionization potential at 24.6 eV – to closely approximate the typical strong field tunneling step, with ion spectra being recorded to measure changes in the rate of double ionized Helium. This will be a multi-dimensional study with the MIR wavelength, XUV photon energies, interferometric delay, and laser intensity all being independent tunable parameters. (ii) We will also study the rate of electron recollision using elliptically polarized MIR light. In this scenario, a delay scan will modulate the relative angle between the XUV polarization, and therefore the initial momentum vector of the photoelectrons, and the instantaneous direction of the MIR field vector. Ken Schafer (LSU) will provide theory support for this program.

Investigations using the LCLS XLEAP. We continue to participate in a LCLS beam time awarded in 2020 but rescheduled for 2021. Our exact involvement in 2021 is still unclear due to COVID restrictions at SLAC. We had planned in 2020 for a student and postdoc to spend 3-4 months each at SLAC involved in recommissioning efforts and attosecond experimental campaigns. We intend on remaining committed to these efforts. The collaboration is led by Dr. James Cryan and Dr. Ago Marinelli.

1.4 Publication Resulting from this Grant from 2018-2020

1A. *"Probing electronic binding potentials with attosecond photoelectron wavepackets"*, D. Kiesewetter *et al.*, Nat. Phys., **14**, 68 (2018). doi: 10.1038/NPHYS4279.

2A. *"Femtosecond profiling of shaped x-ray pulses"*, M. Hoffmann *et al.*, New J. Phys. **20**, 033008 (2018). doi: https://doi.org/10.1088/1367-2630/aab548.

3A. *"Diffractive Imaging of C_{60} Structural Deformations Induced by Intense Femtosecond Midinfrared Laser Fields"*, H. Fuest *et al.*, Physical Review Letters **122**, 053002 (2019). doi: 10.1103/PhysRevLett.122.053002.

4A. *"Probing the interplay between geometric and electronic-structure features via high-harmonic spectroscopy"*, T. T. Gorman *et al.*, J. Chem. Phys. **150**, 184308 (2019). doi: 10.1063/1.5086036.

5A. *"Disentangling Spectral Phases of Interfering Autoionizing States from Attosecond Interferometric Measurements"*, Lou Barreau *et al.*, Phys. Rev. Lett. **122**, 253203 (2019). doi: 10.1103/PhysRevLett.122.253203.

6A. *"Attosecond transient absorption spooktroscopy: a ghost imaging approach to ultrafast absorption spectroscopy"*, Taran Driver *et al.*, Phys. Chem. Chem. Phys. **22**, 2704 (2020). Doi: 10.1039/C9CP03951A.

7A. *"High-power few-cycle Cr: ZnSe mid-infrared source for attosecond soft x-ray physics"*, Vyacheslav Leshchenko *et al.*, Optica **7**, 981 (2020). https://doi.org/10.1364/OPTICA.393377.

8A. *"Clocking Auger electrons",* Nat. Phys., accepted. arXiv preprint arXiv:2003.10398.

Dynamics of Atomic Electrons in Strong-Field Irradiation

J. H. Eberly
Department of Physics and Astronomy
University of Rochester, Rochester, NY 14627
eberly@pas.rochester.edu

Project Scope

Our BES-AMOS work [1, 2, 3, 4] has focused on theoretical questions raised by the initiation of strong-field ionization events, and single, double and multiple ionization processes have been treated in detail. Quantum coherences are particularly interesting and they can be suppressed by insufficient examination and theoretical adoption of pictorial views of electron release under strong irradiation. The most common of these views is the quasi-adiabatic picture of ionization as an event that proceeds as a tunneling process with specific entrance and exit stages. We have steadily developed theoretical approaches that allow avoidance of simplistic pictures, generally relying on *ab initio* Hamiltonian descriptions of dipole-approximate interactions initiated by non-perturbatively strong irradiation.

The outcomes developed by our continuing work in this direction have been recognized in several ways: the designation of our RMP review [5] as an ISI Highly Cited paper, an invitation to contribute to Vrakking's 2018 special issue of the Journal of Physics B [2], and the invitation to present the opening plenary talk [6] at the International Conference on Matter and Radiation at Extremes (2017, Beijing). The driving force of all such related investigations is well understood to be the experimental creativity producing a steady stream of new experimental findings coming from the laboratory availability of short laser pulses with intensities near to, and well above, $I = 0.1$ PW/cm^2, using near-visible wavelengths and also significantly longer and shorter than visible.

Recent Progress: Virtual Detection and Path-Summation

We have carried out an extended exploitation of our theoretical innovation called SENE. It is so-named because it employs a coordination of Schrödinger Equation dynamics and Newton Equation dynamics. The coordination is important becuse it is uniquely controlled by so-called virtual numerical detector (VND) operation [2, 7, 8]. It is initiated by a solution of the time-dependent Schrödinger equation during the early stages of ionization. We have shown that the SENE approach has given us a new avenue of theoretical access to still-obscure characteristics of ionization. These characteristics are important because ionization is the way photons liberate electrons from both atoms and more complex targets, creating quantum correlations that need to be described and exploited experimentally.

What has been missing theoretically is the ability to simulate accurately and also with computational efficiency the quantum nature of electron behavior generated during ionization, without using intuitive assumptions about behavior in the near neighborhood of a "tunnel exit" in the course of ionization. The hypothetical (mainly mythical) tunnel exit plays a basic role in the standard tunneling-based strong field approximation (SFA). The need to avoid such assumptions has been

long noted. A tunneling assumption is especially difficult to maintain for longitudinal ionized-momentum distributions - see Ivanov, Spanner and Smirnova [9]. As we have shown, for example, effects of temporal oscillations will be missed [3].

In order to go forward we have recently created [1] a dramatic extension of the SENE virtual numerical detector method. We have begun to show how to introduce Feynman-type path summation for 10^6 to 10^8 classical numerical trajectory paths. This is already an advance but what is most important is the newly demonstrated ability [1] to work with both the trajectory's momentum and its phase. This phase is lost in the course of virtual numerical detection (VND). The recovery we have achieved is demonstrated in Fig. 1 by the clear appearance of quantum interference fringes in the far-field momentum distribution of the trajectories. Along the way our simulation continues to exploit the huge numerical advantage of accounting for the on-going effect of laser action on the propagating trajectories by using Newtonian rather than Schrödinger evolution.

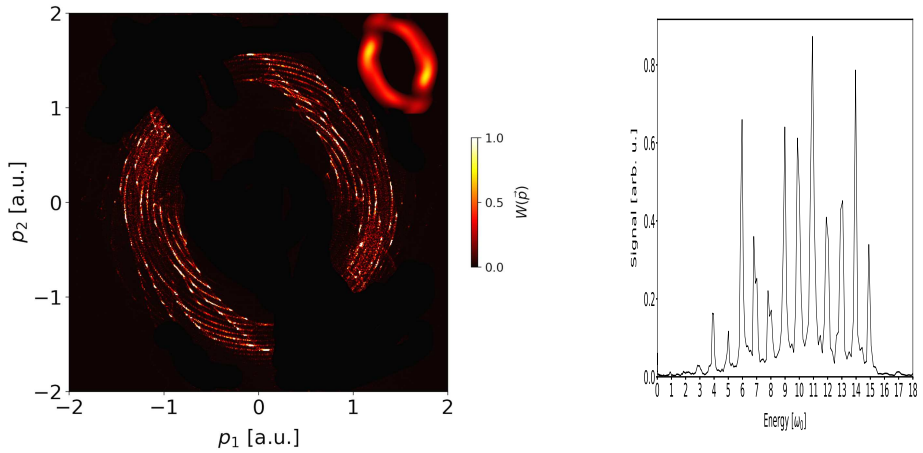

Figure 1: Left panel: two examples of far-field momentum distributions explained in the text. Right panel: A scan across such interfering momenta shown on the left, scaled by energy. The peaks in the continuum are separated by one laser photon energy, exactly correct for an example of above-threshold ionization under circularly polarized irradiation.

Future Plans: Single and Double (or Triple?) Ionization with Phase Capture and Momentum Coherence

Figure 1 shows success in working with phase recovery at its early stage of development. It shows what has been missing from ionization simulations to date. In the left panel of Fig. 1 the momentum-distribution rings embody the coherences that were restored to the outgoing "quantum-classical" electron in its SENE momentum trajectories, as they continue to evolve, post-VND, under the elliptical polarization of a strong applied laser field. The miniaturized version of a momentum distribution is shown super-imposed into the upper right corner of the panel. It was obtained via SENE-VND for the same ionization process, but without recovering phases. Validity of such unphased SENE-VGD work has already been established by comparison with phase-unresolved experimental distributions (see, e.g., [3, 6, 8]).

But the availability of phase-coherent results offers a new range of challenges to experimental work. This feature is most exciting. Phase recovery affords us the ability to extend the numerical detector advantage to more than a single electron. Until now no efficient quantum-accurate multi-electron simulation has been feasible. We have begun such an application.

At the present time it is restricted to one-dimensional evolution, starting with a fully TDSE near-nucleus two-electron wave function under the influence of linearly-polarized light. Each virtual detector records local wave function information, in the SENE-VND way, capturing the 2e probability current and momentum direction at each numerical time step, and thus generating a sequence of classical trajectories. The interaction between a pair of classical virtual electrons (emanating from the same virtual detector in the same numerical time step) is included by assigning them separate individual 1d coordinates x1 and x2. That assignment is then the name of a single Bohmian trajectory, which proceeds to propagate in a two-dimensional phase-space according to the dictates of the *ab initio* soft-core 2e Hamiltonian, with laser and e-e repulsion forces included. The evolution of this single trajectory in x1-x2 space represents a pair of electrons moving in one dimension, Coulomb-repelling each other, as well as responding to the atomic nucleus and the laser field. The two electrons of each co-generated pair continue to "know" and interact with each other, but not with any other virtual pair, throughout the duration of the laser pulse. This will be a primary near-term program goal.

As a closing remark, we emphasize again that in the planned work we will build from a quantum-correct TDSE ionizing initial wave function. We will not need assistance from tunneling or other intuitive and pictorial concepts of ionization. Phase coherence is required, and the path-summation approach provides it. Computational efficiency is automatically captured by adopting our SENE approach (for a collection of details see [1, 2, 10].

Peer-Reviewed Publications Resulting from this Project (2018-2020)

Xu Wang, Justin Tian and J.H. Eberly, (invited) "Virtual Detector Theory for Strong-Field Atomic Ionization", *J. Phys. B* **51**, 084002 (2018), https://doi.org/10.1088/1361-6455/aab5a4.

In the references below the marking * indicates papers supported by the BES-AMOS grant.**

References

[1] ***Rui-Hua Xu, Xu Wang, and J.H. Eberly, "Extended virtual detector theory including quantum interferences," arXiv:2003.05051 (2020) (to be submitted).

[2] ***Xu Wang, Justin Tian and J.H. Eberly, (invited) "Virtual Detector Theory for Strong-Field Atomic Ionization", *J. Phys. B* **51**, 084002 (2018)

[3] ***J. Tian, X. Wang, and J.H. Eberly, "Numerical Detector Theory for the Longitudinal Momentum Distribution of the Electron in Strong Field Ionization," *Phys. Rev. Lett.* **118**, 213201 (2017).

[4] *** Michael G. Pullen, Benjamin Wolter, Xu Wang, Xiao-Min Tong, Michele Sclafani, Matthias Baudisch, Hugo Pires, Claus Dieter Schroeter, Joachim Ullrich, Thomas Pfeifer, Robert Moshammer, J. H. Eberly and Jens Biegert, "Transition from nonsequential to sequential double ionization in many-electron systems", *Phys. Rev. A* **96**, 033401 (2017).

[5] ***W. Becker, X.J. Liu, P.J. Ho and J.H. Eberly, "Theories of Photo-Electron Correlation in Laser-Driven Multiple Atomic Ionization," *Rev. Mod. Phys.* **84**, 1011 (2012). [Invited, ISI Highly Cited Paper]

[6] *** J.H. Eberly, "Where Do the Electrons Come From?", Invited Plenary Lecture, International Conference on Matter and Radiation at Extremes (ICMRE), Beijing CHINA, June 26-30, 2017; and to be published.

[7] Our development of virtual numerical detector (VND) analysis was inspired by B. Feuerstein and U. Thumm: "On the computation of momentum distributions within wavepacket propagation calculations," J. Phys. B 36, 707 (2003).

[8] ***Justin Tian, "Theory of Strong-Field Atomic Ionizations", Ph.D. Dissertation, Department of Physics and Astronomy, University of Rochester (2017).

[9] M. Y. Ivanov, M. Spanner, and O. Smirnova, *J. Mod. Opt.* **52**, 165 (2005). Their remark was: "Identifying the wavepacket dependence on [exit velocity] is much harder. The crucial difficulty stems from the fact that the laser field accelerates the electron while it tunnels out. The velocity distribution along the field is changed continuously during tunneling." They pointed out that it is virtually impossible to separate the initial velocity distribution from the distortions caused by the laser field.

[10] ***Xu Wang, Justin Tian and J.H. Eberly, "Extended Virtual Detector Theory for Strong-Field Atomic Ionization," *Phys. Rev. Lett.* **110**, 243001 (2013).

ECRP: Probing ultrafast XUV/x-ray induced electron correlation in the molecular frame

Principle Investigator: Li Fang
Department of Physics, University of Central Florida, Orlando FL 32816
Email: Li.Fang@ucf.edu

Project Scope:

Electron-electron correlation is a fundamental process where momenta and energies are exchanged in multielectron systems. This project investigates photo-induced electron correlations in molecules in the time domain and in the molecular frames. Specifically, the investigation focuses on the temporal profile of the energy and momentum redistribution during electron correlations, the impact of the electron-electron correlation dynamics on the consequent chemical bond activities, and the dependence of the electron correlation dynamics on molecular orbital properties and molecular axis alignment or orientation. Three phenomena driven by electron correlation will be studied with direct comparison between experimental data and theoretical calculations: 1) autoionization, 2) single- and two- photon double ionization, 3) shake and core-hole decay processes. To achieve the needed temporal resolution and the multiple-observable measurement, ultrafast (atto- and femto- second) lasers and a Cold Target Recoil Ion Momentum Spectrometer (COLTRILMS)-like spectrometer will be used to retrieve the transient 3-dimensioanl momentum as a function of time. The ultrafast lasers to be used include table-top XUV/x-ray attosecond lasers and facility-based free-electron-lasers. The target molecules are prototype or small molecules, such as N_2, CO_2, and C_2H_2.

Future Plans:

The initial phase of the project includes instrumentation development using mostly the PI's start-up fund and partially the equipment funding provided by this grant program. We will continue the construction of the XUV beamline and the spectrometer which are the in-house tools for this project. We will be building a single-shot FROG-type device for pulse duration measurement. Once the commercial pump laser is delivered as expected at the end of the year, we will perform the pulse duration diagnosis and start the sub-project of pulse shortening to single-cycle which will employ hollow fiber spectral broadening and pulse compression using chirped mirrors. Meanwhile, we will carry out experiments, in collaboration at existing attosecond XUV/x-ray beamlines, on autoionization of N_2 and/or C_2H_2. We aim to use laser aligned molecular target in these experiments. The experiment on N_2 will be carried out at an XUV beamline equipped with a magnetic bottle spectrometer and an XUV (~20-50eV)/NIR (800nm) dual-pulse scheme will be applied. The C_2H_2 experiment will be performed at the same beamline with the XUV laser being tuned to a photon energy of ~15 -20eV. Attosecond streaking measurement will be performed. Correspondingly experiments of the same molecular targets will be carried out at an existing XUV beamline that is equipped with a time-of-flight spectrometer for ion measurement. The ion fragmentation information will be combined with the electron data to obtain implicative information of the correlation between the electron and ion dynamics. (We take electron and ion spectra separately at the existing beamlines before the COLTRIMS-like spectrometer is complete and becomes functional.) We expect that LCLS II at high-repetition-rate will become operational next year and will submit proposals when the corresponding submission cycle is open. (The current submission cycle is for standard LCLS configurations, according to the LCLS website.)

Peer-Reviewed Publications Resulting from this Project (Project start date: 9/2020):

No publication to report.

Page is intentionally blank.

Physics of Correlated Systems

Chris H. Greene
Department of Physics & Astronomy, Purdue University, West Lafayette, IN 47907-2036
chgreene@purdue.edu

Project Scope

This project tackles systems, primarily in atomic, molecular, and optical physics as well as chemical physics, which exhibit strong mutual coupling between two or more different degrees of freedom. Such strong coupling or interaction is generally referred to as *correlations* or *entanglement* of those degrees of freedom. Examples include the coupling between spin and orbital angular momenta of a single photoelectron, a strong interaction in heavier atoms, which can be probed by measuring the spin-polarized angular distribution of the ejected particles. Often in the literature, however, the word correlation refers more narrowly to coupling of the spatial degrees of freedom of two or more electrons in the system. In our project, we interpret the phenomenon more broadly, in some cases meaning even the coupling of an electron's motion to two different fields, such as an internal Coulomb field in an atom or molecule and an external electric, magnetic, or electromagnetic field. Each of these different types of correlation can be understood most deeply by developing a theoretical description that is tailored to that specific problem, as opposed to trying to treat them as a perturbative add-on to the standard set of methods that usually start from an independent-particle or mean-field formulation.

This research project concentrates on developing theoretical treatments of such correlated systems, exhibiting correlations between strongly coupled degrees of freedom. Importantly, correlations are not merely an annoyance for theorists: they have a key role in all forms of chemical reactivity and energy transfer. Major challenges still remain even for simple systems such as electron dynamics in an individual atom, negative ion, or small molecule, or in the coupling of electronic and dissociative degrees of freedom in molecules. Hence it is frequently desirable to tackle highly correlated phenomena using a method that builds in the key correlations from the outset. Our studies develop such theoretical techniques and then apply them to problems where the coupling of multiple degrees of freedom has a controlling influence on the phenomena of interest. Some of our theoretical projects are aimed at interpreting experiments that have been carried out which have had only a limited theoretical interpretation or understanding, while others attempt to predict new opportunities for future experiments relating to photofragmentation, chemical reactivity, and energy transfer.

Recent Progress

(i) Few-body collisions in molecular physics and frame transformation theory

Some of the most challenging processes in molecular physics are those that involve the energy interconversion between electronic and vibrational/dissociative degrees of freedom, because such processes inherently hinge on a breakdown of the Born-Oppenheimer approximation. Indeed, there remains a need for a fully quantitative description of electron-nuclear correlation that shows how energy gets interconverted between electronic and nuclear degrees of freedom. At first glance, dissociative recombination might initially seem simple, when the target of the incident electron is a small diatomic or triatomic molecular ion. But it is challenging for standard theoretical methods because there is no simple, direct dissociative pathway to visualize or compute, in contrast to ordinary dissociative recombination or attachment collisions that

follow the Bates-type mechanism. One of the prototype collision systems dominated by indirect recombination is an electron collision with HeH^+ at low energies where there is no identifiable direct dissociative Born-Oppenheimer potential curve.

An exciting development during the past year was the completion and publication of new results obtained for the first time, after years of storage ring construction, with a very cold (<10K) ion storage ring experiment at the Cryogenic Storage Ring (CSR) in Heidelberg. Their experiment measured the dissociative recombination of cryogenic molecular HeH^+ ions that collide with low energy electrons. This permitted the sharpest test of theory yet, as it measured this process at low energy with sufficient energy resolution and sufficiently low rotational temperatures to permit the observation of individual resonances. And in fact their new experiment exposed inaccuracies in previous theory published by many groups including our own. Our new variant of the energy-dependent frame transformation theory has now been implemented in order to quantitatively test the improved theory, in collaboration with the Prague research group of Roman Curik. Following the development and careful benchmarking of the new formulation that we denote as the backpropagated frame transformation method [2], its application to describe the new HeH^+ experiment has proven to give a significant improvement [1] over all previous theoretical implementations of the rovibrational frame transformation method in combination with multichannel quantum defect theory. We are continuing to work on the theory with the Curik group to treat dissociative recombination and vibrational autoionization in systems that have more than one relevant ionic potential curve, as is the case for the gerade symmetry of H_2. This will represent a major expansion of these theoretical capabilities.

Yet another question relates to how much the large mass ratio between the heavy and light particles controls the electron-nuclear correlation phenomena occurring in H_2. Reference [3] by the P.I. with graduate student Michael Higgins in the list of publications below explored this by tackling one of the most extreme mass ratios where the Born-Oppenheimer approximation is likely to be unsuccessful, where the protons are replaced by positrons. In that study, both elastic and inelastic collisions between positronium 1s and positronium 2s atoms were treated in a 4-particle hyperspherical coordinate treatment. Despite having a mass ratio of unity, the Born-Oppenheimer representation, including channel coupling, is nevertheless shown in [3] to successfully describe the inelastic collision physics once nonadiabatic couplings among a few channels are incorporated. This is a fundamental collision process that could be relevant to the eventual creation of a positronium gamma ray laser.

While the rovibrational frame transformation can be viewed as a treatment of correlated electronic and nuclear motions, the correlation of an electron with the fields of two fixed ions or one ion and one atom, e.g. in highly excited states of a diatomic molecule, is a purely electronic problem to an excellent approximation. With postdoc Teri Price, we formulated a first treatment [4] of this class of correlations using the local frame transformation which involves a transformation between spherical and prolate spheroidal coordinates. That study built on the experience that we have gained by developing methods to treat an unusual regime of very high energy states of the H_2^+ molecule, and at very large internuclear distances on the micron scale.[5]

We have benchmarked the simplest version of the frame transformation theory of such collisions involving electron-nuclear correlations, by comparing a semi-realistic model of e-H_2^+ collisions with an essentially exact calculation.[7] The upshot of that study was that in the low energy range, extending over approximately 1 eV or thereabouts, the frame transformation theory

combined with multichannel quantum defect theory does reasonably well in describing the complex resonance structures that an exact calculation produces in a dissociative recombination calculation. The most significant discrepancies are somewhat infrequent isolated occurrences of a low principal quantum number perturbing state that is sometimes located at a slightly shifted incorrect energy, and our current efforts, almost ready to submit for publication, indicate that this small shift can be made nearly exact by implementing an improved energy-dependent frame transformation treatment. In addition to the value of this study [7] in benchmarking the approximate frame transformation theory, it has at the same time provided the first estimate of the ungerade contribution to the H_2^+ dissociative recombination cross section. We view this as a prototype system that will also pay dividends in the study of other systems, especially polyatomic dissociative recombination.

(ii) **Extreme correlation regime in negative ion photodetachment**

Atomic negative ions, even comparatively simple ones possessing just two valence electrons, have for many years served as prototypical systems for the observation of strong electron-electron correlations. One of the most dramatic regimes arises in processes where a negative ion absorbs a photon that excites two or more electrons to a high degree of excitation, after which the system decays by autodetachment, with one electron ejected and the remaining neutral atom left in a highly excited state. [6] An impressive series of experiments in such systems, specifically the alkali-metal negative ions, has been undertaken in recent years by the group of Dag Hanstorp in Gothenberg, Sweden. [See, e.g., Phys. Rev. Lett. 108, 033004 (2012); Eur. Phys. Lett. 106 (2014); Phys. Rev. A 88, 053410 (2013);] Some of their most striking experiments were carried out in the series of negative ions K^-, Na^-, and Cs^-, where absorption of an ultraviolet photon produces high double excitation and autodetachment

These calculations, which were carried out by the P.I. and graduate student Matt Eiles (who completed his PhD in May, 2018, and was a finalist for the DAMOP Thesis Award), required a significant enhancement of our two-electron R-matrix computer codes, in a number of ways.[6] First, to get more (and more accurate) radial basis states, which were needed to reach convergence in these larger box sizes and higher degrees of excitation, we switched over to a B-spline method to solve for the box-confined radial atomic eigenfunctions. This change allowed us to include up to 100 radial functions per partial wave, a major improvement. Second, we implemented an R-matrix propagation scheme to handle the very strong long-range couplings in the Hamiltonian outside the R-matrix box radius, where exchange could be neglected. Ref.[6] achieved quantitative agreement with experiment, even on the comparatively small and sensitive partial photodetachment cross sections that leave the residual atom in states of high energy and angular momentum, and also a detailed physical interpretation.

Future Plans

A graduate student, Yimeng Wang, has nearly completed our first theoretical treatment of 2-photon and 3-photon ionization of atoms with two valence electrons, concentrating on photoelectron angular distributions in the vicinity of high doubly excited states up to the n=3 ionization threshold. That energy range has been important for deriving an understanding of the role of strong final state charge-dipole interactions, a consequence of the so-called 'accidental degeneracy' of the $He^+(n=3)$ levels. Her initial detailed calculations are carried out for atomic helium, focusing on the role of the even parity doubly excited states which have received far less

attention to date than the extensively investigated odd parity J=1 states probed in single photon studies. Once our methodology is verified, we hope to broaden the treatment into the alkaline earth atoms and treat the combination of autoionizing intermediate and final states, whose decay is mediated by either electron-electron interaction or spin-orbit coupling.

A major project that expected to get finished within the coming year is a new full implementation of rovibrational frame transformation theory in the more complex regime where there are multiple Born-Oppenheimer potential curves of the positively charged molecular target ion in a dissociative recombination or photofragmentation process. This major extension of our previous efforts will build on some of our preliminary evidence that a variant of the theory which incorporates the energy-dependence of the fixed nuclei scattering parameters can give improved cross sections for processes such as dissociative recombination and inelastic excitation over a broader energy range. While the simplest (energy-independent) variant of frame transformation theory yielded excellent results over small energy ranges, in comparison with other theories as well as experiment, and permitted the solution of some highly challenging problems such as indirect dissociative recombination in diatomics and polyatomics with up to 5 atoms, its quantitative limitations are still not well understood. Moreover, we anticipate completing a more extensive implementation of the spherical-to-spheroidal coordinate frame transformation to treat highly excited long-range states of the Sr_2^+ molecule.

One project related to ultrafast science we are continuing to work on relates to a recent theoretical treatment by the Dresden group of J.M. Rost, which demonstrated that nonadiabatic turn-on and turn-off of a laser pulse can result in enhanced ionization. Our group has begun an exploration of this phenomenon, in collaboration with the Rost group, to understand its wider applicability as well as its limitations. Preliminary results suggest that there is a quantum mechanical interference of two dominant pathways, which can be sometimes constructive and sometimes destructive.

Peer-Reviewed Publications Resulting from this Project (2018-2020)

[1] *Dissociative recombination of Cold HeH^+ Ions,* Roman Curik, David Hvizdos, and C H Greene, Phys. Rev. Lett. **124**, 043401 (2020); DOI: 10.1103/PhysRevLett.124.043401
[2] *Backpropagated frame transformation theory: A reformulation,* David Hvizdos, C H Greene, and Roman Curik, Phys. Rev. A **101**, 012709 (2020); DOI: 10.1103/PhysRevA.101.012709
[3] *Low-energy scattering properties of ground-state and excited-state positronium collisions,* M. D. Higgins, K. M. Daily, and C H Greene, Phys. Rev. A **100**, 012711-1 to -10 (2019); DOI: 10.1103/PhysRevA.100.012711
[4] *Local frame transformation theory for two classes of diatomic molecules,* T. J. Price and C. H. Greene, Molecular Physics **117**, 3171-3183 (2019); DOI: 10.1080/00268976.2019.1617446
[5] *Semiclassical Treatment of High-Lying Electronic States of H_2^+,* T. J. Price and C. H. Greene, J. Phys. Chem. A **122**, 8565-8575 (2018); DOI: 10.1021/acs.jpca.8b07878
[6] *Extreme correlation and repulsive interactions in highly excited atomic alkali anions,* M. Eiles and C H Greene, Phys. Rev. Lett. **121**, 133401-1 to -6 (2018); DOI: 10.1103/PhysRevLett.121.133401
[7] *Dissociative recombination by frame transformation to Siegert pseudostates: A comparison with a numerically solvable model,* D Hvizdoš, M Vána, K Houfek, C H Greene, T N Rescigno, C. W McCurdy, R Curík Phys. Rev. A **97**, 022704-1 to -12 (2018). DOI: 10.1103/PhysRevA.97.022704

Manipulating and Probing Ultrafast Atomic and Molecular Dynamics

Robert R. Jones, Physics Department, University of Virginia
382 McCormick Road, P.O. Box 400714, Charlottesville, VA 22904-4714
bjones@virginia.edu

I. Project Scope

This project focuses on the exploration and control of dynamics in atoms, small molecules, and micro- or nano-structures driven by strong fields. Our goal is to exploit strong-field processes to implement novel ultrafast techniques for manipulating and probing coherent electronic and nuclear motion within atoms, molecules, and on surfaces. This motion occurs over attosecond to picosecond timescales. Ultimately, we hope to obtain a more complete picture of correlated multi-particle dynamics in molecules and other complex systems.

In our principal experiments, gas phase atoms and molecules are exposed to short pulses of electromagnetic radiation with frequencies ranging from THz into the XUV spectral regions, and with durations from picoseconds to attoseconds. The pulses coherently induce and/or probe dynamics in the electronic, vibrational, and rotational degrees of freedom of the targets. In one line of experiments, we hope to clarify the roles of both electron correlation and coupled electronic-nuclear dynamics in directional multi-electron dissociative ionization of small molecules. In another, in collaboration with the DiMauro-Agostini group at Ohio State, we are developing novel techniques for directly probing the effective electronic potential experienced by an outgoing attosecond photoelectron wavepacket during the first femtosecond, or so, after its release. Lastly, we are exploiting large electric field enhancements near nano- and micro-structured metals to produce high-energy electron bursts which can serve as fast probes of optical fields as well as molecular structure and dynamics.

II. Recent Progress

We previously showed that high-energy (> 5keV) electron bursts can be produced by exposing nano- and micro-structured metals to intense, single-cycle THz pulses [1]. Local THz-field enhancements greater than 3000x have been achieved at the surface of nanotips, enabling tunneling emission and subsequent acceleration of the electrons over subpicosecond time-scales. We are continuing to explore the use of nano- or micro structured metals as a means of greatly enhancing THz field strengths for orienting molecules or influencing strong field electron dynamics. In addition, we are pursuing the use of THz induced electron field-emission as a source of localized subpicosecond electron pulses for inducing and/or probing dynamics in molecules, or on surfaces. During the past year, much of our effort has focused on the development of a new technique that employs electron field emission from nanotips as an *in situ*, sub-wavelength probe of the time-dependent electric field in a focused THz beam in vacuum.

Our ultrafast waveform imaging method utilizes two pulses, with a variable time-delay, and takes advantage of two principal features of high-energy electron field emission driven by intense (near) single-cycle THz pulses. First, the emission of high energy electrons is temporally confined to a brief window near the peak of one half-cycle of the THz field. Second, over a wide range of THz field strengths, both the maximum energy of the emitted electrons and the total high energy electron yield are proportional to the peak electric field at the tip. Accordingly, if a relatively intense single-cycle THz “source” pulse generates high energy electrons from a

nanotip, then when a second relatively weak “signal” waveform is temporally scanned through the source field, the changes in the (net) maximum field at the tip will be directly reflected in the net high-energy electron yield. By repeatedly scanning the relative delay of the signal and source pulses as the spatial position of the nanotip is varied, one can map out the spatio-temporal waveform of the signal field. As an example, images of the time-dependent field along the longitudinal and transverse directions within a focused THz beam, appear in Figure 1. The Gouy phase shift, which occurs along the beam path as one moves through the focus, is clearly visible.

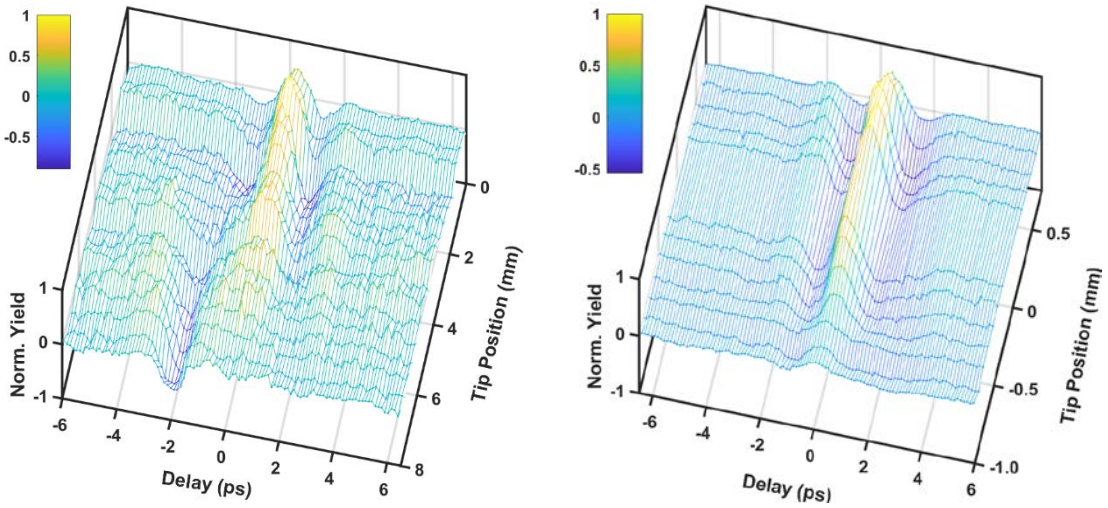

Figure 1: Electric field in a focused THz beam, measured as the variation in the high-energy electron emission from a ~100nm tungsten tip. Changes in the waveform as a function of position along (longitudinal) and across (transverse) the focused beam are shown in the plots on the left and right, respectively.

While non-linear optical techniques, like electro-optic sampling, also allow for full spatio-temporal sampling of THz waveforms, the need to locate a non-linear crystal where the field is to be sampled precludes their use for many potential applications. As an alternative, nano-tips can be easily and finely positioned near other objects, throughout a tight sample volume, and in high-vacuum. A manuscript describing the technique is in preparation.

III. Future Plans

With the slow but steady restart of our laboratory research following the full COVID-19 shutdown, we intend to make progress on several fronts. First, we will characterize the spatial distribution of the high-energy electron emission from THz irradiated nanotips, to determine the utility of this ultrafast electron source for initiating and/or probing molecular dynamics. Second, we hope to return to our investigation [2,3] of the roles of electron correlation [4] and coupled electronic- nuclear dynamics in directional multi-electron dissociative ionization of small molecules, through pump-probe experiments with bichromatic fields. Third, once travel between labs can resume, in collaboration with the DiMauro group at OSU we plan to initiate new time-resolved measurements (such as those described below), to demonstrate the ability of attosecond photo-electrons to capture ultra-fast changes in the molecular binding potentials of their parent ions.

When an attosecond photoelectron wavepacket is created in the presence of an oscillating field, its momentum and acceleration (averaged over the first quarter- oscillation of the dressing field) are directly mapped to the final electron energy spectrum as a function of the delay between the ionizing pulse and the dressing field [a]. Thus, for attosecond XUV photoionization in a near-infrared field, the coarse characteristics (in particular, the average depth U and gradient α) of the binding potential traversed by the electron during the first femtosecond, or so, after its birth can be recovered from the delay-dependent photoelectron spectrum. In collaboration with the DiMauro-Agostini group at OSU, we previously demonstrated this measurement concept using RABBITT+ [a], a modified version of a standard technique originally developed to characterize XUV attosecond pulse trains [5].

Notably, however, our RABBITT+ measurements with atoms did not take advantage of the full power of the approach, namely, that the departing photoelectron captures information on the binding potential during a brief, ~1 fs, interval. Indeed, using the same basic method, it should be possible to monitor changes in molecular binding potentials resulting from additional electronic or nuclear dynamics taking place over longer, or comparable, time scales. Accordingly, we have been planning experiments that can exploit this short measurement window to capture changes in a molecular binding potential due to coherent nuclear dynamics induced by a preceding laser pulse. The measurements will be enabled by the improved electron energy resolution, increased harmonic flux, and enhanced low-energy electron collection efficiency of an updated attosecond beam line at OSU.

We will consider I_2 as an example. We will use a visible, OPA-generated, ~50fs pump pulse at 513 nm to resonantly (and efficiently) excite I_2 molecules in the X $^1\Sigma_g^+$ ground state to B $^3\Pi_u^+$ [6]. This excitation will launch a vibrational wavepacket for which the internuclear separation, R, changes by nearly a factor of 2 (from approximately 5 to 9 a.u.) as the B-state vibrational wavepacket oscillates with a period of 700 fs. The coarse characteristics, U and α, of the electronic binding potential will be probed by performing RABBITT+ measurements at different time delays during the wavepacket evolution. Low energy photoelectrons (and RABBITT+ sidebands) resulting from ionization of the X and B states will be distinguished by the differences in their energies using the improved resolution of the new TOF electron spectrometer. Overlapping TOF signals will be minimized by tuning the wavelength of the OPA generated infrared pulses used for the XUV generation and dressing fields.

Several features make this system an excellent test case for exploring the effectiveness of the time-resolved RABBITT+ probe method. First, the long vibrational period ensures that the wavepacket will be nearly stationary during the 50fs infrared-dressing and XUV ionization pulses available for the RABBITT+ probe. Second, the large changes in R should result in significant, readily detected, changes in the relevant potential parameters. Third, due to the angular dependence of the X→B transition moment, molecules that are excited will be preferentially aligned along the 513nm pump laser polarization. By employing a TOF electron spectrometer with a narrow angular acceptance, and rotating the pump laser polarization, we can choose to measure electrons that are ejected along or perpendicular to the internuclear axis as a function of time delay. Correspondingly, we can characterize the effective potential along, perpendicular to, or at any intermediate angle relative to the molecular axis. Unlike in the previous measurements in Ne and He for which a separate reference atom was used to

determine the XUV phase, here we will seek to determine changes in U and α by comparing the photoelectron spectra as a function of pump-probe delay and/or pump laser polarization.

IV. References

[1] S. Li and R.R. Jones, "High-Energy Electron Emission from Metallic Nano-tips Driven by Intense Single-Cycle Terahertz Pulses," Nat. Comm. **7**, 13405 (2016).

[2] K. J. Betsch, D. W. Pinkham, and R. R. Jones, "Directional Emission of Multiply Charged Ions During Dissociative Ionization in Asymmetric Two-Color Laser Fields," Phys. Rev. Lett. **105**, 223002 (2010).

[3] X. Gong, M. Kunitski, K.J. Betsch, Q. Song, L. Ph. H. Schmidt, T. Jahnke, Nora G. Kling, O. Herrwerth, B. Bergues, A. Senftleben, J. Ullrich, R. Moshammer, G.G. Paulus, I. Ben-Itzhak, M. Lezius, M.F. Kling, H. Zeng, R.R. Jones, and J. Wu, "Multielectron Effects in Strong-field Dissociative Ionization of Molecules," Phys. Rev. A **89**, 043429 (2014).

[4] V. Tagliamonti, H. Chen, and G. N. Gibson, "Multielectron Effects in Charge Asymmetric Molecules Induced by Asymmetric Laser Fields," Phys. Rev. Lett. **110**, 073002 (2013).

[5] P.M. Paul, E.S. Thoma, P. Breger, G. Mullot, F. Auge, Ph. Balcou, H.G. Muller, and P. Agostini, "Observation of a Train of Attosecond Pulses from High Harmonic Generation," Science **292**, 1689 (2001).

[6] V. Tagliamonti, H. Chen, and G. N. Gibson, "Internuclear-separation-resolved asymmetric dissociation of I2 in a two-color laser field," Phys. Rev. A **84**, 043424 (2011).

V. Peer-Reviewed Publications Resulting from this Project (2018-2020)

[a] D. Kiesewetter, R.R. Jones, A. Camper, S.B. Schoun, P. Agostini, and L.F. DiMauro, "Probing Electronic Binding Potentials with Attosecond Photoelectron Wavepackets," Nature Physics **14**, 68 (2018).

Real-time observation of multi-electron processes in atoms and diatomic molecules

Guillaume Marc Laurent (PI)
Department of Physics, Auburn University, Auburn, AL, 36849
Email: glaurent@auburn.edu

Project Scope:

The main goal of this project is to implement a reliable experimental approach to observe, in real-time, electron dynamics in atoms and molecules at the attosecond time scale. Despite significant efforts that are underway, time-resolved studies at the attosecond time scale are still restricted to a few benchmark systems possessing an electronic structure sufficiently simple to make it possible to isolate a particular electronic process and univocally dissect its dynamic [1-7]. We are currently working on the development of an experimental system, which combines high-repetition-rate attosecond sources and sophisticated multi-particle imaging techniques, such as the well-established reaction microscope or COLTRIMS (Cold Target Recoil Ion Momentum Spectroscopy) in order to investigate the correlated electron dynamics in atoms and small molecules. This new capability will offer promising possibilities to yield a deeper insight into atomic and molecular processes and ultimately to identify ways to control them. In addition, we expect that the multi-differential cross section measurements carried out in this project will foster the development of new theoretical models that are essential for a quantitative interpretation of experiments on complex systems.

Recent Progress:

At the beginning of the current report period, our experimental setup, composed of a laser system, an attosecond light source, an XUV/IR interferometer, a velocity-map imaging system, and XUV spectrometer was fully operational. In addition, we have also completed the technical development (stabilization system for the interferometer) required for performing long-term experiments with multi-particle imaging techniques. Over the last year, we have completed two additional mains objectives: (1) we have developed an attosecond pulses shaping technique and used it to control the electron emission from atoms, and (2) we have completed the development of our multi-particle imaging system.

1- Attosecond pulse shaping and control of the electron emission from atoms (Project Leader: J. Vaughan, graduate student)

Coherent control of quantum phenomena in matter through its interaction with light is a fast-growing field in ultrafast science driven by the ultimate goal of controlling the complex dynamical properties of quantum systems at the heart of many scientific fields. Over the last four decades, femtosecond laser technology has led to remarkable advances in our ability to control the ultrafast femtosecond dynamics in a vast number of systems (from simple to complex molecular systems, clusters, nanostructures, ...). With the recent development of extreme

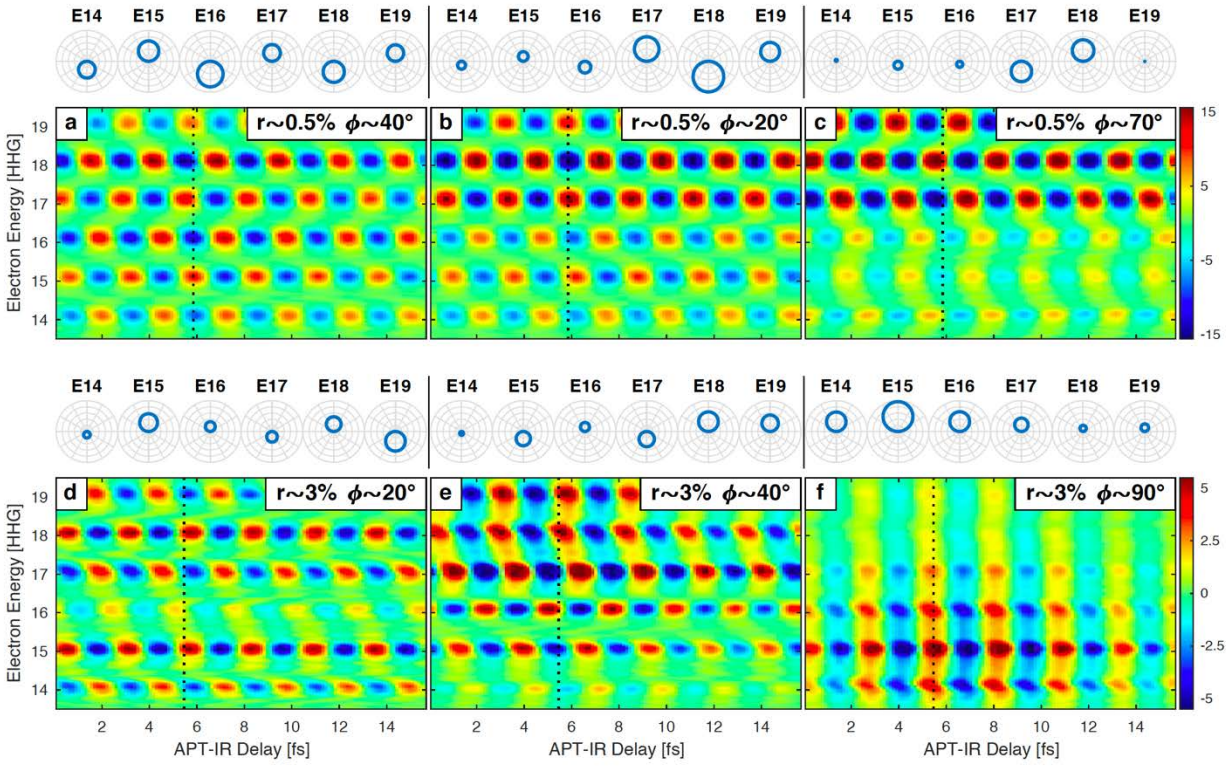

Figure 1: Density plot of the asymmetric component of the photoelectron emission (in %) as a function of the time delay between the APT and IR fields and the photoelectron energy, for different intensity ratio *r* and relative phase ϕ between the two colors of the HHG driving field.

ultraviolet (XUV) light sources with attosecond duration, new capabilities emerge for controlling quantum dynamics in matter with an unprecedented level of precision down to the natural timescale of electron motion. Even though the first attosecond pulses were generated nearly two decades ago, their use for controlling electron dynamics in matter has been elusive so far. Attosecond control has been mostly achieved with pump/probe schemes where an attosecond-pump pulse triggers a given electronic process and a phase-locked femtosecond-probe field is used to steer its dynamics. The system under scrutiny is thus controlled by varying the time delay between the two pulses. Such an approach has been successfully employed to manipulate benchmark systems such as the electronic charge distribution within a molecular target or the photoelectron emission from atoms.

Despite these impressive proofs-of-principle, attosecond control of quantum phenomena in matter is still in its infancy, though, mainly because attosecond pulse shaping techniques are still developing. Even though several schemes have already been reported to tailor both the spectrum and the polarization of these pulses, shaping their spectral phases for attosecond control, on the other hand, still remains a challenging endeavor for the attosecond community. Indeed, the low intensity of the attosecond pulses currently produced via high-harmonic generation (HHG) together with the high absorption rate of XUV radiation by most optical materials circumscribe the use of usual pulse shaping techniques (like chirped mirrors, ...) to manipulate the spectral phase of the pulses after generation. An alternative approach consists of shaping the spectral phases of attosecond pulses directly during the generation process. Within the widely

accepted three-step model describing attosecond pulse generation via high-harmonic generation (1-ionization, 2-propagation in the laser electric field, and 3-recombination), the spectral phases of the frequency components making up the pulse are directly related to the recombination times, which in turn are defined by the electron wavepacket trajectories (also referred to quantum orbits) in the driving laser field. By tailoring the temporal waveform of the femtosecond driving field, the quantum orbits and the recombination times can then be tuned giving some control over the spectral phases of the APT

Two-color femtosecond waveforms made of a fundamental field and its second harmonic have been proved to be very efficient to manipulate quantum orbits in the HHG process. The literature is rich with experimental and theoretical studies reporting the dependence of the resulting APT's spectrum on the temporal profile of such synthetized waveforms. On the other hand, the dependence of the APT's spectral phases on the temporal profile of the two-color field still remains elusive, though. Over the last year, we have investigated how these phases can be manipulated by varying the intensity ratio and the relative phase between the two components of the driving field. We show that the spectral phases exhibit high tunabilty for an intensity ratio between the two colors in the range of 0.1 to 5%. As an application for such a spectral pulse shaping technique, we have performed a coherent control experiment where the photoelectron emission from atoms generated by tailored attosecond pulses is manipulated along the direction of polarization of the light by tuning the spectral phases of the APT. Attosecond pulse trains with tailored spectral components (amplitude and phase) were used to ionize an atomic target in the presence of a weak IR field. An asymmetric electron emission along the polarization vector was produced through the interference between electron wavepackets generated by one- and two-photon transitions [8]. The photoelectron emission pattern was then controlled by tuning the spectral components of the APT (see figure 1).

The results of this work have been presented at the last DAMOP meeting, and they have been recently submitted for publication in a peer-reviewed journal.

2- Completion of the multi-particle imaging system (Project Leader: S. Burrows, graduate student)

Another major part of the project was the development of the multi-particle imaging system (COLTRIMS). This includes the design and assembly of both the spectrometer and the end-station chamber, as well as the development of the data-acquisition system and the data analysis program. The spectrometer has been designed and built in-house and its assembly is currently at the stage of being completed. Concurrently, we have also assembled and tested the data acquisition system and we have developed expertise with the multi-parametric data analysis. It is important to note that the data analysis for COLTRIMS-type experiment is equally time-consuming as setting up the experiment itself. In order to develop our skills with the data analysis program, we have analyzed some photo-ioinization data taken at LBLN and generously provided to us by the research group of T. Weber. Some of the results of the calibration process are shown in figure 2.

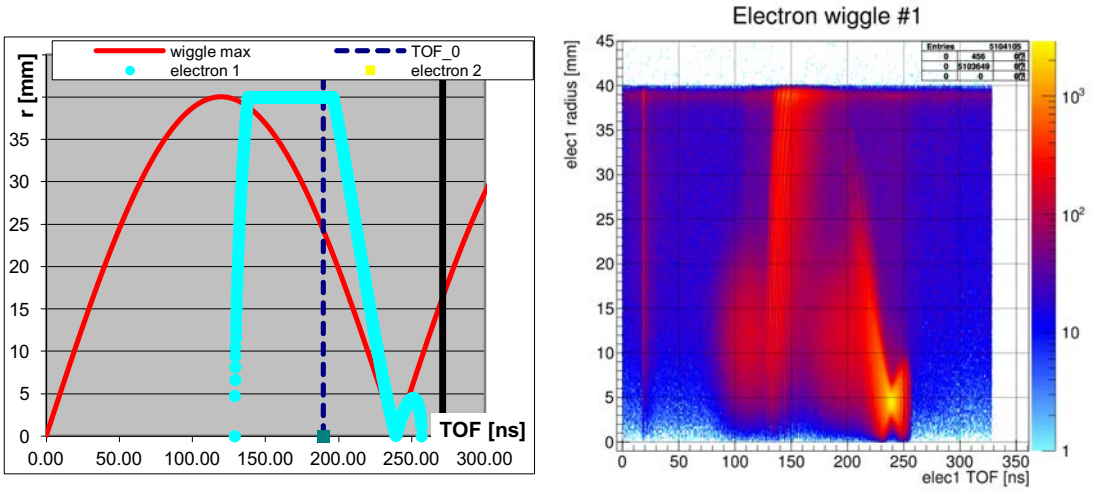

Figure2: Snapshot of the data analysis procedure: calibration of the magnetic field used to confine photoelectrons on the detector. Left: simulated data – Right: experimental data.

Future Plans:

At this point, all the technical development of the project has been completed, which includes the development and characterization of the attosecond source, the development of the stabilized-interferometer system, and the design and assembly of the multi-particle imaging system. For this upcoming year, we then plan to perform measurements of the correlated electron dynamics at the attosecond time scale. Preliminary measurements will be carried out first on benchmark systems (He, Ar …). Then, we will apply our new experimental approach to more complex molecular systems like CO_2, or CH_4.

References:

[1] M. Drescher et al., Nature 419, 803 (2002)
[2] E. Goulielmakis et al., Nature 466, 739 (2010)
[3] M. Schultze et al., 328, 1658 (2010)
[4] K. Klünder et al., Physical Review Letters 106, 143002 (2011)
[5] M. Uiberacker et al., Nature 446, 627 (2007)
[6] P. Eckle et al., Science 322, 1525 (2008)
[7] A. N. Pfeiffer et al., Nature Physics 7, 428 (2011)
[8] G. Laurent et al. Physical Review Letters 109, 083001 (2012).

Peer-Reviewed Publications Resulting from this Project (Project start date: 08/2017)

1- *"Design of an optically-locked interferometer for attosecond pump-probe setups"*, J. Vaughan, J. Bahder, B. Unzicker, D. Arthur, M. Tatum, T. Hart, G. Harrison, S. Burrows, P. Stringer, and G. M. Laurent. Optics Express, **27**, 30989 (2019)

2- *"DAVIS: A Direct Algorithm for Velocity-map Imaging System"*, G. R. Harrison, J. C. Vaughan, B. Hidle, and G. M. Laurent, Journal of Chemical Physics, **148**, 194101 (2018)

Beating Electronic Decoherence

Wen Li, Wayne State University, Detroit, MI, 48202 (wli@chem.wayne.edu)
H. Bernhard Schlegel, Wayne State University, Detroit, MI, 48202 (hbs@chem.wayne.edu)

Program Scope

This research project aims to beat electronic decoherence in molecular systems in two aspects: (1) developing experimental approaches that will capture the extremely fast decoherence process in the time-domain for the first time. (2) devising atomistic schemes that can suppress decoherence and produce long-lived electronic coherence in molecular system. In the past decade, the production and probing of coherent electron motion has been one of the major foci of attosecond spectroscopy. However, only a handful of atomic and molecular systems have been shown experimentally to manifest such dynamics while many more molecular systems have been modeled theoretically to exhibit electronic coherence. Recently, a potential cause for the discrepancy between theory and experiment was suggested by a few theory groups. They proposed that due to the delocalized nature of the nuclear wavepacket and different topologies of potential energy surfaces of the cation states in the Franck-Condon region, electronic decoherence is extremely fast, even before significant nuclear motion can take place. This is significant because long-lived electronic coherence is likely to enable manipulation of electronic and nuclear dynamics to steer chemical reactions, which is a long-standing goal of chemistry and physics. If this decoherence mechanism is confirmed experimentally, another important question arises: is it possible to beat electronic decoherence to produce long-lived electronic motion? The project aims to answer these questions with a joint experimental-theoretical approach.

Recent Progress

The Schlegel group has recently incorporated spin-orbit states in the Time-Dependent Configuration Interaction with Single Excitation and complex absorbing potentials (TDCIS-CAP) method. This will be used to model strong field dynamics of xenon and molecular systems containing heavy atoms such as iodine and bromine.

Future Plans

The Li group will develop two new complementary experimental methods to probe electronic decoherence: a two-beam pump-probe-streaking method and a two-beam pump-probe method. In the first method, by adding a weak orthogonal streaking mid-IR field with a wavelength ~2μm to the established 3D-*2eAS* setup, the time range of the double streaking technique will be increased to ~8 fs while maintaining a resolution of ~200 attoseconds. In the second approach, a strong-field carrier-envelope-phase (CEP)-resolved pump-probe setup will track the charge dynamics at time-delay greater than 3.5 fs while achieving a sub-femtosecond resolution. Combined with kinematically complete coincidence measurements between two electrons and multiple ions, the proposed experiments offer highly differential molecular-frame results that will help unravel complex dynamics. The methods will be applied to study various molecular systems such as methyl iodide and paraxylene and probe decoherence effect.

The Schlegel group will extend the TDCI code to monitor the direction of the ejected electrons, in order to simulate streaking experiments. In the TDCI simulations, ionization is modelled by using a complex absorbing potential (CAP) to remove the part of the wavefunction that has been driven sufficiently far from the molecule. The CAP absorbs electron density in all directions. To obtain directional information, the absorbing potential will be partitioned into 100-200 surface patches and contracted with the one electron density of the time-dependent wavefunction to provide time-dependent directional information for the ejected / absorbed electron density. Since the absorbed wavefunction is a superposition of ground and excited states of the ion, population analysis can be used to partition the density matrix into contributions from the various states of the ion. This analysis will yield channel dependent information for each direction.

Peer-Reviewed Publications Resulting from this Project (Project start date: 09/2020)

No publication to report

Early Career: First-Principles Tools for Nonadiabatic Attosecond Dynamics in Materials

Kenneth Lopata

Department of Chemistry, Center for Computation and Technology,
Louisiana State University, Baton Rouge, LA 70803

klopata@lsu.edu

Project Scope

The response of molecules and materials to intense and/or high energy light underpins a wide range of important processes such as light harvesting, radiation damage, and energy storage. At the atomistic level, many of the underlying mechanisms are poorly understood, especially the electron dynamics during and immediately following interaction with a laser pulse, as well as the resulting electron/lattice dynamics. A promising avenue for measuring these processes is time-resolved X-ray spectroscopy, which exploits both elemental/spatial specificity of X-ray absorption, as well as the ability to make short intense pulses. The resulting time-resolved spectra can be difficult to interpret as they involve features such as intensity modulation, subtle edge energy shifts, and transient pre-edge features. Going from observables as a function of time delay to actual electron dynamics in the system requires first-principles simulations. To address this, the overarching goal of this project is to develop quantum chemistry techniques for simulating attosecond electron dynamics and X-ray observables on equal footing. The primary focus is electronic dynamics and non-adiabatic electron/lattice effects in solid-state materials.

Recent Progress

During the past year of this project, we made progress in four distinct but inter-related directions related to inner shell-probed dynamics:

(I) Reconstructing Electron Dynamics from Time-Resolved X-Ray Absorption

X-ray transient absorption spectroscopy (XTAS) is a promising technique for measuring electron dynamics in molecules and solids with attosecond time resolution. In XTAS, the elemental specificity (and thus spatial localization) of X-ray absorption is exploited to relate modulations in spectra to changes in electron density. Interpreting these effects can be challenging, however, as they involve both intensity and frequency modulations. Simulations are an ideal tool to help “reverse” from time delay to real-time, i.e., reconstructing electron dynamics from the observed transient spectra. In contrast to simulations of the electron dynamics, there has been far less work on computing corresponding attosecond transient X-ray spectra from first-principles.

To address this, we have recently developed a first-principles method for computing attosecond XTAS in a molecules based on real-time time-dependent density functional theory (RT-TDDFT) with constrained DFT to emulate the state of the system following the interaction with a ultraviolet pump laser. Before moving on to more complex systems such as solids, we first validated our technique against a set of molecules including a diatomic (carbon monoxide), a ring with heteroatoms (aminophenol), and a charge transfer dimer (tetracyanoethylene—tetracyanoethylene). Fig. 1 shows the TR-XAS in the aminophenol molecule following a valence $\pi \rightarrow \pi^*$ excitation that results in density oscillations across the molecule. This is a prototypical example of a molecule with two distinct atoms (O and N) that can be probed with XANES. We find a general observation and useful rule of thumb: *the optical density decreases and the frequency blue-shifts at the times when there is an increased electron density around an absorbing atom.*

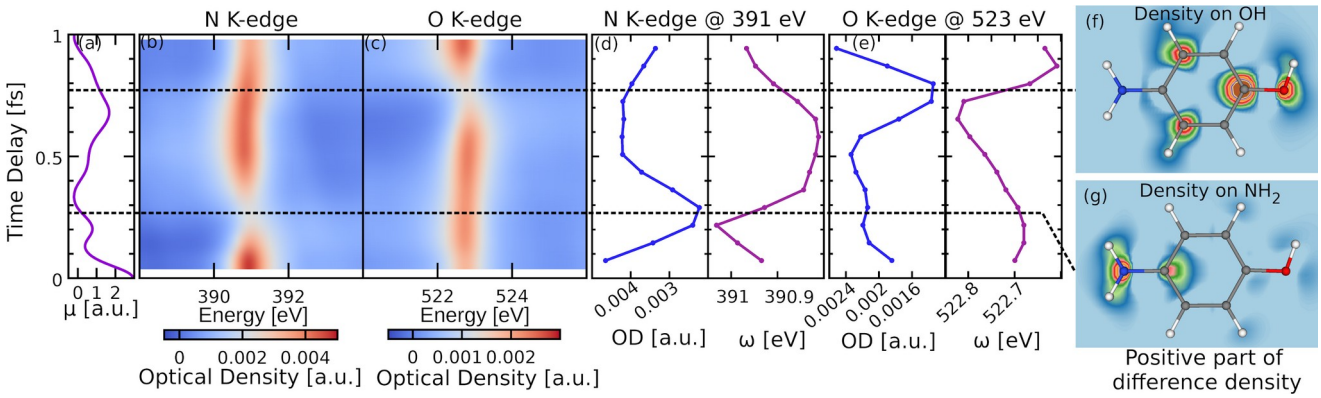

Figure 1: Simulated time-resolved nitrogen and oxygen X-ray absorption in aminophenol following UV pump excitation. The optical density decreases (b,c) and the peak blue-shifts (d,e) with increasing density around the absorbing atom (f,g). These results demonstrate how evolving electron densities can be reconstructed from TR-XAS measurements.

These optical density (OD) modulations can be interpreted in two ways. In a density picture, the increased charge around an atom reduces the transition probability for an inner-shell probe excitation from that atom. In an orbital picture, the OD corresponding to a particular orbital is reduced with increasing population. We also observe pre-edge features arising from transitions to depopulated orbitals. Since these only occur in excited molecules, and these transitions are at frequencies outside of the ground-state absorption, these "background-free" features maybe be advantageous experimentally. We have a publication detailing these findings [Chen2020].

(II) Field-Modulated X-Ray Absorption in Titania

Using our recent implementation [Lopata2020] of spin-orbit real-time TDDFT [Goings2016], we completed our efforts to simulate the effects of static fields on the X-ray absorption of anatase titania (TiO_2). Understanding how external fields can modify the electronic structure of semiconductors, and how this can be probed using x-ray absorption spectroscopy, is a critical first step towards simulating strong-field dynamics and time-resolved probes in these systems. We use a bulk-mimicking cluster approach, which allows for an all-electron simulation and rapid evaluation of hybrid DFT functionals. The experimental bulk anatase structure was cut to yield a Ti-centered finite cluster, which was then passivated with partially charged pseudo-hydrogen atoms at the boundaries. We find that *static field dressing of the system leads to a red-shift in the onset of the t_{2g} peaks and blue-shift in the e_g peaks in the Ti L-edge spectrum*. These shifts, which increase with field intensity, can be attributed to changes in the hybridization of the conduction band (3d) orbitals. These calculations indicate that fields can modify the electronic structure without geometry distortions, which can makes these transient modulations a promising candidate for time-resolved studies such as X-ray transient absorption. These results have been published recently [Darapaneni2020].

(III) Intruder-Free X-Ray Absorption Spectra

Real-time (RT) electronic structure methods, where the wavefunction or density matrix is propagated in time [Li2020], is a natural approach for computing linear-response and time-resolved inner-shell spectra. These approaches, however, can suffer from non-physical "intruder" peaks in their absorption spectrum when using atom-centered basis sets [Kadek2015]. These peaks are typically a result of a transition from a higher inner-shell edge to a high energy virtual state that is unphysically bound due to basis set limitations. This can limit the usefulness of RT methods for computing transient spectra, since an X-ray absorption spectrum might contain numerous spurious peaks or increased absorption amplitude in the spectral range of interest.

To address these issues, we have developed an approach where we use a filtered dipole operator (matrix) to weed out the transition amplitude between all unwanted molecular orbitals. Since this is only applied when computing the expectation value of the dipole moment, it keeps interaction with the laser field untouched. Thus, unlike complex absorbing potentials or phenomenological lifetimes, this method can be safely be utilized for simulating transient absorption spectroscopy. Fig. 2 shows an example of this technique applied to the L-edge spectrum in an argon atom. Traditional RT time-dependent density functional theory (gray line) exhibits two intruder peaks (denoted by stars), whereas our filtered approach (dashed line) gives perfect agreement with the expected linear-response spectrum (green). We have found that *this development is essential for simulating transient absorption in systems with a high density of states* (e.g., silica; discussed below), where the intruder peak problem is otherwise pathological. For this work, we have a completed manuscript that we will be submitting shortly [Yang2020].

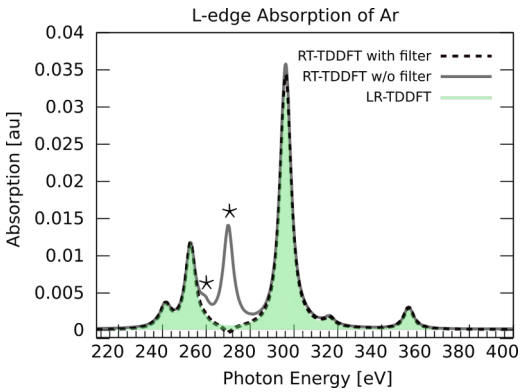

Figure 2: L-edge absorption of an argon atom computed using real-time TDDFT (gray) exhibits non-physical intruder peaks (⋆). Filtering the dipole operator to only include 2p orbitals (dashed) removes these spurious peaks.

(IV) Attosecond Transient Metallization in Insulators

Utilizing many of the tools of strong-field gas-phase studies, condensed matter materials have been the focus of much recent progress for attosecond studies. These experiments have shed light on interesting processes such as ban gap tunneling, carrier transport, high harmonic generation, and strong field damage. As with gas-phase studies, first-principles simulations of the transient spectra are invaluable for interpretation. These simulations can be challenging for conventional methods such as TDDFT, where traditional functionals qualitatively fail. Building on our successes with transient absorption [Chen2020], field-modulated XANES in semiconductors [Darapaneni2020], and our newly developed filtered XANES method [Yang2020] we have shown how transient inner-shell absorption of α-quartz (SiO_2) during a transient metallization process can be simulated from first principles. We use a bulk-mimicking cluster (Fig. 3(a)) and the optimally tuned range-separated hybrid LC-PBE0* to capture band-gap narrowing during interaction with an intense infrared pulse. Our results (Fig. 3(b)) show a drop in the optical density of the lowest energy Si L-edge transition that is correlated with the transient conduction band population. These results are consistent with both the experiment [Schultze 2013], as well as few-band time-dependent Schrodinger equation calculations [Krausz 2014]. Since *this approach requires absolutely no parametrization from experiment*, it is likely to be valuable for interpreting complicated experimental transient spectra without resorting to modeling. We have a completed manuscript draft that will be submitted shortly [Sissay2020].

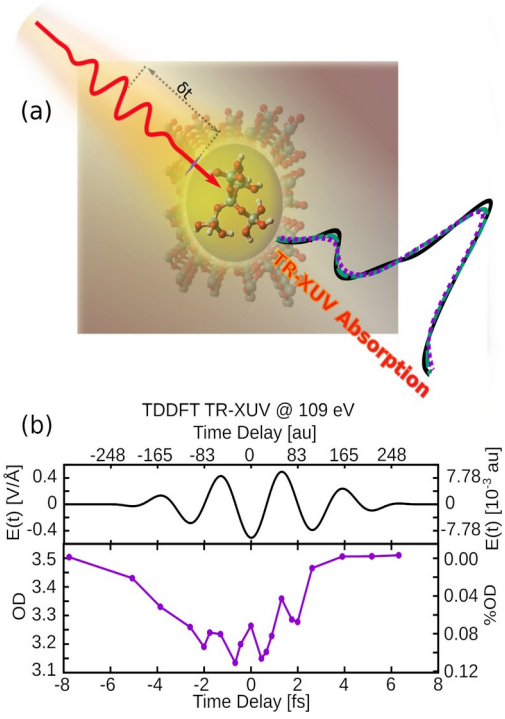

Figure 3: (a) Bulk-mimicking SiO_2 cluster used to compute (b) transient Si L-edge absorption during strong-field induced transient metalization.

Future Plans

In the coming year, we will continue work on simulating transient X-ray absorption in molecules to further validate our observation that local density around an atom can be measured by absorption modulations. We aim to link up with planned future XFEL experiments (e.g., at LCLS). Going forward, the main emphasis will be solid-state systems subjected to fields near their breakdown threshold, starting with diamond which has been studied previously. From a methods standpoint, we will continue to develop improved descriptions of rapid valence excitations, such as using linear-response vectors to initialize the dynamics. Additionally, we will resume implementation of Ehrenfest dynamics, such that coupled electron/nuclear dynamics can be incorporated into both the molecular and solid-state calculations. This will enable us to approximately capture bond softening, as well as compute femtosecond-scale electron-lattice coupled dynamics for materials subjected to fields near the breakdown threshold.

References

[Goings2016] J. Goings, J. Kasper, F. Egidi, S. Sun, X. Li,"Real time propagation of the exact two component time-dependent density functional theory", *J. Chem. Phys.* **145**, 104107 (2016).

[Kadek2015] M. Kadek, L. Konecny, B. Gao, M. Repisky, K. Ruud, “X-ray absorption resonances near $L_{2,3}$-edges from real-time propagation of the Dirac-Kohn-Sham density matrix”, *Phys. Chem. Chem. Phys.* **17**, 22566 (2015).

[Krausz 2014] F. Krausz and M. I. Stockman, “Attosecond metrology: from electron capture to future signal processing”, *Nat. Photon*. **8**, 205 (2014).

[Lopata2020] K. Lopata, M. Sereda, Y. Zhang, N. Govind, "UV-Vis and X-ray $L_{2,3}$ Edge Spectroscopy from Two-Component Relativistic Real-Time Time-Dependent Density Functional Theory" (in preparation).

[Schultze 2013] M. Schultze et al.,"Controlling dielectrics with the electric field of light", *Nature* **493**,75 (2013).

[Sissay2020] A. Sissay, M. Chen, M. Yang, A. Meyer, K. Lopata, “Time-Dependent DFT Simulations of Si L-edge Probed Transient Metallization in Silica” (in preparation).

[Yang2020] M. Yang, A. Sissay, M. Chen, K. Lopata, “Intruder Peak-Free Inner-Shell Spectra using Dipole Filtered Real-Time Methods” (in preparation).

Peer-Reviewed Publications Resulting from this Project (Project start date: 9/2017)

[Chen2020] M. Chen, K. Lopata, “First-Principles Simulations of X-ray Transient Absorption for Probing Attosecond Electron Dynamics”, *J. Chem. Theory Comput.* **16**, 4470–4478 (2020).

[Darapaneni2020] P. Darapaneni, A. M. Meyer, M. Sereda, A. Bruner, J. A. Dorman, K. Lopata, “Simulated Field-Modulated X-ray Absorption in Titania”, *J. Chem. Phys.* **153**, 054110 (2020).

[Li2020] X. Li, N. Govind, C. Isborn, A. E. DePrince III, K. Lopata, “Real-Time Time-Dependent Electronic Structure Theory”, *Chem. Rev.* **120**, 9951–9993 (2020).

[Ranasinghe2019] J. C. Ranasinghe, A. S. Dikkumbura, P. Hamal, M. Chen, R. A. Khoury, H. T. Smith, K. Lopata, L. H. Haber, “Monitoring the Growth Dynamics of Colloidal Gold-Silver Core-Shell Nanoparticles using in-situ Second Harmonic Generation and Extinction Spectroscopy”, *J. Chem. Phys.* **151**, 224701 (2019).

Complexity and Correlated Motion of Electrons in Free and Confined Atomic Systems

Steven T. Manson, Principal Investigator
Department of Physics and Astronomy, Georgia State University, Atlanta, Georgia 30303
(smanson@gsu.edu)

Project Scope

The goals of the research program are: to further understanding of the interaction of radiation with matter; to provide theoretical support to, and collaboration with, various experimental programs that employ latest generation light sources, particularly ALS, APS and LCLS; and to study the properties (especially photoemission) of confined atoms and ions. Specifically, calculations are performed using and upgrading state-of-the-art theoretical methods to help understand the essential physics of the experimental results; to suggest future experimental investigations; and seek out new phenomenology, especially in the areas of attosecond time delay in photoemission (including negative ion photodetachment), outer-shell photoemission in the vicinity of inner-shell thresholds and confined systems. The primary areas of programmatic focus are: many-body and relativistic effects in photoionization; photoabsorption of inner and outer shells of atoms and atomic ions (positive and negative); dynamical properties of atoms endrohedrally confined in buckyballs, primarily C_{60}; and studies of Wigner time delay on the attosecond time scale in photoemission of free and confined atomic systems. Flexibility is maintained to respond to opportunities as they arise.

Recent Progress

A number of aspects of the attosecond dynamics of electrons in the photoemission process, as revealed by Wigner time delay [1,2], were explored. Time delay of photoemission from valence subshells of noble-gas atoms were scrutinized within a relativistic framework [3] with a focus on the variation of time delay in the vicinity of the Cooper minima. It was found that the presence of the Cooper minimum in one photoionization channel has a strong effect on time delay in other channels *via* interchannel coupling, and that relativistic effects strongly affect the time delay in regions of Cooper minima. In addition, we conducted a systematic study of the dipole phase and Wigner time delay in inner-shell photoionization of noble gas atoms from Ne to Xe [4] and found that the time delay, as a function of photoelectron energy, follows more or less a universal shape. And the angular distribution of Wigner time delay was investigated, revealing a strong angular anisotropy of the time delay occurs near Cooper minima while the spin-orbit splitting affects the time delay near threshold [5]. In the vicinity of autoionizing resonances, the time delay spectrum can become quite complicated, exhibiting both positive and negative delays across the resonance profile [6,7]. And aside from the complex energy dependence of time delay across a resonance profile, our work indicates that the angular distribution is also quite complex [8], even to the point that at certain energies, the time delay can be positive in one direction of photoemission, and negative in another direction, a very odd result from a physical point of view.

To obviate the effects of the Coulomb field near threshold, which dominate the time delay for neutral atom photoionization [4-6], we have initiated studies of attosecond time delay in negative ion photodetachment where the emerging photoelectron sees no long-range Coulomb field and low-energy shape resonances are emphasized in the time-delay spectrum. For Cl^- 3*p*, the results show significant differences, both qualitative and quantitative, between the time

delays for Cl^- and (isoelectronic) Ar photoemission at low photoelectron energy [9]; the Wigner time delay in Cl^- exhibits dramatic energy dependence just above threshold, and a rapidly increasing time delay in the vicinity of the shape resonance. A strong angular dependence of time delay has also been found near the threshold region for the Cl^- case and is absent for Ar.

Multielectron correlations in the form of interchannel coupling have been found to be crucial determinants of photoemission time delay for outer subshells in the neighborhood of inner thresholds [10] which suggests that time delay measurements can be used as a sensitive probe of many-body interactions. Thus, we have also initiated investigations of valence photodetachment near inner-shell thresholds [11]. Wigner time delay in photodetachment from the $3p_{3/2}$ and $3p_{1/2}$ subshells of Cl^- has been studied in the vicinity of the $2p_{3/2}$ and $2p_{1/2}$ thresholds, using the relativistic random phase approximation (RRPA). The results show time delay spectra dominated by many-body correlations along with very complicated energy dependence over a broad spectral range, also revealing that relativistic effects are of importance even in the case of a low-Z system. In addition, spin-orbit-interaction-activated interchannel coupling (SOIAIC) [12] has been investigated in the time delay domain for 3*d* photoemission in the isoelectronic sequence I^-, Xe, and Cs^+ using RRPA with relaxation [13]. The results show that SOIAIC becomes more important with increasing nuclear charge, and that time delay is affected more strongly than cross sections or photoelectron angular distribution β parameters.

It has also been found that confinement resonances in the photoionization of endohedrals induce significant resonances in the attosecond time delay of photoelectron emission [14], which suggests that time-domain spectroscopy might be efficacious in studying endohedrals and clusters. And in high-Z atoms, it was found that spin-orbit induced confinement resonances [15] also induce rather significant structures in the Wigner time delay, in the vicinity of these induced resonances, another domain that is ripe for experimental investigations. Also, an investigation of the angular dependence of Wigner time delay has been performed on the 4*d* subshell of $Xe@C_{60}$ and various new phenomena have been uncovered including a new kind of Cooper-like minima in certain of the photoionization channels which can lead to huge time delays and great sensitivity to the details of the confinement [16]; confined Xe 4*d* was chosen because its cross section has already been studied experimentally [17], thereby suggesting the possibility of experimental study of the Wigner time delay of $Xe@C_{60}$.

Our program on confined atoms is aimed at mapping out their properties (especially photoemission) to guide experiment and uncover new phenomena. We have found a huge transfer of oscillator strength from the C_{60} shell, in the neighborhood of the giant plasmon resonance, to the encapsulated atom for both $Ar@C_{60}$ [18] and $Mg@C_{60}$ [19]. And confinement resonances [20], oscillations in the photoionization cross section of an endohedral atom due to interferences in the photoelectron emission from the cavity, were predicted and confirmed experimentally [17]. Further, in the photoionization of endohedral atoms within nested fullerenes, as a result of the multi-walled structure, the confinement resonances become considerably more complicated [21]. In addition, spin-orbit induced confinement resonances in photoionization have been found owing to interchannel coupling between inner-shell spin-orbit split channels in high-Z endohedral atoms [22], an effect which occurs solely owing to relativistic interactions. We have also explored the interatomic Coulomb decay (ICD) in confined atoms and found, owing to hybridization between atomic and shell orbitals, that ICD occurs both ways, from atom to shell and shell to atom, and the rates (widths) are often much larger than the ordinary Auger rates [14-17], making these ICD resonances excellent candidates for experimental study. And to augment the confined atom work, we have performed a density

function theory calculation of the photoionization of all 32 valence levels of free C_{60} with full account of the molecular symmetry [23]; the calculation revealed a wealth of detail on the cross sections and is the most accurate calculation to date.

Since high-Z atoms are excellent laboratories to study the combination of relativistic and many-electron correlation effects in electronic structure and dynamics, a new initiative, properties of superheavy elements, has been started [24,25]. We have studied Z=102, 112 and 118 (the heaviest known element) and significant anomalies in the subshell binding energies are found. Also, the photoionization properties show very large differences as compared to lower-Z atoms in the same column of the periodic table. Specifically, the subshell cross sections are completely dominated by relativistic and many-body interactions. These calculations are of particular interest since experimental studies are now possible [26, 27].

Future Plans

We will continue investigating attosecond time delay in photoemission, including a focus on many-body effects, negative-ion photodetachment, nondipole effects and we will work to further our understanding of how confinement affects time delay. To provide a "road map" for experimental investigations, we will explore photoionization at high energies (tens of keV) to predict where many-body interactions alter simple behavior; preliminary indications are that this can be very significant. In the area of confined atoms, we will expand on our studies of interatomic Coulomb decay (ICD) of resonances. We will also work on ways to enhance the time-dependent local-density approximation to make it more accurate in our calculations of confined atoms and to include relativistic interactions to be able to deal with heavy endohedrals accurately. In addition, we shall focus on taking into account the full molecular symmetry of atomic systems confined in C_{60} to understand the limits of utility of simple models and to deal with off-center endohedral confinement in a realistic manner. And we shall respond to new experimental capabilities and results as they occur.

Peer-Reviewed Publications Resulting from this Project (2018-2020)

● "Wigner-Eisenbud-Smith photoionization time delay due to autoionization resonances," Pranawa C. Deshmukh, Ashish Kumar, Hari R. Varma, Sourav Banerjee, Steven T. Manson, Valeriy K. Dolmatov and Anatoli Kheifets, J. Phys. B **51**, 065108-1-8 (2018).

● "Intershell-correlation-induced time delay in atomic photoionization," D. A. Keating, S. T. Manson, V. K. Dolmatov, A. Mandal, P. C. Deshmukh, Faiza Naseem and A. S. Kheifets, Phys. Rev. A **98**, 013420-1-10 (2018).

● "Interference in electron-molecule elastic scattering," A. S. Baltenkov, S. T. Manson and A. Z. Msezane, J. Phys. B **51**, 205101-1-9 (2018).

● "Strong Dependence of Photoionization Time Delay on Energy and Angle in the Neighborhood of Fano Resonances," S. Banerjee, P. C. Deshmukh, V. K., Dolmatov , S. T. Manson and A. S. Kheifets, Phys. Rev. A **99**, 013416-1-5 (2019).

● "Dominance of Correlation and Relativistic Effects on Photodetchment Time Delay Well Above Threshold," Soumyajit Saha, Pranawa C. Deshmukh, Anatoli S. Kheifets, Valeriy K. Dolmatov, and Steven T. Manson, Phys. Rev. A **99**, 063413-1-6 (2019).

● "Wigner time delay in photodetachment," Soumyajit Saha, Jobin Jose, Pranawa C. Deshmukh, G. Aravind, Valeriy K. Dolmatov, Anatoli S. Kheifets and Steven T. Manson, Phys. Rev. A**99**, 043407-1-8 (2019).

● "X-rays put molecules into a spin," John T. Costello and Steven T. Manson, Proc. Nat. Acad. Sci. **116**, 4772-4773 (2019).

● "Photoionization of C_{60}: Effects of Correlation on cross sections and angular distributions of Valence Subshells," A. Ponzi, S. T. Manson and P. Decleva, J. Phys. Chem. A **124**, 108-125 (2020).

● "Photoemission from hybrid states of $Cl@C_{60}$ before and after a stabilizing electron transfer," Dakota Shields, Ruma De, Mohamed El-Amine Madjet, Steven T. Manson, and Himadri S. Chakraborty, J. Phys. B **53**, 125101-1-8 (2020).

● "Effects of Spin-Orbit Interaction Activated Interchannel Coupling on Photoemission Time Delay," Sourav Banerjee, Pranawa C. Deshmukh, Anatoli S. Kheifets, and Steven T. Manson, Phys. Rev. A **101**, 043411-1-8 (2020).
● "Outer-Shell Photodetachment of Li^- Near Inner-Shell Thresholds," T. W. Gorczyca and S. T. Manson, J. Phys. B **53**, 195203-1-6 (2020).
● "Relativistic and Correlation Effects in the Photoionization Dynamics of Oganesson (Z = 118): Spin-Orbit-Interaction-Activated Interchannel Coupling Effects," J. Jose, S. Baral, P. C. Deshmukh and S. T. Manson, Phys. Rev. A **102**, 022813 (2020).
● "Photoionization of Superheavy Atoms: Correlation and Relativistic Effects," A. K. Razavi, R. K. Hosseini, D. A. Keating, P. C. Deshmukh and S. T. Manson, J. Phys. B **53**, 205203-1-8 (2020).
● "A density functional theory based comparative study of hybrid photoemissions from $Cl@C_{60}$, $Br@C_{60}$ and $I@C_{60}$," D. Shields, R. De, Esam Ali, M. E. Madjet, S. T. Manson, and H. S. Chakraborty, Eur. Phys. J. D (accepted, July 2020).
● "Inner-Shell Photodetachment of Na^- using R-matrix Methods," T. W. Gorczyca, H.-L. Zhou, A. Hibbert, M. F. Hasoglu, and S. T. Manson, Atoms (accepted, Sept., 2020).

References

[1] E. P. Wigner, Phys. Rev. **98**, 145 (1955).
[2] R. Pazourek, S. Nagele and J. Burgdörfer, Rev. Mod. Phys. **87**, 765 (2015) and references therein.
[3] S. Saha, A. Mandal, J. Jose, H. R. Varma, P. C. Deshmukh, A. S. Kheifets, V. K. Dolmatov and S. T. Manson, Phys. Rev. A **90**, 053406 (2014).
[4] A. S. Kheifets, S. Saha, P. C. Deshmukh, D. A. Keating, and S. T. Manson, Phys. Rev. A **92**, 063422 (2015).
[5] A. Kheifets, A. Mandal, P. C. Deshmukh, V. K. Dolmatov, D. A. Keating and S. T. Manson, Phys. Rev. A **94**, 013423 (2016).
[6] P. C. Deshmukh, A. Kumar, H. R. Varma, S. Banerjee, S. T. Manson, V. K. Dolmatov and A. Kheifets, J. Phys. B **51**, 065108 (2018).
[7] U. Fano, Phys. Rev. **124**, 1866 (1961).
[8] S. Banerjee, P. C. Deshmukh, V. K., Dolmatov , S. T. Manson and A. S. Kheifets, Phys. Rev. A **99**, 013416 (2019).
[9] S. Saha, J. Jose, P. C. Deshmukh, G. Aravind, V. K. Dolmatov, A. S. Kheifets and S. T. Manson, Phys. Rev. A**99**, 043407 (2019).
[10] D. A. Keating, S. T. Manson, V. K. Dolmatov, A. Mandal, P. C. Deshmukh, F. Naseem and A. S. Kheifets, Phys. Rev. A **98**, 013420 (2018).
[11] S. Saha, P. C. Deshmukh, A. S. Kheifets, V. K. Dolmatov, and S. T. Manson, Phys. Rev. A **99**, 063413 (2019).
[12] M. Ya. Amusia, L. V. Cernysheva, S. T. Manson, A. Z. Msezane and V. Radojevic, Phys. Rev. Lett. **88**, 093002 (2002).
[13] S. Banerjee, P. C. Deshmukh, A. S. Kheifets, and S. T. Manson, Phys. Rev. A **101**, 043411 (2020).
[14] P. C. Deshmukh, A. Mandal, S. Saha, A. S. Kheifets, V. K. Dolmatov and S. T. Manson, Phys. Rev. A **89**, 053424 (2014).
[15] D. A. Keating, P. C. Deshmukh and S. T. Manson, J. Phys. B **50**, 175001 (2017).
[16] A. Mandal, P. C. Deshmukh, A. S. Kheifets, V. K. Dolmatov and S. T. Manson, Phys. Rev. A **96**, 053407 (2017).
[17] R. A. Phaneuf, A. L. D. Kilcoyne, N. B. Aryal, K. K. Baral, D. A. Esteves-Macaluso, C. M. Thomas, J. Hellhund, R. Lomsadze, T. W. Gorczyca, C. P. Ballance, S. T. Manson, M. F. Hasoglu, S. Schippers, and A. Müller, Phys. Rev. A **88**, 053402 (2013) and references therein
[18] M. E. Madjet, H. S. Chakraborty and S. T. Manson, Phys. Rev. Letters **99**, 243003 (2007).
[19] M. E. Madjet, H. S. Chakraborty, J. M. Rost and S. T. Manson, Phys. Rev. A **78**, 013201 (2008).
[20] V. K. Dolmatov and S. T. Manson, J. Phys. B **41**, 165001 (2008).
[21] V. K. Dolmatov and S. T. Manson, J. Phys. Rev. A **78**, 013415 (2008).
[22] R. De, M. Magrakvelidze, M. E. Madjet, S. T. Manson and H. S. Chakraborty, J. Phys. B **49**, 11LT01 (2016) and references therein.
[23] A. Ponzi, S. T. Manson and P. Decleva, J. Phys. Chem. A **124**, 108 (2020).
[24] A. K. Razavi, R. K. Hosseini, D. A. Keating, P. C. Deshmukh and S. T. Manson, J. Phys. B **53**, 205203 (2020).
[25] J. Jose, S. Baral, P. C. Deshmukh and S. T. Manson, Phys. Rev. A **102**, 022813 (2020).
[26] M. Laatiaoui , A. A. Buchachenko and L. A. Viehland, Phys. Rev. Lett. **125**, 023002 (2020).
[27] M. Laatiaoui , A. A. Buchachenko and L. A. Viehland, Phys. Rev. A **102**, 013106 (2020).

Resolving femtosecond photoinduced energy flow: capture of nonadiabatic reaction pathway topography and wavepacket dynamics from photoexcitation through the conical intersection seam

Principal Investigator: Jeffrey Moses

School of Applied & Engineering Physics, Cornell University
142 Sciences Dr./223 Clark Hall, Ithaca, NY 14853

email: moses@cornell.edu

Project Scope

The dynamics that take place within just tens to hundreds of femtoseconds following the photoexcitation of a molecular chromophore can play a critical role in how the absorbed energy is directed, allowing it to be used for a specific function (photoinduction) or dissipated harmlessly (photoprotection). Underlying these dynamics is the presence of electronic energy degeneracies in the relaxation pathways of the excited chromophores, known as conical intersections (CIs), which mediate nonradiative electronic transitions known as nonadiabatic transitions.

There is already compelling data that nonadiabatic dynamics underlie the energy-managing function of numerous molecules of importance. For example, they are a mediating factor of photochemical energy flow in electrocyclic ring opening reactions, in which the steep potential energy surfaces surrounding the CIs produce swift light-induced chemical action, allowing the envisioning of laser-controlled “molecular motors” at the nanoscale [1,2]. Important examples in biology include the highly effective ultraviolet photoprotection mechanism of DNA [3–5], the efficient phototransduction process of the vertebrate vision response [6], and the photoisomerization of the retinal chromophore underlying channelrhodopsin activation [7,8]. Ultrafast and efficient “photoswitches” based on these natural processes may someday allow controlled manipulation of solar energy or optical control of a wide range of energy management functions, through artificial and biomimetic systems employing optimized nonadiabatic transitions.

Experimental methods, however, have not yet allowed a precisely resolved and complete measurement of the electronic structure during its rapid evolution along the reaction pathway during a nonadiabatic transition – all the way from the Franck-Condon point to the CI seam and finally to the photoproduct. This constitutes a major obstacle to progress in the field, as knowledge of the topography of the reaction pathway and the wavepacket dynamics near the CI will be essential to verifying ab initio theories and to explaining chromophore function, milestones that would inform a wide body of research aiming to efficiently harness the energy of light for practical purposes.

We aim to solve this long-standing problem by establishing a method for direct and complete optical interaction with the evolving electronic structure of a molecule during a nonadiabatic transition, made possible by a multi-octave-spanning light source technology recently developed by our team and capable of providing energetic few-femtosecond probe pulses from visible through mid-IR wavelengths [9]. With a ~10-15-fs instrument response function (IRF), we aim to use visible, near-IR, and mid-IR pulses to measure the changing optical transition frequency across the full reaction pathway,

which varies over several octaves during the few hundred femtosecond transition. Once the primary measurement has been established, we plan to expand the approach to 2D electronic spectroscopy, allowing pump-frequency-resolved (and thus wavepacket-kinetic-energy-resolved) investigation of the complete nonadiabatic reaction pathway.

We plan to use this approach to explore nonadiabatic transitions in three well known photochemical systems with known CIs in the photoreaction pathway and essential and complex femtosecond timescale energy flow dynamics: visual rhodopsin, channelrhodopsin and its mutants, and the DNA nucleobases in monomer and oligomer form. Comparison to ab initio modeling through collaboration with theorists in the field will aid this attempt to empirically provide and explain the reaction pathway topography and complete femtosecond timescale wavepacket dynamics of these samples in solution. If successful, this will help to allow a full physical explanation of their branching ratios and time constants, and will inform a next generation of research aiming to harness and control photoinduced energy flow on a molecular level.

Recent Progress

The initial phase of our program included instrumentation development using the equipment funding provided by this grant program and preliminary experiments to assess and optimize the IRF of our transient absorption pump-probe setup.

We have added two spectrometers with fast array detectors and high dynamic range. In addition to an existing 2D LN2-cooled HgCdTe array (128 x 128 pixel, 2-11 μm sensitivity) detector-based spectrometer, we have added a dual-port spectrometer housing low noise and fast acquisition Si CCD (128 pixel, 200-1000 nm sensitivity) and TE-cooled extended InGaAs CCD (256 pixel, 1000-2200 nm sensitivity) detectors. To allow measurements with adequate sensitivity to resolve a $|\Delta T/T|$ of 1×10^{-4}, we have chosen detectors with high enough well depth, low enough readout noise, and low enough dark noise integrated over 100 μs (our laser pulse interval) to achieve a single-shot dynamic range of 10^4 above the noise floor. Moreover, all three detectors are capable of ≥10 kHz readout speeds – the Si and InGaAs linear arrays at full pixel number, and the 2D HgCdTe array when acquisition is binned down to 96 x 16 pixels.

In order to precisely assess and optimize the IRF, we have been developing methods of *in situ* full pulse amplitude and phase characterization of octave-spanning pulses at the location of the transient absorption experiment. During the reporting period, as planned we implemented and tested a dispersion-scan technique [10] for full pulse amplitude and phase characterization of the broadband pump and probe pulses. The specific technique we sought to establish is a new variant of the dispersion-scan technique in which an inline programmable pulse shaper in a 10-fs near-IR beamline controls the spectral phase of a *10-fs mid-IR* beamline derived from it by our group's pioneered technology of octave-spanning adiabatic frequency downconversion [9]. Since the adiabatic downconversion process possesses a linear spectral phase transfer, scanning the dispersion of the near-IR pulse shaper becomes a method for scanning the dispersion of the mid-IR pulse that contains a bandwidth *spanning a full octave (~2000-4000 nm)*, a process difficult to achieve by other technologies. A further advantage of this approach is *in situ* characterization of the octave-spanning pulses at the location of the transient absorption experiment.

Our initial assessment, however, resulted in a lack of confidence in the robustness of the dispersion scan, and therefore of the characterization method in this new variant. We subsequently turned our investigation to another new technique for full pulse amplitude and phase characterization of ultrashort pulses, the frequency resolved optical switching (FROSt) method [11]. This method in fact employs transient absorption as a temporal pulse gating mechanism, in which an ultrashort pump pulse changes the temporal absorption profile of a thin semiconductor relative to the moving frame of the pulse to be tested. This allows the technique to be particularly suitable for our ultrabroadband transient absorption experiments, as it can be performed *in situ* in the experiment. Since the technique does not rely on a nonlinear conversion process, there is no phase-matching bandwidth limiting its applicability for ultrashort pulses, and the test pulse bandwidth can in fact span the full transmission window of the semiconductor medium. We are collaborating with François Légeré at INRS, Quebec, Canada, to implement this in our laboratory. Our group has already developed a retrieval algorithm, has ordered the components, and is in the process of implementing the experiment.

As part of this effort, we also noted and corrected a flaw of our commercial near-IR 4F pulse shaper design that employs one-dimensional, off-axis parabolic mirrors. This created an aberration on our NIR beam that significantly reduced the conversion efficiency of our adiabatic frequency conversion stage and prevented optimal pulse compression. After studying the origin of this aberration, which was due to residual angular dispersion imparted by the off-axis parabolic mirrors, we redesigned the 4F pulse shapers to use cylindrical mirrors which eliminated the residual angular dispersion. This work represents a notable contribution to the development of technology for ultrabroadband transient optical spectroscopy and was presented at the 2019 Ultrafast Optics Conference [12].

Future Plans

Our next step is to finalize the testing of the pump-probe IRF, and to test the transient absorption experimental apparatus in first experiments. Using FROSt, we will first characterize the IRF of a pump-probe beamline consisting of ~10-fs near-IR (~670-1010 nm) and mid-IR pulses (~2000-4000 nm). We intend to perform a spectroscopy benchmarking experiment on graphene, by observing ultrafast Pauli-blocking using our hyperspectral transient absorption spectroscopy approach. As the sample is much easier to handle than rhodopsin and the spectroscopy signal will have a very high SNR, this is a relatively simple yet scientifically interesting (as it would provide insight into the phenomena of Pauli blocking [13]) stepping stone towards our major program goals of ultrafast transient absorption experiments of the rhodopsins and DNA. We will collaborate with Dr. Giulio Cerullo of Milano Polytechnic to complete these experiments.

We are also continuing the development of our instrumentation. We are currently integrating the new spectrometers into our computer controlled pulse shaping and detection system. On the laser side, we are adding to our existing ~10-fs sources of visible (~450-510 nm), near-IR (~670-1010 nm), and mid-IR pulses (~2000-4000 nm) two new beam-lines covering visible/near-IR (~500-700 nm) and near-IR (~1200-2200 nm) ranges. We have designed and received the adiabatic frequency conversion crystal for the near-IR source and we will implement it after performing a first round of transient

absorption experiments. Eventually, our system will possess nearly three octaves of near-continuous spectral coverage for probing the dynamical transition energy of the rhodopsin chromophore and DNA UV-absorption photosystem.

References

[1] S. Deb and P. M. Weber, Annu. Rev. Phys. Chem. **62**, 19 (2011).

[2] M. P. Minitti, J. M. Budarz, A. Kirrander, J. S. Robinson, D. Ratner, T. J. Lane, D. Zhu, J. M. Glownia, M. Kozina, H. T. Lemke, M. Sikorski, Y. Feng, S. Nelson, K. Saita, B. Stankus, T. Northey, J. B. Hastings, and P. M. Weber, Phys. Rev. Lett. **114**, 255501 (2015).

[3] S. Ullrich, T. Schultz, M. Z. Zgierski, and A. Stolow, Phys. Chem. Chem. Phys. **6**, 2796 (2004).

[4] W. J. Schreier, T. E. Schrader, F. O. Koller, P. Gilch, C. E. Crespo-Hernandez, V. N. Swaminathan, T. Carell, W. Zinth, and B. Kohler, Science **315**, 625 (2007).

[5] B. K. McFarland, J. P. Farrell, S. Miyabe, F. Tarantelli, A. Aguilar, N. Berrah, C. Bostedt, J. D. Bozek, P. H. Bucksbaum, J. C. Castagna, R. N. Coffee, J. P. Cryan, L. Fang, R. Feifel, K. J. Gaffney, J. M. Glownia, T. J. Martinez, M. Mucke, B. Murphy, A. Natan, T. Osipov, V. S. Petrović, S. Schorb, T. Schultz, L. S. Spector, M. Swiggers, I. Tenney, S. Wang, J. L. White, W. White, and M. Gühr, Nat. Commun. **5**, 4235 (2014).

[6] D. Polli, P. Altoè, O. Weingart, K. M. Spillane, C. Manzoni, D. Brida, G. Tomasello, G. Orlandi, P. Kukura, R. A. Mathies, M. Garavelli, and G. Cerullo, Nature **467**, 440 (2010).

[7] D. Urmann, C. Lorenz, S. M. Linker, M. Braun, J. Wachtveitl, and C. Bamann, Photochem. Photobiol. **93**, 782 (2017).

[8] C. Schnedermann, V. Muders, D. Ehrenberg, R. Schlesinger, P. Kukura, and J. Heberle, J. Am. Chem. Soc. **138**, 4757 (2016).

[9] P. Krogen, H. Suchowski, H. Liang, N. Flemens, K.-H. Hong, F. X. Kärtner, and J. Moses, Nat. Photonics **11**, 222 (2017).

[10] B. Alonso, Í. J. Sola, and H. Crespo, Sci. Rep. **8**, 3264 (2018).

[11] A. Leblanc, P. Lassonde, S. Petit, J.-C. Delagnes, E. Haddad, G. Ernotte, M. R. Bionta, V. Gruson, B. E. Schmidt, H. Ibrahim, E. Cormier, and F. Légaré, Opt. Express **27**, 28998 (2019).

[12] D. A. Heberle, C. T. Middleton, N. R. Flemens, and J. Moses, "Understanding chromatic aberrations in 4f few-cycle pulse shapers," in *Ultrafast Optics 2019: Abstract Book*, in *Ultrafast Optics 2019* (SPIE, Bol, Croatia, 2019), Proc. SPIE **11370**, pp. 379-382.

[13] D. Brida, A. Tomadin, C. Manzoni, Y. J. Kim, A. Lombardo, S. Milana, R. R. Nair, K. S. Novoselov, A. C. Ferrari, G. Cerullo, and M. Polini, Nat. Commun. **4**, (2013).

Peer-Reviewed Publications Resulting from this Project (Project start date: 08/2019)

None

Theory and Simulation of Nonlinear X-ray Spectroscopy of Molecules

Shaul Mukamel
University of California, Irvine, CA 92697
smukamel@uci.edu
Progress Report September 2020
DOE DE-FG02-04ER15571

Program Scope

Nonlinear X-ray spectroscopy experiments which use sequences of coherent broadband X-ray pulses are made possible by new ultrafast X-ray free electron laser (XFEL) and high harmonic generation (HHG) sources. These techniques provide unique windows into the motions of electrons and nuclei in molecules and materials and offer novel probes for electron and energy transfer in molecular complexes. This program is aimed at the design of X-ray pulse sequences for probing core and valence electronic excitations, and the development of effective simulation protocols for describing multiple-core excited state energetics and dynamics. Applications are made to detecting strongly coupled electron-nuclear dynamics in molecules through electronic coherence observed in multidimensional broadband stimulated X-ray Raman signals, multidimensional diffraction with coincidence detection, employing stochastic XFEL pulses in nonlinear spectroscopy, and probing time dependent molecular chirality.

Recent Progress

Joint temporal and spectral resolution of stimulated x-ray Raman signals with stochastic free-electron-laser pulses. XFEL pulses are not reproducible from shot to shot. This is a major obstacle for spectroscopy applications which require high temporal and spectral resolutions. Phase control is a crucial requirement of time-resolved coherent nonlinear spectroscopy. We showed that high temporal and spectral resolutions can be obtained with currently available stochastic XFEL pulses. By examining higher-order correlations of signals obtained by averaging over independent pulse realizations, we showed that stimulated x-ray Raman signals with stochastic XFEL pulses can recover the same resolution which normally requires coherent, phase-controlled pulses. This

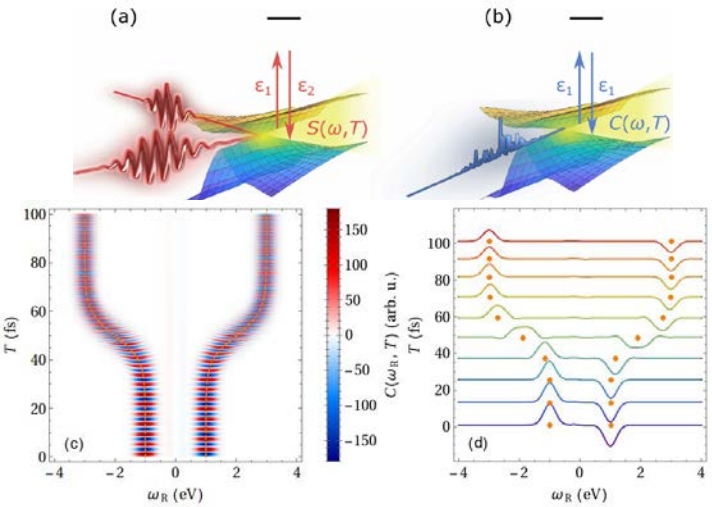

Figure 1: Off-resonant stimulated x-ray Raman signals. (a,b) The dynamics of two molecular potential-energy surfaces are probed by (a) two phase-controlled x-ray pulses and (b) a single stochastic XFEL pulse. (c,d) By taking advantage of the field correlations, joint temporal and spectral resolutions are recovered by a single stochastic XFEL pulse wit no phase control. (c) Simulation of the signal, as a function of the arrival time of the pulse T and the detected Raman frequency ω_R, for a model system with a time-dependent frequency, as exhibited by the orange dashed lines. (d) Sections of the signal at selected time delays T for the same model system, with the time-dependent frequency marked by the orange dots.

scheme is applied to the RNA base uracil passing through a conical intersection, a process where electrons and nuclei are strongly coupled and very high temporal and spectral resolutions are necessary. As shown in Fig. 1, we compare signals obtained by two coherent reproducible x-ray pulses and by a single stochastic XFEL pulse. The XFEL pulse duration determines the high temporal and spectral resolution of the technique, without requiring phase control. The approach can be extended to other time-resolved nonlinear x-ray techniques.

Delocalized current densities with wavevector-resolved x-ray sum-frequency generation in selenophene. XFELs offer intense x-ray pulses at hard-x-ray frequencies of tens of kiloelectronvolts. At such high frequencies, the corresponding wavelength of the x-ray pulse is of the order of fractions of an angstrom and is comparable with the molecular size. The dipole approximation is not applicable at such frequencies, and the x-ray pulse is sensitive to the delocalized charge and current densities of the molecule. We investigate this effect in the resonant x-ray sum-frequency-generation (XSFG) signal of selenophene. The Se K-edge lies at frequencies higher than 12 keV. We employ a description based on the minimal-coupling light–matter interaction Hamiltonian, where the resonant excitation of the molecule is expressed in terms of delocalized transition current densities. By varying the propagation direction of the x-ray pulse, we observe a dependence of the XSFG signal which could not be captured in a multipolar description of the x-ray–molecule interaction. This regime allows the direct access to delocalized transition current densities in molecules.

Frequency-, Time-, and Wavevector-Resolved Ultrafast Incoherent Diffraction of Noisy X-ray Pulses. Bright ultrashort X-ray pulses produced by free electron lasers (FELs) have become an indispensable tool for ultrafast measurements. These sources are usually based on the self-amplified spontaneous emission (SASE) process, which generates strongly fluctuating stochastic radiation. In this work, we developed the statistical approach to wavevector-, time-, and frequency-resolved diffraction signals of stochastic light sources and applied it to thiophenol. Our main finding suggests that frequency dispersion of time-resolved X-ray diffraction can restore the temporal resolution. We further propose to use stochastic sources to enhance the spectral resolution at the expense of the temporal resolution. We have demonstrated how the apparent shortcomings of stochastic X-ray sources with random phase can be turned into a useful tool.

Stimulated X-ray Raman Spectroscopy of Iron-sulfur Complexes. Iron–sulfur complexes play an important role in biological processes such as metabolic electron transport. We simulate the spectra for the stimulated X-ray Raman spectroscopy (SXRS) of the homovalent and mixed-valence [2Fe–2S] complexes and compare them to simulated absorption spectra, using the ab initio DMRG technique. The simulated spectra show clear signatures of the theoretically predicted dense low-lying excited states within the d–d manifold. Furthermore, the difference in spectral intensity between the absorption-active and Raman-active states provides a potential mechanism to selectively excite states by a proper tuning of the excitation pump, to access the electronic dynamics within this manifold.

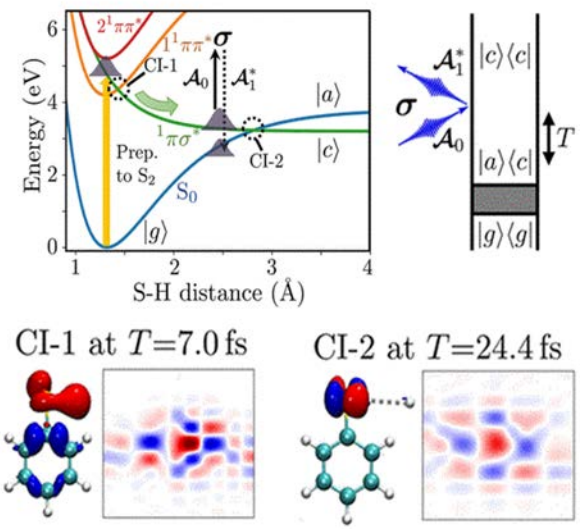

Figure 2: (top) Potential energy surface of thiophenol and the Feynman diagram for the SXRI technique. (bottom) The transition charge densities at the two conical intersections (CI-1 and CI-2) in the photodissociation dynamics of thiophenol and the corresponding SXRI signals (Qx-Qy plane of the diffraction signals).

Stimulated X-ray Raman Imaging of Conical Intersections in thiophenol. Conical intersections (CIs) play a key role in many chemical and biophysical processes. We propose a stimulated X-ray Raman imaging technique for monitoring the real-time and real-space imaging of the transition charge density at the CI. A hybrid X-ray probe field composed of narrowband (probe) and broadband (stimulated emission) pulses then provides a space-resolved image of the electronic coherence thanks to the short wavelength of the X-ray probe field. We applied the technique to probe CI dynamics in the photodissociation of the S–H bond in thiophenol. The transition charge density variation across the CIs is monitored in real-space. More importantly, conical intersections can be distinguished by the diffraction patterns (Fig. 2).

Future Plans

An approach based on the high-order correlations of stochastic XFEL pulses was applied to stimulated x-ray Raman signals, showing that high temporal and spectral resolutions can be achieved without requiring phase-controlled pulses. This approach will be extended to signals with higher numbers of interactions with the stochastic field. Such signals could result from post-processing of the data, or could be the direct outcome of the measurement as, e.g., in four-wave mixing experiments. Averaging over independent pulse realizations provides signals depending on the correlation functions of the stochastic field. This allows one to recover high temporal and spectral resolutions, in spite of the lack of control over the XFEL-pulse phase. We will employ this approach to extend multidimensional nonlinear spectroscopy protocols from the optical to the hard-x-ray regime, by exploiting stochastic XFEL pulses.

Direct time-domain simulation of multidimensional spectroscopy of molecules driven by external fields requires a phase cycling protocol to extract the desired signal as the nonlinear signals are given by sums over Liouville pathways, each representing a different order in the field. We will employ the 9-step phase cycling protocol to calculate the third-order signals of pyrazine and other molecules.

The work on quantum phase-sensitive diffraction and imaging using entangled photons will be extended to other types of entangled light. The SXRS study of visualizing conical intersection passages via vibronic coherence maps will be combined with coherent control protocols aimed at

optimizing the rates and branching ratios of the products. Second order signals such as X-ray SFG in isotropic liquids of chiral molecules will be simulated.

Peer-Reviewed Publications Resulting from the Project (2019-2020)

1. "Quantum phase-sensitive diffraction and imaging using entangled photons", Shahaf Asban, Konstantin E. Dorfman, and, Shaul Mukamel. PNAS (2019) 116, 11673-11678
2. "Quantum diffraction imaging with entangled photons", Shahaf Asban, Konstantin E Dorfman, and Shaul Mukamel. In "Roadmap on Quantum Light Spectroscopy". 2020 J. Phys. B: At. Mol. Opt. Phys.**53**, 072002
3. "Frequency-, time-, and wavevector-resolved ultrafast incoherent diffraction of noisy X-ray pulses", Shahaf Asban, Daeheum Cho, and Shaul Mukamel. J. Phys. Chem. Lett, 10, 5805-5814 (2019)
4. "Probing molecular chirality by orbital angular momentum carrying X-ray pulses", Lyuzhou Ye, Jérémy R. Rouxel, Shahaf Asban, Benedikt Rösner, and Shaul Mukamel. Journal of Chemical Theory and Computation (JCTC) (2019)DOI: 10.1021/acs.jctc.9b00346
5. "Time and frequency resolved transient-absorption and stimulated-Raman signals of stochastic light", Vladimir Al. Osipov, Shahaf Asban, and Shaul Mukamel. JCP Special Issue on "Ultrafast Spectroscopy and Diffraction from XUV to X-ray". 151, 044113 (2019) DOI: 10.1063/1.5109258
6. "Transient X-ray absorption spectral fingerprints of the S_1 dark state in uracil", Weijie Hua, Shaul Mukamel, Yi Luo. J. Phys. Chem Lett (2019), 10, 7172-7178
7. "Stimulated X-ray Raman and Absorption Spectroscopy of Iron-Sulfur Dimers", Daeheum Cho, Jérémy R. Rouxel, Shaul Mukamel, Garnet Kin-Lic Chan, and Zhendong Li. J. Phys. Chem. Lett , 10, 6664-6671(2019) doi: 10.1021/acs.jpclett.9b02414
8. "Molecular Structure and Modeling of Water-Air and Ice-Air Interfaces Monitored by Sum-Frequency Generation", Fujie Tang, Tatsuhiko Ohto, Shumei Sun, Jérémy R. Rouxel, Sho Imoto, Ellen H. G. Backus, Shaul Mukamel, Mischa Bonn, and Yuki Nagata. Chemical Reviews (2020) DOI: 10.1021/acs.chemrev.9b00512
9. "Stimulated X-ray Resonant Raman Imaging of Conical Intersections", Daeheum Cho and Shaul Mukamel. J. Phys. Chem. Lett., 2020, 11, 33-39
10. "Stimulated X-ray Resonant Raman Spectroscopy of Conical Intersections in Thiophenol", Daeheum Cho, Jeremy Rouxel and Shaul Mukamel. J. Phys. Chem. Lett., 2020, 11, 4292–4297
11. "Visualizing Conical Intersection Passages via Vibronic Coherence Maps Generated by Stimulated X-Ray Raman Signals", Daniel Keefer, Thomas Schnappinger, Regina de Vivie-Riedle and Shaul Mukamel. PNAS (2020) doi: 10.1073/pnas.2015988117
12. "Chiral Four-Wave-Mixing signals with circularly-polarized X ray pulses," Jérémy R. Rouxel; Ahmadreza Rajabi; Shaul Mukamel. J. Chem. Theory Comput. 2020, 16, 9, 5784–5791

Theory and Simulation of Ultrafast Multidimensional Nonlinear X-ray Spectroscopy of Molecules

DE-SC0019484

Shaul Mukamel[1,*], Niranjan Govind[2], Sergei Tretiak[3], Marco Garavelli[4]
1) Department of Chemistry and Physics &Astronomy, University of California, Irvine, CA
2) Physical and Computational Sciences Directorate, Pacific Northwest National Laboratory, Richland, WA
3) Theoretical Physics and Chemistry of Materials, Los Alamos National Laboratory, Los Alamos, NM
4) Dipartimento di Chimica Industriale "Toso Montanari", Università di Bologna, Italy
*smukamel@uci.edu

Project Scope

Emerging X-ray free electron laser (XFEL) beam sources offer new types of probes of matter with unprecedented spatial and temporal resolutions. These experimental advances call for robust theoretical and computational tools that provide predictive modeling capacity of the underlying electronic and structural dynamics. The latter are essential for the design of sophisticated multi-pulse experiments and for their interpretation.

This research effort focuses on developing cutting-edge simulation tools for nonlinear multidimensional X-ray/optical spectroscopies. These techniques combine sequences of X-ray and optical pulses to provide a unique experimental toolbox for probing the dynamics of core and valence electronic and vibrational excitations and as well as material structure. These challenges are addressed by three research thrusts, as outlined below.

The team spans the broad and necessary expertise in theoretical spectroscopy, nonlinear optics, quantum chemistry, molecular non-adiabatic dynamics and code development. The nonlinear spectroscopy, real-time electron dynamics, molecular non-adiabatic dynamics focuses on computing the nonlinear response to X-ray pulse sequences, using multidimensional Raman signals and X-ray time resolved diffraction to study non-adiabatic dynamics at conical intersections. Four-wave mixing techniques will be used to study multi-core excitations and electron correlations. Such experiments were so far reported experimentally in the XUV and soft X-rays (at the Fermi facility) providing proof-of-principle for such experiments. LCLS-II will extend these results to the tender and hard X-ray regimes with much finer spatial and temporal resolutions.

This program aims at creating modeling capabilities and making them available to the broad XFEL (e.g LCLS-II) user community to support existing and inspire new innovative experiments. X-ray pulse sequences and experiments for probing core and valence electronic excitations will be designed. Efficient simulation protocols will be designed for the description of multiple-core excited state energetics and dynamics and for the interpretation of their spectroscopic signatures. Nonlinear spectroscopy techniques well established in the visible and the infrared regimes (e.g. time-resolved photoelectron spectroscopy, time-resolved broadband stimulated Raman, and wave mixing) will be extended to the X-ray regime and applied to a large variety of molecular systems, thus laying out XFEL-based multidimensional spectroscopies as a novel diagnostic tool for tracing electronic and structural dynamics in molecular materials.

Recent Progress

- **Thrust 1:** *Methods/Software development and implementation*
  The focus of this Thrust is the integration of the capabilities of software developed by the various groups, and the development of new software, to produce state-of-the-art numerical techniques for the simulation of photo-induced dynamics and different spectroscopic signals.

1. (UNIBO-UCI-PNNL) Completion of the Python-based SPECTRON – NWChem/OpenMolcas interface, named iSPECTRON. A paper highlighting the interface capabilities has been submitted [Segatta2020a]. This interface will be made available to the broader community in the near future. We have completed the implementation of iSPECTRON, a Python-based interface code that allows to parse data from popular quantum chemistry software (as, e.g., NWChem, OpenMolcas, Gaussian, Cobramm, etc.), produce the input files for the simulation of linear and nonlinear spectroscopy of molecules with the Spectron code (developed at UCI), and analyze the spectra with a broad range of tools. Linear and nonlinear vibronic spectra are expressed in term of the electronic eigenstates obtained through quantum chemistry computations, and vibrational/bath effects are incorporated in the framework of the displaced harmonic oscillator model, where all required quantities are computed at the Franck-Condon point. A paper highlighting the interface capabilities has been submitted to the Journal of Computational Chemistry, where the pyrene linear and nonlinear spectra have been computed and analyzed. Regarding nonlinear spectra, iSPECTRON was used to simulate both one-dimensional pump-probe and 2DES spectra, to characterize the spectral diffusion of the main GSB/SE peak and to link the beating along the t_2 time to the actual molecular modes via Fourier transform analysis of the spectra. The effect of the finite time resolution of realistic experiments was also demonstrated.
2. (UNIBO) The established protocol to compute single- and double-core excitations of organic molecules (employing the accurate multi-reference RASSCF/RASPT2 methodology) and a new projection technique that allows one to focus precisely on selected lower-lying valence- and core-excited states, was tested against molecules with various degrees of symmetry. In particular, we have applied this technique to study the carbon K-edge XAS on ethane and fluorine substituted ethanes, as well as 2DCXS in 1,1-difluoroethane, as described in Thrust 2 and 3 sections. Some refinements of the original techniques were introduced, by studying accurate and computationally efficient approaches for the construction of the active spaces when double core excitations have to be computed. L-edge chlorine XAS and XPS spectra were simulated on the chloroquine and hydroxychloroquine molecules, making it necessary to include relativistic corrections to the manifold of states and properties (such as scalar effects and spin-orbit coupling). (see Thrust 3)
3. (LANL-PNNL-UCI) An advanced suite of numerical algorithms able to model mixed quantum-classical dynamics with various accuracies was developed and implemented in the NWChem program. This includes improved Surface Hopping (SH) approaches [Song2020a] as well as accurate Multiconfigurational Ehrenfest *ab-initio* multiple-cloning (MCE-AIMC) formalism [Makhov 2014, Freixas2018]. This NWChem implementation allows simulating multiple-core excited-state dynamics at the TDDFT level. The NWChem SH function contains two different methods to handle decoherence corrections to alleviate inconsistencies due to the classical treatment of nuclei. Advanced algorithms for tracking trivial (unavoided) crossings between noninteracting states have also been developed in both SH and MCE-AIMC approaches. Details of the implementation and applications recently were published for SH [Song2020a] and in

preparation for MCE-AIMC [Song2020b]. Both capabitilies will be available to the broader community in a NWChem release in the near future.

4. (UCI-PNNL) Implementation of excited-state couplings within the TDDFT pseudo-wavefunction framework was completed. This capability, along with others mentioned, will be made available to the community in the near future. This development is being utilized in papers in preparation.

- **Thrust 2:** *New multi-pulse experiments designed to make use of LCLS-II capabilities*

1. (UCI-LANL) *TRUECARS study of conical intersection dynamics*. The synthetic heterodimer shown in Fig. 1a was designed [Hayes2013] as a model to observe coherences and consists of two differently substituted organic monomers A and B that are connected by a semirigid linker. The role of quantum-mechanical coherences in the elementary photophysics of functional optoelectronic molecular materials is currently under active study [Lee2019]. Designing and controlling stable coherences accompanying vibronic dynamics in organic chromophores, is the key for numerous applications. Studying the complex vibronic dynamics of such systems, and predicting experimentally observable signals that visualize them, requires the development and application of novel simulation protocols. Exact quantum dynamics is not feasible for molecules of this size, and the prominent semiclassical surface hopping protocol is not suitable since it does not properly include coherences. In this study, we employ and extend the ab-initio multiple cloning (AIMC) approach [Makhov2014, Freixas2018] based on Ehrenfest trajectories, that naturally includes coherences and decoherence behavior. The AIMC algorithm was modified such that the nuclear overlap $\rho_{\{kl\}}$ (Fig. 1d) could straightforwardly be extracted, and 472 trajectories were launched in the S_2 excited state of the heterodimer, sampling the conical intersection seam. Subsequently, the stimulated X-ray Raman TRUECARS signal [Kowalewski2015, Keefer2020a] given by

$$S(\omega_R, T) = 2I \int_{-\infty}^{\infty} dt\, e^{\{i\omega_R(t-T)\}} \varepsilon_0^*(\omega_R)\varepsilon_1(t-T) \times \rho_{\{kl\}}$$

was calculated, employing a hybrid broadband (ε_0) / narrowband (ε_1) X-ray probing scheme. This technique is available with state-of-the-art free electron laser sources, and monitors coherences without being masked by population contributions (which is usually the case in more traditional Raman-based approaches). The concept of the TRUECARS measurement is sketched in Fig. 1b, and the signal for the trajectory ensemble, which is the experimentally observable scenario, is depicted in Fig. 1c. The signal is visible throughout the dynamics despite the highly heterogeneous contributions from individual trajectories. The coherence is strong from the beginning and survives multiple conical intersection passages until 500 fs. The Wigner spectrogram of the signal [Keefer2020a], shown in Fig. 1f, reveals the transient energy splitting between the electronic states (Fig. 1e), evolving around 0.3 eV throughout the dynamics. This information is directly accessible from the measurement.

Our study tackles multiple important issues in the field. A methodology is developed to simulate the dynamics of vibronic coherence in complex organic chromophores, which are under current extensive study with respect to their photovoltaic activity. On this basis, stimulated X-ray Raman signals are demonstrated to provide an excellent means for directly monitoring these coherences with high temporal and spectral resolution, despite the largely heterogeneous contributions of the relaxation pathways in different parts of the molecular phase space. We show that the frequencies

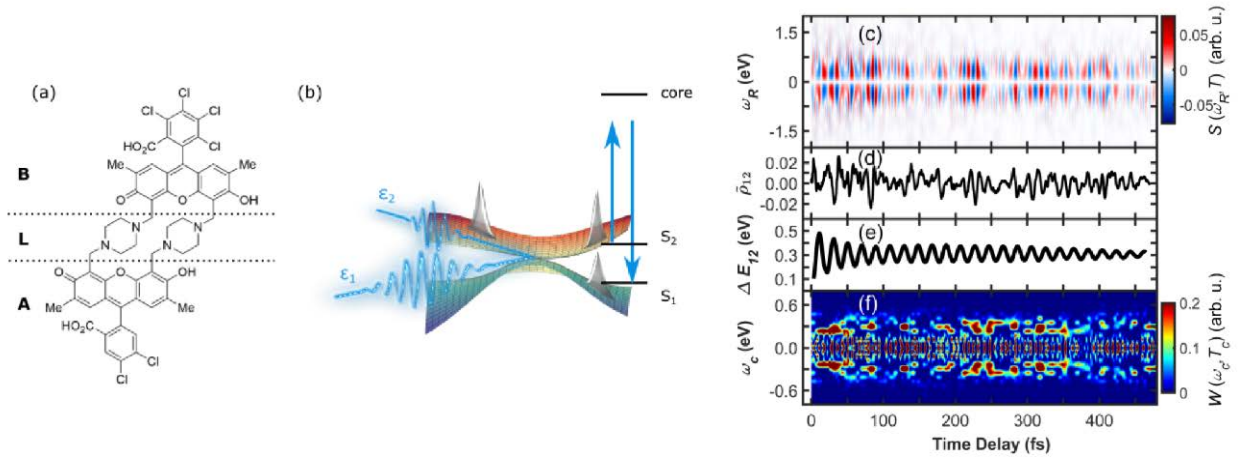

Figure 1: Stimulated *X-ray* Raman spectroscopy on a heterodimer to monitor coherences. a) Molecular structure, with the two monomers A and B and the linker L. b) TRUECARS measurement, employing the *X-ray* fields ε_0 *and* ε_1*, inducing an off-resonant stimulated Raman process to detect coherences between the electronic states. c) TRUECARS signal according to equation (1). d)* Average coherence magnitude over all 472 trajectories. e) Average energy splitting between S_2 and S_1. f) Wigner spectrogram of the TRUECARS signal. The main feature at ω_c = 0.3 eV correctly maps the energy splitting.

of the relevant molecular modes, that experience the excess kinetic energy at the conical intersections, have signatures in the signal. Different types of coherences are revealed by our simulations: one created directly after photoexcitation, and one that emerges only later at the conical intersections. The transient energy splitting between the two participating electronic states is mapped by the experimentally observable distribution of coherence frequencies. We give detailed physical insight into the coherence generation mechanisms and properties and demonstrate how they are captured by the proposed experiment. Our proposed novel technique for probing coherences using state-of-the-art X-ray sources, that are readily available at free-electron lasers, could resolve many of the outstanding issues in this field.

2. (UCI-UNIBO) *Core polaritons in X ray cavities*. Optical cavities in the infrared and visible regime has found tremendous applications in manipulating electronic, optical, and chemical properties of embedded molecules, demonstrated in numerous experiments carried out mainly by the Ebbesen group [Ebbesen2016, Hutchison2012, Thomas2019]. Molecular excitations, be it vibrational or electronic, can mix with the cavity photon modes forming hybrid light-matter states known as

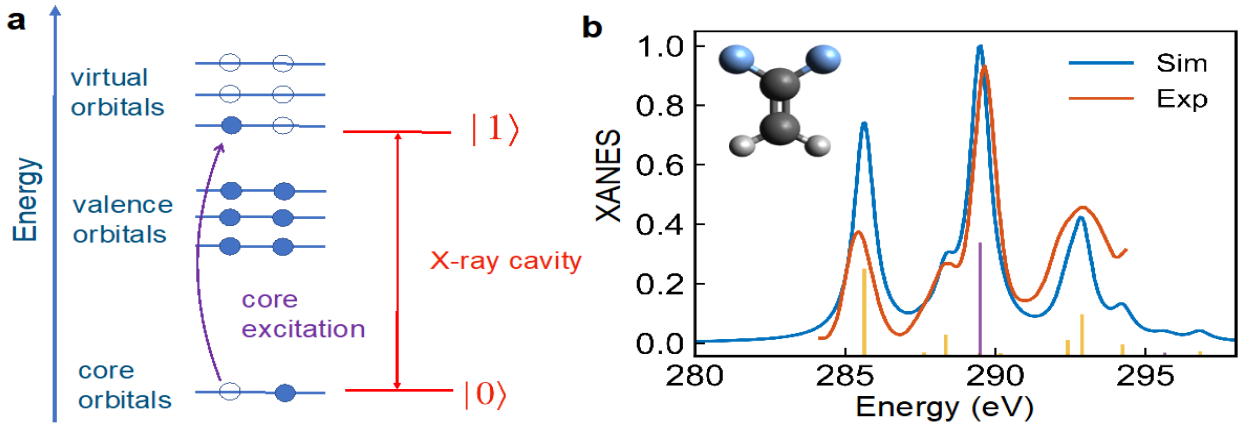

Figure 2: (a) Sketch of core-excitations coupled to an X-ray cavity photon mode. (b) Simulated vs. experimental XANES of 1,1-difluoroethylene in vacuum. Excellent theory-experiment agreent is achieved with the quantum chemistry method outlined in Thrust 1.

polaritons. In a different line of research, X-ray cavities are being used to study Mossbauer resonance of ^{57}Fe at 14.4 keV [Haber2019, Rohlsberger2012].

Here we have explored the influence of X-ray cavities on core-excitations in molecules (Fig. 2a). Specifically, we have studied the linear (XANES) and nonlinear (2DCXS) spectra of 1,1-difluoroethylene in an X-ray cavity [Gu2020a] as it contains two inequivalent carbon atoms with the lowest core-excitations separated by ~3 eV. Chemical shift (Fig. 2b). We have shown that, while core-excitations on different atoms are highly localized and decoupled, they become coupled via the exchange of cavity photons and form hybrid light-matter core-polariton states (Fig. 3b). Core-polaritons are expected to have novel transport and relaxation dynamics resembling those of exciton- and vibrational-polaritons. We have predicted (UCI-UNIBO), for the first time, the creation of such core-polariton states in both XANES (Fig. 3a) and 2DCXS (Fig. 3b), by studying the cavity with different characteristic frequencies and coupling strengths.

UCI developed the formalism and implementations to describe the core-excitation coupled with X-ray cavity photon modes. Quantum chemistry computations of single- and double-core excitations at the carbon K-edge were performed at UNIBO, employing the RASSCF/RASPT2 protocol described in Thrust 1. The QC data are of very high quality, as they can reproduce both position and intensity of the single-core excitations when compared with experimental spectra (Fig. 2b). For double core-excitation different ways of constructing and constraining the active space were studied, in order to achieve both accuracy and computational efficiency. The results of this study have been reported in a paper, recently submitted to Physical Review Letters [Bing2020a].

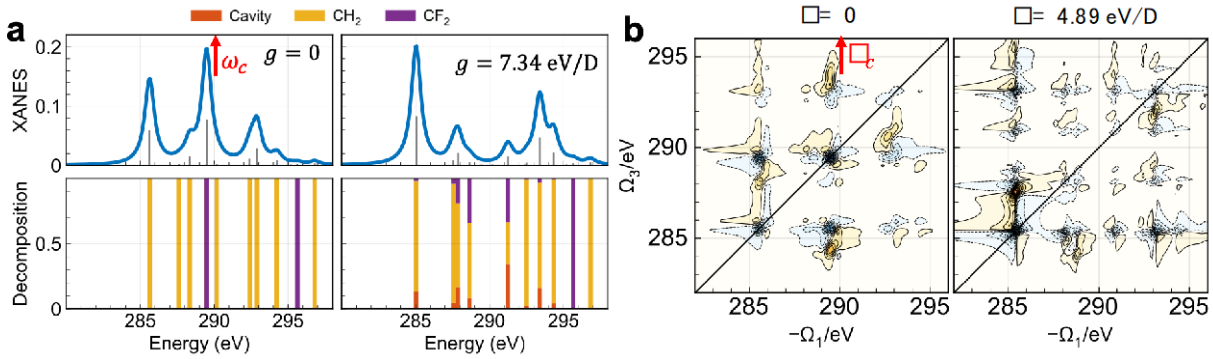

Figure 3: (a) XANES of bare molecules (g=0) and core-polaritons (g=7.34 eV/D). Each peak is decomposed into cavity photon (red), CH_2 (orange), CF_2 (violet) characters. Bare excitations are purely CH2 or CF2 as core-excitations from two carbon core-orbitals are decoupled. In contrast, the core-polaritons contain delocalized excitations involving both K-edges. (b) 2D photon echo signal for bare molecules and core-polaritons. The cross peaks reveal the correlation between core-polariton states.

- **Thrust 3:** *Applications to specific molecular systems*

1. (UNIBO) The XAS simulation protocol (at the RASSCF/RASPT2 level of theory) developed at UNIBO was tested against a variety of simple molecular systems with various degrees of symmetry: the ethane molecule and different fluorine substituted ethanes (at the carbon K-edge). The comparison of simulated and experimental XAS spectra demonstrate the remarkable accuracy of the developed protocol.
2. (UNIBO-UCI) 1,1-difluoroethane was studied by means of linear and nonlinear (2DCXS) spectroscopy to reveal the capability of an X-ray cavity to couple core-level transitions from the two independent carbon centers. The protocol developed by UNIBO to compute single- and

double-core excitations with the ab-initio quantum chemistry software OpenMolcas was tested on fluoroethenes. The fluorine atom was substituted to the hydrogens in various places, modifying the molecular symmetry. In particular, we extensively studied the ethane molecule, and the 1,1-difluoroethane. This molecule was chosen because of its two inequivalent carbon atoms with bound pre- (K-) edge transitions: CH2 around 291 eV and CF2 around 293 eV. The agreement with the experiment is remarkable. A D2h symmetry was employed in the QC computations, allowing to fine-tune the selection of the active orbitals in the different irreducible representations.

3. (UCI-UNIBO) The potential energy surfaces (PESs) of azobenzene were mapped at the RASPT2 level of theory along a few coordinates that are known to be relevant in the light-activated internal conversion processes between the lower lying nπ* excited state and the ground state. Non-adiabatic couplings (NACs) were also computed in the regions where nπ* and S_0 energy gap decreases significantly. PESs and NACs were then fitted and used as input quantities for quantum dynamics (QD) simulations that provides the accurate description of the wave-packet dynamics induced after photo-excitation. Electron densities and transition-densities were computed at the RASSCF level of theory for every grid point, and these serve as the key quantities for the evaluation of X-ray (and electron) time dependent diffraction signals. A paper is in preparation [Keefer2020c].
4. (LANL-PNNL) We have applied the new Surface Hopping formalism and TDDFT level of quantum-chemical simulations using the new NWChem capability to model the photoinduced dynamics of a trans-distyrylbenzene, a small 3-ring oligomer of polyphenylene vinylene (PPV). The results demonstrate the ability of the non-adiabatic algorithm to capture internal conversion spanning multiple excited states with distinct potential energy surfaces, fully corroborating experimental spectroscopic data. Figure 4 illustrates how the electronic energy is being transferred into molecular vibrations through electron-phonon interactions, causing complex dynamics of excited state wavefunction.

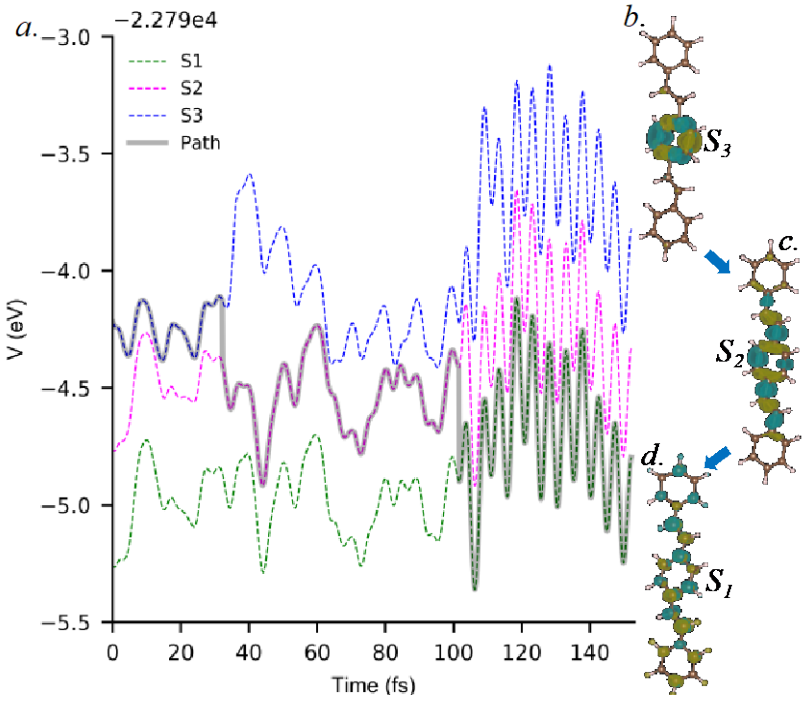

Figure 4: Panel a shows a typical example of photoexcited tragectory in PPV oligomer, demonstrating internal conversion between several excited states (S_3 to S_2 to S_1) over a span of 140 fs. Panels b, c and d show the variability of wavefunction spatial delocatization during this process as revealed by the transition density analysis. [Song 2020a].

5. (UCI-PNNL-LANL-UNIBO) We continue investigation of resonant stimulated X-ray Raman spectroscopy and X-ray and electron diffraction of bimetallic manganese complexes, Hexacyanoferrate complex and cyclooctatetraene is underway (see future plans).

6. (UNIBO-PNNL) Linear and nonlinear spectroscopy of the PBI molecule was studied with theory and experiment, making use of the iSPECTRON interface (see Thrust 1).[Segatta2020b (in preparation)]

Future Plans

- **Thrust 1**

1. (UNIBO) The RASSCF/RASPT2 protocol is being updated. In particular, we are currently exploring a spectroscopy driven selection of the orbitals to be placed in the active space, as it seems possible to choose them with *a-priori* physical insight related to the brightness of the transitions they will be involved in.
2. (UNIBO-UCI) The Spectron code will be debugged and further extended to handle newly developed X-ray spectroscopic techniques, from 2DCXS to TRUECARS.
3. (LANL-PNNL) The MCE-AIMC formalism implementation in NWChem will be debugged, optimized, and applied to representative molecular systems. [Song2020b] Altogether, the implemented non-adiabatic algorithms will extensively expand the capability of the NWChem software packages for use by the broader community.

- **Thrusts 2 and 3**

The new proposed signals will be applied to a broad variety of molecules.We thus combined the two thrusts. Several new molecular targets were identified as promising systems for the application of the novel multidimensional X-ray spectroscopic techniques described earlier. These include large conjugated systems featuring long-range energy transfer and functionalized porphyrins demonstrating charge-transfer dynamics.

1. (UNIBO) Taking advantage of the recent development of the RASSCF/RASPT2 protocol in terms of optimized orbital selection and optimization in 1,1-difluoroethane, we will study double-core excitations of more complex molecules, such as (but not limited to) the ESCA molecule, which has four inequivalent carbon atoms. A range of two-color 2DCXS set-ups will be explored at the carbon K-edge, to evidence the role of double-core excitations from the same core (higher energy probe pulse) and of single-core excitations from valence excited states (lower energy probe pulse).
2. (UCI-UNIBO) The formalism developed to describe polariton states in X-ray cavity will be extended to study molecules with a larger number of x-ray chromophore atoms as in the ESCA molecule, and to explore the cooperative effects in the presence of multiple molecules in different excitation states within a cavity. Cooperative effects can be used to enhance the light-matter coupling strength as it scales with the square root of the number of molecules.
3. (UCI-UNIBO-LANL-PNNL) Based on the results obtained for the azobenzene molecule, a protocol that combines QC data (PESs, NACs and electron densities and transition densities) with QD output for the simulation of X-ray (and electron) diffraction of a photoexcited molecular system will be refined and applied to a variety of molecular targets (such as, but not limited to, the retinal protein and thio-uracils).
4. (UNIBO) Chloroquine and hydroxychloroquine molecules are currently studied in a joint theoretical and experimental work (in collaboration with ELETTRA synchrotron in Trieste, Italy) by means of time-resolved XAS at the chlorine L-edge.
   In the experiment (performed at ELETTRA), a UV pulse is used to induce the population of excited vibrational levels of the ground electronic state, by means of an impulsive stimulated Raman scattering (ISRS) process, and the wave-packet dynamics is monitored by X-ray absorption at the chlorine L-edge, which shows clear pre-edge features around 200 eV whose intensity oscillates

along the pump-probe delay time with a period of 1.6 ps. Simulations of the Cl L-edge bound states is also performed at the RASSCF/RASPT2 level of theory, by accounting for both scalar and spin-orbit relativistic effects. Normal modes calculations of the full chloroquine molecule is carried out, and the X-ray absorption form the chloroquine π-orbitals is evaluated along the low frequency modes (that are known to be populated in the pump-induced impulsive Raman process). The simulations will be able to identify which low frequency mode is possibily activated in the ISRS process, and to demonstrate its role in chaning the intensity of the core-level signals. Based on this results, different configurations (energy, chirp) of the UV pump pulse will be explored, and the same UV-pump X-ray probe strategy will be applied on other molecular systems.

5. (UCI-PNNL) Effect of an X-ray cavity on valence and core-level excitations of model transition metal complexes [Gu2020b]
6. (UCI-PNNL) **Mn mixed-valence complexes**: Fundamental processes such as water oxydation in photosynthesis are catalyzed by enzymes containing manganese clusters. The role played by manganese in these chemical and biological processes, however, is not fully understood. While several techniques, including electron-paramagnetic-resonance spectroscopy and X-ray emission and absorption spectroscopy, have been utilized, they do not provide conclusive time-resolved information about the electron dynamics in the complex.

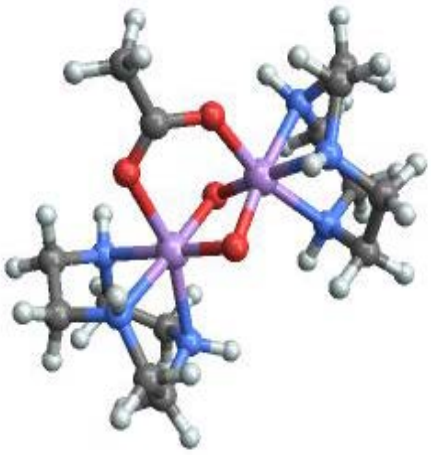

Figure 5: Structure of the Mn complex $[Mn^{III}Mn^{IV}(\mu\text{-}O)_2(\mu\text{-}OAC)(tacn)_2]^{2+}$.

By taking advantage of short, coherent X-ray pulses provided by novel FEL sources, time-resolved stimulated X-ray Raman spectroscopy (SXRS) of manganese complexes will be investigated. SXRS is a pump–probe signal using two X-ray pulses. Each pulse stimulates a Raman transition between the valence and ground states via the resonant excitation of the core states. The transition energies of the core exited states are element specific. By properly tuning the X-ray pulses to given cores, it is thus possible to select valence states preferentially localized around a desired atom in the molecule and strongly coupled to the associated core excited states. By pumping and probing at different sites with X-ray pulses of different colors, this allows one to follow the charge migration of a wavepacket of several valence excited states through the molecule.

TDDFT calculations will be performed at PNNL, in order to provide the transition energies and couplings between core and valence/ground states in selected manganese complexes. This will be employed at UCI for the computation of SXRS signals. A possible candidate, $[Mn^{III}Mn^{IV}$ (μ-O)$_2$(μ-OAC)(tacn)$_2]^{2+}$, is shown in Fig. 5. It contains two Mn atoms in different oxydation states, surrounded by ligand structures containing C, N, and O atoms. By tuning the pump pulse to the transition energies of Mn or N core excited states, different wavepackets of valence excited states are generated. Their evolution is probed at different time delays by tuning the color of the probe pulse to Mn or N core states. This provides access to the valence–core couplings in the molecule, and spatial information about the contributing molecular orbitals. A preliminary SXRS signal is shown in Fig. 6 for pump and probe pulses tuned to the Mn core excited states in $[Mn^{III}Mn^{IV}$ (μ-O)$_2$(μ-OAC)(tacn)$_2]^{2+}$. By using a two-color scheme with pump and probe pulses tuned to different core excited states, SXRS can provide additional information about charge migration between different regions in the complex [Cavaletto2020].

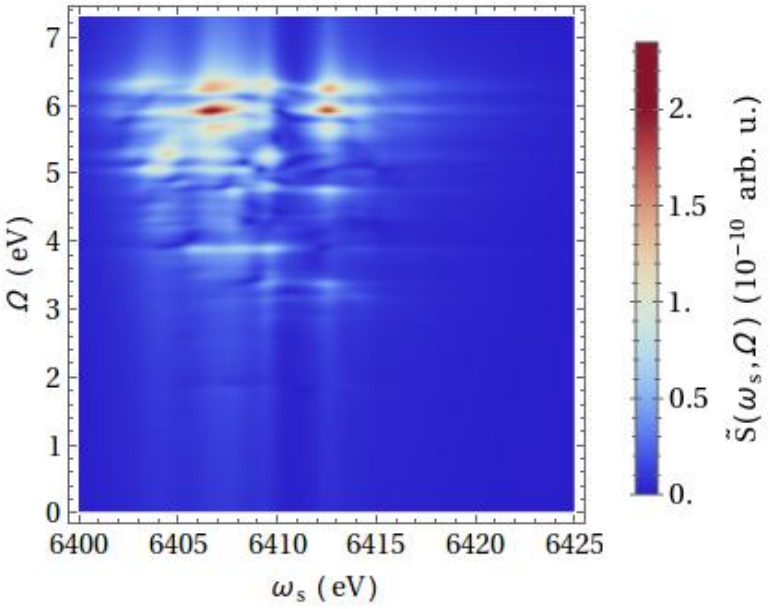

Figure 6: SXRS signal in $[Mn^{III}Mn^{IV}$ (μ-O)$_2$(μ-OAC)(tacn)$_2]^{2+}$ for pump and probe X-ray pulses tuned to the Mn core excited states. The signal is displayed as a function of the X-ray signal frequency ω_s and the optical frequency Ω conjugated to the time delay between pump and probe pulses. Peaks in the signal reveal the couplings between valence states in the wavepacket generated by the pump pulse and the core excited states resonantly excited by the probe pulse.

Time-resolved X-ray diffraction will also be calculated. In such case, the evolution of the wavepacket is observed via the off-resonant diffraction of a delayed X-ray probe. By measuring the strength of the signal as a function of the momentum transfer between incoming and outgoing X-ray radiation, X-ray diffraction can offer snapshots of the evolution of the charge densities in the molecule, with high temporal and spatial resolution. Time-resolved SXRS and X-ray diffraction can thus provide the temporal and spatial information necessary to follow electron dynamics in manganese complexes and shed light on the role of manganese centers in biologically relevant processes. These studies will be further extended to larger two-center transition metal center mixed valence complexes.

7. (UCI-PNNL) **Iron Hexacyanoferrate Complexes:** Ferrous ($[Fe(CN)6]^{4-}$) and ferric ($[Fe(CN)6]^{3-}$) hexacyanide complexes serve as prototypical model systems for understanding the

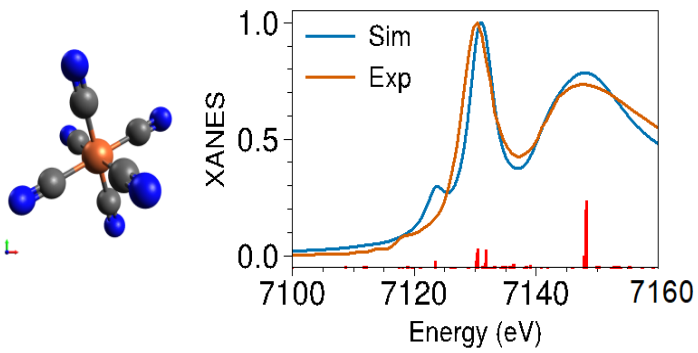

Figure 7: Structure (left) and XANES (right) for ferric hexacynanide. TDDFT simulations of the Fe K-edge are performed at PNNL and nonlinear spectroscopic simulations at UCI.

structure and spectroscopy of Fe(II) and Fe(III) octahedral transition-metal complexes in solution. Structure of the ferric hexacyanide and its XANES in the iron K-edge are shown in Fig. 7 with electronic structure and Fe K-edge simulations performed at PNNL and nonlinear spectroscopic computations at UCI. UCI will further predict the SXRS signal to reveal the correlations between valance excitations and Fe core-excitations. This will be extended to larger transition metal complexes.

8. (LANL-UCI-UNIBO) **Photophysics of cyclooctatetraene:** Cyclooctatetraene (COT) is a unique molecule which has a non-planar and anti-aromatic structure in the ground state, while it gains planarity with a conjugated aromatic π network in the 1st excited state (S_1). It decays back to S_0 through the polyradical S_1/S_0 conical intersection. Although the relaxation of S_1 excited state to S_0 ground state takes several picoseconds, the fate of photoproduct might be determined in the early dynamics within hundreds of femtoseconds, as it is the case of stilbene.

Depending on the UV-irradiation or thermal activation, cyclooctatetraene can undergo various processes such as double bond switching (DBS), ring inversions, semi-bullvalene formation, etc. Direct UV-irradiation of cyclooctatetraene demonstrated potential photoswitch functionality [Garavelli2001, Garavelli2002] (Fig. 8a). The formation of semibulvalene secondary product needs to be suppressed to increase its fatigue resistance. The substitution of H atoms into a donor/acceptor moiety can provide an elaborate control of the electronic current inside the ring as well as a chromophore for X-ray probe (Fig. 8b). Applying the semi-empirical method developed by Tretiak's group would be useful to investigate the excited state dynamics and photo-current of cyclooctatetraene upon UV irradiation given the low computational cost of the semi-empirical simulations.

The mapping of both photochemical and thermal reaction paths (including also Cope rearrangements, valence isomerizations, ring inversions, and double-bond shifting) will allow us to draw a comprehensive reactivity scheme for cyclooctatetraene, which rationalizes the experimental observations and documents the complex network of photochemical and thermal reaction path

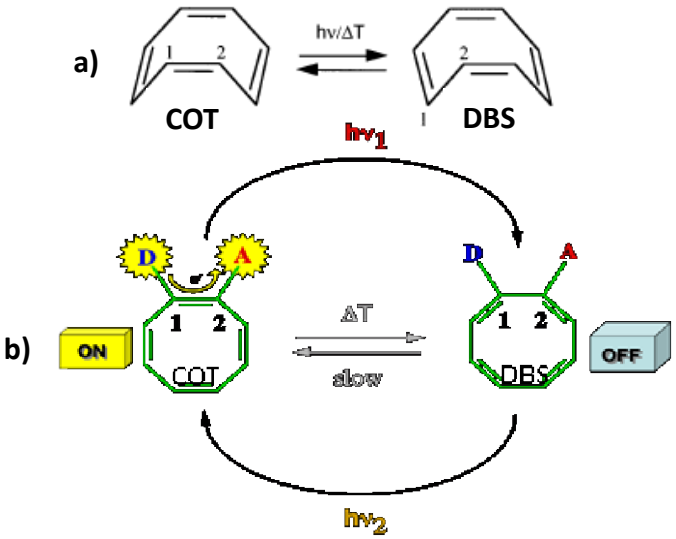

Figure 8: a) Cyclooctatetraene (COT) based photo-switch. B) COT and its double bond shifted (DBS) (photo)product switches on and off by UV or thermal activation.

interconnections. We will use cyclooctatetraene family as testbed systems for applying the developed non-adiabatic algorithms to identify signatures of photoinduced structural transformation in nonlinear spectra (LANL-UCI) and predict a photo-controlled current switch via donor and acceptor substituents (Fig. 8b) (LANL-UNIBO). Signatures of photoinduced structural transformation in nonlinear spectra will be identified.Eventually, time-resolved circular dichroism (TRCD) will be used as a direct measure of the conical intersection (CoIn) and/or the decay of S_1 excited state. Indeed, the circularly polarized light pump can generate a strong electronic ring current for the aromatic S_1 state, while it will be much smaller for the anti-aromatic S_0 ground state. TRCD signals are sensitive to the electronic coherence and their amplitude directly give the magnitude of the ring current. Thus, by comparing the amplitude of signals, we can directly observe the CoIn or the relaxation and decay of the S_1 state.

References

[Ebbesen2016] Ebbesen, T. W. **Hybrid Light–Matter States in a Molecular and Material Science Perspective**, Acc. Chem. Res. 49, 2403–2412 (2016).

[Freixas2018] Freixas, V. M., Fernandez-Alberti, S., Makhov, D. V., Tretiak, S. & Shalashilin, D. **An ab initio multiple cloning approach for the simulation of photoinduced dynamics in conjugated molecules**, Phys. Chem. Chem. Phys. 20, 17762 (2018).

[Garavelli2001] M. Garavelli, et al., **Intrinsically Competitive Photoinduced Polycyclization and Double-Bond Shift through a Boatlike Conical Intersection**, Angew. Chem. Int. Ed., 40, 8, 1466 (2001)

[Garavelli2002] M. Garavelli, et al., **Cyclooctatetraene Computational Photo- and Thermal Chemistry: A Reactivity Model for Conjugated Hydrocarbons**, J. Chem. Theory Comput., 124, 46, 13770 (2002)

[Haber2019] Haber, J. et al. **Spectral Control of an X-ray L -Edge Transition via a Thin-Film Cavity**, Phys. Rev. Lett. 122, 123608 (2019).

[Hayes2013] Hayes, D., Griffn, G. B. & Engel, G. S. **Engineering Coherence Among Excited States in Synthetic Heterodimer Systems**, Science 340, 1431 (2013).

[Hutchison2012] Hutchison, J. A., Schwartz, T., Genet, C., Devaux, E. & Ebbesen, T. W. **Modifying Chemical Landscapes by Coupling to Vacuum Fields.** Angew. Chem. Int. Ed., 51, 1592–1596 (2012).

[Keefer2020a] Keefer, D., Schnappinger, T., de Vivie-Riedle, R. & Mukamel, S. **Visualizing Conical Intersection Passages via Vibronic Coherence Maps Generated by Stimulated Ultrafast X-ray Raman Signals**, P. Natl. Acad. Sci. USA (2020) doi.org/10.1073/pnas.2015988117 .

[Kowalewski2015] Kowalewski, M., Bennett, K., Dorfman, K. E. & Mukamel, S. **Catching Conical Intersections in the Act: Monitoring Transient Electronic Coherences by Attosecond Stimulated X-ray Raman Signals**, Phys. Rev. Lett. 115, 193003 (2015).

[Lee2019] Lee, C., Lee, S., Kim, G.-U., Lee, W. & Kim, B. J. **Recent advances, design guidelines, and prospects of all-polymer solar cells**, Chem. Rev. 119, 8028 (2019).

[Rohlsberger2012] Röhlsberger, R., Wille, H.-C., Schlage, K. & Sahoo, B. **Electromagnetically induced transparency with resonant nuclei in a cavity**, Nature 482, 199–203 (2012).

[Thomas2019] Thomas, A. et al. **Tilting a ground-state reactivity landscape by vibrational strong coupling**, Science 363, 615–619 (2019).

Peer-Reviewed Publications Resulting from this Project (2018-2020)

1. [Asban 2019] Shahaf Asban, Konstantin E. Dorfman, and Shaul Mukamel. "**Quantum phase-sensitive diffraction and imaging using entangled photons**", PROCEEDINGS OF THE NATIONAL ACADEMY OF SCIENCES OF THE UNITED STATES OF AMERICA Volume: 116 Issue: 24 Pages: 11673-11678 DOI: 10.1073/pnas.1904839116
2. [Borrego-Varillas 2019] Rocio Borrego-Varillas, Artur Nenov, Lucia Ganzer, Aurelio Oriana, Cristian Manzon, Alessandra Tolomelli, Ivan Rivalta, Shaul Mukamel, Marco Garavelli and Giulio Cerullo. "**Two-dimensional UV spectroscopy: a new insight into the structure and dynamics of biomolecules**", *Chem. Sci., 10, 9907-9921 (2019)*
3. [Bruner 2019] A. Bruner, S. M. Cavaletto, N. Govind, S. Mukamel, "**Resonant X-ray Sum-Frequency-Generation Spectroscopy of K-edges in Acetyl Fluoride**", JOURNAL OF CHEMICAL THEORY AND COMPUTATION Volume: 15 Issue: 12 Pages: 6832-6839 DOI: 10.1021/acs.jctc.9b00642.

4. [Cho 2019] Daeheum Cho, Jeremy R. Rouxel, Markus Kowalewski, JinYong Lee, and Shaul Mukamel. "**Imaging of transition charge densities involving carbon core excitations by all X-ray sum-frequency generation**", PHILOSOPHICAL TRANSACTIONS OF THE ROYAL SOCIETY A-MATHEMATICAL PHYSICAL AND ENGINEERING SCIENCES Volume: 377 Issue: 2145 Article Number: 20170470 DOI: 10.1098/rsta.2017.0470
5. [Dorfman 2019] Konstantin E. Dorfman, Shahaf Asban, Lyuzhou Ye, Jeremy R. Rouxel, Daeheum Cho, And Shaul Mukamel. "**Monitoring Spontaneous Charge-Density Fluctuations by Single-Molecule Diffraction of Quantum Light**", JOURNAL OF PHYSICAL CHEMISTRY LETTERS Volume: 10 Issue: 4 Pages: 768-773 DOI: 10.1021/acs.jpclett.9b00071
6. [Gu 2020a] Bing Gu, Artur Nenov, Francesco Segatta, Marco Garavelli, and Shaul Mukamel. "**Manipulating core-excitations in molecules by X-ray cavities**", *Phys. Rev. Lett. (Aug submission, 2020)*
7. [Keefer 2020b] Daniel Keefer, Victor M. Freixas, Huajing Song, Sergei Tretiak, Sebastian Fernandez-Alberti, and Shaul Mukamel. "**Monitoring Molecular Vibronic Coherences by Ultrafast X-ray Spectroscopy**", *Nature Comm (Aug 2020 submission)*
8. [Nascimento 2020] Daniel R. Nascimento, Yu Zhang, Uwe Bergmann, Niranjan Govind. "**Near-Edge X-ray Absorption Fine Structure Spectroscopy of Heteroatomic Core-Hole States as a Probe for Nearly Indistinguishable Chemical Environments**", *J. Phys. Chem. Lett.* 11, 2, 556-561 (2020)
9. [Nenov 2019] Artur Nenov, Francesco Segatta, Adam Bruner, Shaul Mukamel, and Marco Garavelli, "**X-ray Linear and Nonlinear spectroscopy of the ESCA molecule**", *J. Chem. Phys*., 151, 114110 (2019)
10. [Osipov 2019] Vladimir Osipov, Shahaf Asban, and Shaul Mukamel. "**Time and frequency resolved transient-absorption and stimulated-Raman signals of stochastic light**", JOURNAL OF CHEMICAL PHYSICS Volume: 151 Issue: 4 Article Number: 044113 DOI: 10.1063/1.5109258
11. [Segatta 2020a] Francesco Segatta, Daniel R. Nascimento, Artur Nenov, Shaul Mukamel, Niranjan Govind, Marco Garavelli, "**iSPECTRON: a simulation interface for linear and non-linear spectra with ab-initio quantum chemistry software**", *J. Chem. Comput.* (Sept. 2020 submission)
12. [Segatta 2020c] Francesco Segatta, Artur Nenov, Silvia Orlandi, Alberto Arcioni, Shaul Mukamel, and Marco Garavelli, "**Exploring the capabilities of optical pump X-ray probe NEXAFS spectroscopy to track photo-induced dynamics mediated by conical intersections**", *Faraday Discuss.*, 221, 245-264 (2020)
13. [Song 2020a] Huajing Song, Sean Fischer, Yu Zhang, Christopher Cramer, Shaul Mukamel, Niranjan Govind, Sergei Tretiak. "**First Principles Non-Adiabatic Excited-State Molecular Dynamics in NWChem**", *just accepted in J. Chem. Theory Comput. (2020) (https://doi.org/10.1021/acs.jctc.0c00295)*
14. [Tollerud 2019] Jonathan Owen Tollerud, Giorgia Sparapassi, Angela Montanaro, Shahaf Asban, Filippo Glerean, Francesca Giusti, Alexandre Marciniak, George Kourousias, Fulvio Bille, Federico Cilento, Shaul Mukamel, Daniele Fausti. "**Femtosecond covariance spectroscopy**", PROCEEDINGS OF THE NATIONAL ACADEMY OF SCIENCES OF THE UNITED STATES OF AMERICA Volume: 116 Issue: 12 Pages: 5383-5386 DOI: 10.1073/pnas.1821048116
15. [Ye 2019a] Lyuzhou Ye, Jeremy R. Rouxel, Shahaf Asban, Benedikt Rosner, and Shaul Mukamel. "**Probing Molecular Chirality by Orbital-Angular-Momentum-Carrying X-ray Pulses**", JOURNAL OF CHEMICAL THEORY AND COMPUTATION Volume: 15 Issue: 7 Pages: 4180-4186 DOI: 10.1021/acs.jctc.9b00346
16. [Ye 2019b] Lyuzhou Ye, Jeremy R. Rouxel, Daeheum Cho, and Shaul Mukamel. "**Imaging electron-density fluctuations by multidimensional X-ray photon-coincidence diffraction**", PROCEEDINGS OF THE NATIONAL ACADEMY OF SCIENCES OF THE UNITED STATES OF AMERICA Volume: 116 Issue: 2 Pages: 395-400 DOI: 10.1073/pnas.1816730116

Manuscripts in preparation

17. [Cavaletto2020] **Resonant stimulated x-ray Raman spectroscopy of bimetallic manganese complexes**, S. M. Cavaletto, D. R. Nascimento, Y. Zhang, N. Govind, S. Mukamel *(2020, in preparation)*
18. [Gu2020b] **Revealing valence- and core-polaritons of iron hexacyanoferrate complexes by nonlinear X-ray spectroscopy** B. Gu, D. R. Nascimento, S. M. Cavaletto, N. Govind, S. Mukamel *(2020, in preparation).*
19. [Keefer2020c] **Monitoring ultrafast photoisomerization of azobenzene by time resolved X-ray diffraction**, D. Keefer, F. Aleotti, J. Rouxel, F. Segatta, B. Gu, A. Nenov, M. Garavell, and S. Mukamel *(2020, in preparation)*
20. [Segatta2020b] **Linear and non-linear spectroscopy of the PBI molecule: theory meets experiments,** F. Segatta, M. Russo, D. N. Nascimento, D. Presti, A. Nenov, M. Maiuri, N. Govind, G. Cerullo and M. Garavelli *(2020, in preparation)*
21. [Song2020b] **The MCE-AIMC formalism implementation in NWChem** H. Song, Victor M. Freixas, S. Fernandez-Alberti, S. Mukamel, N. Govind, S. Tretiak, *(2020, in prepation)*

Quantum Dynamics Probed by Coherent Soft X-Rays

Margaret M. Murnane and Henry C. Kapteyn
JILA and Department of Physics, University of Colorado at Boulder
Phone: (303) 210-0396; E-mail: Margaret.Murnane@colorado.edu

Project Scope

The goal of this research is to develop novel short wavelength quantum light sources, and use them to to understand the dynamic response of quantum systems to short wavelength and strong laser fields. We made exciting advances since 2018, with 15 peer-reviewed publications in top journals such as PRL, Science, Science Advances, Optica, Nature Photonics and elsewhere. Students and postdocs from our group have recently moved to DOE Laboratories (Sandia (2) and Los Alamos (2)). Finally, in other distinct research efforts, we have several collaborations with DOE laboratories, including LBNL and LANL, to develop new imaging methods using electrons and coherent extreme UV (EUV) and soft X-ray (SXR) sources.

Recent Progress

New highly-cascaded VUV sources for probing molecular and material dynamics [1-4]: We made significant advances in developing new light sources in the vacuum ultraviolet (VUV) spectral region (~6–18 eV) — a spectral region uniquely suited to probe physical and chemical processes since the ionization energies of nearly all molecules and materials lie in this energy range. VUV spectroscopies include angle-resolved photoemission spectroscopy (ARPES), which studies the electronic structure of materials and surfaces, and photoionization mass spectroscopy (PIMS), which studies combustion. To date however, few sources of high flux, high repetition rate, femtosecond pulse duration VUV beams were available.

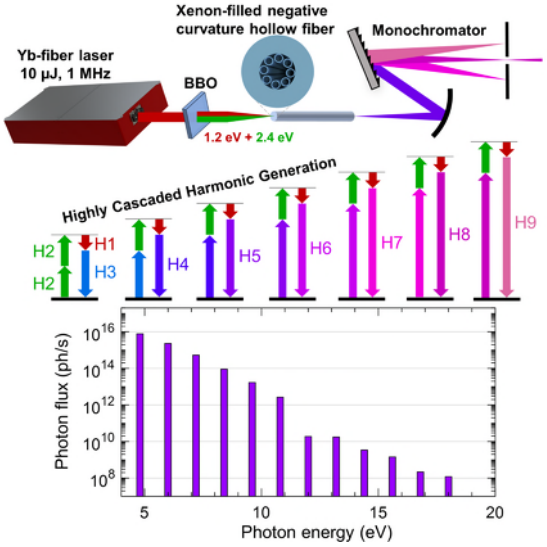

Fig. 1. Highly cascaded harmonic generation is a new and unique high-flux ultrafast VUV source for unique applications in ultrafast photoelectron spectroscopies. Note that the flux at 11-15eV is higher than shown, due to an inefficient monochrometer used for that region.

In recent research, we developed an new VUV light source that is ideal for applications in ARPES and PIMS, with high flux, high repetition rate (100kHz to >MHz), a photon energy range from the UV to 18 eV, with variable energy (~10-40 meV) and time resolution (~50-100 fs).[1] It harnesses a new highly cascaded harmonic generation (HCHG) process (see Fig. 1) where UV and VUV spectral lines are produced through upconversion of an infrared fiber laser such that each harmonic contributes to the cascaded formation of higher harmonics. A significant advantage of this HCHG process is that the peak intensity required for this process is ~10^{12} W/cm^2 - substantially lower (x10-100) than that required for high harmonic generation, and correspondingly lowering the pulse energy needed for VUV generation. This allows us to run up to MHz repetition rates, or lower as needed for delicate samples. And at 10^{12}–10^{16} photons per second, this VUV source can minimize effects such as space-charge, false coincidences, and detector dead times.

This VUV source is ideal for applications in angle-resolved photoemission from quantum materials, and photoionization mass spectrometry of molecules – to understand the fastest femtosecond-to-attosecond charge transfer reactions, for understanding the interaction of light with next-generation photoresists, and for understanding reactions to develop more efficient combustion processes. We are collaborating with Nicole Labbe from CU Boulder Mechanical Engineering and Sandia National Labs on this research. In recent research, we explored enol chemistry, that are found in combustion environments and our atmosphere, and have has garnered increasing attention due to many unanswered questions. The scarcity of experimental data concerning enols means that combustion and atmospheric models lack sufficient constraining parameters, impacting computational predictions. Experimental detection is difficult because mass spectrometry, a powerful tool for probing a wide variety of species, cannot distinguish between enols and their thermodynamically favorable ketone isomers. A solution to this ambiguity is to use tunable VUV light to identify the presence of the enol by its lower ionization energy compared to the isomer. By combining our novel VUV light source with a microreactor, we first explored the formation of vinyl alcohol from acetaldehyde and confirmed that the observed isomerization is indeed unimolecular. Secondly, we observed the thermal tautomerization of acetone to propen-2-ol for the first time. Finally, we observed the thermal tautomerization of cyclohexanone to 1-cyclohexenol and methyl vinyl ketone to 2-hydroxybutadiene. Our measurements can be used to constrain models, inform future experimental studies of enol reactivity, and potentially enhance current understanding of combustion and environmental chemistry. Several other systems have been explored and additional publications are in preparation.

Structured Extreme-Ultraviolet Beams with Spin and Orbital Angular Momentum [5, 6,10,11,12]: In recent research we made significant progress in creating polarization and phase structured HHG beams (spin and orbital angular momentum, SAM and OAM) that can be used to enhance contrast, and to implement unique excitations and probes of chiral structures in molecules, magnetic materials and nanostructures. We demonstrated the first bright, phase-matched, extreme UV (EUV) and soft X-ray HHG beams with circular (or elliptical) polarization, as well as the ability to generate HHG beams with unique polarization and phase structure. These new HHG capabilities are ideal for a suite of ultrafast X-ray absorption spectroscopies, photoelectron spectroscopies and magneto-optic spectroscopies. Moreover, through selection rules, they allow us to sculpt the HHG spectrum, to tailor the spectral, polarization and phase structure for particular applications.

Mapping electron-phonon coupling and hot electron cooling in copper nanoparticles in the warm-dense matter regime: In research in collaboration with LANL and LBNL, we explored a unique method for understanding warm dense matter — a highly-excited state of matter that lies at the confluence of solids, plasmas, and dense liquids. Its physical properties are critical for understanding exotic matter found in astrophysics, planetary, and plasma sciences. However, our knowledge to date has been hindered by the difficulty of probing the strongly-coupled interactions between the electrons and ions, that occur on femtosecond timescales on up. By exciting isolated ~8 nm nanoparticles with a femtosecond laser, we can create uniformly-excited warm-dense matter, and heat electrons to very high temperatures ~10,000 Kelvin. We then measure the instantaneous hot electron temperature and extract the electron-ion coupling and hot electron cooling rates in warm-dense nanomatter for the first time. Comparison with advanced theories confirms that the superheated nanoparticles lie at the boundary between hot solids and plasmas with very strong electron-ion coupling. Our in-situ measurements demonstrate a new route for

exploring the properties of matter in the warm-dense regime and enable benchmarking for current state-of-the-art theories and future developments.

Future work

We will extend structured high harmonic beams from the EUV into the soft x-ray regions and use them to probe dynamics in molecular, nano and materials systems. Ultra-broad bandwidth, ultrafast HHG will be used implement dynamic EUV and soft x-ray spectroscopies in samples excited using mid-IR – UV light. We will also capture dynamics in molecules and nanosystems using photoelectron spectroscopies.

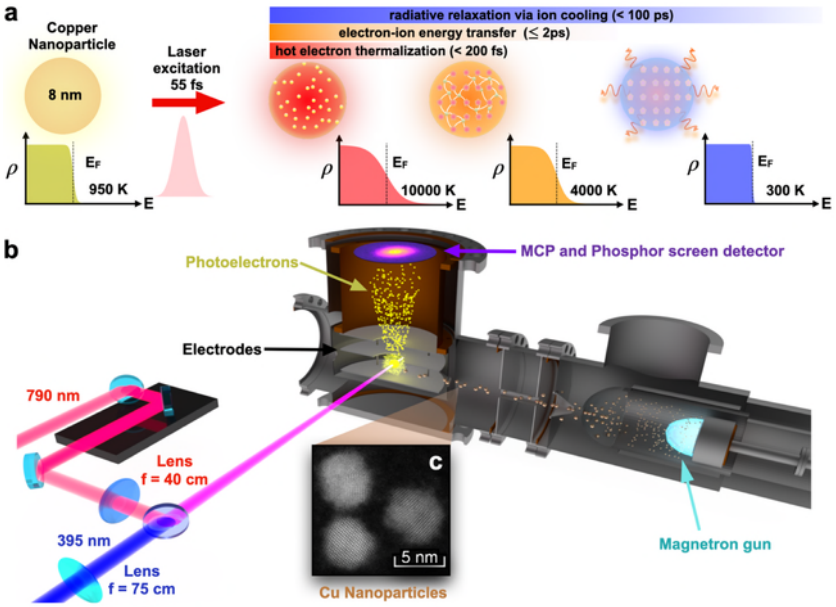

Figure 2. Probing laser excited dynamics of Cu nanoparticles (CuNPs). (a) After excitation by a femtosecond laser, hot electrons thermalize on timescales <200 fs. This is followed by energy transfer from the electron bath to the lattice on timescales up to 2 ps. The corresponding electron Fermi distribution is mapped out using photoelectron spectroscopy and shown in cartoon form. (b) Experimental apparatus for in-sity ultrafast photoelectron spectroscopy of ligand-free Cu nanoparticles. (c) Iset shows a dark-field STEM image of the nanoparticles, confirming the high mono-dispersity and uniform crystal structure.

Peer-Reviewed Publications/Patents Resulting from this Project (2018-2020)

1. D. Couch, D. Hickstein, S. Backus, D. Winters, J. Ramirez, S. Domingue, M. Kirchner, C. Durfee, M. Murnane, H. Kapteyn, "A 1 MHz ultrafast vacuum UV source via highly cascaded harmonic generation in negative-curvature hollow-core fibers," Optica **7**, 832 (2020). doi.org/10.1364/OPTICA.395688

2. Xun Shi, Chen-Ting Liao, Zhensheng Tao, Emma Cating, Margaret Murnane, Carlos Hernandez-Garcia, Henry Kapteyn, "Attosecond light science and its application for probing quantum materials," Invited paper, JPhys Photonics/JPhys B **53**, 184008 (2020). https://doi.org/10.1088/1361-6455/aba2fb

3. D. Couch, Q. Nguyen, A. Liu, D. Hickstein, H. Kapteyn, M. Murnane, N. Labbe, "Detection of the keto-enol tautomerization in acetaldehyde, acetone, cyclohexanone, and methyl vinyl ketone with a novel VUV light source", Proc. Combustion Institute, in press (2020).

4. M. Murnane, X. Shi, H. Kapteyn, "Probing and manipulating magnetic and 2D quantum materials using ultrafast laser and high harmonic sources, in press, Journal of Physics: Condensed Matter, in press (2020).

5. L. Rego, K. Dorney, N. Brooks, Q. Nguyen, C.-T. Liao, J. San Roman, D. Couch, A. Liu, E. Pisanty, M. Lewenstein, L. Plaja, H. C. Kapteyn, M. M. Murnane, C. Hernandez-Garcia, "Generation of extreme-ultraviolet beams with time-varying orbital angular momentum," Science **364**, eaaw9486 (2019). DOI:10.1126/science.aaw9486. *Featured on cover*.

6. K. Dorney, L. Rego, N. J. Brooks, J. San Román, C. Liao, J. Ellis, D. Zusin, C. Gentry, Q. Nguyen, J. Shaw, A. Picón, L. Plaja, H. Kapteyn, M. Murnane, C. Hernández-García, "Helicity in a twist: Controlling the polarization, divergence and vortex charge of attosecond high harmonic beams via all-optical spin-orbit momentum coupling," Nature Photonics. **13**, 123–130 (2019). DOI: 10.1038/s41566-018-0304-3

7. Robert Schoenlein, Thomas Elsaesser, Karsten Holldack, Zhirong Huang, Henry Kapteyn, Margaret Murnane and Michael Woerner, "Recent advances in ultrafast X-ray sources", Phil. Trans. R. Soc. A **377**: 20180384. (2019). https://doi.org/10.1098/rsta.2018.0384

8. F. Bencivenga, R. Mincigrucci, F. Capotondi, L. Foglia, D. Naumenko, A. Maznev, E. Pedersoli, A. Simoncig, F. Caporaletti, V. Chiloyan, R. Cucini, F. Dallari, R. Duncan, T. Frazer, G. Gaio, A. Gessini, L. Giannessi, S. Huberman, H. Kapteyn, J. Knobloch, G. Kurdi, N. Mahne, M. Manfredda, A. Martinelli, M. Murnane, E. Principi, L. Raimondi, S. Spampinati, C. Spezzani1, M. Trovo, M. Zangrando, G. Chen, G. Monaco, K. Nelson, C. Masciovecchio, "Nanoscale transient gratings excited and probed by extreme ultraviolet femtosecond pulses," Science Advances **5**, eaaw5805 (2019). DOI: 10.1126/sciadv.aaw5805

9. E. Pisanty, L. Rego, J. San Roman, A. Picon, K. M. Dorney, H. C. Kapteyn, M. M. Murnane, L. Plaja, M. Lewenstein, C. Hernandez-Garcia, "Conservation of torus-knot angular momentum in high-order harmonic generation," Physical Review Letters **122**, 203201 (2019). DOI:10.1103/PhysRevLett.122.203201

10. D. Popmintchev, B. Galloway, M.C. Chen, F. Dolar, C. Mancuso, L. Miaja-Avila, G. O'Neil, J. Shaw, G. Fan, S. Ališauskas, G. Andriukaitis, T. Balčiunas, O. Mücke, A. Pugzlys, A. Baltuška, H. Kapteyn, T. Popmintchev, M. Murnane, "Near and extended edge X-ray absorption fine structure spectroscopy using ultrafast coherent high harmonic supercontinua", Physical Review Letters **120**, 093002 (2018). *Also featured in Physics, https://physics.aps.org/synopsis-for/10.1103/PhysRevLett.120.093002*

11. P-C. Huang, J. Huang, C. Hernández-García, B. Huang, C. Lu, L. Rego, D. Hickstein, J. Ellis, A. Jaron-Becker, A. Becker, S. Yang, C. Durfee, L. Plaja, H. Kapteyn, M. Murnane, A. Kung, M.-C. Chen, "Polarization Control of Isolated Attosecond Pulses," Nature Photonics **12**, 349 (2018). doi:10.1038/s41566-018-0145-0

12. J. Ellis, K. Dorney, D. Hickstein, N. Brooks, C. Gentry, C. Hernandez-Garcia, D. Zusin, J. Shaw, Q. Nguyen, C. Mancuso, S. Witte, H. Kapteyn, M. Murnane, "High harmonics with spatially varying ellipticity", Optica **5**, 479 (2018).

13. L. Young, K. Ueda, M. Guhr, P. Bucksbaum, M. Simon, S. Mukamel, N. Rohringer, K. Prince, C. Masciovecchio. M. Meyer, A. Rudenko, D. Rolles, C. Bostedt, M. Fuchs, D. Reis, R. Santra, H. Kapteyn, M. Murnane. H. Ibrahim, F. Legare, M. Vrakking, M. Isinger, D. Kroon, M. Gisselbrecht, A. L'Huillier, H. Worner, S. Leone, "Roadmap of ultrafast x-ray atomic and molecular physics", J. Phys. B: At. Mol. Opt. Phys. **51**, 032003 (2018). 10.1088/1361-6455/aa9735

14. L. Martin, R. Bello, C. Hogle, A. Palacios, X. Tong, J. Sanz-Vicario, T. Jahnke, M. Schöffler, R. Dörner, T. Weber, F. Martín, H. Kapteyn, M. Murnane, P. Ranitovic, "Revealing the Role of Electron-Electron Correlations by Mapping Dissociation of Highly Excited D_2^+ using Attosecond XUV Pulses," Physical Review A **97**, 062508 (2018).

15. A. A. Maznev, F. Bencivenga , A. Cannizzo, F. Capotondi, R. Cucini , R. A. Duncan, T. Feurer, T. D. Frazer , L. Foglia , H.-M. Frey, H. Kapteyn, J. Knobloch, G. Knopp, C. Masciovecchio, R. Mincigrucci, G. Monaco, M. Murnane, I. Nikolov, E. Pedersoli , A. Simoncig, A. Vega-Flick, K. A. Nelson, "Generation of coherent phonons by coherent extreme ultraviolet radiation in a transient grating experiment," Appl. Phys. Lett. **113**, 221905 (2018); https://doi.org/10.1063/1.5048023

* Four additional papers are written or in preparation, to be submitted in 2020.

DYNAMICS OF TWO-ELECTRON ATOMIC AND MOLECULAR PROCESSES

Jean Marcel Ngoko Djiokap, P.I.
The University of Nebraska, Department of Physics and Astronomy
855 North 16th Street, 208 Jorgensen Hall, Lincoln, NE 68588-0299
Email: marcelngoko@unl.edu

PROGRAM SCOPE

The goals of this project that started on August 1, 2020 are to develop state-of-the-art numerical toolboxes and theoretical tools to describe, understand, control, and image ultrafast correlated two-electron atomic or molecular processes involving energy and spin angular momentum transfers from intense, short-wavelength, ultrashort, arbitrarily-polarized, external electromagnetic fields eventually delayed in time to matter. More generally, we aim to study the time-dependent correlated dynamics of interacting few-body quantum systems. Investigations of current interest are in the areas of strong field physics, linear attosecond physics, and multiphoton ionization processes. Nearly all proposed projects require large-scale numerical computations, involving, e.g., the direct solution of the full-dimensional time-dependent or time-independent Schrödinger equation for two-electron (or multi-electron) systems interacting with electromagnetic radiation. In some cases, our studies have been stimulated by experimental work carried out by other investigators funded by the DOE AMOS physics program. Principal benefits and outcomes of this research are improved understanding of how to induce and control electron dynamics in atoms and molecules using attosecond pulses, how to transfer energy and spin angular momentum from electromagnetic radiation to matter, how to image electron correlation processes while they occur, and how to characterize the ionizing pulses.

RECENT PROGRESS

A. *Interference of Photoelectron Wave Packets in Ionization of Atoms by Two Time-Delayed Crossing Arbitrarily Polarized Ultrashort Pulses*

Ramsey interferences [1] of the electron wave packets created by photoionization of atoms using two time-delayed, single-color, crossing ultrashort pulses are investigated both analytically using first-order perturbation theory (PT) and numerically by means of *ab-initio* quantum mechanical calculations. The use of orthogonal pulses is shown to lead to two counterintuitive electron phenomena that are absent for co-propagating pulses [2-7]. First, when the initial pulse is linearly-polarized along the propagation direction of the circularly-polarized (CP) later pulse, we find that the circularly polarized single-photon absorption leads to regular single-arm Fermat spiral patterns in the photoelectron momentum distribution. It is shown that such patterns recorded along the surface of a cone with an opening angle θ being above or below the polarization xy-plane of the CP pulse are mirror images. Exquisite control for these one-arm spirals is achieved by varying the relative field amplitude between the two pulses. Second, when two orthogonal pulses are elliptically-polarized with the same or opposite helicity, we determine using PT a correlation between the pulse parameters (ellipticities and intensities) and the detection geometries for which regular (non-distorted) two-arm Fermat spirals or Newton's rings occur in the photoelectron momentum distribution in a plane tilted by an azimuthal angle $\varphi = \pm\psi$ with respect to the zx-plane. Our prediction, illustrated here for the case of single-photon ionization of hydrogen and

helium atoms, is quite general as may hold for any S-state. *(Manuscript in preparation and will be submitted soon.)*

B. *On the Topological Charge of the Transition Amplitude in Ionization of Atoms by Short Pulses*

The concept of electron vortex lines (EVL) [8] is useful in various problems of quantum mechanics. In particular, it has been shown [2-7] that EVL can be seen as spiral patterns in the electron momentum distribution resulting from the ionization of atoms and molecules by a pair of ultrashort laser pulses. These vortices are characterized by the magnitude of the topological charges describing zeros of the transition amplitude. In our work, we analytically evaluate the topological charge (also known as the vortex strength) in the multiphoton regime using perturbation theory (PT). We have found that the topological charge $m(p)$ (where p is the photoelectron momentum) calculated from the transition amplitude for the process of ionization of an atom depends not only on the helicity of the ionizing laser pulses, but also on the initial state of the atom, which has well-defined orbital angular momentum quantum numbers l_i, m_i. For example, for both single-photon and multiphoton single ionization of an atom by either a single short circularly-polarized pulse or a pair of time-delayed co-rotating circularly-polarized single-color pulses, the calculated topological charge $m(p) = m_i - \mu N$ is independent of the photoelectron energy and time delay; however it is determined by the magnetic quantum number m_i of the initial state, the handedness of the circularly-polarized laser pulse $\mu = \pm 1$, as well as the number N of photons absorbed per pulse. The same processes for the cases of time-delayed counter-rotating circularly-polarized single-color or two-color pulses are also investigated. We illustrate these PT predictions by comparing them with the results from solution of the six-dimensional two-electron time-dependent Schrödinger equation for He atom. *(Manuscript in preparation and will be submitted soon.)*

C. *Generation of Torqued-Electronic Vortices*

For the linear (in the pulse intensity) process of single ionization of atoms by a train of n pairs of circularly-polarized attosecond extreme ultraviolet (XUV) unchirped pulses delayed in time by τ, the generation of torqued-electronic vortices resulting from interaction of individual electron vortices or Newton's rings is investigated. Our study is based on both first-order perturbation theory (PT) analysis and solution of the six-dimensional two-electron time-dependent Schrödinger equation (TDSE). The observable is the photoelectron momentum distribution in the laser polarization plane. For this exotic pulse train, the two pulses in each pair are delayed in time by τ_0 and they are either counter-rotating or co-rotating. We also study how the interactions of individual electron vortices or Newton's rings depend upon the pulse ellipticity in a pair of pulses. We first consider the simplest case of only two pairs in the train. Next, we extend our study for $n = 2$ pairs of pulses to the more general case of n pairs of pulses in a train. In each case, the comparison between PT and TDSE results allows us to extract from an analytic expression for the ionization triply differential probability all the parameters in the train of pair of pulses, including the carrier frequencies, durations, helicities, the time delay between two pulses in a pair, and the time delay for successive pairs in the train. *(Manuscript in preparation and will be submitted soon.)*

FUTURE PLANS

In addition to preparing research described above for publication, we are currently investigating five research problems that should be completed in the remainder of the project period:

(a) Electron photoionization for characterization of a train of attosecond pulses or isolated attosecond pulses with time-dependent polarization state.

(b) Effects of attochirp on electron matter-wave vortices. We shall consider first the case of single photoionization of He by a pair of time-delayed, oppositely circularly-polarized attosecond pulses having equal, opposite, or different chirp parameters. Next, we shall consider the investigation C. listed above in the context of chirped pulses.

(c) Double-slit effects in double photoionization of the ground state of the H_2 molecule by few-cycle, elliptically polarized pulses in the high-photon soft X-ray regime within the dipole approximation. The first observable we shall consider is the dynamical electron vortex-shaped momentum distribution produced by time-delayed elliptically-polarized pulses [9], which is a temporal two-slit interference electron phenomenon. The second observable is the angular and momentum distributions exhibiting dichroic phenomena by a single pulse [10]. For perturbative weak pulse intensities, various high pulse carrier frequencies, and different molecular orientation with respect to the light propagation direction, we shall search for particular detection geometries and energy sharing configurations that enable direct observation and control of two-slit effects by tuning the pulse ellipticity.

(d) Resonant harmonic generation (HG) with chirped laser pulses; using the chirp as a means to be on resonance with doubly-excited states of two-electron atoms, such as He and Be.

(e) Effects of the time delay between the two driving laser fields in resonant HG from ground state of He and Be in order to control the multiphoton regime plateau structure [11].

REFERENCES

[1] N.F. Ramsey, "*A Molecular Beam Resonance Method with Separated Oscillating Fields,*" Phys. Rev. **78**, 695 (1950).

[2] J.M. Ngoko Djiokap, S.X. Hu, L.B. Madsen, N.L. Manakov, A.V. Meremianin, and A.F. Starace, "*Electron Vortices in Photoionization by Circularly Polarized Attosecond Pulses,*" Phys. Rev. Lett. **115**, 113004 (2015).

[3] J. M. Ngoko Djiokap, A. V. Meremianin, N. L. Manakov, S. X. Hu, L. B. Madsen, and A. F. Starace, "*Multistart Spiral Electron Vortices in Ionization by Circularly Polarized UV Pulses,*" Phys. Rev. A **94**, 013408 (2016).

[4] D. Pengel, S. Kerbstadt, D. Johannmeyer, L. Englert, T. Bayer, and M. Wollenhaupt, "*Electron Vortices in Femtosecond Multiphoton Ionization*," Phys. Rev. Lett. **118**, 053003 (2017).

[5] D. Pengel, S. Kerbstadt, L. Englert, T. Bayer, and M. Wollenhaupt, "*Control of Three-Dimensional Electron Vortices from Femtosecond Multiphoton Ionization,*" Phys. Rev. A **96**,

043426 (2017).

[6] S. Kerbstadt, K. Eickhoff, T. Bayer, and M. Wollenhaupt, "*Odd Electron Wave Packets from Cycloidal Ultrashort Laser Fields,*" Nat. Comm. **10**, 658 (2019).

[7] S. Kerbstadt, K. Eickhoff, T. Bayer, and M. Wollenhaupt, "*Control of Free Electron Wave Packets by Polarization-Tailored Ultrashort Bichromatic Laser Fields,*" Advances in Physics: X **4**, 1672583 (2019).

[8] I. Bialynicki-Birula, Z. Bialynicki-Birula, and C. Sliwa, "*Motion of Vortex Lines in Quantum Mechanics,*" Phys. Rev. A **61**, 032110 (2000).

[9] J. M. Ngoko Djiokap, A. V. Meremianin, N. L. Manakov, L. B. Madsen, S. X. Hu, and A. F. Starace, "*Dynamical Electron Vortices in Attosecond Double Photoionization of H_2,*" Phys. Rev. A **98**, 063407 (2018).

[10] J. M. Ngoko Djiokap, A. V. Meremianin, N. L. Manakov, L. B. Madsen, S. X. Hu, and A. F. Starace, "*Molecular Symmetry-Mixed Dichroism in Double Photoionization of H_2,*" Phys. Rev. Lett. **123**, 143202 (2019).

[11] J. M. Ngoko Djiokap and A. F. Starace, "*Origin of the Multiphoton-Regime Harmonic-Generation Plateau Structure*," Phys. Rev. A **102**, 013103 (2020).

PEER-REVIEWED PUBLICATIONS RESULTING FROM THIS PROJECT (Project start date: 08/2020)

No publications to report.

"Low-Energy Electron Interactions with Complex Molecules and Biological Targets"

Thomas M. Orlando
School of Chemistry and Biochemistry and School of Physics,
Georgia Institute of Technology, Atlanta, GA 30332-0400
Thomas.Orlando@chemistry.gatech.edu, Phone: (404) 894-4012, FAX: (404) 894-7452

Project Scope: The primary objectives of this program are to investigate the fundamental atomic and molecular physics involved in low-energy (5-250 eV) electron as well as soft x-ray (20-950 eV) interactions with complex molecular targets that have biological relevance and significance. These interactions involve deep and shallow core ionization, Auger processes, interatomic and intermolecular Coulomb decay (ICD), transient negative ion (TNI) formation, dissociative electron attachment (DEA) and shape resonances (SRs). TNIs, ICD, DEA and SRs are inelastic energy-loss events which are extremely sensitive to many body effects and changes in local potentials. All of these energy-loss channels likely contribute significantly to the chemical transformations that occur as a result of the interaction of ionizing radiation. This program uses i) energy-resolved inelastic electron scattering to examine the roles of TNIs, DEA, SRs and ICD in radiation damage of adsorbed/condensed complex biologically relevant molecules as well as ii) strong-field ionization/time-resolved x-ray transient hole absorption and x-ray emission experiments. The latter examines the dynamics of energy exchange and dissipation in complex solutions containing solvated ions.

Recent Progress:.

Task 1. X-ray and low-energy electron induced damage of dAMP: The radiation damage and stimulated desorption of 2'-deoxyadenosine 5'-monophosphate (dAMP), adenosine 5'-monophosphate (rAMP), 2'-deoxycytidine 5'-monophosphate (dCMP) and cytidine 5'-monophosphate (rCMP) deposited on Au have been measured at the Advanced Photon Source (APS) at Argonne National Laboratory using x-rays as both the probe and source of low energy secondary electrons.[1] The fluence dependent behavior of the O-1s, C-1s, and N-1s photoelectron transitions were analyzed to obtain phosphate, sugar and nucleobase damage cross sections. The observed damage and bonding changes were dominated by the inelastic energy-loss channels associated with secondary electron capture and transient negative ion decay. Since the energy distribution of the secondary electrons was unknown, we extended this work at Georgia Tech. by directly irradiating multilayers of dAMP deposited on Au films with a mono-energetic low-energy electron beam tunable from 3 – 25 eV. The damage induced by these electrons was examined using an x-ray photoelectron spectrometer equipped with a low flux impinging x-ray source. Comparison of the O–1s, N–1s and C–1s spectral profiles indicated decomposition of the

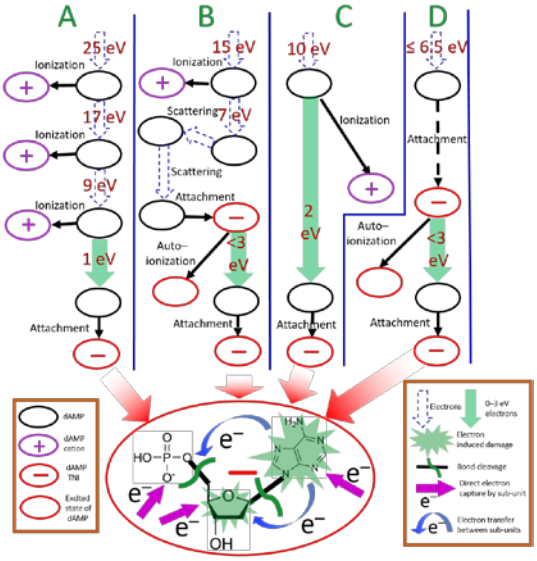

Figure 1. Illustration showing how electrons with different initial energies can undergo a cascade of energy loss processes, most of which eventually generate sub–excitation electrons (< 3 eV). The final TNI of dAMP created by capturing a < 3 eV electron for all these energies is shown enlarged at the bottom, depicting all observed damage sites.

base and sugar as well as cleavage of the glycosidic and phosphate bonds after 3-25 eV irradiation. Comparison of photoelectron spectra decay curves for all incident energies studied showed that *all observed chemical changes can ultimately be attributed to the formation and decay of transient negative ions (TNIs), particularly shape resonances at or below 3 eV.* [2]

Task 2. Low energy electron induced damage of vapor condensed histidine on magnetized cobalt substrates: We have continued our collaboration on x-ray and low-energy electron induced damage of adsorbed molecules of biological relevance[1-5] and completed experiments at the APS on low energy electron induced damage and stimulated desorption of enantiopure L-histidine vapor deposited on a magnetized Co film. In this case, we used the x-rays to both produce low energy secondary electrons and to probe the damage.[6] The histidine coverage was varied between 0.5-1.5 monolayers, and the magnetization direction of the Co film could be flipped *in-situ*, meaning the damage cross-section could be directly compared for both spin-up and spin-down magnetization directions. Reversal of the Co magnetization direction was confirmed using x-ray magnetic circular dichroism (XMCD), and the damage cross-sections were determined by monitoring the strength of the photoelectron peak components as a function incident x-ray fluence. Statistical analysis of the calculated damage cross-sections for >10 points per sample showed a significant difference depending on the magnetization direction. These results show a preferential reaction of spin-down electrons with the L-histidine, with calculated cross-sections on average > 2 times larger under spin-down conditions.

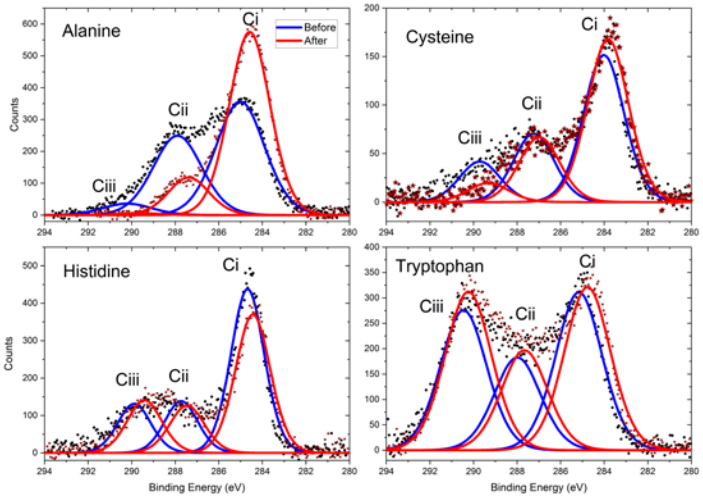

Figure 2. C-1s photoelectron transitions for alanine, cysteine, histidine and tryptophan. These amino acids have functional groups of increasing complexity. Alanine, the simplest amino acid, has the largest damage cross–section while tryptophan appears to be the most stable.

Decomposition of alanine, cysteine, histidine and tryptophan was also measured by irradiating powdered samples with 750 eV X-rays in UHV. Figure 2 shows a clear differential in the profile as well as the stability of the amino acid. The secondary electron fluence dependence of the C-1s photoelectron transition of each amino acid was analyzed to extract photolysis cross–sections of each component of the transition. In addition to the difference in cross–sections between the amino acids, the components differ qualitatively in their dependence on fluence. The amino acids, alanine, cysteine, histidine and tryptophan have functional groups of increasing complexity, hence, comparing their dissociation cross–sections can give an insight into the stability of the molecule in relation to the functional group. Alanine, the simplest amino acid, has the largest damage cross–section while tryptophan appears to be the most stable.

Task 3. Investigating intermolecular Coulomb decay (ICD) at weakly interacting interfaces: We have continued studies of intermolecular Coulomb decay (ICD) in condensed samples composed

of weakly interacting rare gases. Specifically, we probe ICD at interfaces by monitoring the ejected ion masses and kinetic energies as a function of incident electron energy. When using Ar and Kr mixtures, the ICD is initiated by ionization of the Ar-3s level. Previous work has attributed rare gas ion desorption below the double ionization potential to decay of a bi-exciton. Our results suggest this is more likely due to ICD.

Future Plans

- We will expand the ICD work on rare gases to condensed clusters and thin-films of molecules such as water and tetrahydrofuran, a nucleotide sugar surrogate. ICD was demonstrated in XUV photoionization studies of water:tetrahydrofuran clusters. In this work, the amount of water and the role of proton transfer was not clear. Our proposed efforts will compliment these and unravel the relative contributions of energy dissipation via ICD, electron transfer mediated decay and proton transfer.

- Low energy electron damage of amino acids, short peptide sequences, DNA and RNA nucleotides and short DNA and RNA sequences will be examined using Raman micro-spectroscopy, XPS and atomic force microscopy. Damage of films functionalized with amino acids will also be examined to mimic damage of proteins on cancer cell walls. This information will ultimately be valuable to targeted treatment of cancer using radiotherapies.

- A collaboration with the AMOP group at Argonne National Lab. on strong-field ionization/time-resolved x-ray transient hole absorption and x-ray emission experiments to examine the dynamics of energy exchange and dissipation in complex solutions containing solvated ions will begin. Initial efforts will focus on developing a simple liquid jet system and on examing simple (NaCl) aqueous salt solutions. Joint proposals with the Argonne AMOP group for LCLS-II beam-time will also be pursued.

- We ultimately plan to study time-resolved soft- x-ray studies on the ionization and dissociation dynamics of nucleotides and simple amino acids. Therefore, we are working on a technique known as laser induced acoustic desorption (LIAD) as a method to introduce liable biomolecules into the gas-phase for ultrafast ionization dynamics studies. We have launched silica beads from thin-metal foils and are exploring whether nanostructured metal substrates can be used to efficiently produce well defined molecular beams of nucleotides and amino acids for attosecond ionization dynamics studies**.**

References:

1. A. McKee, M. Schaible, S. Kundu, R. Rosenberg and T. M. Orlando, "The role of water and negative ion resonances in X-ray induced damage of dAMP, rAMP, dCMP and rCMP adsorbed on Au coated SiO_2", *J. Chem. Phys*. 150, 204709 (2019) https://doi.org/10.1063/1.5090491
2. S. Kindu, M. J. Schaible, A. D. McKee, and T. M. Orlando, "Direct damage of deoxyadenosine monophosphate by low-energy electrons probed by X-ray photoelectron spectroscopy", *J. Phys. Chem.* B. 124, 9, 1585-1591 (2020), doi.org./10.1021/acs.jpcb.9b08971 (Supplementary Cover Selected)

3. R. A. Rosenberg, J. M. Symonds, K. Vjayalakshmi, D. Mishra, T. M. Orlando, and R. Naaman, "The relationship between interfacial bonding and radiation damage of adsorbed DNA", *Phys. Chem. Chem. Phys*. **16**, 15319-15325 (2014).
4. R. A. Rosenberg, J. M. Symonds, V. Kalyanaraman, T. Z. Markus, T. M. Orlando, R. Naaman, E. a. Medina, F. A. Lopez and V. Muijca, "Kinetic Energy Dependence of Spin Filtering of Electrons Transmitted through Organized Layers of DNA", *J. Phys. Chem. C.* **117,** 22307-22313, (2013).
5. R. Rosenberg, J. M. Symonds, T. Z. Markus, T. M. Orlando and R. Naaman, "The lack of spin selectivity in low-energy electron induced damage of DNA films", *J. Phys. Chem. C.* 117(43), 22307-22313 (2013).
6. M. Schaible, S. Kundu, R. Rosenberg and T. M. Orlando, "Low energy electron induced damage of vapor condensed histidine on magnetized cobalt substrates**"** (in preparation, *J. Chem. Phys. Lett*.)

Peer-reviewed publications resulting from this project (2018-2020)

1. S. Kindu, M. J. Schaible, A. D. McKee, and T. M. Orlando, "Direct damage of deoxyadenosine monophosphate by low-energy electrons probed by x-ray photoelectron spectroscopy", *J. Phys. Chem. B.* 124, 9, 1585-1591 (2020), doi.org./10.1021/acs.jpcb.9b08971 (Supplementary Cover Selected)
2. A. D. McKee, M. Schaible, S. Kundu, R. Rosenberg and T. M. Orlando, "Low energy secondary electron induced damage of condensed nucleotides", *J. Chem. Phys*. 150, 204709 (2019) https://doi.org/10.1063/1.5090491

Presentations acknowledging support from this program

1. T. M. Orlando, "Low-energy electron interactions with complex biomolecules and carcinogenesis", Georgia Tech. Petit Institute for Bioengineering and Biosciences, January 14, 2020. (Recording at https://smartech.gatech.edu/handle/1853/62374)
2. T. M. Orlando, "Low-energy electron interactions with complex molecules and biological targets", DOE Atomic Molecular and Optical Physics PI- Program Meeting, Oct. 28-30, 2019.
3. M. Schaible, S. Kundu, R. Rosenberg and T. M. Orlando, "Low energy electron and electrostatically charged dust grain interactions with organic molecules on airless bodies", EPSC-DPS Joint Meeting, 15-20 Sept. 15-20, 2019, Geneva, Switzerland, id. EPSC-DPS2019-1222. (Travel funded by NASA)
4. T. M. Orlando, "Very low energy (<5 eV) electron induced damage of DNA and RNA nucleotides", Argonne National Laboratory Colloquium, May 1, 2018.

Structure from Fleeting Illumination of Faint Spinning Objects in Flight

A. Ourmazd
Dept. of Physics, University of Wisconsin Milwaukee
3135 N. Maryland Ave, Milwaukee, WI 53211
ourmazd@uwm.edu

Project Scope

The advent of intense, ultrashort pulses of X-rays and electrons has made it possible to obtain two-dimensional snapshots of molecular machines performing their native function. The resulting datasets are, in general, noisy, incomplete, and recorded with substantial timing uncertainty.

We are developing a new generation of machine learning algorithms to recover three-dimensional structure and dynamics from noisy, incomplete data recorded at highly uncertain time points. Combining concepts from machine learning, differential geometry, general relativity, graph theory, and diffraction physics, these techniques promise to revolutionize our understanding of molecular function at the atomic level.

Recent Progress

1. Highly Generalizable Machine-learning Algorithm for Accurate Dynamics (with R. Fung et al.)

In a paper published in *Nature* in 2016 [1], we reported a new and mathematically rigorous machine-learning algorithm for extracting accurate dynamical information from a series of noisy spectral snapshots recorded with substantial timing uncertainty. The power of the algorithm was demonstrated by application to a collection of N_2 molecules undergoing Coulomb explosion on the femtosecond timescale. At the request of, and with funding provided by the Bill and Melinda Gates Foundation, we extended this algorithm to substantially reduce the uncertainty in estimates of the gestational age of individual fetuses, and to predict a personalized forecast of the development of each fetuses. Our algorithm improved the accuracy of gestational age estimates by up to a factor of 5, constituting the first improvement in such estimates since 1812 (not a typo). These results were published in *The Lancet Digital Health* [2]. The ability to extract accurate dynamical information from exploding molecules and unborn fetuses using the same algorithmic approach represents a decisive demonstration of the possibility to develop powerful, mathematically rigorous, and exceptionally generalizable machine learning tools with applications ranging from fundamental science to clinical practice.

2. Extracting Spatio-temporal Information from Complex Dynamical Systems (with D. Giannakis et al.)

Decomposition of signals into their principal components is one of the most widely used techniques for recovering - and understanding - complex phenomena, with Singular Value Decomposition [3] a celebrated example. These so-called eigen-decomposition techniques are linear, in the sense that they assume the data can be described as a flat

manifold, an assumption, which is rarely true. The extension of these approaches to the nonlinear domain [4] has provided unanticipated access to important new insights into the structure [5, 6] and dynamics [1] of molecular machines. Existing eigen-decomposition techniques assume the input data can be expressed as tensor products of temporal and spatial modes. These approaches function poorly when the signal is not separable into such modes. We have developed a data-driven machine learning framework for extracting complex spatiotemporal patterns generated by ergodic dynamical systems [7]. This approach is able to deal efficiently with manifestly non-separable signals. It is thus now possible to express dynamical information in terms of a small number of modes, even for complex signals with intermittency in both space and time.

The algorithm is based on eigen-decomposition of a kernel integral operator acting on a Hilbert space of vector-valued observables of the system, taking values in a space of functions (scalar fields) on a spatial domain. This operator combines the theory of operator-valued kernels for multitask machine learning, with delay-coordinate maps of dynamical systems. The new kernel construction naturally quotients out dynamical symmetries in the data, and asymptotically commutes with the Koopman evolution operator of the system, enabling efficient decomposition of multiscale signals into dynamically intrinsic patterns. The application of this approach to highly complex dynamical systems has demonstrated significant gains in efficient and meaningful decomposition over existing techniques based on scalar-valued kernels.

3. Conical Intersections in Large Molecular Systems (with A. Hosseinizadeh et al.)

Processes involving conical intersections are ubiquitous in physics, chemistry, and biology (see, e.g., [8], [9], and references therein), if only because they represent a vital mechanism for redistributing energy in molecular systems before the onset of irreversible damage. Spectroscopic studies of processes involving conical intersections have reached an unprecedented level of sophistication (see e.g., [10], and references therein). But such experiments have, on the whole, been limited to small molecules. The recent advent of time-resolved serial femtosecond X-ray diffraction (tr-SFX) has dramatically extended the range of amenable systems from simple few-atom molecules to macromolecules, such as the Photoactive Yellow Protein (PYP) [11, 12], and Bacteriorhodopsin [13]. The resulting structural molecular movies reveal, in great detail, difference electron density maps before and after passage through a conical intersection. However, the temporal, and potentially also the spatial resolutions of these molecular movies have been limited by the need to "merge" 2D diffraction snapshots (each inevitably recorded at different timepoints) to form 3D diffraction volumes. Due to XFEL timing jitter, the time-resolution of such molecular movies is limited to ~100fs, which is thought to be long compared with the time needed to "pass through" a conical intersection.

We have developed a new algorithmic approach to recover the full diffraction volume at femtosecond-accurate timepoints without the need to merge data obtained at different (and inaccurately known) times. Preliminary molecular movies already indicate that the

structure-dynamical changes associated with de-excitation via a conical intersection can be mapped with single-femtosecond temporal, and near-atomic spatial resolutions.

Future Plans

Using mathematically rigorous ("AI for Science") machine learning techniques, we plan to develope a new generation of algorithms designed to be robust against the combination of noise, data incompleteness, and timing uncertainty. The power of this approach will be validated in the context of ultrafast dynamics. First, we plan to show that structure-dynamical modes and trajectories of ultrafast de-excitation can be extracted with atomic spatial resolution and single-femtosecond temporal resolution from existing experimental data. This would directly reveal the roles of a large photo-active chromophore and its surrounding in the ultrafast de-excitation dynamics of the chromophore. Second, in combination with tractable and accurate computational methods, we aim to demonstrate that it is possible to determine the topography of the electronic states in the neighborhood of conical intersections. Third, we plan to show that these techniques can be used to determine the key collective variables and boundary conditions controlling the de-excitation dynamics of molecules consisting of thousands of atoms. Finally, we plan to explore whether the combination of data-driven machine learning with existing experimental and theoretical techniques can provide the time resolution of spectroscopy and the spatial resolution of structural methods.

Peer-reviewed Publications Resulting from this Project (2018-2020)

1. Retrieving functional pathways of biomolecules from single-particle snapshots, A. Dashti et al, **Nature Communications 11**, 4734 (2020).
2. Achieving accurate estimates of fetal gestational age and personlized predictions of fetal growth based on data from an international prospective cohort study: a population based machine learning study, Fung et al, **The Lancet Digital Health 2**, E368 (2020).
3. Science in the age of machine learning, A. Ourmazd, **Nature Physics Reviews 2**, 342 (2020) (invited).
4. Cryo-EM, XFELs, and the Structure Conundrum in Structural Biology, A. Ourmazd, **Nature Methods 16**, 941 (2020).
5. Time-Resolved Serial Femtosecond Crystallography at the European XFEL, S. Pandey et al. **Nature Methods 17**, 73 (2020).
6. Spatiotemporal Pattern Extraction by Spectral Analysis of Vector-Valued Observables, D. Giannakis, A. Ourmazd, J. Slawinska, Z. Zhao, **J. Nonlinear Science**, https://doi.org/10.1007/s00332-019-09548-1 (2019).
7. Enzyme intermediates captured "on the fly" by mix-and-inject serial crystallography, J.D. Olmos Jr. et al., **BMC Biology 16**, 59 (2018).
8. Free-electron laser data for multiple-particle fluctuation scattering analysis, K. Pande et al. **Scientific Data**, 5:180201, DOI: 10.1038/sdata.2018,201 (2018)

References

1. Fung, R., et al., *Dynamics from noisy data with extreme timing uncertainty.* Nature, 2016. **532**(7600): p. 471-5.
2. Fung, R. and e. al, *2. Achieving accurate estimates of fetal gestational age and personlized predictions of fetal growth based on data from an international prospective cohort study: a population based machine learning study.* The Lancet DH, 2020. **2**: p. E368 - E375.
3. Aubry, N., R. Guyonnet, and R. Lima, *Spatiotemporal Analysis of Complex Signals - Theory and Applications.* J Stat Phys, 1991. **64**(3-4): p. 683-739.
4. Giannakis, D. and A.J. Majda, *Nonlinear Laplacian spectral analysis for time series with intermittency and low-frequency variability.* Proc Natl Acad Sci U S A, 2012. **109**(7): p. 2222-2227.
5. Dashti, A., et al., *Trajectories of the ribosome as a Brownian nanomachine.* Proc Natl Acad Sci U S A, 2014. **111**(49): p. 17492-7.
6. Hosseinizadeh, A., et al., *Conformational landscape of a virus by single-particle X-ray scattering.* Nat Methods, 2017. **14**(9): p. 877-881.
7. Giannakis, D., et al., *Spatiotemporal Pattern Extraction by Spectral Analysis of Vector-Valued Observables.* Journal of Nonlinear Science, 2019.
8. Domcke, W. and D.R. Yarkony, *Role of conical intersections in molecular spectroscopy and photoinduced chemical dynamics.* Annu Rev Phys Chem, 2012. **63**: p. 325-52.
9. Schuurman, M.S. and A. Stolow, *Dynamics at Conical Intersections.* Annu Rev Phys Chem, 2018. **69**: p. 427-450.
10. Kobayashi, Y., et al., *Direct mapping of curve-crossing dynamics in IBr by attosecond transient absorption spectroscopy.* Science, 2019. **365**(6448): p. 79-83.
11. Pande, K., et al., *Femtosecond structural dynamics drives the trans/cis isomerization in photoactive yellow protein.* Science, 2016. **352**(6286): p. 725-9.
12. Kupitz, C., et al., *Serial time-resolved crystallography of photosystem II using a femtosecond X-ray laser.* Nature, 2014.
13. Nogly, P., et al., *Retinal isomerization in bacteriorhodopsin captured by a femtosecond x-ray laser.* Science, 2018. **361**(6398).

Control of Molecular Dynamics: Algorithms for Design and Implementation

Herschel Rabitz and Tak-San Ho
Princeton University, Frick Laboratory, Princeton, NJ 08540
hrabitz@princeton.edu, tsho@princeton.edu

A. Project Scope:

Activity in quantum control is wide-ranging, from selectively breaking chemical bonds out to rapidly growing initiatives in quantum information science. This research project addresses several key topics in optimal control of complex polyatomic molecular dynamics of many degrees of freedom. Specifically, the collective planned studies explore a number of issues at the foundation of laser control over quantum phenomenon. Such studies involve laboratory experimentation, but there is a great need to design, simulate, and understand the complex dynamical phenomena involved. Thus, the collective studies consider a variety of issues at the foundation of laser control over quantum phenomenon.

B. Recent Progress:

During the current DOE grant period, from October 2019 to September 2020, a broad variety of research topics were pursued in the general area of understanding and controlling dynamics phenomena of few-body out to many-body quantum systems. A summary of these accomplishments is provided below:

[1] Basic theoretical studies. Several research studies were explored, which have significance in all aspects of our current and planned new research program. An initial work in this regard considered the synergistic control capabilities of modeling and experiments carried out in real time in an adaptive control framework. Another study considered the relativistic dynamics of spin ½ particles, building on our prior research in the area of operational dynamical modelling. A series of studies considered the so-called speed limit for controlling quantum systems, which corresponds to the shortest time that quantum control may be carried out without infringing on a loss of controllability of the system.

[2] Exploring control landscapes. We recently arrived at a key theorem based on tools from differential geometry demonstrating that almost all closed systems should be trap free. Although some debate has continued regarding the nature of quantum control landscapes, the overwhelming positive evidence is supportive from quantum control development in general. Another theorem expanded the traditional perspective of linear dipole coupling to now include polarizability effects and numerical studies confirmed favorable topology even when the dipole coupling alone rendered the system not fully controllable. In recent work, we extended this analysis to considering the topology of one quantum system controlling another, which is a circumstance of increasing interest. There remain many open questions about quantum control landscapes that are of both fundamental and practical importance. In a recent work, we considered the landscape of a so-called bipartite system, which consists of a primary system coupled to an environment with the goal of achieving full control of the primary system and decoupling it from the environment at a target time. Our recent work demonstrated that the presence

of saddles could possibly slow down the efficiency of finding an optimal control, but they could not prevent a reasonable algorithm (e.g., gradient-based) from reaching optimal performance. Once again, very favorable topology and landscape features appeared. Satisfaction of these assumptions once again lead to the conclusion of trap-free topology and this was confirmed in numerous simulations.

[3] Consideration of experimental conditions upon the performance of quantum control. Understanding the topology and general features of control landscapes naturally leads to assessing the nature of the performance of potential algorithms to climb the landscapes. We have examined this matter in a study of several algorithms, both in simulation as well as in a collaborative experimental NMR scenario at Princeton; the results clearly show that each algorithm has its own merits best suitable under appropriate conditions. In particular, a stochastic algorithm was tested in a collaborative laboratory study for removal of the hydrogen atom from a phenol group bound to a silicon dioxide surface. Finally, a study of the coherent and incoherent nature of two-photon luminescence from gold nanorods was considered, indicating that both types of signals could be present together, although no direct control was attempted to manipulate these features.

[4] Simulation studies. The control of few-body out to many-body quantum systems is a prime topic of interest. Under weak interactions, the Hartree approximation can be effective as we demonstrated for controlled multiple molecular rotors. Furthermore, in a parallel project, the Magnus expansion was examined for weakly coupled distinct few-body systems with applications to state transfer and entanglement in the presence of strong fields.

[5] Identification of quantum control mechanisms. A common procedure in the laboratory is to perform so-called pump-probe experiments, which can give valuable insights under suitable conditions. However, the real goal is to understand the mechanism created by replacing the pump with the actual optimal control determined typically by learning control. We have begun developing a so-called pulse slicing technique for this procedure and the theoretical tools involved were transferred to the laboratory to examine the dissociative ionization of CH_2BrI. Valuable insights were revealed, which were not understood from the actual control experiments alone. A hallmark of mechanism analysis in considering complex chemical reactions (i.e., with applied fields) is to observe and follow the logical chain of chemical transformations. A study of this type was carried out for the experimental photofragmentation of a complex series of large organometallic molecules.

[6] Theoretical algorithms and tools for modelling analysis. A step in this direction was taken in a recent work deriving an exact optimized effective potential, including with numerical simulations. We have continued to develop a hierarchy of so-called sensitivity analysis techniques. A particular advance during the present research was the introduction of a generalized kernel-based method for global sensitivity analysis that can provide a comprehensive picture of the relationships between multiple observables. As a demonstration of the wide utility of these various model and data analysis tools, they were applied in a medical setting to assess biomedical indicators of autism spectrum

disorder and like foundational tools were also applied to disentangle complex data emanating from LC-MS metabolomics. Finally, mathematical analysis was carried out for the identification of effective Newton-based optimal control applications described by coupled differential-algebraic equations.

[7] Review articles. A review was prepared upon invitation regarding control in a broad area of the sciences, ranging from quantum phenomena out to aspects of biology. Additionally, a comment paper was prepared, relating the impact of quantum learning control principles and quantum control landscapes upon the emerging area of so-called variational quantum algorithms arising in quantum information sciences. Interestingly, the concepts and algorithms we have set out that are commonly used for atomic and molecular quantum control have important significance for the performance of currently operating nascent quantum computing platforms.

C. Future Plans:

During the upcoming year, we will seek a deeper understanding of the fundamental foundations of quantum optimal control, including the topology of the underlying control landscapes. Additionally, we will perform mechanism analysis utilizing algorithms customized to quantum control applications and expand the capability to explore the control complex quantum dynamics phenomena. In regard to the latter item, a new portion of the planned research will be concerned with addressing a long-standing problem of practically solving the many-body quantum dynamics equations, which arise in many scenarios, and particularly in the case of quantum control of polyatomic molecules. We will take a machine learning approach with these “big equations” rather than the standard applications involving big data. An initial study addressed this problem, considering coupled spin systems in a time-independent Hamiltonian and demonstrated that the exponential scaling as normally found in quantum dynamics could be reduced to a polynomial scaling of the number of neural net variables. To this end, we will use the artificial neural network (ANN), for performing large-scale molecular optimal control simulations. Specifically, this research will be an algorithmic development, especially, in the context of machine learning of flexibly parameterized artificial neural networks for enabling polynomial-scaled quantum state representation, accompanied by a set of timely simulations for controlled dynamics of polyatomic molecules.

D. Peer-Reviewed Publications Resulting from this Project (2018-2020)

[1] Dependence of the quantum speed limit on system size and control complexity, J. Lee, C. Arenz, H. Rabitz, B. Russell, New J. Phys. 20, 063002 (2018).
[2] Optimal control of orientation and entanglement for two dipole-dipole coupled quantumplanar rotors, H. Yu, T.-S. Ho, H. Rabitz, PCCP, 20, 13008 (2018).
[3] Exact-exchange optimized effective potential and memory effect in time-dependent density functional theory**,** S.-L. Liao, T.-S. Ho, H. Rabitz, S.-I Chu, Eur. Phys. J. B 91, 147 (2018).
[4] High efficiency classification of children with autism spectrum disorder, G. Li, O. Lee, H. Rabitz, PLoS ONE 13(2):e0192867, February 15, 2018.
[5] Control landscapes for a classof non-linear dynamical systems: sufficient conditions for the absence of traps, B. Russell, S. Vuglar, H. Rabitz, J. Phys. A: Math. Theor. 51,

335103 (2018).
[6] Singularity-free quantum tracking control of molecular rotor orientation, A. Magann, T.-S. Ho, and H. Rabitz, Phys. Rev. A, 98, 043429, (2018).
[7] Reply to comment on “Control landscapes are almost always trap free: a geometric assessment”, B. Russell, R.-B. Wu, and H. Rabitz, J. Phys. A.: Math. Theor., **51**, 508002, (2018).
[8] On lifting operators and regularity of nonsmooth Newton methods for optimal control problems of differential algebraic equations, J. Optim.Theo. Appl., 180, 518 (2019).
[9] Operational dynamical modeling of spin ½ relativistic particles, R. Cabrera, A. Campos, H. Rabitz, and D. Bondar, Eur. Phys. J. Special Topics, 227, 2195 (2019).
[10] Quantum control landscape of bipartite systems, R. Kosut, C. Arenz, and H. Rabitz, J. Phys. A: Math. Theor., **52**, 165305, (2019).
[11] Quantum optimal control of multiple weakly interacting molecular rotors in the time-dependent Hartree approximation, A. Magann, L. Chen, T.-S. Ho, and H. Rabitz, J. Chem. Phys., 150, 164303 (2019).
[12] Peak Annotation and Verification Engine for Untargeted LC-MS Metabolomics L. Wang, X. Xing, L. Chen, L. Yang, X. Su, H. Rabitz, W. Lu, and J. Rabinowitz, Anal. Chem., 91, 1838-1846, (2019).
[13] Dual coherent and incoherent two-photon luminescence in single gold nanorods revealed by polarization and time resolved non-linear autocorrelation, D. Xie, F. Laforge, I. Grigorenko, and H. Rabitz, J. Optical Society of America B, **36**, 1931-1936, (2019).
[14] Assessing the structure of classical molecular optimal control landscapes. C. Joe-Wong, T.-S. Ho, and H. Rabitz, Chem. Phys*. 527*, 110504 (2019).
[15] Inherently trap-free convex landscapes for fully qnatum optimal control. R.-B. Wu, Q. Sun, T.-S. Ho, H. Rabitz, J. Math. Chem*. 57*, 2154 (2019).
[16] Combining the synergistic capabilities of modeling and experiments: Illustration of finding a minimum-time quantum objective. Q.-M. Chen, X. Yang, C. Arenz, R.-B. Wu, X. Peng, I. Pelczer, and H. Rabitz, Phys. Rev. A 101 (2020*)*.
[17] An upper bound on the time required to implement unitary operations. J. Lee, C. Arenz, D. Burgarth, and H. Rabitz, J. Phys. A: Math. Theor. 53, 125304 (2020).
[18] Ultrafast Photofragmentation of Ln(hfac)3 with a Proposed Mechanism for forming High Mass Fluorinated Products. J. Chen, X. Xing, R. Rey-de-Castro, and H. Rabitz, Scientific Reports 10, 7066 (2020).
[19] Optimal control of coupled quantum systems based on the first-order Magnus expansion: Application to multiple dipole-dipole coupled molecular rotors. A. Ma, A. Magann, T.-S. Ho, and H. Rabitz, Phys. Rev. A 102, 013115 (2020).

Atoms and Ions Interacting with Particles and Fields

F. Robicheaux
Purdue University, Department of Physics and Astronomy,
525 Northwestern Ave, West Lafayette IN 47907
(robichf@purdue.edu)

Program Scope

This theory project focuses on the time evolution of systems subjected to either coherent or incoherent interactions represented by fields and particles, respectively. This study is divided into three categories: (1) correlations between two electrons in highly excited states or in double continua, (2) processes for one electron in time dependent or non-separable potentials, and (3) the interaction of atomic electrons with strong electromagnetic fields. Some of the techniques we developed have been used to study collision processes in ions, atoms and molecules. In particular, we have used these techniques to study the correlation between two (or more) continuum electrons and electron impact ionization of small molecules.

Recent Progress (Publications 10/2019-9/2020)

Molecular coherences in strong microwave fields: In Ref. [5], we studied the rotational coherences in large, asymmetric-top molecules with the experimental group of Tim Zwier who is supported by DOE BES Chemical Sciences Division. The experiments found that strong microwave driving a rotational transition would lead to observation of other rotational transitions in the free induction decay (FID). This phenomenon had never been observed before but could be very useful in the characterization of the body frame molecular constants. Our participation involved developing programs to understand possible mechanisms that would lead these extra frequencies in the free induction decay. This was a computational difficult task because the molecules were hot compared to the rotational energy spacings so many asymmetric top rotational states needed to be included in the calculation. The mechanisms theoretically investigated included: long range dipole-dipole interaction, pendular motion in a strong microwave field, turn-on/off effects, collective decay, collision between molecules, collision with background He gas, etc. While we were able to eliminate many possible mechanisms, we were, unfortunately, *not* able to reproduce the experiment even at a qualitative level. Thus, the origin of this useful effect is still a mystery.

X-ray physics: The graduate student Akilesh Venkatesh led a project, Ref. [6], to understand the non-linear Compton scattering of X-rays from bound electrons: 2 photons of frequency ω scatter into one photon of frequency near 2ω. Recent experiments at the LCLS (supported by DOE BES) found an anomalous wavelength shift of the 2ω photons corresponding to an extra several 100 eV transferred to the electron. We solved the time dependent Schrodinger equation for an electron interacting with I~4 X 10^{20} W/cm^2 X-rays of E~9 keV. The properties of the scattered photon were investigated using 1st order perturbation theory in the quantized electromagnetic field but nonperturbative in the incident X-ray field. We attempted to reproduce the angular dependence of the scattered X-rays as well as the outgoing wavelength as a function of scattering angle. While we were able to reproduce the angular dependence, the shift in wavelength did not match the LCLS results. The calculated shift was blue compared to free electrons instead of red, and more than an order of magnitude smaller than seen at the LCLS. Akilesh is exploring further calculations of strong field X-ray/atom interactions.

Fundamental investigations in scattering theory: In 2015 and 2016, we developed with Chris H. Greene's group a method for formulating a wide variety of scattering processes using a method we call generalized local frame-transformation theory. This theory expanded on and made more accurate the local frame-transformation theory introduced by U. Fano and D. Harmin to understand the eigenstates of highly excited alkali atoms in strong electric fields. Since this time, we have been applying this formalism to different problems to understand the strengths and limitations of this theoretical method. Reference [7] generalized this method to accurately treat the perturbation of excited states by another cold atom inside the orbital of the electron. Many interesting effects occur when the excited state has large principle quantum number due to the large number of nearly degenerate states. This approach avoids the use of pseudopotentials and yields analytical expressions for the body-frame reaction matrix. The reaction matrix can be used to obtain the molecular potential energy curves, but equally it can be employed for photodissociation, photoionization, and other processes. Reference [8] used this formalism to predict the existence of a universal class of ultralong-range Rydberg molecular states whose vibrational spectra form trimmed Rydberg series. We used a dressed ion-pair model to capture the physical origin of these exotic molecules. This model accurately predicts the properties of these states and reveals features of ultralong-range Rydberg molecules and heavy Rydberg states with a surprisingly small Rydberg constant.

The graduate student supported by this grant, Akilesh Venkatesh, started research in January 2019 and has been able to very quickly come up to speed. He has finished a project involving strong field X-rays with an electric field of 107 a.u. and frequency ω=340 a.u. to understand non-linear Compton scattering seen at the LCLS and a project involving the orientation and alignment dependence of ionization in collisions between two Rydberg atoms. He is currently investigating basic processes in strong field X-ray scattering.

Future Plans

Atom-atom scattering: The graduate student Akilesh Venkatesh led a project to understand how a pair of atoms interact, leading to ionization. For highly excited atoms, there are quasi-conserved quantum numbers which can govern how (or, even, whether) ionization will occur. Recent experiments explore this regime so modeling the interaction is timely. We found factors of 2-3 variation in ionization versus the alignment and orientation of the states which shows there can be substantial variation in the ionization cross section. The results are available on the arXiv and have been accepted for publication in PRA.

X-ray physics: The graduate student Akilesh Venkatesh will lead a project to understand the possibility for interference between linear Compton and non-linear Compton scattering. Interference can occur when a single photon of frequency 2ω Compton scatters from an electron or two photons of frequency ω non-linearly Compton scatter into a 2ω photon. Since the paths are indistinguishable there will be interference between these processes. We will investigate the angular dependence of the interference as well as the dependence on ω. We will also investigate X-ray scattering where one incoming photon scatters to 2 outgoing photons.

Benchmarking Strong Field Programs: Jens Svensmark and Brett Esry proposed a test problem to benchmark the programs used for calculating the strong laser-atom ionization at 800 nm. They organized this project involving many different theory groups around the world. The goal is to compare the performance of the many different methods being used in the strong field community. The test case they chose was the angular momentum distribution at 0.1 U_p and 10 U_p

for H with the laser at a particular strength and frequency. The calculation was done blind by the different groups and the results sent to Svensmark and Esry to be compared and organized. A paper will be written comparing the different methods.

Peer-Reviewed Publications Resulting from this Project (2018-2020)

[1] X. Wang and F. Robicheaux, “Interference patterns from post-collision interaction in below-threshold photoexcitation Auger processes,” Phys. Rev. A **98**, 013421 (2018).
[2] E.V. Crockett, R.C. Newell, F. Robicheaux, and D.A. Tate, “Heating and cooling of electrons in an ultracold neutral plasma using Rydberg atoms,” Phys. Rev. A **98**, 043431 (2018).
[3] X. Wang and F. Robicheaux, “Angular interferences of sequentially ionized double-continuum wave packets,” Phys. Rev. A **98**, 053407 (2018).
[4] X. Wang and F. Robicheaux, “Ionization from Rydberg atoms and wave packets by scaled terahertz single-cycle pulses,” Phys. Rev. A **99**, 033418 (2019).
[5] A.O. Hernandez-Castillo, C. Abeysekera, F. Robicheaux, and T.S. Zwier, “Propagating molecular rotational coherences through single-frequency pulses in the strong field regime,” J. Chem. Phys. **151**, 084312 (2019).
[6] A. Venkatesh and F. Robicheaux, “Simulation of nonlinear Compton scattering from bound electrons,” Phys. Rev. A **101**, 013409 (2020).
[7] P. Gannakeas, M. T. Eiles, F. Robicheaux, and J. M. Rost, "Generalized local frame-transformation theory for ultralong-range Rydberg molecules," Phys. Rev. A **102**, 033315 (2020).
[8] P. Gannakeas, M. T. Eiles, F. Robicheaux, and J. M. Rost, "Dressed ion-pair states of an ultralong-range Rydberg molecule," Phys. Rev. Lett. **125**, 123401 (2020).

Page is intentionally blank.

Investigating charge transfer and charge migration on the few- to sub-femtosecond time scale

Artem Rudenko[1*], Daniel Rolles[1], Loren Greenman[1], Robin Santra[2,3]
[1] *J. R. Macdonald Laboratory, Department of Physics, Kansas State University, 116 Cardwell Hall, Manhattan, KS 66506*
[2] *Center for Free-Electron Laser Science, Deutsches Elektronen-Synchrotron DESY, 22607 Hamburg, Germany*
[3] *Department of Physics, Universitat Hamburg, Jungiusstrasse 9, 20355 Hamburg, Germany*
[*] rudenko@phys.ksu.edu

Program Scope:

Intramolecular motion of electronic charge is one of the most important primary events in numerous photoinduced processes in physics, chemistry and biology, ranging from photosynthetic light harvesting to x-ray emission from comets and photocatalysis. Understanding charge dynamics at the microscopic level is essential for achieving fundamental insights into these phenomena and, in a longer-term perspective, for improving technological applications related to energy conversion and storage, which rely on charge motion and separation. This project aims at studying ultrafast charge dynamics (charge transfer and charge migration) in gas-phase molecules utilizing novel capabilities provided by the development of the XFEL facilities, and by recent progress in advanced theoretical modelling. This includes time-resolved experiments investigating charge motion triggered by valence and inner-shell photoabsorption, studies of distance-dependent charge transfer processes in dissociating molecules, detailed theoretical simulation of these experiments, and further development of theoretical tools required for the adequate description of the molecular states involved. A basic underlying concept of these studies exploits the fact that x-rays can specifically probe the atomically localized core-level electrons, which makes the XFEL-based techniques sensitive probes of the spatial (element-specific) localization of an electronic wave packet. A particular focus of this project is placed on creating a coherent superposition of molecular states launching a well-defined electron-hole wave-packet, visualizing its evolution in time within the first femtosecond after the photoabsorption, and understanding how subsequent coupling to nuclear motion affects these dynamics. One of the central goals of this program is to identify the observables most sensitive to such ultrafast charge motion [P1-P6] and to develop experimental techniques capable of revealing these observables, often relying on a few-particle coincidence measurements [R1, P7, P8]. Technically, this project relies on the recent development of attosecond x-ray pulses at LCLS [R2], which paves the way towards achieving sub-femtosecond temporal resolution, and on the availability of high repetition rate XFEL facilities such as the European XFEL and later LCLS-II, which makes coincident measurements feasible and efficient.

In order to advance our understanding of different aspects of ultrafast light-driven charge dynamics, we identified four main thrusts, on which we have focused our efforts:

***Thrust 1*:** *Charge transfer and charge migration dynamics following x-ray photoabsorption.*

Thrust 2: *Development of a short-pulse UV source and experiments with UV light.*

Thrust 3: *Studies of distance-dependent charge transfer processes in dissociating molecules*

Thrust 4: *Theory development*

Thrust 1*: *Charge transfer and charge migration dynamics following x-ray photoabsorption
(*Rudenko, Rolles, Greenman, Santra*)

Recent progress

The final goal of this project is to image in real time electronic dynamics unfolding on the time scale of a few hundred attoseconds, before the onset of the nuclear motion. The LCLS is currently the only XFEL facility worldwide that offers attosecond x-ray pulses for user operation. Therefore, because of the LCLS shutdown as well as subsequent COVID-19-related closures and delays, our main efforts in *Thrust 1* of the project during the first two year aimed at developing concepts and tools, which would facilitate x-ray pump – x-ray probe experiments with sub-femtosecond resolution once the corresponding x-ray pulses become available, and on extracting complimentary time-resolved information from coincident measurement with a single x-ray pulse, performed at the LCLS and at the European XFEL (EuXFEL). Finally, we contributed our concepts and ideas to the multi-institutional campaign proposal aimed at utilizing the attosecond capabilities during the upcoming LCLS–II runs, in particular, for the early-phase operations with 120 Hz repetition rate. All four PIs of this project contribute to each of the activities outlined in this section.

Probing ultrafast x-ray induced dynamics via sequential two-photon absorption and ion-electron coincident measurements

To demonstrate the feasibility of mapping light-induced charge dynamics on a few-femtosecond time scale, we proposed and simulated an experimental scheme to launch and detect core-hole wave-packet oscillations in the nitrogen molecule [P1]. The feasibility of such experiments relies on the ability to generate synchronized pairs of attosecond x-ray pulses and to measure the angular correlation between the two photoelectrons, ideally in the molecular frame [P1, R3]. While the attosecond pulse pairs will be available again at the LCLS after its restart, during the first two years of the project, the x-ray pump – x-ray probe option with two separated pulses was not available anywhere worldwide. Fortunately, the retrieval of time-resolved information does not necessarily require a two-pulse pump-probe configuration. In fact, every two- or multi-photon absorption process in the XUV or x-ray domain represents an indirect pump-probe measurement, where the first absorbed photon creates a molecular wave packet, and the following photoabsorption step(s) probe it on the timescale of the pulse. The (average) time delay between the two steps can, in principle, be retrieved from the experimental observables such as, for example, the ion kinetic energy release (KER).

We made the first steps in this direction by measuring in coincidence ions and electrons stemming from two-photon core-shell ionization of N_2 [R1] and O_2 [P7, P8] molecules, and retrieving the photoelectron emission patterns with respect to the positions of the nuclei. Extending a "conventional" molecular-frame measurement concept, where the photoelectrons are measured with respect to the known molecular orientation, we also exploited the relation between the measured ionic KER and the internuclear separation to plot the photoelectron kinetic energy (KE) [R1, P7] and angular distributions [P7, P8] as a function of a bond length. A multidimensional, multiparticle analysis of the data recorded in such measurements is illustrated in Fig. 1 and 2 for the case of O_2 molecule. In this experiment, ions and electrons produced in two-photon photoionization of O_2 by intense ~25 fs, 670 eV pulses of the European XFEL are detected in coincidence using COLTRIMS "reaction microscope" at the Small Quantum System (SQS) end station. Fig. 1 displays the integrated 1D photoelectron spectrum (top) as well as photoelectron-photoelectron (middle) and photoelectron- photoion (bottom) coincidence maps for the events resulting in O^{2+}+O^{2+} ion pair production. The first photon is predominantly absorbed by the carbon 1s shell resulting in a photoelectron line centered at 127 eV (marked 1s in Fig.1), followed by the emission of a fast Auger electron (mostly not detected). If the second photon is absorbed after the Auger decay, it results in somewhat lower photoelectron energy (peak marked PAP for photo-Auger-photo in Fig. 1). If the second photon is absorbed before the Auger decay, two possibilities arise

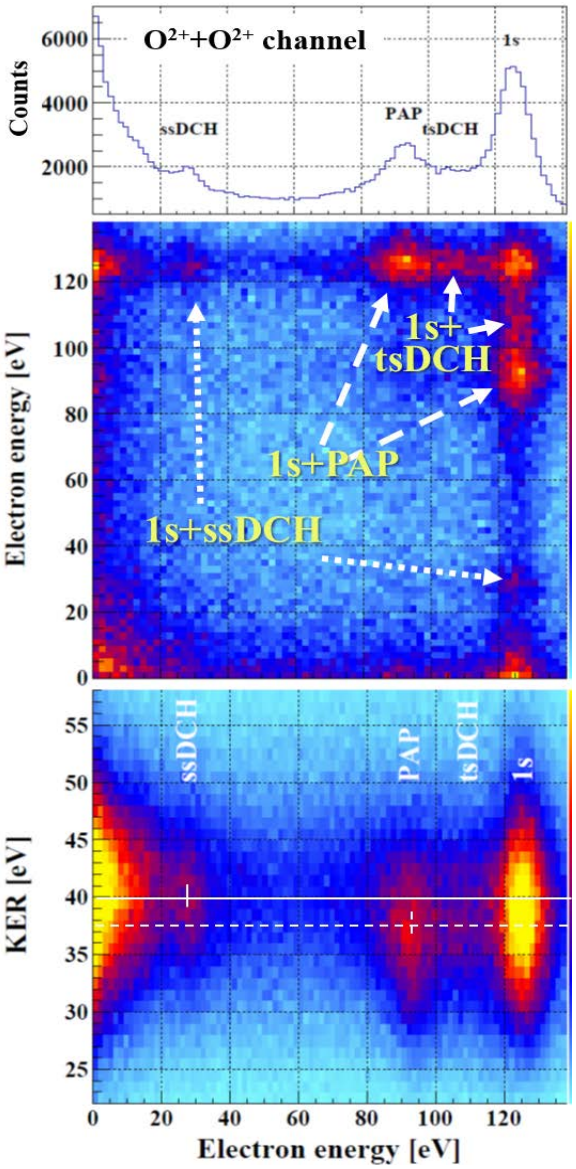

Figure 1: *Photoelectron spectrum and ion KER for O^{2+} + O^{2+} breakup channel after irradiation of O_2 molecules with XFEL pulses at 670 eV photon energies. Top: Integrated electron spectrum measured in coincidence with the two O^{2+} ions. Middle: Energy map for photoelectron-photoelectron coincidences. Bottom: Electron energy as a function of ion KER. Dashed and solid lines mark the positions of the PAP and ssDCH photoelectron peaks, respectively. (From [P8]).*

depending on where it is absorbed, resulting in the so-called single-site or two-site double core-hole (ssDCH and tsDCH) production and yielding very different photoelectron energies (~30 eV and ~110 eV, respectively). The large amount of low-energy electrons is due to other ionization schemes such as double ionization / shakeup process with subsequent Auger decays or ionization by Auger cascades.

The middle panel of Fig. 1 shows a coincidence map of the photoelectron kinetic energies (KE). By filtering the measured dataset on different islands corresponding to different two-photon ionization pathways (marked by the arrows), we are able to extract the molecular-frame photoelectron angular distribution (MFPAD) of the second electron emitted in each of those processes [P5, P11]. Furthermore, each of the photoelectron datasets can be further differentiated as a function of the ion KER using the ion-electron coincidence map shown in the bottom panel. As highlighted by the horizontal lines in this panel, the center of the KER peak corresponding to the PAP feature (dashed line) is ~2.5 eV lower than for ssDCH production (solid line) or tsDCH (the latter is hard to see in this representation). This reflects the characteristic time scale of each process: the DCH states correspond to very small time interval between the two photoabsorption steps, faster than the Auger decay time (i.e., a few fs). Correspondingly, the molecule, on average, reaches the final, quadruply-charged state (after the second Auger decay) at smaller values of the internuclear separation *R* than for the PAP process, where the delay between the two absorption steps is essentially determined by the XFEL pulse duration (~25 fs), as illustrated in Fig. 2a. In [R1], we exploited this relation to observe the KER-dependent shift of the PAP electron for two-photon sequential ionization of N_2 at LCLS, which reflects a change of the electron binding energy in a dissociating molecular ion. In that experiment a significantly longer pulse (~80-90 fs compared to ~25 fs in Fig. 1 and 2), which resulted in a significantly larger change in *R* during the pulse, made this shift observable, in good agreement with the predictions of our model calculation.

While the shift in photoelectron energy as a function of the KER (and, thus, internuclear separation *R*) is not clearly visible for the PAP feature in Fig. 1, the change in R can be resolved in the present

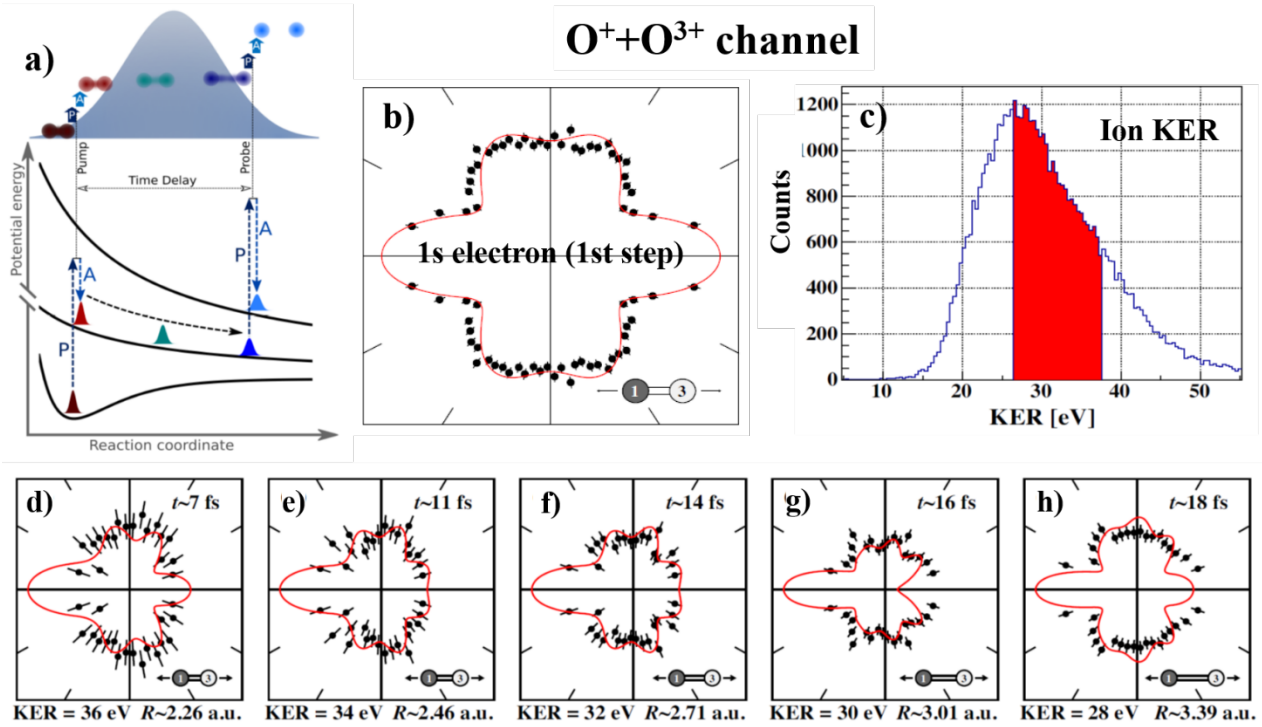

Figure 2: ***a)*** *Schematic of the single-pulse pump-probe scheme.* ***b)*** *Polarization-averaged molecular-frame angular distribution of the first emitted photoelectron.* ***c)*** *Measured KER of the quadruply charged $O^{+}+O^{3+}$ final state. The red-marked area depicts the region of KER used to generate the MPFADs shown in the bottom raw.* ***d-h)****: Polarization-averaged molecular-frame angular distributions of the second photoelectron (PAP channel) for several KERs. In all MFPAD plots the molecule is aligned horizontally with the O^{3+} ion on the right. The theoretical predictions by the model based on the relaxed-core Hartree-Fock approximation (Ph.V. Demekhin, Univ. of Kassel) are overlaid as red lines (see [P7] for details).*

experiment by using the measured MFPADs for different KER values. To illustrate this, we have chosen the asymmetric break-up channel of the quadruply charged O_2 ($O^+ + O^{3+}$), in order to make both of the nuclei distinguishable. While the MFPAD for the first emitted electron (Fig. 2b) is still symmetric, reflecting the 1s ionization of a neutral O_2, the electrons emitted in a second step (PAP channel, Fig. 2d-h) manifest clearly asymmetric MFPADs, reflecting that the second electron is more likely to be emitted from the atom which ends up in a triply charged state. The MFPADs plotted for different KERs thus represent the diffraction pattern of the electron emitted form one and scattered form the other oxygen atom. The internuclear distances *R* and the time delay *t* between the absorption of the first and the second x-ray photon indicated in the figure have been obtained using a simple Coulomb explosion (CE) model. The outcome of the simulation, which is based on these *R* and *t* values (red line) is in qualitative agreement with the experimental data. These results suggest that the measured MFPADs reflect the elongation of the molecular bond by approximately 1.2 a.u. within the duration of the x-ray pulse and, thus, demonstrate the feasibility of photoelectron diffraction imaging of molecular dynamics using high repetition rate XFELs.

Tracing ultrafast intramolecular charge dynamics in multiphoton multiple ionization of molecules

Following our collaborative experimental and theoretical work on tracing ultrafast charge dynamics in iodomethane (CH_3I) and iodobenzene (C_6H_5I) molecules during and after extreme multiphoton ionization by ultraintense hard x-rays at LCLS [R4, R5], we exploited the increase of the repetition rate and the availability of a dedicated "reaction microscope" spectrometer at the SQS end station of the European XFEL to obtain a detailed picture of the intramolecular charge transfer following ionization of iodine-containing molecules by soft x-ray pulses. While in the experiments at

LCLS we mainly focused on the detection of carbon and iodine ions, the parameters available at SQS enabling detecting one or more protons in coincidence with heavier fragments. The outcome of such measurement for CH_3I is illustrated in Fig. 3 and 4. Fig, 3a displays the yield of carbon and iodine ion pairs detected in coincidence after CH_3I ionization by 25 fs, 0.8 mJ x-ray pulses at 2 keV [R6]. One noticeable feature is a noticeable amount of C^{5+} ions, which most likely reflects a non-negligible amount of direct x-ray absorption at the carbon site.

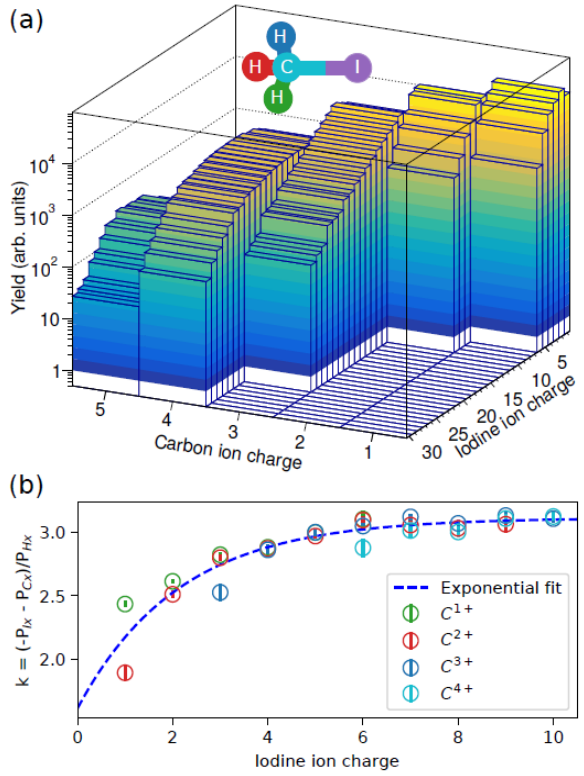

Figure 3: *Fragmentation of CH_3I molecules by 2-keV EuXFEL X-ray pulses.* ***a)*** *Charge state distribution of carbon and iodine ions detected in coincidence.* ***b)*** *Average number of hydrogen ions, k, produced from the fragmentation of a CH_3I molecule for carbon and iodine ion pairs $[I^{m+}, C^{n+}]$ with $m \leq 10$. It is calculated from the measured momenta of I, C and H ions using momentum conservation.*

Fig. 3b displays the estimated number of created protons (k) for each of the I^{m+}, C^{n+} fragmentation pairs, with m set to 10 and n indicated in the figure. Even though protons were also detected in coincidence with heavier fragment pairs, because of the detection efficiency and dead time of the detector, the fraction of events where all three of them could be detected remained rather small. Therefore, to estimate the number k we exploited momentum conservation: along the measured iodine momentum direction (x), the sum of the carbon ion momentum P_{Cx} and the total momentum kP_{Hx} of the k hydrogen ions should be equal to the negative the iodine ion momentum P_{Ix}. Since for the neutral CH_3I the positions of all H atoms are symmetric with respect to C-I axis, their momenta after the rapid fragmentation of a highly charged molecule are, on average, equal to each other and, thus, their number k can be estimated using the measured momentum of only one proton as $k = (P_{Ix} - P_{Cx}) / P_{Hx}$. As can be seen from the figure, the number of protons increases with iodine ion charge state, and then saturates at about 3 above I^{5+}, implying a full fragmentation of the CH_3I molecule without neutral atoms if the iodine ion has more than five charges. This analysis allows us to quantify the number of electrons transferred to the iodine site without the assumption that all three hydrogens are charged.

The ability to measure proton momenta provides an additional sensitive tool for characterizing ultrafast charge rearrangement process during the XFEL fragmentation of molecules. Since these charge dynamics crucially depend on nuclear geometry, i.e., on the (evolving) separation between different atoms, a quantitative understanding of charge rearrangement processes requires a detailed picture of the motion of the nuclei, which can be obtained from the measured ion (in particular, proton) momenta. Fig. 4 displays a set of correlated momentum maps of I, C and H ions for several exemplary charged state combinations. These graphs represent a modified version of the so-called Newton plots, which in this case include the events where at least four ions have been detected in coincidence. Here, the coordinate frame is chosen such that the momentum vector of the I^{n+} fragment points in the positive x direction, all the other momenta are normalized with respect to its magnitude, and the momentum of one detected proton (H_a^+) lies in the top x-y plane. Because of the momentum conservation, the carbon

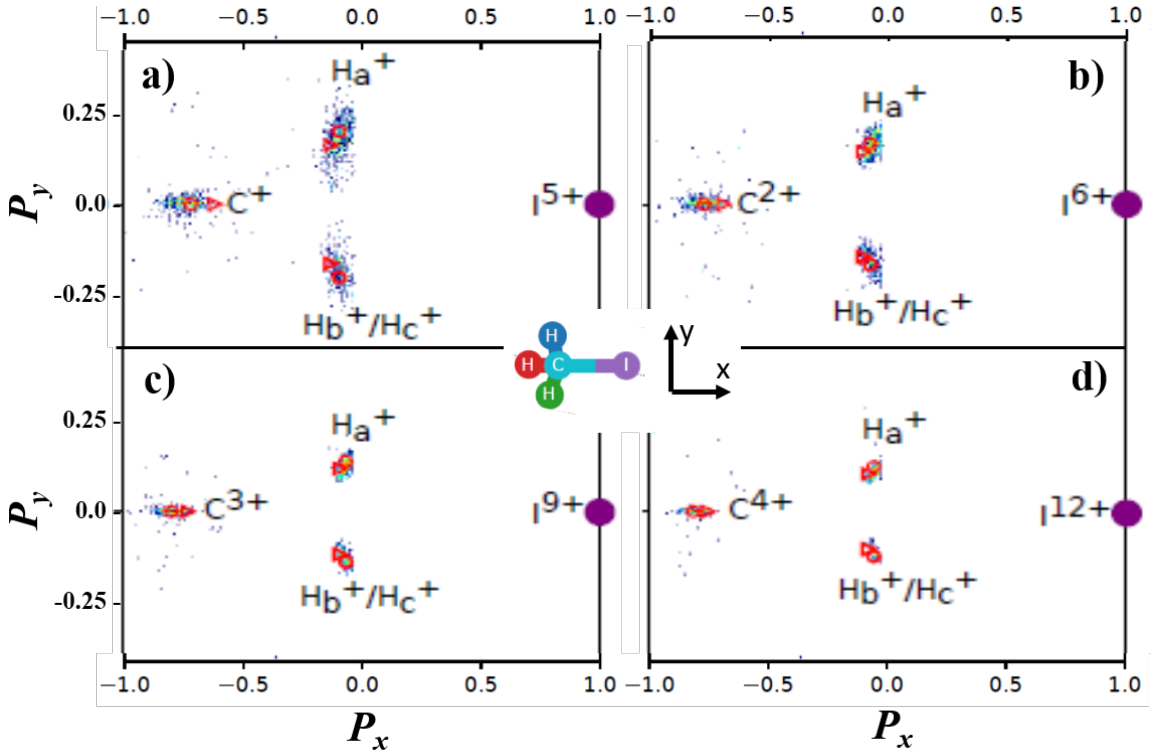

Figure 4: *Modified Newton plots of I^{n+}, C^{m+}, H^+, H^+ coincidence events measured upon CH_3I fragmentation by intense 2 keV EuXFEL pulses (same pulse parameters as in Fig. 3).* ***a)*** *I^{5+}, C^+;* ***b)*** *I^{6+}, C^{2+};* ***c)*** *I^{9+}, C^{3+};* ***d)*** *I^{12+}, C^{4+}. Triangles: the results of the instantaneous Coulomb explosion (CE) simulations. Circles: the results of a CE simulation based on a charge build-up model.*

momentum vector always points in the direction opposite to the iodine. For other protons (H_b^+, H_c^+) the momentum is shown after rotating with respect to x axis until it falls within the x - y plane. As can be seen from the figure, for all charge state combinations the momenta predicted by a straightforward CE model, which assumes instantaneous ionization of the molecule at the equilibrium geometry to the final charge state (triangles in Fig. 4), lie surprisingly close to the experimental data. Still, in a more quantitative consideration, there is a noticeable mismatch between the predictions of the instantaneous CE model and the data, which most likely originates from the time needed for the charge buildup and its redistribution. In order to account for these two time scales, we implement a simple model along the line proposed in [R7], which employs two characteristic parameters to account for the time scale of these two processes. As can be seen from Fig. 4, this model ensures a good quantitative agreement with the data for all charge state combination shown.

For larger systems, momentum maps similar to those shown in Fig. 4 open the way towards studying the charge transfer from the initial absorption site to individual atoms as a function of their position in the molecule. As was theoretically shown in [P9] for the example of iodobenzene, the final charge state for carbon atoms in a benzene ring can be rather inhomogeneous. It is illustrated in Fig. 5, where the average charge for all carbons and hydrogens in C_6H_5I has been simulated as a function of fluence for the conditions of our hard x-ray experiment [R4, R5], where nearly all x-ray absorption occurs at the iodine site. Somewhat counterintuitively, the carbon atoms located closer to the iodine end up with smaller average charge, suggesting that the charge separation due to the Coulomb repulsion after the charge redistribution within the ring plays a more important role than the higher efficiency of the initial charge transfer. In a recent collaborative effort at the EuXFEL (led by R. Boll, T. Jahnke and the PIs of this project), a few-particles correlated momentum maps of ionic fragments have been used to study the position-dependent charge distributions in iodopyridine and iodopyrazine molecules [R8].

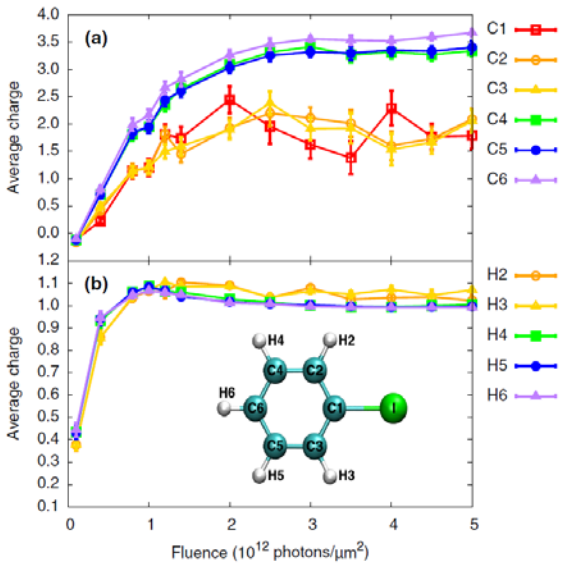

Figure 5: *Simulated average partial charge of (a) carbon and (b) hydrogen atoms for C_6H_5I ionization by 8.3 keV, 30 fs x-ray pulses as a function of fluence (from [P9]).*

The experimental results in [R8] show a trend similar to the results of Fig. 5: the carbon atom closest to the iodine has, on average, the lower charge compared to the other carbons. Besides the insight into charge rearrangement dynamics, the results obtained in [R6, R8] demonstrate that ion momentum imaging with high repetition rate XFELs represents a promising tool for obtaining direct snapshots of (evolving) molecular structure.

Future plans

Even though significat amount of important information and many physical insights can be extracted from single-pulse meausurements combined with coincident few-particle imaging and advanced theoretical modelling, our main priority in *Thrust 1* is to utilize new LCLS attosecond capabilities [R2] for studies of charge dynamics within the first femtosecond after the photoexcitation. Since many experimental and theory groups worldwide (including many within the DOE AMOS program) are interested in such possibilities, these overlapping interests resulted in a joint community proposal for a series of experiments aimed at *real-time observation of ultrafast electron motion using attosecond LCLS pulses* – an effort dubbed "the attosecond campaign", which is led by SLAC researchers J. Cryan, P. Walter and A. Marinelli. This campaign, which is perfectly aligned with the objectives of the *Thrust 1* of our program, was approoved to receive several blocks of beamtime at the LCLS within next couple of years, and the first experiment was initially scheduled for Fall 2020. However, because of the COVID-realated shutdowns, the experiment was postponed and is currently scheduled for April of 2021. The initial measurements will make use of X-ray sensitivity to charge localization for probing the dynamics, and test two complementary methods for launching a coherent electron wave packet: impulsive ionization (core-shell or inner-valence) and impulsive stimulated X-ray Raman scattering [R9]. Besides the experimental preparations, one of the important aspects for the initial attosecond experiments are the expectations for the wave packet produced by either method. Most of the earlier theoretical works describing the prospects of observing such ultrafast electronic motion assumed a fully coherent initial state. However, a recent study by Santra's group [P10] has clearly highlighted the importance of the electronic decoherence (e.g., caused by the interaction of the photoelectron and the cation). This effect, which can unfold on sub-100 as time scale, represents a competing process to the ultrafast correlation-driven electronic dynamics responsble for charge migration. Therefore, one of the of the priorities in the context of attosecond campaign will be understanding the role of electronic decoherence for the conditions of the planned experiments.

***Thrust 2:* <u>*Development of a short-pulsed UV source and experiments with UV light.*</u>**
(*Rolles, Rudenko*)

Recent progress

Because of the LCLS shutdown and since UV pump pulses were not yet available at the EuXFEL, our efforts within *Thrust 2* so far focused on the development of short-pulsed UV source at KSU, on gathering experience with time-resolved imaging of UV-driven photoprocesses, and on experiments with 200 nm pump pulses at FLASH. At KSU, our approach to the experiments with UV light is twofold. First, we commissioned a conventional, crystal-based setup for 3rd and 4th harmonic generation of 800 nm Ti:Sa laser, and employed it in the experiments. In parallel, we developed a

broad-band UV source based on mixing the fundamental and its second harmonic in a gas cell for generating sub-20 fs UV pulses. Using the latter approach and Ar-filled cell, we have generated UV light with 267 nm central wavelength and ~7 nm bandwidth, which for FTL pulses would be sufficient to achieve ~15 fs pulse duration. Currently, the pulses produced by this setup are significantly longer, and the efforts to achieve best possible compression are underway. Meanwhile, we use our crystal-based UV pulses for COLTRIMS experiments on imaging molecular dynamics. We have employed compressed, sub-40 fs 3rd harmonic pulses for several studies of UV-driven dynamics in halomethanes, and, very recently, started first experiments using 4th harmonic light. One example of its application is shown in Fig 6a. which depicts the delay-dependent KER spectrum of $CH_3^+ + I^+$ ions resulting from the B-band photoexcitation in CH_3I by ~85 fs, 200 nm UV pulse probed with double ionization and CE by 25 fs, 800 nm NIR pulses. Because of the predissociative nature of the B-band, its signature in the KER vs. delay spectrum appears as a broad, nearly structures feature, in contrast to rather sharp lines appearing in such spectrum for A-band [R10] or ionic-state [R11] dissociation. As illustrated in Fig. 6b, we complemented this measurement with the experiment at FLASH, where the same 200 nm B-band excitation was probed with core-shell (iodine 4d) ionization by intense, 95 eV XUV pulse [P11].

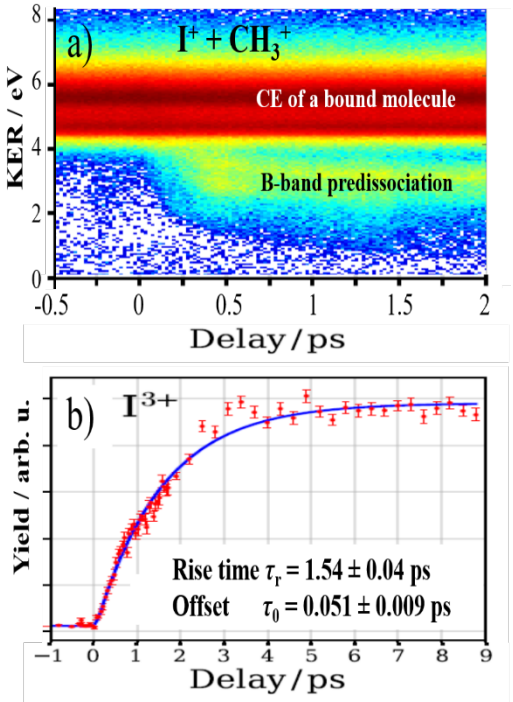

Figure 6: a) *KER spectrum of $CH_3^+ + I^+$ breakup channel for CH_3I as a function of delay between 200nm pump and 800 nm probe pulses at KSU.* ***b)*** *Yield of low-energy I^{3+} ions produced after 4d inner-shell ionization of CH_3I as a function of delay between 200nm pump and 95 eV XUV probe pulses at FLASH (from [P11]).*

Future plans

During the next year, we plan to complete the development of sub-20 fs UV setup at KSU adding the proper pulse compression, and employ these pulses in COLTRIMS experiments at the JRML. We will focus the efforts in *Thrust 2* on studying charge transfer dynamics in bifunctional 2-phenylethyl-N,N-dimethylamine (PENNA) molecule, which is often considered to be a representative model system for charge transfer in larger peptide cations [R12]. The excitation of a few low-lying cationic states in PENNA is expected to result in charge transfer from the phenyl chromophore through a $-CH_2-CH_2-$ bridge to the methylated amine group, unfolding on a 60-80 fs time scale. We plan to induce these dynamics by impulsive two-photon ionization with a broad-band 266 nm pulse, and probe it first with strong-field ionization at KSU, and later with 1s ionization of a nitrogen atom at one of the XFEL facilities. The corresponding proposal for LCLS run 19 will be submitted in October 2020. In addition, following our initial time-resolved experiments employing 200 nm pump pulses, we plan to study wavelength dependence of UV-driven photochemistry using the newly acquired deep UV TOPAS system at KSU.

Thrust 3: ***<u>Studies of distance-dependent charge transfer processes in dissociating molecules</u>***
(Rudenko, Rolles, Santra)

Recent progress

In the previous sections, we discussed intramolecular charge dynamics occurring in bound molecular system before it undergoes fragmentation. However, in x-ray interactions with molecules, electronic dynamics is almost always accompanied by a rapid molecular breakup, such that charge

transfer between different sites of the fragmenting molecule plays an important role for the reaction outcome. Our main goal for *Thrust 3* is therefore to study the functional dependence of the charge transfer rate on distance for several prototypical fragmenting systems. During the last year, we addressed this goal in three different ways, mainly focusing on a prototypical CH_3I molecule. First, we performed an experiment with 800 nm pump at SACLA [R13], which was conceptually similar to our earlier studies [R10, R11], but employed the iodine 4d ionization as a probe and achieved significantly better time resolution. As illustrated in Fig. 7a, in such experiment the charge transfer process is characterized by the delay-dependent yield of the highly charged iodine ions with very low kinetic energies, for which the methyl group remains neutral. Our measurement at SACLA demonstrated that for these conditions, the outcome of the experiment is still consistent with the predictions of the classical over-the-barrier (OTB) model employed in [R10, R11]. Second, using the 200 nm photoexcitation to the CH_3I B-band (discussed in the previous section) as a pump, we looked at similar dynamics for the predissociative precursor state. As can be seen in Fig. 6a, in this case the internuclear separation at a given delay is not well defined, in contrast to the experiments [R10, R11, R13]. The yield of the low-energy I^{3+} ions measured after probing such a wave packet with iodine 4d ionization at FLASH [P11] is shown in Fig. 6b. While the rise time of this signal is determined by the B-state predissociation time (~1.55 ps) and was found to be charge- state independent, the small but clear offset, which increases for larger charge states, reflects the region of small internuclear separations, where at least one electron is always transferred from the methyl group to the iodine ion, and can be still predicted by the classical OTB model.

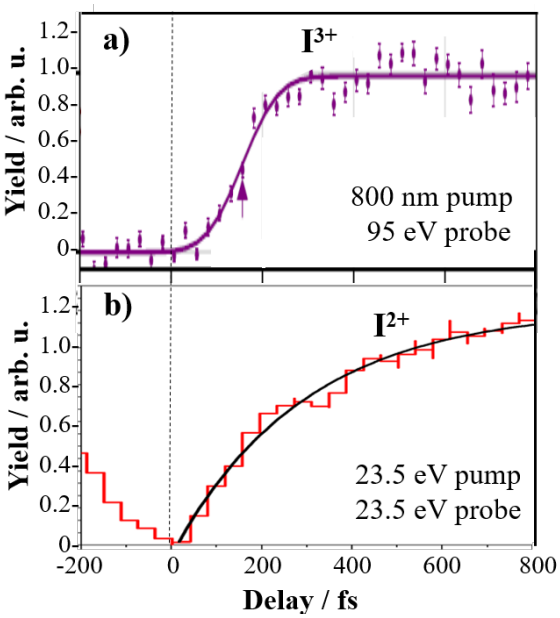

Figure 7: a) *Delay-dependent yield of the low-energy I^{3+} ions from the CH_3I fragmentation by 40 fs, 800 nm pump and 30 fs, 95 eV probe pulses at SACLA. The arrow corresponds to the critical distance predicted by the OTB model. (From [R13]).* ***b)*** *Delay-dependent yield of low-energy I^{2+} ions resulting from CH_3I fragmentation by a pair of 30 fs XUV pulses at 23.5 eV. Black line: exponential fit to the data, yielding the rise time of 292±19 fs.*

Finally, we have studied charge transfer dynamics in dissociating halomethane molecules (CH_3I and CH_2ICl) after valence-shell XUV ionization in the experiment performed at FLASH-II employing XUV pump – XUV probe configuration. The results of this measurement for CH_3I are illustrated in Fig. 7b. In contrast to the experiments discussed above (Fig 6b and 7a), here the photon energy for both the pump and the probe (23.5 eV) is well below the core-shell ionization threshold. Conceptually similar to the measurements discussed before, we trace the signatures of charge transfer by following the delay-dependent yield of low-energy doubly charged iodine ions, which must have a neutral partner. However, in contrast to the step-function-like behavior expected from the OTB model (see, e.g. Fig. 7a), the delay-dependence shown in Fig. 7(b) manifests a steady exponential growth, with a characteristic rise time of ~292 fs. Even though the shape of the curve is somewhat similar to that shown in Fig. 6b, a much shorter rise time, the absence of any detectable offset and the analysis of coincident CE spectra suggest that this behavior is not due to the predissociative precursor state.

Future plans

We are currently working on developing a more quantitative theoretical picture for the experiments on valence ionization of halomethanes. Besides that, we have proposed two experiments aimed to

improve our ability to determine the internuclear separation *R*, and to quantify the charge-transfer rate. The first experiment, proposed for LCLS, will employ iodosilane (SiH_3I) as a target. Compared to CH_3I, SiH_3I offers two advantages. First, its laser-induced dissociation proceeds considerably slower because of the heavier mass of the silicon atom. Second, the silicon atom has considerably more electrons available for transfer to x-ray ionized iodine than the carbon atom in CH_3I. The experiment received beamtime and was initially scheduled for Run 18 at LCLS; however, because of significant delays it was first postponed and then canceled. We are currently discussing options for its implementation in Run 19. In parallel, we have proposed to utilize the high repetition rate and dedicated "reaction microscope" spectrometer at the EuXFEL to perform similar measurements on a deuterated iodomethane (CD_3I). The proposal was approved, and the experiment at the SQS end station is provisionally scheduled for February 2021.

Thrust 4: <u>Theory development</u> (*Greenman, Santra*)

Recent progress

Refining theoretical description of core-shell photoionization

Since the experimental observables exploited in this project almost always involve highly differential measurements of core-shell ionization process, its accurate theoretical modelling is one of the keys to the success of the project. During the last year, we worked on improving several aspects of core-shell ionization description, mainly focusing on issues related to electron-electron correlation. In particular, we developed a procedure that allows the treatment of both delocalized and localized core hole formation in photoionization in single-channel calculations, which is applicable to complex systems where coupled channel photoionization calculations may not be feasible. [P12]. This approach relies on the extension of a recently introduced "overset-grid" implementation of the complex Kohn method [R14] to photoionization. In parallel, we have been exploring the effects of more accurate photoionization continuum state calculations, including the molecular potential, on the angular correlation of the electrons for two-site double core hole states [R3]. The approach based on the molecular potential can be extended to studies of charge migration in rather complex polyatomic molecules after core-shell ionization.

New capabilities and new applications for XMOLECULE

While the current version of XMOLECULE represents a powerful toolkit for detailed simulations of x-ray driven dynamics, which has been successfully applied to explain some of the experimental results obtained within this collaboration [R1, R4, R5], one of the main goal for the theory part is to further enhance its capabilities and range of applications. Recently, several important advances have been made along these lines. First, employing a quantum–classical description of the nuclei by the so-called fewest switches surface hopping algorithm, we have developed a version of XMOLECULE, which is capable of tracing the impact of the photoelectron on electronic coherence of the remaining cation [P10], which is of crucial importance for the studies of ultrafast electronic wave packets responsible for charge migration. Second, XMOLECULE has been adapted to characterize ultrafast charge transfer in molecular systems relevant for photovoltaics by simulating time-resolved x-ray absorption spectra (TRXAS) [P2, P3]. Finally, in a collaboration with a large experimental group led by L. Young, the TRXAS calculated using XMOLECULE has been utilized to study ultrafast proton transfer in valence-ionized liquid water [P4]. Here, XMOLECULE has been employed within in two-layered quantum mechanics / molecular mechanics approach, where a core region is treated quantum-mechanically, and is embedded in a larger region described classically.

Application of XMDYN for studies of charge rearrangement dynamics in complex molecules

While for a rather small polyatomic molecule like H_2O or CH_3I, the XMOLECULE enables the full simulation of molecular interaction with an intense x-ray pulse, for larger systems like iodobenzene (see Fig. 5) including nuclear dynamics is beyond the current computational capabilities. This can be

realized by employing a hybrid quantum-classical approach within XMDYN toolkit [R15]. Here, the neutral atoms, atomic ions and free electrons are treated as classical particles, whereas bound electrons are treated as quantum electrons that are assigned to atomic orbitals of the atomic sites (disregarding molecular states). We have successfully applied this approach to simulate the CE maps and charge rearrangement dynamics for multiple ionization of iodopyridine molecule [R8], including position-resolved charge state distributions for individual nuclei. A very good agreement with experiment is achieved for carbon and proton momenta, suggesting that XMDYN simulation can be used to generate the full numerical movie of ionization and nuclear dynamics. The only serious discrepancy with the experiment is the overestimation of the average carbon charge for high iodine charge states.

Future plans

We will continue to integrate improvements and add-ons into XMOLECULE and XMDYN packages. In particular, based on the results of iodopyridine analysis [R8], the charge transfer description within XMDYN will be refined to achieve better agreement with the experiment. Furthermore, stimulated by intriguing experimental results recently obtained at the EuXFEL on resonantly-enhance x-ray multiphoton ionization (REXMI) of molecules, we will try to extend XMDYN to include bound-bound transitions, which has been recently realized in XATOM, but is currently not feasible for molecular systems. We will also continue working on improving the continuum state description within XMOLECULE. In parallel, we plan to apply XMOLECULE to study a few-femtosecond break-up of higly ionized water molecule, where the experimental results suggest that the proton and electron dynamics are much more interweaved than in the CH_3I example described above in *Thrust 1*. Besides that, the main focus of the whole project will move towards the "attosecond campaign" at LCLS. From the theory side, Santra's group will work on the analysis of decoherence issues for the first experiments planned. In parallel, Greenman's group has started working on simulating electronic dynamics induced by impulsive stimulated X-ray Raman scattering.

Peer-Reviewed Publications Resulting from this Project (Project start date: 09/2018)

[P1] L. Inhester, L. Greenman, A. Rudenko, D. Rolles, and R. Santra, *Detecting coherent core-hole wave-packet dynamics in N_2 by time- and angle-resolved inner-shell photoelectron spectroscopy*, J. Chem. Phys. **151**, 054107 (2019).

[P2] K. Khalili, L. Inhester, C. Arnold, R. Welsch, J.W. Andreasen, and R. Santra, *Hole dynamics in a photovoltaic donor-acceptor couple revealed by simulated time-resolved x-ray absorption spectroscopy*, Struct. Dyn. **6**, 044102 (2019).

[P3] K. Khalili, L. Inhester, C. Arnold, A.S. Gertsen, J.W. Andreasen, and R. Santra, *Simulation of time-resolved x-ray absorption spectroscopy of ultrafast dynamics in article-hole-excited 4-(2-thienyl)-2,1,3-benzothiadiazole*, Struct. Dyn. **7**, 044101 (2020).

[P4] Z.-H. Loh, G. Doumy, C. Arnold, S. H. Southworth, …, R. Santra, and L. Young, *Observation of the fastest chemical processes in the radiolysis of water*, Science **367**, 179 (2020).

[P5] L. Kjellsson, …, G. Doumy, S.H. Southworth, P.J. Ho, A.M. March, …, R. Santra, Z.-H. Loh, S. Coriani, A. I. Krylov, and L. Young, R*esonant Inelastic X-Ray Scattering Reveals Hidden Local Transitions of the Aqueous OH Radical*, Phys. Rev. Lett. **124**, 236001 (2020).

[P6] L. Inhester, Z. Li, X. Zhu, N. Medvedev, T. Wolf, *Spectroscopic Signature of Chemical Bond Dissociation Revealed by Calculated Core-Electron Spectra*, J. Phys. Chem. Lett. **10**, 6536 (2019).

[P7] G. Kastirke, M. Schöefler, …, X. Li, D. Rolles, A. Rudenko, …, P.V. Demekhin, and T. Jahnke, *Photoelectron diffraction imaging of a molecular breakup using an X-ray free-electron laser,* Phys. Rev. X **10**, 021052 (2020).

[P8] G. Kastirke, M. Schöefler, …, X. Li, D. Rolles, A. Rudenko, P.V. Demekhin, and T. Jahnke, *Double core-hole generation in O2 molecules using an x-ray free-electron laser: Molecular-frame photoelectron angular distributions*, Phys. Rev. Lett., accepted (2020).

[P9] Y. Hao, L. Inhester, S.-K. Son, and R. Santra, "*Theoretical evidence for the sensitivity of charge-rearrangement-enhanced x-ray ionization to molecular size"*, Phys. Rev. A **100**, 013402 (2019).
[P10] C. Arnold, C. Lariviere-Loiselle, K. Khalili, L. Inhester, R. Welsch and R. Santra, *Molecular electronic decoherence following attosecond photoionization,* J. Phys. B **53** 164006 (2020).
[P11] R. Forbes, F. Allum, S. Bari, R. Boll, K. Borne, …, D. Rolles, and M. Burt, T*ime-resolved site-selective imaging of predissociation and charge transfer dynamics: the CH_3I B-band,* J. Phys. B, accepted (2020).
[P12] C.A. Marante, L. Greenman, C.S. Trevisan, T.N. Rescigno, C.W. McCurdy,and R.R. Lucchese, *Validity of the static-exchange approximation for inner-shell photoionization of polyatomic molecules*, Phys. Rev. A **102**, 012815 (2020).

References

[R1] X. Li, L. Inhester, …, R. Santra, D. Rolles, A. Rudenko, P. Walter, "*Electron-ion coincidence measurements of molecular dynamics with intense x-ray pulses"*, Scientific Reports, submitted (2020).
[R2] J. Duris, S. Li, T. Driver et al., "*Tunable Isolated Attosecond x-ray Pulses with Gigawatt Peak Power from a Free-Electron Laser*", Nature Photonics **14**, 30 (2020).
[R3] S. Chattopadhyay, L. Inhester, R. Santra, A. Rudenko, D. Rolles, L. Greenman, *Probing core-hole wavepacket dynamics in molecules using angle-resolved photoelectron spectroscopy,* in preparation (2020).
[R4] A. Rudenko, L. Inhester, ..., R. Santra, D. Rolles, *Femtosecond response of polyatomic molecules to ultraintense hard x-rays*, Nature **546**, 129-132 (2017).
[R5] X. Li, L. Inhester, …, R. Santra, D. Rolles, A. Rudenko, *Pulse energy and pulse duration effects in the ionization of iodomethane by ultra-intense hard x-rays*, Phys. Rev. Lett., submitted (2020).
[R6] X. Li, A. Rudenko, ..., D. Rolles, M. Meyer, T. Jahnke and R. Boll, *Coulomb explosion imaging of small polyatomic molecules with ultrashort x-ray pulses*, in preparation (2020).
[R7] K. Motomura, E. Kukk, H. Fukuzawa, …, A. Rudenko, C. Nicolas, X.-J. Liu, …, M. Yabashi, M. Yao, and K. Ueda, *Charge transfer and nuclear dynamics following deep inner-shell multiphoton ionization of CH_3I molecules by X-ray free-electron laser pulses*, J. Phys. Chem. Lett. **6**, 2944 (2015).
[R8] R. Boll, J. Schaefer, …, X. Li, D.Rolles, ..., A.Rudenko, M. Meyer, R. Santra and T. Jahnke, *X-ray induced Coulomb explosion images complex single molecules,* in preparation (2020).
[R9] J. O'Neal, E. G. Champenois, …, A. Picon, A. Marinelli, J. Cryan, *Electronic Population Transfer via Impulsive Stimulated X-Ray Raman Scattering with Attosecond Soft-X-Ray Pulses*, Phys. Rev. Lett. **125**, 073203 (2020).
[R10] R. Boll, B. Erk, R. Coffee, …, D. Rolles, A. Rudenko, *Charge transfer in dissociating iodomethane and fluoromethane molecules ionized by intense femtosecond X-ray pulses***,** Struct. Dyn. **3**, 043207 (2016).
[R11] B. Erk, R. Boll, S. Trippel, ..., D. Rolles, A. Rudenko, *Imaging charge transfer in iodomethane upon x-ray photoabsorption,* Science **345**, 288 (2014).
[R12] B Mignolet, R D Levine and F Remacle, *Charge migration in the bifunctional PENNA cation induced and probed by ultrafast ionization: a dynamical study,* J. Phys. B **47** 124011 (2014).
[R13] F. Allum, …, D. Rolles, A. Rudenko, …, T. Driver, and R. Forbes, *Multi-channel photodissociation and XUV-induced charge transfer dynamics in strong-field ionized methyl iodide studied with time-resolved recoil frame covariance imaging,* Faraday Discussions, submitted (2020).
[R14] L. Greenman, R. R. Lucchese, and C. W. McCurdy, *Variational treatment of electron–polyatomic-molecule scattering calculations using adaptive overset grids,* Phys. Rev. A **96**, 052706 (2017).
[R15] Z. Jurek, S.-K. Son, B. Ziaja, R. Santra, *XMDYN and XATOM: versatile simulation tools for quantitative modeling of X-ray free-electron laser induced dynamics of matter*, J. Appl. Cryst. **49**, 1048 (2016).

Light-induced couplings to study and control electronic interactions and electron-nuclear dynamics

PI: Arvinder Sandhu
Department of Physics and College of Optical Sciences
The University of Arizona
Tucson AZ 85721
asandhu@arizona.edu

Project Scope

In this project we aim to employ light-induced couplings to control correlated and coupled dynamics in atoms and molecules. This will be achieved by by employing tunable, multi-pulse, pump-probe techniques. The overarching goal of our program is to use light fields to understand and predictably control the charge and energy dynamics. Attosecond transient absorption spectroscopy, non-collinear four-wave-mixing, and coincident velocity map imaging form the main experimental techniques utilized on this project.

The topics to be explored in this project include 1) the study of polaritons formed when autoionizing states are coupled by the laser field and the resulting stabilization of ionization channels, 2) the control of interfering ionization pathways and electron-core interactions in the two-color photoionization, 3) the investigation of the electronic correlations and electron-nuclear couplings responsible for charge migration. This project will employ a range of tunable wavelength (600-3400nm) strong fields enabling a systematic study of resonant and non-resonant couplings, leading to new strategies for controlling few-body dynamics in atoms and molecules. The use of multi-pulse schemes provides new control possibilities while also providing means to disentangle the role strong fields in XUV-IR experiments. In the second phase of the project, we will expand our toolkit to employ attosecond soft-x-ray pulses to obtain elemental and chemical sensitivity in the study of charge dynamics.

Recent Progress

We completed a series of measurements demonstrating the formation of polaritonic autoionizing states and ionization stabilization under specific conditions. We obtained new results on the control of phases and amplitudes of two-color ionization into the spin-orbit split continuum. Collaborations with UCF, LBNL, and Purdue theory groups have played a crucial role in the interpretation of results. We are working towards a new experimental setup for attosecond spectroscopy in the soft-x-ray regime. Specifics of our research work are discussed below.

Generation and application of tunable XUV and IR: Our unique experimental approach for attosecond transient absorption and four-wave-mixing emission with fixed XUV spectrum and tunable non-commensurate allowed us to demonstrate control over the time-dependent Autler-Townes splitting and light induced structures in helium [1]. We also investigated linear and nonlinear couplings that govern the temporal and spectral structure of four-wave-mixing emissions. Then we generalized our techniques further by developing a scheme to generate tunable XUV emission through high-order frequency mixing between a strong near-infrared (780 nm) field and a weak shortwave-infrared pulse with adjustable wavelength. In this two-color driving scheme, new harmonics energies are linear combinations of photons from the two fields, providing much higher spectral coverage than single color harmonics and easy tuning to target resonances of

interest. We demonstrated the utility of tunable two-color harmonics in transient absorption spectroscopy and time-resolved photoelectron spectroscopy [3] to address the excited state dynamics which are inaccessible with single-color harmonics. We were able to control of transitions to the light induced states, observe new four-wave-mixing emissions, and selectively address different electronic and vibrational states in atoms and molecules.

Study of autoionizing polaritons and laser induced stabilization:

Using the tunable spectroscopy, we made progress in quantifying the electronic couplings between electronic states and the application of light-induced modifications to control the atomic and molecular autoionization dynamics.

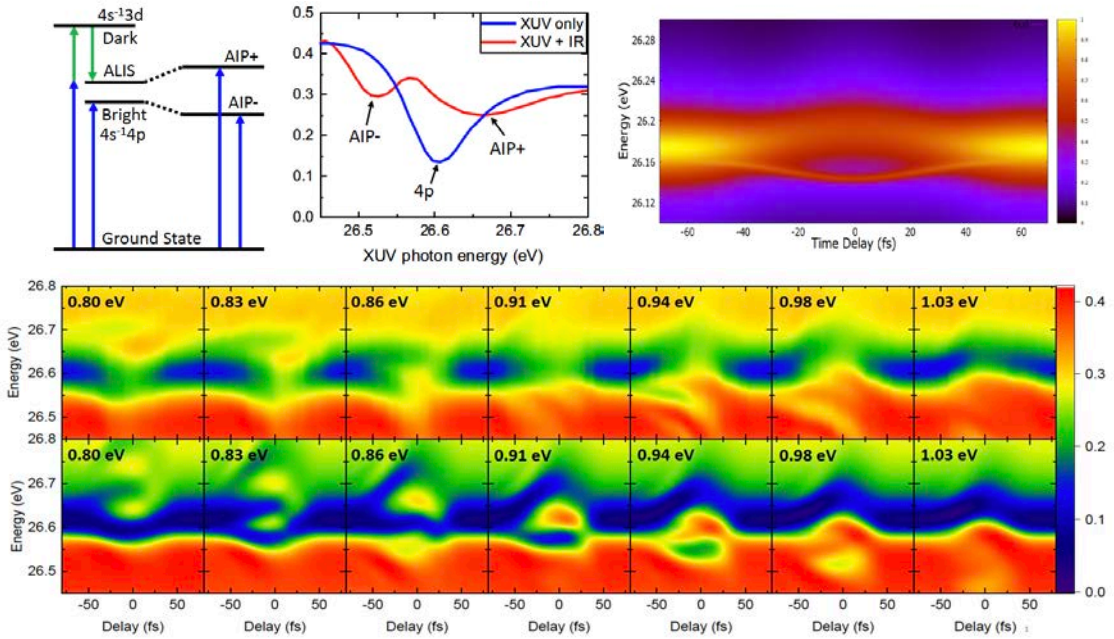

Fig 1. (top panel) Bright ($3s^{-1}$ 4p) and dark ($3s^{-1}$ 3d) autoionizing states (AIS) in Argon. Light induced coupling to the dark state forms autoionizing light induced states (ALIS). Interaction of ALIS and bright AIS generates autoionizing polaritons (AIPs), which manifest in the absorption spectra on the left and right side of the bright resonance. The unequal width of two AIP features indicates different ionization lifetimes. Theoretical modeling shows narrow width for lower AIP band, indicating stabilization against ionization. (Bottom panel) Experimental (above) and theoretical (below) XUV absorption spectra as a function of delay for several values of the IR photon energy, where AIPs show as sidebands above or below the 4p line depending on IR wavelength. Several coherent quantum paths are activated, and interferences determine the structure and lifetimes of AIPs.

Light-induced states are commonly observed in the photoionization spectra of laser-dressed atoms. The properties of autoionizing polaritons, entangled states of light and Auger resonances, however, are largely unexplored. We employed tunable attosecond transient-absorption spectroscopy to study interferences between the dressed autoionizing states in argon, which we control using a tunable femtosecond laser pulse. The avoided crossings between the autoionizing $3s^{-1}4p$ and several dark states lead to the formation of polariton multiplets, whose profiles show evidence of controllable stabilization, due to the competing Auger decay of their constituents. Specifically, the results in Figure 1 show that the line width decreases for one of autoionizing polariton branches, implies a longer lifetime i.e. stabilization against ionization.

We collaborated with Prof. Luca Argenti at the University of Central Florida to theoretically analyze the light induced modifications of electronic interactions and interferences

between active coherent ionization paths. We obtained excellent agreement with ab initio theory and observed the stabilization for one of the polaritonic branches. Our work provides new avenues for the light-induced control of the electronic properties and unlocks the door to applications of autoionizing polaritons in poly-electronic systems. These results are being submitted for publication.

Control of ionization pathways into a spin-orbit split continuum: We used a tunable pump-probe scheme to tailor the electronic wavepacket in neutral argon and then monitor its photoionization into the two channels of a spin-orbit split continua, one of which entails switching of the core spin-orbit state due to interaction with the outgoing electron.

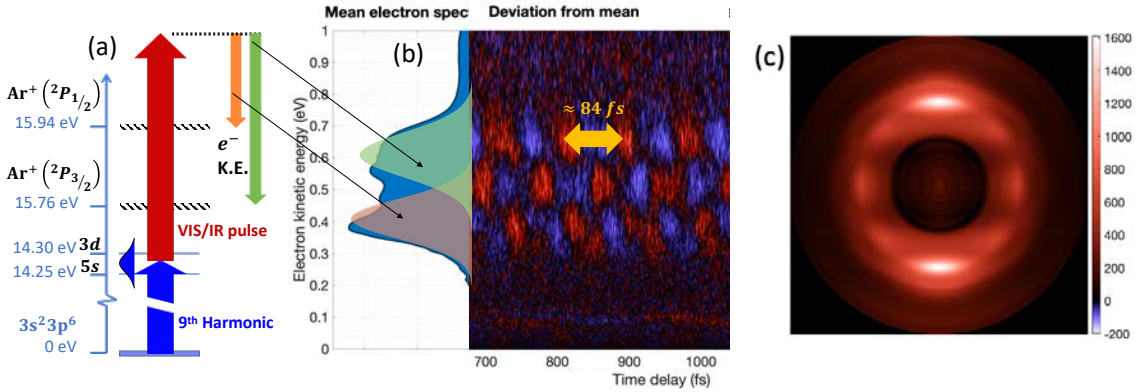

Fig. 2. (a) Two color ionization involving excitation of 3d/5s Rydberg states in Argon and ionization into the split orbit split continuum with one or two tunable IR photons. (b) The beating between ionization pathways is exhibited in both ionization channels with relative phase variation due to electron-core interaction. (c) The photoelectron angular distributions exhibit amplitudes for higher order partial waves due to angular momentum decoupling that occurs when IR field causes m level dependent splitting.

In this study, low-order harmonics were used to prepare a neutral angular Rydberg wavepacket in argon, consisting of *ns* and *nd* states with either J_c=1/2 or 3/2 core. Using the Racah notation for *j*-*l* coupling, such states are labeled as $\left(^{2s+1}L_{J_c}\right) nl\ [K]_J$, where term in the round parenthesis describes core state, *nl* lists the state of the excited electron, *K* is the result of J_c-*l* coupling, and *J* is total angular momentum of the system. We observed that the 9th harmonic can excite a superposition of $\left(^2P_{1/2}\right) 3d\ [3/2]_1$ and $\left(^2P_{1/2}\right) 5s\ [1/2]_1$ states, which beat due to their ~ 48 meV energy separation. When a tunable VIS/IR pulse ionizes the wavepacket, the electron is expected to emerge in the J_c=1/2 continuum. However, due to correlation between the outgoing electron and the core, the electron also appears in the J_c=3/2 continuum with additional 0.18 eV kinetic energy corresponding to the spin-orbit splitting between the ionization thresholds. This is schematically shown in the Figure 2. Simple analysis of the electron kinetic energy spectrum shows peaks corresponding to both channels, and we also observe a quantum beat representing the evolution of *3d*-*5s* wavepacket. Interestingly, the phase of this beat pattern for ionization to the J_c=3/2 channel is different than the J_c=1/2 channel. We are investigating the relationship between the relative phases of the channels and interactions that precipitate the change of ion-core state in one of the exit channels.

Furthermore, we have observed that the angular distributions of various channels exhibit non-zero amplitudes for higher order partial waves that are not allowed in two- or three-photon ionization. This is indicative of the selective excitation of m levels due of the laser field induced splitting of excited states. We are pursuing this in collaboration with Prof. Chris Greene from

Purdue University, who is expert in such MQDT calculations. We will model electron-core interactions in terms of a scattering matrix that will capture the evolution of an entangled system consisting of the Rydberg electron spin and the atomic core through amplitudes and phases for continuum channels corresponding to different core states. We are currently focusing on the role of AC stark splitting in angular momentum decoupling.

Strong-field modification of coupled electron-nuclear dynamics: We continue to pursue the light induced modification of conical intersection between the electronic states of CO_2 molecular ion at ~17 eV energy. The electron hole is driven between the σ and π orbitals by the bending and asymmetric stretch vibrations of this molecule. A delayed NIR pulse excites the hole population to a dissociative state and by monitoring the ion-yield we were able to follow the quantum beating of the electron hole density and its decay with time. Now we are using a 'third' tunable IR control pulse to modify the potential energy landscape of conical intersections. We have observed that the intensity of the NIR field changes the frequency and amplitude of the coherent electron hole beating between the two vibronic states of CO_2^+. We are acquiring additional data at different IR intensities and wavelengths to build a comprehensive picture of this light induced control of conical intersection dynamics. We are using a TIMEPIX based coincidence VMI system for coincident imaging of the electrons and ions for deeper insights into the coupled dynamics.

Future Plans

We will be working on analysis and modeling of the two-color ionization to understand laser induced angular momentum decoupling and electronic interactions in the exit channel. We will also continue the ongoing experimental efforts which aim to study modification of electron nuclear couplings with strong light fields by collecting additional datasets and establishing collaborations for simulating the strong-field modification of potential energy landscape in molecules. We will be investing substantial time to install a new high power, few-cycle MIR laser which will drive the soft-x-ray generation. The additional tunability of light field from 1.6 to 3.4 um will be enabled by this source. The resulting attosecond soft-x-ray capability will allow us to conduct elementally specific probing of charge dynamics in complex molecular systems. The tunable, multi-color and multi-pulse spectroscopy techniques developed in these efforts will enhance the attosecond science toolkit by providing new control knobs.

Peer-Reviewed Publications Resulting from this Project (2018-2020)

1) Nathan Harkema, Jens Baekhoj, Chen-Ting Liao, Mette Gaarde, Ken Schafer, Arvinder Sandhu, "Controlling attosecond transient absorption with tunable, non-commensurate light fields", *Optics Letters* **43**, 3357-3360 (2018).
2) Alexander Plunkett, Nathan Harkema, Robert Lucchese, C. William McCurdy, Arvinder Sandhu, "Ultrafast Rydberg State Dissociation in Oxygen: Identifying the Role of Multielectron Excitations", *Phys. Rev. A* **99**, 063403 (2019).
3) Nathan Harkema, Alexander Plunkett, Arvinder Sandhu, "Tunable high-order frequency mixing for XUV transient absorption and photoelectron spectroscopies", *Optics Express* 19702-19711 (2019).

Transient Absorption and Reshaping of Ultrafast Radiation

DE-SC0010431

Kenneth J. Schafer (kschafe@lsu.edu), Mette B. Gaarde (mgaarde1@lsu.edu)
Department of Physics and Astronomy, Louisiana State University, Baton Rouge, LA 70803

October 2020

Project Scope

Our program is centered around the theoretical study of transient absorption of ultrafast extreme ultraviolet (XUV) radiation by matter interacting with a precisely synchronized near-to-mid infrared (IR) laser pulse, and emphasizes both fundamental theoretical research and a close connection with experimental groups doing attosecond physics [1]. Transient absorption spectroscopy can in principle provide high spectral resolution and high (attosecond) time resolution simultaneously, by spectrally resolving the light transmitted through a sample as a function of delay between the dressing laser pulse and the broadband attosecond EUV probe. As in all transient absorption scenarios, one of the main challenges we confront is the extraction of time-dependent dynamics from delay-dependent information. In addition, we must also account for the reshaping of the broadband XUV light in the macroscopic medium. We study attosecond transient absorption (ATA) using a versatile theoretical treatment that takes account of both the laser-matter interaction at the atomic level via the time-dependent Schrödinger equation (TDSE), as well as propagation of the emitted radiation in the nonlinear medium via the Maxwell wave equation (MWE), often in the single-active electron (SAE) approximation for atomic systems in the gas phase [2][R2,R3]. More recently we have also considered attosecond transient absorption and reflection in condensed phase systems [R4], as well as ATA effects in gases interacting with ultrafast XFEL pulses.

Recent Progress

We have completed a number of research projects, all of them in collaboration with experimental groups carrying out ATA measurements, see [R1-R5] and [3–5]. In this abstract we highlight some of our latest work:

(i) ATA of ultrafast exciton dynamics in condensed phase MgO: In collaboration with the Leone/Neumark experimental group at UC Berkeley, we have considered ultrafast exciton dynamics in a condensed phase system interacting with a moderately intense IR pulse, using attosecond transient reflectivity [R4]. We studied the signature and dynamics of exciton states in the vicinity of the band gap energy. We found that core-level exciton states in MgO have extremely short dephasing lifetimes of just a few femtoseconds; primarily driven by strong and ultrafast exciton-phonon coupling. We also found that the IR pulse gives rise to a Stark shift of the exciton states as well as light-induced states (LIS) in the

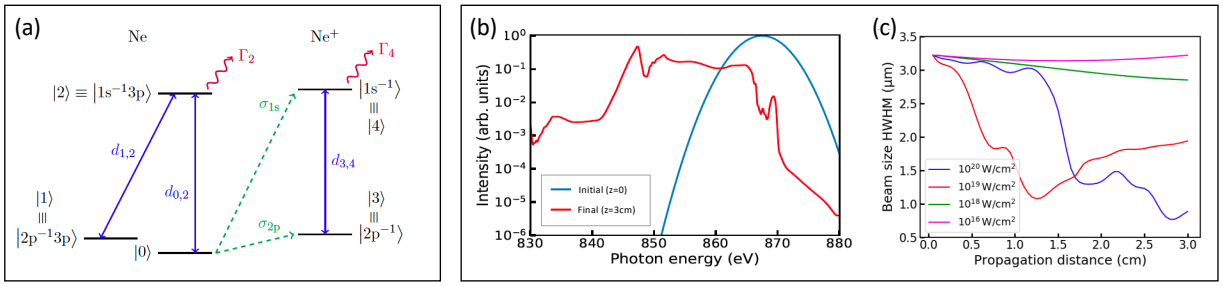

Figure 1: Spatiotemporal reshaping of intense, ultrafast X-ray pulses in resonant neon gas (adapted from [3]): (a) Five-level system used in the calculation. The X-ray pulse is resonant with the ground-$1s^{-1}3p$ transition, and leads to stimulated Raman scattering (SRS) on the $1s^{-1}3p$-$2p^{-1}3p$ and the $1s^{-1}$-$2p^{-1}$ transitions in the neutral and the ion, respectively. The linear absorption and ionization, and nonlinear processes including SRS leads to strong reshaping of the X-ray spectrum (b) as well as the spatial profile (c).

reflectivity spectrum. Similar to the case in atomic systems, these LIS can be understood in terms of IR-induced couplings to dark (dipole-forbidden) exciton states.

In terms of calculations, we developed a simple model in which the excitonic states are described as a three-level system consisting of two bright and one dark state, and the phonon coupling is included as a time-dependent amplitude and phase modulation as described in [6]. We used multi-parameter optimization in comparisons between calculated and measured results in order to extract an estimate for several of the unknown parameters that goes into the model. For example, while the energies of the two bright states are well known from literature (and are clearly visible in the experimental results), both the energy of the dark state and its coupling to the bright states are not. We were able to extract consistent values for these quantities from the modeling coupled with the optimization.

(ii) Linear and nonlinear propagation of intense XFEL pulses through rare gases: In collaboration with the Young experimental group at Argonne National Lab, we have investigated (theoretically) the propagation of intense, ultrafast X-ray pulses through a resonant neon gas. These calculations are part of preparing for experiments scheduled to take place at the European XFEL (currently postponed due to COVID-19), but have also brought interesting insights on their own [3].

We have been studying the Ne/Ne+ five-level system shown in Fig. 1(a). These are the ground state, the core-excited $1s^{-}13p$ state, and the valence-excited $2p^{-}13p$ state in the neutral, and the ground $2p^{-}1$ and excited $1s^{-}1$ states of the ion. We calculate the propagation and reshaping of an intense, sub- or few-femtosecond laser pulse resonant with the ground - $2p^{-}13p$ transition (867 eV) through an atmospheric pressure neon gas, solving simulataneously the TDSE (using the few-level model system) and the MWE. The TDSE solution includes both stimulated emission, absorption, time-dependent ionization (which populates the ionic states) and Auger decay. We find that for intensities above approximately 10^{18} W/cm^2, the X-ray pulse is strongly reshaped in both the temporal, spectral, and spatial

domain, as illustrated in Fig. 1(b,c). At this intensity, the stimulated Raman scattering (SRS) at 850 eV, originating in the neutral $1s^{-}13p$-$2p^{-}13p$ transition and strongly enhanced by the corresponding transition in the ion, rapidly grows with propagation distance. This multi-color, intense X-ray pulse in turn drives complex Rabi cycling which gives rise to the broad bandwidth between 850 and 867 eV visible in the final spectrum in Fig. 1(b). In the spatial domain, we observe both absorption-driven reshaping and refractive-index-driven self-focusing at high intensities, as shown in Fig. 1(c). These results raise interesting prospects for controlling the temporal and spatial properties of intense X-ray pulses.

(iii) Characterization of temporal structure of XUV FEL pulses: The seeded FEL facility FERMI in Milan, Italy generates high intensity, XUV attosecond pulse trains (APT) that have programmable, reproducible wave forms. In collaboration with the Sansone (U. Freiberg) and Mauritsson (Lund U.) experimental groups we have investigated the characterization of XUV APTs produced at FERMI. Because FERMI is seeded by the harmonic of an IR laser, the harmonics that make up the APT are spaced by three IR photons. This presents a challenge when characterizing the temporal structure of the XUV pulses, since the spectral phases of the XUV harmonics pulses must be measured via an interference of processes involving one and two IR photons absorbed or emitted in the continuum. An additional complication is that the delay between the XUV light and the IR dressing laser can be measured but not controlled. The solution, as outlined in [R5], is to plot the correlation between photoelectron sidebands and use the shape of the resulting ellipse to extract the phases. A longer paper outlining the theoretical methods has been submitted [4].

Future Plans

Several projects are in progress or planned for the near future:

(i) Propagation and reshaping of intense X-ray pulses We will continue our studies of temporal and spatial reshaping of intense XFEL pulses in atomic gases. Depending on the central photon energy of the beam time assigned to our experimental collaborators we will either continue with neon studies, or shift to a different atom.

(ii) XFEL characterization, continued work: Continuing our work with the Sansone group on the characterization of high intensity XUV pulses from FERMI, we will collaborate on a run scheduled for December 2020 to study the continuum phase of two IR photon emission/absorption near the ionization threshold of an atomic system. We know from previous work comparing exact TDSE results to strong field approximation simulations that these phases contribute non-trivial effects near threshold [4] and measuring this effect will be the focus of this work.

In a related but separate experiment, J. Mauritsson will lead an FERMI run devoted to studying two photon below threshold absorption (Rabi cycling) in helium. As part of this grant we are providing theoretical support on the design and interpretation of the experiment. The aim is to use the XUV harmonics produced by FERMI to measure the phase of the multiphoton absorption process. This involves measuring the phase of the XUV light just above threshold, and so dovetails nicely with the work on the Sansone experiment.

(iii) Condensed-phase ATA: We will continue studies of ATA in condensed phase materials. We are primarily interested in the development and application of a larger-scale theory framework based on the semiconductor Bloch equations.

Peer-Reviewed Publications Resulting from this Project (2018-2020)

R1 N. Harkema, J. E. Bækhøj, C.-T. Liao, M. B. Gaarde, K. J. Schafer, and A. Sandhu, *Controlling attosecond transient absorption with tunable, non-commensurate light fields*, Opt.Lett. **43**, 3357 (2018).

R2 A. P. Fidler, S. J. Camp, E. R. Warrick, E. Bloch, H. J. B. Marroux, D. M. Neumark, K. J. Schafer, M. B. Gaarde, and S. R. Leone, *Nonlinear XUV Signal Generation Probed by Attosecond Transient Grating Spectroscopy*, Nat. Comm. **10**, 1384 (2019).

R3 E. Simpson, M. Labeye, S. Camp, N. Ibrakovic, S. Bengtsson, A. Olofsson, K. J. Schafer, M. B. Gaarde, and J. Mauritsson, *Probing Stark-induced nonlinear phase variation with opto-optical modulation*, Phys. Rev. A **100**, 023403 (2019).

R4 R. Geneaux, C. J. Kaplan, L. Yue, A. D. Ross, J. E. Bækhøj, P. M. Kraus, H.-T. Chang, A. Guggenmos, M.-Y. Huang, M. Zürch, K. J. Schafer, D. M. Neumark, M. B. Gaarde, and S. R. Leone, *Attosecond time-domain measurement of core-excitonic decay in MgO*, Phys. Rev. Lett. **124**, 207401 (2020)

R5 P. Maroju *et al.*, *Attosecond Pulse-shaping using a seeded Free Electron Laser*, Nature **578**, 386 (2020)

References

[1] M. Wu, S. Chen, S. Camp, K. J. Schafer, and M. B. Gaarde. Theory of strong-field attosecond transient absorption. *J. Phys. B*, 49:062003, 2016.

[2] C.-T. Liao, A. Sandhu, S. Camp, K. J. Schafer, and M. B. Gaarde. Beyond the single-atom response in absorption line shapes: Probing a dense, laser-dressed helium gas with attosecond pulse trains. *Phys. Rev. Lett.*, 114:143002, 2014.

[3] K. Li, M. Labeye, P. Ho, M. B. Gaarde, and L. Young. Resonant propagation of x-rays from the linear to the nonlinear regime. *Phys. Rev. A*, 2020 (submitted).

[4] P. Maroju *et al.* Analysis of two-color photoelectron spectroscopy for attosecond metrology at seeded free-electron lasers. *New J. Phys.*, 2020 (submitted).

[5] J. Klei, R. Pazourek, C. Neidel, A. Rouzee, M. Galbraith, M. B. Gaarde, K. J. Schafer, M. J. J. Vrakking, and J. Mikosch. Analysis of sub-cycle XUV-NIR-induced excitation dynamics in helium by UV photoelectron spectroscopy. *Phys. Rev. A*, (2019, in preparation).

[6] G. D. Mahan. Emission spectra and phonon relaxation. *Phys. Rev. B*, 15:4587, 1977.

Coherent Probes of Molecular Charge Migration

Science Using Ultrafast Probes: DE-SC0012462

Kenneth Schafer[1,*], Mette Gaarde[1], Kenneth Lopata[2],
Louis DiMauro[3], Pierre Agostini[3], Robert Jones[4]
1) Department of Physics and Astronomy, Louisiana State University, Baton Rouge, LA
2) Department of Chemistry, Louisiana State University, Baton Rouge, LA
3) Department of Physics, The Ohio State University, Columbus, OH
4) Department of Physics, University of Virginia, Charlottesville, VA

[*]kschafe@lsu.edu

Project Scope

When forced out of equilibrium, electrons in matter can respond exceedingly fast, on time-scales approaching the attosecond. At this time scale, the dynamics are inherently quantum, and are not yet impacted by the weaker coupling to nuclear degrees of freedom. This response can expose correlations between electrons and holes that are otherwise hidden in the static properties of the system. These correlations, and the dynamics they evoke, can impact fundamental processes, such as charge transport and photoelectric energy conversion. From the perspective of furthering basic science or a desire to manipulate the outcome of a reaction, one needs to understand how attosecond electron-hole dynamics initiate, drive, or steer physical and chemical processes, which may occur on much longer time scales.

The ATTO-CM team is focused on developing and applying coherent probes to directly characterize correlation-driven ultrafast charge migration dynamics that are initiated by different means across molecular families. In this context, charge migration refers to the rapid movement (femtosecond or faster) of positively charged holes in a molecule following localized excitation or ionization. Understanding the mechanisms of this migration, and developing experimental tools for observing it, is crucial to advancing ultrafast science and potential applications across disciplines. The objective of the ATTO-CM team is to advance ultrafast science in the US, at small-, mid- and large-scale facilities, using a concerted effort of theorists and experimentalists. Enabled by an integrated relationship between theory and experiment, our emphasis is on the implementation of high-harmonic spectroscopy and frequency-matched ionization spectroscopy as coherent probes of charge migration dynamics in chemical systems. Our ultimate goal is to develop experimental probes that can provide direct access to specific time-resolved information in a manner that does not require sophisticated modeling for interpretation. For practical implementation, our focus has been to identify parameters to probe and control these dynamics, *e.g.*, molecular alignment and/or functionalization of the target. Charge migration studies are primarily laboratory based but experiments on large-scale facilities, like LCLS, are soon to begin, with the ATTO-CM team participating.

Recent Progress

In our effort to understand and observe charge migration (CM, hereafter) with strong laser fields we have focused our efforts on three main thrusts: “Attochemistry picture of charge migration”, “High-harmonic spectroscopy (HHS)”, and “Frequency-matched Ionization (FMI) spectroscopy”. As demonstrated in what follows, all three nodes of the ATTO-CM network are closely involved in each of the three thrusts defining our program. In brief, our key recent results are:

1. Thrust 1: Attochemistry picture of charge migration – We have focused our efforts on understanding

the chemical/physical properties that makes molecules able to support CM modes [Folorunso 2020, Mauger 2020]. In organic targets, we have identified simple heuristics for CM, including the importance of conjugation and functionalization of the carbon chain. This attochemical expertise will directly guide future HHS and FMI campaigns (Thrusts 2 and 3).

2. Thrust 2: High-harmonic spectroscopy (HHS) – We have published a review article highlighting our major experimental and theoretical achievements on HHS, and their connections to attochemistry (Thrust 1) and molecular alignment/orientation (Thrust 3) [Tuthill 2020]. On the experimental side, we have initiated attosecond spectroscopy through molecular XUV-induced photoionization and investigated the feasibility of two-color HHS phase metrology. On the theory side, we have started HHS simulations in targets that exhibit CM.
3. Thrust 3: Frequency-matched ionization (FMI) spectroscopy– We have combined experiments and theory to investigate CM modes in halogenated carbon rings. Preliminary results show substantial variations in the double:single strong field ionization (SFI) yield ratio in iodobenzene and iodotoluene with laser wavelength, possibly reflecting electron dynamics that are induced, or preferentially detected via double ionization, at specific oscillation periods of the strong field. We are also exploring SFI with asymmetric two-color fields to reveal the orientation-dependence of the SFI signal.

Thrust 1: Attochemistry picture of charge migration

Thrust 1 uses first-principles simulations to address open questions that are critical to the design and interpretation of future charge migration experiments. These include: Which molecules are expected to support CM? Does CM manifest in generic ways so that its periodicity and visibility can be predicted to follow simple rules? Does the way in which CM is initiated influence how it proceeds? Answers to these questions are crucial for ongoing efforts to observe CM using HHS and FMI (Thrusts 2 and 3 below). To this end, the LSU team has performed time-dependent density functional theory (TDDFT) simulations with the goal of predicting and interpreting CM in systematic ways. Two manuscripts summarizing our results are under review [Folorunso 2020, Mauger 2020], with the important findings summarized below.

Molecular Modes of Attosecond Charge Migration: We have focused on a family of organic halogen-functionalized linear molecules to determine the effect of length, bonding, and chemical functionalization on CM. Halohydrocarbons are an ideal framework for CM studies, since localized valence holes can be readily created in these systems via SFI [Sándor 2018, Sándor 2019] and they can be systematically modified in terms of bonding, length, and shape.

Our simulations involve three steps: emulation of a hole via ionization, time propagation, and extraction

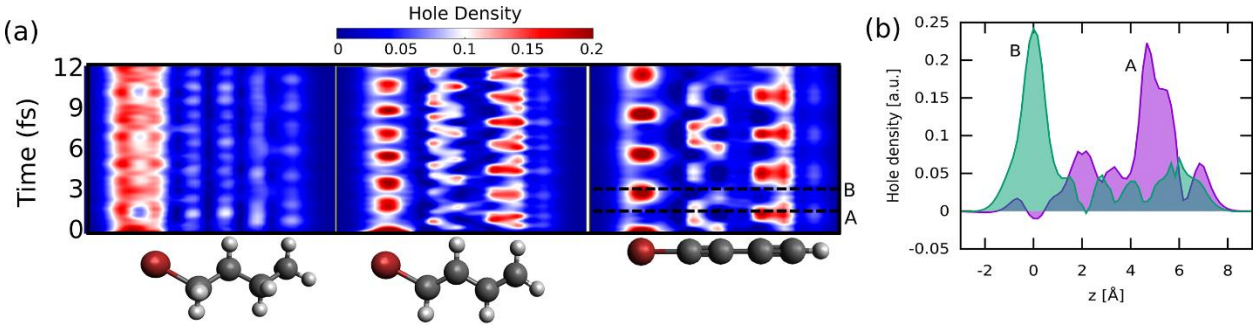

Figure 1: The role of chemical bonding in CM in the family of bromine-functionalized four-carbon chains. (a) Time-dependent hole densities along the chain show the alkane (single bond) does not support CM. In both the alkene (double bonds) and alkyne (triple bonds) cases, CM occurs via hopping, with the C≡C case slower than the C=C case. (b) Snapshots of the hole density along the molecular axis at the times when the hole is on the Br (green) and terminal triple bond (magenta).

of CM modes and metrics from the density. Here we use TDDFT with atom-centered basis sets and hybrid exchange-correlation functionals [Bruner 2017]. To prepare the initial state we use constrained Density Functional Theory (cDFT), which self-consistently computes the density of the system with the requirement of having a localized hole on the halogen. This emulates a rapid SFI process that leaves the system in a non-stationary state with a halogen-localized hole. This is a significant improvement over simply creating ad hoc hole(s) in the ground state Kohn-Sham valence orbital(s), which exhibit significant delocalization errors and gives qualitatively incorrect dynamics. In contrast, the cDFT procedure mixes multiple orbitals, resulting in a more multi-electron, multideterminant-like excitation. We then interpret the resulting dynamics in terms of the hole density, defined as the difference between the neutral ground-state and cation densities. For visualization and analyses we integrate the hole density over the directions transverse to the molecular axis (see Figure 1 (a)). From this we can quantify the CM time, distance, and the corresponding speed.

Our studies of the halohydrocarbon family reveal a set of simple heuristics for CM in these molecules:

- CM requires conjugation and occurs via "hopping" between π bonds: Saturated hydrocarbons do not support charge migration due to their lack of a delocalized π system. In contrast, bromobutadiene/yne exhibits clear CM from the halogen to the terminal double/triple bond. This motion occurs primarily by hopping between the halogen and the double/triple bonds in a molecule, as shown in Figure 1 (a).
- CM occurs at a uniform speed in linear molecules: Our results also show that the CM speed is roughly independent of the molecule's length. For bromopoly-ynes (conjugated triple bonds), holes move with a universal speed of 3.8 Å/fs or 2.6 bonds/fs. This is consistent with particle-like dynamics within a chain and like electron transport in polymers, where the conductivity is an intrinsic property related to the delocalization of the π system.
- Higher Z halogens result in more visible holes throughout the CM process: This is consistent with our previous observations that SFI results in a more localized hole on halomethane's halogen center as one goes down the periodic table [Sándor 2019]. Likewise, we have demonstrated that this gives a more localized hole during the subsequent CM process. This suggests that the "visibility" of CM to experimental probes will increase going from Cl to Br to I.

A manuscript summarizing these findings is under review [Folorunso 2020]. These heuristics form a set of guiding principles, both for identifying molecules to study and for developing the experimental means of measuring CM (Thrusts 2 and 3) going forward.

Nonlinear dynamics of charge migration: The message of the LSU TDDFT simulations is clear: we consistently observe sustained CM modes in halogenated carbon chains. But why does this happen in these systems, and how should we think about these CM modes more generally? To answer these questions, we have investigated the underlying dynamical mechanism(s) that regulate such modes by employing tools from nonlinear dynamics. To begin with, we developed reduced-dimension and simplified-interaction models, which showed interesting modes of CM (see the alternating current-like motion displayed in Figure 2). Through phase space analyses of these models, we find that CM can emerge as a result of the mean-field interaction alone. Our results highlight the central role of dynamical electron-

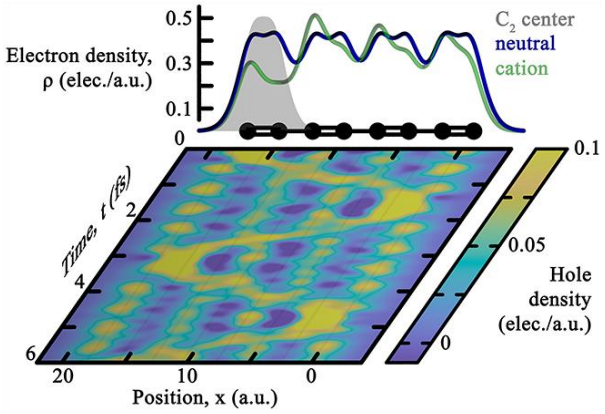

Figure 2: Illustration of an alternating current-like mode of CM in a simplified carbon-chain model. The foreground colormap shows the time-dependent, field-free, migration of the hole following the sudden removal of an electron at one end of the chain (see graphs at the top).

electron coupling and synchronization as the engine for CM dynamics in our carbon-chain models. This is an alternative to, *e.g.*, few-orbital beating mechanisms that have previously been employed [Remacle 2006, Calegari 2014, Ayuso 2017]. Notably we find that one molecule can support several current-like migration modes, depending on the degree of charge localization as well as the location of the hole, with periods varying by several hundred attoseconds. Finally, our analysis reveals the potential for using chemical functionalization to control CM in molecule, an avenue that we will further investigate in the future (see Future Plans). A manuscript summarizing our findings is under review [Mauger 2020].

Taken together, the molecular-mode and nonlinear-dynamics conclusions complement our attochemistry picture of CM and lead to a somewhat surprising corollary: CM should be properly thought of as involving a non-trivial superposition of numerous states rather than a beating between a select few. This principle becomes important as molecular sizes increases and the few state picture inevitably breaks down. Going forward, we will validate and refine this state-agnostic interpretation of charge migration (see Future Plans).

Thrust 2: High-harmonic spectroscopy (HHS)

Thrust 2 of the ATTO-CM network focusses on HHG as a spectroscopic tool for probing charge migration. We recently published a review article on the HHS thrust's work to date [Tuthill 2020]. This review served as a milestone for the collaboration as it highlighted the major experimental and theoretical accomplishments of this thrust while providing an overarching picture of how these new techniques and discoveries fit together. Looking forward, the review also discussed the necessity for a comprehensive approach to CM studies, *e.g.*, including an attochemistry understanding of how the electronic dynamics is regulated (Thrust 1) and matching the probe time-scale to that of the CM mode (Thrust 3).

HHS from TDDFT simulations: The LSU node simulates HHS in real molecules using grid-based TDDFT calculations, as implemented in the open-source code Octopus [Andrade 2015]. In several recent publications [Gorman 2019, Mauger 2019, Tuthill 2020] we have documented meaningful comparisons between ATTO-CM experimental results and theoretical calculations, based on seeding mid-IR HHG with an attosecond pulse train (APT) in order to select the short-trajectory contribution to the harmonic yield. We have recently succeeded in calculating the harmonic response from individual Kohn-Sham orbitals, which has allowed even closer comparison to experimental results.

Recently we have begun HHS calculations in molecules that are undergoing CM. Our first step was to reproduce CM calculations performed with the basis-set-code NWChem, using the grid-based Octopus (this is crucial for HHS calculations in order to incorporate the large excursions of the electron wave packet during the HHG process). While Octopus does not support the computation of cDFT initial conditions described in Thrust 1, we have been able to replicate its effect by matching NWChem-generated initial orbitals to Octopus calculations, and the comparison between the subsequent CM dynamics is excellent, as illustrated in Figure 3 for bromobutadiyne. We have now moved to the second step of calculating HHG from a bromobutadiyne molecule in which CM has been initiated. We are investigating both the effect of the IR+APT pulse on the CM itself, and the effect of the CM on the harmonic spectral amplitude and phase. Our preliminary results are encouraging – we are seeing clear synergies between the CM and the HHG dynamics.

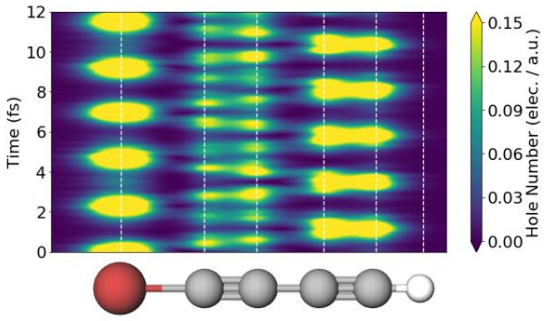

Figure 3: Evolution of the density in the ionized orbital along the carbon-chain axis, like in Figure 1 (a), but computed with the grid-based code Octopus. Compared to NWChem results, the difference in the CM period is due to a different treatment of exchange-correlation.

Attosecond Spectroscopy: Complementary to the OSU node's previous work on accessing CM using HHS, we have also pursued photoelectron analysis of molecules ionized by attosecond XUV radiation. The experiment uses a well-characterized HHG source for conducting RABBITT measurements on the molecule of interest. The RABBITT method allows access to both the amplitude and phase of photo-absorption dipole moment in the target molecule. Also, the target-gas density required is lower than that for HHG, eliminating an issue that has challenged our ability to conduct HHS measurements on the larger molecules that theory has identified as good CM candidates (see Thrust 1 above). In addition, single-photon ionization of molecules using XUV radiation also provides direct access to multiple molecular orbitals. Finally, the experience of using XUV photoionization as a spectroscopic probe will be very useful for future campaigns at the LCLS facility (see Future Plans).

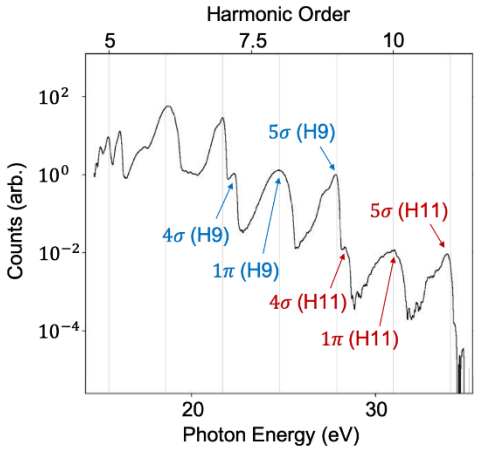

Figure 4: Ionization spectrum of CO induced by the radiation from a 400-nm driven HHG source. The wider harmonic spacing can resolve the contributions from multiple orbitals, here between HH 9 and 11.

The OSU node has chosen to pursue the use of a 400-nm driving field for increased harmonic spectral separation, and thus a higher resolution, as compared to an earlier study that used 800-nm light [Kamalov 2020]. Presently we have studied CO_2, CO, and CH_4 in the absence of an IR-dressing field, and are working towards cataloging common molecules with resolvable orbitals for an HHG comb produced with a 400-nm driving wavelength. A representative photoelectron spectrum of CO is shown in Figure 4. Next, we will reintroduce the dressing field to explore the applicability of RABBITT. In the future, we also plan to extend these results to variable driving-field-wavelengths between 600 and 700 nm using an OPA. This tunable wavelength would allow us to leverage the wavelength-scanning technique previously demonstrated in our HHS results [Gorman 2019] for finer energy resolution.

Two-color HHS phase metrology: Application of HHS using a two-color driving field combined with molecular orientation provides ionization-site selectivity in asymmetric linear molecules, a key requirement for inducing CM in many molecules. As illustrated in Figure 5 the resultant XUV-HHG spectrum has even and odd harmonics, which induces an interference between two-photon and direct-one-photon ionization pathways in the RABBITT scan, otherwise not present with odd-only harmonic spectra. This prevents straightforward phase reconstruction. Alternate methods such as FROG-CRAB [Mairesse 2005], PROOF [Chini 2010], or iPROOF [Laurent 2013] are needed.

In past work, the OSU node has used two-color driving fields to perform attosecond spectroscopy of Ar and He autoionizing resonances [Donsa 2020]. We attempted to use PROOF and iPROOF for phase retrieval, but both methods failed in our application due to a systematic energy-skewing error, caused by our magnetic-bottle electron-spectrometer transfer function. This detector-

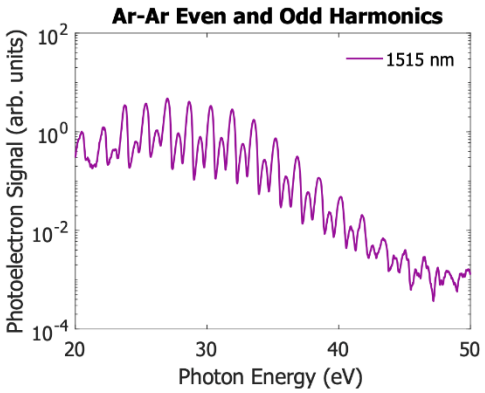

Figure 5: Photoelectron spectrum of Ar ionized with an attosecond pulse train with even and odd harmonics. The XUV light was generated in Ar by a 1515-nm driving field overlapped with its second harmonic (with ≈1% of the fundamental power).

dependent skewing has previously been discussed as a source of error in these algorithms, but has not been explored in depth. We have simulated this energy skewing and its impact on the results of the PROOF, iPROOF, and FROG-CRAB phase-retrieval methods, and plan to better benchmark the allowable detector tolerances for these algorithms. Additionally, with a more comprehensive understanding of these errors, we aim to craft either calibration or post-processing techniques to mitigate the influence of this energy skewing.

Thrust 3: Frequency-matched ionization (FMI) spectroscopy

Through Thrust 3, the ATTO-CM team seeks to determine if periodic electron/hole motion within a molecule, initiated by strong-field single-ionization or electronic excitation, can be detected by observing changes in the double or dissociative ionization yields as the period of the ionizing laser is tuned to match that of the oscillating charge. Accordingly, a major component of this thrust is obtaining a detailed understanding of strong-field single and multiple ionization in molecules. This work plays a central and unifying role across the network, since SFI is the first step in HHG and attosecond pulse generation, and the use of aligned/oriented molecules can play an essential role in inducing, controlling, and probing CM. Indeed, angle-resolved ionization measurements at UVA have verified the accuracy of TDDFT SFI calculations (Thrust 1) at LSU, enabling us to confidently predict aspects of the ionization process that are not directly accessible to experiments. This insight guides the network's development of methods to probe and induce CM. In addition, the alignment/orientation expertise developed at UVA has been valuable for the molecular-frame HHS measurements at OSU (Thrust 2). The optimal molecular species to be studied in ionization measurements at UVA have been informed by calculations of CM modes at LSU, and promising preliminary measurements on FMI using near-IR pulses at UVA will be followed with experiments in the mid-IR at OSU.

Probing CM in Carbon rings using FMI: Numerical simulations performed in Thrust 1 have predicted robust CM oscillations in carbon chains, starting from the assumption that localized holes have been established at defined locations within the molecules. A hypothesis being explored through Thrust 3 is that this coherent hole motion might be detected through a variation in the strong-field double ionization yield as a function of laser wavelength. Assuming the probabilities for strong-field single and double ionization are maximized at the peak field in the laser cycle, the motion of a localized electron hole, created at one field maximum, should influence the double ionization probability that is induced at an integer number of half-cycles later. In particular, one might expect a substantial change in the double (or dissociative) ionization yield if the laser period (or half-period) matches that of the single-ionization induced CM within the molecule.

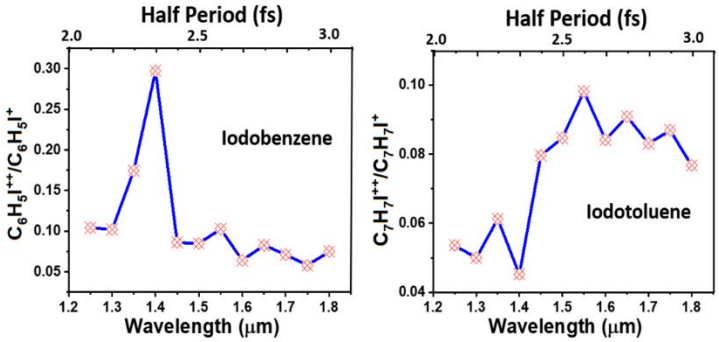

Figure 6: Measured double:single SFI yield ratios vs laser wavelength for iodobenzene (left) and iodotoluene (right) at constant laser energy and approximately constant intensity ~10^{14} W/cm^2. The laser half-period is shown on the upper axis.

Recently, we have measured the wavelength dependence of the double:single SFI yield ratio in functionalized carbon rings, iodobenzene and iodotoluene. Based on TDDFT calculations, we expect that removal of an electron via SFI will create a hole that is preferentially located on the constituent iodine atom, followed by CM with a period of approximately 2.2 fs. Experimentally, we observe significant changes in the double:single parent ion yield when the laser half-period is near this value. However, the responses are quite different for the two molecules. A shown in Figure 6, the ratio in iodobenzene exhibits a pronounced maximum

for laser wavelengths near 1.4 microns, while the iodotoluene ratio shows a step-like increase there. Although very preliminary, these results are intriguing and potentially reflect unexpected differences in the hole creation or subsequent dynamics in the two molecules. We are working to understand the source of these differences and, more generally, determine if FMI is a viable approach for measuring localized CM modes.

SFI of oriented molecules: We have also advanced our focus from alignment-dependent strong-field processes, in which the relative angle between a molecular axis and a laboratory-fixed axis is well-defined, to orientation-dependent phenomena, where the direction of the molecular dipole is known, and controllable. This is significant, as oriented molecular targets open the possibility of using directional fields to drive electrons, bound or continuum, in specific directions within or about the molecule for inducing and probing particular CM modes. Indeed, calculations by the LSU node have made explicit predictions regarding the dependence of SFI on the relative orientation of a molecular dipole and the direction of the applied electric field at the instant of ionization [Sándor 2018, Sándor 2019]. Those predictions have important implications for the ensuing CM dynamics.

Producing a sample of well-oriented molecules in a field-free environment is considerably more difficult than creating a highly-aligned ensemble. Using purely optical techniques based on the application of two-color (ω+2ω) fields, two distinct mechanisms (hyper-Raman excitation and angle-dependent SFI [Znakovskaya 2014]) can coherently redistribute rotational population in molecules, creating wave packets that exhibit preferential orientation at specific times. As with alignment, for symmetric top molecules, the prompt preferential orientation induced by the laser "revives" near integer or (with application of additional control fields) half-integer multiples of the fundamental rotational period T=π/B, where B is the molecular rotational constant. However, unlike the alignment case, the higher-order non-linear processes that enable molecular orientation require substantially higher laser intensities to be effective. As a result, a high degree of orientation is typically accompanied by substantial ionization. Ionization by the orientation pulse makes it much more challenging to accurately extract the angle-dependence of the ionization yield produced by a time-delayed probe when it interacts with the oriented sample near a rotational revival.

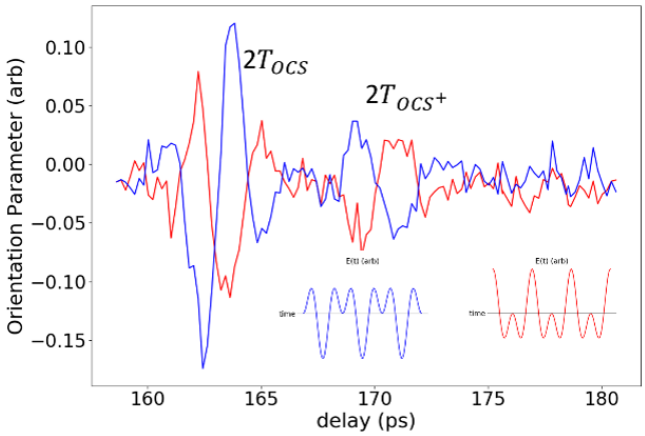

Figure 7: Orientation of OCS as a function of delay after a bichromatic (800nm+400nm) field pulse. The orientation parameter is the normalized difference of S^{3+} ions emitted toward and away from a microchannel plate detector following Coulomb explosion induced by an intense 800-nm pulse. The red and blue curves are near mirror images, showing the degree of orientation near rotational revival times of the neutral ground state and the X-state of the ion, and are produced by bichromatic pulses with opposite peak field directions (see insets). The near single-cycle oscillations in the orientation parameter centered on the two revival times are due to rotational wave packet dynamics in the neutral and ionic species, respectively. The latter reflecting the SFI rate anisotropy in the two-color field.

When a molecule is ionized by an intense, two-color field, the angle-dependent ionization probability is directly reflected in the angular distribution of the resulting ions and the remaining neutrals. The projection from the initial to the final angular distributions creates distinct rotational wave packets in the ions and neutrals. So, if one can separately observe the evolution of the rotational wave packets in the neutral and the ion, through a channel other than single ionization, it should be possible to

cleanly recover the angle-dependent single-ionization probability without directly measuring the single ionization yield.

Figure 7 shows a convenient orientation metric, the normalized difference of S^{3+} fragments (ejected toward and away from an MCP detector), following directional Coulomb explosion of OCS molecules in an intense, 800-nm 35-fs probe, approximately 170 ps after the molecules are exposed to a less intense two-color (800-nm+400-nm) pulse. Substantial variations in this orientation parameter are seen at two distinct delays. These delays correspond to the second integer revival of the ground-state of neutral OCS and the X-state of OCS^+, respectively. In principle, once any residual effects of coherent rotational redistribution via hyper-Raman transitions have been eliminated, the delay-dependence of the orientation parameter during the revivals will reflect the coherent superposition of the neutral and ionic rotational states in the respective wave packets. We intend to exploit this to determine the angle-dependence of the SFI process which created the ions.

Ionization computations with weak-field asymptotic theory: Previously when using basis-set-based TDDFTs, the overlap between field-free ground-state molecular orbitals and the complex absorbing potential used to simulate ionization has limited our ability to reliably compute experimentally-relevant ionization yields at low laser intensities [Sándor 2018]. To overcome this limitation, the LSU node has been working on implementing weak-field asymptotic theory (WFAT) for DFT orbitals. WFAT is an adiabatic method for the calculation of approximate angle-dependent tunnel ionization yields of a molecule under a static electric field. Since it is a time-independent method, it can give inexpensive estimates of angle-dependent ionization rates. While previous studies using WFAT employed Hatree-Fock (HF) orbitals, we have used DFT orbitals in the WFAT-calculated angle-dependent ionization yield, since our aim is to build a WFAT module in the DFT-based NWChem package. This will allow us to use range-separated hybrid functionals, which have been shown to give significantly improved angle-resolved ionization rates. Figure 8 shows our preliminary results, comparing the ionization profiles of benzene (C_6H_6), calculated using WFAT, where the doubly degenerate HOMO orbitals are obtained using both HF and DFT with the B3LYP functional. The comparison is excellent.

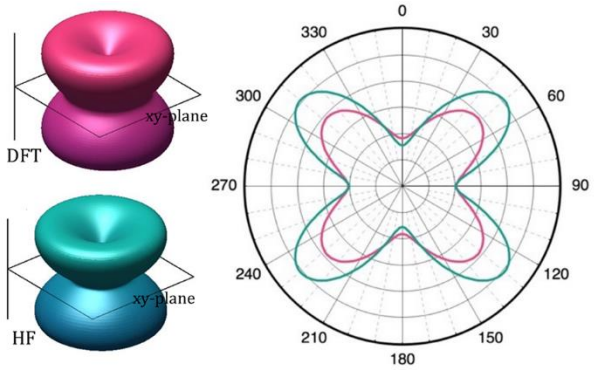

Figure 8: Angle-resolved ionization of C_6H_6 calculated using WFAT. The degenerate HOMO orbitals were obtained using HF and DFT with the B3LYP functional. In the 3D ionization profile (left panels), which is the sum between HOMO and HOMO-1 yields, the molecule lies in the xy-plane and the radial distance on the 3D surfaces gives the total yield when the static field points in that direction. The right panel compares the DFT and HF results in the xz plane.

Cross-training and interactions between the network partners

We have maintained continuous communication between all the nodes of the network, including:

- Frequent zoom meetings between all partners, together with frequent, internode email, phone, *etc.* communications between smaller working groups that target specific tasks.
- An intranet website (with content access restricted to members of the ATTO-CM network), featuring results of common interest, all meeting notes, and many relevant papers. The network also has a cloud storage facility to share, archive and back up data.

These active exchanges maintain a strong collaborative community among the PIs, students and postdocs.

ATTO-CM workshop: The second annual ATTO-CM workshop was held at UVA on February 27-28, 2020. The workshop included oral presentations from all nodes (PIs, students and postdocs) of the network. It also featured contributions from three invited external speakers: Françoise Remacle (Université de Liège), Mauro Nisoli (Politecnico di Milano), and Berny Schlegel, (Wayne State University). Prof Nisoli attended virtually as the COVID-19 pandemic reached Italy one week prior to the meeting. These external speakers were selected for their expertise in theory/experiments related to ultrafast phenomena in AMO in general, and in CM, in particular. For new personnel (one postdoc at each node), the workshop was also a unique opportunity to get a thorough view of the ATTO-CM collaboration and its shared goals. The workshop concluded with a PI meeting during which the long-term directions for the network were reaffirmed and the projects for the next 12-to-18 months were refined. The workshop was very successful (a sentiment that was shared by both collaboration members and external visitors) and it will be held again next year, at OSU.

Future Plans

The continued interactions between the three nodes of the ATTO-CM network is a cornerstone of our collaboration. We fully intend to continue our current interactions, *i.e.*, with regular communication (zoom, emails, shared website, *etc.*) and resume exchange visits between the nodes when it is safe to do so. In what follows, we briefly explain the main avenues we intend to pursue to advance our chances of observing CM with strong laser fields.

Charge-migration compatible molecules

An Attochemistry Picture of Charge Migration: A main focus of the attochemistry thrust is to identify and study molecules for future experiments. Building on recent insights into the effect of molecule length and bonding on CM, we foresee halogen-functionalized organic molecules as the most promising path forward for experimental and theoretical CM campaigns. In the short term, ideal targets should support CM, be non-reactive, be readily purchased/synthesized, and be easily aligned/oriented. Based on the heuristics of CM (described in Thrust 1), linear and ring-shaped halogen-functionalized conjugated molecules are an ideal starting point: Holes can be readily created by SFI, and these holes are predicted to move from the halogens across the chain π-backbone. Going forward, we will expand our studies to more complex systems such as those with donor/acceptor functionalization, where a hole is created on one end of the molecule (*e.g.*, a halogen) and drawn to another end with high hole affinity (*e.g.*, an amino group).

Role of initial condition on charge migration: Our nonlinear dynamical analysis of functional carbon chains (described in Thrust 1) has highlighted the importance of the initial conditions for the subsequent CM motion. Our current method is to specify a localized hole in space that is reminiscent of the hole created by SFI. Although quite successful, our cDFT method can indiscriminately ionize from a wide range of orbitals in the molecule, which necessitates post-processing to extract the CM modes. To address this, we will develop a form of restricted cDFT where only a particular sub-set of the orbitals can ionize. In conjunction with SFI simulations (Thrust 3), this will result in a more physical initial state. Where possible we plan to combine these improvements with our nonlinear analysis of the CM dynamics. Finally, as a first step towards incorporating dephasing effects into the simulations, we will estimate the robustness of a charge migration mode by computing the dynamics for a range of geometries perturbed along selected vibrational modes.

Probing charge migration through high-harmonic spectroscopy

HHS simulation in systems with charge migration: The LSU node will continue HHS investigations on molecules undergoing CM, aiming to identify characteristic features in the harmonic response. This will involve experimenting with the initial conditions for the calculations, as well as the laser wavelength, intensity, and polarization. Alongside these, we will perform companion HHS investigations in the simplified carbon-chain models used for the nonlinear dynamical analysis, which exhibit qualitatively similar CM modes (see

Thrust 1). These simulations are far less computationally demanding than the full-dimensional OCTOPUS one, therefore allowing for a greater flexibility in parameter investigation, but they lack some essential features of their full-dimensional counterparts.

Scattering calculations using Kohn-Sham orbitals: We have initiated a study of whether time-dependent scattering calculations can be used to calculate the recombination dipole moment for the ground state orbital calculated by Octopus. Such calculations could potentially provide a simpler, and computationally less costly, route to qualitatively screen for target-specific amplitude and phase features and guide theoretical and experimental HHS investigations.

HHS of larger molecules: Results from Thrust 1 above have shown that charge migration in larger molecules manifest longer migration times when compared to smaller molecules, *i.e.*, diatomic, triatomics, presently adaptable to our HHS experimental campaigns. Using larger, more complex targets, *e.g.*, benzene [Despre 2015], in experiments brings the technical challenge of working with low vapor pressure liquids at room temperature, while gas-phase HHS requires a high density of molecules to produce a measurable amount of harmonic photons. Thus, we are examining methods to deliver these larger molecules as vapors in the OSU lab at the needed pressures using heat baths and pipes, which were previously demonstrated in the Imperial group [Marangos 2016]. These new delivery methods will also allow us to investigate solvents and solutes that will be studied through the liquid-HHG apparatus (see next) in their vapor form, and use these as references similarly to what was done previously in [Scarborough 2018, Gorman 2019].

HHS in the liquid phase: The OSU node also plans to study larger molecules with HHS performed directly in the condensed phase. We are currently working to construct an experimental apparatus for observing HHG from thin liquid sheets. This apparatus is enabled by newly developed microfluidic nozzles by the DePonte group at SLAC that allow the formation of sub-micron thick flowing liquid sheets [Koralek 2018]. Even with thicker liquid sheets (>100 micron), the DiMauro group has demonstrated that HHG is produced from both water and heavy water when driven by mid-infrared pulses at ~3.5 μm [DiChiara 2009]. This establishes the potential feasibility of HHS on larger molecules in solution.

We expect the liquid-HHS apparatus to be completed by the end of 2020. First experiments will focus on studying the solvent HHG response. Some recent work was performed on HHG from water and simple alcohols [Luu 2018], but characterization is far from complete. To achieve HHS, the solute-molecule HHG contribution must be separated from that of the solvent. This will be the focus of the second round of experiments. Assuming that the solute HHG scales like it would in the gas phase, we expect a considerable portion of the XUV spectrum to only contain HHG contributions from the solute since, so far, common solvents have been shown to have low HHG cutoffs akin to that seen in solids.

Probing charge migration through frequency-matched-ionization spectroscopy

Frequency-Matched Ionization Spectroscopy: The UVA and LSU node will continue their concerted investigations of FMI in organic molecules. This will involve performing measurements and companion CM-mode simulations in the same carbon-ring targets (see Thrust 3 above). While a direct simulation of strong-field induced double ionization (or fragmentation) is not feasible in our TDDFT simulations [Sándor 2018], we expect that our CM metrics, as well as single-ionization computations from molecular cations with CM dynamics (see also next subsection), can yield relevant results when compared to measurements. For oriented target investigations, the LSU node will also perform hyperpolarizability calculations, which are required to accurately separate different contributions to the molecular orientation (see Thrust 3 above), as well as two-color SFI simulations on oriented molecules. Ultimately, by combining our attosecond and SFI simulation methodologies, we will simulate two-color ionization during a CM process, which will allow us to relate observed ionization modulations to the underlying electron dynamics. The most promising molecules/results will be further investigated using mid-IR experimental capabilities at the OSU node.

It is worth noting that our orientation measurements have also revealed revival features associated with excited states of the ion produced by the two-color field. This suggests that, more generally, revival-resolved wave packet spectroscopies could distinguish and characterize angle-dependent ionization from(to) ground and excited states, in the neutral (ion), without the need for electron-ion coincidence detection. Moreover, one might similarly measure angle-dependent double-ionization or dissociative ionization probabilities starting from different initial neutral and ionic levels. Even if the differences in the rotational constants from different states are small, the small differences in revival times can be amplified, simply by moving to later integer revivals. We are excited to explore numerous opportunities afforded by this new approach.

FMI in systems with charge migration: On the theory side, after integrating our WFAT module into NWChem (see Thrust 3 above), we will use it to investigate FMI in molecules that undergo CM. For long-wavelength lasers, we expect a quasi-static ionization process, which justify the use of WFAT. Practically, we will investigate the evolution of ionization signals when varying multiple parameters such as molecular orientation and geometry, laser wavelength and pulse duration, or the relative phase between the CM dynamics and the driving field. In doing so, we will look both at the instantaneous ionization rate, *e.g.*, to identify correlations between a localization of the hole on specific parts of the molecule and ionization bursts, as well as the total ionization yield, integrated over the duration of the pulse, as is measured in experiments.

Attosecond pump-probe spectroscopy at the LCLS: Attosecond science is now a possibility at the LCLS free electron laser, due to the development of XLEAP [Duris 2020], which generates pairs of isolated attosecond soft x-ray pulses, with microjoule-scale energy and controllable delay. This has opened the possibility of studying charge migration using attosecond pump-probe measurements. With its integrated theory-experiments expertise, the ATTO-CM network has become a resource for CM-related studies. In that context, and leveraging the knowledge accumulated across all nodes and thrusts of the collaboration, in Run 18 during the spring of 2021 the DiMauro lab will lead the experimental participation, and Lopata group will lead the theoretical participation, in a larger collaboration that aims to measure charge migration in the aminophenol molecule. Specifically, the charge migration will be initiated by inner valence ionization with a 250 eV attosecond pulse. A hole should then oscillate between the hydroxyl and amino group sides of the ring. A 500 eV attosecond probe pulse will initiate Auger decay. The experiment aims to see whether an oscillation in the Auger-decay signal, due to CM, will be seen as a function of pump-probe delay.

References

[Andrade 2015] X. Andrade *et al.*, “Real-space grids and the Octopus code as tools for the development of new simulation approaches for electronic systems,” Phys. Chem. Chem. Phys. 17, 31371 (2015).

[Ayuso 2017] D. Ayuso *et al.*, “Ultrafast charge dynamics in glycine induced by attosecond pulses,” Phys. Chem. Chem. Phys. 19, 19767 (2017).

[Bruner 2017] A. Bruner *et al.*, “Attosecond Charge Migration with TDDFT: Accurate Dynamics from a Well-Defined Initial State,” J. Phys. Chem. Lett. 8, 3991 (2017).

[Calegari 2014] F. Calegari *et al.*, “Ultrafast electron dynamics in phenylalanine initiated by attosecond pulses,” Science 346, 336 (2014).

[Chini 2010] M. Chini *et al.*, “Characterizing ultra-broadband attosecond lasers,” Opt. Express 18, 13006 (2010).

[Despre 2015] V. Despre *et. al.*, “Attosecond hole migration in benzene molecules surviving nuclear motion,” J. Phys. Chem. Lett. 6, 426 (2015).

[DiChiara 2009] A.D. DiChiara *et al.*, “An investigation of harmonic generation in liquid media with a mid-infrared laser”, Opt. Exp. 17, 200959 (2009).

[Donsa 2020] S. Donsa *et al.*, “Asymmetry in pump-probe photoemission," in preparation (2020).

[Duris 2020] J. Duris *et al.*, “Tunable isolated attosecond X-ray pulses with gigawatt peak power from a free-electron laser”, Nature Photonics 14, 30 (2020).

[Folorunso 2020] A.S. Folorunso *et al.*, "Molecular Modes of Attosecond Charge Migration," under review (2020).

[Kamalov 2020] A. Kamalov *et al.*, "Electron correlation effects in attosecond photoionization of CO_2," Phys. Rev. A. 102, 023118 (2020).

[Koralek 2018] J.D. Koralek *et al.*, "Generation and characterization of ultrathin free-flowing liquid sheets," Nature Comm. 9, 1353 (2018).

[Laurent 2013] G. Laurent *et al.*, "Attosecond pulse characterization," Opt. Express 21, 16914 (2013).

[Luu 2018] T.T. Luu *et al.*, "Extreme-ultraviolet high-harmonic generation in liquids", Nature Comm. 9, 3723 (2018).

[Mairesse 2005] Y. Mairesse *et al.*, "Frequency-resolved optical gating for complete reconstruction of attosecond bursts," Phys. Rev. A 71 011401 (2005).

[Marangos 2016] J.P. Marangos, "Development of high harmonic generation spectroscopy of organic molecules and biomolecules," J. Phys. B. 49, 132001 (2016).

[Mauger 2020] F. Mauger *et al.*, "Nonlinear dynamics of attosecond charge migration in model carbon chains," under review (2020).

[Remacle 2006] F. Remacle *et al.*, "An electronic time scale in chemistry," Proc. Natl. Acad. Sci. USA 103, 6793 (2006).

[Znakovskaya 2014] I. Znakovskaya *et al.*, "Transition between Mechanisms of Laser-Induced Field-Free Molecular Orientation," Phys. Rev. Lett. 112, 113005 (2014).

Peer-Reviewed Publications Resulting from this Project (2018-2020)

[Tuthill 2020] D.R. Tuthill, F. Mauger, T.D. Scarborough, R.R. Jones, M.B. Gaarde, K. Lopata, K.J. Schafer, and L.F. DiMauro, "Multidimensional molecular high-harmonic spectroscopy: a road map for charge migration studies," J. Mol. Spec. 372, 111353 (2020).

[Gorman 2019] T.T. Gorman, T.D. Scarborough, P.M. Abanador, F. Mauger, D. Kiesewetter, P. Sándor, S. Khatri, K. Lopata, K.J. Schafer, P. Agostini, M.B. Gaarde, and L.F. DiMauro, "Probing the interplay between geometric and electronic-structure features via high-harmonic spectroscopy," J. Chem. Phys. 150, 184308 (2019).

[Mauger 2019] F. Mauger, P.M. Abanador, T.D. Scarborough, T.T. Gorman, P. Agostini, L.F. DiMauro, K. Lopata, K.J. Schafer, and M.B. Gaarde, "High-harmonic spectroscopy of transient two-center interference calculated with time-dependent density-functional theory," Struct. Dyn. 6, 044101 (2019).

[Sándor 2019] P. Sándor, A. Sissay, F. Mauger, M.W. Gordon, T.T. Gorman, T.D. Scarborough, M.B. Gaarde, K. Lopata, K.J. Schafer, and R.R. Jones, "Angle-dependent strong-field ionization of halomethanes," J. Chem. Phys. 151, 194308 (2019).

[Abanador 2018] P.M. Abanador, F. Mauger, K. Lopata, M.B. Gaarde, and K.J. Schafer, "Wavelength and intensity dependence of recollision-enhanced multielectron effects in high-harmonic generation," Phys. Rev. A 97, 043414 (2018).

[Kiesewetter 2018] D. Kiesewetter, R.R. Jones, A. Camper, S.B. Schoun, P. Agostini, and L.F. DiMauro, "Probing Electronic Binding Potentials with Attosecond Photoelectron Wavepackets," Nat. Phys. 14, 68 (2018).

[Mauger 2018] F. Mauger, P.M. Abanador, A. Bruner, A. Sissay, M.B. Gaarde, K. Lopata, and K.J. Schafer, "Signature of charge migration in modulation of double ionization," Phys. Rev. A 97, 043407 (2018).

[Sándor 2018] P. Sándor, A. Sissay, F. Mauger, P.M. Abanador, T.T. Gorman, T.D. Scarborough, M.B. Gaarde, K. Lopata, K.J. Schafer and R.R. Jones, "Angle-dependence of Strong-Field Single- and Double-Ionization of Carbonyl Sulfide," Phys. Rev. A 98, 043425 (2018).

[Scarborough 2018] T.D. Scarborough, T.T. Gorman, F. Mauger, P. Sándor, S. Khatri, M.B. Gaarde, K.J. Schafer, P. Agostini, and L.F. DiMauro, "Full Characterization of a Molecular Cooper Minimum Using High-Harmonic Spectroscopy," Appl. Sc. 8, 1129 (2018).

Femtosecond and Attosecond Strong-Fields Processes in Two-Dimensional Finite-Systems: Graphene and Graphene-Like Nanopatches and Polycyclic Molecules

DOE Grant No. DE-FG02-01ER15213

Mark Stockman (PI) and Vadym Apalkov (co-PI)

Department of Physics and Astronomy, Georgia State University, Atlanta, GA 30303

E-mail: vapalkov@gsu.edu

1. Program Scope

The program is aimed at theoretical investigation of a wide range of phenomena induced by ultrafast laser-light excitation of nanostructured or nanosize systems. The program is concentrated on finite nanopatches of two-dimensional materials and large polycyclic molecules. The program is specifically focused on theory of ultrafast processes in strong optical fields in finite systems: nanopatches of two-dimensional materials of hexagonal symmetry and hexagonal polycyclic molecules.

2. Recent Progress and Publications

The recent progress covers the period of 2018-2020 and is illustrated by publications [1-12].

2.1 Topological resonance in Weyl semimetals in circularly-polarized optical pulse [9]

We have shown theoretically that ultrafast electron dynamics in three-dimensional Weyl semimetals, placed in the field of circularly polarized ultrashort optical pulse, is governed by topological resonance, which occurs because of competition between the dynamic phase and the topological phase. When these two phases cancel each other the system exhibits the topological resonance, which results in large residual, i.e., after the pulse, conduction band population. For a Weyl semimetal that consists of two Weyl points at $(\pm k_0, 0,0)$ of reciprocal space, for the pulse propagating along, for example, z direction, the topological resonance results in predominant conduction band population of the region near one of the Weyl points, say W, for $k_z < 0$ and the region near the other Weyl point, W', for $k_z > 0$. Exactly at $k_z = 0$ the conduction band at both Weyl points is equally populated. The reason for such behavior is that for each cross-section $k_z = const$, the Weyl semimetal behaves as a 2D gapped graphene system with the gap that is proportional to k_z. Since the strength of the topological resonance in gapped graphene system increases with the magnitude of the band gap and manifests itself in predominant population of one of the valleys, then similar features of topological resonance is visible in 3D Weyl semimetals. Thus, the dynamics of Weyl semimetals in circularly polarized pulse can be used to study the properties of topological resonance, i.e., its dependence on the band gap, the energy dispersion and profile and intensity of the optical pulse.

2.2 Ultrafast nonlinear absorption in graphene [10]

We have studied theoretically the nonlinear absorption of an ultrafast optical pulse by gapped graphene monolayer. At low field amplitudes, the absorbance in pristine graphene is equal to the universal value of 2.3 %. Although, the ultrafast optical absorption for low field amplitudes is independent on polarization, linear or circular, of the applied optical pulse, for high field amplitudes, the absorption strongly depends on the type of the pulse polarization.

The ultrafast absorption of optical pulses in gapped graphene is determined by specific properties of ultrafast electron dynamics, both intraband and interband, in the field of the pulse. Such dynamics strongly depends on polarization of the optical pulse, whether it is linear or circular.

The fundamental difference between these two types of polarization is that for a single oscillation pulse the electron trajectory in the reciprocal space passes twice though the region with large interband coupling for linear polarization and only once for circular polarization of the pulse. As a result, the interference pattern with the dark and bright fringes is clearly visible in the conduction band population distribution for a linearly polarized pulse, but no such interference is observed at small field amplitudes for a circularly polarized pulse. As a result the absorption of linearly and circularly polarized pulses is quite different. Such difference is well pronounced for relatively large field amplitudes, $> 0.1\ V/A$. Namely, while for a linearly polarized pulse the absorbance as a function of the pulse amplitude is saturated at 1.4 %, for a circularly polarized pulse the absorbance does not show any saturation. The absorbance of a circularly polarized pulse can reach the value of as much as 4 %.

For small field amplitudes, the absorbance for both types of polarization behaves similarly. This is because for such small field amplitudes the size of electron displacement in the reciprocal space is less than or comparable to the size of the region with large interband coupling. In this case, during the whole trajectory, both for linearly and circularly polarized pulses, there is a strong (or weak) interband coupling. Thus no interference pattern can be formed and no difference between the linear and circular polarizations can be observed.

2.3 Anomalous Ultrafast All-Optical Hall Effect in Gapped Graphene [11]

We have proposed an ultrafast all-optical anomalous Hall effect in two-dimensional semiconductors of hexagonal symmetry such as gapped graphene, transition metal dichalcogenides, and hexagonal boron nitride. A gigantic ultrafast all-optical anomalous Hall effect occurs when two strong single-oscillation optical pulses are applied to the gapped graphene or similar hexagonal-symmetry semiconductor materials. These materials possess a broken inversion symmetry and a finite direct bandgap. The two pulses, which generate the anomalous ultrafast Hall effect, are a sequence of a single-cycle chiral pulse followed by a single-cycle linearly-polarized pulse. The chiral pulse breaks down the *T*-reversal symmetry inducing a strong valley polarization, which effectively plays the role of an effective magnetic field. The induction of the strong valley polarization by a fundamentally fastest single oscillation chiral pulse is due to the recently predicted phenomenon of topological resonance. This is a wide-bandwidth, ultrafast effect, which is due to the mutual cancellation of the topological and dynamic phases. The topological resonance is independent of spin of electron and depends on a purely orbital dynamics of electrons in the gapped hexagonal-symmetry monolayers.

The subsequent application of a strong single-oscillation probe pulse that is linearly-polarized along the armchair edge (*y* axis) to such a system, which acquired chirality (a large valley polarization), produces a Hall current in the zigzag direction (*x* axis) transverse to the polarization of the probe pulse.

The fundamental distinction and advantage of this proposed all-optical anomalous Hall effect in 2D hexagonal semiconductors is that it is the fundamentally fastest anomalous effect possible in nature: it takes just a single optical period to induce the strong valley polarization and just one other optical period to read it out. Such a read out can fundamentally be done either by recording the charge transferred after the probe pulse or by observing a THz radiation emitted by the Hall current that is polarized in the *x* direction.

The predicted ultrafast anomalous all-optical Hall effect has a potential to have applications in ultrafast memory and information processing, both classical and quantum.

3. Future Plans

We will develop the comprehensive theory of ultrafast electron dynamic, induced by ultrashort optical pulses, in nanoscale topological systems (quantum dots and quantum molecules). The examples of such systems are nanopatches of graphene-like materials and transition metal dichalcogenides (TMDCs). The developed theory will cover ultrafast valley and spin polarization of the system, generation of electric and spin currents and high harmonic generation. We will also study induced ultrafast light absorption by the systems and manifestation of topology in ultrafast electron dynamics.

4. Peer-Reviewed Publications Resulting from this Project (2018-2020)

[1] S. Azar Oliaei Motlagh, J.-S. Wu, V. Apalkov, and M.I. Stockman, "*Fundamentally fastest optical processes at the surface of a topological insulator*", Phys. Rev. B **98**, 125410 (2018).

[2] H.P. Paudel, V. Apalkov, X. Sun, and M.I. Stockman, "*Plasmon-induced hot carrier transfer to the surface of three-dimensional topological insulators*", Phys. Rev. B **98**, 075428 (2018).

[3] S. Azar Oliaei Motlagh, J-S. Wu, V. Apalkov, and M.I. Stockman, "*Femtosecond valley polarization and topological resonances in transition metal dichalcogenides*", Phys. Rev. B **98**, 081406(R) (2018).

[4] F. Nematollahi, V. Apalkov, and M.I. Stockman, "*Phosphorene in ultrafast laser field*", Phys. Rev. B **97**, 035407 (2018)

[5] S. Azar Oliaei Motlagh, F. Nematollahi, A. Mitra, A.J. Zafar, V. Apalkov, M.I. Stockman, "*Ultrafast optical currents in gapped graphene*", Journal of Physics: Condensed Matter **32** (6), 065305 (2019).

[6] S. Azar Oliaei Motlagh, F. Nematollahi, V. Apalkov, M.I. Stockman, "*Topological resonance and single-optical-cycle valley polarization in gapped graphene*", Physical Review B **100** (11), 115431 (2019).

[7] S. Azar Oliaei Motlagh, V. Apalkov, M.I. Stockman, "*Laser pulse waveform control of Dirac fermions in graphene*", Quantum Nanophotonic Materials, Devices, and Systems, **11091** (2019).

[8] F. Nematollahi, S. A. Oliaei Motlagh, V Apalkov, M.I. Stockman, "*Weyl semimetals in ultrafast laser fields*", Physical Review B **99** (24), 245409 (2019).

[9] F. Nematollahi, Azar Oliaei Motlagh, J.S. Wu, R Ghimire, V. Apalkov, M.I. Stockman, "*Topological resonance in Weyl semimetals in a circularly polarized optical pulse*", Physical Review B **102** (12), 125413 (2020)

[10] Azar Oliaei Motlagh, A.J. Zafar, A. Mitra, V. Apalkov, M.I. Stockman, "*Ultrafast strong-field absorption in gapped graphene*", Physical Review B **101** (16), 165433 (2020).

Submitted Manuscripts

[11] Azar Oliaei Motlagh, V. Apalkov, M.I. Stockman, "Anomalous Ultrafast All-Optical Hall Effect in Gapped Graphene", arXiv: **2007.12757** [cond-mat.mes-hall], 1-8 (2020) (submitted to Physical Review Research).

[12] P. Kumar, T.M. Herath, V. Apalkov, M.I. Stockman, "*Bilayer graphene in strong ultrafast laser fields*", arXiv: **2004.09732** [cond-mat.mes-hall], 1-11 (2020) (submitted to Physical Review B)

Complete spectroscopy in the attosecond regime

Carlos A. Trallero
Department of Physics, University of Connecticut, Storrs, CT 06268
carlos.trallero@uconn.edu

Project Scope

The main scope of my research is to perform coherent measurements of the time dependent molecular structure with femto and attosecond time resolution. Such complete measurements involve time-resolved phase and amplitude maps of the quantum state of molecules and atoms.

Recent progress

Electronic flow control with $w - 3w$ synthesies pulses timed through ionization

We measured harmonics generated with synthesized $\omega - 3\omega$ pulses centered at 800 and 266 nm respectively in unison with in-situ ionization yields. Theoretically it has been proposed that this frequency combination will provide much higher XUV yields and cutoffs compared to single frequencies. However, such predicted results depend on very stringent relative phase control over the synthesized pulse. Because ionization rate in atoms, for a fixed pulse duration, depends only on peak intensity, ionization yields recorded as function of delay between ω and 3ω provides an absolute field phase calibration. We then use this well characterized phase point to determine the influence of electron trajectories on the harmonic yields.

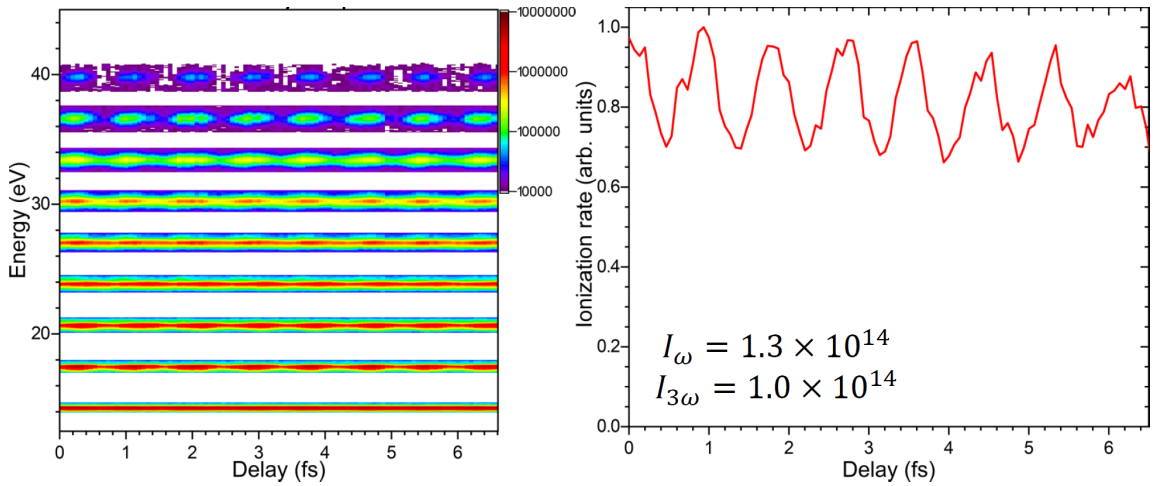

Figure 1: Left: Harmonic yields as a function of delay between the ω and 3ω fields. Right: Ionization yield recorded in parallel with the harmonic signal. The intensities used for both fields are shown as an inset in the right panel. Oscillations in both harmonics and ion signals are observed.

To generate the $\omega - 3\omega$ laser fields, we developed a very stable two-color interferometer. For our two-color measurements to be successful, we need to have a stability between the two arms that is "much" less than the period of the shortest wavelength driving field, which is 0.9 fs for the 266-nm field. To achieve this stability, we vibrationally isolated the interferometer from

the optics table. We measure the stability by propagating a frequency doubled continuous wave ND:YAG laser through the interferometer and image the spatial interference at the exit. Finally, we extract the phase of the image using Fourier analysis. This method yields a timing jitter between the arms that has a root-mean-square error (RMSE) of 50 as over 170 seconds, which is significantly smaller than the period of the 266-nm laser pulse.

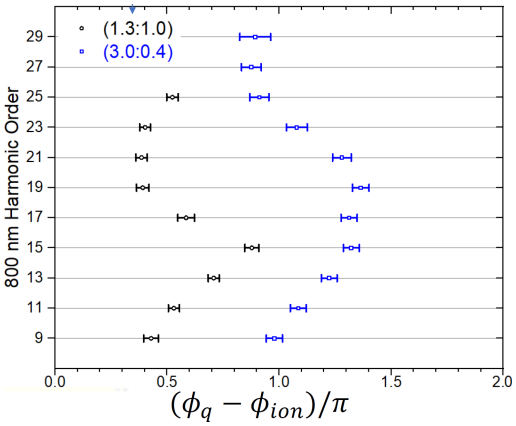

Figure 2: Phase difference between the maximum harmonic and ionization yield for all measured harmonics. The experiments were repeated at two different intensity ratios between the 800 and 266 nm fields.

Yields of the harmonics as a function of delay between the two fields is shown in the left panel of Fig. 1. As expected, we observed oscillations in the harmonic yield with a period of 3ω, visible for all harmonics except for the ones below threshold. In unison with the harmonic yield we also measure ionization through a chaneltron placed at the interaction region where harmonics are generated. Experimental measurements are shown in the left panel of Fig. 1. This is one the key measurements of our experiment because, ionization is maximum when the synthesized electric field has the highest strength. Thus, the peaks in the ionization produce an absolute time stamp for ionization and a relative time for the generation of the harmonics. Since both yields oscillate with the same period, we use a $\cos(3\omega + \phi)$ where ϕ is the phase of the oscillation.

The difference in phases relative to the ionization yield gives us a direct measurement of the timing of the harmonics generation relative to the optimum ionization time, or peak field maximum. A plot of the phase dependence for each harmonic is shown in Fig. 2 for two different intensity ratios between the 800 nm and the 266 nm. Using this phase map and completely classical electron trajectories we can establish how electron flow control maximizes the yield for each harmonic and what trajectory it follows.

Phase matching conditions for the generation of high harmonics with Bessel beams

Bessel-like beams present a lot of potential for strong field science. We have generated high harmonics using Bessel beams giving us great insight on phase matching conditions. In these experiments harmonics are generated within a thin jet and the focus position is scanned relative to the jet. As in the previous experiments we also measure the ionization in parallel with the harmonics. Our Bessel beams are generated with a combination of lens and axicon. For non-perfect, real-life axicons, the center part of the near-field mode profile has oscillations, with the highest peak intensity reached just before the donut mode is realized. However, in our experiments the ionization and harmonic yields are maximum near the tip of the axicon (away from the donut mode). We have now established that this occurs due to volume averaging. For the harmonics, there is a higher number of emitters, even though the maximum peak intensity is lower at the point in space. These conclusions are also corroborated by numerical simulations of the beam profile.

New lab

Most of the academic 2019-2020 year was spent dealing with a move to our new lab space and re-installing the new laser and experimental apparatuses. The main laser consists of a commercial Continuum USA Ti:Sapphire system that was recently upgraded to deliver up to 20 mJ of energy, 16 fs pulses at 1 kHz repetition rate. The 16 fs pulses out of the amplifier are reached with the combination of a Mazzler-Dazzler pulse shapers. The laser can feed an asymmetric dual high energy optical parametric amplifier (OPA). The OPA has two arms fed by a common white-light seed and has two arms one being more energetic than the other. Currently we have measured a combined 5 mJ of energy per pulse. Of particular relevance for this grant is the generation of carrier-envelope-phase stable idlers that are also phase locked respect to each other. We have measured phase-locking stability over a day with RMS noise of 120 mrads.

Future work

We will continue our development of transient absorption spectroscopy methods with Bessel beams applied to the study of aligned molecules an inner shell dynamics. Currently we are working on several excitation schemes, some of which involve field-free alignment of molecular targets. For this, we have already purchased and tested an Even-Lavie valve. Thanks to the high power of our laser we can have several schemes in which multiple pulses can be used for alignment/excitation.

New laser system

In the Spring of 2021, we will install a new laser source that will open many new possibilities. This laser system was made possible through a DURIP, an ONR and AFOSR grants. The laser produces 300 W or average power and will have several modes of operation with continuously tunable repetition rates from 25 kHz to 200 kHz and possible pulse duration as short as 4fs. We have tested 300 W long term stability at 25 and 200 kHz.

Peer-Reviewed Publications Resulting from this Project (Project start date August 16th 2018)

- Generation and control of phase-locked Bessel beams with a persistent noninterfering region, Z. Rodnova, Tobias Saule, Richard Sadlon, Edward McManus, Nicholas May, Xiaoming Yu, Sina Shahbazmohamadi, and Carlos A. Trallero-Herrero, Journal of the Optical Society of America B, https://doi.org/10.1364/JOSAB.400801

Page is intentionally blank.

Structural Molecular Dynamics Using Ultrafast Gas X-Ray Scattering

Peter M. Weber
Department of Chemistry
Brown University, Providence, Rhode Island 02912
Peter_Weber@brown.edu

I. Project Scope

Understanding the structures and chemical dynamics of molecules in their excited states is of great importance for basic energy science and myriad applications within and outside of chemistry and related molecular sciences. This project develops two experimental tools and applies them to explore both the *nuclear dynamics*, i.e. the geometrical arrangement of atomic nuclei in molecules, and *electron dynamics*, i.e. the time evolution of electron probability density distributions during chemical reactions. The experimental approach focuses on ultrafast time resolved gas phase X-ray scattering, which is pursued at the LCLS light source at SLAC National Accelerator Laboratory. The X-ray scattering experiments are prepared and complemented by time-resolved Rydberg fingerprint spectroscopy experiments, which are conducted at Brown University. Both methods are sensitive to the structures of molecules in excited states with a time resolution of <100 fs. Because the experimental methods are complementary, their coordinated application to the same systems provides deeper insights into the molecular dynamics than each technique would give in isolation.

The experiments explore molecular phenomena associated with the nuclear and electron structural dynamics of molecules during reactions. This includes the motions through conical intersections, charge delocalization, the fracture of chemical bonds, vibrational motions and the propagation and spreading of wave packets. Model systems for those investigations include medium-sized organic systems such as cyclohexadiene, trimethyl amine, N-methylmorpholine, N,N-dimethylpiperazine, and 1,2-dithiane. Those systems are deliberately chosen to broaden the investigations beyond standard prototypes. By focusing on structurally well-defined molecules, the project advances our knowledge of molecules in excited electronic states and their chemical reaction dynamics. This aids numerous applications and provides benchmark data that support the continued development of computational methods.

II. Recent Progress

Successful beam times at LCLS, in particular LR83 in March 2018, has led to several important advances as reported previously:

- We have measured complete, time-dependent excited state structures of polyatomic molecules. These are largely experimental structures, with only the electronic correction terms derived from theory.[8]
- We learned how to determine the spatial orientation of transition dipole moments within the molecular frame from the anisotropy of the transition dipole moment.[2]
- We developed codes to calculate the total scattering signal from molecules in excited states.[3]
- We observed ultrafast molecular dynamics in trimethyl amine, N-methylmorpholine and 1,3-cyclohexadiene. [4]

The general principle of these experiments is shown in figure 1: the molecules are excited by an optical laser pulse to an excited state, a process that initiates the reaction. The time-evolving molecular structures are probed by scattering an X-ray pulse that arrives a short time after the excitation pulse. The scattering pattern is measured on the detector, and its analysis leads to the structure as a function of time. By sequencing the time-dependent molecular structures we obtain a 'molecular movie' showing the motions of atoms while reactions proceed.

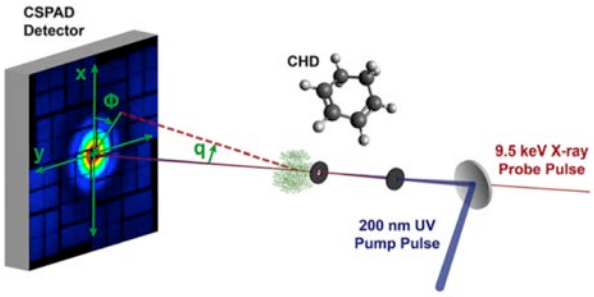

Figure 1: Experimental scheme: The molecules in the interaction region are intercepted by a linearly polarized UV laser (blue) and, at some time delay, by the X-ray pulse (red). Absorption of the UV pump pulse launches the structural molecular response. The X-ray probe is variably delayed with respect to the UV pump pulse to image the time-dependent dynamics. Scattering signals are captured by the detector.

X-ray scattering is sensitive to the electron density distributions. Since the core electrons are tightly, and nearly spherically, distributed about the atomic nuclei (except for hydrogen atoms), the X-ray scattering pattern yields the atomic positions. The valence electrons also contribute to the scattering signal, but their spatial distributions depend on the chemical bonding. We have now succeeded in observing both the nuclear and the electronic structure parts.

The Deep-UV Photo-Induced Dynamics of 1,3-Cyclohexadiene (CHD)

The CHD molecule is a favorite prototype molecule for the observation of chemical reaction dynamics because the reaction proceeds ballistically through a series of potential energy surfaces. In most experiments, exposure to 266 nm radiation leads to the excitation of the 1B state. The time-evolving wave packet encounters the conical intersection with the 1A state from underneath, which propels the wavepacket in an off-symmetry direction.

With 200 nm excitation, a molecular Rydberg state is initially excited. The wavepacket transitions to the repulsive surface, but since the coupling of a Rydberg state with a valence state is much smaller, the wavepacket is not pushed out of the plane of symmetry. Instead, travel on the repulsive surface tends to focus it into the symmetry plane. We discovered that in contradiction to standard Woodward-Hoffmann rules, this mechanism leads dominantly to a transition back to the potential energy well of the reactant CHD molecule.[9]

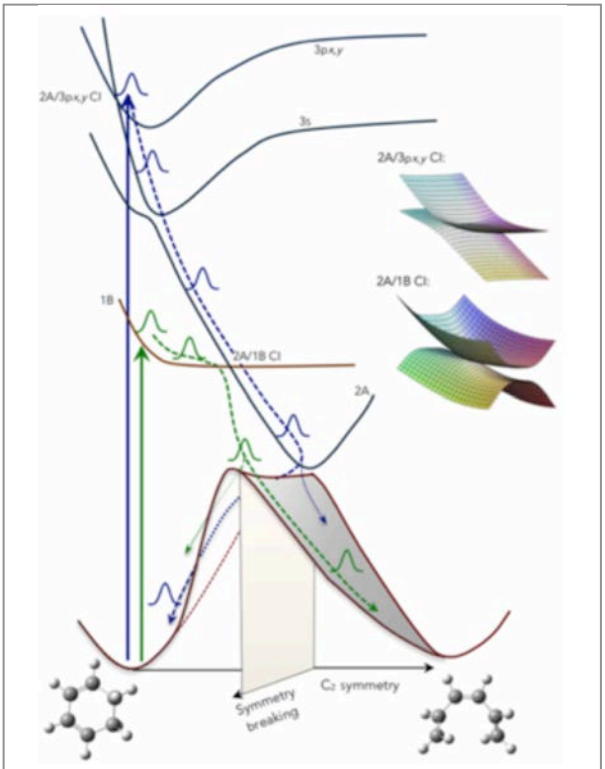

Figure 2: The potential energy surfaces of CHD allow for reversion to the ground state of the reactant molecule, favored when the wavepacket is close to the plane of symmetry, or ring opening to the HT product molecule, favored when the wavepacket is off symmetry. We found that 200 nm excitation predominantly leads to the former.

The experiment revealed how excitation to different states, and the topology of the potential energy surfaces, controls the outcome of the chemical reaction. Future experiments are planned to study the reaction dynamics at multiple wavelengths.

Electron Density Distributions from X-Ray Scattering

When a molecule interacts with light, its electrons can absorb energy from the electromagnetic field by rapidly rearranging their positions. This constitutes the first step of photochemical and photophysical processes that include primary events in human vision and photosynthesis. Since X-ray scattering signals directly relate to the distribution of electrons around nuclei and in chemical bonds, electronic excitation is expected to alter a molecule's scattering pattern. The effect is subtle, since one-photon excitation primarily changes the spatial distribution of one electron while leaving the others largely untouched. Nevertheless, it is an effect that must be considered in evaluating scattering signals from molecules in excited states.

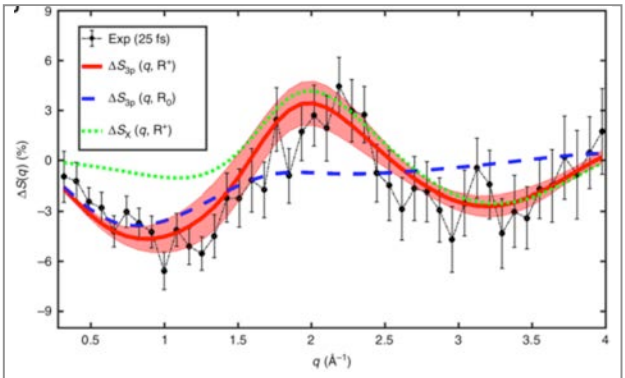

Figure 3: Fractional difference signals, ΔS(q), shown in percent, for optical excitation of CHD at 200 nm. The experimental signal at 25 fs delay time is shown in black with 1σ error bars. The corresponding theoretical $\Delta S_{3p}(q,R^+)$ signal for the electronic 3p state is shown in red with the shaded region accounting for the sampling of geometries in the excited state. For comparison, theoretical signals for the ground electronic state (X) at the 3p geometry, dotted green line $\Delta S_X(q,R^+)$, and for the excited 3p state at equilibrium geometry, dashed blue line $\Delta S_{3p}(q,R_0)$, are included. Both the electronic and the nuclear terms are needed to accurately simulate excited state scattering signals.

Excitation of 1,3-cyclohexadiene at 200 nm leads to a Rydberg state with an appreciable lifetime.[9] Optical excitation removes an electron from the highest occupied molecular orbital and places it into a 3p Rydberg state. We measured the X-ray scattering pattern at the 25 fs time delay, Figure 3, and found that to explain the observed signal, both the nuclear and the electron terms must be included. The nuclear and electronic effects are treated as additive terms

$$\Delta S_{\mathrm{exc}}(q,\mathbf{R}') = \Delta S_{\mathrm{exc}}^{\mathrm{elec}}(q,\mathbf{R}') + \Delta S^{\mathrm{nucl}}(q,\mathbf{R}'),$$

where the first term is the electronic contribution, $\Delta S_{\mathrm{exc}}^{\mathrm{elec}}(q,\mathbf{R}')$, defined by the difference in scattering from the excited and ground electronic states at a single molecular geometry $\mathbf{R}'$. The nuclear contribution, $\Delta S^{\mathrm{nucl}}(q,\mathbf{R}')$, on the other hand, represents the contribution to the scattering as if the molecular geometry was deformed $\mathbf{R}_0 \rightarrow \mathbf{R}'$ on the ground electronic state. On a formal level, this decomposition of $\Delta S_{\mathrm{exc}}(q,\mathbf{R}')$ does not involve any approximation regarding the scattering process itself.[10]

Thus, ultrafast non-resonant x-ray scattering is capable of resolving changes in electron density due to transitions between electronic states. The experiment probes the rearrangement of electrons when gas-phase CHD molecules are optically excited from the ground electronic state to a low-lying Rydberg state. Given the upcoming improvements in XFEL repetition rate, time-resolution, and mean photon energy, and the ongoing development of robust methods for data analysis that may come to include sophisticated tools from modern charge density analysis, ultrafast X-ray scattering may become a powerful and versatile tool for chemical research.

III. Future Plans

We are continuing to analyze data sets obtained at LCLS in March 2018. We have unraveled the complex kinetics of dithiane upon optical excitation, and we have observed the ultrafast structural signature of charge delocalization in dimethyl piperazine. Manuscripts about that work are being prepared.

Several beam times are on the docket, albeit with as of yet uncertain timing. We anticipate using the shorter optical pulses we are implementing at the CXI endstation, which will enable us to better resolve the reaction dynamics. Our goal is to image the molecules as they transition through conical intersections. Future beam times also will use tunable, short-pulsed UV excitation. We are also working with our collaborators (Centurion, Rudenko, Rolles, Lopata) on MeV electron and other experiments.

Finally, we continue to develop codes to calculate X-ray and electron scattering patterns. We are developing codes to calculate time-dependent scattering patterns off molecular ions, which can be related to both the ongoing X-ray and the MeV electron experiments.

IV. Peer-Reviewed Publications resulting from this Project (2018-2020)

1. “Putting the Disulfide Bridge at Risk - How UVC Radiation Leads to Ultrafast Rupture of the S-S bond” M. A.B. Larsen et al., *ChemPhysChem* **2018** *19*, DOI: 10.1002/cphc.201800610.
2. “Determining Orientations of Optical Transition Dipole Moments using Ultrafast X-Ray Scattering,” Haiwang Yong et al., *J. Phys. Chem. Lett.* **2018**, 9, 22, 6556-6562, DOI: 10.1021/acs.jpclett.8b02773
3. “Ab initio calculation of total scattering from molecules”, Andrés Moreno Carrascosa et al., *Journal of Chemical Theory and Computation*, 15, 5, 2836-2846, **2019**, DOI: 10.1021/acs.jctc.9b00056
4. “Simplicity beneath Complexity: Counting Molecular Electrons Reveals Transients and Kinetics of Photodissociation Reactions”, Jennifer M. Ruddock et al., *Angewandte Chemie International Edition*, **2019**, 58, 6371 –6375, DOI: 10.1002/anie.201902228
5. “The photochemical ring-opening of 1,3-cyclohexadiene imaged by ultrafast electron diffraction” T. J. A. Wolf et al., *Nature Chemistry*, **11**, 504–509 (**2019**), DOI: 10.1038/s41557-019-0252-7
6. “Femtosecond Molecular Movie Reveals Vibrational Coherence and Dephasing” Brian Stankus et al., *Nature Chemistry*, 11, 716–721 (**2019**). DOI: 10.1038/s41557-019-0291-0.
7. “Roadmap on photonic, electronic and atomic collision physics I. Light-matter interaction,” Kiyoshi Ueda et al., *J. Phys. B: At. Mol. Opt. Phys*. 52, 171001 (**2019**). DOI: 10.1088/1361-6455/ab26d7
8. “Scattering off Molecules far from Equilibrium,” Haiwang Yong et al., *J. Chem. Phys*., 151, 084301 (**2019**). DOI: 10.1063/1.5111979.
9. “A Deep UV Trigger for Ground-State Ring-Opening Dynamics of 1,3-Cyclohexadiene,” Jennifer M. Ruddock et al., *Science Advances*, 5, eaax6625 (**2019**). DOI: 10.1126/sciadv.aax6625
10. “Observation of the molecular response to light upon photoexcitation” Haiwang Yong et al., *Nature Communications*, 11, 2157 (**2020**). DOI 10.1038/s41467-020-15680-4.
11. “Ultrafast X-ray and Electron Scattering of Free Molecules: a Comparative Evaluation” Lingyu Ma et al, Structural Dynamics, **7**, 034102 (**2020**); PMCID: PMC7316516; https://doi.org/10.1063/4.0000010.

Combining High Level *Ab Initio* Calculations with Laser Control of Molecular Dynamics

Thomas Weinacht
Department of Physics and Astronomy
Stony Brook University
Stony Brook, NY
thomas.weinacht@stonybrook.edu

and

Spiridoula Matsika
Department of Chemistry
Temple University
Philadelphia, PA
smatsika@temple.edu

1 Project Scope

We use intense, shaped, ultrafast laser pulses to follow and control molecular dynamics and high level *ab initio* calculations to interpret the dynamics and guide the control.

2 Recent Progress

Our scientific focus over the past year has been on coupled electron-nuclear dynamics and correlated electron dynamics in small organic molecules. In the past year we have made significant progress along the following fronts:

2.1 Excited State Dynamics in Conjugated Systems

One of the questions that we set out to address in the previous grant period was how the structure of conjugated systems affects their excited state dynamics. In order to expand our understanding of photoisomerization with two double bonds, we studied cis,cis-1,3-cyclooctadiene (COD), a molecule similar to cyclohexadiene (CHD) and butadiene, for which there have been a number of studies, but larger and more flexible. We made used both trajectory surface hopping (TSH) calculations and UV-pump VUV-probe time resolved photoelectron spectroscopy (TRPES).

The TSH calculations reveal that COD has a very short excited state lifetime, with decay to the ground state occurring through conical intersections (CIs). Several CIs were located accessible with small or no barriers. Fig. 1 shows these barrierless pathways to three important CIs. The CIs help us understand the main nuclear motions involved in non-adiabatic transitions to the ground state. Fig. 1 shows the main distortions responsible for the dynamics, which involve twisting along only one double bond or both of them. For the case of twisting along both double bonds, the dynamics show that the main distortions involve twisting of one double bond at a time (local) followed by pyramidalization of a carbon belonging to that double bond (similar to ethylene). Only about 16% of transitions occur through a non-local or delocalized twisting of both double bonds (third pathway in Fig. 1). Several products formed on the ground state have also been observed, including cis,trans COD and 3-methylenecycloheptene (3-MCH, a seven membered ring with one of the carbon atoms pushed out of the original eight membered ring).

Our calculations and analysis indicate that the internal conversion dynamics for photo-excited COD are highly non-local, with trajectories exploring many different geometries at which non-adiabatic coupling drives hopping between electronic states. The results of this work provide insight about both the effect of conjugation on dynamics as well as the effect of additional low frequency degrees of freedom. The same chromophoric unit (two conjugated double bonds in this case) does not always result in the same excited state dynamics, i.e. CHD and COD behave differently while COD and butadiene are much more similar. In addition, the low frequency degrees of freedom can also have an important effect on the dynamics by providing flexibility to the system. These observations can be useful as we try to expand our understanding of excited state dynamics and find relationships between structure and dynamics.

TRPES measurements of COD are shown in Fig. 2. A 4.75 eV deep UV pump pulse launched a vibrational wavepacket on the first electronically excited state, and the ensuing dynamics were

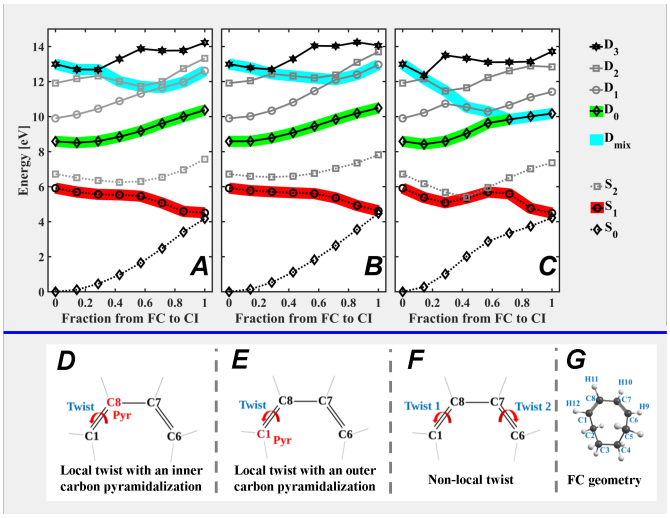

Figure 1: Electronic state energies from Franck Condon (FC) to CIs. Top three panels: Neutral (dashed lines) and cationic (solid lines) electronic states from the FC region to different CIs. **A**: local CI with inner carbon pyramidalization. **B**: local CI with outer carbon pyramidalization. **C**: non-local CI (both double bonds twisted). Four important states, S_0, S_1, D_0, D_3, are shown in black, while the other states are plotted in gray. Three thick colored lines highlight the states involved in the dynamics: S_1 (red), D_0 (green) and D_{mix} (cyan). Panels **D, E**, and **F** indicate the related structural changes corresponding to panels **A**, **B**, and **C**, respectively. A cartoon depiction of the molecule in the Franck-Condon geometry is shown in panel **G**.

probed *via* ionization using a 7.92 eV probe pulse. The experimental results indicate the wavepacket undergoes rapid internal conversion to the ground state in under 100 fs.

The qualitative features of the photoelectron spectrum compared to the calculations reveal interesting features of the electronic structure. The photoelectron spectrum shown in Fig. 2 can be decomposed into two different peaks that behave differently with time. The higher energy peak shifts systematically towards lower energy as a function of pump-probe delay times, while the lower energy peak does not shift significantly with pump-probe delay. These features are explained by calculating the ionic states which are ionized and the Dyson norms which predict the ionization probabilities along the different pathways for relaxation. These calculations predict that ionization from the S_1 state will lead to two different ionic states, D_0 and D_3. The higher energy ionic state, D_3, is almost parallel to S_1 as a function of the deactivation coordinate (see Fig. 1) and this leads to the low energy potential energy surface feature that does not change much with pump probe delay. D_0 on the other hand increases in separation from S_1 along the deactivation coordinate, and this leads to the high energy peak which moves to lower energies as a function of pump probe delay. So, the calculations are able to explain qualitatively the features of the TRPES.

2.2 Uracil Excited State Dynamics

We studied the excited state dynamics of uracil, which is a nucleobase found in RNA. Although theory and experiment have shed a significant light in understanding the photoexcited dynamics of uracil, there are still disagreements in the literature about specific details. In order to examine how the dynamics are influenced by the underlying electronic structure theory, we have performed non-adiabatic excited state dynamics simulations of uracil using on-the-fly trajectory surface hopping methodology on potential energy surfaces calculated at different electronic structure theory levels (CASSCF, MRCIS, XMS-CASPT2, TD-DFT). These simulations reveal that the dynamics are very sensitive to the underlying electronic structure theory, with the multi-reference theory levels that include dynamic correlation predicting that there is no trapping on the absorbing S_2 state, in

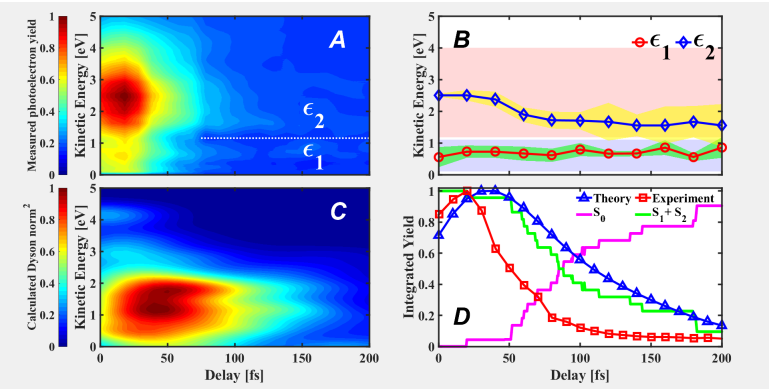

Figure 2: TRPES of cc-COD with UV-pump and VUV probe. Panels **A** and **C** show the measured and calculated TRPES respectively. The low and high KE peak regions of panel **A** are labeled as ϵ_1 and ϵ_2. Panel **B** shows the peak locations as a function of pump probe delay. Panel **D** shows the state populations, the calculated ionization yield, and the experimental ionization yield (energy integrated TRPES measurement).

contrast with predictions from lower level electronic structure results. The dynamics are instead governed by ultrafast decay to the ground state or trapping on the dark S_1 state.

2.3 Strong Field Molecular Double Ionization

Our earlier work on double ionization of a series of organic molecules suggested that conjugation played an important role in enhancing the double ionization yield. Subsequent coincidence measurements showed a difference in the electron correlation for dissociative non-dissociative double ionization, but many of the details were obscured by state and angle averaging of the double ionization yield. In order to address this issue, we are currently working on the double ionization of D_2O and Formaldehyde, for which the measurement of three body dissociation and comparison with trajectory calculations on the dication, allow us interpret angle and state resolved yields.

3 Future Plans

We have several goals for the immediate future:

1. Combine the trajectory surface hopping calculations, TRPES measurements and UED measurements for COD to form a complete picture of the excited state dynamics.

2. Carry out structure and dynamics calculations for the double ionization of Formaldehyde. Combine with measurements to arrive at a molecular frame, state resolved picture of the strong field double ionization.

3. Revisit the excited state dynamics of uracil with our new calculations and TRPES measurements.

4 Peer-Reviewed Publications Resulting from this Project (2018-2020)

- "Quadruple coincidence measurement of electron correlation in strong-field molecular double ionization", Arthur Zhao, Chuan Cheng, Spiridoula Matsika and Thomas Weinacht, *Phys. Rev. A*, **97**,043412, (2018)

- "Real-Time Adjustable, 11 Microsecond FWHM, > 5 KHz Piezo Electric Actuated Pulsed Atomic Beam Source", Anthony Catanese, Spencer Horton, Yusong Liu and Thomas Weinacht, *Review of Scientific Instruments*, in press (2018)

- "Strong and Weak-Field Ionization in Pump-Probe Spectroscopy", Spencer L. Horton, Yusong Liu, Pratip Chakraborty, Philipp Marquetand, Tamas Rozgonyi, Spiridoula Matsika, and Thomas Weinacht, *Phys. Rev. A*, **98**, 053416, (2018)

- "Electron correlation in channel resolved strong field molecular double ionization", Chuan Cheng, Patricia Vindel Zandbergen, Spiridoula Matsika, and Thomas Weinacht, *Phys. Rev. A*, **100**, 053405 (2019)

- Excited State Dynamics of cis,cis-1,3-Cyclooctadiene: UV Pump VUV Probe Time Resolved Photoelectron Spectroscopy Yusong Liu, Pratip Chakraborty, Spiridoula Matsika and Thomas Weinacht *J. Chem. Phys.*, **153**, 074301, (2020)

- "The Generality of the GUGA MRCI Approach in COLUMBUS for Treating Complex Quantum Chemistry", Hans Lischka, Ron Shepard, Thomas Müller, Péter G. Szalay, Russel M. Pitzer, Adelia J. A. Aquino, Mayzza M. Arajo do Nascimento, Mario Barbatti, Lachlan T. Belcher, Itamar Borges Jr., Scott R. Brozell, Anita Das, Silmar A. do Monte, Leticia Gonzalez, William L. Hase, Gary Kedziora, Fabris Kossoski, Francisco B. C. Machado, Spiridoula Matsika, Dana Nachtigallova, Reed Nieman, Markus Oppel, Felix Plasser, Rene F. K. Spada, Eric A. Stahlberg, Elizete Ventura, David R. Yarkony *J. Chem. Phys.*, **152**, 134110, (2020)

- "Excited State Dynamics of cis,cis-1,3-Cyclooctadiene: UV pump VUV Probe Time Resolved Photoelectron Spectroscopy" Yusong Liu, Pratip Chakraborty, Spiridoula Matsika and Thomas Weinacht. *J. Chem. Phys.*, **153**, 074301 (2020)

- "Excited State Dynamics of cis,cis-1,3-Cyclooctadiene: Non-adiabatic Trajectory Surface Hopping" Pratip Chakraborty, Yusong Liu, Thomas Weinacht, Spiridoula Matsika. *J. Chem. Phys.*, 152, 174302 (2020)

- "Spectroscopic and structural probing of excited state molecular dynamics with time-resolved photoelectron spectroscopy and ultrafast electron diffraction" Yusong Liu, Spencer Horton, Jie Yang, J. Pedro F. Nunes, Xiaozhe Shen, Thomas J. A. Wolf, Ruaridh Forbes, Chuan Cheng, Bryan Moore, Martin Centurion, Kareem Hegazy, Renkai Li, Ming-Fu Lin, Albert Stolow, Paul Hockett, Tamás Rozgonyi, Philipp Marquetand, Xijie Wang, and Thomas Weinacht *Phys. Rev. X*, **10**, 021016, (2020)

- "Simultaneous Observation of Nuclear and Electronic Dynamics by Ultrafast Electron Diffraction", Jie Yang, Xiaolei Zhu, J. Pedro F. Nunes, Jimmy K. Yu, Robert M. Parrish, Thomas J. A. Wolf, Martin Centurion, Markus Guhr, Renkai Li, Yusong Liu, Bryan Moore, Mario Niebuhr, Suji Park, Xiaozhe Shen, Stephen Weathersby, Thomas Weinacht, Todd J. Martinez, Xijie Wang *Science*, 368, 886, (2020)

- "Angle-dependent strong-field ionization and fragmentation of carbon dioxide using rotational wave-packets" Huynh Lam, Suresh Yarlagadda, Anbu Venkatachalam, Tomthin Nganba Wangjam, Rajesh K. Kushawaha, Chuan Cheng, Peter Svihra, Andrei Nomerotski, Thomas Weinacht, Daniel Rolles and Vinod Kumarappan. *Phys. Rev. A* accepted, (2020)

- "Effect of Dynamic Correlation on the Ultrafast Relaxation of Uracil in the Gas Phase", Pratip Chakraborty, Yusong Liu, Thomas Weinacht, and Spiridoula Matsika, *F*araday Disucssions, submitted, (2020)

AMOS PI Meeting
October 26-28, 2020

Thomas Allison
Stony Brook University
thomas.allison@stonybrook.edu

Vadym Apalkov
Georgia State University
vapalkov@gsu.edu

Luca Argenti
University of Central Florida
luca.argenti@ucf.edu

Polly Arnold
Lawrence Berkeley National Laboratory
PLA@lbl.gov

Andreas Becker
University of Colorado, Boulder
andreas.becker@colorado.edu

Itzik Ben-Itzhak
Kansas State University
ibi@phys.ksu.edu

Nora Berrah
University of connecticut
nora.berrah@uconn.edu

Cosmin Blaga
Kansas State University
blaga@phys.ksu.edu

Philip Bucksbaum
SLAC National Accelerator Laboratory
phb@slac.stanford.edu

Martin Centurion
University of Nebraska, Lincoln
martin.centurion@unl.edu

Lan Cheng
Johns Hopkins University
lcheng24@jhu.edu

Michael Chini
University of Central Florida
michael.chini@ucf.edu

Amy Cordones-Hahn
SLAC National Accelerator Laboratory
acordon@slac.stanford.edu

James Cryan
SLAC National Accelerator Laboratory
jcryan@slac.stanford.edu

Steven Cundiff
University of Michigan
cundiff@umich.edu

Marcos Dantus
Michigan State University
dantus@msu.edu

Louis DiMauro
Ohio State University
dimauro.6@osu.edu

Gilles Doumy
Argonne National Laboratory
gdoumy@anl.gov

Joseph Eberly
University of Rochester
eberly@pas.rochester.edu

Brett Esry
Kansas State University
esry@phys.ksu.edu

Li Fang
University of Central Florida
li.fang@ucf.edu

Chris Fecko
U.S. Department of Energy
Christopher.Fecko@science.doe.gov

Bob Forrey
National Science Foundation
rforrey@nsf.gov

Mette Gaarde
Louisiana State University
mgaarde1@lsu.edu

AMOS PI Meeting
October 26-28, 2020

Kelly Gaffney
SLAC National Accelerator Laboratory
kgaffney@slac.stanford.edu

Marco Garavelli
Bologna University
marco.garavelli@unibo.it

Bruce Garrett
U.S. Department of Energy
bruce.garrett@science.doe.gov

Oliver Gessner
Lawrence Berkeley National Laboratory
ogessner@lbl.gov

Shambhu Ghimire
SLAC National Accelerator Laboratory
shambhu@slac.stanford.edu

Tais Gorkhover
SLAC National Accelerator Laboratory
taisgork@slac.stanford.edu

Niri Govind
Pacific Northwest National Laboratory
niri.govind@pnnl.gov

Chris Greene
Purdue University
chgreene@purdue.edu

Loren Greenman
Kansas State University
lgreenman@phys.ksu.edu

Tony Heinz
SLAC National Accelerator Laboratory
tony.heinz@stanford.edu

Phay Ho
Argonne National Laboratory
pho@anl.gov

Edward Hohenstein
SLAC National Accelerator Laboratory
egh4@slac.stanford.edu

Cynthia Jenks
Argonne National Laboratory
cjenks@anl.gov

Robert Jones
University of Virginia
rrj3c@virginia.edu

Henry Kapteyn
University of Colorado
kapteyn@jila.colorado.edu

Jeffrey Krause
U.S. Department of Energy
Jeff.Krause@science.doe.gov

Vinod Kumarappan
Kansas State University
vinod@phys.ksu.edu

Guillaume Laurent
Auburn University
glaurent@auburn.edu

Peter Lee
U.S. Department of Energy
peter.lee@science.doe.gov

Stephen Leone
LBNL/University of California, Berkeley
srl@berkeley.edu

Elliane Lessner
U.S. Department of Energy
Eliane.Lessner@science.doe.gov

Wen Li
Wayne State University
wli@chem.wayne.edu

Chii Dong Lin
Kansas State university
cdlin@phys.ksu.edu

Kenneth Lopata
Louisiana State University
klopata@lsu.edu

AMOS PI Meeting
October 26-28, 2020

Robert Lucchese
Lawrence Berkeley National Laboratory
rlucchese@lbl.gov

Vyacheslav Lukin
National Science Foundation
vlukin@nsf.gov

Steven Manson
Georgia State University
smanson@gsu.edu

Anne Marie March
Argonne National Laboratory
amarch@anl.gov

Todd Martinez
SLAC National Accelerator Laboratory
toddjmartinez@gmail.com

Spiridoula Matsika
Temple University
smatsika@temple.edu

Bill McCurdy
Lawrence Berkeley National Laboratory
cwmccurdy@lbl.gov

Grace Metcalfe
Air Force Office of Scientific Research
grace.metcalfe@us.af.mil

Jeffrey Moses
Cornell University
moses@cornell.edu

Shaul Mukamel
University of California, Irvine
smukamel@uci.edu

Margaret Murnane
University of Colorado
Margaret.Murnane@colorado.edu

Adi Natan
SLAC National Accelerator Laboratory
natan@slac.stanford.edu

Daniel Neumark
LBNL/University of California, Berkeley
dneumark@berkeley.edu

Jean Marcel Ngoko Djiokap
University of Nebraska, Lincoln
marcelngoko@unl.edu

Thomas Orlando
Georgia Institute of Technology
thomas.orlando@chemistry.gatech.edu

Abbas Ourmazd
University of Wisconsin, Milwaukee
ourmazd@uwm.edu

Mick Pechan
U.S. Department of Energy
michael.pechan@science.doe.gov

Herschel Rabitz
Princeton University
hrabitz@princeton.edu

David Reis
SLAC National Accelerator Laboratory
dreis@stanford.edu

Thomas Rescigno
Lawrence Berkeley National Laboratory
tnrescigno@lbl.gov

Francis Robicheaux
Purdue University
robichf@purdue.edu

Daniel Rolles
Kansas State University
rolles@phys.ksu.edu

Artem Rudenko
Kansas State University
rudenko@phys.ksu.edu

Arvinder Sandhu
University of Arizona
asandhu@email.arizona.edu

Robin Santra
DESY/University of Hamburg
robin.santra@cfel.de

Kenneth Schafer
Louisiana State University
kschafe@lsu.edu

H. Bernhard Schlegel
Wayne State University
hbs@chem.wayne.edu

Robert Schoenlein
SLAC National Accelerator Laboratory
rwschoen@slac.stanford.edu

Tom Settersten
U.S. Department of Energy
thomas.settersten@science.doe.gov

Wade Sisk
U.S. Department of Energy
wade.sisk@science.doe.gov

Daniel Slaughter
Lawrence Berkeley National Laboratory
DSSlaughter@lbl.gov

Steve Southworth
Argonne National Laboratory
southworth@anl.gov

Uwe Thumm
Kansas State University
thumm@phys.ksu.edu

Carlos Trallero
University of Connecticut
carlos.trallero@uconn.edu

Sergei Tretiak
Los Alamos National Laboratory
serg@lanl.gov

Xijie Wang
SLAC National Accelerator Laboratory
wangxj@slac.stanford.edu

Peter Weber
Brown University
peter_weber@brown.edu

Thorsten Weber
Lawrence Berkeley National Laboratory
TWeber@lbl.gov

Thomas Weinacht
Stony Brook University
thomas.weinacht@stonybrook.edu

Thomas Wolf
SLAC National Accelerator Laboratory
thomas.wolf@stanford.edu

Linda Young
Argonne National Laboratoy
young@anl.gov